ECOLOGY AND PHYSIOLOGY OF NITRIFICATION

EDITED BY: Laura E. Lehtovirta-Morley, Sebastian Lücker, Holger Daims, Annette Bollmann, Anne E. Taylor and Peter Bottomley

PUBLISHED IN: Frontiers in Microbiology and Frontiers in Marine Science

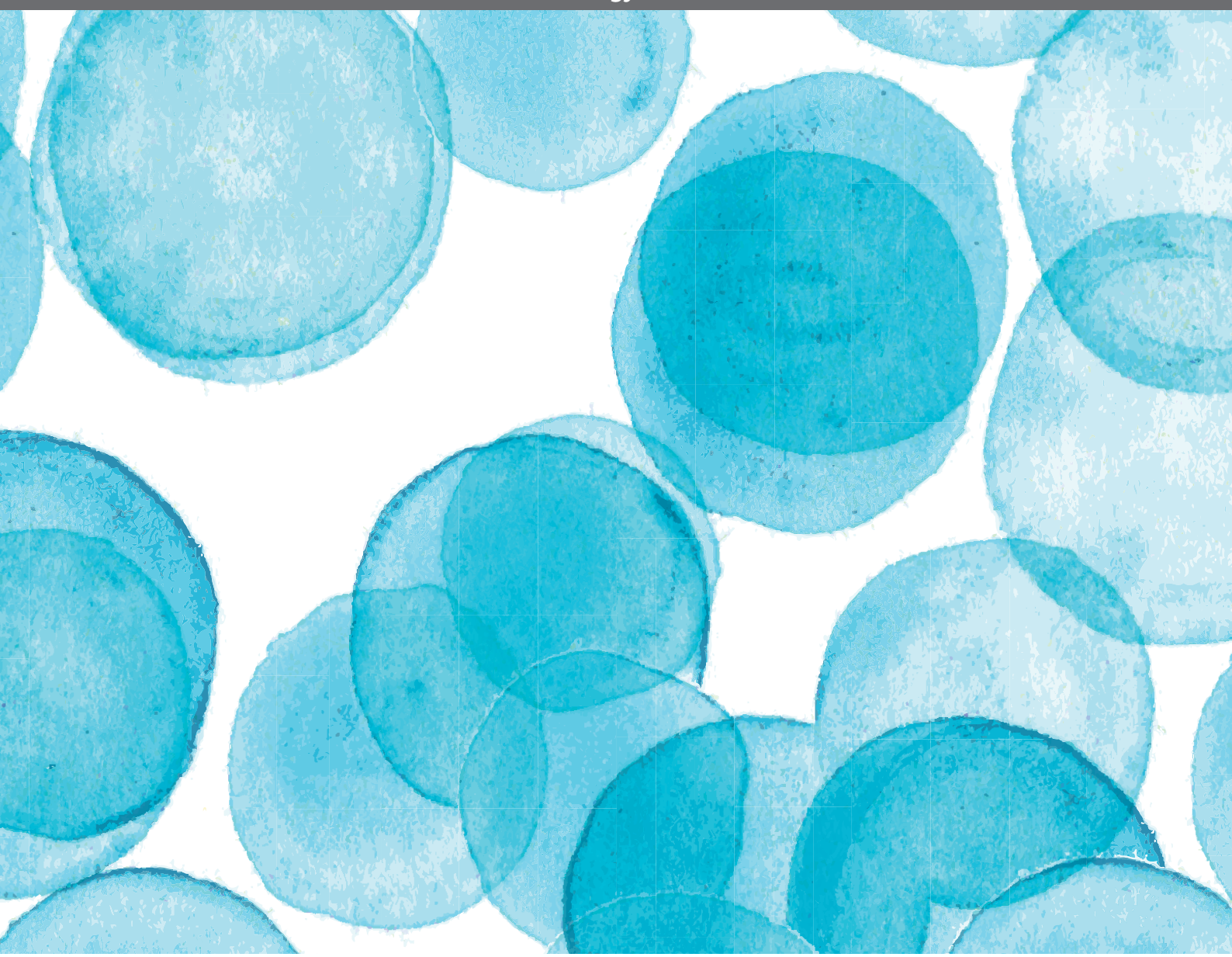

frontiers Research Topics

frontiers

ISSN 1664-8714
ISBN 978-2-88971-752-1
DOI 10.3389/978-2-88971-752-1

About Frontiers

Frontiers is more than just an open-access publisher of scholarly articles: it is a pioneering approach to the world of academia, radically improving the way scholarly research is managed. The grand vision of Frontiers is a world where all people have an equal opportunity to seek, share and generate knowledge. Frontiers provides immediate and permanent online open access to all its publications, but this alone is not enough to realize our grand goals.

Frontiers Journal Series

The Frontiers Journal Series is a multi-tier and interdisciplinary set of open-access, online journals, promising a paradigm shift from the current review, selection and dissemination processes in academic publishing. All Frontiers journals are driven by researchers for researchers; therefore, they constitute a service to the scholarly community. At the same time, the Frontiers Journal Series operates on a revolutionary invention, the tiered publishing system, initially addressing specific communities of scholars, and gradually climbing up to broader public understanding, thus serving the interests of the lay society, too.

Dedication to Quality

Each Frontiers article is a landmark of the highest quality, thanks to genuinely collaborative interactions between authors and review editors, who include some of the world's best academicians. Research must be certified by peers before entering a stream of knowledge that may eventually reach the public - and shape society; therefore, Frontiers only applies the most rigorous and unbiased reviews.
Frontiers revolutionizes research publishing by freely delivering the most outstanding research, evaluated with no bias from both the academic and social point of view. By applying the most advanced information technologies, Frontiers is catapulting scholarly publishing into a new generation.

What are Frontiers Research Topics?

Frontiers Research Topics are very popular trademarks of the Frontiers Journals Series: they are collections of at least ten articles, all centered on a particular subject. With their unique mix of varied contributions from Original Research to Review Articles, Frontiers Research Topics unify the most influential researchers, the latest key findings and historical advances in a hot research area! Find out more on how to host your own Frontiers Research Topic or contribute to one as an author by contacting the Frontiers Editorial Office: frontiersin.org/about/contact

ECOLOGY AND PHYSIOLOGY OF NITRIFICATION

Topic Editors:
Laura E. Lehtovirta-Morley, University of East Anglia, United Kingdom
Sebastian Lücker, Radboud University Nijmegen, Netherlands
Holger Daims, University of Vienna, Austria
Annette Bollmann, Miami University, United States
Anne E. Taylor, Oregon State University, United States
Peter Bottomley, Oregon State University, United States

Citation: Lehtovirta-Morley, L. E., Lücker, S., Daims, H., Bollmann, A., Taylor, A. E., Bottomley, P., eds. (2021). Ecology and Physiology of Nitrification. Lausanne: Frontiers Media SA. doi: 10.3389/978-2-88971-752-1

Table of Contents

frontiers in Marine Science

ORIGINAL RESEARCH
published: 26 May 2020
doi: 10.3389/fmars.2020.00360

Imprint of Trace Dissolved Oxygen on Prokaryoplankton Community Structure in an Oxygen Minimum Zone

Luis Medina Faull[1], Paraskevi Mara[2], Gordon T. Taylor[1] and Virginia P. Edgcomb[2]*

[1] School of Marine and Atmospheric Sciences, Stony Brook University, Stony Brook, NY, United States, [2] Department of Geology and Geophysics, Woods Hole Oceanographic Institution, Woods Hole, MA, United States

The Eastern Tropical North Pacific (ETNP) is a large, persistent, and intensifying oxygen minimum zone (OMZ) that accounts for almost half of the total area of global OMZs. Within the OMZ core (∼350–700 m depth), dissolved oxygen is typically near or below the analytical detection limit of modern sensors (∼10 nM). Steep oxygen gradients above and below the OMZ core lead to vertical structuring of microbial communities that also vary between particle-associated (PA) and free-living (FL) size fractions. Here, we use 16S amplicon sequencing (iTags) to analyze the diversity and distribution of prokaryotic populations between FL and PA size fractions and among the range of ambient redox conditions. The hydrographic conditions at our study area were distinct from those previously reported in the ETNP and other OMZs, such as the ETSP. Trace oxygen concentrations (∼0.35 μM) were present throughout the OMZ core at our sampling location. Consequently, nitrite accumulations typically reported for OMZ cores were absent as were sequences for anammox bacteria (Brocadiales genus *Candidatus* Scalindua), which are commonly found across oxic-anoxic boundaries in other systems. However, ammonia-oxidizing bacteria (AOB) and archaea (AOA) distributions and maximal autotrophic carbon assimilation rates (1.4 μM C d^{-1}) coincided with a pronounced ammonium concentration maximum near the top of the OMZ core. In addition, members of the genus *Nitrospina*, a dominant nitrite-oxidizing bacterial (NOB) clade were present suggesting that both ammonia and nitrite oxidation occur at trace oxygen concentrations. Analysis of similarity test (ANOSIM) and Non-metric Dimensional Scaling (nMDS) revealed that bacterial and archaeal phylogenetic representations were significantly different between size fractions. Based on ANOSIM and iTag profiles, composition of PA assemblages was less influenced by the prevailing depth-dependent biogeochemical regime than the FL fraction. Based on the presence of AOA, NOB and trace oxygen in the OMZ core we suggest that nitrification is an active process in the nitrogen cycle of this region of the ETNP OMZ.

Keywords: eastern tropical north pacific, oxygen minimum zones, prokaryoplankton community structure, oxygen gradients, nitrification

OPEN ACCESS

Edited by:
Sebastian Lücker, Radboud University Nijmegen, Netherlands

Reviewed by:
J. Michael Beman, University of California, Merced, United States
Xin Sun, Princeton University, United States

****Correspondence:***
Gordon T. Taylor
gordon.taylor@stonybrook.edu

Specialty section:
This article was submitted to Aquatic Microbiology, a section of the journal Frontiers in Marine Science

Received: *13 January 2020*
Accepted: *28 April 2020*
Published: *26 May 2020*

Citation:
Medina Faull L, Mara P, Taylor GT and Edgcomb VP (2020) Imprint of Trace Dissolved Oxygen on Prokaryoplankton Community Structure in an Oxygen Minimum Zone. Front. Mar. Sci. 7:360. doi: 10.3389/fmars.2020.00360

INTRODUCTION

In response to ongoing climate change and localized human activities, concentrations of dissolved oxygen have been declining in the open ocean and in coastal marine systems (Breitburg et al., 2018). Estimated oxygen loss from the open ocean during the past 60 years exceeds 2% (Schmidtko et al., 2017), creating concerns about the consequences of oxygen-depleted zone expansion (Paulmier and Ruiz-Pino, 2009). Open ocean OMZs form when high surface primary production fuels biological oxygen demand in subsurface waters that exceeds rates of physical ventilation at depth. Oxygen concentrations in OMZ water columns can have steep gradients (oxycline) above and below the oxygen-depleted core creating hypoxic (typically between 2 and ∼90 μM), suboxic (<2 μM) and anoxic (below detection limit (∼10 nM) layers of varying dimensions (Bertagnolli and Stewart, 2018). Oxygen gradients lead to vertical structuring of metazoan and microbial communities and biogeochemical processes along these extensive oxyclines (Belmar et al., 2011).

Some of the highest rates of nitrogen loss have been recorded in OMZs of the Eastern Tropical North Pacific (ETNP) and South Pacific (ETSP) (Callbeck et al., 2017; Penn et al., 2019), the permanently stratified Cariaco Basin (Montes et al., 2013), the Arabian Sea (Ward et al., 2009), and the OMZ of the Benguela upwelling system (Kuypers et al., 2005). In these systems, the microbial processes of canonical denitrification (heterotrophic reduction of nitrate to nitrogen intermediates and often to dinitrogen gas) and anammox (anaerobic ammonium oxidation) lead to nitrogen losses that can potentially limit primary production (Ward et al., 2007). Moreover, oceanic nitrous oxide emissions (a potent greenhouse gas) from microbial denitrification occurring in OMZs is estimated to account for at least one third of global natural nitrous oxide emissions (Naqvi et al., 2010).

The ETNP OMZ is a large, persistent, and intensifying oxygen minimum zone that accounts for almost half of the total area of global OMZs, is located between 0–25°N latitude and 75 and 180°W longitude (Paulmier and Ruiz-Pino, 2009; Schmidtko et al., 2017). Due to their ecological importance, the biogeochemistry and microbial diversity of different ETNP OMZ regions have been studied intensively (e.g., Beman and Carolan, 2013; Duret et al., 2015; Ganesh et al., 2015; Chronopoulou et al., 2017; Pack et al., 2015; Peng et al., 2015). Previous studies report that dissolved oxygen in this OMZ core (∼250–750 m depth) is typically near or below analytical detection limits (∼10 nM) (Tiano et al., 2014; Garcia-Robledo et al., 2017). However, along the northern margin of the ETNP's OMZ (study site location ∼22°N) oxygen concentrations at 500 m can reach annual averages between 10 and 20 μM (Paulmier and Ruiz-Pino, 2009; Data from World Ocean Atlas 2013)[1]. During the field campaign reported herein, we measured oxygen in the OMZ core at sufficient concentrations (0.35 μM) to support aerobic microbial processes, such as ammonium and nitrite oxidation, and partially inhibit important anaerobic microbial processes. Aerobic microbial processes have been detected previously in seemingly suboxic or anoxic layers of the ETNP OMZ (Peng et al., 2015; Garcia-Robledo et al., 2017; Penn et al., 2019). However, factors controlling the distribution and activities of specific functional groups of microorganisms in OMZs are not yet fully understood.

The presence of nitrifiers where oxygen is undetectable in an OMZ can be explained by recent shifts in the vertical position of the oxycline due to episodic vertical oxygen ventilation, which can lead to ephemeral trace oxygen levels within OMZ cores (Muller-Karger et al., 2001; Ulloa et al., 2012; Garcia-Robledo et al., 2017). Such transient conditions can be exploited by aerobic or microaerophilic populations, including nitrifiers. Moreover, sinking particles from the epipelagic (aggregated cells, fecal pellets, and complex organic materials) can contain trace levels of oxygen (Ganesh et al., 2014). Thus, oxygen and aerobic microbes can be transported to otherwise anoxic waters, temporarily allowing aerobic metabolisms to occur in association with particles. Particles are known to be hotspots of microbial biogeochemical cycling (Simon et al., 2002; Ganesh et al., 2014) and can support contrasting anaerobic or aerobic microbial processes that are not observed in the free-living state (Alldredge and Cohen, 1987; Wright et al., 2012; Suter et al., 2018).

In the present study, we investigate prokaryotic communities occupying the northern margin of the ETNP's OMZ and environmental factors that likely influence their vertical distributions using 16S amplicon sequencing (iTags) coupled with multivariate statistics. We examined two size fractions; the free-living (0.2–2.7 μm) fraction, and the particle-associated fraction (>2.7 μm, capturing particles as well as protistan cells) at multiple depths along the oxycline that correspond to distinct redox conditions.

MATERIALS AND METHODS

Sampling and Analytical Procedures

A 28-day oceanographic expedition starting from Manzanillo, Mexico and returning to San Diego, CA was conducted onboard the R/V *Sikuliaq*, from 19 January to 15 February 2017 (UNOLS cruise number SKQ201701S). Sampling of OMZ waters was conducted off the Baja California Peninsula. Among the 16 stations occupied during this cruise, Station #12 (21.6°N 117.8°W) was the source of all samples analyzed for this study. This station is located at the northern margin of the ETNP OMZ, approximately 350 nautical miles (∼650 km) offshore from the Baja California Peninsula (**Figure 1**). At this station, hydrographic data were obtained using a conductivity-temperature-depth (CTD) system (Seabird 3 temperature sensor, Seabird nine digital pressure sensor, and a Seabird four conductivity sensor), a Seapoint fluorimeter (range: 0.01 to 125 μg Chla L^{-1}), and a RI.NKO III series optical oxygen sensor (JFE Advantech Co., Ltd.), all mounted on a rosette. The oxygen sensor was calibrated by the two point calibration method using air-bubbled water for 100% DO saturation and a dilute sodium sulfite solution for 0% DO saturation. Water samples for biological and chemical analyses were collected in 10-liter Niskin bottles on the rosette.

[1]https://www.nodc.noaa.gov/OC5/woa13/

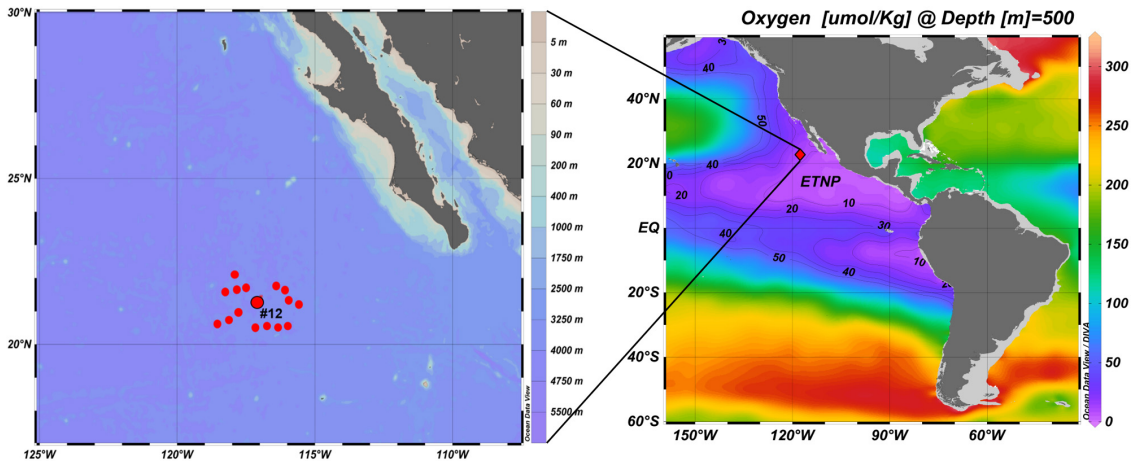

FIGURE 1 | Locations of 16 ETNP stations occupied during the cruise. Station #12 (21.6°N 117.8°W) was the source of the samples analyzed for this study (prepared using Ocean Data View, Schlitzer, R., ODV, https://odv.awi.de, 2018).

From Niskin bottles, 2–5 L of water from 10 depths were directly passed through a 2.7 μm hydrophilic glass fiber filter (EMD Millipore, Burlington, MA, United States) and then through an in-line 0.2 μm Millipore® Sterivex™ filter (EMD Millipore, Burlington, MA, United States) to collect material for 16S amplicon sequencing (iTags). The >2.7 μm filters primarily captured the particle and protist-associated cells ("PA" fraction) and the 0.2 μm filter primarily captured free-living cells (0.2–2.7 μm = "FL" fraction). The 10 depths sampled targeted different biogeochemical regimes (**Table 1**); including normoxic conditions below the photic zone (=115 μM O_2, "O"), upper oxycline (114–5 μM O_2, "UOC"), the OMZ core (0.35–5 μM O_2, "OMZc"), lower oxycline (5–50 μM O_2, "LOC"), and deep normoxic (>50 μM O_2, "DO") samples. Two biological replicates were processed from each of the 10 sampled depths. Filters were immediately preserved for nucleic acid extraction by adding 1.8 ml sterile DNA lysis buffer (50 mM Tris-HCL, 40 mM EDTA, 0.73 M sucrose) through the inlet of the Sterivex filter using a micropipette. The Sterivex filter was sealed with parafilm. Glass fiber filters were transferred into sterile 4 ml cryovials and were immersed in the lysis buffer. Sterivex and glass fiber filters were stored at −80°C.

TABLE 1 | Oxygen concentrations and collection depths for ENTP samples.

Oxygen condition	Depth (m)	Oxygen concentration (μM)
Oxic (O)	106	203
Oxic (O)	125	153
Oxic (O)	150	115
Upper Oxycline (UOC)	200	70
OMZ core (OMZc)	500	0.35
OMZ core (OMZc)	640	0.86
OMZ core (OMZc)	650	0.92
OMZ core (OMZc)	700	2.30
Lower Oxycline (LOC)	900	7.23
Deep Oxic (DO)	2,500	90

FL = 0.2–2.7 μm size fraction; PA = >2.7 μm size fraction.

Photoautotrophic and chemoautotrophic production were measured using bulk community ^{13}C-bicarbonate incorporation according to Fisher and Haines (1979) and Sambrotto et al. (2015). A CTD cast was performed to obtain the irradiance profile based on the attenuation of PAR just prior to the collection of water for productivity measurements. For photoautotrophic ^{13}C-assimilation, water from five depths (corresponding to 100, 55, 30, 10, and 1.5% of surface irradiance) was dispensed into 2 L transparent polycarbonate (PC) bottles. Incubation bottles were covered with neutral density plastic screen to simulate *in situ* irradiance levels and were incubated for 24 h in an on-deck incubator. The incubators were continuously flushed with surface seawater to maintain *in situ* mixed layer temperature (at ∼23°C) which was monitored throughout the experiments. Water for dark ^{13}C-assimilation was collected the same way at six depths (100, 200, 500, 650, 750, and 1500 m) and incubated with ^{13}C-bicarbonate for 24 h in 2 L PC bottles in the dark at *in situ* temperature. After incubation, particulate material was collected on GF/F filters (previously combusted) under gentle vacuum. Total carbon content and ^{13}C/^{12}C ratios of the samples were measured by a continuous flow isotope ratio mass spectrometer at the UC Davis stable isotope facility[2].

Water for nutrients (nitrate, nitrite, phosphate and ammonium) was collected at 20 depths that included normoxic conditions within and below the photic zone, upper and lower oxycline depths, OMZ core, and deep normoxic waters. These samples were analyzed by continuous flow analysis (CFA) at the Instrumental Analysis Laboratory, School of Marine and Atmospheric Sciences, Stony Brook University, following methods of Gordon et al. (1993).

To enumerate total prokaryoplankton abundances, 200 ml samples from 20 depths throughout the water column were

[2]https://stableisotopefacility.ucdavis.edu/

preserved with 2% borate-buffered formaldehyde in high density polyethylene (HDPE) bottles and stored at 4°C. Back in the laboratory, subsamples were filtered, and all filters were stained with 1 μg/ml (final concentration) 4′,6-diamidino-2-phenylindole (DAPI) and abundances of DAPI-positive cells were quantified using an epifluorescence microscope with a UV excitation filter set (Porter and Feig, 1980).

Nucleic Acid Extraction and Sequencing

For DNA extractions, we used a modification of the Somerville et al. (1988) protocol appropriate for extracting DNA from glass fiber filters. To improve handling and increase the extraction yield, we transferred the glass fiber filters from the 4 ml cryovials that were collected onboard, into 15 ml sterile Falcon tubes. Glass fiber and Sterivex filters were immersed in 40 μl lysozyme solution (50 mM) for 1 h in a 37°C shaker incubator. Lysozyme solution contained 2 mg lysozyme in 40 μl DNA lysis buffer; 50 mM Tris-HCL, 40 mM EDTA, 0.73 M sucrose). After the lysozyme treatment, 100 μl of Proteinase K solution (20 mg/ml) and 100 μl of 20% SDS were added to both types of filters and the tubes were shaken in the incubator for an additional 2 h at 55°C. After the Proteinase K incubation, crude lysates from each glass fiber and Sterivex filter were transferred to separate 15 ml sterile Falcon tubes. Both filter types were rinsed twice with 1 ml lysis buffer and incubated during each rinse for 15 min at 55°C in a shaker incubator. After rinsing, lysate fluids were combined with the crude lysate from their respective Sterivex and glass fiber filters. DNA extraction of the lysates was performed using a phenol-chloroform protocol. Bacterial and archaeal 16S rRNA gene fragments were PCR amplified from the samples using the primers: 515F-Y (5′-GTGYCAGCMGCCGCGGTAA) and 926R (5′-CCGYCAATTYMTTTRAGTTT[GT2]) (Parada et al., 2016). PCR products were sequenced at Georgia Genomics and Bioinformatics Core Facility (U. of Georgia) using llumina MiSeq PE300 and barcoded primers.

Sequence Analysis

Sequence analysis was performed using Quantitative Insights Into Microbial Ecology (QIIME) v1.9.1 software (Caporaso et al., 2010). Raw sequence reads were processed through Trim Galore[3], FLASH (Magoč and Salzberg, 2011) and FASTX_Toolkit[4] for trimming and removal of low quality/short reads. During quality control, sequences shorter than 250 nucleotides were removed. Operational Taxonomic Unit (OTU) clusters were constructed at 97% similarity with the script pick_otus.py within QIIME (Caporaso et al., 2010) v1.9.1 software and "uclust". All sequence data generated in this study has been deposited into Sequence Read Archive (SRA) GenBank under the accession numbers SRR10173043-SRR10172999.

Statistical Analysis

The normalized relative abundance table of OTUs present in each sample was obtained using QIIME v1.9.1. Non-Metric Dimensional Scaling (nMDS) and Analysis of Similarities test (ANOSIM) were conducted based on this relative abundance OTU table using R (version 3.2.1).

Bubble plots were created in R (version 3.2.1) to present diversity in each sample at two taxonomic levels (Phylum, Order) using the Vegan package, version 2.3–2. First, OTUs were segregated by FL and PA size fractions (0.2–2.7 μm and >2.7 μm) and analyzed separately. Relative abundances of individual OTUs from replicate biological samples were averaged and then normalized using the Hellinger transformation (Clarke et al., 2013). Only OTUs with >0.1% average relative abundance in at least one sample were included.

nMDS analysis of all samples was performed in R using the same version and package above. Input for these analyses was a Bray-Curtis dissimilarity matrix of the Hellinger-transformed OTU tables. For nMDS analyses, stress values are reported as a measure of goodness of fit. To assess the influence of biotic and abiotic factors on sample ordination, vectors representing contextual data (oxygen, nutrients, DIC assimilation, total prokaryoplankton counts, etc.) were fit to the ordination plots using goodness of fit statistics (r^2 and p-value) as indicators for each vector.

Finally, in order to assess if groups of OTUs were significantly different among water samples from different redox regimes (O, UOC, LOC, OMZc, and DO) and size fractions, ANOSIM tests between groups was performed using the dissimilarity matrix as input (Clarke et al., 2013).

RESULTS AND DISCUSSION

Hydrographic and Geochemical Setting

The hydrographic conditions at our study area were distinct from those previously reported in the ETNP (Podlaska et al., 2012) and other OMZs, such as the ETSP (Bristow et al., 2016). Oxygen profiles measured *in situ* from all 16 stations occupied during the cruise, consistently indicated trace oxygen was present in the OMZ core of this region. The minimum oxygen concentrations within the water column varied between 0.28 and 0.38 μM, revealing the presence of trace oxygen even in OMZ core waters (∼350–700 m). In addition, nitrite did not accumulate within the OMZ core at station #12, indicating the presence of microoxic conditions during the period of our cruise. The presence/absence of nitrite accumulation has been used previously to indicate anoxia in OMZs (Ulloa et al., 2012; Peng et al., 2015; Sun et al., 2019).

Vertical profiles of temperature, salinity, and water density (Sigma-t) for our master station (#12) are presented in **Figure 2A**. The surface layer was well-mixed to 100 m, below which a steep thermocline appears where temperatures dropped from ∼23 to 12°C between 100 and 250 m, and declined more gradually to ∼2°C by 2,500 m. Salinity values were highest in surface waters (34.25 PSU), decreasing down to ∼150 m (33.60 PSU), and then gradually increasing toward a maximum of 34.60 PSU by ∼400 m. In general, seawater density (Sigma-t) increased gradually from 100 to 2,500 m reflecting decreasing temperature and increasing salinity. At station #12, a narrow peak in oxygen concentration was observed below the well-oxygenated mixed

[3]http://www.bioinformatics.babraham.ac.uk/projects/trim_galore/
[4]http://hannonlab.cshl.edu/fastx_toolkit/

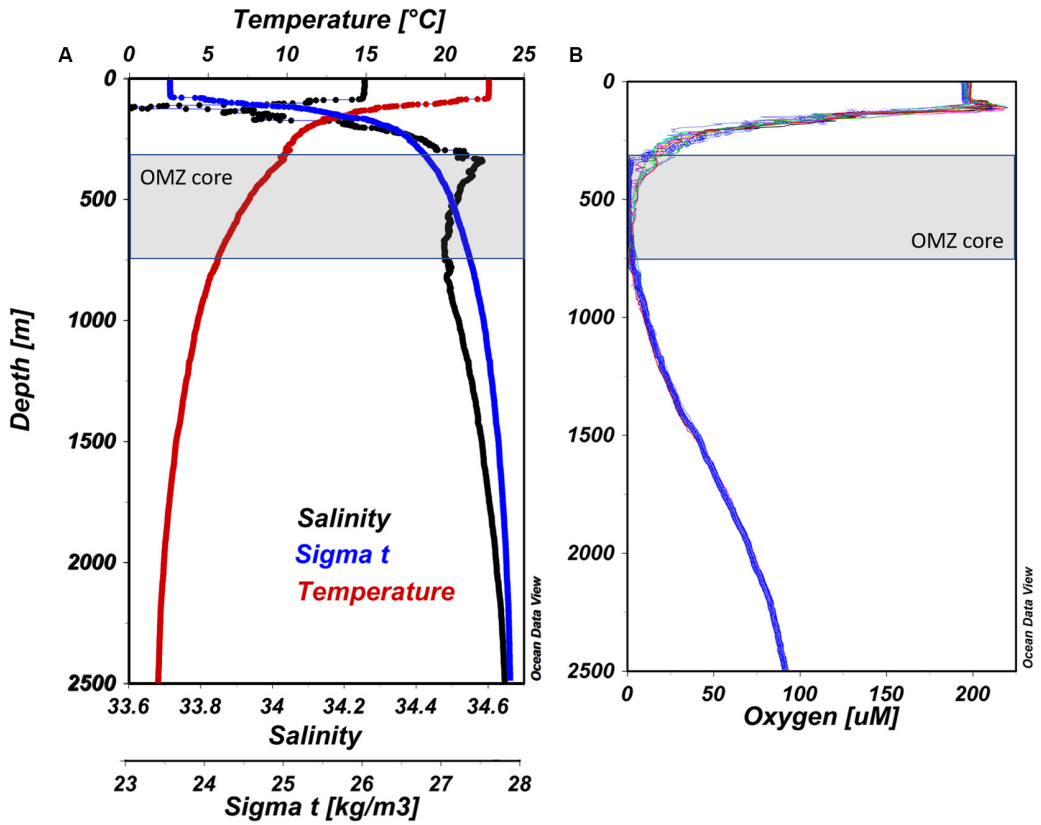

FIGURE 2 | (A) Vertical profiles of CTD sensor data from ETNP station #12. Temperature, salinity, and Sigma-t are presented as red, black, and blue lines, respectively. **(B)** Vertical profiles of dissolved oxygen concentration from all stations surveyed at the cruise. Blue solid line represent station #12 (prepared using Ocean Data View, Schlitzer, R., ODV, https://odv.awi.de, 2018).

layer at 120 m (220 μM O_2; **Figure 2B**), which coincided with a deep chlorophyll *a* (Chl *a*) fluorescence maximum at 106 m. A steep oxycline was observed between 200 and ∼350 m, above the OMZ core which extended from 350 to ∼700 m. Below ∼700 m depth, oxygen gradually increased to 69 μM at 2,500 m.

The well-mixed surface layer (100 m) in this region is subject to high rates of primary production that influence nutrient concentrations. Phosphate and nitrate concentrations (**Figures 3A,B**) were lowest in the surface layer (0 – ∼100 m), and increased steeply from 150 to 250 m, followed by more gradual increases down to ∼900 m. Nitrite distributions were distinct from other nutrients, exhibiting maximum concentration at 150 m (∼1 μM N) and secondary peaks at 25 and 250 m (**Figure 3B**). Ammonium was only detected at 150 m (∼0.7 μM N) and 500 m (0.4 μM N; **Figure 3A**).

Biological variables measured at station #12 suggest intense microbial activity just above the upper oxycline (100–150 m) down into the OMZ core (500 m). Dark and light dissolved inorganic carbon assimilation (DIC assimilation), fluorescence, a proxy of Chl *a* indicative of phytoplankton biomass, and total prokaryoplankton concentrations are shown in **Figure 4**. A very pronounced fluorescence peak (∼0.7 relative fluorescence units) was observed at 106 m and corresponded with maximum representation of OTUs belonging to the cyanobacterial Subsection I (*Prochlorococcus*). The highest prokaryotic abundances were measured in surface waters (6.8×10^8 cells L^{-1}; **Figure 4**). In general, cell concentrations decreased with depth, but secondary peaks were observed coincident with the 106 m fluorescence peak and just above the OMZ core (300 m).

The maximum DIC assimilation (1.4 μM C d^{-1}) was observed in the OMZ core at 500 m, coinciding with one of the ammonium concentrations peaks (**Figures 3B**, **4**). Similar to the present study, Podlaska et al. (2012) reported maximum DIC assimilation rates varying between 0.02 and 6.4 μM C d^{-1} among four ETNP stations 7° south of the current study. These rates are considerably faster than those reported for nitrifiers in normoxic regions, such as in the mesopelagic Atlantic Ocean, 0.03–10.4 nM C d^{-1} (Pachiadaki et al., 2017) or South China Sea and the Western Pacific Ocean, 0.008–1.31 nM C d^{-1} (Zhang et al., 2020). The disparity between these putatively nitrifier-driven rates may simply be explained by ammonium distributions. NH_4^+ concentrations in the ETNP studies varied between 400 and 2500 nM-N with depth-dependent peaks (Podlaska et al., 2012; this study). Whereas at those normoxic sites, NH_4^+ concentrations were only on the order of 30–50 nM-N through the depths sampled (Zhang et al., 2020). At two of Podlaska et al.'s (2012) stations, they

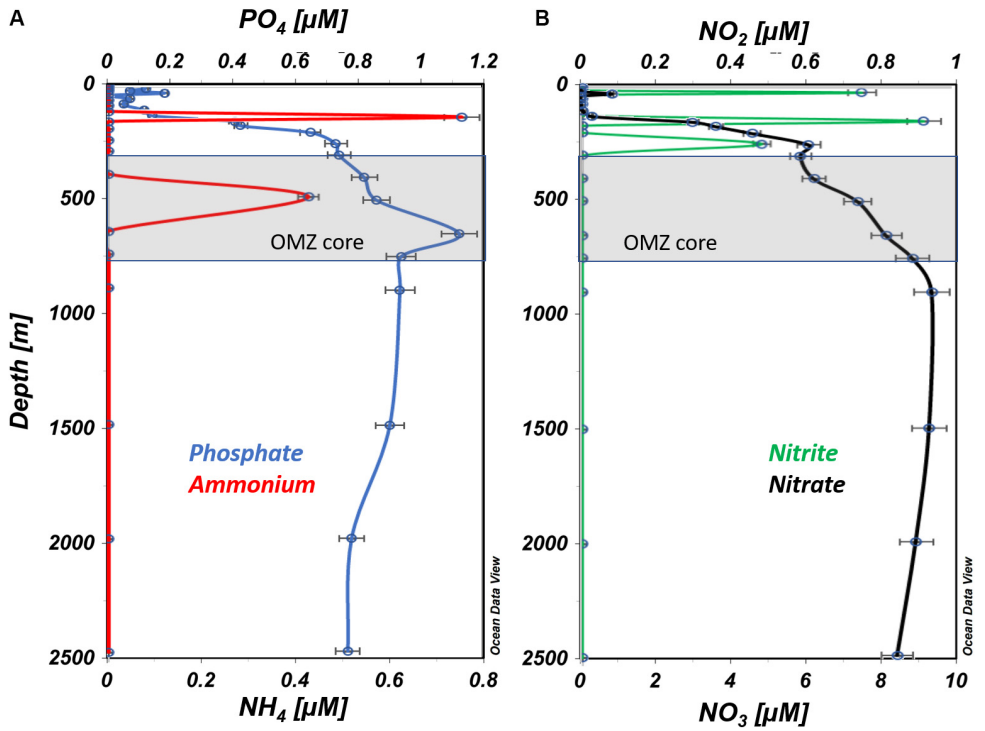

FIGURE 3 | Vertical profiles of nutrient concentrations from ETNP station #12. **(A)** Ammonium and phosphate are presented in blue and red, respectively. **(B)** Nitrate and nitrite are presented in black and green, respectively (prepared using Ocean Data View, Schlitzer, R., ODV, https://odv.awi.de, 2018).

showed that 30 μM NH_4^+ amendments could stimulate DIC assimilation by 1.5 to 33-fold among samples from four to six depths. Observed stimulations suggest nitrifying activity in this system is ammonium limited.

Accumulation of ammonium often results from remineralization of sinking organic material that reaches depth from more productive surface waters (Lam et al., 2011; Beman and Popp, 2012). Alternatively, ammonium enrichments can be generated by excretion from vertically migratory mesozooplankton. In fact, during our cruise Wishner et al. (2018) conducted mesozooplankton surveys using a 1-m^2 MOCNESS net and observed an abundance peak of the copepod, *Lucicutia hulsemannae*, between 500 and 600 m. It is likely that the ammonium enrichment observed at 500m during the current study combined with the presence of trace oxygen fueled chemoautotrophic production by nitrifiers. In the photic zone, a smaller peak of DIC assimilation was observed at 90 m (0.38 μM C d^{-1}) just above the Chl *a* peak where OTUs affiliated with the cyanobacterial Subsection I (*Prochlorococcus*) were most highly represented.

Size Partitioning of Prokaryotic Assemblages

Microbial phylogenetic composition, cell abundances, depth distributions, and activities can vary widely among size-fractionated samples in OMZs (Ganesh et al., 2014; Suter et al., 2018). Ganesh et al. (2014) observed distinct phylogenetic compositions of PA and FL assemblages in the ETSP. These differences suggested that many PA prokaryoplankton taxa are specialists favoring biogeochemical conditions in the detritosphere and prefer surface attachment, association with protists, or growth in biofilms. Furthermore, particles that have been colonized in surface waters and sink through the OMZ likely contain prokaryotic assemblages phylogenetically distinct from the surrounding waters from which they are collected (Suter et al., 2018).

In the present study, two size fractions (0.2–2.7 μm and >2.7 μm) of the microbial community from each depth were analyzed. ANOSIM tests results (R value = 0.67, $p < 0.001$) revealed that bacterial and archaeal taxonomic representation was significantly different between the FL and PA size fractions. **Supplementary Figure 1** shows the nMDS for all samples based on the relative abundances of 463 OTUs, clearly showing community differences among the size fractions (FL and PA).

Size partitioning of prokaryote assemblages is evident in the average relative abundances of bacterial and archaeal iTags at the phylum taxonomic level (**Figure 5**). Of the 17 main groups with average relative abundances above 0.1% in at least one sample, only Proteobacteria and Thaumarchaeota were abundant in both size fractions and under all redox conditions. The top three most abundant bacterial classes were alpha-, gamma- and delta-proteobacteria with alpha-proteobacteria dominating bacterial inventories at all depths. Signatures of cyanobacteria and/or chloroplasts were only abundant in the surface waters in both size fractions. Marinimicrobia (SAR 406) and Euryarchaeota

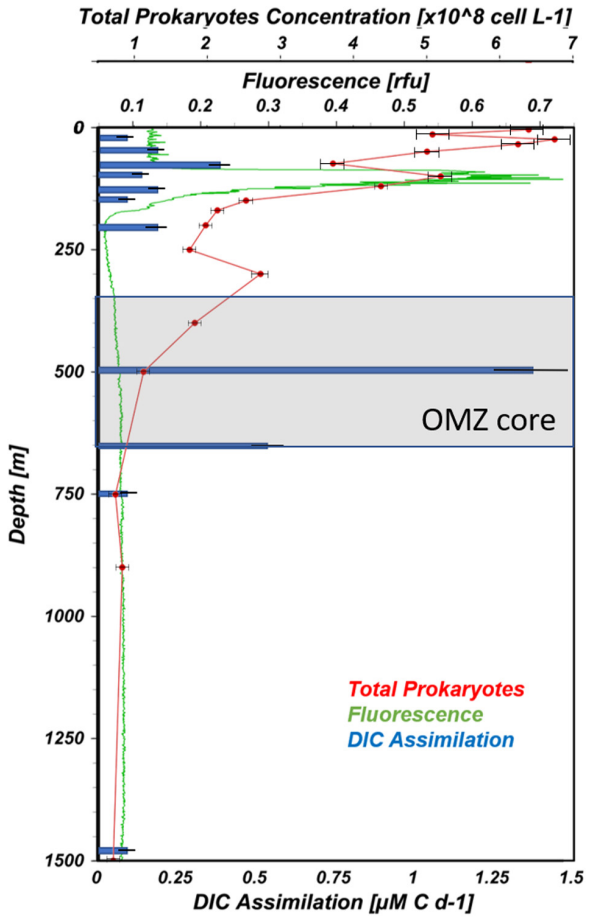

FIGURE 4 | Vertical profiles of biological variables from ETNP station #12. Total prokaryoplankton, fluorescence, and DIC assimilation are presented as red, green and blue lines, respectively (prepared using Ocean Data View, Schlitzer, R., ODV, https://odv.awi.de, 2018).

were abundant throughout the water column in the FL fraction, while Planctomycetes and Bacteroidetes were also abundant throughout all depths in the PA fraction. Firmicutes were most highly represented in the PA fraction at 150 and 500 m depth.

Anaerobacillus sp. (Bacillaceae) comprised 75% of the OTUs belonging to the Firmicutes in the PA fraction at 150 m (O) and 500 m (OMZc). The four known species within this genus are strictly anaerobic, heterotrophic, diazotrophic bacteria that possess the *nifH* gene which is a widely sequenced marker gene for nitrogen fixation (Zavarzina et al., 2009; Wang et al., 2015). Although our study lacks metagenomic and metatranscriptomic data on *nifH,* we hypothesize nitrogen fixation is possibly carried out by particle-associated *Anaerobacillus* species at 150 and 500 m, the NH_4 maxima. This highlights the potential importance of particle-associated microorganisms in OMZ water columns and can offer an explanation for how anaerobic nitrogen fixation can occur at the same depths as microaerophilic nitrifiers that oxidize ammonium to nitrite.

We postulate that the ammonium peak observed at 500 m supports ammonium oxidation (the first step of nitrification) if AOB, AOA and trace oxygen are present. In fact, our iTag data reveal an abundant, well-described AOA, Marine Group I (Thaumarchaeota) OTU in the FL and PA fractions of OMZ core (**Figures 6**, **7**) coincident with the 500 m ammonium maximum (0.4 µM) and oxygen minimum (0.35 µM). Marine Group I were also abundant in the UOC and DO in both size fractions in our station. BLASTn analysis revealed many of our Marine Group I SSU signatures were affiliated with uncultured archaeon clones L4, L5, and L6 (100% query coverage; 97.1% percentage ID and *e*-value 0). Zou et al. (2019) determined that these clones are affiliated with AOA, providing indirect evidence that our Marine Group I signatures are also largely AOAs. Other phylogenetic studies from oxygen minimum zones and seasonally stratified anoxic basins reveal that Marine Group I is well represented in the oxycline and is believed to be a major driver of nitrification in the oceans (Pitcher et al., 2011; Swan et al., 2014). Studies of the Chilean OMZ showed that AOA and NOB could be responsible for ammonium and nitrite oxidation rates between 0.16 and 1 µM N d^{-1} at very low oxygen levels (5–30 nM) if oxygen fluxes are sufficient (Ward et al., 1989; Molina et al., 2010; Bristow et al., 2016). Elsewhere in the ETNP, Peng et al. (2015) reported that AOA dominated ammonia oxidation over AOB within the oxycline. Likewise, Podlaska et al. (2012) suggested that ammonium and nitrite oxidation were important in the upper oxycline, OMZ core, and deep waters at their ETNP stations, based on metabolic activity and nitrogen species profiles. Considering that our iTag library revealed AOA in the OMZ core and that nitrification can occur at trace oxygen concentrations, we posit that ammonium oxidation was an active process in the OMZ core at this site in the ETNP.

Similarly, based on a sharp decrease in nitrite concentrations below 150 m (**Figure 3**) and evidence of nitrite-oxidizing taxa in our iTAG libraries, we hypothesize that nitrite oxidation must be an active process where traces of oxygen are present. Four genera are recognized to be responsible for nitrite oxidation in the ocean; *Nitrobacter* (alpha-proteobacteria), *Nitrococcus* (gamma-proteobacteria), *Nitrospina* (Nitrospinae) and *Nitrospira* (Nitrospirae). However, several studies report the last two as the most common groups in the open ocean (Levipan et al., 2014; Pachiadaki et al., 2017; Sun et al., 2019). We did not recover any *Nitrococcus* or *Nitrobacter* sequences in our iTag libraries. *Nitrospina* sp. was the dominant NOB taxon in the oxic layer (150 m), UOC, OMZ core and deep waters, appearing primarily in the FL fraction (**Figure 6**), but also in the PA fraction (**Figure 7**) to a lesser extent. Although *Nitrospira* OTUs were found in the oxic layer and OMZ core their average relative abundances were less than 0.1% in all samples (FL and PA fractions).

Nitrospinae is a cosmopolitan chemoautotrophic bacterial clade present in major oxygenated mesopelagic water masses (e.g., Pachiadaki et al., 2017). Although, the type species for the Nitrospinae phylum (*Nitrospina gracilis*) was described to be strictly aerobic (Lücker et al., 2013), it has been found to be present and active in OMZ locations and in an anoxic basin (Rodriguez-Mora et al., 2013; Bristow et al., 2016; Sun et al., 2019). Suter et al. (2018) found a relatively high abundance

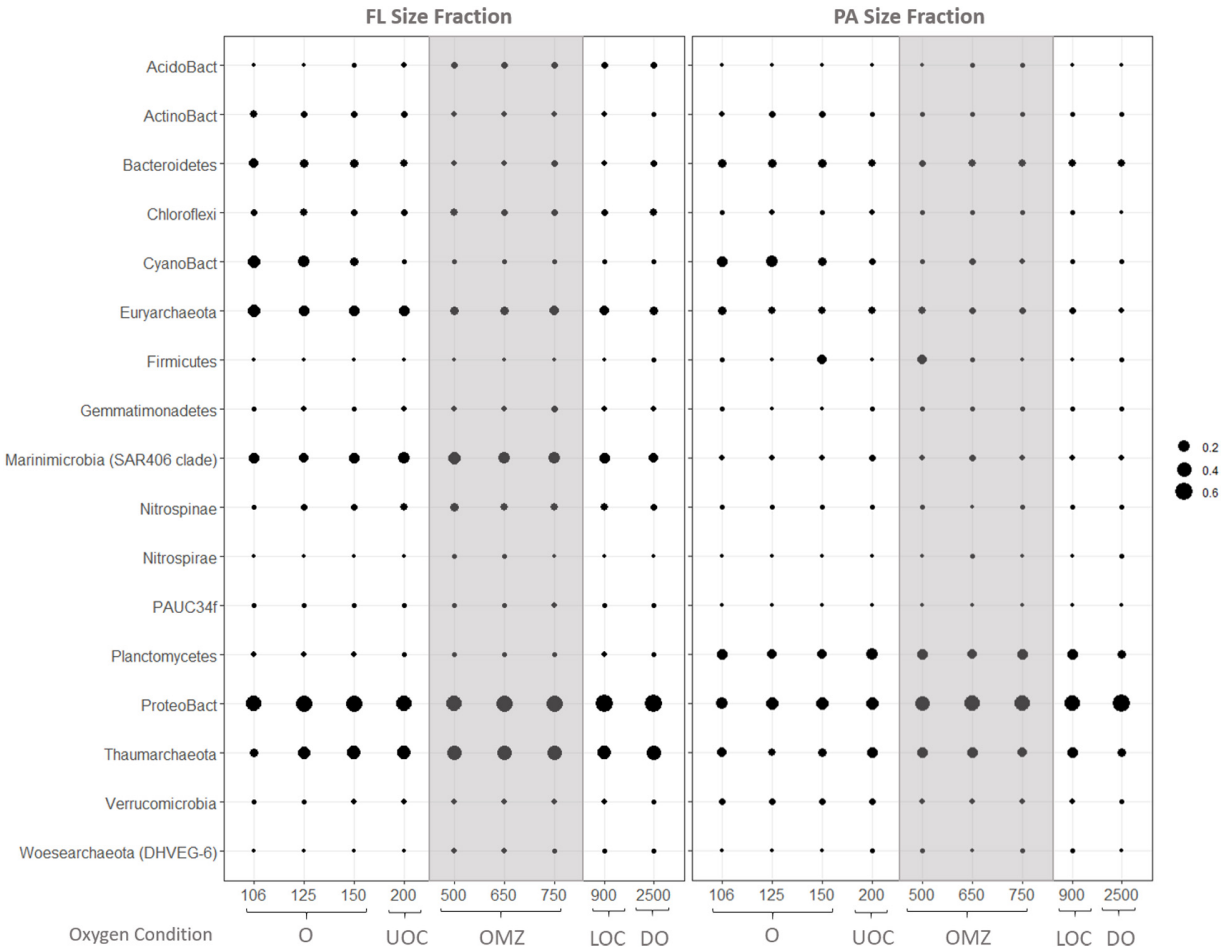

FIGURE 5 | Average relative abundances of iTags in the FL (left) and PA (right) size fractions at coarse phylogenetic resolution. Samples in each panel are organized from left to right by depth, spanning from the oxic (O), upper oxycline (UOC), oxygen minimum zone core (OMZc), lower oxycline (LOC) and deep oxic (DO) depths. Bubbles are the average relative abundances.

of Nitrospinae along the oxycline of the Cariaco Basin, where oxygen concentrations declined from ∼120 to 0.4 μM, but they were absent in anoxic and euxinic layers, suggesting an adaptation to low but non-zero oxygen conditions. Studies in coastal habitats and in open ocean waters showed that abundances and distributions of Nitrospinae correlated with those of AOA, implicating metabolic interdependence between members of these clades (Mincer et al., 2007; Santoro et al., 2010). Furthermore, *Nitrospina gracilis*' genome encodes for a cytochrome *cbb3*-type terminal oxidase with high O_2 affinity and for nitrite and ammonia transporters that enable *Nitrospina* to sustain respiration and assimilatory nitrogen uptake in low-oxygen environments (Lücker et al., 2013). If the Nitrospinae detected at our station are similarly adapted, then it is plausible that these aerobes are actively oxidizing nitrite in the OMZ core where oxygen concentrations average 0.35 μM O_2. This proposition is also consistent with evidence for microaerophilic respiration (nitrite oxidation) at functionally anoxic depths from the Peruvian OMZs and ETNP (Kalvelage et al., 2015; Sun et al., 2017). Thus, we suggest that coupled ammonia and nitrite oxidations likely play an important role in nitrogen cycling in the OMZ core at this location when traces of oxygen are present.

Oxygen Effect on Prokaryoplankton Assemblage Composition

Distributions of bacterial and archaeal OTUs appeared to be strongly influenced by vertical oxygen distributions. ANOSIM tests were performed to compare taxonomic compositions of both size fractions and of waters from oxic (O), upper oxycline (UOC), oxygen minimum zone core (OMZc), lower oxycline (LOC) and deep oxic (DO) layers. For the FL fraction, the ANOSIM R value (0.80, $p < 0.001$) suggests a strong dissimilarity among prokaryotic assemblages along the redox gradient. nMDS ordination of OTUs in the FL fraction (**Figure 8A**) reveals that groups living in well-oxygenated surface waters (O) are significantly different from those in underlying layers. The goodness of fit (r^2 and p-values) of each environmental variable vector in the ordination space for the

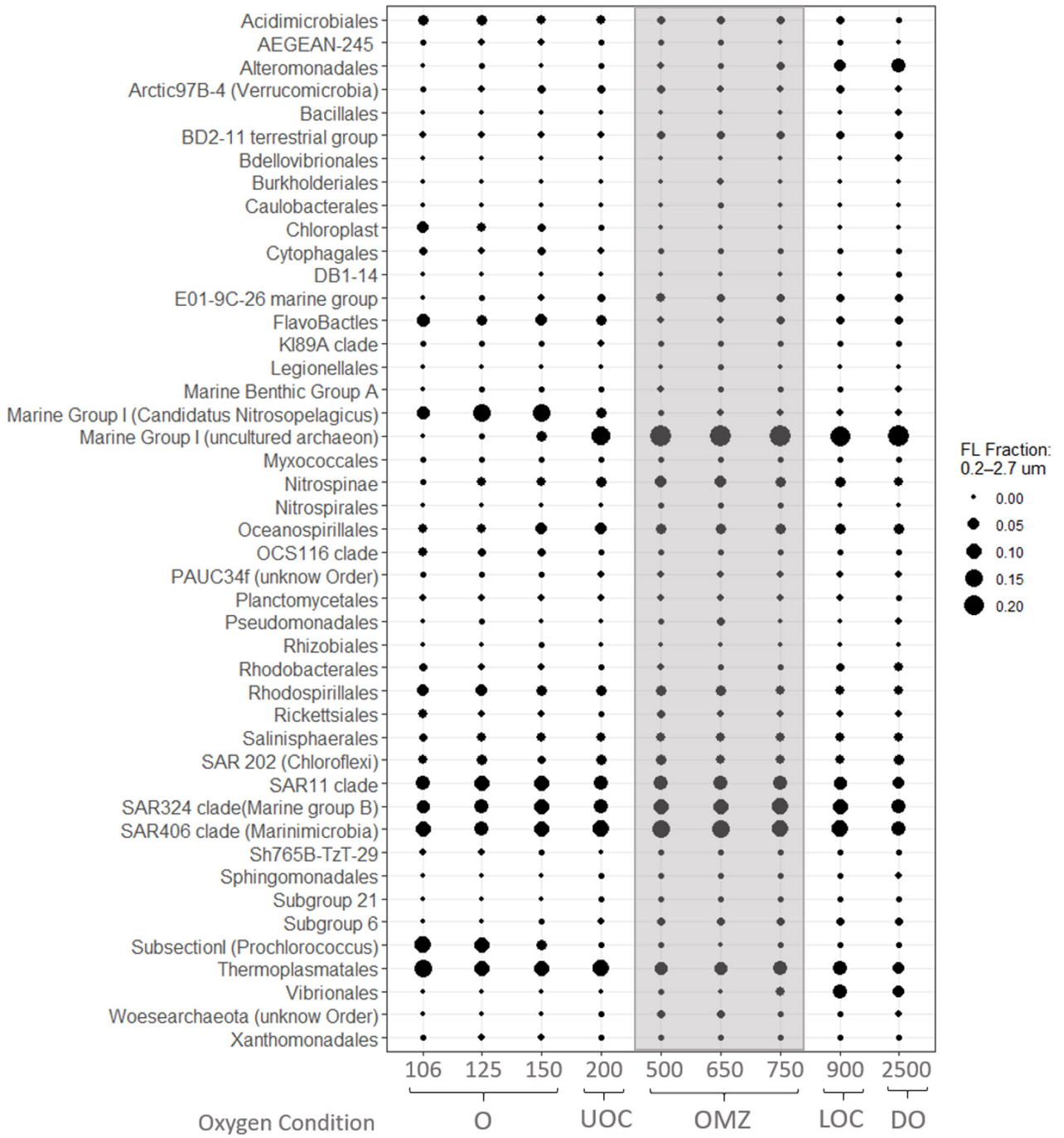

FIGURE 6 | Average relative abundances of iTags at taxonomic level of Order from the 0.2–2.7 μm (FL) size fraction. Samples in each panel are organized from left to right by depth, spanning the oxic (O), Upper oxycline (UOC), oxygen minimum zone core (OMZc), Lower Oxycline (LOC) and deep oxic (DO) depths. Bubbles are the average relative abundances in the FL fraction.

FL prokaryoplankton assemblage shows that OTU distributions are strongly influenced by oxygen (r^2 = 0.85; $p < 0.001$), nitrite (r^2 = 0.92; $p < 0.001$), and ammonium (r^2 = 0.91; $p < 0.001$) concentrations.

As expected for surface waters, recovered sequences in the FL fraction were dominated by OTUs of cyanobacteria mainly affiliated with *Prochlorococcus*. Other notable OTUs present in the FL fraction from the surface waters included the autotroph *Candidatus* Nitrosopelagicus (Thaumarchaeota), and OTUs from the heterotrophic clade of Flavobacteriales (**Figure 6**). Both *Candidatus* Nitrosopelagicus and Flavobacteriales (**Figure 6**) were abundant in our oxic water samples and co-occurred with

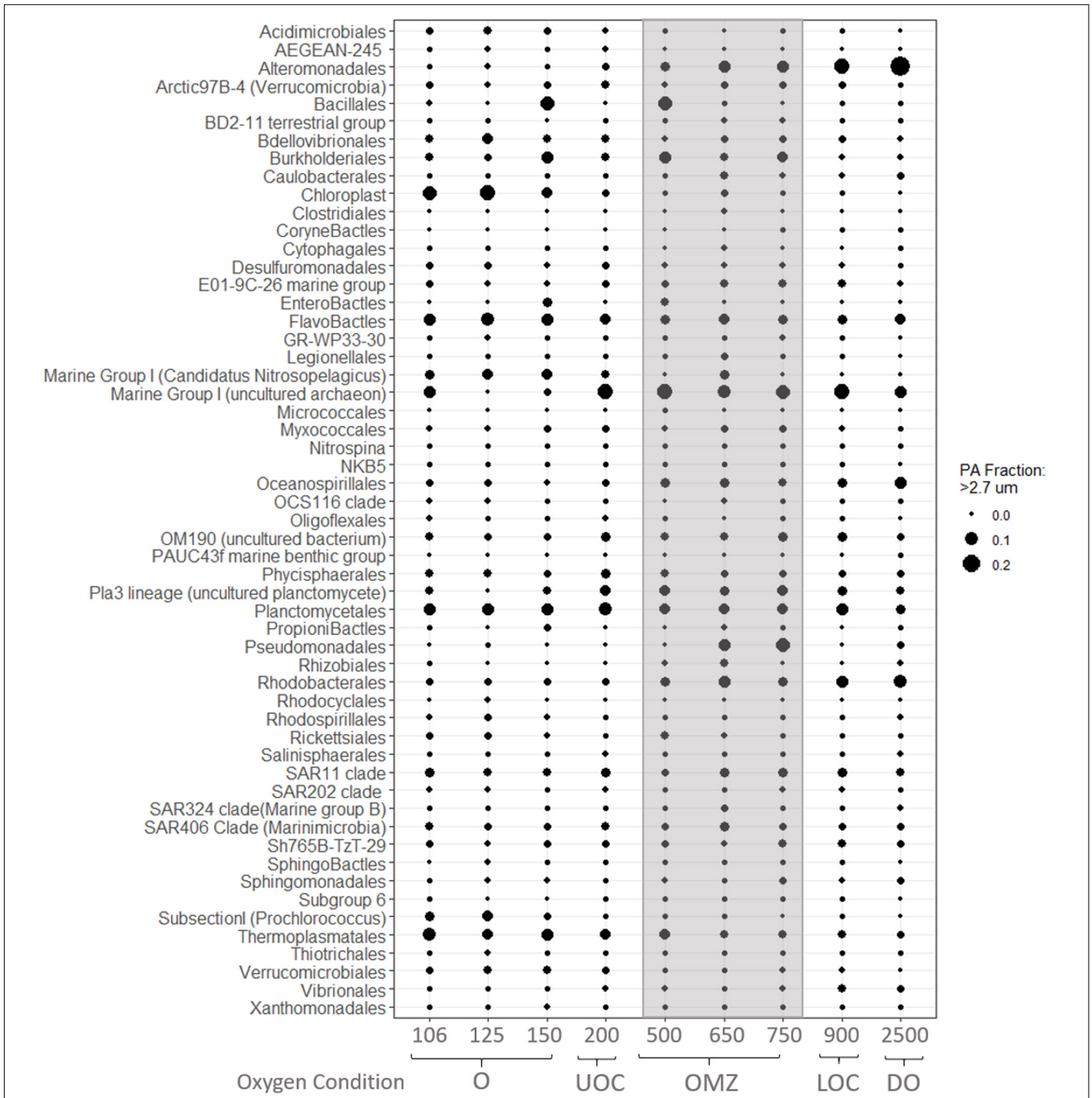

FIGURE 7 | Average relative abundances of iTags at the taxonomic level of Order from the PA fraction. Samples in each panel are organized from left to right by depth, spanning from samples in the oxic (O), upper oxycline (UOC), oxygen minimum zone core depleted (OMZc), lower oxycline (LOC) and deep oxic (DO) depths. Bubbles are the average relative abundances in the PA fraction.

the higher nitrite and ammonium concentrations observed near the base of the euphotic zone (150 m) (**Figure 3**).

Thaumarchaeota are the major ammonia oxidizers in the oceans that aerobically oxidize ammonia to nitrite. The presence of *Candidatus* Nitrosopelagicus in the FL fraction in the oxic layer may indicate active ammonia oxidation with concomitant production of nitrite near the base of the euphotic zone. Highly represented Flavobacteriales in the FL fraction of the oxic layer is consistent with observations from other studies in the ETNP OMZ (Fuchsman et al., 2017). The presence of Flavobacteriales in epipelagic waters of the seasonal deep OMZ in the Gulf of Alaska was reported to be a response to phytoplankton blooms (Muck et al., 2019). Other studies have shown that increased abundances of Flavobacteriales in epipelagic waters are

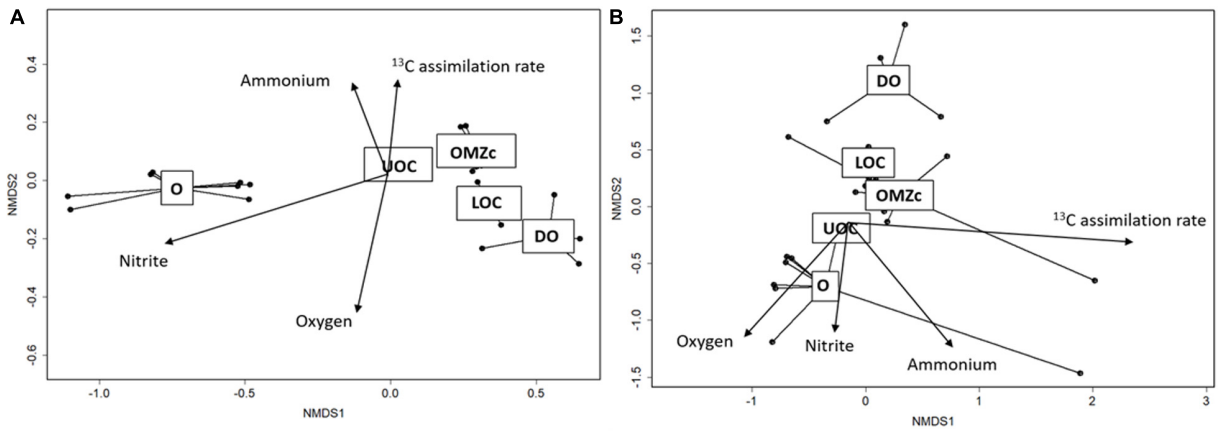

FIGURE 8 | (A) Ordination (nMDS) plot of OTUs in the FL fraction. Stress for this analysis was 4%. Overlain vectors correspond to O_2, nitrate, nitrite concentrations and ^{13}C assimilation. r^2 and p-values of each vector are: O_2: $r^2 = 0.85$; $p < 0.00001$, nitrate: $r^2 = 0.93$; $p < 0.00001$, nitrite: $r^2 = 0.16$; $p < 0.130$ and ^{13}C assimilation: r^2: = 0.30; $p < 0.017$. **(B)** Ordination (nMDS) plot of OTUs in the PA size fraction. Stress for this analysis was 8%. r^2 and p-values of each vector are: O_2: $r^2 = 0.32$; $p < 0.001$, nitrite: $r^2 = 0.50$; $p < 0.001$, ammonium: $r^2 = 0.16$; $p < 0.128$ and ^{13}C assimilation rate: $r^2 = 0.25$; $p < 0.005$. Dots represent each of the 26 samples. Samples in the ordination space segregated by oxygen conditions (O = oxic, UOC = upper oxycline, OMZc = oxygen minimum zone core, LOC = lower oxycline and DO = deep oxic).

significantly related with phytoplankton-derived polysaccharides and decomposition of algal-derived organic matter (Teeling et al., 2012; Taylor et al., 2014).

Members of the Vibrionales and Alteromonadales were highly represented in the deep oxic FL samples, but not in the surface water libraries (**Figure 6**). Specific ecotypes of Alteromonadales in deep waters are considered to have an important ecological role in denitrification and in the degradation of recalcitrant compounds in sinking particles found at meso- and bathypelagic depths (Martinez et al., 2008). We hypothesize that they play a similar role in our 900 and 2,500 m samples. Within the Vibrionaceae family, *Vibrio* and *Photobacterium* were the most highly represented genera. Some *Vibrio* and *Photobacterium* species can be free-living, while others are bioluminescent symbionts occupying light organs of deep-sea fishes (Haygood, 1990). The Vibrionales whose signatures we detected at 900 and 2,500 m could be symbionts of deep-sea fishes or free-living bacteria.

In the FL fraction, SAR11, SAR324 (Marine Group B) and SAR406 (Marinimicrobia) clades were abundant throughout the water column (**Figure 6**). Wright et al. (2012) reported that OTUs representing the SAR11 and SAR324 clades dominated suboxic and anoxic environments in other OMZs and suggested that members of these clades could have overlapping habitat preferences. Within single-cell amplified genomes, Tsementzi et al. (2016) identified SAR11 lineages that carry adaptions for low oxygen. These include genes for respiratory nitrate reductases (*nar*) that represented ∼40% of the *nar* transcripts identified in the ETNP OMZ off Mexico. The vertical distribution of these SAR11 *nar* transcripts was similar to that reported by Ganesh et al. (2015), showing a *nar* expression peak in the OMZ core. Furthermore, phylogenetic analysis revealed affiliation with facultative aerobic gamma-proteobacteria, Deferribacteres and *Geobacter* sp. (delta-proteobacteria), all of which are known nitrate-reducers (Tsementzi et al., 2016). Marinimicrobia and SAR324 clades identified in the Northeastern subarctic Pacific OMZ and the seasonally anoxic Saanich Inlet have been reported to commonly encode for key enzymes in denitrification, i.e., nitrate reductases (*nar*), nitrous oxide reductases (*nos*), and nitrite reductases (*nir*) genes (Hawley et al., 2017). While observed high relative abundances of SAR11, SAR324 (Marine Group B), and SAR406 (Marinimicrobia) at all depths is not definitive evidence of their specific activity, we hypothesize that these clades may be contributing to denitrification at this site.

The PA size fraction also showed vertical structuring of prokaryotic assemblages along the redox gradient. The goodness of fit (r^2 and p-values) of each vector representing contextual variables in the ordination space with PA prokaryoplankton assemblage showed that OTU distributions had significant, but weaker correlations than those observed for the FL fraction with oxygen ($r^2 = 0.32$, $p < 0.001$), nitrite ($r^2 = 0.50$, $p < 0.001$), ammonium ($r^2 = 0.50$, $p < 0.001$). The ANOSIM R value (0.26) suggests that biogeochemical conditions exert selective pressures on both FL and PA assemblages, but the pressures on PA were weaker. The observed weaker vertical zonation of PA assemblage composition may simply be explained by sinking particles being colonized in surface waters, where most form, and sinking downward with shallow water assemblages. Alternatively, it may be indicative of particles from different depths sharing greater similarities in their chemical microenvironments than experienced in the surrounding waters by the FL fraction. Support for these hypotheses will be evaluated below.

Not unexpectedly, the PA fraction yielded sequences of chloroplasts from larger eukaryotic species, such as *Eucampia Antarctica,* and several uncultured Prymnesiophytes (C19847, C5574). Also, Enterobacteriales and Firmicutes of the order Bacilliales were highly represented in oxic waters (150 m; **Figure 7**). The PA fraction in the OMZc and LOC samples

was dominated by iTags from Rhizobiales, Burkholderiales and Pseudomonadales, members of which are well-known chemoorganotrophic denitrifiers (**Figure 7**). The relative abundances of Rhodobacteriales, Oceanospirillales, and Marine Group I (Thaumarchaeota) OTUs increased from the UOC and reached a maximum in the OMZc and deep oxic waters (**Figure 7**). Alteromonadales was another group that appeared to prefer conditions in the PA fraction of OMZc, LOC and deep oxic samples, with maximum iTag representation at 2,500 m (**Figure 8**).

Planctomycetes were abundant in the PA fraction under all redox conditions and largely absent in the FL fraction. Of the 491 OTUs recovered in this study, 10% belonged to this group. The two most numerically important classes within the Planctomycetes phylum were the Phycisphaerae (13 OTUs) and Planctomycetacia (23 OTUs). *Blastopirellula*, *Gemmata*, *Planctomyces*, and *Rhodopirellula* were the most abundant genera. These genera include heterotrophic, non-annamox species that can cope with low oxygen concentrations, but are obligate aerobes (Woebken et al., 2007).

Planctomycetes are widely distributed in marine environments with a prominent role in anaerobic ammonia oxidation. However, anammox Planctomycetes are only found within the genetically and metabolically distinct order, Brocadiales (Woebken et al., 2007; Fuerst and Sagulenko, 2011). The metabolic and genetic differences between anammox and non-anammox Planctomycetes involve the absence of C1 metabolic genes, absence of almost any planctomycete-specific genes (e.g., sulfatases that breakdown of sulfated polysaccharides and are involved in carbon recycling), and absence of paralogous gene families (probably involved in internal compartmentalization) in anammox planctomycetes (Woebken et al., 2007). Notably, no sequences of anammox bacteria belonging to "*Candidatus* Brocadiales' order or genus "*Candidatus* Scalindua" were recovered in our survey. This clade, however, is commonly reported from other ETNP locations (e.g., Rush et al., 2012; Ganesh et al., 2018) and from other oxygen-depleted systems, such as the ETSP (Stevens and Ulloa, 2008) or anoxic basins (Cernadas-Martín et al., 2017). While the absence of proof is not proof of absence, failure to recover "*Candidatus* Scalindua" sequences in our iTag libraries suggests either that this group was rare at this location in the ETNP during the sampled period or that our vertical sampling resolution was insufficient to capture a narrow anammox layer.

We hypothesize that denitrification dominated N_2 production over anammox at the master station during our study period. Our iTag data reveal the presence of well-known denitrifiers in both size fractions and the complete absence of anammox bacterial sequences. Generally, higher rates of anammox (N_2 production) are observed in anoxic, non-sulfidic systems, but denitrification dominates where hydrogen sulfide is produced (Thamdrup, 2012). We speculate that hydrogen sulfide production at this ETNP site is negligible because OTUs belonging to sulfur cycling organisms were not recovered at relative abundances exceeding 0.1% of total sequences in any library. Episodic input of new organic matter to the ETSP OMZ was determined to favor production of N_2O and N_2 via denitrification, with anammox bacteria oxidizing ammonium at a slower rate (Dalsgaard et al., 2012). It is possible that prior to our cruise an oxygen ventilation event occurred, leading to ephemeral trace oxygen levels and introduction of new organic matter within the OMZ core. Some denitrifying microorganism are known to be facultative aerobes, having the ability to colonize biogenic particles in oxic waters. As these particles sink into the OMZ and organic matter is remineralized, localized anoxia can develop within particles when microbial respiration exceeds diffusive O_2 influx. Such conditions enable facultative aerobic microbes to occupy different niches within particles, conducting a range of anaerobic processes, including denitrification (Arístegui et al., 2009). Trace oxygen present in the OMZ core at the master station may have been sufficient to inhibit anammox bacteria leaving denitrification as the sole pathway for the production of N_2O and N_2.

The ability to denitrify is broadly polyphyletic within the domain Bacteria and therefore, denitrification genes (e.g., *nar*, *nor*, *nir*, and *nos*) are present in a range of organisms with widely different denitrification regulatory phenotypes (Bergaust et al., 2011). Dalsgaard et al. (2014) suggested that denitrification in OMZs results from individual processes catalyzed by different groups of coexisting microorganisms. This suggests that a functional group of diverse denitrifying taxa can develop an ecological "bet hedging" strategy in which an array of different ecophysiotypes are poised to respond to transient changes in redox conditions. Similar to Dalsgaard et al.'s (2014) proposal for the anoxic OMZ off Chile, we hypothesize that "bet hedging" strategies were operative at our master ETNP station. However, this hypothesis requires further investigation.

Organization of prokaryoplankton assemblages in response to biogeochemical gradients will depend upon how dependent, adaptable, or sensitive different groups are to any of a myriad of environmental variables. Our statistical analyses of iTag profiles revealed that PA assemblages were less influenced by the biogeochemical regime of surrounding waters than FL fraction assemblages. Particles are known to offer unique biogeochemical and physical microenvironments (Alldredge and Cohen, 1987; Ganesh et al., 2014). However, the degree to which PA assemblage composition changes among depths in OMZs in response to biogeochemical conditions in ambient waters remains an open question (Ganesh et al., 2014). Our results suggest that surrounding biogeochemical conditions in the ETNP's OMZ do, in fact, influence observed structure of PA assemblages, i.e., shallow oxic, oxycline, core, and deep oxic assemblages were distinct from one another (**Figures 7**, **8B**). If most sinking particles were formed in surface waters and microbial assemblages were essentially established there, then PA assemblages among depths would likely exhibit a higher similarity than evident in **Figure 8B**. Alternatively, particles may be generated at different depths by aggregation processes or release by vertically migrating zooplankton (Simon et al., 2002; Wishner et al., 2018). For slowly sinking particles generated in shallow waters, chance collisions with microorganisms and colonization by chemotactic attraction may be sufficiently frequent to shift assemblage composition as particles sink further into the OMZ (Stocker, 2012). In these cases, PA assemblages are likely to be dissimilar among depths.

Provenance of the particles captured in each of our PA samples cannot be determined with available data. Furthermore, we have no information on prokaryotes associated with protists captured in our PA size fraction. Therefore, we cannot determine to what degree differences in PA assemblages observed through the water column are driven by particle sources/quality, protist-prokaryotic associations, colonization in transit, or both ambient and particle biogeochemical regimes. Clearly, further focused studies are necessary to assess the relative contributions of these variables to prokaryote assemblage composition in size-fractionated samples.

CONCLUSION

Our study site in the ETNP was characterized by a steep vertical oxygen concentration gradient that strongly influenced prokaryotic assemblage composition. Bacterial and archaeal OTUs were strongly segregated between the FL and PA size fractions at all depths sampled, with environmental conditions having a stronger influence on the FL fraction. In contrast to other ETNP OMZ studies, our location on the northern margin had a suboxic core (350–700 m), maintaining low oxygen concentrations (0.35–2.30 μM) and exhibiting very limited nitrite accumulation only in the upper oxycline. Prokaryoplankton assemblages within the core were distinct from those previously reported from other regions in the ETNP and the ETSP OMZs, and from truly anoxic water columns, such as the Cariaco Basin and Black Sea. Three major groups; SUP 05, artic96BD-19 (both gamma-proteobacteria), and *Candidatus* Scalindua (Brocadiales), commonly abundant in OMZs and anoxic environments, were completely undetected in our iTag libraries (Stevens and Ulloa, 2008; Podlaska et al., 2012; Beman and Carolan, 2013; Cernadas-Martín et al., 2017; Suter et al., 2018). While taxon abundance and activity are not always linked, scarcity of these key players at this site suggests chemoautotrophic oxidation of sulfur and anammox were not important processes at the time of sampling this site.

We detected the presence of ammonia-oxidizing archaea in the OMZ core which suggests that aerobic ammonium oxidation occurs at low oxygen concentrations (<2 μM). We hypothesize that at the time of sampling oxygen supply to the OMZ core was sufficient to support ammonium and nitrite oxidation and to inhibit other important anaerobic processes. Microaerophilic nitrifiers may play an important role in nitrogen cycling in some regions of the ETNP OMZ. Furthermore, the growing ETNP literature illustrates that distributions of hydrographic and geochemical properties within this OMZ vary geographically and temporally. Accounting for this variability is crucial to understanding how the expansion of the OMZ regions will affect future marine environments.

DATA AVAILABILITY STATEMENT

All iTag sequence data generated in this study have been deposited into Sequences Read Archive (SRA) GenBank under the accession numbers SRR10173043–SRR10172999.

AUTHOR CONTRIBUTIONS

All authors participated in experimental design. LM and PM collected samples, performed experiments, and conducted the data analysis. LM took the lead on manuscript writing with contributions from all authors.

FUNDING

This project resulted from a cruise of opportunity and was not expressly funded by any particular project. Projects which contributed to travel and sequencing costs had no funds allocated to publication costs and expired over a year ago. As I am a very active member of the Frontiers in Marine Science Editorial Board. I was granted one free submission and now request a waiver of the Article Processing Charges for this article.

ACKNOWLEDGMENTS

We thank the cruise's chief scientists, Drs. Karen Wishner and Brad Seibel, for their invitation to participate in the cruise and for providing the logistics necessary to transport materials and equipment used during the expedition. We also thank Elizabeth Suter and Maria Pachiadaki for their inputs in the manuscript and data analysis. Thanks to the captain and crews of the R/V Sikuliaq (University of Alaska). This communication benefited greatly from insightful suggestions provided by our reviewers (JB and XS). This work was partially supported by the National Science Foundation (NSF) grants (OCE-1336082 to VE and OCE-1335436 and OCE-1259110 to GT).

SUPPLEMENTARY MATERIAL

The Supplementary Material for this article can be found online at: https://www.frontiersin.org/articles/10.3389/fmars.2020.00360/full#supplementary-material

REFERENCES

Alldredge, A., and Cohen, Y. (1987). Can microscale chemical patches persist in the sea? microelectrode study of marine snow, fecal pellets. *Science* 235, 689–691. doi: 10.1126/science.235.4789.689

Arístegui, J., Gasol, J. M., Duarte, C. M., and Herndl, G. J. (2009). Microbial oceanography of the dark ocean's pelagic realm. *Limnol. Oceanogr.* 54, 1501–1529. doi: 10.4319/lo.2009.54.5.1501

Belmar, L., Molina, V., and Ulloa, O. (2011). Abundance and phylogenetic identity of archaeoplankton in the permanent oxygen minimum zone of the eastern tropical South Pacific. *FEMS Microbiol. Ecol.* 78, 314–326. doi: 10.1111/j.1574-6941.2011.01159.x

Beman, J. M., and Carolan, M. T. (2013). Deoxygenation alters bacterial diversity and community composition in the ocean's largest oxygen minimum zone. *Nat. Commun.* 4:2705. doi: 10.1038/ncomms3705

Beman, M., and Popp, B. (2012). Quantification of ammonia oxidation rates and ammonia-oxidizing archaea and bacteria at high resolution in the Gulf of of California and Eastern Tropical North Pacific Ocean. *Limnol. Oceanogr.* 57, 711–726. doi: 10.4319/lo.2012.57.3.0711

Bergaust, L., Bakken, L. R., and Frostegård, Å. (2011). Denitrification regulatory phenotype, a new term for the characterization of denitrifying bacteria. *Biochem. Soc. Trans.* 39, 207–212. doi: 10.1042/BST0390207

Bertagnolli, A. D., and Stewart, F. J. (2018). Microbial niches in marine oxygen minimum zones. *Nat. Rev. Microbiol.* 16, 723–729. doi: 10.1038/s41579-018-0087-z

Breitburg, D., Levin, L. A., Oschlies, A., Grégoire, M., Chavez, F. P., and Conley, D. J. (2018). Declining oxygen in the global ocean and coastal waters. *Science* 359:eaam7240. doi: 10.1126/science.aam7240

Bristow, L. A., Dalsgaard, T., Tiano, L., Mills, D. B., Bertagnolli, A. D., Wright, J. J., et al. (2016). Ammonium and nitrite oxidation at nanomolar oxygen concentrations in oxygen minimum zone waters. *Proc. Natl. Acad. Sci. U.S.A.* 113, 10601–10606. doi: 10.1073/pnas.1600359113

Callbeck, C. M., Lavic, G., Stramma, L., Kuypers, M. M., and Bristow, L. A. (2017). Enhanced nitrogen loss by eddy-induced vertical transport in the offshore Peruvian oxygen minimum zone. *PLoS One* 12:e0170059. doi: 10.1371/journal.pone.0170059

Caporaso, J. G., Kuczynski, J., Stombaugh, J., Bittinger, K., Bushman, F. D., Costello, E. K., et al. (2010). QIIME allows analysis of high-throughput community sequencing data. *Nat. Methods* 7, 335–336.

Cernadas-Martín, S., Suter, E. A., Scranton, M. I., Astor, Y., and Taylor, G. T. (2017). Aerobic and anaerobic ammonium oxidizers in the Cariaco Basin: distributions of major taxa and nitrogen species across the redoxcline. *Aquat. Microb. Ecol.* 79, 31–48. doi: 10.3354/ame01817

Chronopoulou, P., Shelley, F., Pritchard, W. J., Maanoja, S. T., and Trimmer, M. (2017). Origin and fate of methane in the Eastern Tropical North Pacific oxygen minimum zone. *Nat. Publ. Gr.* 11, 1386–1399. doi: 10.1038/ismej.2017.6

Clarke, K., Gorley, R. N., Somerrfield, P. J., and Warwick, R. M. (2013). *Change in Marine Communities: An Approach to Statistical Analysis and Interpretation*, 3nd Edn. Plymouth: PRIMER-E.

Dalsgaard, A., Thamdrup, B., Farias, L., and Revsbech, N. P. (2012). Anammox and denitrification in the oxygen minimum zone of the Eastern South Pacific. *Limnol. Oceanogr.* 57, 1331–1346. doi: 10.4319/lo.2012.57.5.1331

Dalsgaard, T., Stewart, F. J., Thamdrup, B., De Brabandere, L., Revsbech, N. P., Ulloa, O., et al. (2014). Oxygen at nanomolar levels reversibly suppresses process rates and gene expression in anammox and denitrification in the oxygen minimum zone off northern Chile. *mBio* 5:e01966-14. doi: 10.1128/mBio.01966-14

Duret, M., Pachiadaki, M. G., Sarode, N., Christaki, U., and Edgcomb, V. P. (2015). Size-fractionated diversity of eukaryotic microbial communities in the Eastern Tropical North Paciic oxygen minimum zone. *FEMS Microbiol. Ecol.* 91:fiv037. doi: 10.1093/femsec/fiv037

Fisher, T., and Haines, E. (1979). A comment on the calculation for stable isotopes1 of atom percent enrichment. *Limnol. Oceanogr.* 24, 593–595. doi: 10.4319/lo.1979.24.3.0593

Fuchsman, C. A., Devol, A. H., Saunders, J. K., McKay, C., and Rocap, G. (2017). Niche partitioning of the N Cycling microbial community of an offshore oxygen deficient zone. *Front. Microbiol.* 8:2384. doi: 10.3389/fmicb.2017.02384

Fuerst, J., and Sagulenko, E. (2011). Beyond the bacterium: planctomycetes challenge our concepts of microbial structure and function. *Nat. Rev. Microbiol.* 9, 403–413. doi: 10.1038/nrmicro2578

Ganesh, S., Bertagnolli, A. D., Bristow, L. A., Padilla, C. C., Blackwood, N., Aldunate, M., et al. (2018). Single cell genomic and transcriptomic evidence for the use of alternative nitrogen substrates by anammox bacteria. *ISME J.* 12, 2706–2722. doi: 10.1038/s41396-018-0223-9

Ganesh, S., Bristow, L. A., Larsen, M., Sarode, N., Thamdrup, B., and Stewart, F. J. (2015). Size-fraction partitioning of community gene transcription and nitrogen metabolism in a marine oxygen minimum zone. *ISME J.* 9, 2682–2696. doi: 10.1038/ismej.2015.44

Ganesh, S., Parris, D. J., DeLong, E. F., and Stewart, F. J. (2014). Metagenomic analysis of size-fractionated picoplankton in a marine oxygen minimum zone. *ISME J.* 8, 187–211. doi: 10.1038/ismej.2013.144

Garcia-Robledo, E., Padilla, C. C., Aldunate, M., Stewart, F. J., Ulloa, O., Paulmier, A., et al. (2017). Cryptic oxygen cycling in anoxic marine zones. *Proc. Natl. Acad. Sci. U.S.A.* 114, 8319–8324. doi: 10.1073/pnas.1619844114

Gordon, L., Jennings, J. Jr., Ross, A., and Krest, J. (1993). *A Suggested Protocol for Continuous Flow Automated Analysis of Seawater Nutrients (Phosphate, Nitrate, Nitrite and Silicic Acid). WOCE Operation Manual 91-1.* Washington, DC: US WHP Office, 1989–1991.

Hawley, A. K., Nobu, M. K., Wright, J. J., Durno, W. E., Morgan-lang, C., Sage, B., et al. (2017). Diverse Marinimicrobia bacteria may mediate coupled biogeochemical cycles along eco-thermodynamic gradients. *Nat. Commun.* 8:1507. doi: 10.1038/s41467-017-01376-9

Haygood, M. G. (1990). Relationship of the luminous bacterial symbiont of the Caribbean flashlight fish, Kryptophanaron alfredi (family Anomalopidae) to other luminous bacteria based on bacterial luciferase (luxA) genes. *Arch. Microbiol.* 154, 496–497.

Kalvelage, T., Lavik, G., Jensen, M. M., Revsbech, N. P., Löscher, C., Schunck, H., et al. (2015). Aerobic microbial respiration in oceanic oxygen minimum zones. *PLoS One* 10:e0133526. doi: 10.1371/journal.pone.0133526

Kuypers, M. M., Lavik, G., Woebken, D., Schmid, M., Fuchs, B. M., Amann, R., et al. (2005). Massive nitrogen loss from the Benguela upwelling system through anaerobic ammonium oxidation. *Proc. Nat. Acad. Sci. U.S.A.* 102, 6478–6483. doi: 10.1073/pnas.0502088102

Lam, P., Jensen, M., Kopck, A., Lettmann, K., Plancherel, Y., Lavik, G., et al. (2011). Origin and fate of the secondary nitrite maximum in the Arabian Sea Biogeosciences Origin and fate of the secondary nitrite maximum in the Arabian Sea. *Biogeosciences* 8, 1565–1577. doi: 10.5194/bg-8-1565-2011

Levipan, H. A., Molina, V., and Fernandez, C. (2014). Nitrospina-like bacteria are the main drivers of nitrite oxidation in the seasonal upwelling area of the Eastern South Pacific (Central Chile 36°S). *Environ. Microbiol. Rep.* 6, 565–573. doi: 10.1111/1758-2229.12158

Lücker, S., Nowka, B., Rattei, T., Spieck, E., and Daims, H. (2013). The genome of *Nitrospina gracilis* illuminates the metabolism and evolution of the major marine nitrite oxidizer. *Front. Microbiol.* 4:27. doi: 10.3389/fmicb.2013.00027

Magoč, T., and Salzberg, S. L. (2011). FLASH: fast length adjustment of short reads to improve genome assemblies. *Bioinformatics* 27, 2957–2963. doi: 10.1093/bioinformatics/btr507

Martinez, E. I., Martin, A. B., D'Auria, G., Mira, A., Ferriera, S., Johnson, J., et al. (2008). Comparative genomics of two ecotypes of the marine planktonic copiotroph Alteromonas macleodii suggests alternative lifestyles associated with different kinds of particulate organic matter. *ISME J.* 2, 1194–1212. doi: 10.1038/ismej.2008.74

Mincer, T. J., Church, M. J., Taylor, L. T., Preston, C., Karl, D. M., and Delong, E. F. (2007). Quantitative distribution of presumptive archaeal and bacterial nitrifiers in Monterey Bay and the North Pacific Subtropical Gyre. *Environ. Microbiol.* 9, 1162–1175. doi: 10.1111/j.1462-2920.2007.01239.x

Molina, V. L., Belmar, L., and Ulloa, O. (2010). High diversity of ammonia-oxidizing archaea in permanent and seasonal oxygen-deficient waters of the eastern South Pacific. *Environ. Microbiol.* 12, 2450–2465. doi: 10.1111/j.1462-2920.2010.02218.x

Montes, E., Altabet, M. A., Muller-Karger, F. E., Scranton, M. I., Thunell, R., Benitez-Nelson, C., et al. (2013). Biogenic nitrogen gas production at the oxic-anoxic interface in the Cariaco Basin, Venezuela. *Biogeosciences* 10, 267–279. doi: 10.5194/bg-10-267-2013

Muck, S., De Corte, D., Clifford, E. L., Bayer, B., Herndl, G. J., and Sintes, E. (2019). Niche Differentiation of aerobic and anaerobic ammonia oxidizers in a high latitude deep oxygen minimum zone. *Front. Microbiol.* 10:2141. doi: 10.3389/fmicb.2019.02141

Muller-Karger, F., Varela, R., Thunell, R., Scranton, M., Bohrer, R., Taylor, G., et al. (2001). Annual cycle of primary production in the Cariaco Basin: response to upwelling and implications for vertical export. *J. Geophys. Res.* 106, 4527–4542. doi: 10.1029/1999JC000291

Naqvi, S. W. A., Bange, H. W., Farías, L., Monteiro, P. M. S., Scranton, M. I., and Zhang, J. (2010). Marine hypoxia/anoxia as a source of CH_4 and N_2O. *Biogeosciences* 7, 2159–2190. doi: 10.5194/bg-7-2159-2010

Pachiadaki, M. G., Sintes, E., Bergauer, K., Brown, J. M., Record, N. R., Swan, et al. (2017). Major role of nitrite-oxidizing bacteria in dark ocean carbon fixation. *Science* 358, 1046–1051. doi: 10.1126/science.aan8260

Pack, M. A., Heintz, M. B., Reeburgh, W. S., Trumbore, S. E., Valentine, D. L., Xu, X., et al. (2015). Methane oxidationin the eastern tropical North

PacificOcean water column. *J. Geophys. Res. Biogeosci.* 120, 1078–1092. doi: 10.1002/2014JG002900

Parada, A. E., Needham, D. M., and Fuhrman, J. A. (2016). Every base matters: assessing small subunit rRNA primers for marine microbiomes with mock communities, time series and global field samples. *Environ. Microbiol.* 18, 1403–1414. doi: 10.1111/1462-2920.13023

Paulmier, A., and Ruiz-Pino, D. (2009). Oxygen minimum zones (OMZs) in the modern ocean. *Prog. Oceanogr.* 80, 113–128. doi: 10.1016/j.pocean.2008.08.001

Peng, X., Fuchsman, C. A., Jayakumar, A., Oleynik, S., Martens-Habbena, W., Devol, A. H., et al. (2015). Ammonia and nitrite oxidation in the Eastern Tropical North Pacific. *Glob. Biogeochem. Cycles* 29, 2034–2049. doi: 10.1002/2015gb005278

Penn, J., Weber, T., Chang, B. T., and Deutsch, C. (2019). Microbial ecosystems dynamics drive fluctuating nitrogen lost in marine anoxic zones. *Proc. Nat. Acad. Sci. U.S.A.* 116, 7220–7225. doi: 10.1073/pnas.1818014116

Pitcher, A., Villanueva, L., Hopmans, E. C., Schouten, S., Reichart, G. J., and Sinninghe Damsté, J. S. (2011). Niche segregation of ammonia-oxidizing archaea and anammox bacteria in the Arabian Sea oxygen minimum zone. *ISME J.* 5, 1896–1904. doi: 10.1038/ismej.2011.60

Podlaska, A., Wakeham, S. G., Fanning, K. A., and Taylor, G. T. (2012). Deep-Sea Research I Microbial community structure and productivity in the oxygen minimum zone of the eastern tropical North Pacific. *Deep Res. Part I* 66, 77–89. doi: 10.1016/j.dsr.2012.04.002

Porter, K. G., and Feig, Y. S. (1980). The use of DAPI for identifying and counting aquatic microflora. *Limnol. Oceanogr.* 25, 943–948. doi: 10.4319/lo.1980.25.5.0943

Rodriguez-Mora, M. J., Madrid, V. M., Taylor, G. T., Scranton, M., and Chistoserdov, A. (2013). Bacterial community composition in a large marine anoxic basin: a Cariaco Basin time-series survey. *FEMS Microbiol. Ecol.* 84, 625–639. doi: 10.1111/1574-6941.12094

Rush, D., Wakeham, S. G., Hopmans, E. C., Schouten, S., and Sinninghe Damsté, J. S. (2012). Biomarker evidence for anammox in the oxygen minimum zone of the Eastern Tropical North Pacific. *Org. Geochem.* 53, 80–87. doi: 10.1016/j.orggeochem.2012.02.005

Sambrotto, R. N., Burdloff, D., and McKee, K. (2015). Spatial and year-to-year patterns in new and primary productivity in sea ice melt regions of the eastern Bering Sea. *Deep Res. Part II Top. Stud. Oceanogr.* 134, 86–99. doi: 10.1016/j.dsr2.2015.07.011

Santoro, A. E., Casciotti, K. L., and Francis, C. A. (2010). Activity, abundance and diversity of nitrifying archaea and bacteria in the central California Current. *Environ. Microbiol.* 12, 1989–2006. doi: 10.1111/j.1462-2920.2010.02205.x

Schmidtko, S., Stramma, L., and Visbeck, M. (2017). Decline in global oceanic oxygen content during the past five decades. *Nature* 542, 335–339. doi: 10.1038/nature21399

Simon, M., Grossart, H., Schweitzer, B., and Ploug, H. (2002). Microbial ecology of organic aggregates in aquatic ecosystems. *Aquat. Microb. Ecol.* 28, 175–211. doi: 10.3354/ame028175

Somerville, C, Knight, I. T., Straube, W. L., and Colwell, R. R. (1988). Simple, rapid method for direct isolation of nucleic acids from aquatic environments. *App. Environ. Microbiol.* 55, 548–554.

Stevens, H., and Ulloa, O. (2008). Bacterial diversity in the oxygen minimum zone of the eastern tropical South Pacific. *Environ. Microbiol.* 10, 1244–1259. doi: 10.1111/j.1462-2920.2007.01539.x

Stocker, R. (2012). Marine microbes see a sea of gradients. *Science* 338, 628–633. doi: 10.1126/science.1208929

Sun, X., Ji, Q., Jayakumar, A., and Ward, B. B. (2017). Dependence of nitrite oxidation on nitrite and oxygen in low-oxygen seawater. *J. Geophys. Res. Lett.* 44, 7883–7891. doi: 10.1002/2017GL074355

Sun, X., Kop, L., Lau, M., Frank, J., Jayakumar, A., Lucker, S., et al. (2019). Uncultured Nitrospina-like species are major nitrite oxidizing bacteria in oxygen minimum zones. *ISME J.* 13, 2391–2402. doi: 10.1038/s41396-019-0443-7

Suter, E. A., Pachiadaki, M., Taylor, G. T., Astor, Y., and Edgcomb, V. P. (2018). Free-living chemoautotrophic and particle-attached heterotrophic prokaryotes dominate microbial assemblages along a pelagic redox gradient. *Environ. Microbiol.* 20, 693–712. doi: 10.1111/1462-2920.13997

Swan, B. K., Chaffin, M. D., Martinez-Garcia, M., Morrison, H. G., Field, E. K., and Poulton, N. J. (2014). Genomic and metabolic diversity of Marine Group I Thaumarchaeota in the mesopelagic of two subtropical gyres. *PLoS One* 9:e95380. doi: 10.1371/journal.pone.0095380

Taylor, J. D., Cottingham, S. D., Billinge, J., and Cunliffe, M. (2014). Seasonal microbial community dynamics correlate with phytoplankton-derived polysaccharides in surface coastal waters. *ISME J.* 8, 245–248. doi: 10.1038/ismej.2013.178

Teeling, H., Fuchs, B. M., Becher, D., Klockow, C., Gardebrecht, A., Bennke, C. M., et al. (2012). Substrate-controlled succession of marine bacterioplankton populations induced by a phytoplankton bloom. *Science* 336, 608–611. doi: 10.1126/science.1218344

Thamdrup, B. (2012). New pathways and processes in the global nitrogen cycle. *Annu. Rev. Ecol. Evol. Syst.* 43, 407–428. doi: 10.1146/annurev-ecolsys-102710-145048

Tiano, L., Garcia-Robledo, E., Dalsgaard, T., Devol, A. H., Ward, B. B., Ulloa, O., et al. (2014). Oxygen distribution and aerobic respiration in the north and south eastern tropical Pacific oxygen minimum zones. *Deep Res. Part I Oceanogr. Res. Pap.* 94, 173–183. doi: 10.1016/j.dsr.2014.10.001

Tsementzi, D., Wu, J., Deutsch, S., Nath, S., Rodriguez, L. M., Burns, A. S., et al. (2016). SAR11 bacteria linked to ocean anoxia and nitrogen loss. *Nature* 536, 179–183. doi: 10.1038/nature19068

Ulloa, O., Canfield, D. E., DeLong, E. F., Letelier, R. M., and Stewart, F. J. (2012). Microbial oceanography of anoxic oxygen minimum zones. *Proc. Natl. Acad. Sci. U.S.A.* 109, 15996–16003. doi: 10.1073/pnas.1205009109

Wang, J. P., Liu, B., Liu, G. H., Ge, C. B., Chen, Q. Q., Zhu, Y. J., et al. (2015). Genome sequence of *Anaerobacillus macyae* JMM-4T (DSM 16346), the first genomic information of the newly established genus *Anaerobacillus*. *GenomeA* 3, 4–5. doi: 10.1128/genomeA.00922-15

Ward, B., Capone, D. G., and Zehr, J. P. (2007). What ' s new in the nitrogen cycle? *Oceanogrphy* 20, 101–109.

Ward, B. B., Devol, A. H., Rich, J. J., Chang, B. X., Bulow, S. E., Naik, H., et al. (2009). Denitrification as the dominant nitrogen loss process in the Arabian Sea. *Nat. Lett.* 461, 78–81. doi: 10.1038/nature08276

Ward, B. B., Glover, H. E., and Lipschultz, F. (1989). Chemoautotrophic activity and nitrification in the oxygen minimum zone off Peru. *Deep Sea Res. Part A* 36, 1031–1051. doi: 10.1016/0198-0149(89)90076-9

Wishner, K. F., Seibel, B. A., Roman, C., Deutsch, C., Outram, D., Shaw, C. T., et al. (2018). Ocean deoxygenation and zooplankton: very small oxygen differences matter. *Sci. Adv.* 4:eaau5180. doi: 10.1126/sciadv.aau5180

Woebken, D., Teeling, H., Wecker, P., Dumitriu, A., Kostadinov, I., DeLong, E. F., et al. (2007). Fosmids of novel marine Planctomycetes from the Namibian and Oregon coast upwelling systems and their cross-comparison with planctomycete genomes. *ISME J.* 11, 419–435. doi: 10.1038/ismej.2007.63

Wright, J. J., Konwar, K. M., and Hallam, S. J. (2012). Microbial ecology of expanding oxygen minimum zones. *Nat. Rev. Microbiol.* 10, 381–394. doi: 10.1038/nrmicro2778

Zavarzina, D. G., Tourova, T. P., Kolganova, T. V., Boulygina, E. S., and Zhilina, T. N. (2009). Description of *Anaerobacillus alkalilacustre* gen. nov., sp. nov.-Strictly anaerobic diazotrophic bacillus isolated from soda lake and transfer of *Bacillus arseniciselenatis*, *Bacillus macyae*, and *Bacillus alkalidiazotrophicus* to *Anaerobacillus* as the new combinations *A. arseniciselenatis* comb. nov., *A. macyae* comb. nov., and *A. alkalidiazotrophicus* comb. nov. *Microbiology* 78, 723–773.

Zhang, Y., Qin, W., Hou, L., Zakem, E. J., Wan, Z., Zhao, Z., et al. (2020). Nitrifier adaptation to low energy flux controls inventory of reduced nitrogen in the dark ocean. *Proc. Natl. Acad. Sci. U.S.A.* 117, 4823–4830. doi: 10.1073/pnas.1912367117

Zou, D., Li, Y., Kao, S.-J., Liu, H., and Li, M. (2019). Genomic adaptation to eutrophication of ammonia-oxidizing archaea in the Pearl River estuary. *Environ. Microb.* 21, 2320–2332. doi: 10.1111/1462-2920.14613

Conflict of Interest: The authors declare that the research was conducted in the absence of any commercial or financial relationships that could be construed as a potential conflict of interest.

frontiers in Microbiology

ORIGINAL RESEARCH
published: 10 July 2020
doi: 10.3389/fmicb.2020.01541

Hurricane Disturbance Stimulated Nitrification and Altered Ammonia Oxidizer Community Structure in Lake Okeechobee and St. Lucie Estuary (Florida)

Justyna J. Hampel[1,2], Mark J. McCarthy[2], Sanni L. Aalto[3] and Silvia E. Newell[2]*

[1] School of Ocean Science and Engineering, The University of Southern Mississippi, Ocean Springs, MS, United States, [2] Department of Earth and Environmental Sciences, Wright State University, Dayton, OH, United States, [3] Section for Aquaculture, The North Sea Research Centre, DTU Aqua, Technical University of Denmark, Hirtshals, Denmark

OPEN ACCESS

Edited by:
Sebastian Lücker, Radboud University Nijmegen, Netherlands

Reviewed by:
Huiluo Cao, The University of Hong Kong, Hong Kong
Hidetoshi Urakawa, Florida Gulf Coast University, United States

***Correspondence:**
Justyna J. Hampel
justyna.hampel@usm.edu

Specialty section:
This article was submitted to Aquatic Microbiology, a section of the journal Frontiers in Microbiology

Received: *21 April 2020*
Accepted: *12 June 2020*
Published: *10 July 2020*

Citation:
Hampel JJ, McCarthy MJ, Aalto SL and Newell SE (2020) Hurricane Disturbance Stimulated Nitrification and Altered Ammonia Oxidizer Community Structure in Lake Okeechobee and St. Lucie Estuary (Florida). Front. Microbiol. 11:1541. doi: 10.3389/fmicb.2020.01541

Nitrification is an important biological link between oxidized and reduced forms of nitrogen (N). The efficiency of nitrification plays a key role in mitigating excess N in eutrophic systems, including those with cyanobacterial harmful algal blooms (cyanoHABs), since it can be closely coupled with denitrification and removal of excess N. Recent work suggests that competition for ammonium (NH_4^+) between ammonia oxidizers and cyanoHABs can help determine microbial community structure. Nitrification rates and ammonia-oxidizing archaeal (AOA) and bacterial (AOB) community composition and gene abundances were quantified in Lake Okeechobee and St. Lucie Estuary in southern Florida (United States). We sampled during cyanobacterial (*Microcystis*) blooms in July 2016 and August 2017 (2 weeks before Hurricane Irma) and 10 days after Hurricane Irma made landfall. Nitrification rates were low during cyanobacterial blooms in Lake Okeechobee and St. Lucie Estuary, while low bloom conditions in St. Lucie Estuary coincided with greater nitrification rates. Nitrification rates in the lake were correlated ($R^2 = 0.94$; $p = 0.006$) with AOA *amoA* abundance. Following the hurricane, nitrification rates increased by an order of magnitude, suggesting that nitrifiers outcompeted cyanobacteria for NH_4^+ under turbid, poor light conditions. After Irma, AOA and AOB abundances increased in St. Lucie Estuary, while only AOB increased in Lake Okeechobee. AOA sequences clustered into three major lineages: *Nitrosopumilales* (NP), *Nitrososphaerales* (NS), and *Nitrosotaleales* (NT). Many of the lake OTUs placed within the uncultured and uncharacterized NS δ and NT β clades, suggesting that these taxa are ecologically important along this eutrophic, lacustrine to estuarine continuum. After the hurricane, the AOA community shifted toward dominance by freshwater clades in St. Lucie Estuary and terrestrial genera in Lake Okeechobee, likely due to high rainfall and subsequent increased turbidity and freshwater loading from the lake into the estuary. AOB community structure was not affected by the disturbance. AOA communities were consistently more diverse than AOB, despite fewer

sequences recovered, including new, unclassified, eutrophic ecotypes, suggesting a wider ecological biogeography than the oligotrophic niche originally posited. These results and other recent reports contradict the early hypothesis that AOB dominate ammonia oxidation in high-nutrient or terrestrial-influenced systems.

Keywords: AOA, AOB, eutrophication, harmful algal blooms, hurricane, nitrification

INTRODUCTION

Canonical nitrification is a two-step process in which ammonium (NH_4^+) is oxidized to nitrite (NO_2^-), and NO_2^- is further oxidized to nitrate (NO_3^-). Nitrification is a key pathway in the nitrogen (N) cycle as the sole biological link between oxidized and chemically reduced N forms, and it is often closely coupled to removal of excess N via denitrification (An and Joye, 2001). Thus, nitrification is a critical link in the ability of eutrophic ecosystems to mitigate excess N loads via coupling with denitrification.

The first step of nitrification, ammonia oxidation, is performed by ammonia-oxidizing archaea (AOA) and bacteria (AOB). Although AOA and AOB coexist in the environment, they generally exhibit niche separation (Prosser and Nicol, 2012; Hink et al., 2018). Previous studies on nitrifier community structure have posited that trophic status of the ecosystem defines the dynamics between AOA and AOB, based mostly on differences in substrate affinity for NH_4^+ and half-saturation constants (K_m; Martens-Habbena et al., 2009; Bristow et al., 2016). Traditionally, AOB were thought to be more abundant in nutrient rich waters and soils (Jia and Conrad, 2009; Verhamme et al., 2011; Hou et al., 2013), while AOA were assumed to be more abundant in the oligotrophic open ocean (Francis et al., 2005; Könneke et al., 2005; Newell et al., 2011; Beman et al., 2012). However, a comprehensive phylogenetic analysis of >33,000 archaeal *amoA* sequences showed that AOA are ubiquitous, widespread, and highly diverse, and current knowledge on the physiology of cultured AOA does not represent predominant clades in the environment (Alves et al., 2018). Recently, various AOA clades from *Nitrososphaerales*, *Nitrosotaleales*, and *Nitrosopumilales* orders have shown to be highly abundant in shallow, eutrophic waters affected by agriculture runoff and cyanobacterial blooms (Zeng et al., 2012; Damashek et al., 2015; Hampel et al., 2018; Li et al., 2018), and wastewater treatment plants (Alves et al., 2018), where depth distribution of AOA ecotypes may not be applicable, and NH_4^+ concentrations often exceed those in the oligotrophic ocean by orders of magnitude. Thus, some AOA clades likely inhabit a more eutrophic niche than previously determined in ocean water column studies (Santoro et al., 2010; Sintes et al., 2013), but more work is needed to understand active ecotypes in shallow, freshwater systems.

Environmental controls on nitrification have been studied extensively in marine and coastal ecosystems (Beman et al., 2012; Horak et al., 2013; Urakawa et al., 2014; Damashek et al., 2016; Santoro et al., 2017), while studies in freshwater systems (Hugoni et al., 2013; Vissers et al., 2013; Bollmann et al., 2014; Hayden and Beman, 2014), particularly eutrophic systems, have received less attention (Hampel et al., 2018) and are often limited to sediment studies (Hou et al., 2013; Yao et al., 2018). Work in marine and coastal environments has shown that oxygen, temperature, salinity, light, turbidity, top-down grazing pressure (Lavrentyev et al., 1997; Jochem et al., 2004), and ambient NH_4^+ concentrations can all influence nitrification rates (Heiss and Fulweiler, 2016; Damashek and Francis, 2018). However, in eutrophic lakes, competition for NH_4^+ between nitrifiers and photoautotrophs, including bloom-forming cyanobacteria (cyanoHABs), may be more important than ambient NH_4^+ concentrations (which can be very high). Nitrifiers and cyanobacteria are both highly competitive for NH_4^+ and urea, and while cyanobacteria can assimilate N_2 and NO_3^-, nitrifiers cannot. Cyanobacteria can also thrive in high light conditions, which may inhibit nitrifiers (Hayden and Beman, 2014). A recent study showed that this competition can reduce nitrification efficiency (Hampel et al., 2018), potentially impacting the capacity for denitrification and removal of excess N.

We examined environmental controls on nitrification rates and ammonia oxidizer community structure along a freshwater-estuarine continuum during cyanoHABs and before and after passage of a major hurricane. Lake Okeechobee and the St. Lucie Estuary (Florida) provide an opportunity to investigate the impacts of dissolved inorganic N (DIN) concentrations, salinity, cyanoHABs, and physical disturbance (hurricane passage) on nitrification. Lake Okeechobee has experienced toxic cyanoHABs for decades (James et al., 2009), resulting in myriad negative effects on the downstream St. Lucie Estuary. To prevent flooding, nutrient-laden water from Lake Okeechobee is released into St. Lucie Estuary via a canal system, reducing salinity and increasing nutrient concentrations and turbidity (Lapointe et al., 2012; Phlips et al., 2012). Toxic *Microcystis* blooms in St. Lucie Estuary have been observed on numerous occasions (Phlips et al., 2012), including during a massive bloom in 2016, which led the State of Florida to declare a state of emergency (Kramer et al., 2018).

On September 10th, 2017, Hurricane Irma made landfall in the Florida Keys as a Category 4 hurricane (sustained winds >210 km h^{-1}) and moved through central Florida with sustained winds of ∼65 km h^{-1} in the Okeechobee region (Hampel et al., 2019) and maximum winds up to ∼100 km h^{-1} (SFWMD). High winds and precipitation runoff have major impacts on hydrology, microbial and phytoplankton community structure, sediments, and nutrients, including reducing salinity in estuaries, often leading to stratification and bottom-water hypoxia (Paerl et al., 2001). Hurricane winds also produce strong currents and seiches, which resuspend sediments and increase total suspended solids (TSS) and turbidity in the water column (James et al., 2008). Short-term hurricane effects on cyanoHABs include decreased NH_4^+ uptake rates and microcystin synthetase gene abundance (Hampel et al., 2019). Previous studies showed decreased AOA abundance and diversity after an oil spill (Newell et al., 2014)

and increased AOB abundance after storm disturbance (Happel et al., 2018). However, very little is known about storm effects on nitrification and ammonia oxidizer community structure in freshwater and estuary ecosystems (Bouskill et al., 2011; Newell et al., 2014; Happel et al., 2018).

Despite its ecological importance, nitrification in eutrophic, cyanoHABs-dominated systems remains understudied. The goal of this study was to quantify nitrification rates and *amoA* gene abundance, and investigate ammonia oxidizer community structure, along a freshwater-estuarine continuum in central Florida during cyanoHABs in 2016 and 2017 and before and after Hurricane Irma passage. We hypothesized that nitrification rates would be lower during cyanoHABs due to resource competition and that hurricane disturbance would further decrease nitrification rates and the abundance of ammonia oxidizers. We also speculated that there would be a shift in *amoA* community structure as an immediate response to hurricane disturbance. Climate change predictions forecast escalation of eutrophication, cyanoHABs, and the intensity of large-scale extreme weather events (Paerl et al., 2019). Thus, understanding the effects of these disturbances on nitrification and ammonia oxidizer communities is important for constructing and validating ecosystem models used to evaluate ecosystem resilience and inform management action in eutrophic waters.

MATERIALS AND METHODS

Sampling

Lake and estuary water samples were collected on July 25–27, 2016, August 22–24, 2017, and September 20–21, 2017. The July 2016 sampling occurred during a large cyanoHAB in both systems (Kramer et al., 2018). In August 2017, sampling occurred 2 weeks before Hurricane Irma passed over the Okeechobee region as a Category 3 hurricane. The September 2017 sampling occurred 10 days after Hurricane Irma passed through south and central Florida. In July 2016, sampling was conducted at two stations in Lake Okeechobee, L004 (surface and bottom water) and LZ40 (surface and bottom water), and four stations in the St. Lucie Estuary following a freshwater to marine salinity gradient from SLE80, SLE2, SLE4, and SLE8 (surface water only; **Figure 1**). In August 2017, L004 (surface and bottom water) and a northern lake station (SAV165, surface water only) were sampled, along with SLE80, SLE5, and SLE7 in the estuary. Post-hurricane sampling was hindered by flooding and included stations L004, LZ40, and LOBG (nearshore in the south) in the lake (surface water only), and SLE5 and SLE7 in the estuary.

Water for nutrient analyses was filtered in the field to 0.2 μm with pre-rinsed syringe filters (Nylon) into 15 ml polypropylene tubes and frozen upon return to the laboratory. Water for nitrification experiments was collected with a van Dorn water sampler into 5 L cubitainers and returned to the lab for incubations. Physicochemical parameters were measured with a YSI multisensor sonde in July 2016 and August 2017, and a Manta 2 multiparameter sonde in September 2017. Dissolved nutrient analyses included NH_4^+, NO_2^-, NO_3^-, orthophosphate (ortho-P), and urea were analyzed using a Lachat Quickchem 8500 FIA nutrient analyzer. Turbidity and TSS measurements were obtained from the DB Hydro database[1] and collected by South Florida Water Management District (SFWMD) according to standard EPA protocols.

DNA Collection and Extraction

Environmental DNA was collected in August and September 2017. Samples were hand filtered in the field with 0.2 μm Sterivex filters (SVGP01015; MilliporeSigma, MA, United States). Samples were preserved in the field with ∼2 mL of Ambion RNAlater (Invitrogen, Carlsbad, CA, United States). The volume of site water pushed through Sterivex filters in August 2017 ranged from 120–240 ml. However, due to increased turbidity after the hurricane, only 45–60 ml of water was filtered in September for stations L004, LZ40, SLE5, and SLE7. An exception was station LOBG, where 300 ml of water were filtered. Preserved filters were frozen at −80°C until analysis.

Filter cartridges were thawed on ice in the lab, and RNAlater in the Sterivex filters was removed by pushing 10 ml of Phosphate Buffer Saline 1× Solution (Fisher BioReagents, United States) through the filter. DNA was extracted using the Gentra PureGene kit (Qiagen Inc., United States). Lysis buffer (0.9 ml) and Proteinase K (10 μl) were added to the filters, and the samples were incubated for 1 h at 55°C and 1 h at 65°C, repeated twice, in a hybridization oven at 90 rpm (Newell et al., 2011; Hampel et al., 2018).

amoA Gene Abundance

Quality and quantity of the extracted DNA were measured spectrophotometrically (NanoDrop 2000, Thermo Scientific). There are limitations to using the NanoDrop at low DNA concentrations, but our samples had consistently high concentrations (>10 ng/μL). Archaeal *amoA* was quantified with Arch-amoAF and Arch-amoAR primers, and bacterial *amoA* was quantified with amoAF and amoA2R primers (**Supplementary Table S4**; Rotthauwe et al., 1997; Francis et al., 2005). Archaeal and bacterial *amoA* qPCR standards were prepared by cloning the fragment of interest with the TOPO TA Cloning Kit (Invitrogen, United States), inserting it into a competent cell plasmid (One Shot *E. coli* cells, Invitrogen, United States), and isolating the plasmid containing the *amoA* gene using the UltraClean Standard Mini Plasmid Prep Kit (Mo Bio Laboratories Inc., Carlsbad, CA, United States). Each qPCR run included three no template controls (NTC), six standards from serial dilution in triplicate, and the environmental DNA samples in triplicate. Each sample and standard received 10 μl of Luna Universal qPCR Master Mix (New England Biolabs Inc., United States), 0.5–1 μl of each 10 μM primer, and 20–35 ng of DNA template.

amoA qPCR protocols followed methods of Bollmann et al. (2014; and **Supplementary Table S4**), followed by melting curve analysis to ensure a single product. Automatic settings for the thermocycler (Realplex, Eppendorf) were used to determine threshold cycle (Ct values), efficiency (93–98%), and a standard

[1]https://www.sfwmd.gov/science-data/dbhydro

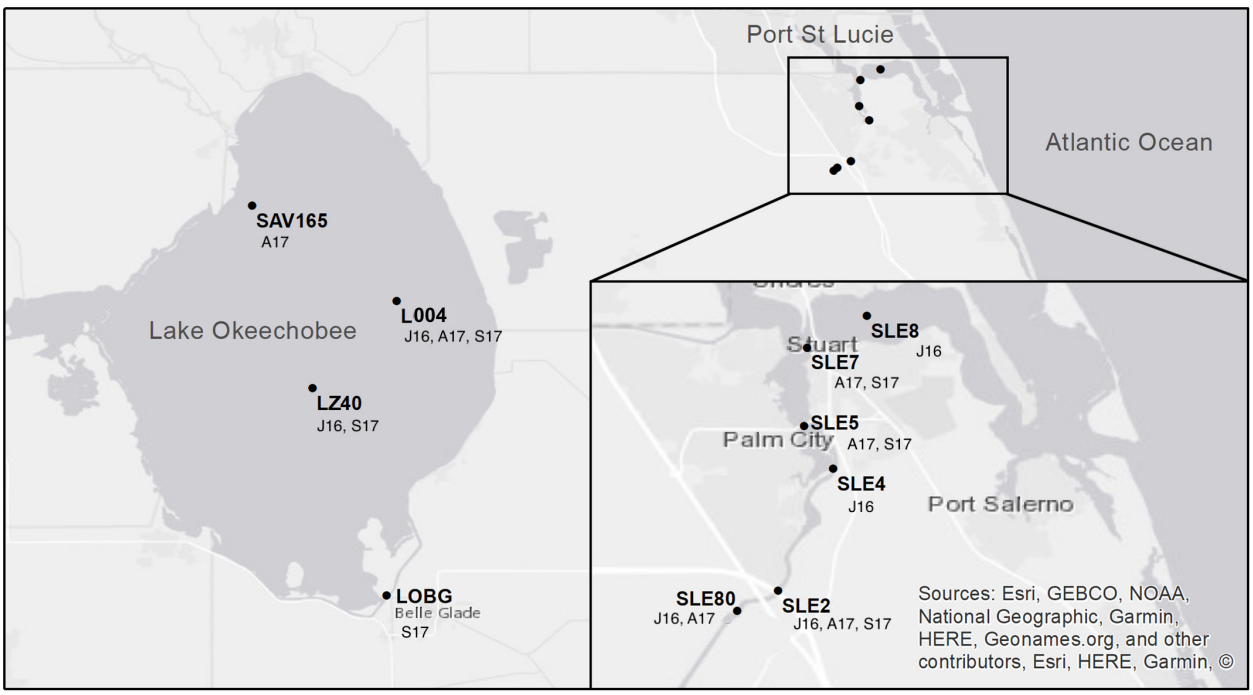

FIGURE 1 | Map of sampling locations in Lake Okeechobee and St. Lucie Estuary. Annotations indicate sampling date (J16, July 2016; A17, August 2017; S17, September 2017). Modified from Hampel et al. (2019).

curve with R^2 values ≥0.99. Gene copy number was calculated as (ng * number mol $^{-1}$)/(bp * ng g^{-1} * g mol^{-1} of bp) and is reported in *amoA* gene copies ml^{-1} of sample water.

amoA Amplicon Sequencing and Analysis

Barcoded amplicons for AOA and AOB were prepared by using a two-step PCR approach (Herbold et al., 2015). In the first PCR, bacterial and archaeal *amoA* fragments were amplified using the standard procedures and primers listed above, with a decreased number of cycles (24 cycles). In the second PCR, the first-step PCR product was used as a template for eight cycle amplification with a primer consisting of the barcodes and Illumina adapters (**Supplementary Table S4**). The barcoded amplicons were sequenced on an Illumina MiSeq for paired end sequencing (2 × 300 bp PE). Barcoding, cleaning, quantification, and pooling was conducted at the Ohio State Molecular and Cellular Imaging Center, and the Illumina MiSeq Reagent kit v3, paired end 300 sequencing kit, and the Illumina Nextera XT index kit v2 for indexing the libraries were used. Raw sequence data analysis was conducted using Mothur pipeline (version 1.42.3; Schloss et al., 2009). Sequences were assembled into contigs, and adapters and primers were removed. Sequences longer than 555 bp for AOA, and 475 bp for AOB, and low-quality sequences with more than one mismatch in barcode/primer sequences, were removed in Mothur. Frameshift errors in unique archaeal and bacterial reads were corrected using the FunGene FrameBot tool (Wang et al., 2013), and sequence alignment was conducted using aligned archaeal or bacterial *amoA* sequences retrieved from the FunGene database (Aalto et al., 2018). Chimeric sequences were removed using Uchime in Mothur (Edgar et al., 2011), and sequences were clustered into OTUs at 95% sequence identity.

The taxonomic assignment of archaeal and bacterial sequences was completed in Mothur using the Alves et al. (2018) comprehensive AOA *amoA* database and custom AOB *amoA* reference libraries, which were collected from sequences and their taxonomies in the Nucleotide database (Aalto et al., 2018) at a 95% cutoff (Beman and Francis, 2006; Frank et al., 2016; Aalto et al., 2018). Phylogenetic analysis was conducted in MEGA X, where sequences were aligned using the multiple sequence alignment tool, ClustalW, to align representative and reference sequences. Maximum likelihood phylogenetic trees were constructed with 1000 bootstrap replicates using the Tamura-Nei nucleotide substitution model in MEGA X (Kumar et al., 2018). The phylogenetic tree was edited and annotated using iTOL v.5 (Letunic and Bork, 2019). Raw sequences were submitted to NCBI's Sequence Read Archive under BioProject #PRJNA592084.

Nitrification Rates

Nitrification rates were measured using the $^{15}NH_4^+$ tracer addition method (Ward, 2008; Newell et al., 2013; Heiss and Fulweiler, 2016). Five hundred ml of water from each station was distributed into acid-washed, 1 L polycarbonate bottles and enriched with 98% $^{15}NH_4Cl$ (Isotec) at final concentrations of 0.25 μM (2016) or 0.5 μM (2017). Amended water was mixed thoroughly by inverting 10 times and distributed into

three, acid-washed 125 ml polycarbonate incubation bottles. Unamended control samples for each station were distributed into 125 ml incubation bottles. Initial samples (T_0) were filtered to 0.22 μm with syringe filters into 50 ml polycarbonate tubes and frozen until analysis, and final samples (T_f) were collected after incubating for 20 h at near *in situ* light and temperature in a laboratory incubator.

Accumulation of $^{15}NO_3^-$ was measured using the Cd reduction/NaN_3 reduction method (McIlvin and Altabet, 2005; Heiss and Fulweiler, 2016). Approximately 25 ml from each sample was filtered (0.2 μm syringe filter) into 50 ml centrifuge tubes. NO_3^- was reduced to NO_2^- by addition of 100 mg of MgO, 6.6 g of NaCl, and 0.75–1 g of acidified Cd powder to each sample, followed by a 17 h incubation on a shaker table (McIlvin and Altabet, 2005). Samples were centrifuged at 1000 × *g* for 15 min, and 7.5 ml of supernatant was carefully transferred into 12 ml Exetainers.

NOx (including cadmium-reduced NO_2^-) was further reduced to N_2O with the NaN_3 method (McIlvin and Altabet, 2005; Newell et al., 2011; Hampel et al., 2018). Briefly, each sample was treated (with gastight syringe) with 0.25 ml of a 1:1 (v:v) solution of 2 M NaN_3:20% CH_3COOH solution (Ar-purged) and incubated for 1 h at 30°C (McIlvin and Altabet, 2005). NO_2^- in the sample from Cd reduction was transformed chemically to N_2O. After a 1 h incubation, the reaction was stopped with an injection of 0.15 ml of 10 M NaOH. Samples were inverted and sent to the University of California Davis Stable Isotope Facility for isotopic analysis of $^{45/44}N_2O$ using a Thermo Finnigan GasBench + PreCon trace gas concentration system interfaced to a Thermo Scientific Delta V Plus isotope-ratio mass spectrometer (Bremen, Germany). Nitrification rates were corrected for NaN_3 reduction efficiency (determined from reduced standards), and $^{15}NO_3^-$ production was calculated as:

$$\text{Nitrification (in nmol L}^{-1}\text{d}^{-1}) = ((^{15}N/^{14}N^*[NO_3^-])_{24h} - (^{15}N/^{14}N^*[NO_3^-])_{0h})/\alpha^* t$$

Where $\alpha = [^{15}NH_4^+]/([^{15}NH_4^+] + [^{14}NH_4^+])$.

Statistical Analysis

Statistical analysis was conducted using RStudio software (Version 1.1.463). First, environmental data, nitrification rates, and *amoA* abundance were checked for normality using the Shapiro-Wilk test. After determining that the data were not normally distributed, the Kendall correlation method for non-parametric data was used to determine correlations between parameters. Wilcoxon and Kruskal-Wallis tests for non-parametric data were used to determine differences between sampling events. Additionally, a stepwise multiple-regression model for nitrification rates was constructed using the MASS package (R Version 7.3). The best-fitting model was selected based on the minimum Akaike's information criteria (AIC; Akaike, 1987). All non-normally distributed variables were log(x + 1)-transformed prior to running the model to normalize the data for parametric analysis.

Community structure analysis and visualization was performed using phyloseq (Version 1.28.0; McMurdie and Holmes, 2013), vegan (Version 2.5-2; Oksanen et al., 2018), and ggplot2 (Version 3.2.0; Wickham, 2016) packages in RStudio. Alpha diversity was calculated for bacterial and archaeal data. Bray-Curtis dissimilarity analysis was used to evaluate variability of communities across samples, using non-metric multidimensional scaling (NMDS; **Supplementary Figure S1**). Differences in the AOA and AOB community structure between sampling events were tested separately with permutational multivariate analysis of variance (PERMANOVA; Anderson, 2001; adonis in vegan package), followed by the homogeneity of dispersion test using the betadisper function. Relationships between sequencing data and environmental variables were evaluated using the Constrained Analysis of Principal Coordinates (CAP) ordinations after removing missing values from environmental data (**Supplementary Figure S2**).

RESULTS

Physical and Biogeochemical Parameters

Environmental data have been reported previously (Hampel et al., 2019) and are presented here in **Supplementary Tables S1**, **S2**. Water temperature in the lake and estuary was uniform across all sampling events. After the hurricane, salinity and NH_4^+ concentrations decreased in the estuary (p = 0.03, p = 0.08, respectively), while conductivity (p = 0.005), turbidity (p = 0.001), TSS (p = 0.005), and NO_3^- concentrations (p = 0.001) increased (**Supplementary Tables S1**, **S2**). Post-hurricane, lake turbidity (p = 0.04) and NO_3^- concentration (p = 0.05) increased. In the lake, chlorophyll *a* (chl *a*) concentration was higher during the August 2017 bloom than during the 2016 bloom and decreased after the hurricane (**Supplementary Table S1**). In the estuary, chl *a* concentrations decreased along the salinity gradient and were lowest following the hurricane (**Supplementary Table S2**).

Nitrification Rates

Nitrification rates in the lake in July 2016 varied between the eastern (L004; **Figure 1**) and central lake stations (LZ40; **Figure 2A**). Nitrification rates were higher in bottom water (2 m) at L004 (98.8 ± 5.11 nmol L^{-1} d^{-1}; mean ± SE) compared to surface water (∼0.2 m; 10.5 ± 1.6 nmol L^{-1} d^{-1}; p = 0.03). In contrast, nitrification rates in the bottom water at LZ40 were undetectable, and low rates were measured in surface water (2.04 ± 0.52 nmol L^{-1} d^{-1}). Nitrification rates in the lake in August 2017 were only measurable in surface water and were slightly lower than those measured in 2016 (0.78 ± 0.82 nmol L^{-1} d^{-1} at SAV165 to 2.14 ± 0.02 nmol L^{-1} d^{-1} at L004; **Figure 2A**). However, after the hurricane, nitrification rates increased by 2–3 orders of magnitude (p = 0.003) at L004 (1280 ± 71.3 nmol L^{-1} d^{-1}) and LZ40 (168 ± 96.1 nmol L^{-1} d^{-1}).

In July 2016, nitrification rates in the estuary increased along the salinity gradient, with undetectable rates at the most upstream site (SLE80) and greatest rates at the most saline site (SLE8; 79.4 ± 0.01 nmol L^{-1} d^{-1}; **Figure 2B**). In August

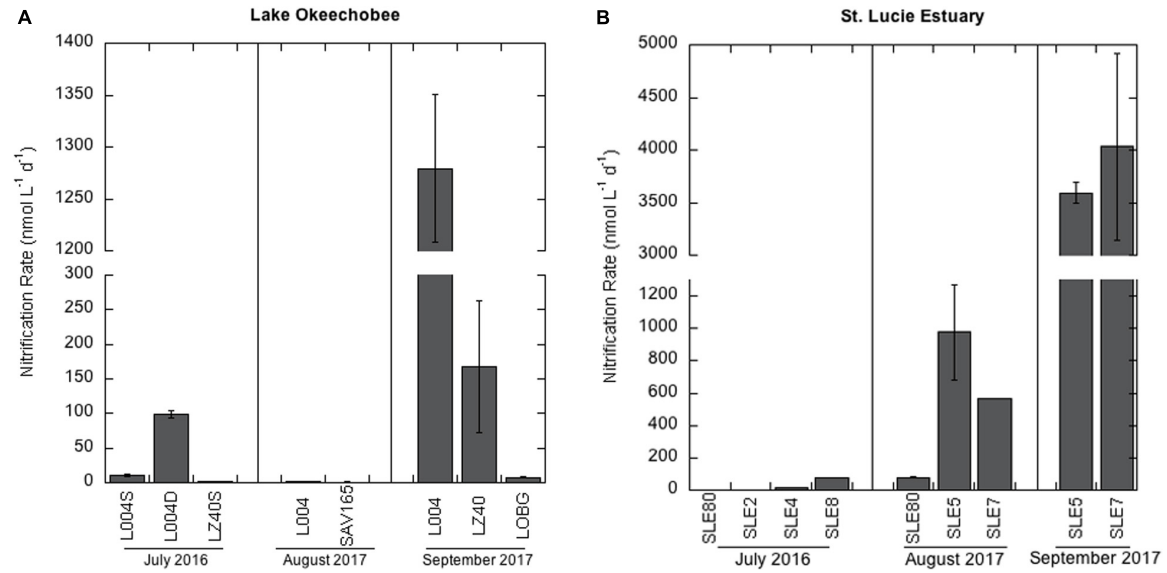

FIGURE 2 | Nitrification rates ± one standard error in: **(A)** Lake Okeechobee and **(B)** St. Lucie Estuary. Note the scale difference between **(A)** and **(B)**.

2017, nitrification rates in the estuary were higher than in 2016 ($p = 0.06$). Again, the lowest rates were observed upstream near the St. Lucie canal (SLE80; 79.1 ± 2.22 nmol L^{-1} d^{-1}), and greatest rates were observed downstream at SLE5 (978 ± 294 nmol L^{-1} d^{-1}; $p = 0.04$) and SLE7 (563 ± 0.4 nmol L^{-1} d^{-1}; $p < 0.001$; **Figure 2B**). Following the hurricane, nitrification rates increased at both upstream (SLE5: 3590 ± 98.9 nmol L^{-1} d^{-1}) and downstream stations (SLE7: 4030 ± 888 nmol L^{-1} d^{-1}; **Figure 2B**; $p < 0.001$). Overall, nitrification rates in the estuary exceeded those in the lake on all occasions. Nitrification rates were negatively correlated with temperature and dissolved oxygen (DO; Kendall, $p = 0.03$; **Table 1**) and positively correlated with ambient NO_3^- concentrations (Kendall, $p = 0.001$). Additionally, the best-fitting multiple regression model for nitrification revealed that ambient NO_3^- concentration, turbidity, and salinity were the best predictors for nitrification rates in the lake and estuary (Adj. $R^2 = 0.99$; **Supplementary Table S3**).

amoA Abundance

In the lake in August 2017, AOA (mean = 8.21 ± 0.70 × 10^5; range: 8.21 × 10^4–1.83 × 10^6) exceeded AOB abundance (mean = 1.54 ± 0.29 × 10^4; range: 2.31–3.29 × 10^3) at all stations, with AOA abundance 1–3 orders of magnitude higher (**Figure 3A**). Following the hurricane, AOA abundance (mean = 3.06 ± 1.32 × 10^6; range: 4.32 × 10^4–5.73 × 10^6) was also higher than AOB (mean = 4.87 ± 0.43 × 10^4; range: 2.07–9.35 × 10^4) at all stations, except near the lake shore (LOBG; **Figure 3A**). AOB abundance increased after Hurricane Irma in the lake ($p = 0.05$), while AOA abundance did not change. Lake nitrification rates were correlated with AOA *amoA* copy numbers (**Figure 4**; $R^2 = 0.94$, $p = 0.006$), while no pattern was observed between nitrification rates and lake AOB or estuarine ammonia oxidizers (**Supplementary Figure S3**).

In the estuary in August 2017, AOA abundance (mean = 5.36 ± 4.39 × 10^4; range: 7.10 × 10^3–1.29 × 10^5) exceeded AOB (mean = 2.07 ± 0.36 × 10^4; range: 5.25 × 10^2–9.37 × 10^3) at all stations except upstream (SLE80). AOA abundance was slightly lower than in the lake, while AOB abundances were comparable to those measured in the lake (**Figure 3B**). After Hurricane Irma, *amoA* gene copies for both AOA and AOB increased, and AOA (mean = 2.71 ± 0.63 × 10^5; range: 7.65 × 10^4–4.65 × 10^5) outnumbered AOB (mean = 1.03 ± 0.13 × 10^5; range: 5.06 × 10^4–1.56 × 10^5) at all stations (**Figure 3B**). AOA abundance in both the lake and estuary were negatively correlated with temperature and ambient NH_4^+ concentration and positively correlated with TSS (Kendall, $p = 0.003$; **Table 1**). AOB abundance was positively correlated with conductivity (Kendall, $p = 0.03$).

Ammonia Oxidizer Community Structure

Following the quality control steps in Mothur, frameshift in FrameBot, and chimera removal, we retrieved 3,699 unique *amoA* sequences for AOA and 17,030 for AOB. *amoA* sequences grouped into 574 and 101 OTUs (95% similarity) for AOA and AOB, respectively. We observed a shift in the AOA community after the hurricane (**Figure 5**; PERMANOVA, $F = 2.763$, $p = 0.03$), while the AOB community changed only marginally ($F = 1.592$, $p = 0.08$).

Ammonia-oxidizing archaeal sequences grouped phylogenetically into the lineages and clades of *Nitrososphaerales* (NS), *Nitrosotaleales* (NT), and *Nitrosopumilales* (NP): NP η (*Nitrosotenuis* spp.), NP γ 2.1 (*Nitrosopumilus* spp.), NP γ 2.2 (*Nitrosoarchaeum* spp.), and NP δ (**Figure 6**). Sequences from the lake and estuary were mostly phylogenetically distinct, as OTUs present only in the lake were phylogenetically close to NS and NT orders, while the estuarine-only OTUs assigned to the NP γ 2.1 clade.

TABLE 1 | Details of Kendall correlation for non-parametric data analysis of environmental parameters, geochemical rates, and *amoA* gene abundance in Lake Okeechobee and St. Lucie Estuary.

		Temp.	DO	Salinity	NH_4^+	NO_3^-	Cond.	Turbidity	TSS
Nitrification	Kendall T	**−0.58**	**−0.38**	0.39	0.08	**0.58**	0.29	0.23	0.00
	p-value	**0.002**	**0.03**	0.09	0.65	**0.001**	0.110	0.45	1.00
AOA	Kendall T	**−0.51**	0.37	**−0.40**	**−0.73**	0.24	0.17	0.52	**0.68**
	p-value	**0.04**	0.12	0.32	**0.003**	0.32	0.47	0.09	**0.003**
AOB	Kendall T	**−0.04**	**−0.11**	**−0.60**	0.02	0.28	**0.53**	0.33	0.29
	p-value	0.85	0.65	0.14	0.92	0.24	**0.03**	0.29	0.36

Correlations where p < 0.05 are presented in bold. Temp., temperature; DO, dissolved oxygen; Cond., conductivity; TSS, total suspended solids.

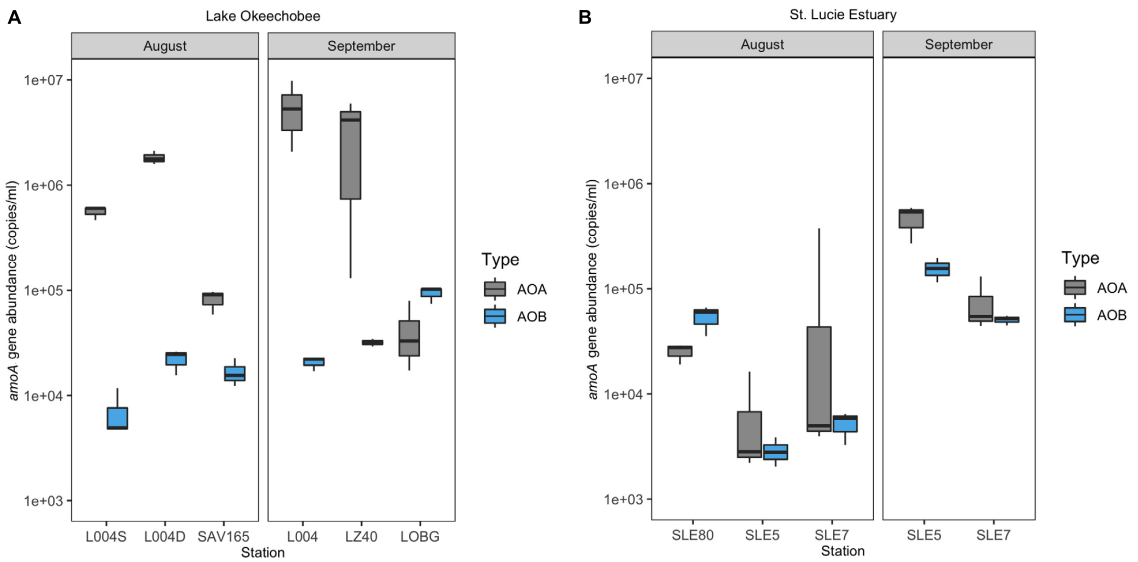

FIGURE 3 | Ammonia oxidizer abundance (*amoA* gene) ± one standard error in Lake Okeechobee **(A)** and St. Lucie Estuary **(B)** before and after Hurricane Irma.

Before the hurricane, AOA were dominated by unclassified NP γ 2.2 (*Nitrosoarchaeum* spp.) in the lake and NP γ 2,1 (*Nitrosopumilus* spp.) OTUs in the estuary (**Figure 5A**). After the hurricane, AOA in the lake shifted to NP η 1.1 (*Ca. Nitrosotenuis cloacae*) OTUs in the central lake (L004, LZ40), while most OTUs from the nearshore station (LOBG) clustered within the NS δ clade. The post-hurricane AOA community in the estuary shifted to higher relative abundances of NP η 1.1 (*Ca. N. cloacae*) upstream (SLE5) and NP η 1.1 and NP γ 2.2 OTUs downstream (SLE7).

Ammonia-oxidizing bacterial sequences were not as clearly separated by sampling location as AOA sequences and were placed phylogenetically into the *Nitrosomonas* clusters, with most of the OTUs close to *Nitrosomonas ureae*, and some estuary-only OTUs close to *Nitrosomonas nitrosa* (**Figure 7**). Before the hurricane, AOB communities were dominated by *Nitrosomonas oligotropha* in the upstream estuary (SLE80 and SLE5) and by unclassified *Nitrosomonas* groups in the lake (**Figure 5B**). After the hurricane, both lake and estuary AOB communities shifted to a higher proportion of *Nitrosomonas oligotropha*.

Overall, despite an order of magnitude fewer sequences, AOA were more diverse than AOB (p = 0.009; **Figure 8**). AOB alpha diversity increased after the hurricane in both systems (p = 0.02), while AOA diversity remained unchanged (**Figure 8**). Constrained Analysis of Principal coordinates (CAP) for AOA showed separation by sampling month and the effects of hurricane disturbance (**Supplementary Figure S2A**). CAP1 (57.9% variance explained) was driven by salinity (r = −0.95), NH_4^+ concentration (r = −0.91), and turbidity (r = 0.77), which were also affected by the hurricane, while CAP2 (25.9% variance explained) was driven primarily by NO_3^- (r = −0.61) and DO concentrations (r = 0.53). For AOB communities (**Supplementary Figure S2B**), CAP1 (35.2% variance explained) was associated with salinity (r = 0.80), NH_4^+ concentration (r = 0.76), and nitrification rate (r = −0.63), while CAP2 (20.7% variance) was associated with salinity (r = 0.54) and turbidity (r = −0.51).

DISCUSSION

Nitrification During Cyanobacterial Blooms

Nitrification rates in both the lake and estuary varied between sampling events (**Figure 2**). Nitrification rates in Lake Okeechobee were low during cyanoHABs in 2016

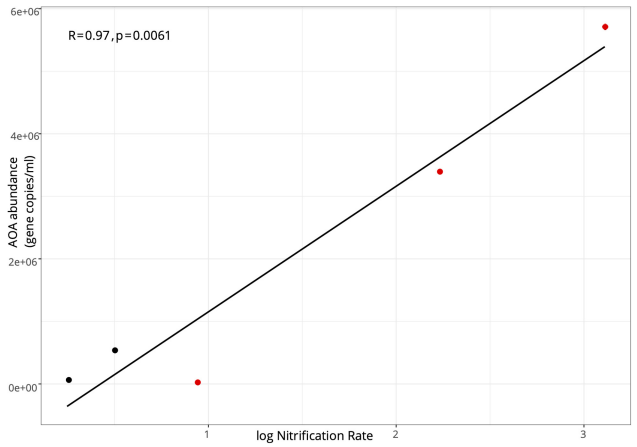

FIGURE 4 | Pearson correlation between the abundance of ammonia oxidizing archaea *amoA* functional gene and log-transformed nitrification rates in Lake Okeechobee. Black points indicate samples collected in August 2017; red points indicate samples collected in September 2017.

and 2017 (**Figure 2A**), similar in magnitude to those from oligotrophic Lake Superior (Small et al., 2013), and lower than those previously measured in spring in Lake Okeechobee (James et al., 2009). Competition for NH_4^+ between nitrifiers and photoautotrophs, including cyanobacteria, may inhibit nitrification during severe cyanoHABs, which were observed in Lake Okeechobee in 2016 (Kramer et al., 2018; Hampel et al., 2019). NH_4^+ is the most energetically favorable N form for primary producers, including non-N_2 fixing cyanobacteria (e.g., *Microcystis*), which often outcompete other algal groups (e.g., Blomqvist et al., 1994) and ammonia oxidizers for NH_4^+. Nitrifiers have a lower substrate affinity and higher K_m (Martens-Habbena et al., 2009) for NH_4^+ than *Microcystis* (Nicklisch and Kohl, 1983; Baldia et al., 2007). In Lake Okeechobee, nitrification accounted for <1% of total NH_4^+ uptake and was likely suppressed by competition with *Microcystis* (Hampel et al., 2019). Suppression of nitrification due to competition for NH_4^+ between *Microcystis* and ammonia oxidizers has also been observed in hypereutrophic Lake Taihu (China), where nitrification rates during massive *Microcystis* blooms were equally as low as reported here in Lake Okeechobee, but increased when the bloom was less pronounced (Hampel et al., 2018).

Water column nitrification measurements in lakes are scarce compared to open ocean and coastal marine systems, but the rates measured here are comparable to other systems. In the estuary, nitrification rates in 2016 ranged from undetectable to 79.4 ± 0.02 nmol L^{-1} d^{-1} and increased along the salinity gradient (**Figure 2B**). These rates are similar to those measured in other coastal marine systems (Horak et al., 2013; Damashek et al., 2016; Heiss and Fulweiler, 2016; Laperriere et al., 2018). Undetectable and low nitrification rates in the upstream estuary are likely due to the presence of cyanoHABs during sampling and increased competition for NH_4^+. High photoautotrophic NH_4^+ uptake rates (2.32 μmol L^{-1} h^{-1}; Hampel et al., 2019), coincident with high *Microcystis* cell densities in the upstream estuary (Kramer et al., 2018), suggest that nitrifiers were outcompeted for

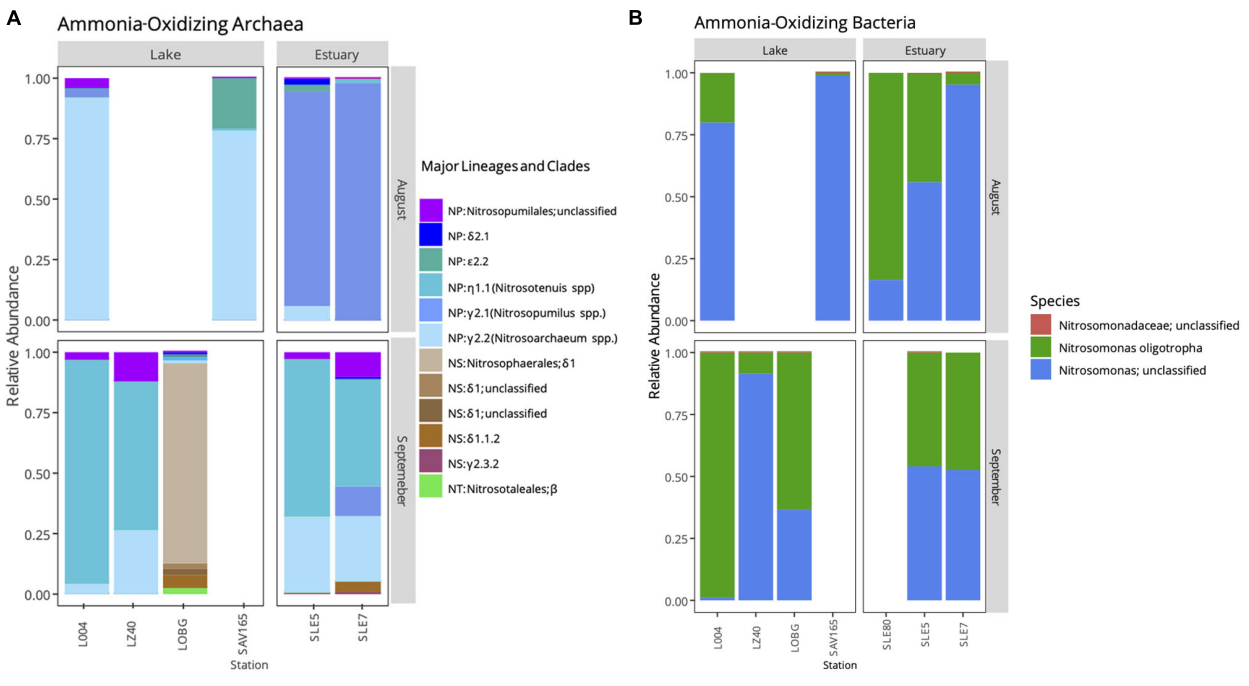

FIGURE 5 | Relative abundance of ammonia-oxidizing archaea **(A)** and bacteria **(B)** in Lake Okeechobee and St. Lucie Estuary before (August) and after (September) hurricane disturbance. AOA represent three major lineages: *Nitrosopumilales* (NP), *Nitrososphaerales* (NS), and *Nitrosotaelales* (NT). Lineages are divided into clades (Greek letters) and numbers (genera).

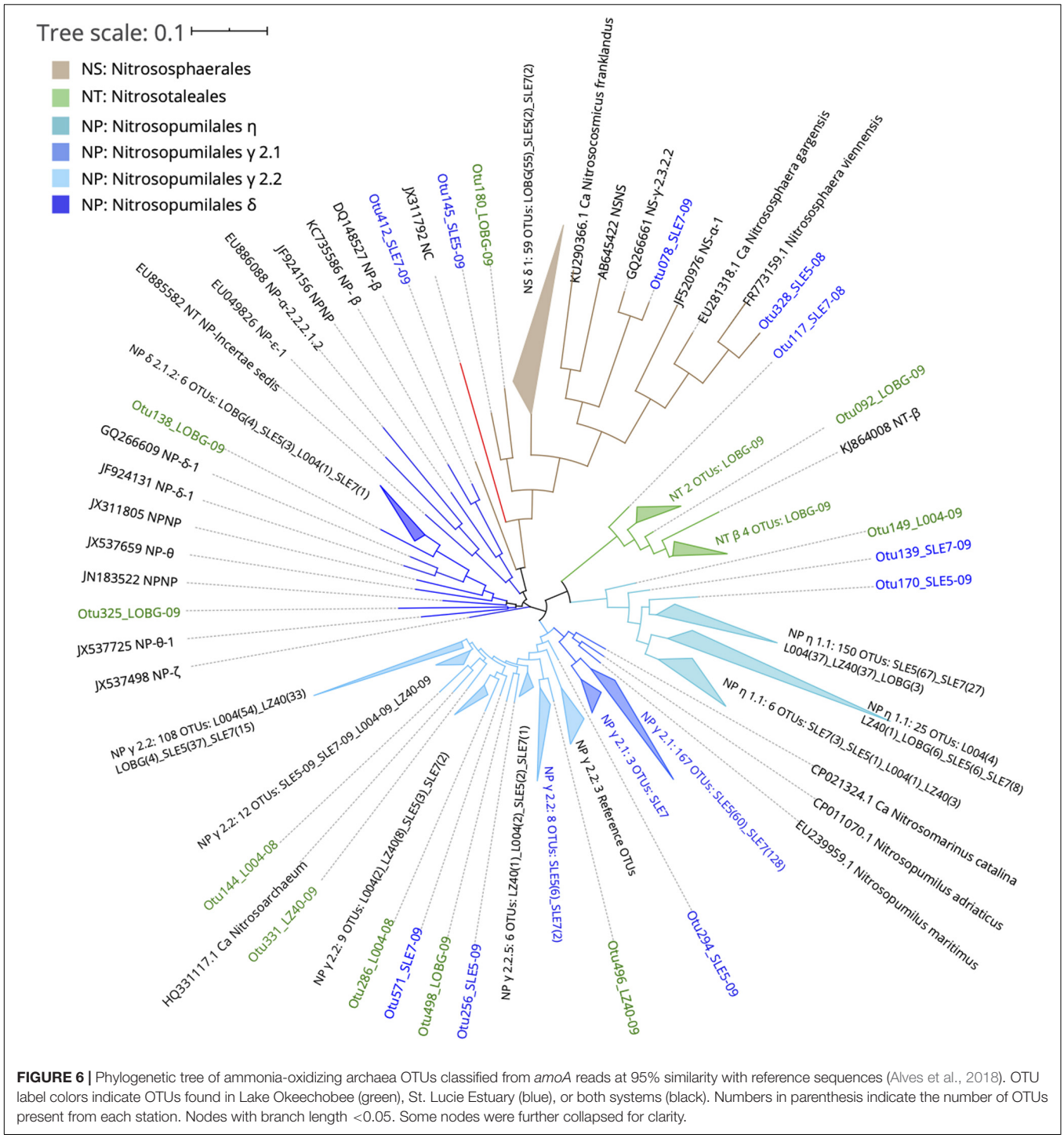

FIGURE 6 | Phylogenetic tree of ammonia-oxidizing archaea OTUs classified from *amoA* reads at 95% similarity with reference sequences (Alves et al., 2018). OTU label colors indicate OTUs found in Lake Okeechobee (green), St. Lucie Estuary (blue), or both systems (black). Numbers in parenthesis indicate the number of OTUs present from each station. Nodes with branch length <0.05. Some nodes were further collapsed for clarity.

NH_4^+. In contrast, the bloom was less pronounced downstream (Kramer et al., 2018), and photoautotrophic NH_4^+ uptake rates were lower (1.11 μmol L^{-1} h^{-1}; Hampel et al., 2019), which may help explain the increase in nitrification rates along the salinity gradient.

Before the hurricane, flows of lake water into the estuary were low in 2017, and cyanoHABs were mostly constrained to the lake (Hampel et al., 2019). Nitrification rates in the estuary were an order of magnitude higher in August 2017 than in the previous year (**Figure 2B**). The highest nitrification rates were observed at the more saline SLE5 and SLE7 (563–978 nmol L^{-1} d^{-1}; **Figure 2B**), and nitrification accounted for 3–7% of total NH_4^+ uptake, suggesting a more effective competition for NH_4^+. Nitrification rates of this magnitude have been observed in other high-nutrient environments, such as the Eastern Tropical South Pacific (Lipschultz et al., 1990), the hypoxic zone in

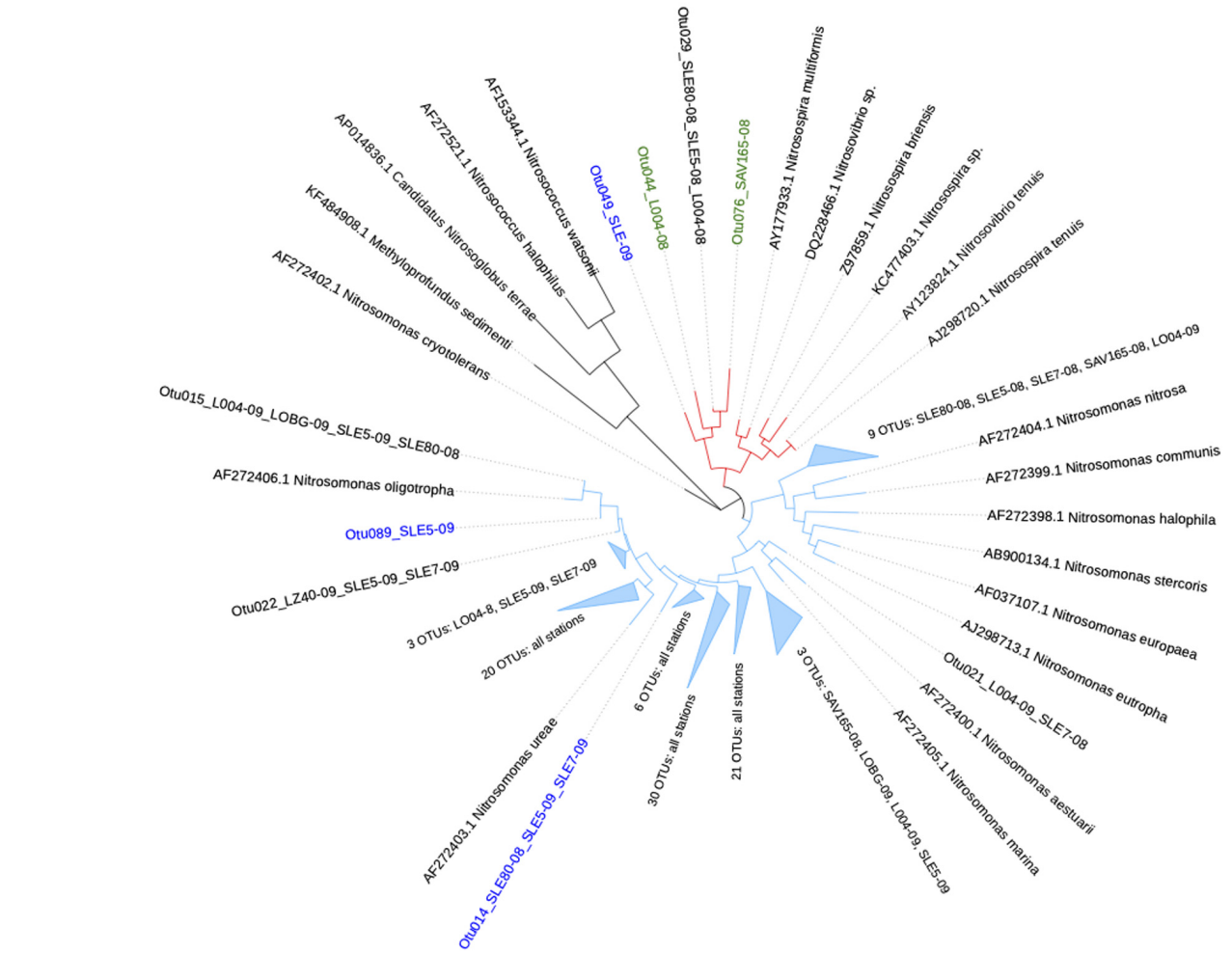

FIGURE 7 | Phylogenetic tree of ammonia-oxidizing bacteria OTUs classified from *amoA* reads at 95% similarity. OTU label colors indicate OTUs found in Lake Okeechobee (green), St. Lucie Estuary (blue), or both systems (black). Numbers in parenthesis indicate the number of OTUs present from each station. Nodes with branch length <0.05. Some nodes were further collapsed for clarity.

the Gulf of Mexico (Bristow et al., 2015), coastal Georgia (United States; Tolar et al., 2017), and Hood Canal, Puget Sound (United States; Urakawa et al., 2014). These results illustrate indirect downstream consequences of HABs along the hydrologic continuum, where HABs and nutrient loading upstream in the estuary can suppress nitrification (as seen in 2016), therefore potentially reducing N removal via denitrification.

Nitrification Following Hurricane Irma

After the hurricane, nitrification rates in both systems increased by an order of magnitude or more (**Figure 2**). In the lake, nitrification rates were up to 1280 nmol L^{-1} d^{-1} (**Figure 2A**). Nitrification rates on this scale in natural, freshwater systems have, to our knowledge, only been reported in Lake Taihu (Hampel et al., 2018) and Lake Mendota (Hall, 1986). In the estuary, nitrification rates after the hurricane ranged from 3590–4030 nmol L^{-1} d^{-1}, much higher than rates reported previously in oligotrophic and some eutrophic estuarine systems (Horak et al., 2013; Bronk et al., 2014; Urakawa et al., 2014; Heiss and Fulweiler, 2016). Rates in this range were previously measured in the Chang Jiang (Yangtze) River plume (Hsiao et al., 2014), eutrophic Elbe estuary (Sanders et al., 2018), Pearl River estuary (Dai et al., 2008), and northern Gulf of Mexico (Carini et al., 2010). The dramatic increase in nitrification following the hurricane may be related to sediment resuspension caused by high winds, introducing benthic nitrifiers and NH_4^+ accumulated in sediments into the water column. With more favorable

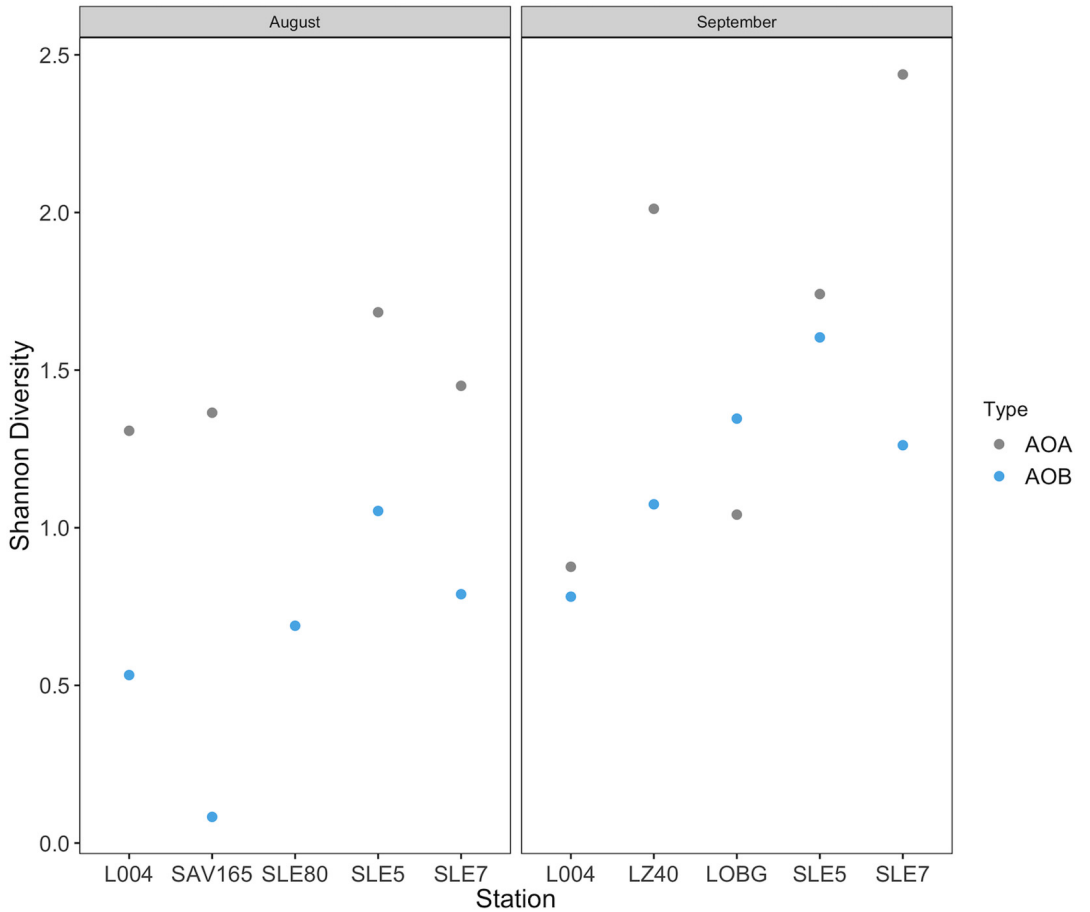

FIGURE 8 | Shannon diversity before and after Hurricane Irma in Lake Okeechobee and St. Lucie Estuary for ammonia oxidizing archaea and ammonia oxidizing bacteria.

oxygen conditions in the water column, a fresh supply of NH_4^+, and higher turbidity, photoautotrophs may have experienced light limitation (James et al., 2008), thus releasing competitive pressure and allowing nitrification to increase (Wengrove et al., 2015).

A comprehensive review of nitrification in estuaries reported a trend of elevated nitrification rates at Estuary Turbidity Maxima (ETM; Damashek and Francis, 2018), some of which were also associated with turbid waters and strong wind events (Hsiao et al., 2014; Happel et al., 2018; Laperriere et al., 2018; Sanders et al., 2018). NH_4^+ released from resuspended sediments can thus lead to nitrification "hot spots" (Percuoco et al., 2015; Damashek et al., 2016). Hurricanes are also accompanied by increased rainfall, leading to larger runoff and increased nutrient concentrations in the water column (Havens et al., 2001; James et al., 2008). High turbidity in the water column may limit photoautotrophic access to light, thus favoring nitrifiers, which are chemolithoautotrophic and do not require light. Microcystin synthetase (*mcyD*) abundance and chl *a* levels decreased following the hurricane (Hampel et al., 2019), supporting this interpretation. In the estuary, nitrification accounted for 60–90% of total NH_4^+ uptake after the hurricane, further supporting the idea that turbid conditions favored nitrifiers.

Ammonia-Oxidizer Community Structure and Abundance

For most sampling events, AOA abundance was greater than AOB (**Figure 3**). While AOA are generally more abundant than AOB in the open ocean, estuarine ammonia-oxidizing communities are more complex and dynamic, with different systems exhibiting AOA dominance (Beman and Francis, 2006; Horak et al., 2013), AOB dominance (Bernhard et al., 2010), or interchanging spatial dominance of AOA and AOB (Santoro et al., 2008; Zhang et al., 2014). Salinity can help shape ammonia oxidizer community structure (Caffrey et al., 2007; Mosier and Francis, 2008; Santoro et al., 2008). AOB often dominate lower salinity regions of estuaries, while AOA are more abundant in more marine areas (Bouskill et al., 2012), but this pattern is not universal (Mosier and Francis, 2008; Santoro et al., 2008). In the estuary, AOB abundance was only greater than AOA at the upstream, lower salinity site (SLE80).

Despite AOA outnumbering AOB in many systems, AOB abundance has more often correlated positively with nitrification rates (Bernhard et al., 2010; Zeng et al., 2012; Damashek et al., 2015; Hampel et al., 2018). However, the only observed relationship between *amoA* abundance and nitrification rate was between AOA *amoA* copy number and log-transformed nitrification rates in Lake Okeechobee (R^2 = 0.94; **Figure 4** and **Supplementary Figure S3**). A relationship between AOA *amoA* abundance and potential nitrification rates in sediments was reported in hypereutrophic Lake Taihu (Zeng et al., 2012), but we are not aware of any similar relationship reported in a eutrophic lake water column to date.

This study presents a remarkable phylogenetic diversity of recovered AOA OTUs, with close relatives from three of the four major lineages (Alves et al., 2018). Unlike AOB, AOA rarefaction curves (**Supplementary Figure S4**) did not plateau, suggesting that much of the diversity for AOA was not characterized. Despite the relatively low number of AOA sequences recovered, AOA were still more abundant and diverse than AOB. The low number of sequences, but high diversity and abundance, justifies not rarefying our sequences in the downstream analysis. Recent studies suggest that normalizing sequences via rarefaction can result in discarding important reads and introduces more bias (McMurdie and Holmes, 2014). Overall, the high diversity (even at comparatively low abundance) of AOA sequences along with strong correlation with nitrification rates emphasizes the possible importance of AOA in eutrophic systems and their contribution to nitrification.

The high abundance and diversity of AOA, and strong relationship with nitrification rates within Lake Okeechobee, is puzzling considering the reported oligotrophic nature of AOA (Martens-Habbena et al., 2009; Bollmann et al., 2014; Kits et al., 2017). We suggest that AOA in these eutrophic ecosystems might have evolved from niche differentiation and could represent a new, eutrophic ecotype, separate from oligotrophic AOA (Beman et al., 2008; Sintes et al., 2013; Santoro et al., 2017). High phylogenetic diversity of AOA in this and other studies (Alves et al., 2018; Cheung et al., 2019; Zhao et al., 2020) suggests that broad classification into shallow and deep marine and terrestrial ecotypes is insufficient, and many *amoA* clades represent ecotype intra-diversity, perhaps dictated by other environmental conditions beyond depth, salinity, and pH.

The majority of lake-only AOA OTUs clustered within the NS δ clade, the most abundant clade in the Alves et al. (2018) database that still lacks cultivated representatives. Although little is known about the physiological characteristics of the NS δ clade, it is abundant in soils, freshwater water columns and sediments, marine sediments, wastewater treatment plants, and salt lakes, suggesting an exceptional versatility of habitats for this group. A BLAST search of the representative sequences from this clade matched with previous studies from sludges (Xia et al., 2019), soils (Li et al., 2015; Zhong et al., 2016), and streams affected by wastewater treatment plants (Merbt et al., 2015). Other lake OTUs clustered in NT β and NP δ and η. The NT β clade has no isolated representative and is mostly present in freshwaters, soils, and sediments, while NP δ is also uncharacterized, with sequences from freshwater, estuarine, and marine environments (Alves et al., 2018). These lake-only OTUs, particularly from the NS δ clade at LOBG, could belong to a eutrophic AOA ecotype that has adapted to high NH_4^+ concentrations, but evidence from the literature is lacking on AOA communities in lakes. The NH_4^+ concentration at this station during sampling was ∼20 μM (**Supplementary Table S1**), which greatly exceeds typical concentrations in the ocean. This eutrophic AOA ecotype may be able to outcompete AOB in eutrophic freshwater systems, as suggested from our results in Lake Okeechobee. Similar conclusions were reached in the eutrophic Pearl River estuary (Zou et al., 2019), but genomic adaptations of AOA in eutrophic systems and their contributions to nitrification remain an intriguing knowledge gap requiring further investigation.

Few studies have documented changes in ammonia oxidizer community structure following disturbances in aquatic systems. Responses of ammonia oxidizers to various perturbations differ and include increased AOB diversity or abundance (wastewater, Aalto et al., 2018; flow restriction, Bernhard et al., 2015; flooding, Bouskill et al., 2011; storms, Kan, 2018), decreased AOA diversity or abundance (storms, Happel et al., 2018; hurricanes, Newell et al., 2014), or little to no effect (oil spill, Bernhard et al., 2019; oil spill, Marton et al., 2015). Here, we observed substantial hurricane impacts on the abundance, community composition, and diversity of ammonia oxidizers. In the lake, only AOB abundance increased after the hurricane, while in the estuary, we observed the opposite, with AOA abundance increasing. AOB communities were more diverse following the hurricane, while AOA diversity increased in the estuary but decreased in the lake (**Figure 8**). These results agree with those from a previous study in the Gulf of Mexico (Newell et al., 2014), where benthic AOA communities were less diverse following Hurricanes Ike and Gustav, suggesting a weak resistance to disturbance. Increased AOB abundance in our study also supports disturbance studies in boreal lake sediments (Aalto et al., 2018) and estuaries (Happel et al., 2018), where AOB diversity and/or abundance increased at affected sites, suggesting that AOB are more adaptable to disruptive events (Aalto et al., 2018).

Hurricane disturbance caused a significant shift in AOA community structure in both systems (**Figure 5A**). In the lake, the community changed from high abundance of low-salinity tolerant NP γ 2.2 (*Nitrosoarchaeum* spp.) to dominance by NP η 1.1 (*Ca. Nitrosotenuis cloacae*) in the central lake (L004, LZ40) and NS δ OTUs at the littoral station (LOBG). *Ca. Nitrosotenuis cloacae* was enriched from a wastewater treatment plant and exhibits intolerance to high salinity, and phylogenetically related strains of NP η have been found in lakes and rivers (Li et al., 2016; Alves et al., 2018). *Nitrososphaera* are often present in soils and sediments (Alves et al., 2018; Li et al., 2018); thus, their high abundance at the littoral station after the hurricane is likely due to sediment resuspension or soil runoff from heavy rainfall. A significant shift in the community was also observed in the estuary, from the salinity tolerant *Nitrosopumilus* spp. (NP γ 2.1) to salinity intolerant *Nitrosoarchaeum* spp. (NP γ 2.2) and *Ca. Nitrosotenuis cloacae* (NP η 1.1), likely reflecting population transfer via water discharges from the lake into the estuary.

In contrast, AOB communities after the hurricane exhibited no community composition changes. The majority of the sequences from both systems were unclassified *Nitrosomonas* and *Nitrosomonas oligotropha* (**Figures 5B**, **7**). A BLAST search of unclassified *Nitrosomonas* consensus sequences revealed that sequences from this study matched with those from other eutrophic systems, such as the Chang Jiang River basin (Jiang et al., 2017), Lake Taihu (Zeng et al., 2012; Zhao et al., 2013; Liu and Yang, 2019), San Francisco Bay (Damashek et al., 2015), an aquaculture system (Bartelme et al., 2017), and wastewater/sludge bioreactors (Wells et al., 2009; Wu et al., 2013; Zhang et al., 2018). Overall, a high abundance of *Nitrosomonas*-like AOB is expected due to NH_4^+-rich, eutrophic conditions (Stein et al., 2007; Prosser et al., 2014; Sedlacek et al., 2019) and have been found in many eutrophic natural environments (Zhang et al., 2014; Damashek et al., 2015) and N-rich engineered systems (Zhang et al., 2014; Bartelme et al., 2017). However, some *Nitrosomonas* species are adapted to lower NH_4^+ environments. Representative sequences from this study matched *Nitrosomonas sp.* Is79, an ammonia oxidizer found in low NH_4^+ freshwater environments (Bollmann et al., 2013). Additionally, sequences in this study classified as *Nitrosomonas oligotropha,* which is also adapted to lower trophic conditions (French et al., 2012). In the estuary, we observed an increase in *Nitrosomonas oligotropha* after the hurricane, possibly due to reduced salinity (Mosier and Francis, 2008), sediment resuspension, and lower nutrient concentrations (NH_4^+ and ortho-P; **Supplementary Table S2**).

The increased nitrifier abundance, shift in AOA community structure, and higher nitrification rates post-hurricane were likely caused by a combination of physicochemical factors, resuspension of benthic nitrifiers into the water column, and reduced competition with cyanobacteria. Environmental parameters explaining variance in nitrifier community structure were salinity, turbidity, and NH_4^+ and NO_3^- concentrations (**Supplementary Figure S2**). All of these factors were affected by the hurricane disturbance (**Supplementary Tables S1**, **S2**). The presence of primarily soil and sediment nitrifiers in water column samples likely contributed to increased nitrification rates, along with reduced competition with *Microcystis*. The shift (PERMANOVA; $p = 0.003$) in AOA community structure, but not AOB, might indicate that AOA have lower resistance to disturbance than AOB (Bowen et al., 2011; Shade et al., 2011, 2012), but a follow-up study would be required to assess resilience.

CONCLUSION

This study evaluated the effects of cyanoHABs and Hurricane Irma on water column nitrification rates and ammonia oxidizer community structure along a freshwater-estuarine continuum. We show that nitrification rates were lower during cyanoHABs, increasing by an order of magnitude when cyanoHABs were less abundant in the estuary the following year. We also show that several OTUs from Lake Okeechobee belong to the uncultured NS δ clade, which is versatile and appears to be ecologically important in eutrophic systems. Following Hurricane Irma, nitrification rates increased by an order of magnitude or more, coincident with increased turbidity and conductivity and decreased salinity and cyanoHABs. We also observed a substantial shift in AOA community structure immediately after the hurricane, suggesting weaker resistance to disturbance than AOB.

This study contributes to the growing literature showing high abundance of AOA in eutrophic waters relative to AOB and presents a strong relationship between AOA abundance and nitrification rates. Given their relatively recent discovery and large gaps in knowledge of AOA physiology, many open questions and suggestions for future research remain:

(1) AOA appear to be adapted to a wider range of trophic conditions than previously thought. The high abundance and diversity of AOA in eutrophic systems, and low number of cultured species (NS δ, NT β, NP δ), suggest that trophic adaptation and niche differentiation are likely, beyond the oceanic/terrestrial ecotype differentiation;
(2) AOB alpha diversity increased after the hurricane, while the AOA community shifted dominance. However, it is not certain which of these groups was responsible for the increase in nitrification rates in the estuary after the hurricane;
(3) Our results present short-term effects of hurricane and cyanoHAB disturbances on nitrification rates and ammonia oxidizer community structure. Studies focused on longer term effects should explore resilience of the ammonia oxidizer community and temporal scales of community recovery. The limited scope of the present study leaves open whether and/or how quickly the community might return to the pre-hurricane state, when turbidity is either flushed or settles to the sediment surface. Current climate change projections forecast amplification of hurricane events and increased eutrophication, and understanding the role of nitrification in converting chemically reduced N forms to oxidized N, and providing substrate for N removal via denitrification, may present valuable opportunities to constrain system N budgets.

DATA AVAILABILITY STATEMENT

The datasets presented in this study can be found in online repositories. The names of the repository/repositories and accession number(s) can be found in the article/ **Supplementary Material**.

AUTHOR CONTRIBUTIONS

JH, MM, and SN designed the study and collected samples. JH analyzed the samples. SA helped with sequence analysis. JH, SN, and MM interpreted results. All authors contributed to writing and revising the manuscript.

FUNDING

This work was funded by Florida Sea Grant (Project PD-16-10), the Wright State Women in Science Giving Circle, and the Eppley Foundation.

ACKNOWLEDGMENTS

We thank the South Florida Water Management District, especially Therese East, for providing lab space, boat access, and assistance with incubations. We thank Dr. Annette Bollmann for her insights to sequencing approach. We also thank Captain David Lauer for boat access on Lake Okeechobee after Hurricane Irma, Daniel Hoffman, Justin Myers, and Ashlynn Boedecker for help with sample analyses, and Megan Reed and Donnie Peterson for help with field sampling. We thank Richard Doucett and the UC Davis Stable Isotope Facility for processing nitrification samples. We thank the instructors and teaching assistants at STAMPS 2019 MBL workshop for providing valuable advice and tips regarding microbiome data analysis.

SUPPLEMENTARY MATERIAL

The Supplementary Material for this article can be found online at: https://www.frontiersin.org/articles/10.3389/fmicb.2020.01541/full#supplementary-material

REFERENCES

Aalto, S. L., Saarenheimo, J., Mikkonen, A., Rissanen, A. J., and Tiirola, M. (2018). Resistant ammonia-oxidizing archaea endure, but adapting ammonia-oxidizing bacteria thrive in boreal lake sediments receiving nutrient-rich effluents: AOA and AOB in wastewater-influenced sediments. *Environ. Microbiol.* 20, 3616–3628. doi: 10.1111/1462-2920.14354

Akaike, H. (1987). "Factor analysis and AIC," in *Selected Papers of Hirotugu Akaike*, eds E. Parzen, K. Tanabe, and G. Kitagawa (New York, NY: Springer), 371–386. doi: 10.1007/978-1-4612-1694-0_29

Alves, R. J. E., Minh, B. Q., Urich, T., von Haeseler, A., and Schleper, C. (2018). Unifying the global phylogeny and environmental distribution of ammonia-oxidising archaea based on *amoA* genes. *Nat. Commun.* 9:1517.

An, S., and Joye, S. B. (2001). Enhancement of coupled nitrification-denitrification by benthic photosynthesis in shallow estuarine sediments. *Limnol. Oceanogr.* 46, 62–74. doi: 10.4319/lo.2001.46.1.0062

Anderson, M. J. (2001). A new method for non-parametric multivariate analysis of variance. *Aust. Ecol.* 26, 32–46. doi: 10.1111/j.1442-9993.2001.01070.pp.x

Baldia, S. F., Evangelista, A. D., Aralar, E. V., and Santiago, A. E. (2007). Nitrogen and phosphorus utilization in the cyanobacterium *Microcystis aeruginosa* isolated from Laguna de Bay, Philippines. *J. Appl. Phycol.* 19, 607–613. doi: 10.1007/s10811-007-9209-0

Bartelme, R. P., McLellan, S. L., and Newton, R. J. (2017). Freshwater recirculating aquaculture system operations drive biofilter bacterial community shifts around a stable nitrifying consortium of ammonia-oxidizing *Archaea* and comammox *Nitrospira*. *Front. Microbiol.* 8:101. doi: 10.3389/fmicb.2017.00101

Beman, J. M., and Francis, C. A. (2006). Diversity of ammonia-oxidizing archaea and bacteria in the sediments of a hypernutrified subtropical estuary: Bahia del Tobari, Mexico. *Appl. Environ. Microbiol.* 72, 7767–7777. doi: 10.1128/aem.00946-06

Beman, J. M., Popp, B. N., and Francis, C. A. (2008). Molecular and biogeochemical evidence for ammonia oxidation by marine Crenarchaeota in the Gulf of California. *ISME J.* 2, 429–441. doi: 10.1038/ismej.2007.118

Beman, M., Popp, B. N., and Alford, S. E. (2012). Quantification of ammonia oxidation rates and ammonia-oxidizing archaea and bacteria at high resolution in the Gulf of California and eastern tropical North Pacific Ocean. *Limnol. Oceanogr.* 57, 711–726. doi: 10.4319/lo.2012.57.3.0711

Bernhard, A. E., Chelsky, A., Giblin, A. E., and Roberts, B. J. (2019). Influence of local and regional drivers on spatial and temporal variation of ammonia-oxidizing communities in Gulf of Mexico salt marshes. *Environ. Microbiol. Rep.* 11, 825–834.

Bernhard, A. E., Dwyer, C., Idrizi, A., Bender, G., and Zwick, R. (2015). Long-term impacts of disturbance on nitrogen-cycling bacteria in a New England salt marsh. *Front. Microbiol.* 6:46. doi: 10.3389/fmicb.2015.00046

Bernhard, A. E., Landry, Z. C., Blevins, A., de la Torre, J. R., Giblin, A. E., and Stahl, D. A. (2010). Abundance of ammonia-oxidizing archaea and bacteria along an estuarine salinity gradient in relation to potential nitrification rates. *Appl. Environ. Microbiol.* 76, 1285–1289. doi: 10.1128/AEM.02018-09

Blomqvist, P., Petterson, A., and Hyenstrand, P. (1994). Ammonium-nitrogen: a key regulatory factor causing dominance of non-nitrogen-fixing cyanobacteria in aquatic systems. *Arch. Hydrobiol.* 132, 141–164.

Bollmann, A., Bullerjahn, G. S., and McKay, R. M. (2014). Abundance and diversity of ammonia-oxidizing archaea and bacteria in sediments of trophic end members of the Laurentian Great Lakes, Erie and superior. *PLoS One* 9:97068. doi: 10.1371/journal.pone.0097068

Bollmann, A., Sedlacek, C., Norton, J., Norton, J. M., Laanbroek, H. J., Suwa, Y., et al. (2013). Complete genome sequence of *Nitrosomonas* sp. Is79, an ammonia oxidizing bacterium adapted to low ammonium concentrations. *Stand. Genomic Sci.* 7, 469–482.

Bouskill, N. J., Eveillard, D., Chien, D., Jayakumar, A., and Ward, B. B. (2012). Environmental factors determining ammonia-oxidizing organism distribution and diversity in marine environments: ammonia-oxidizers across aquatic environmental gradients. *Environ. Microbiol.* 14, 714–729. doi: 10.1111/j.1462-2920.2011.02623.x

Bouskill, N. J., Eveillard, D., O'Mullan, G., Jackson, G. A., and Ward, B. B. (2011). Seasonal and annual reoccurrence in betaproteobacterial ammonia-oxidizing bacterial population structure. *Environ. Microbiol.* 13, 872–886. doi: 10.1111/j.1462-2920.2010.02362.x

Bowen, J. L., Ward, B. B., Morrison, H. G., Hobbie, J. E., Valiela, I., Deegan, L. A., et al. (2011). Microbial community composition in sediments resists perturbation by nutrient enrichment. *ISME J.* 5, 1540–1548. doi: 10.1038/ismej.2011.22

Bristow, L. A., Dalsgaard, T., Tiano, L., Mills, D. B., Bertagnolli, A. D., Wright, J. J., et al. (2016). Ammonium and nitrite oxidation at nanomolar oxygen concentrations in oxygen minimum zone waters. *Proc. Natl. Acad. Sci. U.S.A.* 113, 10601–10606. doi: 10.1073/pnas.1600359113

Bristow, L. A., Sarode, N., Cartee, J., Caro-Quintero, A., Thamdrup, B., and Stewart, F. J. (2015). Biogeochemical and metagenomic analysis of nitrite accumulation in the Gulf of Mexico hypoxic zone: nitrite accumulation in hypoxic zones. *Limnol. Oceanogr.* 60, 1733–1750. doi: 10.1002/lno.10130

Bronk, D. A., Killberg-Thoreson, L., Sipler, R. E., Mulholland, M. R., Roberts, Q. N., Bernhardt, P. W., et al. (2014). Nitrogen uptake and regeneration (ammonium regeneration, nitrification and photoproduction) in waters of the West Florida Shelf prone to blooms of *Karenia brevis*. *Harmful Algae* 38, 50–62. doi: 10.1016/j.hal.2014.04.007

Caffrey, J. M., Bano, N., Kalanetra, K., and Hollibaugh, J. T. (2007). Ammonia oxidation and ammonia-oxidizing bacteria and archaea from estuaries with differing histories of hypoxia. *ISME J.* 1, 660–662. doi: 10.1038/ismej.2007.79

Carini, S. A., McCarthy, M. J., and Gardner, W. S. (2010). An isotope dilution method to measure nitrification rates in the northern Gulf of Mexico and other eutrophic waters. *Cont. Shelf Res.* 30, 1795–1801. doi: 10.1016/j.csr.2010.08.001

Cheung, S., Mak, W., Xia, X., Lu, Y., Cheung, Y., and Liu, H. (2019). Overlooked genetic diversity of ammonia oxidizing archaea lineages in the global oceans. *J. Geophys. Res. Biogeosci.* 124, 1799–1811.

Dai, M., Wang, L., Guo, X., Zhai, W., Li, Q., and He, B. (2008). Nitrification and inorganic nitrogen distribution in a large perturbed river/estuarine system: the

Pearl River Estuary, China. *Biogeosciences* 5, 1227–1244. doi: 10.5194/bg-5-1227-2008

Damashek, J., Casciotti, K. L., and Francis, C. A. (2016). Variable nitrification rates across environmental gradients in turbid, nutrient-rich estuary waters of San Francisco bay. *Estuar. Coast.* 39, 1050–1071. doi: 10.1007/s12237-016-0071-7

Damashek, J., and Francis, C. A. (2018). Microbial nitrogen cycling in estuaries: from genes to ecosystem processes. *Estuar. Coast.* 41, 626–660. doi: 10.1007/s12237-017-0306-2

Damashek, J., Smith, J. M., Mosier, A. C., and Francis, C. A. (2015). Benthic ammonia oxidizers differ in community structure and biogeochemical potential across a riverine delta. *Front. Microbiol.* 5:743. doi: 10.3389/fmicb.2014.00743

Edgar, R. C., Haas, B. J., Clemente, J. C., Quince, C., and Knight, R. (2011). UCHIME improves sensitivity and speed of chimera detection. *Bioinformatics* 27, 2194–2200. doi: 10.1093/bioinformatics/btr381

Francis, C. A., Roberts, K. J., Beman, J. M., Santoro, A. E., and Oakley, B. B. (2005). Ubiquity and diversity of ammonia-oxidizing archaea in water columns and sediments of the ocean. *Proc. Natl. Acad. Sci. U.S.A.* 102, 14683–14688. doi: 10.1073/pnas.0506625102

Frank, I. E., Turk-Kubo, K. A., and Zehr, J. P. (2016). Rapid annotation of nifH gene sequences using classification and regression trees facilitates environmental functional gene analysis. *Environ. Microbiol. Rep.* 8, 905–916. doi: 10.1111/1758-2229.12455

French, E., Kozlowski, J. A., Mukherjee, M., Bullerjahn, G., and Bollmann, A. (2012). Ecophysiological characterization of ammonia-oxidizing archaea and bacteria from freshwater. *Appl. Environ. Microbiol.* 78, 5773–5780. doi: 10.1128/aem.00432-12

Hall, G. H. (1986). "Nitrification in lakes," in *Nitrification*, 1st Edn, ed. J. I. Prosser (Washington, DC: IRL Press), 127–156.

Hampel, J. J., McCarthy, M. J., Gardner, W. S., Zhang, L., Xu, H., Zhu, G., et al. (2018). Nitrification and ammonium dynamics in Taihu Lake, China: seasonal competition for ammonium between nitrifiers and Cyanobacteria. *Biogeosciences* 15, 733–748. doi: 10.5194/bg-15-733-2018

Hampel, J. J., McCarthy, M. J., Reed, M. H., and Newell, S. E. (2019). Short term effects of Hurricane Irma and cyanobacterial blooms on ammonium cycling along a freshwater–estuarine continuum in south Florida. *Front. Mar. Sci.* 6:640. doi: 10.3389/fmars.2019.00640

Happel, E., Bartl, I., Voss, M., and Riemann, L. (2018). Extensive nitrification and active ammonia oxidizers in two contrasting coastal systems of the Baltic Sea. *Environ. Microbiol.* 20, 2913–2926. doi: 10.1111/1462-2920.14293

Havens, K. E., Jin, K.-R., Rodusky, A. J., Sharfstein, B., Brady, M. A., East, T. L., et al. (2001). Hurricane effects on a shallow lake ecosystem and its response to a controlled manipulation of water level. *Sci. World J.* 1, 44–70. doi: 10.1100/tsw.2001.14

Hayden, C. J., and Beman, J. M. (2014). High abundances of potentially active ammonia-oxidizing bacteria and archaea in oligotrophic, high-altitude lakes of the Sierra Nevada, California, USA. *PLoS One* 9:e111560. doi: 10.1371/journal.pone.0111560

Heiss, E. M., and Fulweiler, R. W. (2016). Coastal water column ammonium and nitrite oxidation are decoupled in summer. *Estuar. Coast. Shelf Sci.* 178, 110–119. doi: 10.1016/j.ecss.2016.06.002

Herbold, C. W., Pelikan, C., Kuzyk, O., Hausmann, B., Angel, R., Berry, D., et al. (2015). A flexible and economical barcoding approach for highly multiplexed amplicon sequencing of diverse target genes. *Front. Microbiol.* 6:731. doi: 10.3389/fmicb.2015.00731

Hink, L., Gubry-Rangin, C., Nicol, G. W., and Prosser, J. I. (2018). The consequences of niche and physiological differentiation of archaeal and bacterial ammonia oxidisers for nitrous oxide emissions. *ISME J.* 12, 1084–1093. doi: 10.1038/s41396-017-0025-5

Horak, R. E., Qin, W., Schauer, A. J., Armbrust, E. V., Ingalls, A. E., Moffett, J. W., et al. (2013). Ammonia oxidation kinetics and temperature sensitivity of a natural marine community dominated by Archaea. *ISME J.* 7, 2023–2033.

Hou, J., Song, C., Cao, X., and Zhou, Y. (2013). Shifts between ammonia-oxidizing bacteria and archaea in relation to nitrification potential across trophic gradients in two large Chinese lakes (Lake Taihu and Lake Chaohu). *Water Res.* 47, 2285–2296. doi: 10.1016/j.watres.2013.01.042

Hsiao, S. S. Y., Hsu, T. C., Liu, J. W., Xie, X., Zhang, Y., Lin, J., et al. (2014). Nitrification and its oxygen consumption along the turbid Chang Jiang River plume. *Biogeosciences* 11, 2083–2098. doi: 10.5194/bg-11-2083-2014

Hugoni, M., Etien, S., Bourges, A., Lepère, C., Domaizon, I., Mallet, C., et al. (2013). Dynamics of ammonia-oxidizing Archaea and Bacteria in contrasted freshwater ecosystems. *Res. Microbiol.* 164, 360–370. doi: 10.1016/j.resmic.2013.01.004

James, R. T., Havens, K., Zhu, G., and Qin, B. (2009). Comparative analysis of nutrients, chlorophyll and transparency in two large shallow lakes (Lake Taihu, P.R. China and Lake Okeechobee, USA). *Hydrobiologia* 627, 211–231. doi: 10.1007/s10750-009-9729-5

James, T. R., Chimney, M. J., Sharfstein, B., Engstrom, D. R., Schottler, S. P., East, T., et al. (2008). Hurricane effects on a shallow lake ecosystem, Lake Okeechobee, Florida (USA). *Fundam. Appl. Limnol.* 172, 273–287. doi: 10.1127/1863-9135/2008/0172-0273

Jia, Z., and Conrad, R. (2009). Bacteria rather than Archaea dominate microbial ammonia oxidation in an agricultural soil. *Environ. Microbiol.* 11, 1658–1671. doi: 10.1111/j.1462-2920.2009.01891

Jiang, X., Wu, Y., Liu, G., Liu, W., and Lu, B. (2017). The effects of climate, catchment land use and local factors on the abundance and community structure of sediment ammonia-oxidizing microorganisms in Yangtze lakes. *AMB Express* 7:173.

Jochem, F. J., Lavrentyev, P. J., and First, M. R. (2004). Growth and grazing rates of bacteria groups with different apparent DNA content in the Gulf of Mexico. *Mar. Biol.* 145, 1213–1225. doi: 10.1007/s00227-004-1406-7

Kan, J. (2018). Storm events restructured bacterial community and their biogeochemical potentials. *J. Geophys. Res. Biogeosci.* 123, 2257–2267.

Kits, K. D., Sedlacek, C. J., Lebedeva, E. V., Han, P., Bulaev, A., Pjevac, P., et al. (2017). Kinetic analysis of a complete nitrifier reveals an oligotrophic lifestyle. *Nature* 549, 269–272. doi: 10.1038/nature23679

Könneke, M., Bernhard, A. E., José, R., Walker, C. B., Waterbury, J. B., and Stahl, D. A. (2005). Isolation of an autotrophic ammonia-oxidizing marine archaeon. *Nature* 437, 543–546. doi: 10.1038/nature03911

Kramer, B. J., Davis, T. W., Meyer, K. A., Rosen, B. H., Goleski, J. A., Dick, G. J., et al. (2018). Nitrogen limitation, toxin synthesis potential, and toxicity of cyanobacterial populations in Lake Okeechobee and the St. Lucie River Estuary, Florida, during the 2016 state of emergency event. *PLoS One* 13:e0196278. doi: 10.1371/journal.pone.0196278

Kumar, S., Stecher, G., Li, M., Knyaz, C., and Tamura, K. (2018). MEGA X: molecular evolutionary genetics analysis across computing platforms. *Mol. Biol. Evol.* 35, 1547–1549. doi: 10.1093/molbev/msy096

Laperriere, S. M., Nidzieko, N. J., Fox, R. J., Fisher, A. W., and Santoro, A. E. (2018). Observations of variable ammonia oxidation and nitrous oxide flux in a eutrophic estuary. *Estuar. Coast.* 42, 33–44. doi: 10.1007/s12237-018-0441-4

Lapointe, B. E., Herren, L. W., and Bedford, B. J. (2012). Effects of hurricanes, land use, and water management on nutrient and microbial pollution: St. Lucie estuary, Southeast Florida. *J. Coast. Res.* 285, 1345–1361. doi: 10.2112/jcoastres-d-12-00070.1

Lavrentyev, P. J., Gardner, W. S., and Johnson, J. R. (1997). Cascading trophic effects on aquatic nitrification: experimental evidence and potential implications. *Aquat. Microb. Ecol.* 13, 161–175. doi: 10.3354/ame013161

Letunic, I., and Bork, P. (2019). Interactive tree of life (iTOL) v4: recent updates and new developments. *Nucleic Acids Res.* 47, W256–W259.

Li, H., Weng, B. S., Huang, F. Y., Su, J. Q., and Yang, X. R. (2015). pH regulates ammonia-oxidizing bacteria and archaea in paddy soils in Southern China. *Appl. Microbiol. Biotechnol.* 99, 6113–6123. doi: 10.1007/s00253-015-6488-2

Li, M., Wei, G., Shi, W., Sun, Z., Li, H., Wang, X., et al. (2018). Distinct distribution patterns of ammonia-oxidizing archaea and bacteria in sediment and water column of the Yellow River estuary. *Sci. Rep.* 8:1584. doi: 10.1038/s41598-018-20044-6

Li, Y., Ding, K., Wen, X., Zhang, B., Shen, B., and Yang, Y. (2016). A novel ammonia-oxidizing archaeon from wastewater treatment plant: its enrichment, physiological and genomic characteristics. *Sci. Rep.* 6:23747.

Lipschultz, F., Wofsy, S. C., Ward, B. B., Codispoti, L. A., Friedrich, G., and Elkins, J. W. (1990). Bacterial transformations of inorganic nitrogen in the oxygen-deficient waters of the Eastern Tropical South Pacific Ocean. *Deep Sea Res. A Oceanogr. Res. Pap.* 37, 1513–1541. doi: 10.1016/0198-0149(90)90060-9

Liu, T. T., and Yang, H. (2019). An RNA-based quantitative and compositional study of ammonium-oxidizing bacteria and archaea in Lake Taihu, a eutrophic freshwater lake. *FEMS Microbiol. Ecol.* 95:fiz117.

Martens-Habbena, W., Berube, P. M., Urakawa, H., de la Torre, J. R., and Stahl, D. A. (2009). Ammonia oxidation kinetics determine niche separation of nitrifying Archaea and Bacteria. *Nature* 461, 976–979. doi: 10.1038/nature08465

Marton, J. M., Roberts, B. J., Bernhard, A. E., and Giblin, A. E. (2015). Spatial and temporal variability of nitrification potential and ammonia-oxidizer abundances in Louisiana salt marshes. *Estuar. Coast.* 38, 1824–1837. doi: 10.1007/s12237-015-9943-5

McIlvin, M. R., and Altabet, M. A. (2005). Chemical conversion of nitrate and nitrite to nitrous oxide for nitrogen and oxygen isotopic analysis in freshwater and seawater. *Anal. Chem.* 77, 5589–5595. doi: 10.1021/ac050528s

McMurdie, P. J., and Holmes, S. (2013). phyloseq: an R package for reproducible interactive analysis and graphics of microbiome census data. *PLoS One* 8:e61217. doi: 10.1371/journal.pone.0061217

McMurdie, P. J., and Holmes, S. (2014). Waste not, want not: why rarefying microbiome data is inadmissible. *PLoS Comput. Biol.* 10:e1003531. doi: 10.1371/journal.pcbi.1003531

Merbt, S. N., Auguet, J. C., Blesa, A., Martí, E., and Casamayor, E. O. (2015). Wastewater treatment plant effluents change abundance and composition of ammonia-oxidizing microorganisms in Mediterranean urban stream biofilms. *Microb. Ecol.* 69, 66–74. doi: 10.1007/s00248-014-0464-8

Mosier, A. C., and Francis, C. A. (2008). Relative abundance and diversity of ammonia-oxidizing archaea and bacteria in the San Francisco Bay estuary. *Environ. Microbiol.* 10, 3002–3016. doi: 10.1111/j.1462-2920.2008.01764.x

Newell, S. E., Babbin, A. R., Jayakumar, A., and Ward, B. B. (2011). Ammonia oxidation rates and nitrification in the Arabian Sea: Arabian Sea ammonia oxidation and nitrification. *Glob. Biogeochem. Cycles* 25:GB4016. doi: 10.1029/2010GB003940

Newell, S. E., Eveillard, D., McCarthy, M. J., Gardner, W. S., Liu, Z., and Ward, B. B. (2014). A shift in the archaeal nitrifier community in response to natural and anthropogenic disturbances in the northern Gulf of Mexico. *Environ. Microbiol. Rep.* 6, 106–112. doi: 10.1111/1758-2229.12114

Newell, S. E., Fawcett, S. E., and Ward, B. B. (2013). Depth distribution of ammonia oxidation rates and ammonia-oxidizer community composition in the Sargasso Sea. *Limnol. Oceanogr.* 58, 1491–1500. doi: 10.4319/lo.2013.58.4.149

Nicklisch, A., and Kohl, J. G. (1983). Growth kinetics of *Microcystis aeruginosa* (Kütz) Kütz as a basis for modelling its population dynamics. *Int. Rev. Gesamten Hydrobiol. Hydrogr.* 68, 317–326. doi: 10.1002/iroh.19830680304

Oksanen, J., Blanchet, F. G., Friendly, M., Kindt, R., Legendre, P., McGlinn, D., et al. (2018). *R Package 'Vegan'* (Vienna). (accessed October, 2019). doi: 10.1002/iroh.19830680304

Paerl, H. W., Bales, J. D., Ausley, L. W., Buzzelli, C. P., Crowder, L. B., Eby, L. A., et al. (2001). Ecosystem impacts of three sequential hurricanes (Dennis, Floyd, and Irene) on the United States' largest Lagoonal estuary, Pamlico Sound, NC. *Proc. Natl. Acad. Sci. U.S.A.* 98, 5655–5660. doi: 10.1073/pnas.101097398

Paerl, H. W., Havens, K. E., Hall, N. S., Otten, T. G., Zhu, M., Xu, H., et al. (2019). Mitigating a global expansion of toxic cyanobacterial blooms: confounding effects and challenges posed by climate change. *Mar. Freshw. Res.* 71, 579–592. doi: 10.1071/mf18392

Percuoco, V. P., Kalnejais, L. H., and Officer, L. V. (2015). Nutrient release from the sediments of the Great Bay Estuary, NH USA. *Estuar. Coast. Shelf Sci.* 161, 76–87. doi: 10.1016/j.ecss.2015.04.006

Phlips, E. J., Badylak, S., Hart, J., Haunert, D., Lockwood, J., O'Donnell, K., et al. (2012). Climatic influences on autochthonous and allochthonous phytoplankton blooms in a subtropical estuary, St. Lucie Estuary, Florida, USA. *Estuar. Coast.* 35, 335–352. doi: 10.1007/s12237-011-9442-2

Prosser, J. I., Head, I. M., and Stein, L. Y. (2014). "The family *Nitrosomonadaceae*," in *The Prokaryotes: Alphaproteobacteria and Betaproteobacteria*, eds E. Rosenberg, E. F. DeLong, S. Lory, E. Stackebrandt, and F. Thompson (Berlin: Springer), 901–918. doi: 10.1007/978-3-642-30197-1_372

Prosser, J. I., and Nicol, G. W. (2012). Archaeal and bacterial ammonia-oxidisers in soil: the quest for niche specialisation and differentiation. *Trends Microbiol.* 20, 523–531. doi: 10.1016/j.tim.2012.08.001

Rotthauwe, J.-H., Witzel, K.-P., and Liesack, W. (1997). The ammonia monooxygenase structural gene amoA as a functional marker: molecular fine-scale analysis of natural ammonia-oxidizing populations. *Appl. Environ. Microbiol.* 63, 4704–4712. doi: 10.1128/aem.63.12.4704-4712.1997

Sanders, T., Schöl, A., and Dähnke, K. (2018). Hot spots of nitrification in the Elbe estuary and their impact on nitrate regeneration. *Estuar. Coast.* 41, 128–138. doi: 10.1007/s12237-017-0264-8

Santoro, A. E., Casciotti, K. L., and Francis, C. A. (2010). Activity, abundance and diversity of nitrifying archaea and bacteria in the central California Current. *Environ. Microbiol.* 12, 1989–2006. doi: 10.1111/j.1462-2920.2010.02205.x

Santoro, A. E., Francis, C. A., de Sieyes, N. R., and Boehm, A. B. (2008). Shifts in the relative abundance of ammonia-oxidizing bacteria and archaea across physicochemical gradients in a subterranean estuary. *Environ. Microbiol.* 10, 1068–1079. doi: 10.1111/j.1462-2920.2007.01547.x

Santoro, A. E., Saito, M. A., Goepfert, T. J., Lamborg, C. H., Dupont, C. L., and DiTullio, G. R. (2017). Thaumarchaeal ecotype distributions across the equatorial Pacific Ocean and their potential roles in nitrification and sinking flux attenuation. *Limnol. Oceanogr.* 62, 1984–2003. doi: 10.1002/lno.10547

Schloss, P. D., Westcott, S. L., Ryabin, T., Hall, J. R., Hartmann, M., Hollister, E. B., et al. (2009). Introducing mothur: open-source, platform-independent, community-supported software for describing and comparing microbial communities. *Appl. Environ. Microbiol.* 75, 7537–7541. doi: 10.1128/aem.01541-09

Sedlacek, C. J., McGowan, B., Suwa, Y., Sayavedra-Soto, L., Laanbroek, H. J., Stein, L. Y., et al. (2019). A physiological and genomic comparison of *Nitrosomonas* cluster 6a and 7 ammonia-oxidizing bacteria. *Microb. Ecol.* 78, 985–994. doi: 10.1007/s00248-019-01378-8

Shade, A., Peter, H., Allison, S. D., Baho, D., Berga, M., Bürgmann, H., et al. (2012). Fundamentals of microbial community resistance and resilience. *Front. Microbiol.* 3:417. doi: 10.3389/fmicb.2012.00417

Shade, A., Read, J. S., Welkie, D. G., Kratz, T. K., Wu, C. H., and McMahon, K. D. (2011). Resistance, resilience and recovery: aquatic bacterial dynamics after water column disturbance. *Environ. Microbiol.* 13, 2752–2767. doi: 10.1111/j.1462-2920.2011.02546.x

Sintes, E., Bergauer, K., De Corte, D., Yokokawa, T., and Herndl, G. J. (2013). Archaeal amoA gene diversity points to distinct biogeography of ammonia-oxidizing *Crenarchaeota* in the ocean. *Environ. Microbiol.* 15, 1647–1658. doi: 10.1111/j.1462-2920.2012.02801.x

Small, G. E., Bullerjahn, G. S., Sterner, R. W., Beall, B. F. N., Brovold, S., Finlay, J. C., et al. (2013). Rates and controls of nitrification in a large oligotrophic lake. *Limnol. Oceanogr.* 58, 276–286. doi: 10.4319/lo.2013.58.1.0276

Stein, L. Y., Arp, D. J., Berube, P. M., Chain, P. S., Hauser, L., Jetten, M. S., et al. (2007). Whole-genome analysis of the ammonia-oxidizing bacterium, *Nitrosomonas eutropha* C91: implications for niche adaptation. *Environ. Microbiol.* 9, 2993–3007. doi: 10.1111/j.1462-2920.2007.01409.x

Tolar, B. B., Wallsgrove, N. J., Popp, B. N., and Hollibaugh, J. T. (2017). Oxidation of urea-derived nitrogen by Thaumarchaeota-dominated marine nitrifying communities: oxidation of urea-derived nitrogen in the sea. *Environ. Microbiol.* 19, 4838–4850. doi: 10.1111/1462-2920.13457

Urakawa, H., Martens-Habbena, W., Huguet, C., de la Torre, J. R., Ingalls, A. E., Devol, A. H., et al. (2014). Ammonia availability shapes the seasonal distribution and activity of archaeal and bacterial ammonia oxidizers in the Puget Sound Estuary. *Limnol. Oceanogr.* 59, 1321–1335. doi: 10.4319/lo.2014.59.4.1321

Verhamme, D. T., Prosser, J. I., and Nicol, G. W. (2011). Ammonia concentration determines differential growth of ammonia-oxidising archaea and bacteria in soil microcosms. *ISME J.* 5, 1067–1071. doi: 10.1038/ismej.2010.191

Vissers, E. W., Anselmetti, F. S., Bodelier, P. L., Muyzer, G., Schleper, C., Tourna, M., et al. (2013). Temporal and spatial coexistence of archaeal and bacterial *amoA* genes and gene transcripts in Lake Lucerne. *Archaea* 2013:289478.

Wang, Q., Quensen, J. F., Fish, J. A., Lee, T. K., Sun, Y., Tiedje, J. M., et al. (2013). Ecological patterns of nifH genes in four terrestrial climatic zones explored with targeted metagenomics using FrameBot, a new informatics tool. *mBio* 4:e00592-13.

Ward, B. B. (2008). "Nitrification in marine systems," in *Nitrogen in the Marine Environment*, 2nd Edn, D. Capone, D. Bronk, M. Mulholland, and E. Carpenter (Amsterdam: Elsevier).

Wells, G. F., Park, H. D., Yeung, C. H., Eggleston, B., Francis, C. A., and Criddle, C. S. (2009). Ammonia-oxidizing communities in a highly aerated full-scale activated sludge bioreactor: betaproteobacterial dynamics and low relative

abundance of Crenarchaea. *Environ. Microbiol.* 11, 2310–2328. doi: 10.1111/j.1462-2920.2009.01958.x

Wengrove, M. E., Foster, D. L., Kalnejais, L. H., Percuoco, V., and Lippmann, T. C. (2015). Field and laboratory observations of bed stress and associated nutrient release in a tidal estuary. *Estuar. Coast. Shelf Sci.* 161, 11–24. doi: 10.1016/j.ecss.2015.04.005

Wickham, H. (2016). *ggplot2: Elegant Graphics for Data Analysis*. New York, NY: Springer-Verlag.

Wu, Y. J., Whang, L. M., Fukushima, T., and Chang, S. H. (2013). Responses of ammonia-oxidizing archaeal and betaproteobacterial populations to wastewater salinity in a full-scale municipal wastewater treatment plant. *J. Biosci. Bioeng.* 115, 424–432. doi: 10.1016/j.jbiosc.2012.11.005

Xia, H., Wu, Y., Chen, X., Huang, K., and Chen, J. (2019). Effects of antibiotic residuals in dewatered sludge on the behavior of ammonia oxidizers during vermicomposting maturation process. *Chemosphere* 218, 810–817. doi: 10.1016/j.chemosphere.2018.11.167

Yao, L., Chen, C., Liu, G., and Liu, W. (2018). Sediment nitrogen cycling rates and microbial abundance along a submerged vegetation gradient in a eutrophic lake. *Sci. Total Environ.* 616, 899–907. doi: 10.1016/j.scitotenv.2017.10.230

Zeng, J., Zhao, D.-Y., Huang, R., and Wu, Q. L. (2012). Abundance and community composition of ammonia-oxidizing archaea and bacteria in two different zones of Lake Taihu. *Can. J. Microbiol.* 58, 1018–1026. doi: 10.1139/w2012-078

Zhang, X., Zheng, S., Zhang, H., and Duan, S. (2018). Autotrophic and heterotrophic nitrification-anoxic denitrification dominated the anoxic/oxic sewage treatment process during optimization for higher loading rate and energy savings. *Bioresour. Technol.* 263, 84–93. doi: 10.1016/j.biortech.2018.04.113

Zhang, Y., Xie, X., Jiao, N., Hsiao, S. Y., and Kao, S. J. (2014). Diversity and distribution of amoA-type nitrifying and nirS-type denitrifying microbial communities in the Yangtze River estuary. *Biogeosciences* 11, 2131–2145. doi: 10.5194/bg-11-2131-2014

Zhao, D., Zeng, J., Wan, W., Liang, H., Huang, R., and Wu, Q. L. (2013). Vertical distribution of ammonia-oxidizing archaea and bacteria in sediments of a eutrophic lake. *Curr. Microbiol.* 67, 327–332. doi: 10.1007/s00284-013-0369-7

Zhao, R., Dahle, H., Ramírez, G. A., and Jørgensen, S. L. (2020). Indigenous ammonia-oxidizing archaea in oxic subseafloor oceanic crust. *Msystems* 5:e00758-19.

Zhong, W., Bian, B., Gao, N., Min, J., Shi, W., Lin, X., et al. (2016). Nitrogen fertilization induced changes in ammonia oxidation are attributable mostly to bacteria rather than archaea in greenhouse-based high N input vegetable soil. *Soil Biol. Biochem.* 93, 150–159. doi: 10.1016/j.soilbio.2015.11.003

Zou, D., Li, Y., Kao, S. J., Liu, H., and Li, M. (2019). Genomic adaptation to eutrophication of ammonia-oxidizing archaea in the Pearl River estuary. *Environ. Microbiol.* 21, 2320–2332. doi: 10.1111/1462-2920.14613

Conflict of Interest: The authors declare that the research was conducted in the absence of any commercial or financial relationships that could be construed as a potential conflict of interest.

frontiers in Microbiology

ORIGINAL RESEARCH
published: 10 July 2020
doi: 10.3389/fmicb.2020.01522

Defining Culture Conditions for the Hidden Nitrite-Oxidizing Bacterium *Nitrolancea*

Eva Spieck[1], Katharina Sass[1], Sabine Keuter[1], Sophia Hirschmann[1], Michael Spohn[2], Daniela Indenbirken[2], Linnea F. M. Kop[3], Sebastian Lücker[3] and Alejandra Giaveno[4]*

[1] Department of Microbiology and Biotechnology, Universität Hamburg, Hamburg, Germany, [2] Technology Platform Next Generation Sequencing, Heinrich Pette Institut, Hamburg, Germany, [3] Department of Microbiology, IWWR, Radboud University, Nijmegen, Netherlands, [4] PROBIEN (CONICET-UNCo), Departamento de Química, Facultad de Ingeniería, Universidad Nacional del Comahue, Neuquén, Argentina

Nitrification is a key process for N-removal in engineered and natural environments, but recent findings of novel nitrifying microorganisms with surprising features revealed that our knowledge of this functional guild is still incomplete. Especially nitrite oxidation – the second step of nitrification – is catalyzed by a phylogenetically diverse bacterial group, and only recently bacteria of the phylum *Chloroflexi* have been identified as thermophilic nitrite-oxidizing bacteria (NOB). Among these, *Nitrolancea hollandica* was isolated from a laboratory-scale nitrifying bioreactor operated at 35°C with a high load of ammonium bicarbonate. However, its distribution remains cryptic as very few closely related environmental 16S rRNA gene sequences have been retrieved so far. In this study, we demonstrate how such thermophilic NOB can be enriched using modified mineral media inoculated with samples from a wastewater side-stream reactor operated at 39.5°C. Distinct cultivation conditions resulted in quick and reproducible high enrichment of two different strains of *Nitrolancea*, closely related to *Nl. hollandica*. The same cultivation approach was applied to a complex nitrite-oxidizing pre-enrichment at 42°C inoculated with biomass from a geothermal spring in the Copahue volcano area in Neuquen, Argentina. Here, an additional distinct representative of the genus *Nitrolancea* was obtained. This novel species had 16S rRNA and nitrite oxidoreductase alpha subunit (*nxrA*) gene sequence identities to *Nl. hollandica* of 98.5% and 97.2%, respectively. A genomic average nucleotide identity between the Argentinian strain and *Nl. hollandica* of 91.9% indicates that it indeed represents a distinct species. All *Nitrolancea* cultures formed lancet-shaped cells identical to *Nl. hollandica* and revealed similar physiological features, including the capability to grow at high nitrite concentrations. Growth was optimal at temperatures of 35–37°C and was strongly enhanced by ammonium supplementation. Genomic comparisons revealed that the four *Nitrolancea* strains share 2399 out of 3387 orthologous gene clusters and encode similar key functions. Our results define general growth conditions that enable the selective enrichment of *Nitrolancea* from artificial and natural environments. In most natural habitats these NOB apparently are of low abundance and their proliferation depends on the balanced presence of nitrite and ammonium, with an optimal incubation temperature of 37°C.

Keywords: nitrification, nitrite oxidation, *Nitrolancea*, cultivation, wastewater treatment plant, geothermal springs

OPEN ACCESS

Edited by:
Thomas E. Hanson, University of Delaware, United States

Reviewed by:
Lisa Y. Stein, University of Alberta, Canada
Petra Pjevac, University of Vienna, Austria

****Correspondence:***
Eva Spieck
eva.spieck@uni-hamburg.de

Specialty section:
This article was submitted to Microbial Physiology and Metabolism, a section of the journal Frontiers in Microbiology

Received: *22 April 2020*
Accepted: *12 June 2020*
Published: *10 July 2020*

Citation:
Spieck E, Sass K, Keuter S, Hirschmann S, Spohn M, Indenbirken D, Kop LFM, Lücker S and Giaveno A (2020) Defining Culture Conditions for the Hidden Nitrite-Oxidizing Bacterium Nitrolancea. Front. Microbiol. 11:1522. doi: 10.3389/fmicb.2020.01522

INTRODUCTION

As important part of the global nitrogen cycle, nitrification converts reduced nitrogen species into oxidized forms, namely ammonium (−III) to nitrite (+III) and further to nitrate (+V). In wastewater treatment plants, nitrification is essential to remove N-compounds like ammonium and nitrite, and to provide nitrate as electron acceptor for denitrification. In agricultural, but also natural systems, nitrification causes nitrogen loss due to leaching of negatively charged nitrate ions and emission of gaseous N-compounds produced by denitrifying bacteria.

Both steps of nitrification are performed by distinct groups of bacteria or archaea (Koops and Pommerening-Röser, 2005; Spieck and Bock, 2005; Stieglmeier et al., 2014), but the traditional differentiation into ammonia and nitrite oxidizers has been overturned with the discovery of comammox *Nitrospira*, which can perform the complete oxidation of ammonia to nitrate (Daims et al., 2015; van Kessel et al., 2015).

Nitrite-oxidizing bacteria (NOB) from six genera belonging to four different phyla have been isolated so far. These are *Nitrobacter, Nitrotoga* and *Nitrococcus* within the *Alpha-*, *Beta-* and *Gammaproteobacteria*, respectively (Spieck and Bock, 2005; Alawi et al., 2007), *Nitrospira* and *Nitrospina*, which belong to separate phyla (Ehrich et al., 1995; Lücker et al., 2013), and the moderate thermophilic NOB *Nitrolancea*, which is phylogenetically affiliated with the *Chloroflexi* (Sorokin et al., 2012, 2014). The latter phylum also contains novel thermophilic nitrite oxidizers that have been highly enriched from hot springs at Yellowstone National Park (Spieck et al., 2020). Indications for further marine NOB have been obtained by metagenomics studies (Lüke et al., 2016; Ngugi et al., 2016; Sun et al., 2019).

Nitrolancea hollandica has been isolated from a lab-scale nitrifying bioreactor receiving a high load of ammonium bicarbonate and operating at 35°C (Vejmelkova et al., 2012). It has a high tolerance against nitrite as typical for *r*-strategists among the NOB (Andrews and Harris, 1986; Nowka et al., 2015), which appears to correlate with the cytoplasmic localization of the key enzyme nitrite oxidoreductase (NXR) (Spieck et al., 1998; Lücker et al., 2010). The genomic organization of the *nxr* genes in *Nitrolancea* is very similar to those in *Nitrobacter, Nitrococcus* (Sorokin et al., 2012) and the recently described *Candidatus* (*Ca.*) Nitrocaldera (Spieck et al., 2020). In contrast, NOB containing a periplasmic NXR like *Nitrospira* (Spieck et al., 1996) are mostly inhibited by high substrate concentrations (Off et al., 2010). This distinct *Nitrospira*-type NXR is closely related to that of anaerobic ammonium-oxidizing (anammox) bacteria (Lücker et al., 2010), while the cytoplasmic *Nitrobacter*-type NXR is closely related to dissimilatory nitrate reductases (NAR) of nitrate-reducing microorganisms (Kirstein and Bock, 1993).

The low substrate affinity of *Nl. hollandica* ($K_{m\ (nitrite)}$ = 1 mM; Sorokin et al., 2012) posed the question of its natural niche. Nitrite is an intermediate of nitrification, denitrification and nitrate reduction to ammonium. It can accumulate when these processes are imbalanced, an effect that can be exaggerated by abiotic factors like pH, temperature or certain operational modes in reactor systems (Philips et al., 2002).

Temperature is a main factor shaping the community structure of nitrite-oxidizing bacteria and variations of this incubation parameter have resulted in the discovery of novel NOB (Alawi et al., 2007; Lebedeva et al., 2008). Nitrite oxidation at elevated temperature was found to be performed by *Nitrospira* (Lebedeva et al., 2005, 2011; Courtens et al., 2016), a common NOB in geothermal habitats (Marks et al., 2012; Edwards et al., 2013), or novel NOB of the *Chloroflexi* phylum (Spieck et al., 2020).

Based on the observed properties, the natural habitat of *Nl. hollandica* has been proposed to feature high temperatures as well as high ammonium and nitrite concentrations, as present for instance in compost or dung (Sorokin et al., 2012). *Nitrolancea*-like 16S rRNA gene sequences have only rarely been detected in specialized incubations of water or soil samples (Sorokin et al., 2018). These include soil columns used for aquifer treatment (Friedman et al., 2018), 1,3-dichloropropene fumigated soil (Fang et al., 2019), and manure composting (Zhang et al., 2016). A closely related 16S rRNA gene sequence (JN087902) has been detected in a SHARON (single reactor system for high activity ammonium removal over nitrite) reactor in Korea running at elevated temperature, a system with conditions comparable to the source of *Nl. hollandica*. Furthermore, recent surveys revealed the presence of this NOB in four Danish enhanced biological phosphorus removal (EBPR) systems and an N-removal plant in China (Speirs et al., 2019). Additionally, *Nitrolancea*-like 16S rRNA gene sequences have been found in reactors used for partial nitrification (Yu et al., 2018, 2020) and in free nitrous acid (FNA) treated wastewater (Wang et al., 2020). However, so far it is unclear what the lower temperature limit for proliferation of this moderate thermophilic NOB is and if *Nitrolancea* is present and active in full-scale nitrifying sludge systems especially as activated sludge does not contain ammonium or nitrite in the high concentrations apparently required by *Nitrolancea* to be competitive.

Apart from engineered systems, 16S rRNA gene sequences distantly related to *Nitrolancea* were found in warm natural environments, like the Atacama Desert (Orlando et al., 2010, EU603380) and the Kalahari (Elliott et al., 2014). These findings raise the question whether geothermal habitats might be suitable habitats for *Nitrolancea,* too. Therefore, in this study the geothermal area Las Máquinas in Argentina was investigated for the presence of nitrifying microorganisms. This region belongs to the Copahue-Caviahue system, which is mostly located in the Neuquen Province in Northern Patagonia and is characterized by a high biodiversity (Chiacchiarini et al., 2010; Urbieta et al., 2012, 2015a,b; Giaveno et al., 2013; Willis Poratti et al., 2016).

In the present study, three new representatives of *Nitrolancea* were selectively enriched under comparable conditions, and two pure cultures were obtained. Two of the enrichment cultures originated from a full-scale centrate treatment reactor at a wastewater treatment plant (WWTP) in Hamburg, Germany, and one from the geothermal Las Máquinas area in Argentina. The obtained species were compared to the type strain *Nl. hollandica* with regard to their genomic, phenotypic and physiological features.

MATERIALS AND METHODS

Sampling

WWTP Hamburg-Dradenau, Germany

On May 22, 2017, a centrate treatment side-stream reactor (3300 m^3) at the full-scale WWTP Hamburg-Dradenau was sampled (sample Z2; **Supplementary Figure S1A**). The centrate originated from centrifuged digested sludge and contained high ammonium (38 mM) and nitrite (44 mM), and low nitrate (9 mM) concentrations, and had a temperature of 39.5°C and a pH of 6.5–6.9 on the sampling day. In the treatment reactor, this liquid was mixed with activated sludge from the nitrification stage (approx. 30% v/v) and was supplied with 2 mg O_2 l^{-1}. The HRT was 1 day. The solids content and chemical oxygen demand (COD) amounted to 550 mg l^{-1} and 1750 mg l^{-1}, respectively. Subsequent to this "Store and treat" (SAT) procedure, patent-registered by the HSE (Hamburger Stadtentwässerung), the reactor effluent was applied for anammox treatment.

Las Máquinas, Argentina

The Copahue volcano (37°51′S, 71°10.2′W; 2977 m a.s.l), the Rio Agrio (pH 0.5–7) and Caviahue Lake (pH 2.1–3.7) are geographical landmarks that frame a geothermal field, which is composed of five hydrothermal sites: Las Máquinas, Las Maquinitas, Anfiteatro, Termas de Copahue (in Argentina) and Chancho-Co (in Chile). The Las Máquinas area contains many thermal fluid emission systems, consisting of fumaroles, boiling-bubbling water and mud pools with wide ranges of pH (2–7) and temperature (30–90°C). The chemical composition of the fumaroles, which are mainly fed by meteoric water (Chiodini et al., 2015), showed that the main emitted gas is CO_2, followed by minor concentrations of N_2, H_2, CH_4, and H_2S. CO and He concentrations are <1 ppm. Ammonium as a substrate for nitrification was detected in concentrations between 0 and 20 mM at different sampling sites of Las Máquinas, whereas nitrite and nitrate occurred between 0 and 6 μM (unpublished results).

In December 2008 (sample E2) and in March 2011 (sample A4), two mud pools in the geothermal area Las Máquinas, Argentina, were sampled. Both sampling sites were characterized by high sulfate concentrations (**Supplementary Table S1**). For sample E2 (**Supplementary Figure S1B**), red to brownish sediment was removed at a site that had a temperature of 40°C, a pH of 2.5–3.0 and an ammonium content of 0.6 mM. The sampling site of A4 (**Supplementary Figure S1C**) had a temperature of 45°C, a pH of 6.0 and ammonium was below the detection limit. Sample aliquots were transported at ambient temperature by courier to the University of Hamburg, Germany. Temperature, pH, and electric conductivity were measured *in situ* in each sample point using specific electrodes (Thermo Scientific Orion 5-Star Plus benchtop multifunction meter, electrode Orion 9142BN, Waltham, MA, United States). Water samples for metal analysis were filtered using 0.2 μm membrane filters (Cellulose acetate, Sartorius, Göttingen, Germany) and their concentrations (**Supplementary Table S1**) determined by atomic absorption spectrophotometry (AAS; Merodio and Martínez, 1985). To quantify anions, a standard turbidimetric assay for the determination of sulfate with $BaCl_2$ (Kolmert et al., 2000) and a titration of chloride ions with mercuric nitrate solution using diphenyl carbazide indicator were used (APHA et al., 1992).

Cultivation Media

The enrichments were performed in 0.05 to 0.15 l batch cultures in mineral salts medium with the following composition: 0.007 g l^{-1} $CaCO_3$, 0.5 g l^{-1} NaCl, 0.05 g l^{-1} $MgSO_4 \times 7\ H_2O$, and 0.15 g l^{-1} KH_2PO_4 dissolved in distilled water. If not stated otherwise, 0.02–0.2 g l^{-1} $NaNO_2$ (0.29 – 2.9 mM) were supplied as energy source. The trace element solution (1 ml l^{-1}) contained 33.8 mg l^{-1} $MnSO_4 \times H_2O$, 49.4 mg l^{-1} H_3BO_3, 43.1 mg l^{-1} $ZnSO_4 \times 7\ H_2O$, 37.1 mg l^{-1} $(NH_4)_6Mo_7O_{24}$, 973.0 mg l^{-1} $FeSO_4 \times 7\ H_2O$, and 25.0 mg l^{-1} $CuSO_4 \times 5\ H_2O$. The pH was adjusted to 8.0 and changed to 7.4–7.6 2 days after autoclaving. In order to enrich *Nitrolancea*, NH_4Cl was added in concentrations between 0.5 and 10 mM (**Supplementary Table S2**). When bicarbonate (0.5 mM) was included, the pH had to be adjusted to 6.7 to reach a final pH of 7.4–7.6 after autoclaving. For growth of the centrate-derived cultures, and the Argentinian cultures from 2018 on, trace elements according to Widdel and Bak (1991) were added to the medium (1 ml l^{-1}): 100 mg l^{-1} $MnCl_2 \times 4\ H_2O$, 30 mg l^{-1} H_3BO_3, 144 mg l^{-1} $ZnSO_4 \times 7\ H_2O$, 36 mg l^{-1} $Na_2MoO_4 \times 2\ H_2O$, 2.1 g l^{-1} $FeSO_4 \times 7\ H_2O$, 2 mg l^{-1} $CuCl_2 \times 2\ H_2O$, 190 mg l^{-1} $CoCl_2 \times 6\ H_2O$, and 24 mg l^{-1} $NiCl_2 \times 6\ H_2O$.

Enrichment

WWTP Hamburg-Dradenau

Two batches of mineral NOB medium (see above) containing 3 mM $NaNO_2$ and 3 mM NH_4Cl were inoculated (1% v/v) with the centrate sample Z2 on June 22, 2017, and incubated without agitation at 42°C and 46°C, respectively. A transfer was performed on October 23, 2017, and the incubation temperature was lowered to 37°C. In the following, the cultures grew very well and nitrite concentrations supplied to the medium were continuously increased (**Supplementary Table S2**).

Copahue – Argentina

A 0.5 ml aliquot of sample E2 (spring water with sediment) was inoculated into a 100 ml Erlenmeyer flask with 50 ml mineral unbuffered AOB medium (Krümmel and Harms, 1982) containing 0.5 mM ammonium as substrate. When ammonium was depleted, it was replenished to 400–500 μM with sterile 5 M NH_4Cl solution. Ammonium measurements were done with Quantofix test stripes (Macherey-Nagel, Düren, Germany). The pH was manually adjusted to approx. 7.4 with 5% (w/v) $NaHCO_3$ solution. For sample A4, 1 ml was inoculated in 100 ml mineral medium for NOB with 0.3 mM nitrite as substrate in a 250 ml screw cap Schott bottle. Both cultures were grown at 42°C under static conditions and evaporation was compensated for with sterile distilled water. Both cultures were regularly transferred with 1% (v/v) inoculum into mineral NOB media containing different concentrations of ammonium and nitrite with or without addition of 0.5 mM bicarbonate, and incubated under different conditions, as detailed in **Supplementary Table S2**.

Isolation Attempts

Cells from the enrichment cultures Z2.3.3 and A4.5.1 (**Supplementary Table S2**) were manually separated by an optical tweezers system (PALM MicroTweezers, Carl Zeiss Microscopy GmbH, Munich, Germany). Cells were visualized by bright-field microscopy at 1000× magnification (Axio Observer.Z1, Carl Zeiss, Jena, Germany), trapped with an infrared laser (1064 nm, 3 W) and separated by micromanipulation (PatchMan NP2, CellTram Vario, Eppendorf, Hamburg, Germany). Separated cells were transferred to NOB medium (0.5 mM $NaNO_2$, 0.5 mM NH_4Cl and 0.5 mM $NaHCO_3$) in 1.5 ml Eppendorf tubes, and incubated at 37°C. A total of 10 and 20 tubes for enrichments Z2.3.3 and A4.5.1, respectively, were inoculated with single cells or short chains resembling *Nitrolancea* by morphology. After nitrite consumption, active cultures were transferred twice to 5ml tubes (10% inoculum) and lastly into 100 ml Erlenmeyer flasks with 75 ml NOB medium. Additional attempts to eliminate accompanying heterotrophic bacteria were serial tenfold dilutions for cultures Z2.3.3 and A4.5.2 in three to four parallels in mineral NOB medium containing 0.5 mM $NaNO_2$, 0.5 mM NH_4Cl and 0.5 mM $NaHCO_3$, and incubated at 37°C. All investigations of *Nitrolancea* were done on enrichment cultures.

Purity Tests

The purity of the cultures (in terms of absence of heterotrophs) was tested repeatedly by incubating culture aliquots in complex liquid medium (0.5 g l^{-1} bactopeptone, 0.5 g l^{-1} yeast extract, 0.5 g l^{-1} meat extract, 0.584 g l^{-1} NaCl in distilled water, pH 7.4), and on solid RT (2.5 g l^{-1} meat extract, 2.5 g l^{-1} casamino acids, 0.5 g l^{-1} yeast extract, 1.0 g l^{-1} KH_2PO_4, 0.5 g l^{-1} NaCl, pH 7.4, 15.0 g l^{-1} agar in distilled water), R2A (half-strength; 0.25 g l^{-1} yeast extract, 0.25 g l^{-1} proteose peptone, 0.25 g l^{-1} casamino acids, 0.25 g l^{-1} glucose, 0.25 g l^{-1} soluble starch, 0.25 g l^{-1} Na-pyruvate, 0.15 g l^{-1} K_2HPO_4, 0.025 g l^{-1} $MgSO_4 \times 7\ H_2O$, pH 7.4, 15.0 g l^{-1} agar in distilled water) or mixotrophic NOB medium (0.2 g l^{-1} $NaNO_2$, 0.15 g l^{-1} yeast extract, 0.15 g l^{-1} bactopeptone, 0.055 g l^{-1} sodium pyruvate, trace elements [see mineral medium above], pH 8.0, 13 g l^{-1} agarose in distilled water).

Physiological Experiments

Growth of *Nitrolancea* was investigated in batch cultures, using 100 ml mineral medium in 300 ml Erlenmeyer flasks under static conditions at 37°C. Cultures were inoculated with 1% (v/v). To test for nitrite consumption as indication for growth, the Griess-Ilosvay spot test was used (Schmidt and Belser, 1994) or nitrite and nitrate were determined qualitatively with analytical test stripes (Merck KGaA, Germany). Nitrite concentrations for physiological experiments were measured by the HPLC technique.

Chemical Analyses

Nitrite and nitrate were determined quantitatively by HPLC via ion pair chromatography on a LiChrospher RP-18 column (125 × 4 mm; Merck) with UV detection in an automated system (Hitachi LaChrom Elite; VWR International GmbH, Darmstadt, Germany). Data acquisition and processing of nitrite and nitrate concentrations was performed with the integrated software EZChrom Elite 3.3.2.

Growth Characteristics

Nitrite consumption, nitrate production, cell numbers and protein content of cultures of A4.5.2 and Z2.3.4 were determined to calculate generation times (d^{-1}) as well as protein and cell yield per mmol nitrite. Cells were counted using a Thoma cell chamber (0.02 mm depth), and protein content was quantified by fluorescence using the NanoOrange protein quantitation kit (Thermo Fisher Scientific, Waltham, MA, United States).

Activity Measurements and Oxidation Kinetics

Nitrite-dependent oxygen consumption of cells from culture of A4.5.2 (1 replicate) and culture Z2.3.4 (2 biological replicates) was measured following Nowka et al. (2015), using a micro-respiration system (Unisense AS, Denmark) consisting of a 1-channel oxygen sensor amplifier (OXY-Meter), a Clark-type oxygen microsensor (OX-MR), 2 ml glass chambers with glass stoppers, glass coated magnets and a stirring system. Cells were grown at 37°C in mineral medium as described above, with 10 mM and 35 mM (A4.5.2) or 5 mM and 15 mM (Z2.3.4) ammonium and nitrite, respectively. 12–48 h after nitrite was depleted, cells were added to the chambers, which were sealed and mounted on a stirring rack in a water bath at 37°C. The oxygen microsensor was inserted through a capillary hole inside the glass stopper. After an initial equilibration period of 15–30 min, the measurements were started by adding nitrite from stock solutions through a second capillary hole using a syringe. Nitrite oxidation kinetics were estimated from oxygen consumption rates at varying defined nitrite concentrations using the R-package "drc" (Ritz et al., 2015), which fits Michaelis-Menten kinetic to the data with the following equation: $V = (V_{max} \times [S])/(K_m + [S])$, where V is activity, V_{max} is maximum specific activity (μmol mg protein^{-1} h^{-1}), K_m is the half-saturation constant for nitrite oxidation (μM), and [S] is concentration of nitrite (μM). For cell specific V_{max}, the calculated maximum activity was translated to fmol NO_2^- cell^{-1} h^{-1}.

Microscopic Investigations

For electron microscopy, cells were collected by centrifugation (13,000 × *g* for 15 min), fixed with 2.5% (v/v) glutaraldehyde as well as 2% (w/v) osmium tetroxide, and embedded in a mixture of Spurr and acetone as described previously (Spieck and Lipski, 2011). Thin sections were stained with 2% (w/v) uranyl acetate and 2% (w/v) lead citrate. Microscopic examination was carried out with a transmission electron microscope (Zeiss model Leo 906E with a CCD camera model 794). For the visualization of whole cells, 3 μl concentrated biomass was pipetted on EM grids (300 mesh, Stork Veco B.V, Netherlands) and stained with 2% (w/v) uranyl acetate. 4′-6′-diamidino-2-phenylindole (DAPI) stained cells were observed using a confocal laser scanning microscope LSM 800 (Zeiss, Jena, Germany) and Plan-Apochromat 63x and 100 × 1.4 oil objectives.

Fluorescence *in situ* Hybridization

Cells were pelleted at 10°C and 13,000 × *g* for 15 min, washed with 0.9% (w/v) NaCl and fixed with 1:1 (v/v) 96% ethanol:PBS as described previously (Amann et al., 1995). After dehydration in 50, 80 and 96% ethanol for 3 min each (Manz et al., 1992), cells were hybridized overnight in hybridization buffer containing 20% formamide with the FITC-labeled universal bacterial probe EUB338 (Amann et al., 1990) and the Cy3-labeled probe Ntlc804 specific for *Nitrolancea* (Sorokin et al., 2012). Cells were embedded in Citifluor AF1 (Citifluor Ltd., London, United Kingdom) prior to microscopic observation at the LSM 800 (Zeiss). Signal specificity was ensured by performing negative control hybridizations using the NON-338 probe labeled in Cy3 (Wallner et al., 1993).

DNA Extraction

DNA for PCR and Illumina sequencing was extracted with the PowerSoil DNA isolation Kit (MO BIO Laboratories, Inc., Carlsbad, CA, United States) according to manufacturer's instructions with slight modifications except for cultures E2 and A4.1: Before cell disruption via vortexing (step 5), Proteinase K (1 mg ml^{-1}), lysozyme (4 mg ml^{-1}) and RNase A (1 mg ml^{-1}) were added. The vortexing step was extended to 30 min at 37°C.

PCR

The presence of *Nitrolancea* was tested for with specific primer sets for 16S rRNA and *nxrA* genes (**Supplementary Table S3**) and subsequent gel electrophoresis. Presence of NOB belonging to *Nitrospira* was checked using the *nxrB*-targeted primer set NxrB-169f/NxrB-638r (Pester et al., 2014). The following PCR program was used: initial denaturation at 94°C, 5 min; 32 cycles consisting of 30 s denaturation at 94°C, 30 s annealing at 55°C (16S rRNA gene), 60°C (*nxrA*) or 56°C (*nxrB*) and 3.5 min (for *Nitrolancea* primers) or 45 s (*Nitrospira* primers) elongation at 72°C; final elongation at 72°C, 20 min.

Amplicon Sequencing

For selected cultures, 10 ng of genomic DNA were used for 16S rRNA gene amplicon sequencing at MR DNA (Molecular Research LP, Shallowater, TX, United States). For the cultures E2 and A4.1, amplicons were generated using the primers 341F and 785R (Herlemann et al., 2011), followed by 454 pyrosequencing (300 bp, 3000 reads per sample). For all other cultures the primers 515F and 806R (Caporaso et al., 2011) were used with subsequent Illumina MiSeq sequencing (2 × 300 bp, 20000 reads per sample). Operational taxonomic units (OTUs) were obtained from the preprocessed sequences using the *de novo* OTU picking workflow in qiime (v1.9.1) (Caporaso et al., 2010), and summarized and visualized by the QIIME *summarize_taxa_through_plots.py* script. Illumina sequences were processed, classified and summarized by MR DNA (Dowd et al., 2008). In short, paired-end sequences were joined and depleted of barcodes, followed by removal of sequences <150 bp or with ambiguous base calls. Sequences were denoised, OTUs generated and chimeras removed. OTUs were defined by clustering at 3% divergence (97% similarity). Final OTUs were taxonomically classified using BLASTn against a curated database derived from NCBI and RDPII.[1, 2]

Metagenomic Sequencing

DNA was fragmented using a Bioruptor (Diagenode, Seraing, Belgium). Libraries for Illumina HiSeq sequencing were generated using the NEBNext Ultra DNA Library Prep Kit for Illumina (New England Biolabs, Ipswich, MA, United States) as per manufacturer's recommendations. Size and quality of the libraries were visualized on a Bioanalyzer High Sensitivity Chip (Agilent Technologies, Santa Clara, CA, United States). Diluted libraries were multiplex sequenced on the Illumina HiSeq 2500 instrument (Illumina, St. Diego, CA, United States) by paired-end sequencing (2 × 100 bp [metagenomes 40 and 51] or 2 × 250 bp [metagenome 35] on the Illumina MiSeq platform (Illumina, St. Diego, CA, United States). For sequencing of the metagenomes A2, Z2, and Z4, library preparation was done using the Nextera XT kit (Illumina, San Diego, CA, United States) according the manufacturer's instructions. Tagmentation was performed starting with 1 ng of DNA, followed by incorporation of the indexed adapters and amplification of the library. After purification of the amplified library using AMPure XP beads (Beckman Coulter, Indianapolis, IA, United States), libraries were checked for quality and size distribution using the Agilent 2100 Bioanalyzer and the High sensitivity DNA kit. Quantitation of the library was performed by Qubit with the dsDNA HS Assay Kit (Thermo Fisher Scientific Inc., Waltham, MA, United States). The libraries were pooled, denatured and sequenced on a Illumina MiSeq (San Diego, CA, United States). Paired end sequencing of 2 × 300 bp was performed using MiSeq Reagent Kit v3 (San Diego, CA, United States) according to the manufacturer's protocol.

Metagenome Assembly and Binning

Adapter removal, contaminant filtering and quality trimming of the Illumina HiSeq and MiSeq paired-end sequencing reads was performed using BBDUK (BBTOOLS version 37.76). Terminal base calls with a quality score < Q17 were trimmed and the reads with a mean quality score of ≤Q20 were discarded. The processed HiSeq reads with a length of ≥70 bp were then corrected for sequencing errors using BayesHammer (Nikolenko et al., 2013). Additional filtering parameters were applied to the MiSeq reads (k = 23, mink = 11, hdist = 1, ktrim = r, tbo = t, maxns = 0, tossjunk = t) and only reads with a length of ≥150 bp were kept. The corrected reads were assembled using metaSPAdes v3.11.1 (Nurk et al., 2017) with default settings. For the samples sequenced with HiSeq, the reads for all samples were co-assembled with iterative assemblies using kmer sizes of 21, 33, 55, 77, 99, and 127, whereas for the MiSeq reads, the assemblies were performed separately for each sample with kmer sizes of 21, 33, and 55. Trimmed HiSeq reads were mapped back to the metagenome separately for each sample using Burrows-Wheeler Aligner (BWA v0.7.17) (Li and Durbin, 2009), employing the "mem" algorithm. For samples sequenced with MiSeq, reads were

[1] www.ncbi.nlm.nih.gov

[2] http://rdp.cme.msu.edu

mapped back to the metagenomes using the minimap2 (v2.16-r922) preset for genomic short-read mapping (Li, 2018). The sequence mapping files were handled and converted as needed using SAMtools 1.6 (Li et al., 2009). The MiSeq metagenomes were manually binned using anvi'o (v5, Eren et al., 2015) and taxonomically classified using the 'classify workflow' of GTDB-Tk (version 0.3.2, Parks et al., 2018). Subsequently, the *Nitrolancea*-like bins were annotated using Prokka (version 1.12-beta, Seemann, 2014) with the RefSeq bacterial nr protein database as a reference and the Kyoto Encyclopedia of Genes and Genomes (KEGG). The completeness and redundancy of the bins was assessed using the checkM 'lineage' workflow (Parks et al., 2015).

Phylogenetic Analyses

The average nucleotide identity (ANI) between the recovered *Nitrolancea* genomes and the genome of *Nl. hollandica* was calculated using orthoANI (Lee et al., 2016).

Sequences (16S rRNA and *nxrA*) were aligned using the multiple sequence alignment web server T-Coffee (Notredame et al., 2000). Subsequently, maximum-likelihood trees were calculated using Mega-X (Kumar et al., 2018) with 1000 bootstraps.

Genome Comparison

The orthologous gene clusters were identified using the OrthoVenn 2 web service tool (Xu et al., 2019) with an *E*-Value of 1e-2 and an inflation value of 1.5.

RESULTS

Selective Enrichment of Nitrolancea

The enrichment process of *Nitrolancea* from WWTP centrate and geothermal mud pool samples was monitored by specific PCR, fluorescence *in situ* hybridization (FISH; **Supplementary Table S3**), and 16S rRNA gene amplicon and metagenomic sequencing. Additional details on the enrichment process can be found in the **Supplementary Material**.

As shown by amplicon sequencing, the microbial community of the original centrate treatment reactor sample Z2 was dominated by *Proteobacteria* (56%), *Bacteriodetes* (22%) and *Firmicutes* (10%). *Chloroflexi* were present at low amounts (2%; **Supplementary Figure S2**), but none of these sequences were affiliated with the genus *Nitrolancea*. Members of the nitrifying genera *Nitrosomonas* and *Nitrosovibrio* were detected (2.1 and 0.7%, respectively), but no known nitrite oxidizer could be identified.

Over a period of only 4 months, *Nitrolancea* could be selectively enriched from 1.4 to 24% (**Supplementary Table S2**). Different isolation attempts were performed to increase the relative abundance of *Nitrolancea*-like bacteria in the nitrite-oxidizing cultures. For Z2, incubations with increasing substrate concentrations (up to 70 mM nitrite) revealed a very high enrichment of lancet-shaped cells (**Figure 1a**) and combination with the use of an optical tweezers system or serial dilution series increased the enrichment further (**Figure 1b**). Two consecutive dilution series with growth up to the dilution 10^{-8} and 10^{-6}, respectively, lead to a pure culture of *Nitrolancea* strain Z based on purity tests using four different complex media.

Unlike the centrate treatment reactor sample, the primary nitrite-oxidizing enrichment of Las Máquinas (A4.1) grown at 42°C was dominated by members of the phylum *Chloroflexi* (45%), followed by *Deinococcus-Thermus* (28%) and *Proteobacteria* (22%) according to 16S rRNA amplicon sequencing (**Supplementary Figure S2**). This enrichment had been supplied with 0.3 mM of nitrite without ammonium addition. *Nitrolancea* abundances increased to 14.1% after the culture had been repeatedly replenished with nitrite over a period of 4 years and increased further to 44% after using high substrate concentrations (30 mM) and adding ammonium (**Supplementary Table S2**). Manual sorting of cells from this enrichment with the optical tweezers system generated six follow-up cultures that, however, all still contained several accompanying heterotrophic bacteria (not shown). Meanwhile, the parallel culture A4.5.2, which received 40 mM nitrite in addition to the ammonium and bicarbonate also present in A4.5.1, was nearly pure as shown by inoculation of four different complex media and FISH (**Figure 1c**) and only tiny colonies grew on half-strength R2A plates. These heterotrophic bacteria were lost upon another serial dilution to the step 10^{-7} (A4.5.3) and the strain deemed isolated. The novel *Nitrolancea* strain was provisionally designated as *Ca.* Nitrolancea copahuensis based on 16S rRNA gene and whole-genome dissimilarity to *Nl. hollandica* (see below).

Notably, in an ammonia-oxidizing culture that had been inoculated with an earlier sample from Las Maquinas (E2) with 0.5 mM ammonium, but without nitrite addition, *Nitrolancea*-like NOB were also co-enriched with unknown ammonia-oxidizing microorganisms. This culture was dominated by *Chloroflexi* (34%), *Proteobacteria* (40%) and *Actinobacteria* (21%), while *Nitrolancea*-like bacteria constituted nearly 20% of the microbial community after 3.5 years of incubation at 42°C. Contrastingly, no *Nitrolancea*-like sequences could be detected in a parallel nitrite-oxidizing culture of E2, which was grown without ammonium addition at 42°C (not shown).

Regarding other known NOB, *Nitrospira* were nearly absent in all centrate treatment reactor enrichments and constituted only 0.3% of the retrieved amplicon sequences in the Argentinian cultures A4.2, A4.3 and A4.4 (**Supplementary Table S2**). *Nitrobacter*-like 16S rRNA gene sequences amounted to 0.8% in the centrate cultures Z2.1 and Z2.2 (not shown). In the Argentinian A4 cultures, *Nitrobacter* was undetectable, but constituted a tiny fraction in culture E2 (0.05%).

Morphology and Ultrastructure

Light and transmission electron microscopy of the nitrite-oxidizing enrichment cultures that had been inoculated with biomass from the Hamburg-Dradenau centrate treatment reactor and from Las Máquinas revealed *Nitrolancea*-like cells with characteristic tapered ends (**Figure 2**) similar to those of *Nl. hollandica* (Sorokin et al., 2012), but smaller in size (**Table 1**). The lancet shape was less pronounced in A4 cultures, where most cells had an ovoid shape (**Figure 2F**). *Nitrolancea*-like bacteria in all cultures appeared as single cells, or formed pairs and short chains.

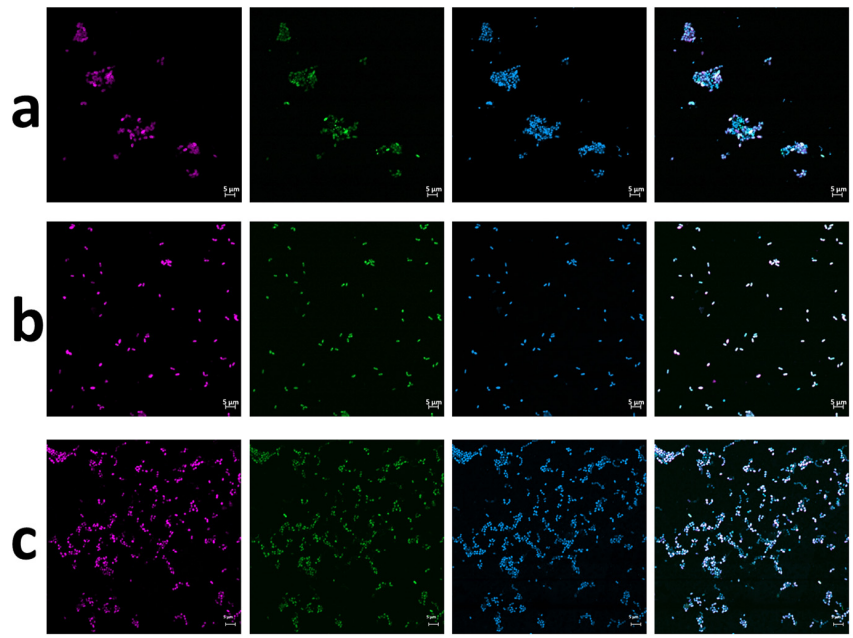

FIGURE 1 | FISH micrographs of culture Z2.3.3 **(a)** before and **(b)** after 10^{-8} dilution and **(c)** of culture A4.5.2. From left to right: *Nitrolancea*-like bacteria detected with probe Ntlc804 labeled in Cy3 (red); all bacteria detected with EUB338 labeled in FITC (green); all cells stained with DAPI (blue); overlay of all three channels.

In late nitrite-oxidizing cultures, cells of *Nitrolancea* aggregated to roundish flocs, whereas in primary enrichments of cultures E2 and A4 tiny yellow to orange particles accumulated.

The *Nitrolancea*-like cells in both incubation series had the typical Gram-positive type complex cell wall, including a regular proteinaceous surface layer (**Figure 2C**), which is a common component of archaeal and bacterial cell walls (Rachel et al., 1997). This protein layer is easily disrupted during the embedding process (**Figures 2D,F**), resulting in loss of the typical cell morphology. As described for *Nl. hollandica*, the novel *Nitrolancea* strains did not possess carboxysomes or intracytoplasmic membrane systems. However, in some cells membrane invaginations as described by Sorokin et al. (2014) were observed at the cell poles (not shown).

Physiology

As also known for *Nl. hollandica,* cells of both *Nitrolancea* enrichments derived from the samples Z2 and A4 were able to grow lithoautotrophically with nitrite as energy source and CO_2 as carbon source. Nitrite was oxidized aerobically and stoichiometrically to nitrate with a minimum generation time of 53 h (culture Z2.3.4; **Figure 3A**) or 43 h (culture A4.5.2; **Figure 4A**).

In the beginning of the cultivation process, the Z2.2 culture was tested for its ammonium requirements. Growth was slow in ammonium-free medium and was clearly accelerated by the addition of 0.5 – 3 mM ammonium (not shown). Consequently, all mineral NOB media were prepared with the addition of ammonium. Fascinatingly, NH_4Cl concentrations up to 500 mM could be tolerated, although consumption of 3 mM nitrite took 4 months. Addition of 250 mM ammonium caused slight inhibition only (**Figure 3C**). In accordance with *Nl. hollandica*, the cultures derived from the centrate were able to grow in the presence of very high nitrite concentrations and completely oxidized up to 150 mM nitrite within several months. Growth occurred between 22 and 43°C and with a delay at 19 and 45°C. Nitrite was oxidized optimally at 37°C (**Figure 3D**). Additionally, the influence of aeration and bicarbonate supplementation on growth and activity were tested. The highest nitrite oxidation rates were obtained when cells were incubated in Erlenmeyer flasks without agitation and were further accelerated by addition of 0.5 mM $NaHCO_3$ (**Figure 3B**).

The nitrite oxidation rates of the *Nitrolancea* cultures obtained from Las Máquinas (A4.4) increased with increasing substrate concentrations (1–10 mM $NaNO_2$) without a prolonged lag-phase (**Figure 4B**). The nitrite tolerance level was 40 mM. Nitrite was also oxidized slowly in medium without ammonium, but optimal growth depended on the addition of up to 50 mM NH_4Cl (**Figure 4C**). The ammonium tolerance limit was 500 mM. Growth of the Argentinian *Nitrolancea* strain was observed between 22 and 45°C, delayed at 19°C, and with an optimum growth temperature of 35–37°C (**Figure 4D**). A comparison of key parameters between *Nl. hollandica* and the strains investigated here is shown in **Table 1**.

Nitrite oxidation kinetics were determined by microsensor-based oxygen consumption measurements in the different *Nitrolancea* cultures (**Supplementary Figure S3**). Both representatives revealed moderate substrate affinities with apparent half-saturation constants (K_m) of 0.12–0.45 mM nitrite for *Nl. hollandica* strain Z and 0.22 mM for *Nl. copahuensis* (**Supplementary Table S4**). The maximum specific activity (V_{max}) was relatively low (11.1–26.8 μmol nitrite mg

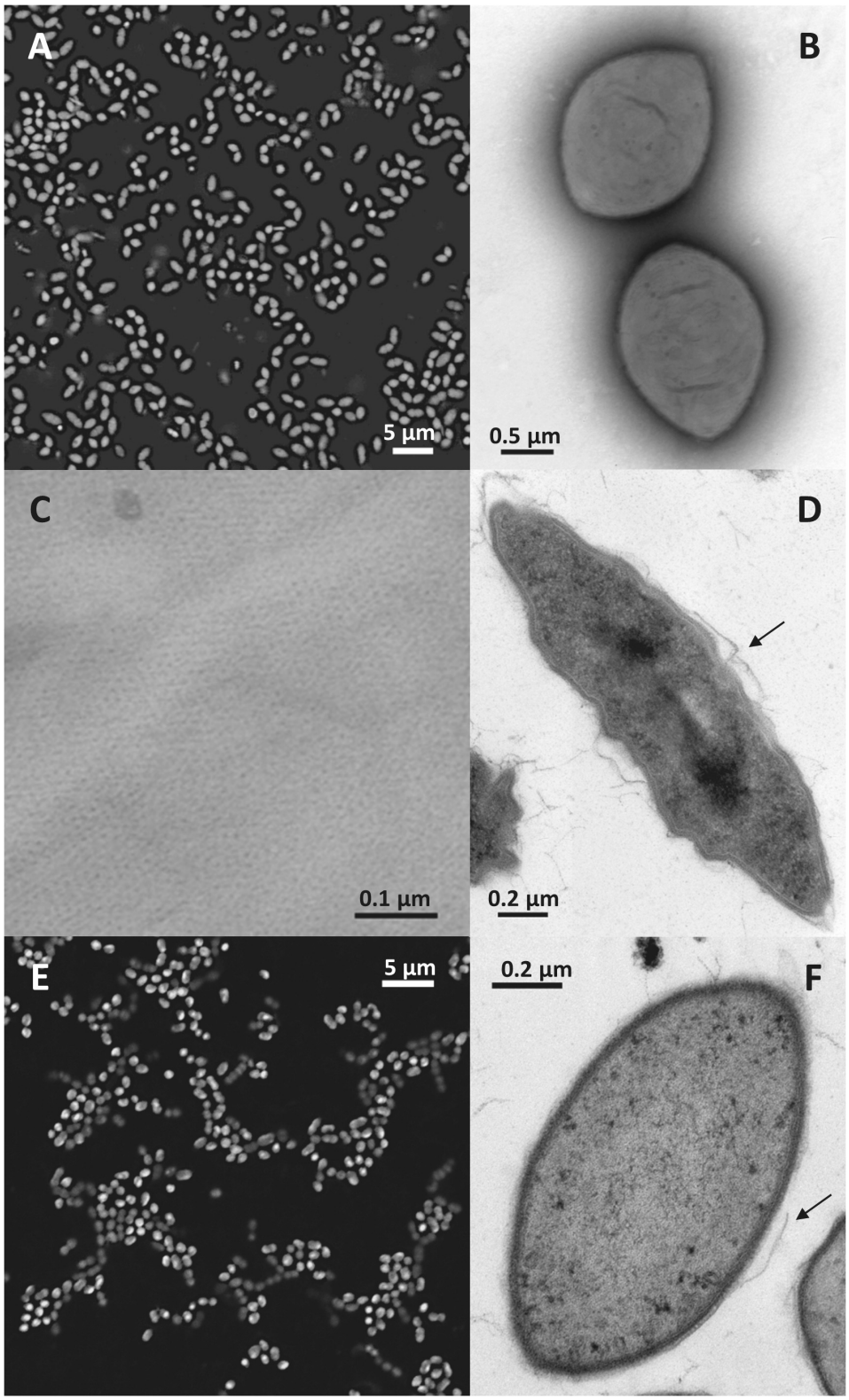

FIGURE 2 | *Nitrolancea*-like cells in the nitrite-oxidizing enrichments derived from centrate **(A–D**; culture Z2.3.3) and of Las Máquinas **(E,F)**. **(A)** Cell shape of *Nitrolancea hollandica* strain Z stained with DAPI. **(B)** Negatively stained cells showing the tapered ends in detail, stained with uranyl acetate. **(C)** Regular protein layer of the cell wall. **(D)** Electron micrograph of an ultrathin section. **(E)** Fluorescence micrograph of culture A4.4 stained with DAPI. **(F)** Ultrathin section of culture A4.3. The arrows indicate where the disrupted external protein layer is detached from the cell wall.

TABLE 1 | Comparison of morphological, physiological and genomic features of the novel *Nitrolancea* strains and *Nl. hollandica*.

Feature	*Nl. hollandica* strain Z*	*Ca.* Nl. copahuensis	*Nl. hollandica*
Morphology	Ovoid rods with tapered ends	Ovoid rods with tapered ends	Ovoid rods with tapered ends
Size [μm]	1.3–1.5 × 1.6–2.3	1.1 × 1.7	1–1.2 × 2–4
Temperature optimum	37°C	35–37°C	40°C
Temperature range for growth	19–45°C	19–45°C	20–46°C
Nitrite tolerance	150 mM	40 mM	75 mM
Nitrite optimum	3–10 mM	3–10 mM	5–20 mM
Km value (nitrite)	0.12–0.45 mM	0.22 mM	1 mM
μ_{max} (nitrite) h^{-1}	0.013	0.016	0.019
NxrA copies	2/4 (Z2/Z4)	2	4
Ammonium requirement	+	+	+
Ammonium optimum	5–20 mM	5–25 mM	5 mM
Ammonium tolerance	500 mM	500 mM	>200 mM
CO_2 fixation	Calvin cycle	Calvin cycle	Calvin cycle
Rubisco	Type I	Type I	Type I
Isolation source	Centrate treatment reactor	Geothermal spring	Bioreactor

**Without differentiation between the genotypes Z2 and Z4.*

protein^{-1} h^{-1}). Growth yields ranged from 0.17 to 0.88 mg protein mmol nitrite^{-1}.

Genomic Analyses

Biomass of cultures Z2.2, Z2.3.2, and A4.4 was used for metagenomic sequencing (**Table 2**). The draft genomes of the three resulting *Nitrolancea* strains described here (Z2, Z4, A2) could be assembled into 48 to 150 contigs. These high-quality draft genomes ranged in size from 3.19 to 3.45 Mbp and had G+C contents between 62.7 and 62.9 mol%. The number of predicted coding sequences was between 3023 and 3235, including 40 to 46 tRNAs.

After assembly and binning of the *Nitrolancea* strains, comparative genomics revealed that two highly similar strains (Z2 and Z4) were enriched from the centrate treatment reactor sample, while the strain A2 obtained from sample A4 was clearly distinct (see below). The comparison of these metagenome-assembled genomes (MAGs) with *Nl. hollandica* revealed 2399 conserved clusters out of in total 3387 orthologous gene clusters within the four *Nitrolancea* strains (**Figure 5**). The type strain *Nl. hollandica* exhibits 14 unique gene clusters that were absent in the genomes of the three novel strains, which, on the contrary, shared 131 of orthologous clusters. Additionally, the Argentinian strain A2 contained 6 unique gene clusters, while the two genomes obtained from the centrate enrichment cultures in total had 109 clusters not present in the other *Nitrolancea* strains.

Phylogenetic and sequence similarity-based analysis of the 16S rRNA genes of the novel *Nitrolancea* strains (**Supplementary Table S5**, **Figure 6**) revealed a close affiliation with the previously described type strain *Nl. hollandica* (Sorokin et al., 2014). *Ca.* Nitrolancea copahuensis had a 16S rRNA gene sequence identity of 98.5% to *Nl. hollandica*, whereas the two centrate strains were almost identical to the type strain (99.9 and 100% identity). Comparison of the NxrA sequences of the novel strains and *Nl. hollandica* revealed high amino acid identities (**Supplementary Table S5**, **Supplementary Figure S4**). Furthermore, the draft genome sequences of the centrate strains and *Nl. hollandica* had high average nucleotide identity (ANI) values of 99.2 and 99.3%, respectively, which was only 91.9% for the geothermal strain (**Supplementary Table S6**). The two draft genomes from the centrate enrichments were almost identical and had an ANI value of 99.96%. Thus, based on 16S rRNA gene and ANI similarity, Z2 and Z4 belong to the species *Nl. hollandica*, while the Argentinian strain A2 had 16S rRNA and ANI identity values below the species threshold of 98.7–99.0% (Stackebrandt and Ebers, 2006) and 95% (Rodriguez-R and Konstantinidis, 2016), respectively. Consequently, this strain represents a separate species within the genus *Nitrolancea*.

The genomic data was furthermore mined to reconstruct the core metabolic pathways of the three novel *Nitrolancea* strains (**Table 3**). Genes encoding all proteins of the Calvin cycle for CO_2 fixation, but not for carboxysomes have been identified. The potential for nitrite and formate oxidation was also present and the genomes contained additional non-operonal *nxrA* copies, as has been observed for *Nl. hollandica* (Sorokin et al., 2012). The A2 and Z2 genomes contained only one orphan *nxrA* gene, while the Z4 genome encoded 3 additional NxrA copies. All other NXR subunits were not duplicated and encoded within a highly conserved operon (**Supplementary Figure S5**). Furthermore, genes for a NO-forming nitrite reductase (*narK*) and the cytoplasmic assimilatory nitrate reductase (*nasAB*) were detected in the three analyzed genomes, but not for assimilatory nitrite reductases (*nirA or nirBD*) or dissimilatory nitrite reduction to ammonium (*nrfA*).

Additionally, all *Nitrolancea* genomes encoded an aerobic-type CO dehydrogenase, cyanase and an [NiFe]-hydrogenase. Based on the genomic data, all strains have the potential to grow heterotrophically and to use thiosulfate for energy conservation. So far, none of these phenotypes could be observed in growth experiments with *Nl. hollandica* (Sorokin et al., 2012). Within the sulfur metabolism, the assimilatory sulfate reduction pathway involving sulfate adenylyltransferase (*sat*), adenylyl-sulfate kinase (*cysC*), phosphoadenosine phosphosulfate reductase (*cysH*) and ferredoxin-dependent sulfite reductase (*sir*) could be identified in the three analyzed genomes, along with genes encoding thiosulfate sulfurtransferases (*glpE*, *sseA*) and a putative sulfite oxidase (*sorA*).

DISCUSSION

The first isolate of *Nitrolancea* was only described in 2012 (Sorokin et al., 2012). Growth depended on the use of a modified NOB medium (Spieck and Lipski, 2011), as *Nl. hollandica* grew optimally in mineral medium containing high substrate concentrations of 20 to 50 mM KNO_2 and supplementation of 5 mM NH_4HCO_3. Unexpectedly for a nitrite-oxidizing

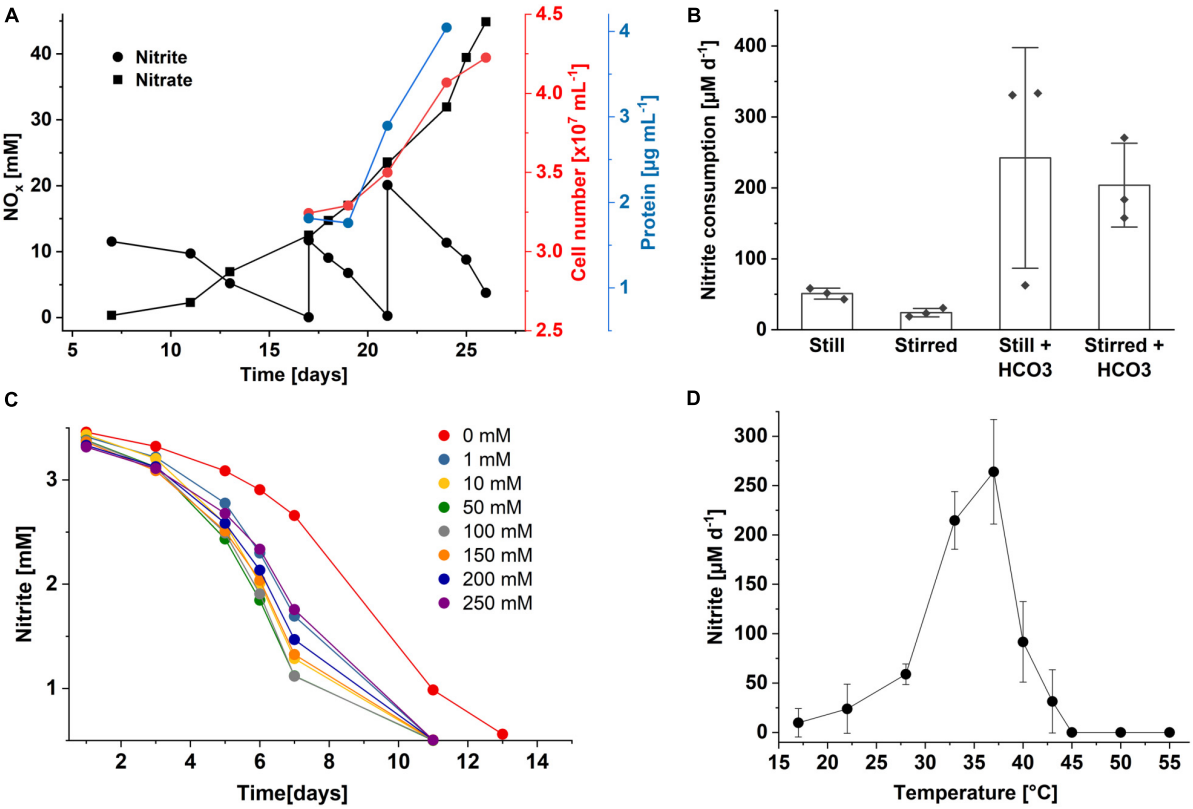

FIGURE 3 | Growth characteristics of *Nitrolancea hollandica* strain Z. **(A)** Stoichiometric oxidation of nitrite to nitrate leading to increase in cell number and biomass. **(B)** Nitrite consumption of enrichment culture Z2.3.3 under different incubation conditions at 37°C: without agitation (still) or stirred at approx. 120 rpm, and with or without the addition of 0.5 mM $NaHCO_3$. Bars represents the mean ± standard error of biological triplicates, diamonds indicate individual data points; **(C)** nitrite oxidation over time in medium supplemented with 3 mM nitrite and different ammonium concentrations (0 – 250 mM); **(D)** nitrite oxidation rates per day at different temperatures. The rates were determined for the period between day 3 and 10 after inoculation (2.5 mM initial nitrite concentration). Data represents the mean ± standard error of biological triplicates. For all incubations, medium was inoculated with 1% (v/v) enrichment culture of **(A)** Z2.3.4, **(B,D)** Z2.3.3 or **(C)** Z2.3.1.

organism, *Nl. hollandica* depends on ammonium as N-source and accordingly its genome did not encode any enzymes for nitrite reduction to ammonium (Sorokin et al., 2012). This absence of assimilatory nitrite reduction pathways was recently also observed in other thermophilic NOB within the phylum *Chloroflexi* (Spieck et al., 2020), and some *Nitrotoga* species are apparently dependent on ammonium addition, too (Ishii et al., 2017; Wegen et al., 2019). In contrast, the early *Nitrolancea* enrichments obtained in this study were able to oxidize nitrite also without ammonium addition, although no assimilatory nitrite reductase genes were detected in their genomes. However, it is likely that these *Nitrolancea* strains were provided with ammonium or organic N-sources by the accompanying heterotrophs present in the cultures, as the ability for growth without ammonium addition was lost upon increased purity of the cultures.

The optimal growth conditions for the novel *Nitrolancea* strains were assessed by testing different incubation temperatures, as well as nitrite and ammonium concentrations. Although *Nitrolancea* has been described as NOB, that requires high substrate concentrations, early enrichments from Las Máquinas were done at very low nitrite availability (**Supplementary Table S2**). Nevertheless, once an active culture was obtained, an increase of substrate concentrations was observed to be beneficial for the selective enrichment of *Nitrolancea*-like NOB. High ammonium concentrations can also enhance proliferation of *Nitrolancea*, as was observed in culture A4.4. However, we cannot exclude that this effect was caused by growth stimulation of accompanying bacteria. After initial cultivation at 42°C, reducing the incubation temperatures to the apparent optimum of 37°C led to a reliable enrichment of *Nitrolancea*-like cells from both sample locations (**Supplementary Table S2**). Intriguingly, this cultivation strategy resulted in the successful enrichment of two novel *Nl. hollandica* strains from the centrate treatment reactor, even though no *Nitrolancea*-like 16S rRNA gene sequences were detected in the original sample. This finding indicates that these NOB are more widely distributed than previously assumed, albeit at very low numbers. The minimum temperature for growth for *Nitrolancea* derived from the centrate reactor as well as from the geothermal mud pool was 19°C, but related 16S rRNA gene sequences were also found in a bioreactor system operated at 12°C (Yu et al., 2018). Therefore, the environmental distribution of these NOB seems not to be restricted to thermophilic conditions.

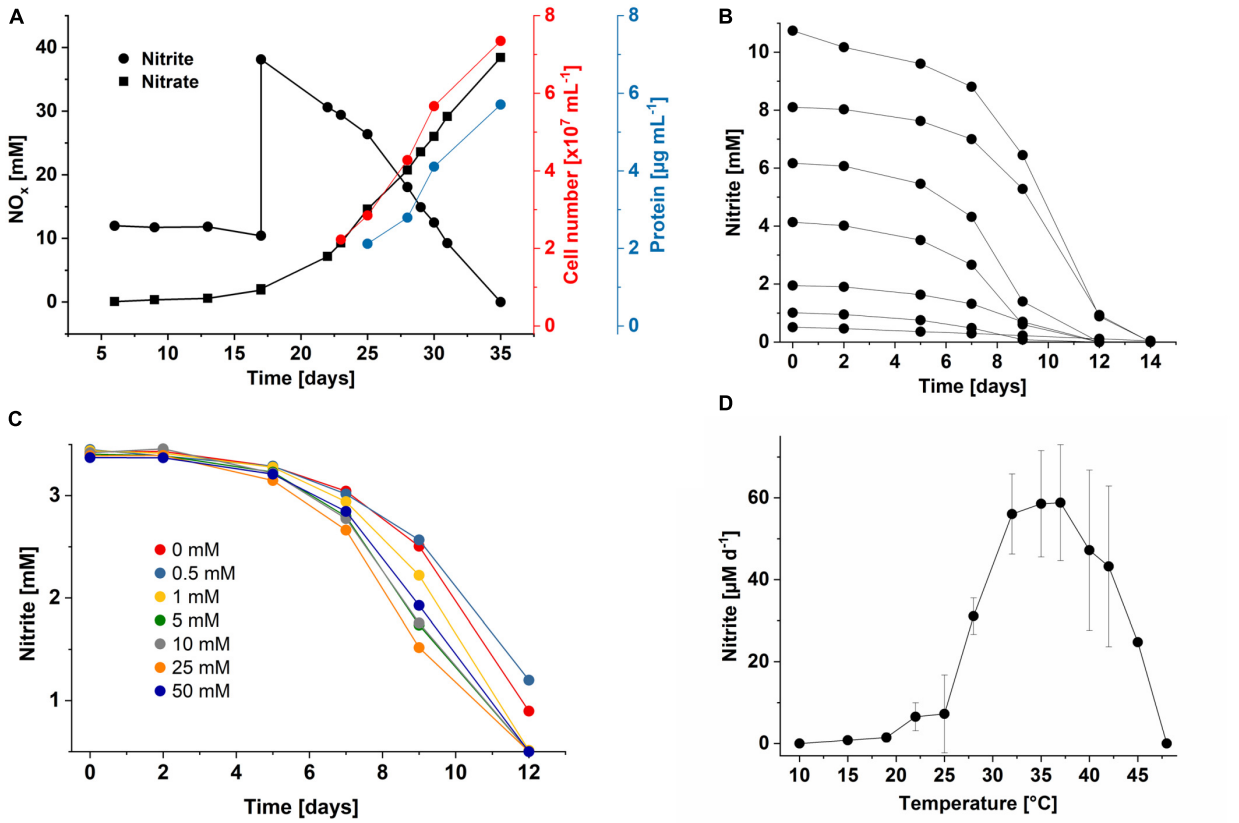

FIGURE 4 | Growth characteristics of *Ca.* Nitrolancea copahuensis. **(A)** Stoichiometric oxidation of nitrite to nitrate leading to increase in cell number and biomass. **(B)** Substrate consumption test with different initial nitrite concentrations in culture A4.4, showing the rapid consumption of nitrite. Reduced nitrite oxidation was still observed at up to 40 mM nitrite (not shown). **(C)** Nitrite consumption of culture A4.4 in medium supplemented with different ammonium concentrations (0 to 50 mM). **(D)** Influence of temperature on nitrite oxidation in culture A4.5.1 with 0.5 mM nitrite. Nitrite oxidation rates were determined for the period between day 4 and 11 after inoculation. Data represents the mean ± standard error of biological triplicates. At 42°C, two biological replicates were incubated.

TABLE 2 | Genome characteristics of the four *Nitrolancea* strains as predicted using PROKKA (Version 1.12).

Genomic feature	*Nl. hollandica* Z2	*Nl. hollandica* Z4	*Ca.* Nl. copahuensis A2	*Nl hollandica* Lb
Genome size	3 193 324 bp	3 450 053 bp	3 385 528 bp	3 888 104 bp
G+C value (genome)	62.9%	62.9%	62.7%	62.6%
CDS	3023	3235	3232	3946
Contigs	150	140	48	736
tRNA	41	40	46	67
tmRNA	1	1	1	1
Completeness	99.7%	98.1%	96.3%	
Contamination	0%	0%	0%	

Fast and reproducible initial enrichment of *Nitrolancea* spp. was achieved by designing a standard medium consisting of a mineral salt solution supplemented with 3 mM $NaNO_2$, 3 mM NH_4Cl and, as observed in later cultivation approaches, 0.5 mM $NaHCO_3$. The positive effect of bicarbonate probably is due to resulting elevated CO_2 concentrations within the cell, which might reduce the reaction of ribulose 1,5-bisphosphate carboxylase/oxygenase (RuBisCO) with the competing substrate O_2 and thus increase carbon fixation efficiency in the absence of other CO_2-concentrating mechanisms like carboxysomes (Price et al., 2008). In this study, a preference for a reduced oxygen supply (**Figure 3B**) of *N. hollandica* strain Z was found and culturing was done without agitation. Accordingly, *Nitrolancea*-like sequences have been detected in a reactor treating synthetic low-strength wastewater at low dissolved oxygen contents (Yu et al., 2020).

The proliferation of the different *Nitrolancea* strains at nitrite concentrations between 3 and 40 and even 70 mM, respectively, matches the extremely high half-saturation constant (K_m) for nitrite determined for *Nl. hollandica* (Sorokin et al., 2012). The

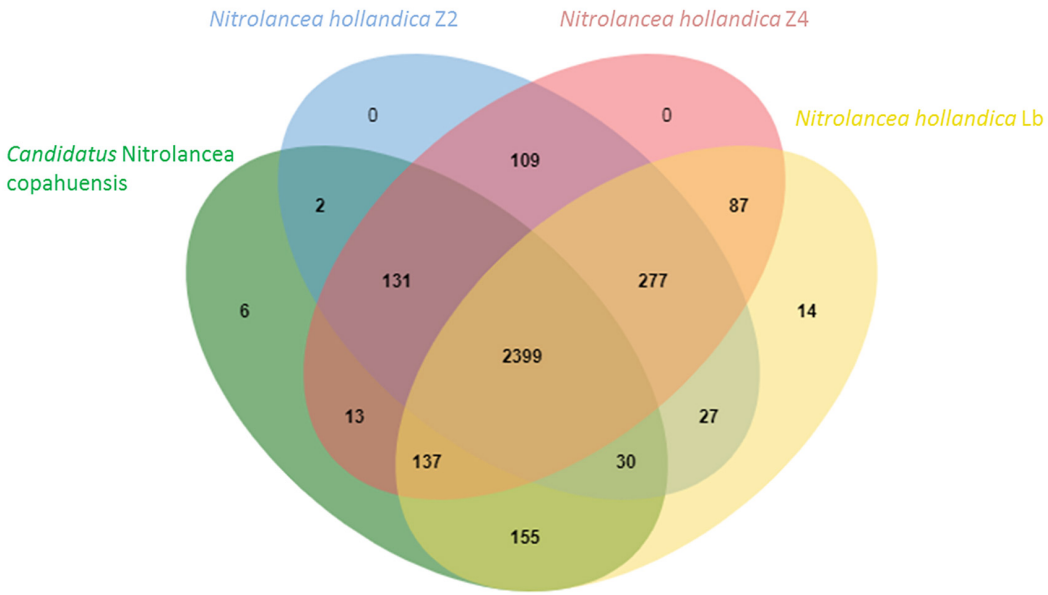

FIGURE 5 | Venn diagram indicating the number of shared orthologous clusters among the genomes of *Nitrolancea hollandica* and the *Nitrolancea* strains obtained from the nitrite-oxidizing enrichments A4.4 (A2), Z2.2 (Z2) and Z2.3.2 (Z4). The diagram was plotted by using OrthoVenn2 (Xu et al., 2019).

K_m of this strain was found to be 1 mM nitrite, which corresponds to the lowest substrate affinity of any NOB determined so far and is in line with the high substrate concentrations present in the bioreactor *Nl. hollandica* was isolated from. The *Nitrolancea* cultures investigated here revealed a higher affinity for nitrite, although there was a great variance between values for strain Z and only one measurement was done for *Nl. copahuensis*. Nevertheless, our preliminary results suggest that the K_m value of *Nitrolancea* is in the range of the different *Nitrobacter* species (Nowka et al., 2015). This higher substrate affinity fits with the presence of *Nitrolancea* in the geothermal area of Las Máquinas, where nitrite is rarely detected as usual for most natural systems. Nevertheless, high substrate concentrations are necessary for optimal growth of *Nitrolancea* and nitrite was oxidized slowly when present in low concentrations (**Figures 4B,D**).

Comparing the genomes and NxrA gene sequences from the different enrichments, it has become obvious that distinct representatives of *Nitrolancea* grew depending on the respective medium (for instance 3 mM vs. 60 mM nitrite for strains Z2 and Z4). Similarly, the representatives of *Nitrolancea* enriched from the Las Máquinas samples differed in the initial enrichments E2 and A4.4 in AOB and NOB medium, respectively (**Supplementary Figure S4**). The *nxrA* gene within the metagenome 40 of the culture E2 is non-operonal, whereas in close vicinity to the *nxrA* gene of the metagenome 35 a cytochrome *c* was found. Therefore, the initial samples must have contained a microdiversity of *Nitrolancea* strains, which selectively proliferate once their special demands were met.

Nitrolancea-like 16S rRNA gene sequences have only occasionally been detected in full-scale nitrifying activated sludge systems so far (Speirs et al., 2019). The *Nitrolancea*-typical marker fatty acid 12-methyl octadecanoic acid (18:0 12methyl) (Sorokin et al., 2012) was measured in low amounts (0.2% of total fatty acids) in activated sludge of the Hamburg-Dradenau WWTP by Kruse et al. (2013). The abundance of 12-methyl octadecanoic acid increased slightly to 0.7% after incubations with nitrite at 28°C and 32°C, which confirms the preference of *Nitrolancea* for elevated temperatures. However, similar glycolipids are also characteristic for other thermophilic *Chloroflexi*, like for instance *Thermomicrobium*, which has also been detected in WWTPs based on 16S rRNA gene sequences (Spieck et al., 2020). Therefore, it is still speculative if *Nitrolancea* also occurs in activated sludge, which was used as inoculum for the centrate reactor.

The geothermal area in Las Máquinas apparently offers beneficial conditions for *Nitrolancea*-like NOB, as revealed by our 16S rRNA amplicon data (**Supplementary Figure S2**, **Supplementary Table S2**) although closely related sequences have not been detected in this area previously (Urbieta et al., 2015a). Elevated ammonium or nitrite concentrations could not be measured at the sampling sites, thus posing the question if alternative substrates might have enabled proliferation of *Nitrolancea*. Some NOB are metabolically versatile and can use simple organic carbon compounds like formate, hydrogen, and even ammonia as additional energy sources (Koch et al., 2014, 2015; Daims et al., 2015; van Kessel et al., 2015). Furthermore, different NOB possess the genetic potential to use various sulfur compounds (Starkenburg et al., 2008; Lücker et al., 2013; Boddicker and Mosier, 2018; Kitzinger et al., 2018; Palomo et al., 2018) and the oxidation of sulfide has been demonstrated for *Nitrococcus mobilis* (Füssel et al., 2017). In the Las Máquinas area, a highly active sulfur cycle is

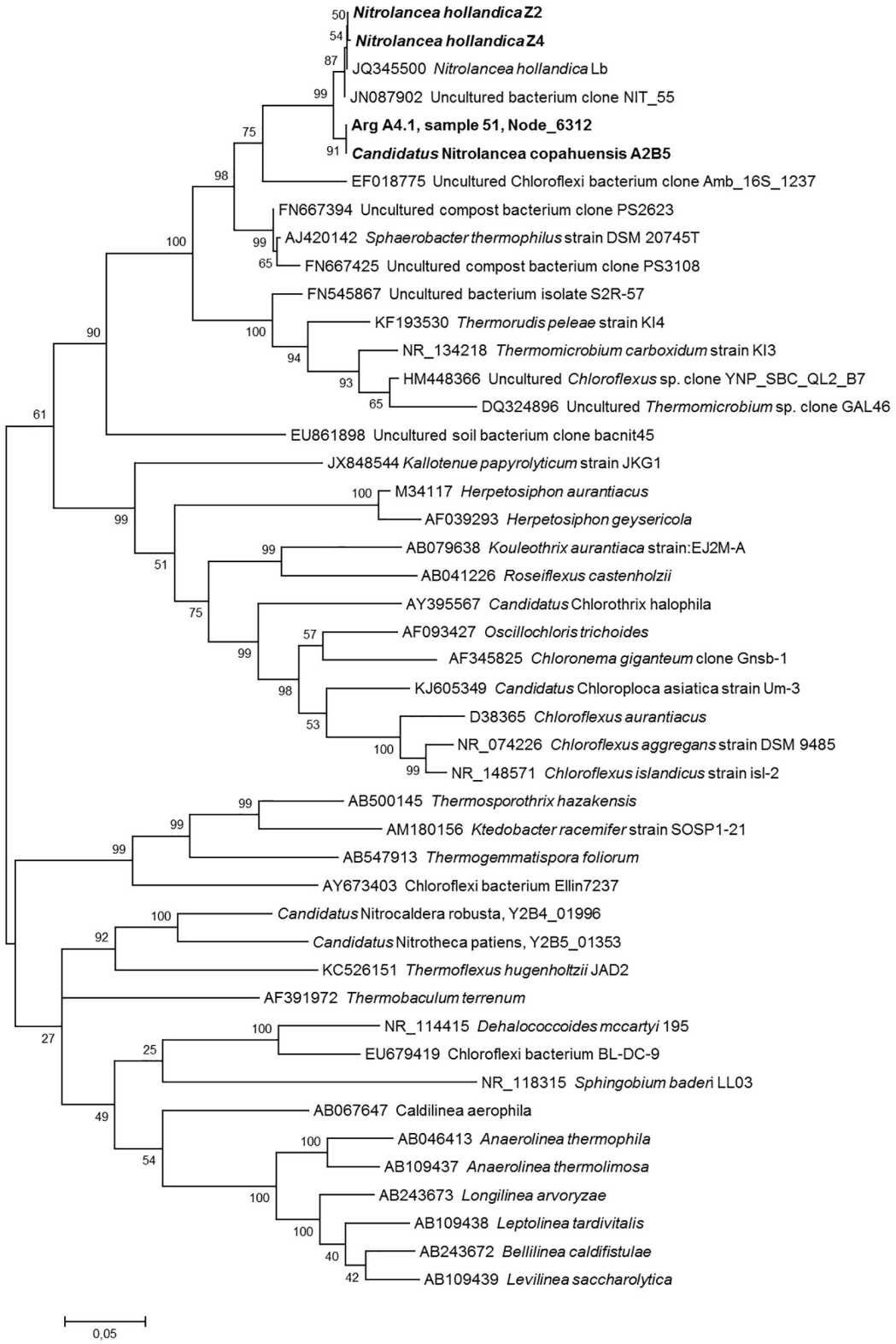

FIGURE 6 | Phylogenetic relationship of the *Nitrolancea* strains based on 16S rRNA gene sequences. Maximum likelihood tree indicating the affiliation of the 16S rRNA genes identified in the centrate treatment reactor and Argentinian enrichment cultures. Statistical branching support values based on 1000 bootstraps are indicated on the nodes. The alignment contained 1703 valid positions used for tree calculation. Sequences obtained in this study are shown in bold. The scale bar represents the expected changes per nucleotide. For designation of cultures see **Supplementary Table S2**.

TABLE 3 | Comparison of key functions predicted for the four *Nitrolancea* strains using PROKKA (Version 1.12) and the Kyoto Encyclopedia of Genes and Genomes (KEGG).

Predicted function	*Nitrolancea hollandica*	*Ca.* Nl. copahuensis A2	*Nl. hollandica* Z2	*Nl. hollandica* Z4
Heterotrophy	yes*	yes	yes	yes
Carbon fixation	Calvin cycle	Calvin cycle	Calvin cycle	Calvin cycle
Carbon monoxide dehydrogenase	yes*	yes	yes	yes
Formate dehydrogenase	yes	yes	yes	yes
Hydrogenase	yes	yes	not complete	yes
Nitrite oxidation	yes	yes	yes	yes
Assimilatory nitrite reduction	no	no	no	no
Assimilatory nitrate reduction	yes	yes	yes	yes
Sulfite oxidation	no	no	no	no
Urea degradation	no	no	no	no
Cyanate degradation	yes	yes	yes	yes
Siderophore transport	yes	yes	no	yes
Flagellum	no	no	no	no
Secretion system	Sec + Tat	Sec + Tat	Sec + Tat	Sec + Tat

**Could not be functionally confirmed (Sorokin et al., 2012).*

present (Giaveno et al., 2013; Urbieta et al., 2014) and the ability of *Nitrolancea* species to oxidize thiosulfate should be tested in further studies. The ability for cyanate degradation might provide an alternative source to generate ammonia for N-assimilation.

In conclusion, we physiologically and genomically characterized three novel representatives affiliated with the genus *Nitrolancea*, which we enriched from a centrate treatment reactor at the WWTP Hamburg-Dradenau and the geothermal area Las Máquinas in Neuquen-Argentina. One of these strains represents a new species within the genus *Nitrolancea*. We provisionally refer to this strain as, *Candidatus* Nitrolancea copahuensis' (co.pa.hu.en'sis. N.L.fem.adj. copahuensis pertaining to the Copahue region in North-Patagonia, Argentina).

The strain is a mesophilic, aerobic, chemolithoautotrophic bacterium, which stoichiometrically converts nitrite to nitrate and uses carbon dioxide as carbon source. Forms short rods with tapered ends; Gram-positive. Requires ammonium supplementation and tolerates high nitrite and ammonium concentrations. Optimum growth temperature is 35–37°C. DNA G+C content is 62.7 mol%. Originated from a hot spring in the geothermal field Las Máquinas, Neuquen-Argentina.

DATA AVAILABILITY STATEMENT

The datasets generated for this study are available in the European Nucleotide Archive (ENA) under accession numbers ERS4399870, ERS4399871, ERS4399872, ERS4647270-74, ERS4648393-96, and LR794103-5. Strain availability will be performed upon request.

AUTHOR CONTRIBUTIONS

AG performed the sampling. ES, SK, and SL designed the research. SH worked on the *Nitrolancea* enrichments. ES and KS isolated the nitrite oxidizers and performed FISH. SK did physiological experiments. DI performed genome sequencing. MS, LK, and SL analyzed the data. ES, KS, SK, LK, AG, and SL wrote the manuscript. All authors read and agreed on the final manuscript.

FUNDING

This work was funded by the Deutsche Forschungsgemeinschaft (DFG, German Research Foundation grant SP 667/7-1+2, grant SP 667/10-1+2, and grant SP 667/11-1) and Netherlands Organization for Scientific Research (Grants 016.Vidi.189.050 and SIAM Gravitation Grant 024.002.002).

ACKNOWLEDGMENTS

We thank the Government of the Province of Neuquen for allowing sampling in the protected natural area Copahue geothermal park and Edgardo Donati and Wolfgang Sand for providing samples from Las Máquinas. HSE is appreciated for the support in getting samples from Hamburg-Dradenau. Elke Woelken is acknowledged for excellent technical help in electron microscopy and Theo van Alen for sequencing. We are grateful that Katja Wendt, Kristina Detzel, Katrin Petersen as well as Laura Nissen did initial cultivation and laboratory work. We also thank Malik Alawi, Lia Burkhardt, and Kerstin Reumann for sequencing assistance.

SUPPLEMENTARY MATERIAL

The Supplementary Material for this article can be found online at: https://www.frontiersin.org/articles/10.3389/fmicb.2020.01522/full#supplementary-material

REFERENCES

Alawi, M., Lipski, A., Sanders, T., Eva-Maria-Pfeiffer, and Spieck, E. (2007). Cultivation of a novel cold-adapted nitrite oxidizing betaproteobacterium from the Siberian Arctic. *ISME J.* 1, 256–264. doi: 10.1038/ismej.2007.34

Amann, R. I., Krumholz, L., and Stahl, D. A. (1990). Fluorescent-oligonucleotide probing of whole cells for determinative, phylogenetic, and environmental studies in microbiology. *J. Bacteriol.* 172, 762–770. doi: 10.1128/jb.172.2.762-770.1990

Amann, R. I., Ludwig, W., and Schleifer, K. H. (1995). Phylogenetic identification and *in situ* detection of individual microbial cells without cultivation. *Microbiol. Rev.* 59, 143–169. doi: 10.1128/mmbr.59.1.143-169.1995

Andrews, J. H., and Harris, R. F. (1986). "r- and K-selection and microbial ecology," in *Advances in Microbial Ecology*, ed. K. C. Marshall, (Boston, MA: Springer US), 99–147. doi: 10.1007/978-1-4757-0611-6_3

APHA, AWWA, and WPCF. (1992). *Métodos Normalizados Para el Análisis de Aguas Potables y Residuales*. Madrid: Díaz de Santos, 1715.

Boddicker, A. M., and Mosier, A. C. (2018). Genomic profiling of four cultivated *Candidatus* Nitrotoga spp. predicts broad metabolic potential and environmental distribution. *ISME J.* 12, 2864–2882. doi: 10.1038/s41396-018-0240-248

Caporaso, J. G., Kuczynski, J., Stombaugh, J., Bittinger, K., Bushman, F. D., and Costello, E. K. (2010). QIIME allows analysis of high-throughput community sequencing data. *Nat. Met.* 7, 335–336. doi: 10.1038/nmeth.f.303

Caporaso, J. G., Lauber, C. L., Walters, W. A., Berg-Lyons, D., Lozupone, C. A., and Turnbaugh, P. J. (2011). Global patterns of 16S rRNA diversity at a depth of millions of sequences per sample. *Proc. Natl. Acad. Sci. U.S.A.* 108(Suppl. 1), 4516–4522. doi: 10.1073/pnas.1000080107

Chiacchiarini, P., Lavalle, L., Giaveno, A., and Donati, E. (2010). First assessment of acidophilic microorganisms from geothermal Copahue-Caviahue system. *Hydrometallurgy* 104, 334–341. doi: 10.1016/j.hydromet.2010.02.020

Chiodini, G., Cardellini, C., Lamberti, M. C., Agusto, M., Caselli, A., Liccioli, C., et al. (2015). Carbon dioxide diffuse emission and thermal energy release from hydrothermal systems at Copahue-Caviahue volcanic complex (Argentina). *J. Volcanol. Geoth. Res.* 304, 294–303. doi: 10.1016/j.jvolgeores.2015.09.007

Courtens, E. N., Spieck, E., Vilchez-Vargas, R., Bodé, S., Boeckx, P., Schouten, S., et al. (2016). A robust nitrifying community in a bioreactor at 50°C opens up the path for thermophilic nitrogen removal. *ISME J.* 10, 2293–2303. doi: 10.1038/ismej.2016.8

Daims, H., Lebedeva, E. V., Pjevac, P., Han, P., Herbold, C., Albertsen, M., et al. (2015). Complete nitrification by *Nitrospira* bacteria. *Nature* 528, 504–509. doi: 10.1038/nature16461

Dowd, S. E., Sun, Y., Secor, P. R., Rhoads, D. D., Wolcott, B. M., James, G. A., et al. (2008). Survey of bacterial diversity in chronic wounds using pyrosequencing, DGGE, and full ribosome shotgun sequencing. *BMC Microbiol.* 8:43. doi: 10.1186/1471-2180-8-43

Edwards, T. A., Calica, N. A., Huang, D. A., Manoharan, N., Hou, W., Huang, L., et al. (2013). Cultivation and characterization of thermophilic *Nitrospira* species from geothermal springs in the US Great Basin, China, and Armenia. *FEMS Microbiol. Ecol.* 85, 283–292. doi: 10.1111/1574-6941.12117

Ehrich, S., Behrens, D., Lebedeva, E., Ludwig, W., and Bock, E. (1995). A new obligately chemolithoautotrophic, nitrite-oxidizing bacterium, *Nitrospira moscoviensis* sp. nov. and its phylogenetic relationship. *Arch. Microbiol.* 164, 16–23. doi: 10.1007/bf02568729

Elliott, D. R., Thomas, A. D., Hoon, S. R., and Sen, R. (2014). Niche partitioning of bacterial communities in biological crusts and soils under grasses, shrubs and trees in the Kalahari. *Biodivers. Conserv.* 23, 1709–1733. doi: 10.1007/s10531-014-0684-688

Eren, A. M., Esen, O. C., Quince, C., Vineis, J. H., Morrison, H. G., Sogin, M. L., et al. (2015). Anvi'o: An advanced analysis and visualization platform for 'omics data. *PeerJ* 2015, e1319. doi: 10.7717/peerj.1319

Fang, W., Yan, D., Huang, B., Ren, Z., Wang, X., Liu, X., et al. (2019). Biochemical pathways used by microorganisms to produce nitrous oxide emissions from soils fumigated with dimethyl disulfide or allyl isothiocyanate. *Soil Biol. Biochem.* 132, 1–13. doi: 10.1016/j.soilbio.2019.01.019

Friedman, L., Mamane, H., Avisar, D., and Chandran, K. (2018). The role of influent organic carbon-to-nitrogen (COD/N) ratio in removal rates and shaping microbial ecology in soil aquifer treatment (SAT). *Wat. Res.* 146, 197–205. doi: 10.1016/j.watres.2018.09.014

Füssel, J., Lücker, S., Yilmaz, P., Nowka, B., van Kessel, M. A. H. J., Bourceau, P., et al. (2017). Adaptability as the key to success for the ubiquitous marine nitrite oxidizer *Nitrococcus*. *Sci. Adv.* 3:e1700807. doi: 10.1126/sciadv.1700807

Giaveno, M. A., Urbieta, M. S., Ulloa, J. R., Toril, E. G., and Donati, E. R. (2013). Physiologic versatility and growth flexibility as the main characteristics of a novel thermoacidophilic *Acidianus* strain isolated from Copahue geothermal area in Argentina. *Microb. Ecol.* 65, 336–346. doi: 10.1007/s00248-012-0129-124

Herlemann, D. P., Labrenz, M., Jürgens, K., Bertilsson, S., Waniek, J. J., and Andersson, A. F. (2011). Transitions in bacterial communities along the 2000 km salinity gradient of the Baltic Sea. *ISME J.* 5, 1571–1579. doi: 10.1038/ismej.2011.41

Ishii, K., Fujitani, H., Soh, K., Nakagawa, T., Takahashi, R., and Tsuneda, S. (2017). Enrichment and physiological characterization of a cold-adapted nitrite-oxidizing *Nitrotoga* sp. from an eelgrass sediment. *Appl. Environ. Microbiol.* 83:e00549-17. doi: 10.1128/AEM.00549-17

Kirstein, K., and Bock, E. (1993). Close genetic relationship between *Nitrobacter hamburgensis* nitrite oxidoreductase and *Escherichia coli* nitrate reductases. *Arch. Microbiol.* 160, 447–453. doi: 10.1007/BF00245305

Kitzinger, K., Koch, H., Lücker, S., Sedlacek, C. J., Herbold, C., Schwarz, J., et al. (2018). Characterization of the first "*Candidatus* Nitrotoga" isolate reveals metabolic versatility and separate evolution of widespread nitrite-oxidizing bacteria. *mBio* 9:e01186-18. doi: 10.1128/mBio.01186-18

Koch, H., Galushko, A., Albertsen, M., Schintlmeister, A., Gruber-Dorninger, C., Lücker, S., et al. (2014). Microbial metabolism: Growth of nitrite-oxidizing bacteria by aerobic hydrogen oxidation. *Science* 345, 1052–1054. doi: 10.1126/science.1256985

Koch, H., Lücker, S., Albertsen, M., Kitzinger, K., Herbold, C., Spieck, E., et al. (2015). Expanded metabolic versatility of ubiquitous nitrite-oxidizing bacteria from the genus *Nitrospira*. *Proc. Natl. Acad. Sci. U.S.A.* 112, 11371–11376. doi: 10.1073/pnas.1506533112

Kolmert, A., Wikström, P., and Hallberg, K. (2000). A fast and simple turbidimetric method for the determination of sulfate in sulfate-reducing bacterial cultures. *J. Microbiol. Meth.* 41, 179–184. doi: 10.1016/S0167-7012(00)00154-158

Koops, H.-P., and Pommerening-Röser, A. (2005). "The lithoautotrophic ammonia-oxidizing bacteria," in *Bergey's Manual of Systematic Bacteriology*, eds D. J. Brenner, N. R. Krieg, J. T. Staley, and G. M. Garrity, (Boston, MA: Springer), 778–811. doi: 10.1007/0-387-28021-9_18

Krümmel, A., and Harms, H. (1982). Effect of organic matter on growth and cell yield of ammonia-oxidizing bacteria. *Arch. Microbiol.* 133, 50–54. doi: 10.1007/bf00943769

Kruse, M., Zumbrägel, S., Bakker, E., Spieck, E., Eggers, T., and Lipski, A. (2013). The nitrite-oxidizing community in activated sludge from a municipal wastewater treatment plant determined by fatty acid methyl ester-stable isotope probing. *Syst. Appl. Microbiol.* 36, 517–524. doi: 10.1016/j.syapm.2013.06.007

Kumar, S., Stecher, G., Li, M., Knyaz, C., and Tamura, K. (2018). MEGA X: Molecular evolutionary genetics analysis across computing platforms. *Mol. Biol. Evol.* 35, 1547–1549. doi: 10.1093/molbev/msy096

Lebedeva, E. V., Alawi, M., Fiencke, C., Namsaraev, B., Bock, E., and Spieck, E. (2005). Moderately thermophilic nitrifying bacteria from a hot spring of the Baikal rift zone. *FEMS Microbiol. Ecol.* 54, 297–306. doi: 10.1016/j.femsec.2005.04.010

Lebedeva, E. V., Alawi, M., Maixner, F., Jozsa, P. G., Daims, H., and Spieck, E. (2008). Physiological and phylogenetic characterization of a novel lithoautotrophic nitrite-oxidizing bacterium, "*Candidatus* Nitrospira bockiana. *Int. J. Syst. Evol. Microbiol.* 58, 242–250. doi: 10.1099/ijs.0.65379-65370

Lebedeva, E. V., Off, S., Zumbrägel, S., Kruse, M., Shagzhina, A., Lücker, S., et al. (2011). Isolation and characterization of a moderately thermophilic nitrite-oxidizing bacterium from a geothermal spring. *FEMS Microbiol. Ecol.* 75, 195–204. doi: 10.1111/j.1574-6941.2010.01006.x

Lee, I., Kim, Y. O., Park, S. C., and Chun, J. (2016). OrthoANI: an improved algorithm and software for calculating average nucleotide identity. *Int. J. Syst. Evol. Microbiol.* 66, 1100–1103. doi: 10.1099/ijsem.0.000760

Li, H. (2018). Minimap2: Pairwise alignment for nucleotide sequences. *Bioinformatics* 34, 3094–3100. doi: 10.1093/bioinformatics/bty191

Li, H., and Durbin, R. (2009). Fast and accurate short read alignment with Burrows-Wheeler transform. *Bioinformatics* 25, 1754–1760. doi: 10.1093/bioinformatics/btp324

Li, H., Handsaker, B., Wysoker, A., Fennell, T., Ruan, J., Homer, N., et al. (2009). The Sequence Alignment/Map format and SAMtools. *Bioinformatics* 25, 2078–2079. doi: 10.1093/bioinformatics/btp352

Lücker, S., Nowka, B., Rattei, T., Spieck, E., and Daims, H. (2013). The genome of *Nitrospina gracilis* illuminates the metabolism and evolution of the major marine nitrite oxidizer. *Front. Microbiol.* 4:27. doi: 10.3389/fmicb.2013.00027

Lücker, S., Wagner, M., Maixner, F., Pelletier, E., Koch, H., Vacherie, B., et al. (2010). A *Nitrospira* metagenome illuminates the physiology and evolution of globally important nitrite-oxidizing bacteria. *Proc. Natl. Acad. Sci. U.S.A.* 107, 13479–13484. doi: 10.1073/pnas.1003860107

Lüke, C., Speth, D. R., Kox, M. A. R., Villanueva, L., and Jetten, M. S. M. (2016). Metagenomic analysis of nitrogen and methane cycling in the Arabian Sea oxygen minimum zone. *PeerJ* 4:e1924. doi: 10.7717/peerj.1924

Manz, W., Amann, R., Ludwig, W., Wagner, M., and Schleifer, K. H. (1992). Phylogenetic oligodeoxynucleotide probes for the major subclasses of *proteobacteria*: problems and solutions. *Syst. Appl. Microbiol.* 15, 593–600. doi: 10.1016/s0723-2020(11)80121-9

Marks, C. R., Stevenson, B. S., Rudd, S., and Lawson, P. A. (2012). *Nitrospira*-dominated biofilm within a thermal artesian spring: a case for nitrification-driven primary production in a geothermal setting. *Geobiology* 10, 457–466. doi: 10.1111/j.1472-4669.2012.00335.x

Merodio, J. C., and Martínez, J. M. (1985). Análisis químico de componentes mayoritarios en rocas silicatadas. *Rev. Asoc. Argentina Mineral. Petrol.* 16, 7–16.

Ngugi, D. K., Blom, J., Stepanauskas, R., and Stingl, U. (2016). Diversification and niche adaptations of *Nitrospina*-like bacteria in the polyextreme interfaces of Red Sea brines. *ISME J.* 10, 1383–1399. doi: 10.1038/ismej.2015.214

Nikolenko, S. I., Korobeynikov, A. I., and Alekseyev, M. A. (2013). BayesHammer: Bayesian clustering for error correction in single-cell sequencing. *BMC Genomics* 14:S7. doi: 10.1186/1471-2164-14-S1-S7

Notredame, C., Higgins, D. G., and Heringa, J. (2000). T-coffee: A novel method for fast and accurate multiple sequence alignment. *J. Mol. Biol.* 302, 205–217. doi: 10.1006/jmbi.2000.4042

Nowka, B., Daims, H., and Spieck, E. (2015). Comparison of oxidation kinetics of nitrite-oxidizing bacteria: Nitrite availability as a key factor in niche differentiation. *Appl. Environ. Microbiol.* 81, 745–753. doi: 10.1128/AEM.02734-2714

Nurk, S., Meleshko, D., Korobeynikov, A., and Pevzner, P. A. (2017). MetaSPAdes: A new versatile metagenomic assembler. *Genome Res.* 27, 824–834. doi: 10.1101/gr.213959.116

Off, S., Alawi, M., and Spieck, E. (2010). Enrichment and physiological characterization of a novel *Nitrospira*-like bacterium obtained from a marine sponge. *Appl. Environ. Microbiol.* 76, 4640–4646. doi: 10.1128/AEM.03095-3099

Orlando, J., Alfaro, M., Bravo, L., Guevara, R., and Carú, M. (2010). Bacterial diversity and occurrence of ammonia-oxidizing bacteria in the Atacama Desert soil during a "desert bloom" event. *Soil Biol. Biochem.* 42, 1183–1188. doi: 10.1016/j.soilbio.2010.03.025

Palomo, A., Pedersen, A. G., Fowler, S. J., Dechesne, A., Sicheritz-Pontén, T., and Smets, B. F. (2018). Comparative genomics sheds light on niche differentiation and the evolutionary history of comammox *Nitrospira*. *ISME J.* 12, 1779–1793. doi: 10.1038/s41396-018-0083-83

Parks, D. H., Chuvochina, M., Waite, D. W., Rinke, C., Skarshewski, A., Chaumeil, P. A., et al. (2018). A standardized bacterial taxonomy based on genome phylogeny substantially revises the tree of life. *Nat. Biotechnol.* 36:996. doi: 10.1038/nbt.4229

Parks, D. H., Imelfort, M., Skennerton, C. T., Hugenholtz, P., and Tyson, G. W. (2015). CheckM: Assessing the quality of microbial genomes recovered from isolates, single cells, and metagenomes. *Genome Res.* 25, 1043–1055. doi: 10.1101/gr.186072.114

Pester, M., Maixner, F., Berry, D., Rattei, T., Koch, H., Lücker, S., et al. (2014). NxrB encoding the beta subunit of nitrite oxidoreductase as functional and phylogenetic marker for nitrite-oxidizing *Nitrospira*. *Environ. Microbiol.* 16, 3055–3071. doi: 10.1111/1462-2920.12300

Philips, S., Laanbroek, H. J., and Verstraete, W. (2002). Origin, causes and effects of increased nitrite concentrations in aquatic environments. *Rev. Environ. Sci. Biotechnol.* 1, 115–141. doi: 10.1023/A:1020892826575

Price, G. D., Badger, M. R., Woodger, F. J., and Long, B. M. (2008). Advances in understanding the cyanobacterial CO2-concentrating-mechanism (CCM): functional components, Ci transporters, diversity, genetic regulation and prospects for engineering into plants. *J. Exp. Bot.* 59, 1441–1461. doi: 10.1093/jxb/erm112

Rachel, R., Pum, D., Šmarda, J., Šmajs, D., Komrska, J., Krzyzánek, V., et al. (1997). II. Fine structure of S-layers. *FEMS Microbiol. Rev.* 20, 13–23. doi: 10.1111/j.1574-6976.1997.tb00302.x

Ritz, C., Baty, F., Streibig, J. C., and Gerhard, D. (2015). Dose-response analysis using R. *PLoS One* 10:e0146021. doi: 10.1371/journal.pone.0146021

Rodriguez-R, L. M., and Konstantinidis, K. T. (2016). The enveomics collection: a toolbox for specialized analyses of microbial genomes and metagenomes. *PeerJ* 4:e1900v1.

Schmidt, E. L., and Belser, L. W. (1994). "Autotrophic nitrifying bacteria," in *Methods of Soil Analysis*, eds B. P. Weaver, and J. S. Angle, (Madison, WI: Soil Science Society of America), 159–177. doi: 10.2136/sssabookser5.2.c10

Seemann, T. (2014). Prokka: Rapid prokaryotic genome annotation. *Bioinformatics* 30, 2068–2069. doi: 10.1093/bioinformatics/btu153

Sorokin, D. Y., Lücker, S., and Daims, H. (2018). "Nitrolancea," in *Bergey's manual of systematics of Archaea and Bacteria*, eds W. B. Whitman, F. Rainey, P. Kämpfer, M. Trujillo, J. Chun, P. DeVos, et al. (Hoboken, NJ: Wiley), 1–6. doi: 10.1002/9781118960608.gbm01563

Sorokin, D. Y., Lücker, S., Vejmelkova, D., Kostrikina, N. A., Kleerebezem, R., Rijpstra, W. I. C., et al. (2012). Nitrification expanded: discovery, physiology and genomics of a nitrite-oxidizing bacterium from the phylum *Chloroflexi*. *ISME J.* 6, 2245–2256. doi: 10.1038/ismej.2012.70

Sorokin, D. Y., Vejmelkova, D., Lücker, S., Streshinskaya, G. M., Rijpstra, W. I. C., Sinninghe Damsté, J. S., et al. (2014). *Nitrolancea hollandica* gen. nov., sp. nov., a chemolithoautotrophic nitrite-oxidizing bacterium isolated from a bioreactor belonging to the phylum Chloroflexi. *Int. J. Syst. Evol. Microbiol.* 64, 1859–1865. doi: 10.1099/ijs.0.062232-62230

Speirs, L. B. M., Rice, D. T. F., Petrovski, S., and Seviour, R. J. (2019). The phylogeny, biodiversity, and ecology of the *Chloroflexi* in activated sludge. *Front. Microbiol.* 10:2015. doi: 10.3389/fmicb.2019.02015

Spieck, E., Aamand, J., Bartosch, S., and Bock, E. (1996). Immunocytochemical detection and location of the membrane-bound nitrite oxidoreductase in cells of *Nitrobacter* and *Nitrospira*. *FEMS Microbiol. Lett.* 139, 71–76. doi: 10.1111/j.1574-6968.1996.tb08181.x

Spieck, E., and Bock, E. (2005). "The lithoautotrophic nitrite-oxidizing bacteria," in *Bergey's Manual of Systematic Bacteriology*, eds D. J. Brenner, N. R. Krieg, J. T. Staley, and G. M. Garrity, (Boston, MA: Springer), 149–153. doi: 10.1007/0-387-28021-9_19

Spieck, E., Ehrich, S., Aamand, J., and Bock, E. (1998). Isolation and immunocytochemical location of the nitrite-oxidizing system in *Nitrospira moscoviensis*. *Arch. Microbiol.* 169, 225–230. doi: 10.1007/s002030050565

Spieck, E., and Lipski, A. (2011). "Cultivation, growth physiology, and chemotaxonomy of nitrite-oxidizing bacteria," in *Methods in Enzymology*, ed. M. G. Klotz, (Burlington: Academic Press), 109–130. doi: 10.1016/b978-0-12-381294-0.00005-5

Spieck, E., Spohn, M., Wendt, K., Bock, E., Shively, J., Frank, J., et al. (2020). Extremophilic nitrite-oxidizing *Chloroflexi* from Yellowstone hot springs. *ISME J.* 14, 364–379. doi: 10.1038/s41396-019-0530-539

Stackebrandt, E., and Ebers, J. (2006). Taxonomic parameters revisited: Tarnished gold standards. *Microbiol. Today* 33, 152–155.

Starkenburg, S. R., Larimer, F. W., Stein, L. Y., Klotz, M. G., Chain, P. S., Sayavedra-Soto, L. A., et al. (2008). Complete genome sequence of *Nitrobacter hamburgensis* X14 and comparative genomic analysis of species within the genus *Nitrobacter*. *Appl. Environ. Microbiol.* 74, 2852–2863. doi: 10.1128/AEM.02311-2317

Stieglmeier, M., Alves, R. J. E., and Schleper, C. (2014). "The phylum Thaumarchaeota," in *The Prokaryotes: Other major lineages of Bacteria and the Archaea*, eds E. Rosenberg, E. F. DeLong, S. Lory, E. Stackebrandt, and F. Thompson, (Berlin: Springer), 347–362. doi: 10.1007/978-3-642-38954-2_338

Sun, X., Kop, L. F. M., Lau, M. C. Y., Frank, J., Jayakumar, A., Lücker, S., et al. (2019). Uncultured *Nitrospina*-like species are major nitrite oxidizing bacteria

in oxygen minimum zones. *ISME J.* 13, 2391–2402. doi: 10.1038/s41396-019-0443-447

Urbieta, M. S., González-Toril, E., Bazán, ÁA., Giaveno, M. A., and Donati, E. (2015a). Comparison of the microbial communities of hot springs waters and the microbial biofilms in the acidic geothermal area of Copahue (Neuquén, Argentina). *Extremophiles* 19, 437–450. doi: 10.1007/s00792-015-0729-722

Urbieta, M. S., Porati, G., Segretín, A., González-Toril, E., Giaveno, M., and Donati, E. (2015b). Copahue geothermal system: A volcanic environment with rich extreme prokaryotic biodiversity. *Microorganisms* 3, 344–363. doi: 10.3390/microorganisms3030344

Urbieta, M. S., González Toril, E., Aguilera, A., Giaveno, M. A., and Donati, E. (2012). First prokaryotic biodiversity assessment using molecular techniques of an acidic river in Neuquén, Argentina. *Microb. Ecol.* 64, 91–104. doi: 10.1007/s00248-011-9997-9992

Urbieta, M. S., Toril, E. G., Alejandra Giaveno, M., Bazán, ÁA., and Donati, E. R. (2014). Archaeal and bacterial diversity in five different hydrothermal ponds in the Copahue region in Argentina. *Syst. Appl. Microbiol.* 37, 429–441. doi: 10.1016/j.syapm.2014.05.012

van Kessel, M. A. H. J., Speth, D. R., Albertsen, M., Nielsen, P. H., Op Den Camp, H. J. M., Kartal, B., et al. (2015). Complete nitrification by a single microorganism. *Nature* 528, 555–559. doi: 10.1038/nature16459

Vejmelkova, D., Sorokin, D. Y., Abbas, B., Kovaleva, O. L., Kleerebezem, R., Kampschreur, M. J., et al. (2012). Analysis of ammonia-oxidizing bacteria dominating in lab-scale bioreactors with high ammonium bicarbonate loading. *Appl. Microbiol. Biotechnol.* 93, 401–410. doi: 10.1007/s00253-011-3409-x

Wallner, G., Amann, R., and Beisker, W. (1993). Optimizing fluorescent in situ hybridization with rRNA-targeted oligonucleotide probes for flow cytometric identification of microorganisms. *Cytometry* 14, 136–143. doi: 10.1002/cyto.990140205

Wang, B., Wang, Z., Wang, S., Qiao, X., Gong, X., Gong, Q., et al. (2020). Recovering partial nitritation in a PN/A system during mainstream wastewater treatment by reviving AOB activity after thoroughly inhibiting AOB and NOB with free nitrous acid. *Environ. Int.* 139:105684. doi: 10.1016/j.envint.2020.105684

Wegen, S., Nowka, B., and Spieck, E. (2019). Low temperature and neutral pH define "*Candidatus* Nitrotoga sp." *as a competitive nitrite oxidizer in coculture with Nitrospira defluvii*. *Appl. Environ. Microbiol.* 85:e02569-18. doi: 10.1128/AEM.02569-2518

Widdel, F., and Bak, F. (1991). "Gram-negative mesophilic sulfate-reducing bacteria," in *The Prokaryotes: a Handbook on the Biology of Bacteria*, eds A. Balows, H. G. Trüper, M. Dworkin, W. Harder, and K. H. Schleifer, (New York, NY: Springer), 3352–3379. doi: 10.1007/978-1-4757-2191-1_21

Willis Poratti, G., Yaakop, A. S., Chan, C. S., Urbieta, M. S., Chan, K. G., Ee, R., et al. (2016). Draft genome sequence of the sulfate-reducing bacterium *Desulfotomaculum copahuensis* strain CINDEFI1 isolated from the geothermal Copahue system, Neuquén, Argentina. *Genome Announc.* 4:e00870-16. doi: 10.1128/genomeA.00870-816

Xu, L., Dong, Z., Fang, L., Luo, Y., Wei, Z., Guo, H., et al. (2019). OrthoVenn2: a web server for whole-genome comparison and annotation of orthologous clusters across multiple species. *Nucleic Acids Res.* 47, W52–W58. doi: 10.1093/nar/gkz333

Yu, H., Meng, W., Song, Y., and Tian, Z. (2018). Understanding bacterial communities of partial nitritation and nitratation reactors at ambient and low temperature. *Chem. Eng. J.* 337, 755–763. doi: 10.1016/j.cej.2017.10.120

Yu, H., Tian, Z., Zuo, J., and Song, Y. (2020). Enhanced nitrite accumulation under mainstream conditions by a combination of free ammonia-based sludge treatment and low dissolved oxygen: reactor performance and microbiome analysis. *RSC Adv.* 10, 2049–2059. doi: 10.1039/C9RA07628J

Zhang, J., Sun, Z., Zhong, X., Huang, Y., Tan, L., Tang, Y., et al. (2016). Maturity and microbial community structure dynamics during simulated windrow composting of solid fraction of dairy manure. *Chin. J. Appl. Environ. Biol.* 22, 423–429.

Conflict of Interest: The authors declare that the research was conducted in the absence of any commercial or financial relationships that could be construed as a potential conflict of interest.

frontiers in Microbiology

ORIGINAL RESEARCH
published: 22 July 2020
doi: 10.3389/fmicb.2020.01737

Enrichment of Comammox and Nitrite-Oxidizing *Nitrospira* From Acidic Soils

*Yu Takahashi[1], Hirotsugu Fujitani[2], Yuhei Hirono[3], Kanako Tago[4], Yong Wang[4], Masahito Hayatsu[4] and Satoshi Tsuneda[1]**

[1] Department of Life Science and Medical Bioscience, School of Advanced Science and Engineering, Waseda University, Tokyo, Japan, [2] Department of Biological Sciences, Faculty of Science and Engineering, Chuo University, Tokyo, Japan, [3] Institute of Fruit Tree and Tea Science, National Agriculture and Food Research Organization (NARO), Shimada, Japan, [4] Institute for Agro-Environmental Sciences, National Agriculture and Food Research Organization (NARO), Tsukuba, Japan

In agricultural soils fertilized with a high amount of ammonium nitrogen, the pH decreases because of the oxidation of ammonia by nitrifiers. Molecular-based analyses have revealed that members of the genus *Nitrospira* dominate over other nitrifiers in some acidic soils. However, terrestrial *Nitrospira* are rarely cultivated and little is known about their ecophysiology. In addition, recent studies discovered a single microbe with the potential to oxidize both ammonia and nitrite (complete ammonia oxidizer; comammox) within *Nitrospira*, which had been previously recognized as a nitrite oxidizer. Despite their broad distribution, there are no enrichment samples of comammox from terrestrial or acidic environments. Here, we report the selective enrichment of both comammox and nitrite-oxidizing *Nitrospira* from the acidic soil of a heavily fertilized tea field. Long-term enrichment was performed with two individual continuous-feeding bioreactors capable of controlling ammonia or nitrite concentration and pH. We found that excessive ammonium supply was a key factor to enhance the growth of comammox *Nitrospira* under acidic conditions. Additionally, a low concentration of nitrite was fed to prevent the accumulation of free nitrous acid and inhibition of cell growth under low pH, resulting in the selective enrichment of nitrite-oxidizing *Nitrospira*. Based on 16S rRNA gene analysis, *Nitrospira* accounting for only 1.2% in an initial soil increased to approximately 80% of the total microorganisms in both ammonia- and nitrite-fed bioreactors. Furthermore, *amoA* amplicon sequencing revealed that two phylotypes belonging to comammox clade A were enriched in an ammonia-fed bioreactor. One group was closely related to previously cultivated strains, and the other was classified into a different cluster consisting of only uncultivated representatives. These two groups coexisted in the bioreactor controlled at pH 6.0, but the latter became dominant after the pH decreased to 5.5. Additionally, a physiological experiment revealed that the enrichment sample oxidizes ammonia at pH <4, which is in accordance with the strongly acidic tea field soil; this value is lower than the active pH range of isolated acid-adapted nitrifiers. In conclusion, we successfully enriched multiple phylotypes of comammox and nitrite-oxidizing *Nitrospira* and revealed that the pH and concentrations of protonated N-compounds were potential niche determinants.

Keywords: acidic soil, nitrifying bacteria, nitrification, *Nitrospira*, comammox, cultivation, enrichment, low pH

OPEN ACCESS

Edited by:
Laura E. Lehtovirta-Morley, University of East Anglia, United Kingdom

Reviewed by:
Baozhan Wang, Nanjing Normal University, China
Aqiang Ding, Chongqing University, China

****Correspondence:***
Satoshi Tsuneda
stsuneda@waseda.jp

Specialty section:
This article was submitted to Microbial Physiology and Metabolism, a section of the journal Frontiers in Microbiology

Received: *25 March 2020*
Accepted: *02 July 2020*
Published: *22 July 2020*

Citation:
Takahashi Y, Fujitani H, Hirono Y, Tago K, Wang Y, Hayatsu M and Tsuneda S (2020) Enrichment of Comammox and Nitrite-Oxidizing Nitrospira From Acidic Soils. Front. Microbiol. 11:1737. doi: 10.3389/fmicb.2020.01737

INTRODUCTION

Nitrification is an important reaction composing the global nitrogen cycle. In soil ecosystems, nitrification acts as a production route of nitrate, a nitrogen source of soil plants. Despite the importance of nitrification, supplementation with excessive nitrogen fertilizers over-activates nitrification and induces environmental problems. Too much nitrate produced by nitrification leaches into groundwater, causing pollution and the economic loss of fertilizers (Schlesinger, 2009). Furthermore, excessive nitrification also causes the release of nitrous oxide, a greenhouse gas (Wrage et al., 2001) and soil acidification (Vitousek et al., 1997). In particular, acidic soils (defined as pH <5.5) are known to show the same or higher nitrification rate as neutral soils (Booth et al., 2005). Moreover, soils with lower pH were reported to generate more nitrous oxide (Mørkved et al., 2007; Liu et al., 2010; Bakken et al., 2012).

Traditionally, nitrification had been thought to consist of two independent steps: ammonia oxidation (NH_3 to NO_2^-) and nitrite oxidation (NO_2^- to NO_3^-). The first step is catalyzed by ammonia-oxidizing bacteria (AOB) and ammonia-oxidizing archaea (AOA), while the second step is carried out by nitrite-oxidizing bacteria (NOB). Molecular approaches revealed that AOA predominated among ammonia oxidizers in soils (Leininger et al., 2006) including acidic soils (Nicol et al., 2008; Zhang et al., 2012). In addition, a strain of acidophilic AOA, "*Candidatus* Nitrosotalea devanaterra" was isolated from acidic soil (Lehtovirta-Morley et al., 2011) and physiologically characterized (Lehtovirta-Morley et al., 2014). Although these studies supported the importance of AOA in nitrification in acidic soils, AOB was reported to outnumber AOA in some acidic soils (Long et al., 2012; Petersen et al., 2012; Wertz et al., 2012). Furthermore, a strain of acid-tolerant AOB, "*Candidatus* Nitrosoglobus terrae" was isolated from the acidic soil of a tea field (Hayatsu et al., 2017). This study proved that the phylogenetically novel AOB classified into *Gammaproteobacteria* were more abundant than other ammonia oxidizers in some tea fields (Hayatsu et al., 2017). In contrast, for acidophilic NOB, *Nitrobacter* sp. Io acid was isolated from acidic forest soil (Hankinson and Schmidt, 1988). All of the acid-tolerant isolates of NOB were classified into the genus *Nitrobacter*: *Nitrobacter* sp. Io acid (Hankinson and Schmidt, 1988), *Nitrobacter winogradskyi* (Bock and Heinrich, 1969), and *Nitrobacter* strain NHB1, co-cultured with AOB (De Boer et al., 1991). However, *Nitrospira*, a different genus of NOB, outnumbers *Nitrobacter* in other acidic soils (Wertz et al., 2012; Stempfhuber et al., 2017). Moreover, in several studies cultivating samples from wastewater treatment plants and soilless medium-based horticulture systems, *Nitrospira* became dominant in acidic cultures at pH <5 (Tarre and Green, 2004; Cytryn et al., 2012). Although these cultures were not from soils, such previous reports support that uncultivated *Nitrospira* could contribute to nitrification in acidic environments.

Recent studies found a complete ammonia oxidizer (comammox) in the genus *Nitrospira*; this novel bacterium oxidizes both ammonia and nitrite in a single cell (Daims et al., 2015; van Kessel et al., 2015). Comammox *Nitrospira* is phylogenetically diverse and separated into two sister clades named as clade A and B, based on ammonia monooxygenase subunit A (*amoA*) gene sequence (Daims et al., 2015). Since this discovery, many studies have investigated the potential metabolisms and environmental distributions of comammox based on molecular biological techniques such as metagenomics (Palomo et al., 2016, 2018; Bartelme et al., 2017; Camejo et al., 2017; Wang et al., 2017; Orellana et al., 2018). Based on these metagenomic datasets, quantitative PCR primers targeting comammox were designed (Pjevac et al., 2017). In a study using this primer set, comammox was reported to be the most dominant in nitrifying bacteria communities in acidic soils at pH 4.0–7.0 (Hu and He, 2017). While the importance of comammox and nitrite-oxidizing *Nitrospira* in acidic soils has been clarified as described above, cultivation of these bacteria has hardly been attempted. Only one study obtained an isolate of comammox, *Nitrospira inopinata*, from a biofilm sustained in thermal waters at pH 7.5 (Daims et al., 2015; Dimitri et al., 2017). Also, "*Candidatus* Nitrospira nitrosa" and "*Candidatus* Nitrospira nitrificans" were enriched from a recirculation aquaculture system biofilter in a sequencing batch reactor operated at pH 6.99 (van Kessel et al., 2015). Other culture samples of comammox were obtained from wastewater treatment plants (Camejo et al., 2017; Roots et al., 2019) nitrifying granules (Fujitani et al., 2013), and river sediments (Yu et al., 2018). On the basis of these cultivation researches and genomic studies, physiological and biochemical characteristics of comammox *Nitrospira* have been speculated. Comammox *Nitrospira* is presumed to have advantage over other nitrifiers under low dissolved oxygen concentration and adapted to slow growth in oligotrophic environments (Koch et al., 2019). However, all the comammox cultures were incubated with a neutral or alkaline medium. For this reason, culture samples allowing the study of the acid-adaptation and ecology of comammox *Nitrospira* in acidic soils have not been obtained yet.

In this study, we focused on the cultivation of comammox and nitrite-oxidizing *Nitrospira* from acidic soils. The soil sample was collected from a tea field. Tea fields are supplemented with higher amount of N fertilizer than typical croplands and the excessive fertilization causes N-related problems, such as nitrate leaching (Hirono et al., 2009), soil acidification, and N_2O production (Tokuda and Hayatsu, 2004). Using two types of bioreactors, we enriched both comammox and nitrite-oxidizing *Nitrospira* at pH 5.5. During a long-term enrichment process over 2 years, the microbial community was analyzed by 16S rRNA gene and *amoA* gene amplicon sequencing. Furthermore, ammonia oxidation activity tests using the enrichment samples were performed to investigate adaptation to different pH and ammonia concentrations.

MATERIALS AND METHODS

Soil Samples

Following our previous study (Hayatsu et al., 2017) soil samples were collected in August 2017 from tea field plots supplemented with N fertilizer of 506 kg N ha^{-1} $year^{-1}$ at Kanaya Tea Research

Station, Institute of Fruit Tree and Tea Science, NARO, in Japan (34°48′28.2″N 138°07′55.9″E). Soil samples were immediately stored at −80°C or 4°C. Molecular analyses were performed on the samples stored at −80°C. The characteristics of the soils are shown in **Supplementary Table S1**. Samples stored at 4°C were used for incubation within a month of sampling.

Continuous-Feeding Incubation

Following our previous research (Fujitani et al., 2013) two types of continuous-feeding bioreactors were set up to selectively enrich comammox and nitrite-oxidizing *Nitrospira*. A 13 g soil sample was suspended in an inorganic medium and incubated in batch culture. As biomass carriers for soil bacteria, non-woven fabrics were sunk in the medium. To attach the biomass to the non-woven fabrics, the suspended soil sample was statically incubated without exchanging the medium. The pH in the medium was manually kept under 6.0 and the concentration of NH_4Cl in the medium was kept under 0.4 mM. After pre-incubation for a month, the non-woven fabrics and supernatant in the batch culture were transferred to a bioreactor. Subsequently, inorganic medium containing NH_4Cl was continuously supplied into the continuous-feeding bioreactor (day 0 of continuous-feeding incubation). The biomass was maintained on the non-woven fabrics to prevent microorganisms to be washed out from the bioreactor. On day 25, part of the biomass in the NH_4Cl-fed bioreactor was transplanted to the other bioreactor, and a medium containing $NaNO_2$ was supplied continuously.

The components of inorganic medium supplied into the NH_4Cl-fed and $NaNO_2$-fed bioreactors are shown in **Supplementary Tables S2, S3**, respectively. The capacity of both bioreactors was 1.0 L and the inorganic media were supplied at a rate of 3.0 L day^{-1}. The bioreactors were operated in a dark room maintained at 23°C and were supplied with excess oxygen by aeration. The inorganic media and pH adjustment chemicals were supplied by tubing pumps (ATTO Co., Tokyo, Japan) into the bioreactors. The influx of pH adjustment chemicals was automatically operated by digital pH controllers (Nissin Rika Co., Tokyo, Japan), which are able to measure the pH values in the bioreactors and control the flux in real time. $NaHCO_3$ and HCl were used as pH adjustment chemicals for the NH_4Cl- and $NaNO_2$-fed bioreactors, respectively.

During continuous-feeding incubation of the NH_4Cl-fed bioreactor, the NH_4Cl concentration in the supplied medium increased in a stepwise way from 0.07 to 0.14, 0.71, 1.4, 2.1, 7.1, 18, 29, 39, and 50 mM (day 0–206). The inflow NH_4Cl concentration was determined, following our previous study (Hayatsu et al., 2017). From day 206 to the end of the experiment, the concentration was maintained at 50 mM. The pH in the NH_4Cl-fed bioreactor was controlled at pH 6.0 ± 0.2 from day 0 to 373. On day 374, after the stable nitrification was observed at pH 6.0, the pH value was decreased to 5.5 ± 0.2, and kept a constant level until the end of the experiment. Likewise, the concentration of $NaNO_2$ in the medium supplied into the $NaNO_2$-fed bioreactor was increased in a stepwise manner from 0.07 to 0.14, 0.29, 0.43, 0.71, 1.8, 2.9, and 3.9 mM (day 25–150), following our previous research (Fujitani et al., 2013). Thereafter, the concentration was maintained for a while, but was again reduced from 3.9 to 1.8, 0.71, and 0.36 mM at last from day 310 to 387 to reduce the stress on the biomass. The pH in the $NaNO_2$-fed bioreactor was controlled at pH 6.0 ± 0.2 from day 0 to 303. The pH value was decreased to 5.5 ± 0.2 on day 304 and kept at a constant level until the end of the experiment.

Chemical Analyses During Continuous-Feeding Incubation

For each culture condition, the culture solution in each bioreactor was collected and sterilized by passing through 0.22 μm polyethersulfone membrane filters (Millipore, Eschborn, Germany). These solution samples were stored at −20°C until chemical analyses to measure the total ammonia–nitrogen (NH_4^+ + NH_3), nitrite–nitrogen (NO_2^-–N), and nitrate–nitrogen (NO_3^-–N) concentrations. The total ammonia–nitrogen concentration was measured using the indophenol blue method (Kandeler and Gerber, 1988) with a PowerWave HT microplate spectrophotometer (BioTek Instruments Inc., Winooski, VT, United States) using the absorbance at 630 nm as an index. The nitrite–nitrogen and nitrate–nitrogen concentrations were measured using an IC-2010 ion chromatography system (Tosoh Co., Tokyo, Japan). Based on the measured values, the concentrations of free ammonia (NH_3) and free nitrite (HNO_2) were calculated according to the method of a previous study (Anthonisen et al., 1976).

Microscopic Observation

The cell suspensions were collected from non-woven fabrics in bioreactors on days 84, 228, 319, and 791. The samples were fixed and stored at −20°C until observation. The fixed samples were sonicated with a Q55 homogenizer (Qsonica LLC., Newtown, CT, United States) at 20% amplitude for 30 s to disperse bacterial aggregates. The sonicated samples were dropped onto slide glasses and stained using fluorescence *in situ* hybridization (FISH) as described in a previous study (Amann et al., 1990). Oligonucleotide probes binding specifically to 16S rRNA of *Nitrospira* lineage II, *Nitrospira* lineage I, *Nitrobacter*, and betaproteobacterial AOB were labeled with hydrophilic sulfoindocyanine dye (Cy3) (**Supplementary Table S4**). These probes were added to the slide glasses and hybridized at 46°C for 2.5 h. Furthermore, all bacteria were stained with SYTOX Green nucleic acid stain (Life Technologies, Carlsbad, CA, United States). The stained samples were observed with an Axioskop 2 Plus fluorescence microscope (Carl Zeiss, Oberkochen, Germany).

DNA Extraction

Genomic DNA was extracted from the initial soil samples used for cultivation and cell suspensions collected from the bioreactors. The extraction was performed using the FastDNA SPIN Kit for Soil (MP Biomedicals, Irvine, CA, United States) according to the protocol of the manufacturer. The extracted DNA was stored at −20°C until amplicon sequencing.

Amplicon Sequencing of 16S rRNA Gene and *amoA* Gene

Amplicon sequencing targeting the variable regions V7 and V8 of the 16S rRNA gene was performed with primers with added adapter sequences (**Supplementary Table S5**). The extracted genomic DNA was amplified by PCR using Ex Taq (Takara Bio Inc., Shiga, Japan). The amplicon was sequenced by the Ion Torrent Personal Genome Machine sequencer (Life Technologies, Carlsbad, CA, United States) (McDonald et al., 2012). Sequence data were processed with CLC Genomics Workbench v5.5.1 (CLC bio, Aarhus, Denmark). The barcode sequences, sequences of inappropriate length (<250 bp or >350 bp), sequences with low-quality scores (limit = 0.005), and sequences containing ambiguous nucleotides (five nucleotides at most) were trimmed. The processed sequences were analyzed using QIIME (Caporaso et al., 2010) and sequences with 98% or more homology were compiled as operational taxonomic units (OTUs) using the UCLUST algorithm (Edgar, 2010). One representative sequence was extracted from each OTU, and the sequences were assigned referring to the SILVA database version 132 (Quast et al., 2013). Sequences sharing less than 80% homology with the references were defined as unclassified. To investigate the phylogeny of OTUs in more detail, sequences of OTUs classified as nitrifiers were analyzed using the Basic Local Alignment Search Tool (BLAST) server[1] of the National Center for Biotechnology Information (NCBI).

Likewise, adapter sequences were added to a primer pair targeting the *amoA* gene of comammox (**Supplementary Table S5**). PCR amplification, sequencing, and trimming procedures were the same as those for the 16S rRNA gene, except for trimming and compiling. The sequences of inappropriate length (<150 bp or >250 bp) were trimmed and sequences with homology of 97% or more were summarized as OTUs.

Phylogenetic Analyses

The sequences of 16S rRNA genes classified into each lineage of the genus *Nitrospira* were searched on the nucleotide database of NCBI[2]. Based on these sequences and representative sequences of OTUs obtained in this study, phylogenetic analysis was performed using MEGA7 software (Shindo et al., 2006). The collected sequences were aligned and a phylogenetic tree was constructed using the neighbor-joining method (Saitou and Nei, 1987) and the bipartition confidence was evaluated at 1,000 bootstraps (Felsenstein, 1985).

The whole genome sequences of cultivated comammox, metagenome-assembled genomes (MAGs) constructed from environmental samples and clone sequences of the *Nitrospira amoA* gene detected in cultured samples were searched for in the NCBI nucleotide database, and AmoA amino acid sequences were collected. In case coding sequences (CDSs) of *amoA* were not annotated in the GenBank entry on the database, the MAG sequences were downloaded and CDSs were annotated using Prokka (version 1.13) (Seemann, 2014). To obtain AmoA amino acid sequences of enriched comammox and to correct the frame-shift of those sequences, the nucleotide sequences of OTUs were translated using the FrameBot tool (Wang et al., 2013) referring to the AmoA sequence of *Nitrospira inopinata*. The phylogenetic tree based on AmoA amino acid sequences was constructed using the same method as that for the 16S rRNA genes.

Nitrification Experiments of NH_4Cl-Fed Enrichment

To examine the effect of NH_4Cl concentration on the nitrification activity, a batch culture test was performed. An enrichment sample was collected from the NH_4Cl-fed bioreactor on day 749 and washed using centrifugation (2,900 × *g*, 10 min). The fresh inorganic medium described above was added to the sample and the bacterial pellet was dispersed with a Q55 homogenizer (Qsonica LLC, Newtown, CT, United States) for 30 s at 20% amplitude. The suspended sample was transferred into test tubes containing inorganic medium adjusted to pH 5.5, containing 0, 12.5, 25, 50, 75, 100, 200, or 300 mM NH_4Cl. The test tubes were incubated for three days in a dark room maintained at 23°C. The test was performed with three biological replicates. The supernatant of the medium in the tubes was collected and stored at −20°C until chemical analyses.

To examine the effect of pH on nitrification activity, another batch culture test was performed. The method for preparing bacterial suspension was as described above, except for the sampling was performed on day 849. The sample was transferred into test tubes with inorganic medium containing 12.5 mM NH_4Cl, adjusted to pH 3.0, 4.0, 5.0, 6.4, 7.5, or 9.0. As buffers of the medium, 80 mM 2-morpholinoethanesulfonic acid (MES) for pH 5.0, 4-(2-hydroxyethyl)-1-piperazine-ethanesulphonic acid (HEPES) for pH 6.4, and 25 mM N-cyclohexyl-3-aminopropanesulfonic acid (CAPS) for pH 7.5 and 9.0 were mixed. The concentration of CAPS was adjusted to the condition described in a previous report (Dai et al., 2012). The media for the pH 3.0 and 4.0 tests were unbuffered. The tubes were incubated for 2 days and collected samples were stored as described above.

Chemical Analyses for Nitrification Experiments

The nitrite concentrations of culture samples were measured using the Griess test (Griess-Romijn, 1966) using the absorbance at 560 nm as the index. As described in a previous study (Miranda et al., 2001) nitrate concentrations were determined by reducing nitrate to nitrite with vanadium chloride (III) and measured using the Griess test. The absorbance was measured using a PowerWave HT microplate spectrophotometer (BioTek Instruments Inc., Winooski, VT, United States).

RESULTS AND DISCUSSION

Water Quality During Continuous-Feeding Incubation

At the start of the continuous-feeding incubation in the NH_4Cl-fed bioreactor, the medium was maintained at around pH 6.0.

[1] https://blast.ncbi.nlm.nih.gov/Blast.cgi

[2] https://www.ncbi.nlm.nih.gov/nucleotide/

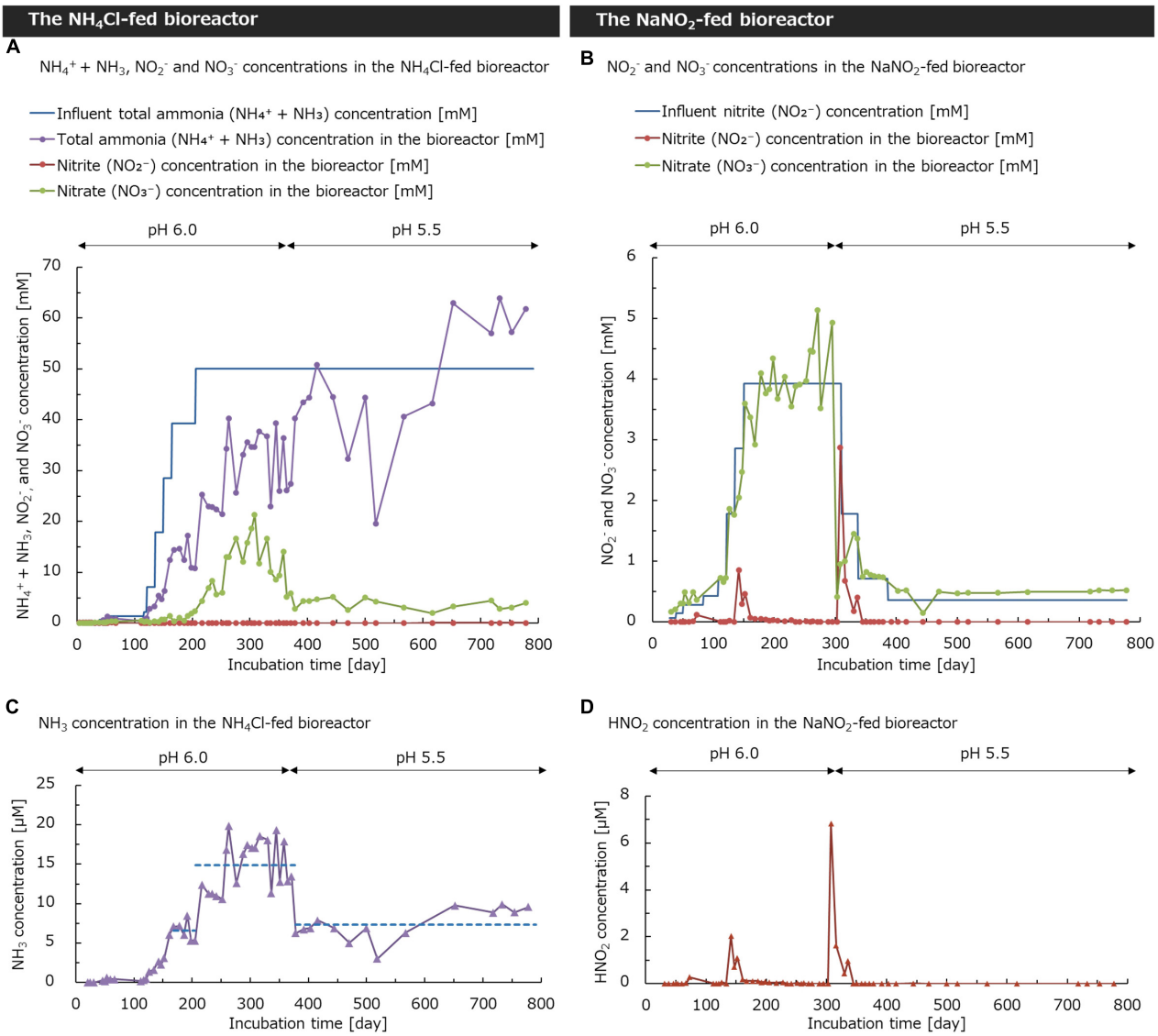

FIGURE 1 | Total ammonia, nitrite, and nitrate concentrations in the **(A)** NH_4Cl-fed bioreactor and **(B)** $NaNO_2$-fed bioreactor. The theoretically calculated concentration of NH_3 in the NH_4Cl-fed bioreactor and HNO_2 in the $NaNO_2$-fed bioreactor are shown in **(C,D)**, respectively. The dashed lines in **(C)** show the average value of each period. The pH values in the NH_4Cl-fed bioreactor and $NaNO_2$-fed bioreactor were changed from 6.0 to 5.5 on days 374 and 304, respectively.

Under acidic conditions, the concentration of free ammonia (NH_3) decreased exponentially as the pH decreased, owing to protonation from ammonia to ammonium (NH_4^+) (pKa = 9.25) (De Boer and Kowalchuk, 2001). Ammonia, not ammonium, is known as the substrate of ammonia monooxygenase (Suzuki et al., 1974; Galloway et al., 2008). Considering the decrease in ammonia concentration caused by protonation, an excessive amount of ammonium was supplied into the bioreactor to enrich the comammox *Nitrospira*. The concentration of NH_4Cl in the supplied medium was increased in a stepwise way. On day 165–205, when the bioreactor was supplied with the medium containing 39 mM NH_4Cl, the nitrate (NO_3^-) concentration in the bioreactor increased to 1.3 ± 0.8 mM on average, which shows an increase in nitrification activity (**Figure 1A**). After the further increase in supplied NH_4Cl concentration to 50 mM, the NO_3^- concentration in the bioreactor reached 11.2 ± 4.9 mM during days 206–373. Although the total ammonia (NH_4^+ + NH_3) in the bioreactor was not completely oxidized to nitrate, a low concentration of NO_3^- was stably produced by nitrification. Based on this result, the influent concentration of NH_4Cl was fixed at 50 mM in the subsequent incubation. To enrich the nitrifiers adapted to a more acidic condition, we decreased the pH from 6.0 to 5.5, in which most of the isolated ammonia oxidizers cannot grow (De Boer and Kowalchuk, 2001). After the decrease in pH during days 374–791, the NO_3^- concentration in the bioreactor reduced to 3.7 ± 1.0 mM, indicating the suppression of nitrification activity. However, in acidic soils, high concentration of ammonium accumulated (**Supplementary**

Table S1). On the other hand, nitrate concentration in soils was two orders of magnitude less than that of ammonium. Thus, the culture condition with low pH and high influent concentration of ammonia could reproduce the environment in acidic soils, although ammonia in the bioreactor was not completely oxidized. Furthermore, the concentration of NO_2^- was maintained at under 0.2 mM throughout the cultivation process. This result was also in accordance with the low nitrite concentration in soils (Kowalchuk and Stephen, 2001).Throughout the incubation, the measured concentration of total ammonia ($NH_4^+ + NH_3$) in the bioreactor was not stable. This is considered to be due to the high reagent blank of the indophenol blue method (Willason and Johnson, 1986; Aminot et al., 1997; Kérouel and Aminot, 1997). Moreover, the stoichiometric ratio of ammonia consumption and nitrate generation was not consistent. This inconsistency could be caused by the consumption of ammonia as nitrogen source or denitrification converting nitrate to gaseous nitrogen.

A part of the biomass in the NH_4Cl-fed bioreactor was transferred to the $NaNO_2$-fed bioreactor on day 25. The medium in the bioreactor was maintained at around pH 6.0. Under low pH conditions, the concentration of free nitrous acid (HNO_2) increases because of the protonation of NO_2^- (pKa = 3.3). Considering that even low concentrations of HNO_2 suppress nitrification (Anthonisen et al., 1976) the concentration of NO_2^- in the bioreactor was controlled to be as low as possible to avoid the accumulation of HNO_2. The concentration of $NaNO_2$ in the supplied medium was increased in a stepwise way but controlled carefully to completely oxidize all NO_2^- in the bioreactor. Therefore, NO_2^- was completely oxidized to NO_3^- and the NO_3^- concentration in the bioreactor increased as the influent concentration of NO_2^- increased during days 28–303 (**Figure 1B**). On day 304, the pH was reduced from 6.0 to 5.5. Therefore, the concentration of NO_2^- in the bioreactor rapidly increased to 2.9 mM on day 308. The decrease in nitrite oxidation activity could be due to the increase in HNO_2 with the change in pH. To avoid the accumulation of HNO_2 in the bioreactor, we step-wisely reduced the $NaNO_2$ concentration in the supplied medium from 3.93 mM to 0.36 mM during days 310–387. Just after decreasing the inflow NO_2^- concentration from 3.93 mM to 1.79 mM, NO_3^- concentration in the bioreactor partially recovered. Furthermore, as the NO_2^- concentration in the inflow medium decreased, the NO_2^- concentration in the bioreactor gradually decreased to reach 0 mM. These results suggest that the nitrite-oxidation activity in the $NaNO_2$-fed bioreactor was recovered by adjusting the NO_2^- concentration in the supplied medium, although the oxidation was temporarily inhibited by a decrease in pH. Therefore, we presumed that the sharp decrease in the nitrite oxidation rate could be caused not only by the change in pH, but also by the increase in HNO_2 concentration.

To investigate the relationship between the nitrification activity and the concentration of NH_3 or HNO_2, the theoretical concentration of NH_3 in the NH_4Cl-fed bioreactor and HNO_2 concentration in the $NaNO_2$-fed bioreactor were calculated according to the method of a previous study (Anthonisen et al., 1976). In the NH_4Cl-fed bioreactor controlled at pH 6.0 until day 373, the NH_3 concentration in the bioreactor increased as the concentration of NH_4Cl in the supplied medium increased (**Figure 1C**). When the medium containing 39 mM NH_4Cl was supplied during days 165–205, the average NH_3 concentration was 6.6 ± 1.2 μM. Afterward, the NH_4Cl concentration in the supplied medium increased to 50 mM on day 206 and the average NH_3 concentration in the bioreactor increased to 14.9 ± 3.2 μM during days 206–373. On day 374, the pH was decreased from 6.0 to 5.5; concurrently the NH_3 concentration also decreased and kept constant at 7.4 ± 2.0 μM until day 791. Based on this result, the decrease in the nitrification rate after pH change is considered to be partly caused by the decreasing concentration of free ammonia, the substrate for nitrification.

Furthermore, in the $NaNO_2$-fed bioreactor controlled at pH 6.0, HNO_2 temporarily increased up to 2.0 μM on day 142 (**Figure 1D**). This was due to the sudden increase in the influent NO_2^- concentration. However, at this point, the nitrification rate increased rapidly and the NO_2^- concentration in the bioreactor decreased immediately by day 161. From this result, the nitrifier community in the bioreactor would be still active under the conditions of 1.1 μM HNO_2 on day 161. In contrast, the nitrification activity decreased immediately after the pH was reduced from 6.0 to 5.5 on day 304. Simultaneously, the HNO_2 concentration increased to 6.8 μM on day 308 and remained in the bioreactor until day 336. During this period, nitrification in the bioreactor did not recover unless the influent NO_2^- concentration was reduced. Although 6.8 μM of HNO_2 inhibited nitrification in the bioreactor, the nitrifier community would be still active under pH 5.5. Consequently, it is considered that HNO_2, rather than low pH, suppressed the nitrification activity.

Morphology of Nitrifiers

The non-woven fabrics in both bioreactors became brown colored with the biomass (**Supplementary Figure S1**). The cell suspensions collected from the bioreactors formed flocs visible to naked eyes. The morphological feature of these flocs was similar to an enrichment culture of *Nitrospira* in a previous report (Spieck et al., 2006).

In the NH_4Cl-fed bioreactor, *Nitrospira* lineage II and betaproteobacterial AOB grew remarkably (**Figure 2A**). On day 84, several cells of *Nitrospira* lineage II aggregated and formed small colonies. Such small colonies gathered to form larger dense aggregates on day 228 and 319. Until day 319, those aggregates were mainly composed of *Nitrospira* lineage II cells. However, on day 791, *Nitrospira* lineage II were co-aggregated with colonies of other bacteria. This morphological change in *Nitrospira* lineage II might be caused by the pH decrease. The co-aggregates containing *Nitrospira* lineage II resembled the structures observed in the culture incubating "*Ca.* Nitrospira nitrosa" and "*Ca.* Nitrospira nitrificans" (van Kessel et al., 2015) rather than the small microcolonies of *Nitrospira inopinata* (Daims et al., 2015). In contrast, betaproteobacterial AOB grew throughout the incubation. As in *Nitrospira* lineage II, aggregates mainly composed of AOB cells were observed on day 319 at pH 6.0. However, AOB adhered to other bacteria on day 791 at pH 5.5. Such a co-aggregation of betaproteobacterial AOB with other bacteria was induced by pH reduction in a previous study (De Boer et al., 1991). Unlike the significant growth of *Nitrospira*

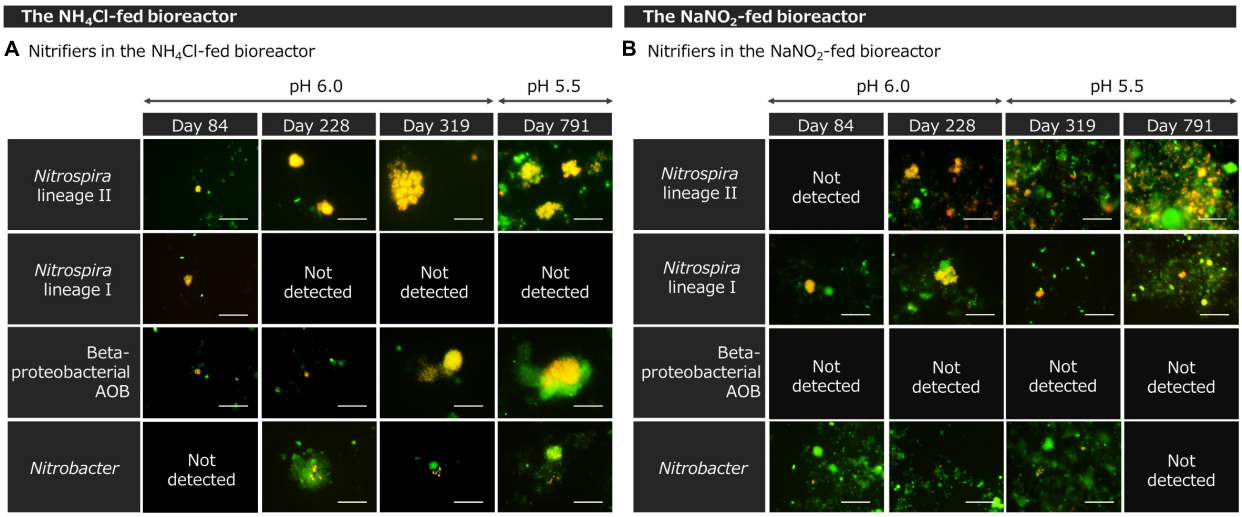

FIGURE 2 | Fluorescence in situ hybridization (FISH) images of enrichment samples from **(A)** the NH_4Cl-fed bioreactor and **(B)** $NaNO_2$-fed bioreactor. All bacteria were stained with SYTOX Green (green). Only targeted cells were labeled with FISH probes (red) and two colors were merged into yellow. The scale bars represent 10 μm.

lineage II and AOB, *Nitrospira* lineage I and *Nitrobacter* were hardly observed throughout the incubation.

Bacteria in the $NaNO_2$-fed bioreactor formed strongly aggregated structures with widths of several tens of micrometers (**Figure 2B**). On day 228, after the stepwise increase in the influent $NaNO_2$ concentration, dozens of *Nitrospira* lineage II cells formed colonies. On day 319, just after changing the pH from 6.0 to 5.5, *Nitrospira* lineage II decreased and its colonies became smaller. However, on day 791, after the $NaNO_2$ concentration in the bioreactor was kept low, *Nitrospira* lineage II grew again. At pH 5.5, *Nitrospira* lineage II aggregated with other bacteria and formed a complex structure. This aggregation is considered to be an adaptation to lower pH or higher concentrations of HNO_2. *Nitrospira* was reported to increase the production of extracellular polymeric substances to form aggregates under high nitrite concentrations (Nowka et al., 2015). The structure of *Nitrospira* lineage I aggregates was similar to that of lineage II. Furthermore, betaproteobacterial AOB was under the detection limit of microscopic observation throughout the incubation. In addition, only a small number of *Nitrobacter* cells were observed as a part of the aggregates.

16S rRNA Gene-Based Bacterial Community

Based on the V7–V8 region of the 16S rRNA gene, the bacterial community structure in the bioreactors was analyzed at the family level. In the initial soil sample, the family *Nitrospiraceae* including comammox accounted for 1.2% of the total bacteria, which was the largest among nitrifying bacteria (**Figure 3**). In contrast, the family *Nitrosomonadaceae* including betaproteobacterial AOB and the family *Bradyrhizobiaceae* including the genus *Nitrobacter* occupied <0.1% of the total bacteria in the initial soil sample.

In the NH_4Cl-fed bioreactor, the nitrification activity increased during days 165–205 when the medium containing 39 mM NH_4Cl was supplied. At the same time, the relative abundance of family *Nitrospiraceae* also increased and reached 60.1% by day 206 (**Figure 3A**). After that, the abundance of *Nitrospiraceae* fluctuated within 55.8–92.9%, but consistently accounted for more than half of the whole bacterial population, regardless of the pH change. Although another nitrifier oxidizing ammonia, *Nitrosomonadaceae* also increased in number, the abundance remained <8.4% throughout the incubation. The relative abundance of *Bradyrhizobiaceae* including *Nitrobacter* also remained <7.3%. Considering that a small number of AOB existed and a small number of NO_2^- were produced in the bioreactor, some bacteria of the family *Nitrospiraceae* would function as *Nitrospira* oxidizing only NO_2^- and not NH_3. However, based on the great difference between the proportion of *Nitrosomonadaceae* and that of *Nitrospiraceae*, most of the *Nitrospiraceae* in the bioreactor was assumed to function as comammox *Nitrospira* oxidizing NH_3 to NO_3^-. Since the family *Nitrospiraceae* became dominant in the bioreactor and maintained a stable proportion, the culture condition in this study was considered to be suitable for cultivating *Nitrospiraceae* from an acidic soil. In addition, an isolate of acidophilic AOA from acidic soils was reported to be deactivated at pH 6.0 (Lehtovirta-Morley et al., 2014). Thus, the initial culture condition at pH 6.0 might eliminate AOA in the soils. However, we did not try to detect AOA in the enrichment sample with molecular biological techniques such as quantitative PCR. Therefore, note that the possibility of ammonia oxidation by AOA cannot be denied. Moreover, even though *Nitrospiraceae* was enriched with inorganic medium, some heterotrophic bacteria such as *Rhodanobacteraceae* remained in the bioreactor. *Rhodanobacteraceae* is known as a heterotrophic denitrifying bacterium (Kostka et al., 2012). Those bacteria might consume

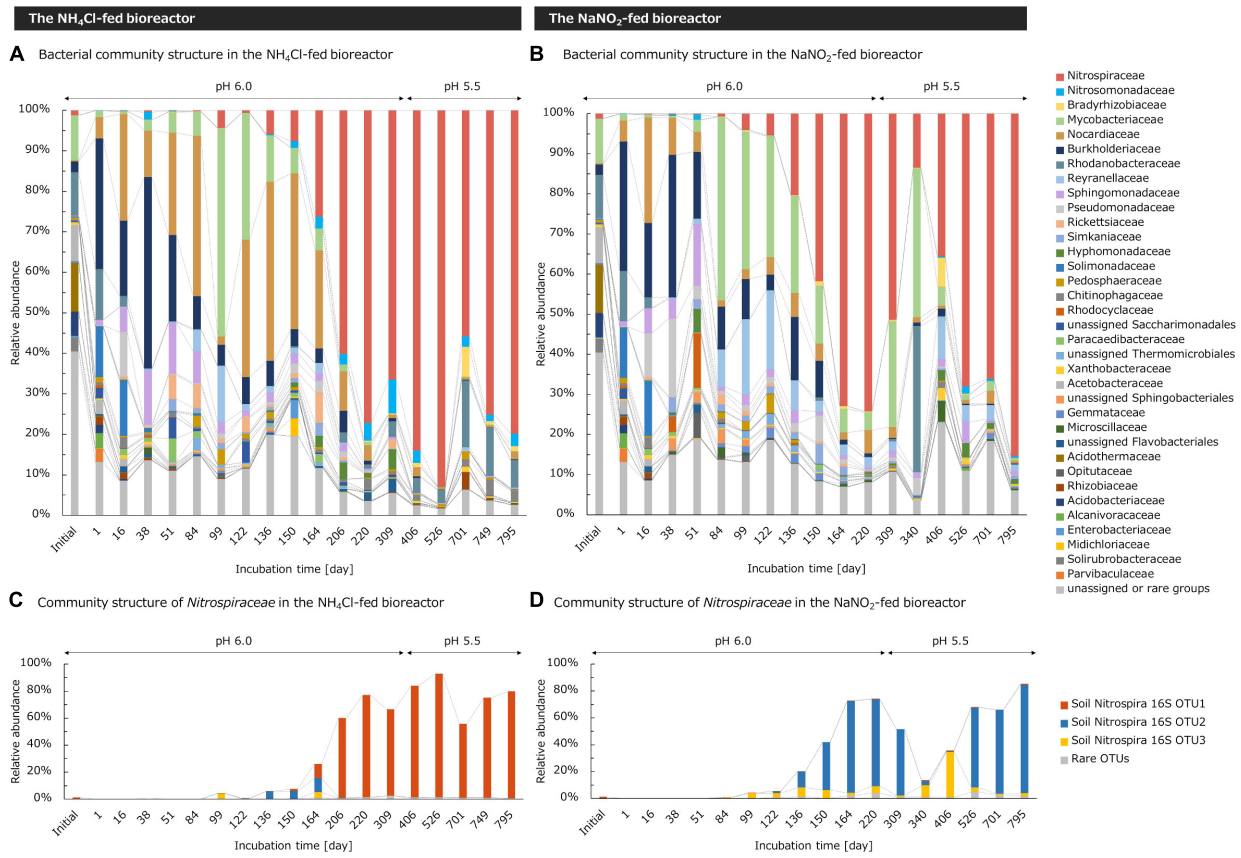

FIGURE 3 | Taxonomic assignments of 16S rRNA gene sequences of enrichment cultures in **(A,C)** the NH_4Cl-fed bioreactor and **(B,D)** $NaNO_2$-fed bioreactor. **(A,B)** Relative abundances of taxonomic groups were analyzed at the family classification level. Unassigned taxon and phylogenetic groups occupying <3% of the total bacteria in all samples were integrated to "unassigned or rare groups." **(C,D)** Relative abundances of taxonomic groups in the family *Nitrospiraceae* were analyzed at the OTU level. OTUs occupying <2% of the total bacteria in all samples were integrated into "rare OTUs."

NH_3 as nitrogen source or reduce NO_3^- by denitrification to contribute to the inconsistency of stoichiometric ratio of ammonia consumption and nitrate generation (**Figure 1A**).

Likewise, in the $NaNO_2$-fed bioreactor controlled at pH 6.0, the relative abundance of *Nitrospiraceae* increased as the influent NO_2^- concentration gradually increased up to 3.93 mM during days 28–150. After that, the pH in the bioreactor and influent NO_2^- concentration kept a constant level until day 303. In this period, the relative abundance of family *Nitrospiraceae* increased to 72.9% on day 164 and remained an almost constant abundance until day 220 (**Figure 3B**). However, the nitrification activity of the bioreactor decreased after the pH was decreased from 6.0 to 5.5 on day 304. Concurrently, the proportion of *Nitrospiraceae* decreased from 51.4% on day 309 to 13.5% on day 340. In contrast, the abundance of the family *Bradyrhizobiaceae*, including *Nitrobacter*, increased from 0.32% on day 309 to 7.20% on day 406 following the pH change. This different response between *Nitrospira* and *Nitrobacter* to pH change is considered to be due to the relatively higher resistance of *Nitrobacter* to HNO_2 (Blackburne et al., 2007). After the decrease in HNO_2 concentration in the bioreactor, the nitrification was reactivated and the relative abundance of *Nitrospiraceae* recovered to 35.6% on day 406. During days 526–795, the bioreactor operated under a stable environment, and the abundance of *Nitrospiraceae* reached to the range of 66.1%–85.4%. In the environment with a low concentration of HNO_2, however, the relative abundance of *Bradyrhizobiaceae* was always <1%, much lower than that of *Nitrospiraceae*. From this viewpoint, *Nitrospira* was assumed to be the main contributor to NO_2^- oxidation in the bioreactor at pH 5.5, except for under high concentrations of HNO_2. In addition, despite the absence of ammonium in the inflow medium supplied to the bioreactor, the family *Nitrosomonadaceae* consisting of AOB grew and comprised 1.82% of the bacterial community on day 526. Although AOB needs NH_3 as a substrate to grow, most of them are known to produce NH_3 by degrading urea (Koper et al., 2004; Norton et al., 2008). Therefore, AOB in the bioreactor might degrade the small amount of urea provided by bacteria coexisting in the bioreactor, which was a limited proportion of the biomass.

Furthermore, community structures of the families *Nitrospiraceae*, *Nitrosomonadaceae*, and *Bradyrhizobiaceae* were analyzed at the level of OTUs. *Nitrospiraceae* was mainly composed of three OTUs. Before the cultivation, the most abundant of the three OTUs was soil Nitrospira 16S OTU1,

which accounted for 1.0% of the whole bacterial community in the initial soil sample (**Figure 3C**). Considering that the relative proportion of *Nitrospiraceae* was 1.19% and the total abundance of *Nitrospiraceae*, *Nitrosomonadaceae*, and *Bradyrhizobiaceae* was only 1.25%, soil Nitrospira 16S OTU1 was regarded as the dominant bacteria in the community of nitrifiers in the initial soil sample. In the NH_4Cl-fed bioreactor, soil Nitrospira 16S OTU1, OTU2, and OTU3 coexisted until day 164, however, soil Nitrospira 16S OTU1 was enriched and accounted for more than half of the bacterial community during days 206–795 (**Figure 3C**). Based on this result, the continuous-feeding bioreactor supplied with an inorganic medium containing excessive NH_4Cl at pH 5.5–6.0 seemed to be suitable for enrichment of the major group of *Nitrospira* in acidic soil. On the other hand, the other two OTUs were enriched in the $NaNO_2$-fed bioreactor. Soil Nitrospira 16S OTU2, accounting for only 0.02 % in the initial soil, became dominant in the bioreactor on day 164 (**Figure 3D**). In contrast, the relative abundance of soil Nitrospira 16S OTU3 was lower than 7% throughout the incubation except under high HNO_2 concentrations. After the pH change and the accumulation of HNO_2 in the bioreactor, soil Nitrospira 16S OTU3 increased its proportion to 8.7% and 33.8% on days 340 and 406, respectively. Afterward, the soil Nitrospira 16S OTU3 decreased and soil Nitrospira 16S OTU2 became dominant in the bioreactor again. From this result, the factor deciding the niche differentiation between soil Nitrospira 16S OTU2 and OTU3 would be the tolerance to HNO_2, rather than the pH.

The composition of the family *Nitrosomonadaceae* was also analyzed at the OTU level. The cultivated *Nitrosomonadaceae* was mainly composed of two OTUs. In the NH_4Cl-fed bioreactor, soil Nitrosospira 16S OTU1 classified into the genus *Nitrosospira* was enriched (**Supplementary Figure S2A**). This OTU accounted for 0.011% of the total bacterial community in the initial soil and was the dominant OTU of the family *Nitrosomonadaceae* accounting for 0.032%. In the $NaNO_2$-fed bioreactor, soil Nitrosospira 16S OTU2 was enriched, but this group was not detected in the initial soil sample (**Supplementary Figure S2B**). In contrast to *Nitrosomonadaceae*, the communities of family *Bradyrhizobiaceae* in the two bioreactors were composed of a common OTU assigned to the genus *Nitrobacter* (**Supplementary Figure S3**). This OTU, named soil Nitrobacter 16S OTU1, was the major OTU in *Bradyrhizobiaceae* throughout the cultivation and accounted for 0.032% of the total bacterial community in the initial soil.

16S rRNA Gene-Based Phylogenetic Analyses

A phylogenetic tree of *Nitrospira* based on the 16S rRNA gene sequence was constructed referring to OTUs retrieved from amplicon sequencing and sequences registered in the NCBI nucleotide database. Therefore, soil Nitrospira 16S OTU1 and OTU2 were classified into *Nitrospira* lineage II (**Figure 4**). Soil Nitrospira 16S OTU1 was grouped within the cluster including "*Candidatus* Nitrospira nitrificans" (van Kessel et al., 2015), an enriched strain of comammox *Nitrospira*, while soil Nitrospira 16S OTU2 was closely related to *Nitrospira japonica*, an isolated strain of nitrite-oxidizing *Nitrospira* (Ushiki et al., 2013). On the other hand, soil Nitrospira 16S OTU3 was classified into lineage I and was closely related to *Nitrospira* sp. ND1 (Fujitani et al., 2013).

In the $NaNO_2$-fed bioreactor, soil Nitrospira 16S OTU2 classified into lineage II and soil Nitrospira 16S OTU3 classified into lineage I competed with one another during the continuous-feeding incubation (**Figure 3D**). Soil Nitrospira 16S OTU2 did not decrease its relative abundance with exposure to 2.03 μM HNO_2 during days 142–152, but decreased just after being exposed to 6.8 μM HNO_2 on day 308 (**Figures 1D**, **3D**); meanwhile, the relative abundance of soil Nitrospira 16S OTU3 increased. From these results, *Nitrospira* lineage II in the bioreactor was presumed to be advantageous under low concentrations of NO_2^- regardless of pH change; however, it was more sensitive to HNO_2 than lineage I. By contrast, lineage I was estimated to be favorable under relatively high concentrations of HNO_2 and tolerated 6.8 μM HNO_2 (**Table 1**). Moreover, a similar niche differentiation between the two lineages was reported in previous studies cultivating *Nitrospira* from activated sludge under different NO_2^- concentrations (Maixner et al., 2006; Fujitani et al., 2013). Furthermore, the concentration of diluted oxygen (Park and Noguera, 2008) and usability of organic substrates (Gruber-Dorninger et al., 2015) were reported as the niche differentiation factors between the two lineages. However, all of these theories are based on experiments using samples from wastewater treatment systems. Therefore, the enrichment sample obtained in this study would provide important information to reveal the factors influencing the niche differentiation between the two lineages in acidic conditions and soil environments.

While *Nitrospira* lineage I contains only nitrite-oxidizing *Nitrospira*, lineage II also includes comammox. Soil *Nitrospira* 16S OTU1 was enriched in the NH_4Cl-fed bioreactor but was rarely detected in the $NaNO_2$-fed bioreactor (**Figure 3**). Furthermore, according to metagenomic studies, comammox *Nitrospira* are known to lack assimilatory nitrite reductase or cyanate hydratase genes for generating ammonia, while nitrite-oxidizing *Nitrospira* do contain these genes and are able to grow in inorganic media containing only NO_2^- as a nitrogen source (Palomo et al., 2018). In contrast, most of the comammox genomes harbor urease genes to produce ammonia through urea degradation (Palomo et al., 2018), which might enable the growth of comammox depending on urea produced by other bacteria. However, urea-dependent ammonia oxidation is known to take longer than ammonia oxidation under NH_4Cl supplementation (Pommerening-Roser and Koops, 2005). Based on these facts, soil Nitrospira 16S OTU1 could be composed of comammox *Nitrospira*. In contrast, soil Nitrospira 16S OTU2 enriched in the $NaNO_2$-fed bioreactor was thought to mainly include nitrite-oxidizing *Nitrospira*. However, note that the phylogenetic position does not directly support the function of complete ammonia oxidation (Pjevac et al., 2017).

To investigate the phylogenetical positions of OTUs classified into the genera *Nitrosospira* and *Nitrobacter*, the related sequences were searched using NCBI BLAST. Soil Nitrosospira 16S OTU1 was 100% identical to the 16S rRNA gene sequence of *Nitrosospira lacus* strain APG3. This strain was reported

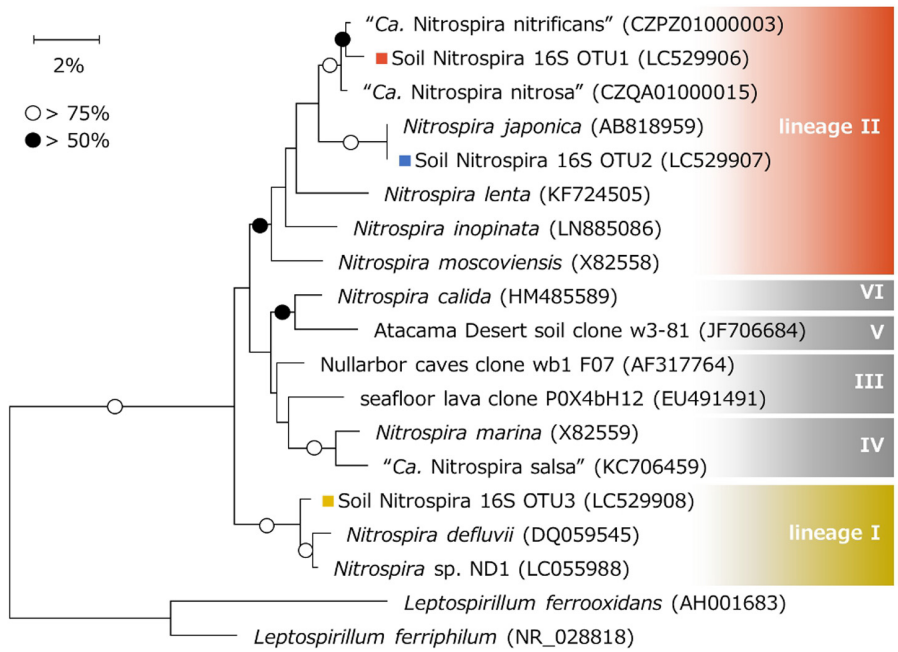

FIGURE 4 | Phylogenetic tree based on the 16S rRNA gene sequences of *Nitrospira*. Phylogenetic analysis was performed using the neighbor-joining method with 1000 bootstraps. Bootstrap values of >75% or >50% are indicated as open or closed circles, respectively. Sequences of *Leptospirillum* were used to root the tree. Colored squares show the OTUs obtained in this study.

TABLE 1 | Features of the OTUs obtained from amplicon sequencing of the 16S rRNA gene and comammox *amoA* gene.

OTU	Soil Nitrospira 16S OTUs			Soil Nitrospira amoA OTUs			
	OTU1	OTU2	OTU3	OTU1	OTU3	OTU4	OTU2
Source bioreactor	NH_4Cl-fed	$NaNO_2$-fed		NH_4Cl-fed			
Major function	Comammox	Nitrite oxidation		Comammox			
Phylogenetic group[a]	lineage II		lineage I	Uncultivated			Cultivated
The minimum tolerable pH[b]	pH 5.5			pH 5.5			pH 6.0
Tolerable HNO_2 concentration[c]		Low	High				
Favorable NH_3 concentration[d]				Low			High

The gray cells represent common features of several OTUs. Empty cells represent no data. [a]*OTUs were classified based on phylogenetic analyses of the 16S rRNA gene sequences (**Figure 4**) and AmoA amino acid sequences (**Figure 6**).* [b]*All soil Nitrospira 16S OTUs were detected throughout the incubation regardless of the pH decrease from 6.0 to 5.5 (**Figures 3C,D**). Likewise, soil Nitrospira amoA OTU1, OTU3, and OTU4 were detected at pH 5.5 (**Figure 5**). On the other hand, soil Nitrospira amoA OTU2 was detected at only pH 6.0 (**Figure 5**).* [c]*Soil Nitrospira 16S OTU2 decreased its relative abundance with exposure to 6.8 μM HNO_2 on day 308 (**Figures 1D**, **3D**); meanwhile, the relative abundance of soil Nitrospira 16S OTU3 increased. From these results, soil Nitrospira 16S OTU3 would be tolerable to relatively high concentration of HNO_2.* [d]*The concentration of NH3 in the NH_4Cl-fed bioreactor was 6.6 ± 1.2 μM during days 165–205 (**Figure 1C**). Just after this period, on day 206, soil Nitrospira amoA OTU1 dominated among the comammox community (**Figure 5**). Afterwards, the NH3 concentration increased to 14.9 ± 3.2 μM during days 206–373 (**Figure 1C**). In this period, soil Nitrospira amoA OTU2 became dominant instead (**Figure 5**). Thus, soil Nitrospira amoA OTU2 could be adapted to relatively high NH3 concentration.*

to grow under a wide range of pH values (5–9) (Urakawa et al., 2015). Although APG3 was isolated from a freshwater lake (Garcia et al., 2013), closely related *Nitrosospira* was also detected in a soil (Zhang et al., 2015). In contrast, soil Nitrosospira 16S OTU2 cultivated in the $NaNO_2$-fed bioreactor was closely related to *Nitrosospira* sp. EnI299 enriched from fertilized soil (Tourna et al., 2010). Moreover, soil Nitrobacter 16S OTU1 was 100% identical to the 16S rRNA gene sequence of *Nitrobacter* sp. Io acid and *Nitrobacter vulgaris*. *Nitrobacter* sp. Io acid was isolated from an acidic forest soil and showed nitrite-oxidizing activity at pH 3.5–7.0 (Hankinson and Schmidt, 1988). *Nitrobacter vulgaris* DSM10236 was cultivated in media with neutral or mildly alkaline pH, such as 7.4 or 8.6 (Reshetilov et al., 2011). For a different strain of the same species, *Nitrobacter vulgaris* strain mesi survived in a fairly wide range of pH values (6.0–9.2) (Laanbroek and Schotman, 1991). Therefore, the adaptable pH range for *Nitrobacter* depends on each strain and it is difficult to distinguish the range based solely on the 16S rRNA gene sequence at this point.

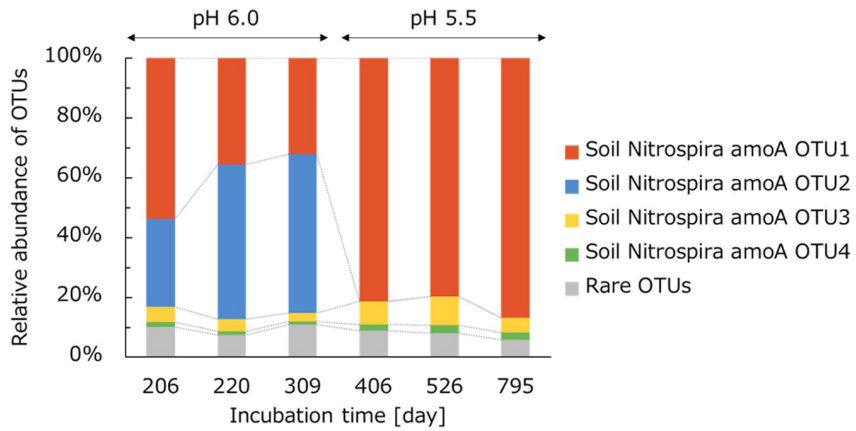

FIGURE 5 | Relative abundance of taxonomic groups in comammox *Nitrospira* in the NH_4Cl-fed bioreactor. Taxonomic groups were analyzed based on comammox amoA gene sequences at the OTU classification level. OTUs occupying <2% of the total comammox community in all samples were integrated into "rare OTUs."

amoA Gene-Based Bacterial Community of Comammox *Nitrospira*

As described above, *Nitrospira* lineage II includes both comammox and nitrite-oxidizing *Nitrospira*; it is difficult to distinguish these two groups based on 16S rRNA gene sequences (Pjevac et al., 2017). To analyze the phylogenetic features of comammox *Nitrospira* specifically, an amplicon sequencing targeted at the comammox *amoA* gene was performed. However, the comammox *amoA* gene in the extracted DNA samples was not amplified before day 206 (data not shown). The impossibility of amplification could be due to the low abundance of comammox *Nitrospira* and low PCR efficiency of barcode-attached primers. The relative abundance of each OTU was calculated as a proportion to the total reads of comammox *amoA* sequences. The comammox *Nitrospira* community in the NH_4Cl-fed bioreactor was mainly composed of four OTUs. Other OTUs accounting for less than 2% of all samples were integrated into "rare OTUs." Especially, two OTUs, named soil Nitrospira amoA OTU1 and soil Nitrospira amoA OTU2 were dominant (**Figure 5**). During days 206–309, the pH in the bioreactor was controlled at 6.0 and the concentration of NH_4Cl in the influx medium was maintained at 50 mM. In this period, the relative abundance of soil Nitrospira amoA OTU2 slowly increased, while that of soil Nitrospira amoA OTU1 decreased (**Figure 5**). After the pH change from 6.0 to 5.5, however, soil Nitrospira amoA OTU2 was not detected and soil Nitrospira amoA OTU1 became dominant instead.

The dynamics of the relative abundances of comammox OTUs caused by the pH change indicated that the soil Nitrospira amoA OTU2 activity was suppressed or completely inhibited at pH 5.5. The acidic condition stresses microorganisms by affecting pH homeostasis or decreasing HCO_3^- as a carbon source (Lehtovirta-Morley et al., 2016; Herbold et al., 2017). Thus, the pH decrease might suppress the growth of Nitrospira amoA OTU2. The concentration of NH_3 in the bioreactor controlled at pH 5.5 during days 374–791 corresponded to the value at pH 6.0 during days 165–205 (**Figure 1C**). Just after this period, on day 206, soil Nitrospira amoA OTU2 accounted for a high proportion of the comammox community. Based on this trend, the decrease in NH_3 concentration caused by the pH change on day 374 would not be critical to the nitrification activity of soil Nitrospira amoA OTU2. Indeed, soil Nitrospira amoA OTU2 was unable to grow under pH 5.5 like typical ammonia oxidizers (De Boer and Kowalchuk, 2001). Instead, soil Nitrospira amoA OTU1 became dominant under relatively acidic conditions at pH 5.5.

Moreover, unlike the dynamic change in the comammox *amoA* gene-based community structure, 16S rRNA gene-based analysis of the *Nitrospira* community showed no significant change before and after the pH decrease (**Figure 3C**). The gap between these two analyses was considered to be caused by the difference in the similarities of nucleotide sequences. Partial 16S rRNA gene sequences of nitrifiers have high similarities, and thus, it is difficult to distinguish between closely related bacteria. In contrast, functional marker genes are considered to be suitable for analyzing the diversity in detail and characterizing the phenotypic features (Norton et al., 2002). Especially, the *amoA* gene has been used as a suitable functional marker gene to analyze the phylogeny of comammox *Nitrospira* because it enables comammox and nitrite-oxidizing *Nitrospira* to be differentiated (Yu et al., 2018). In this study, analysis based on the *amoA* gene sequence detected several groups of comammox *Nitrospira*. Generally, genomes of comammox *Nitrospira* harbor one single copy of the *amoA* gene (Palomo et al., 2018). Therefore, several types of comammox were presumed to exist in the bioreactor. Even though *amoA* gene sequences detected in this experiment were classified into different OTUs, amplicon sequencing of the 16S rRNA gene found only one OTU in the NH_4Cl-fed bioreactor. This could be because the phylogenetically distinct types of comammox at the *amoA* gene level shared a high proportion of 16S rRNA gene sequences, and they were grouped into an identical OTU. This impossibility of linking each *amoA* OTU with one specific 16S rRNA gene sequence could be solved by using a single-cell isolation system combined with the *de novo* assembly of single-cell genomes (Chitsaz et al., 2011).

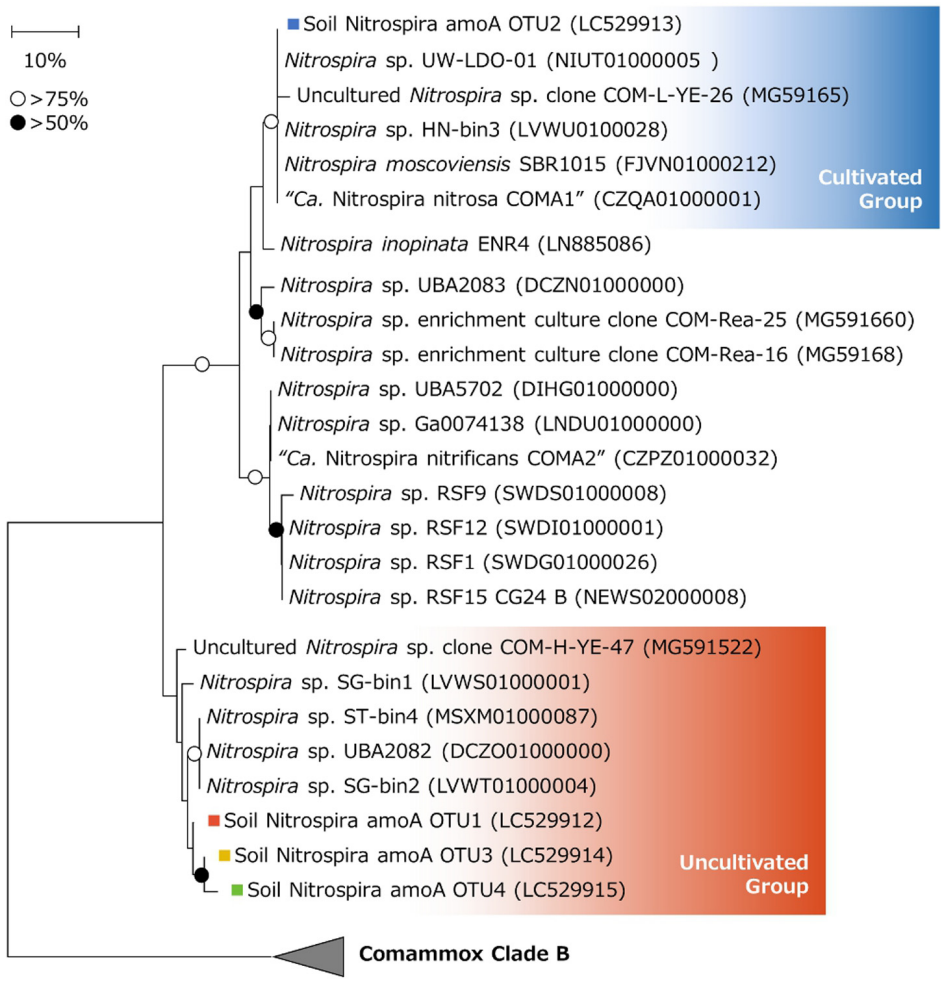

FIGURE 6 | Phylogenetic tree of comammox clade A based on AmoA amino acid sequences translated from nucleotide sequences. Phylogenetic analysis was performed using the neighbor-joining method with 1000 bootstraps. Bootstrap values of >75% or >50% are indicated as open or closed circles, respectively. Colored squares show the OTUs obtained in this study. Comammox clade B sequences (NEWT02000035, NEWR02000002, OEKW00000000, and OELE00000000) were used as outgroups.

AmoA-Based Phylogenetic Analysis of Comammox *Nitrospira*

The nucleotide sequences of comammox *amoA* OTUs were translated into amino acid sequences. A phylogenetic tree was constructed by referring to these translated sequences and those registered in the NCBI database. Comammox AmoA are known to be divided into two clades, and the primer pair used in this study was able to amplify the *amoA* genes of both clade A and B (Fowler et al., 2018). However, all of the detected OTUs were classified into clade A. Looking in further detail, soil Nitrospira amoA OTU2 and other OTUs were classified into different branches of clade A (**Figure 6**). The phylogenetical gap between these two groups corresponded to the difference in low pH adaptation; soil Nitrospira amoA OTU2 was deactivated at pH 5.5, while the other three OTUs survived (**Table 1**). Moreover, soil Nitrospira amoA OTU2 was grouped into the same branch with a cultivated comammox *Nitrospira* reported in previous studies (Daims et al., 2015; van Kessel et al., 2015; Camejo et al., 2017; Yu et al., 2018). On the other hand, soil Nitrospira amoA OTU1, OTU3, and OTU4 were classified into another branch with uncultured *Nitrospira*. Genes encoding AmoA of those *Nitrospira* were detected in drinking water (Wang et al., 2017), marine sediments (Parks et al., 2017) and river sediments (Yu et al., 2018). In the study cultivating sediments by Yu et al., uncultured *Nitrospira* sp. Clone COM-H-YE-47 was found. Interestingly, however, no identical *amoA* gene sequence was detected in a NH_4Cl-fed bioreactor incubating the sediment sample (Yu et al., 2018). From these results, it could be inferred that the continuous-feeding bioreactor in this study enabled the enrichment of a group of comammox *Nitrospira* that were fastidious and not cultivated in previous studies. Furthermore, these enriched comammox *Nitrospira* were not only physiologically novel, but also phylogenetically distinct from the strains cultivated in previous researches.

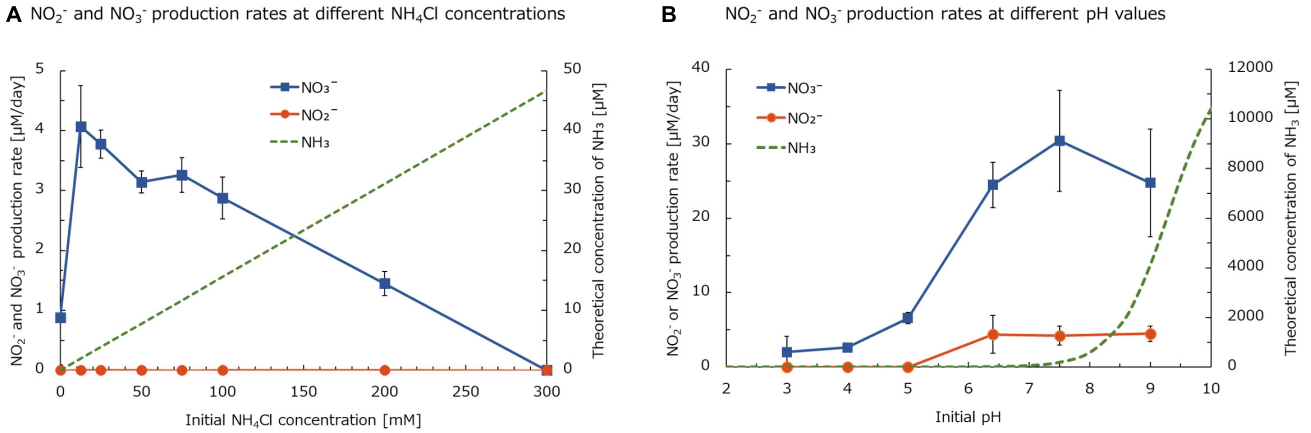

FIGURE 7 | (A) NO_2^- and NO_3^- production rates of the enrichment sample from the NH_4Cl-fed bioreactor at different NH_4Cl concentrations. The initial pH of media was adjusted to 5.5. **(B)** NO_2^- and NO_3^- production rates of the enrichment sample from the NH_4Cl-fed bioreactor at different pH values. The medium was supplemented with 12.5 mM of NH_4Cl. Data show means and error bars show standard deviation of biological triplicates. Green dashed lines show the theoretically calculated concentrations of NH_3.

Effect of the NH_4Cl Concentration and pH on the Nitrification Activity of the Enrichment Sample

To evaluate the nitrification activity of the enrichment sample in the NH_4Cl-fed bioreactor, the culture sample was collected on day 749 and the activity was tested under different NH_4Cl concentrations. The initial pH of the medium was adjusted to pH 5.5, the same value as the medium in the bioreactor. Furthermore, the NH_4Cl concentration in the medium was adjusted at 0, 12.5, 25, 50, 75, 100, 200, or 300 mM. After three days of incubation, NO_3^- was accumulated in the samples, but NO_2^- was rarely detected (**Figure 7A**). This result indicated that all the oxidized ammonia was converted to nitrate. Even in the sample not supplemented with NH_4Cl, NO_3^- was slightly generated. This is likely because a small amount of ammonium was produced by the degradation of organic nitrogen such as cyanate or urea. Considering the culture sample containing heterotrophic bacteria other than chemolithoautotrophic nitrifiers, the amount of organic nitrogen generated from the biomass could not be negligible.

The NO_3^- production rate was the highest at a NH_4Cl concentration of 12.5 mM (**Figure 7A**). The theoretical concentration of free ammonia (NH_3) under this condition was calculated to be 1.94 μM. This value is smaller than 33.3 μM, the half saturation constant (K_m) of NH_3 reported for "*Ca.* Nitrosoglobus terrae", AOB isolated from acidic soil (Hayatsu et al., 2017). On the other hand, AOA isolated from acidic soil, "*Ca.* Nitrosotalea devanaterra", showed the highest growth rate with 0.18 nM NH_3 (Lehtovirta-Morley et al., 2011). Therefore, the optimum NH_3 concentration for comammox *Nitrospira* enriched in this study would be higher than that for AOA but lower than that for AOB cultured from acidic soils. Based on these results, the niche differentiation among terrestrial comammox *Nitrospira*, AOB, and AOA is considered to partly depend on a favorable NH_3 concentration. This trend corresponds to the difference in affinity for NH_3, described in a previous study testing the physiological characteristics of *Nitrospira inopinata* (Dimitri et al., 2017). Moreover, the K_m value of NH_3 reported for *Nitrospira inopinata* is around 49 to 83nM (Dimitri et al., 2017). Although this value is lower than 1.94 μM, the optimum concentration for the enrichment in this study, it is still larger than that of terrestrial AOA.

Furthermore, the nitrification rate of the enrichment from the NH_4Cl-fed bioreactor decreased as the initial NH_4Cl concentration increased (**Figure 7A**). The enrichment was still active at 200 mM NH_4Cl. However, the nitrification activity was inhibited by 300 mM NH_4Cl, which was equivalent to 46.7 μM NH_3 at pH 5.5. This value almost matches the K_m of NH_3 for "*Ca.* Nitrosoglobus terrae", as described above (Hayatsu et al., 2017). Considering that an acid-adapted AOB could tolerate this amount of NH_3, the nitrification at pH 5.5 in this experiment was mainly performed by comammox rather than AOB, although the inhibition of comammox *Nitrospira* caused by a high concentration of NH_3 has not been reported by physiological experiments with pure cultures.

Moreover, to investigate the adaptation to pH change, the nitrification activity of the enrichment sample from the NH_4Cl-fed bioreactor was tested under a variety of pH values. After 2 days of incubation, the decrease in pH was kept within 1.0 in all samples (data not shown). The enrichment sample oxidized NH_3 to NO_3^- at a wide range of pH values (3.0–9.0). Within pH 6.4–9.0, NH_3 was not completely oxidized and NO_2^- was accumulated in the culture (**Figure 7B**). However, at this pH range, NH_3 was oxidized relatively faster than at pH 3.0–5.0. Under higher pH conditions, the concentration of NH_3

increases because of deprotonation. Especially at pH 7.5 and 9.0, the theoretical concentration of NH_3 was 192 and 4,122 μM, respectively. These values are much higher than the 46.7 μM inhibiting the nitrification activity of the enrichment at pH 5.5 (**Figure 7A**). Based on these results, the nitrifier oxidizing NH_3 to NO_3^- at pH 7.5–9.0 would be different from the major nitrifier oxidizing NH_3 at pH 5.5.

According to the 16S rRNA gene-based analysis, betaproteobacterial AOB enriched in the bioreactor was closely related to *Nitrosospira lacus*. *Nitrosospira lacus* was reported to oxidize NH_3 under a broad range of pH values (5–9) (Urakawa et al., 2015). Furthermore, the NH_3 oxidation activity of *Nitrosospira lacus* sharply decreased at pH 6 (Ishii et al., 2017). This trend corresponds to the low NO_3^- production rate at pH 3.0–5.0 in this study (**Figure 7B**). On the other hand, the slow NO_3^- production at pH 3.0–5.0 would be carried out by comammox *Nitrospira*. The NO_3^- production rate in this pH range was almost equivalent to the rate at pH 5.5 measured in the former experiment (**Figure 7A**). Therefore, NH_3 might be mainly oxidized by comammox *Nitrospira* and *Nitrosospira* at pH 3.0–5.0 and 6.4–9.0, respectively. Thus, the gap in the NH_3 oxidation rate between these two pH ranges might be caused by the difference in the maximum oxidation rate between AOB and comammox *Nitrospira*. According to a previous report, the maximum rate of ammonia oxidation of *Nitrosomonas europaea*, a strain of betaproteobacterial AOB, was several times higher than that of *Nitrospira inopinata* (Dimitri et al., 2017). From these results, the rapid NH_3 oxidation at pH 6.4–9.0 was considered to be caused by AOB, although the relative abundance of *Nitrosospira* was lower than that of *Nitrospira* in the enrichment sample. Within pH 6.4–9.0, NO_2^- was accumulated in the medium, which also supports two-step oxidation from NH_3 to NO_3^- via NO_2^- by AOB and NOB. Considering the accumulation of NO_2^- in this experiment, the NOB activity in the enrichment sample might not be sufficient to completely oxidize NO_2^-. This could be partly because the abundance of *Nitrobacter* was lower than that of *Nitrosospira* in the enrichment sample. On the other hand, NO_2^- was not detected at pH 3.0–5.0. This result suggests that the complete nitrification occurred at pH 3.0–5.0. However, NO_2^- can be converted to NO_3^- abiotically at pH < 3.3 (Cai et al., 2001). Thus, the complete nitrification at pH 3.0 is still debatable.

In this study, NH_3 oxidation at pH 3.0–5.0 seemed to be carried out by comammox *Nitrospira*. According to previous studies, ammonia oxidizers cultured from acidic soils, "*Ca.* Nitrosoglobus terrae" and "*Ca.* Nitrosotalea devanaterra", were unable to oxidize NH_3 at pH 3.5. From these results, comammox *Nitrospira* enriched in this study would have an equal or higher tolerance to low pH as acid-adapted AOB and AOA. Even though the contribution of each microbe to the nitrification in this experiment was still unclear, this study gives evidence of the ability of diverse nitrifying bacteria communities in soil to adapt to a wide range of pH values.

CONCLUSION

In this study, we selectively enriched both comammox and nitrite-oxidizing *Nitrospira* from acidic soils of a tea field fertilized with a large amount of nitrogen. A phylogenetical analysis based on the 16S rRNA gene revealed the niche differentiation between nitrite-oxidizing *Nitrospira* lineage I and lineage II depending on the HNO_2 concentration rather than pH. Moreover, the amplicon sequencing targeting the *amoA* gene detected OTUs related to uncultivated comammox *Nitrospira*. The enrichment sample of comammox *Nitrospira* showed nitrification activity even at pH 3–4. Therefore, the enriched comammox *Nitrospira* was not only phylogenetically novel, but also might possess the potential to adapt to low pH.

Although *Nitrospira*, as either comammox or NOB, is still difficult to cultivate, physiological studies are necessary to understand their characteristics. This study provides a scientific basis to establish a cultivation method for *Nitrospira* from acidic soils. Furthermore, the enrichment sample enables us to examine the metabolism of *Nitrospira* by comprehensive analyses based on metatranscriptomics or metaproteomics. These approaches could reveal the still unknown acid-adaptation mechanisms of *Nitrospira* and the regulation factors that affect these systems.

DATA AVAILABILITY STATEMENT

The amplicon sequence data have been deposited in DDBJ Sequence Read Archive with BioProject number PRJDB9437. The OTUs acquired from amplicon sequencing based on the 16S rRNA gene and amoA gene were registered at DDBJ/ENA/GenBank with accession numbers LC529906, LC529907, LC529908, LC529909, LC529910, LC529911, LC529912, LC529913, LC529914, and LC529915.

AUTHOR CONTRIBUTIONS

YT, HF, and ST contributed to the conception and design of the study, analyzed the phylogenetical and physiological data, and wrote the manuscript with help from all co-authors. YT cultivated the soil sample and performed all of the experiments using enrichment cultures. YH collected the soil sample. KT, YW, and MH analyzed and identified the chemical characteristics of the soil sample. All authors contributed to the article and approved the submitted version.

FUNDING

This study was supported by the Japan Society for the Promotion of Science with KAKENHI (19K16218) (to HF), the Mayekawa Houonkai Foundation with Scientific Research Grant (A16034) (to HF), and the Waseda

University Grant for Special Research Projects (2019C-275) for supporting this research.

ACKNOWLEDGMENTS

We thank Dr. Toshi Urakawa (Florida Gulf Coast University, Fort Myers, FL, United States) for offering advice to this research. We also would like to thank Kento Ishii for scientific discussion. Furthermore, we would like to thank Editage (www.editage.com) for English language editing.

SUPPLEMENTARY MATERIAL

The Supplementary Material for this article can be found online at: https://www.frontiersin.org/articles/10.3389/fmicb.2020.01737/full#supplementary-material

REFERENCES

Amann, R. I., Krumholz, L., and Stahl, D. A. (1990). Fluorescent-oligonucleotide probing of whole cells for determinative, phylogenetic, and environmental studies in microbiology. *J. Bacteriol.* 172, 762–770. doi: 10.1128/jb.172.2.762-770.1990

Aminot, A., Kirkwood, D. S., and Kérouel, R. (1997). Determination of ammonia in seawater by the indolphenol-blue method: evaluation of the ICES NUTS I/C 5 questionnaire. *Mar. Chem.* 56, 59–75. doi: 10.1016/s0304-4203(96)00080-1

Anthonisen, A. C., Loehr, R. C., Prakasam, T. B. S., and Srinath, E. G. (1976). Inhibition of nitrification by ammonia and nitrous acid. *J. Water Pollut. Control Federation* 48, 835–852.

Bakken, L. R., Bergaust, L., Liu, B., and Frostegård, Å (2012). Regulation of denitrification at the cellular level: a clue to the understanding of N2O emissions from soils. *Philos. Trans. R. Soc. BBiol. Sci.* 367, 1226–1234. doi: 10.1098/rstb.2011.0321

Bartelme, R. P., McLellan, S. L., and Newton, R. J. (2017). Freshwater recirculating aquaculture system operations drive biofilter bacterial community shifts around a stable nitrifying consortium of ammonia-oxidizing archaea and comammox *Nitrospira*. *Front. Microbiol.* 8:101. doi: 10.3389/fmicb.2017.00101

Blackburne, R., Vadivelu, V. M., Yuan, Z., and Keller, J. (2007). Kinetic characterisation of an enriched *Nitrospira* culture with comparison to Nitrobacter. *Water Res.* 41, 3033–3042. doi: 10.1016/j.watres.2007.01.043

Bock, E., and Heinrich, G. (1969). Morphological and physiological studies of Nitrobacter winogradskyi Buch. *Archiv. Mikrobiolo.* 69, 19–59.

Booth, M. S., Stark, J. M., and Rastetter, E. (2005). Controls on nitrogen cycling in terrestrial ecosystems: a synthetic analysis of literature data. *Ecol. Monogr.* 75, 139–157. doi: 10.1890/04-0988

Cai, Q., Zhang, W., and Yang, Z. (2001). Stability of nitrite in wastewater and its determination by ion chromatography. *Anal. Sci.* 17, 917–920.

Camejo, P. Y., Domingo, J. S., McMahon, K. D., and Noguera, D. R. (2017). Genome-enabled insights into the ecophysiology of the comammox bacterium "candidatus *Nitrospira* nitrosa". *mSystems* 2:e00059-17. doi: 10.1128/mSystems.00059-17

Caporaso, J. G., Kuczynski, J., Stombaugh, J., Bittinger, K., Bushman, F. D., Costello, E. K., et al. (2010). QIIME allows analysis of high-throughput community sequencing data. *Nat. Methods* 7, 335–336.

Chitsaz, H., Yee-Greenbaum, J. L., Tesler, G., Lombardo, M. J., Dupont, C. L., Badger, J. H., et al. (2011). Efficient *de novo* assembly of single-cell bacterial genomes from short-read data sets. *Nat. Biotechnol.* 29, 915–921 . doi: 10.1038/nbt.1966

Cytryn, E., Levkovitch, I., Negreanu, Y., Dowd, S., Frenk, S., and Silber, A. (2012). Impact of short-term acidification on nitrification and nitrifying bacterial community dynamics in soilless cultivation media. *Appl. Environ. Microbiol.* 78, 6576–6582. doi: 10.1128/aem.01545-12

Dai, G. Z., Shang, J. L., and Qiu, B. S. (2012). Ammonia may play an important role in the succession of cyanobacterial blooms and the distribution of common algal species in shallow freshwater lakes. *Global Change Biol.* 18, 1571–1581. doi: 10.1111/j.1365-2486.2012.02638.x

Daims, H., Lebedeva, E. V., Pjevac, P., Han, P., Herbold, C., Albertsen, M., et al. (2015). Complete nitrification by *Nitrospira bacteria*. *Nature* 528, 504–509. doi: 10.1038/nature16461

De Boer, W., Gunnewiek, P. J. A. K., Veenhuis, M., Bock, E., and Laanbroek, H. J. (1991). Nitrification at low pH by aggregated chemolithotrophic bacteria. *Appl. Environ. Microbiol.* 57, 3600–3604. doi: 10.1128/aem.57.12.3600-3604.1991

De Boer, W., and Kowalchuk, G. A. (2001). Nitrification in acid soils: micro-organisms and mechanisms. *Soil Biol. Biochem.* 33, 853–866. doi: 10.1016/s0038-0717(00)00247-9

Dimitri, K., Sedlacek, C. J., Lebedeva, E. V., Han, P., Bulaev, A., Pjevac, P., et al. (2017). Kinetic analysis of a complete nitrifier reveals an oligotrophic lifestyle. *Nature* 549, 269–272. doi: 10.1038/nature23679

Edgar, R. C. (2010). Search and clustering orders of magnitude faster than BLAST. *Bioinformatics* 26, 2460–2461. doi: 10.1093/bioinformatics/btq461

Felsenstein, J. (1985). Confidence limits on phylogenies: an approach using the bootstrap. *Evolution* 39, 783–791. doi: 10.1111/j.1558-5646.1985.tb00420.x

Fowler, S. J., Palomo, A., Dechesne, A., Mines, P. D., and Smets, B. F. (2018). Comammox *Nitrospira* are abundant ammonia oxidizers in diverse groundwater-fed rapid sand filter communities. *Environ. Microbiol.* 20, 1002–1015. doi: 10.1111/1462-2920.14033

Fujitani, H., Aoi, Y., and Tsuneda, S. (2013). Selective enrichment of two different types of *Nitrospira*-like nitrite-oxidizing bacteria from a wastewater treatment plant. *Microb. Environ.* 28, 236–243. doi: 10.1264/jsme2.me12209

Galloway, J. N., Townsend, A. R., Erisman, J. W., Bekunda, M., Cai, Z., Freney, J. R., et al. (2008). Transformation of the nitrogen cycle: recent trends, questions, and potential solutions. *Science* 320, 889–892. doi: 10.1126/science.1136674

Garcia, J. C., Urakawa, H., Le, V. Q., Stein, L. Y., Klotz, M. G., and Nielsen, J. L. (2013). Draft genome sequence of *Nitrosospira* sp. strain *APG3*, a psychrotolerant ammonia-oxidizing bacterium isolated from sandy lake sediment. *Genome Announc.* 1:e00930-13. doi: 10.1128/genomeA.00930-13

Griess-Romijn, E. (1966). *Physiological and Chemical Tests for Drinking Water, in NEN 1056, IV-2*. Rijswijk: Nederlands Normalisatie Instituut.

Gruber-Dorninger, C., Pester, M., Kitzinger, K., Savio, D. F., Loy, A., Rattei, T., et al. (2015). Functionally relevant diversity of closely related *Nitrospira* in activated sludge. *ISME J.* 9, 643–655. doi: 10.1038/ismej.2014.156

Hankinson, T. R., and Schmidt, E. L. (1988). An acidophilic and a neutrophilic Nitrobacter strain isolated from the numerically predominant nitrite-oxidizing population of an acid forest soil. *Appl. Environ. Microbiol.* 54, 1536–1540. doi: 10.1128/aem.54.6.1536-1540.1988

Hayatsu, M., Tago, K., Uchiyama, I., Toyoda, A., Wang, Y., Shimomura, Y., et al. (2017). An acid-tolerant ammonia-oxidizing γ-proteobacterium from soil. *ISME J.* 11, 1130–1141. doi: 10.1038/ismej.2016.191

Herbold, C. W., Lehtovirta-Morley, L. E., Jung, M. Y., Jehmlich, N., Hausmann, B., Han, P., et al. (2017). Ammonia-oxidising archaea living at low pH: insights from comparative genomics. *Environ. Microbiol.* 19, 4939–4952. doi: 10.1111/1462-2920.13971

Hirono, Y., Watanabe, I., and Nonaka, K. (2009). Trends in water quality around an intensive tea-growing area in Shizuoka. *Jpn. Soil Sci. Plant Nutr.* 55, 783–792. doi: 10.1111/j.1747-0765.2009.00413.x

Hu, H. W., and He, J. Z. (2017). Comammox—a newly discovered nitrification process in the terrestrial nitrogen cycle. *J. Soils and Sediments* 17, 2709–2717. doi: 10.1007/s11368-017-1851-9

Ishii, K., Fujitani, H., Soh, K., Nakagawa, T., Takahashi, R., and Tsuneda, S. (2017). Enrichment and physiological characterization of a coldadapted nitrite-oxidizing Nitrotoga sp. from an eelgrass sediment. *Appl. Environ. Microbiol.* 83:AEM.00549-17. doi: 10.1128/AEM.00549-17

Kandeler, E., and Gerber, H. (1988). Short-term assay of soil urease activity using colorimetric determination of ammonium. *Biol. Fertil. Soils* 6, 68–72.

Kérouel, R., and Aminot, A. (1997). Fluorometric determination of ammonia in sea and estuarine waters by direct segmented flow analysis. *Mar. Chem.* 57, 265–275. doi: 10.1016/s0304-4203(97)00040-6

Koch, H., van Kessel, M., and Lücker, S. (2019). Complete nitrification: insights into the ecophysiology of comammox *Nitrospira*. *Appl. Microbiol. Biotechnol.* 103, 177–189. doi: 10.1007/s00253-018-9486-3

Koper, T. E., El-Sheikh, A. F., Norton, J. M., and Klotz, M. G. (2004). Urease-encoding genes in ammonia-oxidizing bacteria. *Appl. Environ. Microbiol.* 70, 2342–2348. doi: 10.1128/aem.70.4.2342-2348.2004

Kostka, J., Green, S., Rishishwar, L., Om Prakash Katz, L., Mariño-Ramírez, L., Jordan, K., et al. (2012). Genome sequences for six rhodanobacter strains, isolated from soils and the terrestrial subsurface, with variable denitrification capabilities. *J. Bacteriol.* 194, 4461–4462. doi: 10.1128/jb.00871-12

Kowalchuk, G. A., and Stephen, J. R. (2001). Ammonia-oxidizing bacteria: a model for molecular microbial ecology. *Annu. Rev. Microbiol.* 55, 485–529. doi: 10.1146/annurev.micro.55.1.485

Laanbroek, H. J., and Schotman, J. M. T. (1991). Effect of nitrite concentration and pH on most probable number enumerations of non-growing Nitrobacter spp. *FEMS Microbiol. Ecol.* 8, 269–277. doi: 10.1111/j.1574-6941.1991.tb01772.x

Lehtovirta-Morley, L. E., Ge, C., Ross, J., Yao, H., Nicol, G. W., and Prosser, J. I. (2014). Characterisation of terrestrial acidophilic archaeal ammonia oxidisers and their inhibition and stimulation by organic compounds. *FEMS Microbiol. Ecol.* 89, 542–552. doi: 10.1111/1574-6941.12353

Lehtovirta-Morley, L. E., Sayavedra-Soto, L. A., Gallois, N., Schouten, S., Stein, L. Y., Prosser, J. I., et al. (2016). Identifying potential mechanisms enabling acidophily in the ammonia-oxidizing archaeon "Candidatus Nitrosotalea devanaterra". *Appl. Environ. Microbiol.* 82, 2608–2619. doi: 10.1128/aem.04031-15

Lehtovirta-Morley, L. E., Stoecker, K., Vilcinskas, A., Prosser, J. I., and Nicol, G. W. (2011). Cultivation of an obligate acidophilic ammonia oxidizer from a nitrifying acid soil. *Proc. Natl. Acad. Sci. U.S.A.* 108, 15892–15897. doi: 10.1073/pnas.1107196108

Leininger, S., Urich, T., Schloter, M., Schwark, L., Qi, J., Nicol, G. W., et al. (2006). Archaea predominate among ammonia-oxidizing prokaryotes in soils. *Nature* 442, 806–809. doi: 10.1038/nature04983

Liu, B., Mørkved, P. T., Frostegård, A., and Bakken, L. R. (2010). Denitrification gene pools, transcription and kinetics of NO, N2O and N2 production as affected by soil pH. *FEMS Microbiol. Ecol.* 72, 407–417. doi: 10.1111/j.1574-6941.2010.00856.x

Long, X., Chen, C., Xu, Z., Oren, R., and He, J. Z. (2012). Abundance and community structure of ammonia-oxidizing bacteria and archaea in a temperate forest ecosystem under ten-years elevated CO2. *Soil Biol. Biochem.* 46, 163–171. doi: 10.1016/j.soilbio.2011.12.013

Maixner, F., Noguera, D. R., Anneser, B., Stoecker, K., Wegl, G., Wagner, M., et al. (2006). Nitrite concentration influences the population structure of *Nitrospira*-like bacteria. *Environ. Microbiol.* 8, 1487–1495. doi: 10.1111/j.1462-2920.2006.01033.x

McDonald, D., Price, M. N., Goodrich, J., Nawrocki, E. P., DeSantis, T. Z., Probst, A., et al. (2012). An improved Greengenes taxonomy with explicit ranks for ecological and evolutionary analyses of bacteria and archaea. *ISME J.* 6, 610–618. doi: 10.1038/ismej.2011.139

Miranda, K. M., Espey, M. G., and Wink, D. A. (2001). A rapid, simple spectrophotometric method for simultaneous detection of nitrate and nitrite. *Nitric Oxide Biol. Chem.* 5, 62–71. doi: 10.1006/niox.2000.0319

Mørkved, P. T., Dörsch, P., and Bakken, L. R. (2007). The N2O product ratio of nitrification and its dependence on long-term changes in soil pH. *Soil Biol. Biochem.* 39, 2048–2057. doi: 10.1016/j.soilbio.2007.03.006

Nicol, G. W., Leininger, S., Schleper, C., and Prosser, J. I. (2008). The influence of soil pH on the diversity, abundance and transcriptional activity of ammonia oxidizing archaea and bacteria. *Environ. Microbiol.* 10, 2966–2978. doi: 10.1111/j.1462-2920.2008.01701.x

Norton, J. M., Alzerreca, J. J., Suwa, Y., and Klotz, M. G. (2002). Diversity of ammonia monooxygenase operon in autotrophic ammonia-oxidizing bacteria. *Arch. Microbiol.* 177, 139–149. doi: 10.1007/s00203-001-0369-z

Norton, J. M., Klotz, M. G., Stein, L. Y., Arp, D. J., Bottomley, P. J., Chain, P. S. G., et al. (2008). Complete genome sequence of *Nitrosospira* multiformis, an ammonia-oxidizing bacterium from the soil environment. *Appl. Environ. Microbiol.* 74, 3559–3572. doi: 10.1128/aem.02722-07

Nowka, B., Off, S., Daims, H., and Spieck, E. (2015). Improved isolation strategies allowed the phenotypic differentiation of two *Nitrospira* strains from widespread phylogenetic lineages. *FEMS Microbiol. Ecol.* 91:fiu031.

Orellana, L. H., Chee-Sanford, J. C., Sanford, R. A., Löffler, F. E., and Konstantinidis, K. T. (2018). Year-round shotgun metagenomes reveal stable microbial communities in agricultural soils and novel ammonia oxidizers responding to fertilization. *Appl. Environ. Microbiol.* 84:e01646-17. doi: 10.1128/AEM.01646-17

Palomo, A., Jane Fowler, S., Gülay, A., Rasmussen, S., Sicheritz-Ponten, T., and Smets, B. F. (2016). Metagenomic analysis of rapid gravity sand filter microbial communities suggests novel physiology of *Nitrospira* spp. *ISME J.* 10, 2569–2581. doi: 10.1038/ismej.2016.63

Palomo, A., Pedersen, A. G., Fowler, S. J., Dechesne, A., Sicheritz-Pontén, T., and Smets, B. F. (2018). Comparative genomics sheds light on niche differentiation and the evolutionary history of comammox *Nitrospira*. *ISME J.* 12, 1779–1793. doi: 10.1038/s41396-018-0083-3

Park, H. D., and Noguera, D. R. (2008). *Nitrospira* community composition in nitrifying reactors operated with two different dissolved oxygen levels. *J. Microbiol. Biotechnol.* 18, 1470–1474.

Parks, D. H., Rinke, C., Chuvochina, M., Chaumeil, P. A., Woodcroft, B. J., Evans, P. N., et al. (2017). Recovery of nearly 8,000 metagenome-assembled genomes substantially expands the tree of life. *Nat. Microbiol.* 2, 1533–1542. doi: 10.1038/s41564-017-0012-7

Petersen, D. G., Blazewicz, S. J., Firestone, M., Herman, D. J., Turetsky, M., and Waldrop, M. (2012). Abundance of microbial genes associated with nitrogen cycling as indices of biogeochemical process rates across a vegetation gradient in Alaska. *Environ. Microbiol.* 14, 993–1008. doi: 10.1111/j.1462-2920.2011.02679.x

Pjevac, P., Schauberger, C., Poghosyan, L., Herbold, C. W., van Kessel, M. A. H. J., Daebeler, A., et al. (2017). AmoA-targeted polymerase chain reaction primers for the specific detection and quantification of comammox *Nitrospira* in the environment. *Front. Microbiol.* 8:1508. doi: 10.3389/fmicb.2017.01508

Pommerening-Roser, A., and Koops, H. P. (2005). Environmental pH as an important factor for the distribution of urease positive ammonia-oxidizing bacteria. *Microbiol. Res.* 160, 27–35. doi: 10.1016/j.micres.2004.09.006

Quast, C., Pruesse, E., Yilmaz, P., Gerken, J., Schweer, T., Yarza, P., et al. (2013). The SILVA ribosomal RNA gene database project: improved data processing and web-based tools. *Nucleic Acids Res.* 41, D590–D596.

Reshetilov, A. N., Iliasov, P. V., Knackmuss, H. J., and Boronin, A. M. (2011). The nitrite oxidizing activity of nitrobacter strains as a base of microbial biosensor for nitrite detection. *Anal. Lett.* 33, 29–41. doi: 10.1080/00032710008543034

Roots, P., Wang, Y., Rosenthal, A. F., Griffin, J. S., Sabba, F., Petrovich, M., et al. (2019). Comammox *Nitrospira* are the dominant ammonia oxidizers in a mainstream low dissolved oxygen nitrification reactor. *Water Res.* 157, 396–405. doi: 10.1016/j.watres.2019.03.060

Saitou, N., and Nei, M. (1987). The neighbor-joining method: a new method for reconstructing phylogenetic trees. *Mol. Biol. Evol.* 4, 406–425.

Schlesinger, W. H. (2009). On the fate of anthropogenic nitrogen. *Proc. Natl. Acad. Sci. U.S.A.* 106, 203–208. doi: 10.1073/pnas.0810193105

Seemann, T. (2014). Prokka: rapid prokaryotic genome annotation. *Bioinformatics* 30, 2068–2069. doi: 10.1093/bioinformatics/btu153

Shindo, J., Okamoto, K., and Kawashima, H. (2006). Prediction of the environmental effects of excess nitrogen caused by increasing food demand with rapid economic growth in eastern Asian countries, 1961-2020. *Ecol. Modelling* 193, 703–720. doi: 10.1016/j.ecolmodel.2005.09.010

Spieck, E., Hartwig, C., McCormack, I., Maixner, F., Wagner, M., Lipski, A., et al. (2006). Selective enrichment and molecular characterization of a previously uncultured *Nitrospira*-like bacterium from activated sludge. *Environ. Microbiol.* 8, 405–415. doi: 10.1111/j.1462-2920.2005.00905.x

Stempfhuber, B., Richter-Heitmann, T., Bienek, L., Schöning, I., Schrumpf, M., Friedrich, M., et al. (2017). Soil pH and plant diversity drive co-occurrence patterns of ammonia and nitrite oxidizer in soils from forest ecosystems. *Biol. Fertil. Soils* 53, 691–700. doi: 10.1007/s00374-017-1215-z

Suzuki, I., Dular, U., and Kwok, S. C. (1974). Ammonia or ammonium ion as substrate for oxidation by *Nitrosomonas europaea* cells and extracts. *J. Bacteriol.* 120, 556–558. doi: 10.1128/jb.120.1.556-558.1974

Tarre, S., and Green, M. (2004). High-rate nitrification at low pH in suspended- and attached-biomass reactors. *Appl. Environ. Microbiol.* 70, 6481–6487. doi: 10.1128/aem.70.11.6481-6487.2004

Tokuda, S., and Hayatsu, M. (2004). Nitrous oxide flux from a tea field amended with a large amount of nitrogen fertilizer and soil environmental factors controlling the flux. *Soil Sci. Plant Nutr.* 50, 365–374. doi: 10.1080/00380768.2004.10408490

Tourna, M., Freitag, T. E., and Prosser, J. I. (2010). Stable isotope probing analysis of interactions between ammonia oxidizers. *Appl. Environ. Microbiol.* 76, 2468–2477. doi: 10.1128/aem.01964-09

Urakawa, H., Garcia, J. C., Nielsen, J. L., Le, V. Q., Kozlowski, J. A., Stein, L. Y., et al. (2015). *Nitrosospira lacus* sp. nov., a psychrotolerant, ammonia-oxidizing bacterium from sandy lake sediment. *Int. J. Syst. Evol. Microbiol.* 65, 242–250. doi: 10.1099/ijs.0.070789-0

Ushiki, N., Fujitani, H., Aoi, Y., and Tsuneda, S. (2013). Isolation of *Nitrospira* belonging to sublineage II from a wastewater treatment plant. *Microbes Environ.* 28, 346–353. doi: 10.1264/jsme2.me13042

van Kessel, M. A. H. J., Speth, D. R., Albertsen, M., Nielsen, P. H., Op Den Camp, H. J. M., Kartal, B., et al. (2015). Complete nitrification by a single microorganism. *Nature* 528, 555–559. doi: 10.1038/nature16459

Vitousek, P. M., Aber, J. D., Howarth, R. W., Likens, G. E., Matson, P. A., Schindler, D. W., et al. (1997). Human alteration of the global nitrogen cycle: Sources and consequences. *Ecol. Appl.* 7, 737–750. doi: 10.1890/1051-0761(1997)007[0737:haotgn]2.0.co;2

Wang, Y., Ma, L., Mao, Y., Jiang, X., Xia, Y., Yu, K., et al. (2017). Comammox in drinking water systems. *Water Res.* 116, 332–341. doi: 10.1016/j.watres.2017.03.042

Wang, Q., Quensen, J. F. III., Fish, J. A., Lee, T. K., Sun, Y., Tiedje, J. M., et al. (2013). Ecological patterns of nifH genes in four terrestrial climatic zones explored with targeted metagenomics using framebot, a new informatics tool. *mBio* 4:e00592-13. doi: 10.1128/mBio.00592-13

Wertz, S., Leigh, A. K., and Grayston, S. J. (2012). Effects of long-term fertilization of forest soils on potential nitrification and on the abundance and community structure of ammonia oxidizers and nitrite oxidizers. *FEMS Microbiol. Ecol.* 79, 142–154. doi: 10.1111/j.1574-6941.2011.01204.x

Willason, S. W., and Johnson, K. S. (1986). A rapid, highly sensitive technique for the determination of ammonia in seawater. *Mar. Biol.* 91, 285–290. doi: 10.1007/bf00569445

Wrage, N., Velthof, G. L., Van Beusichem, M. L., and Oenema, O. (2001). Role of nitrifier denitrification in the production of nitrous oxide. *Soil Biol. Biochem.* 33, 1723–1732. doi: 10.1016/s0038-0717(01)00096-7

Yu, C., Hou, L., Zheng, Y., Liu, M., Yin, G., Gao, J., et al. (2018). Evidence for complete nitrification in enrichment culture of tidal sediments and diversity analysis of clade a comammox *Nitrospira* in natural environments. *Appl. Microbiol. Biotechnol.* 102, 9363–9377. doi: 10.1007/s00253-018-9274-0

Zhang, J., Dai, Y., Wang, Y., Wu, Z., Xie, S., and Liu, Y. (2015). Distribution of ammonia-oxidizing archaea and bacteria in plateau soils across different land use types. *Appl. Microbiol. Biotechnol.* 99, 6899–6909. doi: 10.1007/s00253-015-6625-y

Zhang, L. M., Hu, H. W., Shen, J. P., and He, J. Z. (2012). Ammonia-oxidizing archaea have more important role than ammonia-oxidizing bacteria in ammonia oxidation of strongly acidic soils. *ISME J.* 6, 1032–1045. doi: 10.1038/ismej.2011.168

Conflict of Interest: The authors declare that the research was conducted in the absence of any commercial or financial relationships that could be construed as a potential conflict of interest.

frontiers in Microbiology

ORIGINAL RESEARCH
published: 28 July 2020
doi: 10.3389/fmicb.2020.01710

Nitrogen Isotope Fractionation During Archaeal Ammonia Oxidation: Coupled Estimates From Measurements of Residual Ammonium and Accumulated Nitrite

*Maria Mooshammer[1†], Ricardo J. E. Alves[2†], Barbara Bayer[2†], Michael Melcher[2], Michaela Stieglmeier[2], Lara Jochum[3], Simon K.-M. R. Rittmann[2], Margarete Watzka[1], Christa Schleper[2], Gerhard J. Herndl[2,4] and Wolfgang Wanek[1]**

[1] Centre for Microbiology and Environmental Systems Science, University of Vienna, Vienna, Austria, [2] Department of Functional and Evolutionary Ecology, University of Vienna, Vienna, Austria, [3] LMU – Max von Pettenkofer Institute for Hygiene and Medical Microbiology, Ludwig Maximilian University of Munich, Munich, Germany, [4] Department of Marine Microbiology and Biogeochemistry, Royal Netherlands Institute for Sea Research (NIOZ), Utrecht University, Utrecht, Netherlands

OPEN ACCESS

Edited by:
Laura E. Lehtovirta-Morley,
University of East Anglia,
United Kingdom

Reviewed by:
Soo-Je Park,
Jeju National University, South Korea
Anne E. Taylor,
Oregon State University,
United States
Karen L. Casciotti,
Stanford University, United States

***Correspondence:**
Wolfgang Wanek
wolfgang.wanek@univie.ac.at

†Present address:
Maria Mooshammer,
Department of Environmental Science, Policy, and Management, University of California, Berkeley, Berkeley, CA, United States
Ricardo J. E. Alves,
Lawrence Berkeley National Laboratory, Climate and Ecosystem Sciences Division, Earth and Environmental Sciences, Berkeley, CA, United States
Barbara Bayer,
Department of Ecology, Evolution and Marine Biology, University of California, Santa Barbara, Santa Barbara, CA, United States

Specialty section:
This article was submitted to Microbial Physiology and Metabolism, a section of the journal Frontiers in Microbiology

Received: 18 February 2020
Accepted: 29 June 2020
Published: 28 July 2020

The naturally occurring nitrogen (N) isotopes, ^{15}N and ^{14}N, exhibit different reaction rates during many microbial N transformation processes, which results in N isotope fractionation. Such isotope effects are critical parameters for interpreting natural stable isotope abundances as proxies for biological process rates in the environment across scales. The kinetic isotope effect of ammonia oxidation (AO) to nitrite (NO_2^-), performed by ammonia-oxidizing archaea (AOA) and ammonia-oxidizing bacteria (AOB), is generally ascribed to the enzyme ammonia monooxygenase (AMO), which catalyzes the first step in this process. However, the kinetic isotope effect of AMO, or ε_{AMO}, has been typically determined based on isotope kinetics during product formation (cumulative product, NO_2^-) alone, which may have overestimated ε_{AMO} due to possible accumulation of chemical intermediates and alternative sinks of ammonia/ammonium (NH_3/NH_4^+). Here, we analyzed ^{15}N isotope fractionation during archaeal ammonia oxidation based on both isotopic changes in residual substrate (RS, NH_4^+) and cumulative product (CP, NO_2^-) pools in pure cultures of the soil strain *Nitrososphaera viennensis* EN76 and in highly enriched cultures of the marine strain *Nitrosopumilus adriaticus* NF5, under non-limiting substrate conditions. We obtained ε_{AMO} values of 31.9–33.1‰ for both strains based on RS ($\delta^{15}NH_4^+$) and showed that estimates based on CP ($\delta^{15}NO_2^-$) give larger isotope fractionation factors by 6–8‰. Complementary analyses showed that, at the end of the growth period, microbial biomass was ^{15}N-enriched (10.1‰), whereas nitrous oxide (N_2O) was highly ^{15}N depleted (−38.1‰) relative to the initial substrate. Although we did not determine the isotope effect of NH_4^+ assimilation (biomass formation) and N_2O production by AOA, our results nevertheless show that the discrepancy between ε_{AMO} estimates based on RS and CP might have derived from the incorporation of ^{15}N-enriched residual NH_4^+ after AMO reaction into microbial biomass and that N_2O production did not affect isotope fractionation estimates significantly.

Keywords: ammonia oxidation, nitrification, nitrous oxide, stable isotope fractionation, Thaumarchaeota

INTRODUCTION

Knowledge of natural ^{15}N abundances and of nitrogen (N) isotope fractionation effects associated with key microbial N transformation processes has contributed greatly to our understanding of the marine N cycle (Casciotti and Buchwald, 2012; Buchwald and Casciotti, 2013) and of terrestrial gaseous N emissions (Houlton and Bai, 2009), namely atmospheric N_2O sources and sinks (Yoshida and Toyoda, 2000), and biological N fixation (Vitousek et al., 2013). The oxidation of NH_4^+ to NO_2^-—the first and rate-limiting step in nitrification—is a central process in the marine and terrestrial N cycles, as well as the major driver of a large N isotope effect that leads to formation of ^{15}N-depleted products such as NO, N_2O, NO_2^-, and NO_3^-, while residual NH_4^+ becomes ^{15}N-enriched during that process (Mariotti et al., 1981; Sigman and Casciotti, 2001). A detailed understanding of N isotope effects of the range of N transformation processes is thus critical for adequate biological interpretation of natural ^{15}N isotope patterns in the environment (Casciotti, 2016).

Besides the recently discovered comammox bacteria (Daims et al., 2015; van Kessel et al., 2015), ammonia oxidation is catalyzed by both ammonia-oxidizing archaea (AOA) and ammonia-oxidizing bacteria (AOB), with different relative contributions across ecosystems and environmental conditions (Prosser and Nicol, 2012; Prosser et al., 2019). On a cellular level, ammonia oxidation is a multi-step process that comprises different enzymatic reactions and chemical equilibrium processes, which can all contribute to the N isotope fractionation effects inferred from extracellular N pools (Casciotti et al., 2003; Santoro and Casciotti, 2011). The isotopic fractionation effect (ε) of ammonia oxidizers has been typically inferred based on changes in $\delta^{15}N$ of the cumulative product (CP) NO_2^- (ε_{CP}), and attributed to the initial enzymatic step catalyzed by the ammonia monooxygenase (AMO) enzyme, defined as ε_{AMO}. However, ε_{CP} estimates reflect the combined fractionation effects of the isotope equilibrium between NH_4^+ and NH_3 [NH_3, the proposed substrate for ammonia oxidation, is depleted in ^{15}N relative to NH_4^+ (Hermes et al., 1985)], the AMO-catalyzed reaction, and accumulation of several intermediates derived from subsequent enzymatic processes (Casciotti et al., 2003). For instance, ε_{CP} estimates may be affected by the accumulation of essential intermediates, such as hydroxylamine (NH_2OH) and by the production of gaseous N by-products (nitric oxide, NO; and nitrous oxide, N_2O), which may represent further ^{15}N fractionation steps. Consequently, this could result in a difference of kinetic isotope effect estimates derived from residual substrate (RS) and CP (Casciotti et al., 2003). Not only could these "leakage" processes alter CP-based estimates of ε_{AMO}, but their different contributions to ammonia utilization and to ε_{CP} may also underlie the large differences observed in ε_{AMO} between ammonia-oxidizing organisms (Mariotti et al., 1981; Yoshida, 1988; Casciotti et al., 2003; Santoro and Casciotti, 2011).

Estimates of isotope effects based on the change in $\delta^{15}NH_4^+$ (ε_{RS}) can circumvent many of the expected biases associated with ε_{CP}, as they are not affected by the multiple subsequent equilibria, enzymatic transformations, and intermediate N pools, as discussed but not quantified previously (Casciotti et al., 2003; Santoro and Casciotti, 2011). However, to our knowledge, only one study has determined the isotope fractionation factors based on concurrent measurements of changes in isotopic composition of RS and CP of ammonia oxidation, namely in cultures of the AOB *Nitrosomonas europaea* (Mariotti et al., 1981). This study found no difference between ε_{RS} and ε_{CP}, suggesting that ammonia oxidation can be effectively regarded as a "one-step process," where the AMO-catalyzed reaction constitutes the rate-limiting and sole isotope fractionation step. On the other hand, AOB and AOA seem to harbor fundamentally distinct ammonia oxidation pathways and exhibit different yields of gaseous N compounds per mole of NH_4^+ consumed (Walker et al., 2010; Kozlowski et al., 2016). Importantly, the enzyme hydroxylamine dehydrogenase (HAO), which performs the second step in ammonia oxidation of AOB, has not been identified in AOA, and thus it remains unclear how NH_2OH is converted to NO_2^- in AOA (Walker et al., 2010; Kerou et al., 2016). Moreover, a recent study has provided evidence that the bacterial HAO oxidizes NH_2OH to NO rather than to NO_2^-, as generally assumed, with the latter resulting from non-enzymatic oxidation of NO by oxygen (Caranto and Lancaster, 2017). Previous studies have shown that NO is also an essential intermediate in ammonia oxidation by AOA, as their growth and activity is highly sensitive to exposure to an NO scavenger (Shen et al., 2013; Kozlowski et al., 2016).

Here, we tested whether the kinetic isotope effect of archaeal ammonia oxidation based on CP ($\delta^{15}NO_2^-$) alone might be biased, by comparing the isotope fractionation factors inferred from both RS and CP pools. For this, we determined the kinetic isotope effects during growth of two phylogenetically and ecologically distinct AOA: the axenic strain *Nitrososphaera viennensis* EN76 (Stieglmeier et al., 2014a), isolated from soil, and the highly enriched marine strain *Nitrosopumilus adriaticus* NF5 (Bayer et al., 2016). This is also the first study of ^{15}N isotope fractionation of ammonia oxidation by an AOA strain in pure culture. All previous studies of kinetic isotope effects of AOA have been performed with enrichment cultures with varying degrees of enrichment (Santoro and Casciotti, 2011; Nishizawa et al., 2016) and bacterial contaminants that may have contributed to the variation in isotope effects through consumption of and inputs to the same N pools.

MATERIALS AND METHODS

Pure cultures of *N. viennensis* EN76 were cultivated in freshwater medium and incubated at 37°C, as described by Tourna et al. (2011). In a first experiment, quadruplicate cultures were supplemented with 1 mM NH_4^+ and 0.1 mM pyruvate; in a second experiment, quadruplicate cultures were supplemented with 2 mM NH_4^+ and 0.5 mM pyruvate to generate higher cell biomass and sufficient N_2O concentrations for isotopic analysis, in order to determine their potential effect on ε_{AMO}. Quadruplicate enrichment

cultures of *N. adriaticus* NF5 were cultivated in Synthetic Crenarchaeota Medium (SCM) at 30°C as described by Bayer et al. (2016). The medium was supplemented with 1 mM NH_4^+ and 5% (v/v) autoclaved seawater, which was sterile-filtered (0.22 μm GTTP, Millipore). Kanamycin at a final concentration of 100 μg ml^{-1} was used to inhibit bacterial contaminants. At the time of the experiment (January 2013), the enrichment level of strain NF5 was ∼95%, as it contained a heterotrophic non-nitrifying/non-denitrifying contaminant of the alphaproteobacterial species *Oceanicaulis alexandrii* (Bayer et al., 2019).

Ammonia-oxidizing archaea growth was monitored by measuring nitrite production using the Griess method (Hood-Nowotny et al., 2010), coupled to NH_4^+ consumption determined using the Berthelot method for *N. viennensis* cultures (Hood-Nowotny et al., 2010) and the o-Phthalaldehyde (OPA) method for *N. adriaticus* cultures (Goyal et al., 1988). $\delta^{15}NH_4^+$ was quantified by microdiffusion (Sørensen and Jensen, 1991) with subsequent analysis on a continuous-flow isotope ratio mass spectrometer consisting of an elemental analyzer (EA1110, CE Instruments) coupled via a ConFlo III interface (Finnigan MAT, Thermo Fisher Scientific) to the isotope ratio mass spectrometer (IRMS; DeltaPLUS, Finnigan MAT, Thermo Fisher Scientific). $\delta^{15}NO_2^-$ was determined based on the reduction of NO_2^- to N_2O by azide under acidified conditions (Lachouani et al., 2010). Concentrations and isotopic ratios of N_2O were determined using a purge-and-trap GC/IRMS system (PreCon - GasBench II headspace analyzer, Delta Advantage V IRMS; Thermo Fischer Scientific, Vienna, Austria). For NH_4^+ and NO_2^- isotope measurements, we included blanks, concentration standards, and isotope standards varying in natural ^{15}N abundance together with the samples through the full microdiffusion and azide procedures to allow corrections for blank contribution, incomplete reaction, and procedural isotope fractionation (Lachouani et al., 2010). Nitrogen content and $\delta^{15}N$ signature of AOA biomass were determined by EA-IRMS as described above. $\delta^{15}N$ signatures [‰ vs. AIR] were calculated relative to the ratio R (^{15}N:^{14}N) of the atmospheric N_2 standard (AIR), as $\delta^{15}N = (R_{sample}/R_{standard} - 1) \times 1000$.

Isotope fractionation factors (ε) were calculated based on the Rayleigh closed system isotope fractionation, based on changes in the isotopic compositions of RS (i.e., NH_4^+) and CP (i.e., NO_2^-) (Mariotti et al., 1981):

$$10^3 \ln \frac{10^{-3}\delta_{RS} + 1}{10^{-3}\delta_{S0} + 1} = \varepsilon \ln(f) \quad (1)$$

$$\delta_{CP} - \delta_{S0} = -\varepsilon f \frac{\ln(f)}{(1-f)}, \quad (2)$$

where δ_{S0} is $\delta^{15}N$ of initial NH_4^+, δ_{RS} is $\delta^{15}NH_4^+$, δ_{CP} is $\delta^{15}NO_2^-$ and f is the fraction of the initial [NH_4^+] remaining in the culture. Plots of $10^3 \frac{10^{-3}\delta_{RS}+1}{10^{-3}\delta_{S0}+1}$ versus $\ln(f)$ and of $\delta_{CP} - \delta_{S0}$ versus $f\frac{\ln(f)}{(1-f)}$ yield linear relations, with the slope representing the kinetic isotope effect based on the isotopic change in substrate (ε_{RS}) and product (ε_{AP}), respectively. Uncertainties of ε are expressed as standard error of the slope. Differences in isotope fractionation effects between cultures were assessed by testing significant differences between their regression plots, using R (R Development Core Team, 2012).

RESULTS AND DISCUSSION

Based on the oxidation of NH_3/NH_4^+ to NO_2^-—a typical proxy for ammonia oxidizer growth, as it strongly correlates with growth rates (Stieglmeier et al., 2014a; Bayer et al., 2016)—all cultures showed growth curves typical for batch cultures of AOA, reaching stationary phase after 7 days for *N. adriaticus*, and after 3–4 days for *N. viennensis* cultures (**Figures 1A–C**). Nitrogen isotope fractionation was reflected in both the substrate (i.e., NH_4^+) and the product (i.e., NO_2^-) of ammonia oxidation, and followed typical Rayleigh isotope fractionation kinetics for closed systems (**Figures 1D–F**): NH_4^+ became increasingly ^{15}N-enriched with the fraction of NH_4^+ oxidized, while NO_2^- was strongly ^{15}N-depleted after correction for NO_2^- deriving from the inoculum. With an increasing fraction of NH_4^+ oxidized, $\delta^{15}NO_2^-$ converged toward the isotopic signature of the initial NH_4^+. Both *N. adriaticus* and *N. viennensis* (including cultures grown on 1 and 2 mM NH_4^+) exhibited ^{15}N isotope fractionation factors based on substrate (ε_{RS}) between 31.9 and 33.1‰, and based on product (ε_{CP}) between 37.7 and 49.1‰ (**Figures 2A–F**). We found no significant difference between the isotope fractionation factors of the different AOA cultures studied here based on $\delta^{15}N$ evolution of the substrate (ε_{RS}; comparison of slopes, df = 2, F = 0.519, p = 0.598) or the product (ε_{CP}; comparison of slopes, df = 2, F = 2.380, p = 0.102). The N isotope fractionation factors based on $\delta^{15}NO_2^-$ (ε_{CP}) were larger than those based on $\delta^{15}NH_4^+$ (ε_{RS}) by 8.0, 5.8, and 5.9‰ for *N. adriaticus*, and for *N. viennensis* grown on 1 mM or 2 mM NH_4^+, respectively.

Nitrogen isotope fractionation has been studied in several AOB strains, but only in three marine and one thermophilic AOA enrichment cultures. These AOA enrichment cultures showed average N isotope fractionation factors between 22 and 25‰ at low substrate concentrations, and up to 32.0‰ at higher ammonium concentrations (Santoro and Casciotti, 2011; Nishizawa et al., 2016, measured via the isotopic composition of the product nitrite; see **Table 1**). These estimates are in the same range as the reported average isotope effects for different AOB strains, i.e., 14–38‰ (Delwiche and Steyn, 1970; Mariotti et al., 1981; Casciotti et al., 2003). ^{15}N isotope fractionation factors of *N. viennensis* and *N. adriaticus* are in the upper range, or higher, than those previously reported for AOA, which might be due to the higher ammonia concentrations applied in our study (1–2 mM in our study vs. 200 μM in Nishizawa et al., 2016; 10–75 μM in Santoro and Casciotti, 2011). Previous studies have indicated that higher initial ammonia concentrations lead to more stable

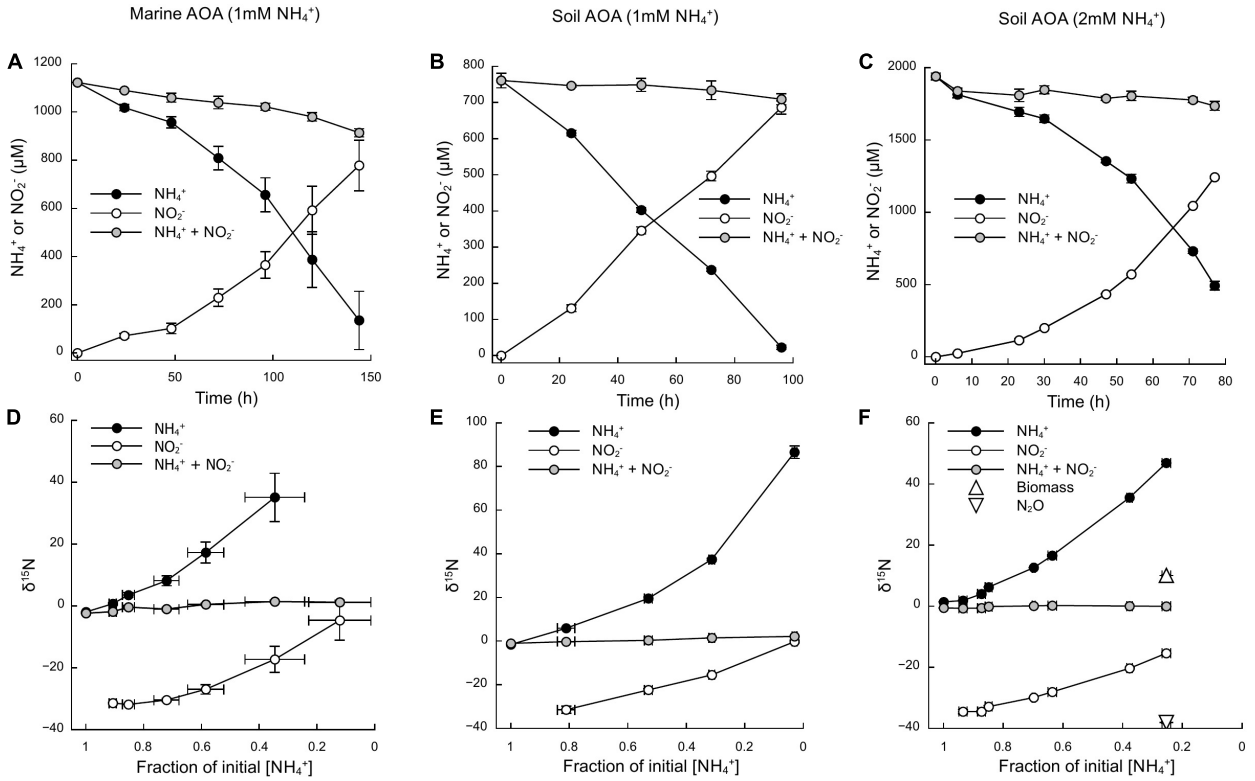

FIGURE 1 | Ammonia oxidation and isotopic signature of NH_4^+ and NO_2^- of a marine (*N. adriaticus* NF5 enrichment culture) and a soil (*N. viennensis* EN76) AOA. **(A–C)** Time course of NH_4^+ oxidation to NO_2^-. **(D–F)** Isotopic composition of NH_4^+ and NO_2^- as a function of initial NH_4^+ oxidized. Some error bars are smaller than the symbol.

and higher ^{15}N isotope fractionation (Casciotti et al., 2003; Santoro and Casciotti, 2011).

We also measured ε_{AMO} based on changes in $\delta^{15}NH_4^+$ (i.e., the residual substrate) to both circumvent and assess potential biases associated with estimates based on $\delta^{15}NO_2^-$ (i.e., the cumulative product). It should be noted, however, that different apparent isotope effects in whole cells may also be observed in the NH_4^+ pool, despite constant AMO enzyme-level isotope effects, depending, for example, on the balance between ammonia oxidation rates and ammonia diffusion across the S-layer (i.e., outermost cell envelope component in AOA) (Casciotti et al., 2003; Li et al., 2018). Published models of AOA and AOB metabolism favor the hypothesis of a (pseudo-)periplasmic location of the ammonia oxidation process (Arp and Stein, 2003; Walker et al., 2010; Simon and Klotz, 2013). However, AOA and AOB harbor very distinct NH_3/NH_4^+ transport systems (Offre et al., 2014), whose role in ammonia oxidation and contribution to observed differences in ^{15}N isotope fractionation remain unclear (Arp and Stein, 2003). At low ammonia concentrations, ammonia oxidation rates are expected to become limited by NH_4^+ transport/NH_3 diffusion, resulting in the convergence of the isotope effect toward that of NH_4^+/NH_3 equilibrium (if NH_3 is mainly taken up by the cells) or NH_4^+/NH_3 transport. The NH_4^+/NH_3 equilibrium isotope effect has been estimated to be 19.2‰ in aqueous solution (Hermes et al., 1985), whereas secondary active ammonium (AMT) transporters, which are highly expressed in AOA (Carini et al., 2017), have been shown to exert isotope fractionation of around 13–15‰, due to deprotonation of NH_4^+ during transport (Ariz et al., 2018). It is unlikely that ammonia oxidation has been limited by NH_3 availability in our study, because of the high substrate concentrations used, which are well above the K_m of the AMO of *N. viennensis* (5.4 µM NH_3 + NH_4^+; Kits et al., 2017) and that of the marine strain *Nitrosopumilus maritimus* strain SCM1 (0.13 µM NH_3 + NH_4^+; Martens-Habbena et al., 2009), which is closely related to *N. adriaticus*. Furthermore, Nishizawa et al. (2016) estimated that, when NH_3 concentrations in the pseudo-periplasm are lower than in the medium under laboratory conditions, cell-specific NH_3 diffusion rates into the pseudo-periplasm are higher than cell-specific ammonia oxidation rates. It has also been proposed that the charged S-layer proteins of AOA enhance the diffusion of charged solutes, such as NH_4^+, which concentrates NH_4^+ in the pseudo-periplasmic space near the active site of the AMO (Li et al., 2018), where then the equilibrium reaction between NH_4^+ and NH_3 is relatively fast and considered not to be rate-limiting.

Even if ammonia oxidation was not limited by periplasmatic NH_3 availability, the apparent isotope effect of the AMO can

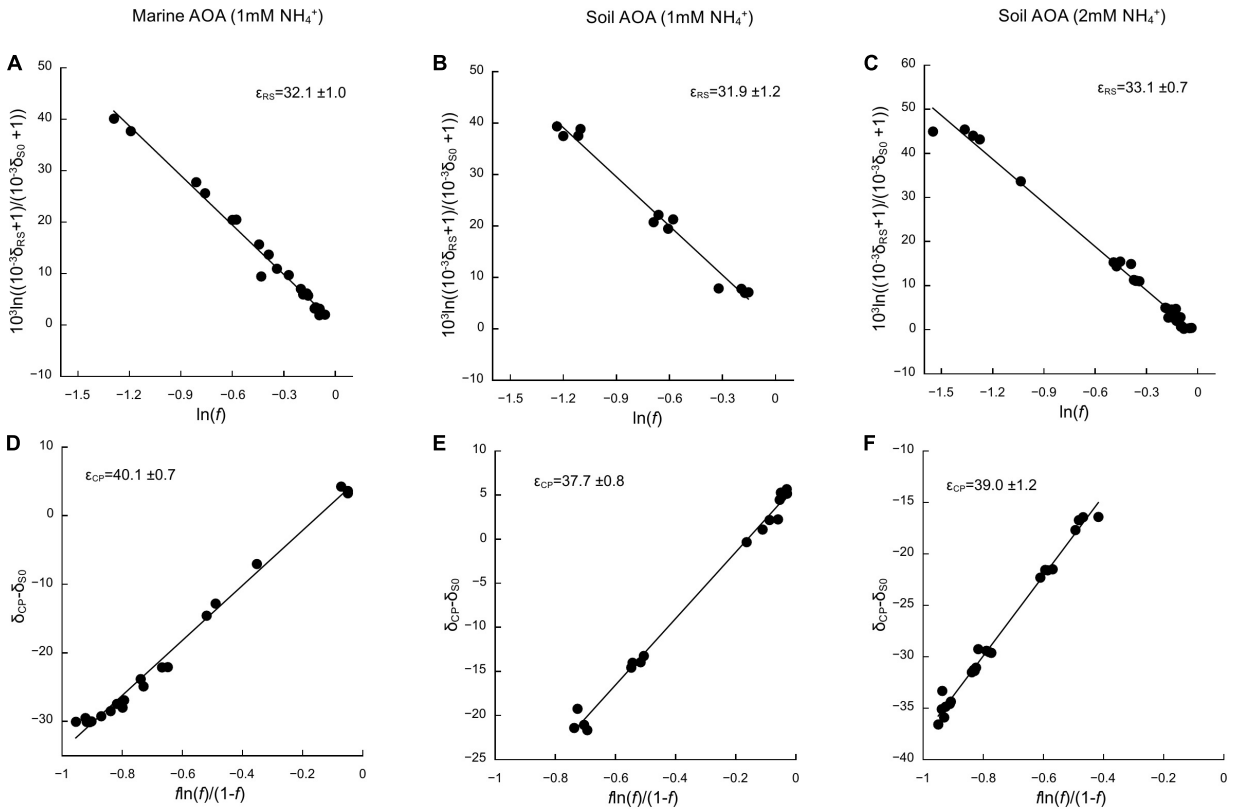

FIGURE 2 | Kinetic isotope effects of the marine AOA *N. adriaticus* and the soil AOA *N. viennensis*. Isotope fractionation factors (ε_{RS} and ε_{CP}) were calculated based on changes in **(A–C)** δ^{15}N-NH_4^+ (δ_{RS}) and **(D–F)** δ^{15}N-NO_2^- (δ_{CP}), using linear regressions of $10^3 \frac{10^{-3}\delta_{RS}+1}{10^{-3}\delta_{S0}+1}$ versus ln(f) and $\delta_{CP} - \delta_{S0}$ versus $f \frac{\ln(f)}{(1-f)}$, respectively, as described in Mariotti et al. (1981). δ_{S0} is δ^{15}N of initial NH_4^+ and f is the fraction of the initial [NH_4^+] remaining in the culture. Uncertainties of ε_{RS} and ε_{CP} are expressed as SE of the slope. We used multiple-point estimates because they have lower uncertainty than single-point analyses.

also be underestimated due to concurrent NH_4^+ assimilation, which has a smaller isotope effect. This process would alter observed ε_{RS} estimates in proportion to the amount of NH_4^+ assimilated and the isotope effect for NH_4^+ assimilation (4–27‰; Hoch et al., 1992). Therefore, we also measured δ^{15}N of the cell biomass at the end of incubation of *N. viennensis* grown on 2 mM NH_4^+ (**Figures 1F**, **3**). Although it is impossible to infer directly the contribution of N assimilation to ε_{RS} from just one end-point measurement, we propose that N assimilation substantially contributed to the decrease of ε_{RS} relative to ε_{CP} in our study, as biomass was ^{15}N-enriched by ∼10‰ compared to initial NH_4^+. Biomass N represented 3.1% (±0.3 SE) of ammonia oxidized by *N. viennensis* grown on 2 mM NH_4^+. Although dissolved inorganic N (DIN) concentrations (sum of [NH_4^+] and [NO_2^-]) were relatively constant over the course of ammonia oxidation, we recovered only 81.9% (±1.5 SE) of the initial DIN by the end of incubation of *N. adriaticus*, and 94.7% (±3.4 SE) and 90.7% (±1.1 SE) of *N. viennensis* grown on 1 mM NH_4^+ or 2 mM NH_4^+, respectively. In *N. adriaticus* cultures, assimilation of N by contaminant bacteria likely did not contribute substantially to the lower ε_{RS} relative to ε_{CP}, due to the high enrichment level of the culture (95%) at the time of the experiment, and the fact that ε_{RS} of *N. adriaticus* was similar to that of *N. viennensis* in pure culture. In addition, the ^{15}N-enrichment of *N. viennensis*' biomass shows that AMO preferentially, and primarily, reacts on pseudo-periplasmatic NH_3, causing ^{15}N-enrichment of the residual ammonia, which is subsequently assimilated into biomass. We thus propose that under substrate replete conditions, the observed isotope effects of ε_{RS} of 31.9–33.1‰ primarily reflect the kinetic isotope effect of the AMO-catalyzed reaction, modified by the NH_4^+/NH_3 equilibrium isotope effect (19.2‰; Hermes et al., 1985) and decreased by the contribution of the lower kinetic isotope effect of NH_4^+ assimilation for anabolic purposes (4–27‰; Hoch et al., 1992). Moreover, it should be noted that some ammonia oxidizers use distinct pathways of NH_4^+ assimilation, even among just AOA, which may contribute to different kinetic isotope effects. For instance, some members of the AOA genus *Candidatus* Nitrosocosmicus appear to assimilate NH_4^+ via glutamate synthase (GOGAT), whereas all other known AOA use the glutamate dehydrogenase (GDH) pathway (Alves et al., 2019).

Despite these potential isotope fractionation effects on the RS level, a higher ε_{CP} relative to ε_{RS} may also result from accumulation of metabolic intermediates, allowing for at least

TABLE 1 | Compilation of published kinetic isotope effects of AOA and AOB.

Source	AOA/AOB	Strain	Initial [NH_4^+] (mM)	Other conditions	ε_{RS}		ε_{CP}	
					Mean	SD	Mean	SD
This study	AOA	*Nitrosopumilus adriaticus* NF5	1		32.1	1.0	40.1	0.7
	AOA	*Nitrososphaera viennensis* EN76	1		31.9	1.2	37.7	0.8
	AOA	*Nitrososphaera viennensis* EN76	2		33.1	0.7	39.0	1.2
Santoro and Casciotti (2011)	AOA	Marine AOA enrichment CN25†	0.01–0.075				22	5
		Marine AOA enrichment CN75					21	10
		Marine AOA enrichment CN150					22	5
Nishizawa et al. (2016)	AOA	*Candidatus* Nitrosocaldus sp.	0.2				22.0	5.0
		Candidatus Nitrosocaldus sp.	14				24.7	2.1
Mariotti et al. (1981)	AOB	*Nitrosomonas europaea*	4.7–25		34.7	2.5	31.9	6.4
Delwiche and Steyn (1970)	AOB	*Nitrosomonas europaea*					26.0	5.6
Yoshida (1988)	AOB	*Nitrosomonas europaea*	38	pO_2 low			24.6	
	AOB	*Nitrosomonas europaea*	38	pO_2 medium			29.0	
	AOB	*Nitrosomonas europaea*	38	pO_2 high			32.0	
Casciotti et al. (2003)	AOB	*Nitrosomonas marina*	2				14.2	3.6
		Nitrosomonas sp. C-113a	2				19.1	1.2
		Nitrosospira tenuis	1				24.6	1.4
		Nitrosomonas eutropha	1				32.8	1.7
		Nitrosomonas europaea	1				38.2	1.6
Casciotti et al. (2010)	AOB	*Nitrosomonas* sp. C-113a	0.005–0.05				30–46	
	AOB	*Nitrosococcus oceani*	0.005–0.05				30–46	
	AOB	*Nitrospira briensis*	0.005–0.05				30–46	

†*Currently designated as Candidatus Nitrosopelagicus brevis CN25 (Santoro et al., 2015).*

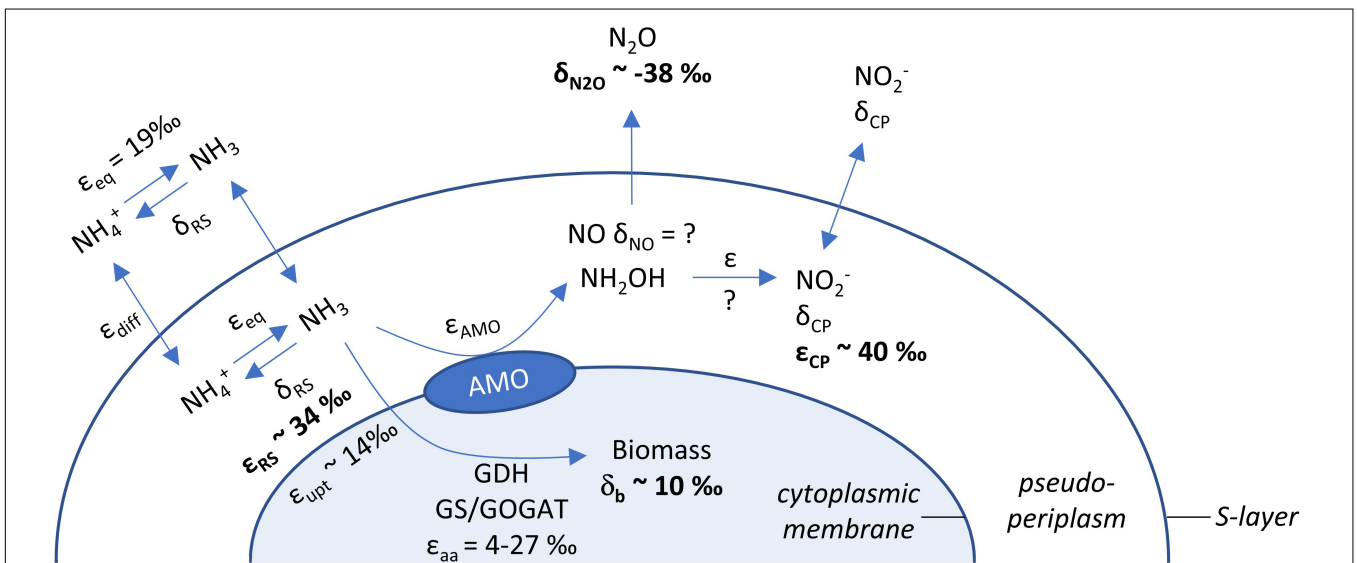

FIGURE 3 | Schematic overview of processes and isotope fractionation effects involved in ammonia oxidation, growth and intermediate formation of the soil AOA *N. viennensis*. $\delta^{15}N$ values are given for endpoint measurements of N_2O and biomass, while average kinetic isotope effects of ammonia oxidation are presented for substrate (NH_4^+, ε_{RS}) and product (NO_2^-, ε_{CP}). Literature values for isotope fractionation of NH_3/NH_4^+ equilibration (ε_{eq}; causing ^{15}N depletion of NH_3), for secondary active NH_4^+ uptake (ε_{upt}) and ammonia assimilation (ε_{aa}) are presented as well. The identity of the enzyme oxidizing NH_2OH to NO_2^- and its inherent isotope fractionation are currently unknown for AOA.

TABLE 2 | Nitrogen pools for *N. viennensis* culture grown on 2 mM NH_4^+.

	N pool (μM)	δ^{15}N of N pool (‰)	Percent of missing N pool	Percent of ammonia oxidized
Missing	204.4 (±25.2)	−7.6 (±5.2)		
Biomass	38.8 (±3.4)	10.1 (±0.1)	22.8 (±4.1)	3.1 (±0.3)
N_2O-N	6.5 (±0.2)	−38.1 (±0.3)	3.5 (±0.4)	0.5 (±0.1)
Unaccounted	139.2 (±27.1)	−18.5 (±1.7)	73.7 (±4.5)	

The missing N pool is N that was not present at NH_4^+ and NO_2^- at the last sampling time point when biomass and N_2O was collected for isotope analysis. We used a mass balance approach to calculate $\delta^{15}N$ of the missing and unaccounted N pool. Standard errors are given in parentheses.

a second ^{15}N isotope fractionation step to be observed. First, accumulation of NH_2OH, or any other intermediate, has not been observed in AOA cells, and the coupled activities of AMO and hydroxylamine oxidoreductase (yet unknown in AOA) are assumed to maintain NH_2OH at low steady-state concentrations. Therefore, isotope effects associated with NH_2OH oxidation should have a limited impact on $\delta^{15}NO_2^-$. Second, any process that adds an additional isotope fractionation step, either prior, or subsequent, to NO_2^- formation, such as the production of the gases NO and N_2O, may result in an under- or overestimation of the kinetic isotope fractionation factor. The effect of N_2O and NO production on $\delta^{15}NO_2^-$ will depend on their formation pathways, and respective isotope effects and by-product yields. In the *N. viennensis* culture grown on 2 mM NH_4^+, we measured cumulative N_2O at the end of the incubation, which represented 0.5% (±0.01 SE) of the NH_4^+ oxidized, or 3.5% (±0.4 SE) of the "missing" N pool. N_2O yields of AOA are generally low. For example, *N. viennensis* has been shown to produce N_2O at rates of about 0.1% of those of ammonia oxidation when grown on 1 mM NH_4^+/NH_3 (Stieglmeier et al., 2014b), whereas the marine AOA *N. maritimus* SCM1 produces even less (0.002–0.03%; Löscher et al., 2012). Here, the cumulative N_2O of the *N. viennensis* culture had a $\delta^{15}N$ of −38.1‰ (±0.3 SE) (**Figures 1F**, **3**), which was more ^{15}N-depleted than previously observed for AOA enrichment cultures. AOA have been shown to produce N_2O with $\delta^{15}N$ signatures ranging between −35 and −13‰ in soil enrichment cultures and −9‰ in marine enrichment cultures (Santoro et al., 2011; Jung et al., 2014), while N_2O produced by AOB tends to have lower $\delta^{15}N$, ranging between −66‰ (*Nitrosomonas europaea*; Yoshida, 1988) and −10‰ (*Nitrosomonas marina*; Frame and Casciotti, 2010). Furthermore, by-products that are more ^{15}N-depleted than the main product of ammonia oxidation (i.e., NO_2^-) would decrease the apparent kinetic isotope effect of AMO (ε_{CP}), instead of increasing it. Using an isotopic mass balance approach, we calculated that the missing N pool (i.e., the NH_4^+ taken up which was not oxidized to NO_2^-), would need to have a $\delta^{15}N$ of −18.5‰ (±1.7 SE) in order to account for the difference in isotope fractionation between ε_{RS} and ε_{CP} (**Table 2**). Therefore, the $\delta^{15}N_2O$ signature of −38.1‰ cannot explain the observed large isotope fractionation based on $\delta^{15}NO_2^-$, since the N_2O produced would need to be a larger contributor to the "missing" N pool, as well as to be ^{15}N-enriched relative to NO_2^-.

Nitric oxide is an important intermediate in the ammonia oxidation pathway, particularly in that of AOA. Unlike in AOB, NO is a necessary co-reactant for the oxidation of NH_2OH to NO_2^- in AOA, despite being produced in relatively small amounts (Kozlowski et al., 2016). Although the $\delta^{15}N$ signature of NO produced by AOA has not yet been determined, Yoshida (1988) found that NO produced during nitrification by *N. europaea* had a $\delta^{15}N$ between 0 and +20‰. The production of such ^{15}N-enriched NO could significantly contribute to the observed overestimation of ε_{CP} in AOA.

CONCLUSION

In conclusion, our results show that, under non-limiting substrate conditions, the ε_{AMO} of two phylogenetically and ecologically distinct AOA strains was 31.9–33.1‰ based on $\delta^{15}NH_4^+$, whereas the more commonly estimated ε_{AMO} based on $\delta^{15}NO_2^-$ was higher (37.7–40.1‰). Thus, NH_4^+ assimilation, but not N_2O production, significantly affected the isotope fractionation factor of AMO estimated for *N. viennensis* (**Figure 3**). Although the potential role of NO in this context remains to be tested, isotopic analysis of this molecule is difficult and therefore future measurements of ε_{AMO} may rely on coupled estimates from $\delta^{15}NH_4^+$ and $\delta^{15}NO_2^-$.

DATA AVAILABILITY STATEMENT

The raw data supporting the conclusion of this article have been deposited at DRYAD (doi: 10.5061/dryad.0gb5mkkz1).

AUTHOR CONTRIBUTIONS

WW designed the study. MMo, RA, BB, MMe, MS, LJ, SR, and MW performed the experiments. MMo, RA, BB, MS, and LJ analyzed the data. GH and CS provided the resources and strains. MMo, RA, and WW wrote the manuscript with contributions from all co-authors.

FUNDING

This study was funded by the Austrian Science Fund (FWF; project P28037-B22). Open access funding was provided by University of Vienna.

ACKNOWLEDGMENTS

We thank the students of the course "Stable Isotopes in Ecology" of the years 2012–2014 at the University of Vienna, who contributed to the sample analyses and discussion of the data.

REFERENCES

Alves, R. J. E., Kerou, M., Zappe, A., Bittner, R., Abby, S. S., Schmidt, H., et al. (2019). Ammonia oxidation by the arctic terrestrial thaumarchaeote Ca. Nitrosocosmicus arcticus is stimulated by increasing temperatures. *Front. Microbiol.* 10:1571. doi: 10.3389/fmicb.2019.01571

Ariz, I., Boeckstaens, M., Gouveia, C., Martins, A. P., Sanz-Luque, E., Fernández, E., et al. (2018). Nitrogen isotope signature evidences ammonium deprotonation as a common transport mechanism for the AMT-Mep-Rh protein superfamily. *Sci. Adv.* 4:eaar3599. doi: 10.1126/sciadv.aar3599

Arp, D. J., and Stein, L. Y. (2003). Metabolism of inorganic N compounds by ammonia-oxidizing bacteria. *Crit. Rev. Biochem. Mol. Biol.* 38, 471–495. doi: 10.1080/10409230390267446

Bayer, B., Pelikan, C., Bittner, M. J., Reinthaler, T., Könneke, M., Herndl, G. J., et al. (2019). Proteomic response of three marine ammonia-oxidizing archaea to hydrogen peroxide and their metabolic interactions with a heterotrophic alphaproteobacterium. *mSystems* 4:e00181-19. doi: 10.1128/mSystems.00181-19

Bayer, B., Vojvoda, J., Offre, P., Alves, R. J. E., Elisabeth, N. H., Garcia, J. A. L., et al. (2016). Physiological and genomic characterization of two novel marine thaumarchaeal strains indicates niche differentiation. *ISME J.* 10, 1051–1063. doi: 10.1038/ismej.2015.200

Buchwald, C., and Casciotti, K. L. (2013). Isotopic ratios of nitrite as tracers of the sources and age of oceanic nitrite. *Nat. Geosci.* 6, 308–313. doi: 10.1038/ngeo1745

Caranto, J. D., and Lancaster, K. M. (2017). Nitric oxide is an obligate bacterial nitrification intermediate produced by hydroxylamine oxidoreductase. *Proc. Natl. Acad. Sci. U.S.A.* 114, 8217–8222. doi: 10.1073/pnas.1704504114

Carini, P., Dupont, C., and Santoro, A. E. (2017). Correlated expression of archaeal ammonia oxidation machinery across disparate environmental and culture conditions. *BioRxiv* [Preprint]. doi: 10.1101/175141

Casciotti, K. L. (2016). Nitrogen and oxygen isotopic studies of the marine nitrogen cycle. *Ann. Rev. Mar. Sci.* 8, 379–407. doi: 10.1146/annurev-marine-010213-135052

Casciotti, K. L., and Buchwald, C. (2012). Insights on the marine microbial nitrogen cycle from isotopic approaches to nitrification. *Front. Microbiol.* 3:356. doi: 10.3389/fmicb.2012.00356

Casciotti, K. L., McIlvin, M., and Buchwald, C. (2010). Oxygen isotopic exchange and fractionation during bacterial ammonia oxidation. *Limnol. Oceanogr.* 55, 753–762. doi: 10.4319/lo.2010.55.2.0753

Casciotti, K. L., Sigman, D. M., and Ward, B. B. (2003). Linking diversity and stable isotope fractionation in ammonia-oxidizing bacteria. *Geomicrobiol. J.* 20, 335–353. doi: 10.1080/01490450303895

Daims, H., Lebedeva, E. V., Pjevac, P., Han, P., Herbold, C., Albertsen, M., et al. (2015). Complete nitrification by Nitrospira bacteria. *Nature* 528:504. doi: 10.1038/nature16461

Delwiche, C. C., and Steyn, P. L. (1970). Nitrogen isotope fractionation in soils and microbial reactions. *Environ. Sci. Technol.* 4, 929–935. doi: 10.1021/es60046a004

Frame, C. H., and Casciotti, K. L. (2010). Biogeochemical controls and isotopic signatures of nitrous oxide production by a marine ammonia-oxidizing bacterium. *Biogeosciences* 7, 2695–2709. doi: 10.5194/bg-7-2695-2010

Goyal, S. S., Rains, D. W., and Huffaker, R. C. (1988). Determination of ammonium ion by fluorometry or spectrophotometry after on-line derivatization with o-phthalaldehyde. *Anal. Chem.* 60, 175–179. doi: 10.1021/ac00153a016

Hermes, J. D., Weiss, P. M., and Cleland, W. W. (1985). Use of nitrogen-15 and deuterium isotope effects to determine the chemical mechanism of phenylalanine ammonia-lyase. *Biochemistry* 24, 2959–2967. doi: 10.1021/bi00333a023

Hoch, M. P., Fogel, M. L., and Kirchman, D. L. (1992). Isotope fractionation associated with ammonium uptake by a marine bacterium. *Limnol. Oceanogr.* 37, 1447–1459. doi: 10.4319/lo.1992.37.7.1447

Hood-Nowotny, R., Umana, N. H.-N., Inselbacher, E., Oswald- Lachouani, P., and Wanek, W. (2010). Alternative methods for measuring inorganic, organic, and total dissolved nitrogen in soil. *Soil Sci. Soc. Am. J.* 74:1018. doi: 10.2136/sssaj2009.0389

Houlton, B. Z., and Bai, E. (2009). Imprint of denitrifying bacteria on the global terrestrial biosphere. *Proc. Natl. Acad. Sci. U.S.A.* 106, 21713–21716. doi: 10.1073/pnas.0912111106

Jung, M.-Y., Well, R., Min, D., Giesemann, A., Park, S.-J., Kim, J.-G., et al. (2014). Isotopic signatures of N 2 O produced by ammonia-oxidizing archaea from soils. *ISME J.* 8, 1115–1125. doi: 10.1038/ismej.2013.205

Kerou, M., Offre, P., Valledor, L., Abby, S. S., Melcher, M., Nagler, M., et al. (2016). Proteomics and comparative genomics of Nitrososphaera viennensis reveal the core genome and adaptations of archaeal ammonia oxidizers. *Proc. Natl. Acad. Sci. U.S.A.* 113, E7937–E7946. doi: 10.1073/pnas.1601212113

Kits, K. D., Sedlacek, C. J., Lebedeva, E. V., Han, P., Bulaev, A., Pjevac, P., et al. (2017). Kinetic analysis of a complete nitrifier reveals an oligotrophic lifestyle. *Nature* 549:269. doi: 10.1038/nature23679

Kozlowski, J. A., Stieglmeier, M., Schleper, C., Klotz, M. G., and Stein, L. Y. (2016). Pathways and key intermediates required for obligate aerobic ammonia-dependent chemolithotrophy in bacteria and Thaumarchaeota. *ISME J.* 10, 1836–1845. doi: 10.1038/ismej.2016.2

Lachouani, P., Frank, A. H., and Wanek, W. (2010). A suite of sensitive chemical methods to determine the δ15N of ammonium, nitrate and total dissolved N in soil extracts. *Rapid Commun. Mass Spectrom.* 24, 3615–3623. doi: 10.1002/rcm.4798

Li, P.-N., Herrmann, J., Tolar, B. B., Poitevin, F., Ramdasi, R., Bargar, J. R., et al. (2018). Nutrient transport suggests an evolutionary basis for charged archaeal surface layer proteins. *ISME J.* 12, 2389–2402. doi: 10.1038/s41396-018-0191-0

Löscher, C. R., Kock, A., Koenneke, M., LaRoche, J., Bange, H. W., and Schmitz, R. A. (2012). Production of oceanic nitrous oxide by ammonia-oxidizing archaea. *Biogeosciences* 9, 2419–2429. doi: 10.5194/bg-9-2419-2012

Mariotti, A., Germon, J. C., Hubert, P., Kaiser, P., Letolle, R., Tardieux, A., et al. (1981). Experimental determination of nitrogen kinetic isotope fractionation: some principles; illustration for the denitrification and nitrification processes. *Plant Soil* 62, 413–430. doi: 10.1007/bf02374138

Martens-Habbena, W., Berube, P. M., Urakawa, H., José, R., and Stahl, D. A. (2009). Ammonia oxidation kinetics determine niche separation of nitrifying Archaea and Bacteria. *Nature* 461:976. doi: 10.1038/nature08465

Nishizawa, M., Sakai, S., Konno, U., Nakahara, N., Takaki, Y., Saito, Y., et al. (2016). Nitrogen and oxygen isotope effects of ammonia oxidation by thermophilic Thaumarchaeota from a geothermal water stream. *Appl. Environ. Microbiol.* 82, 4492–4504. doi: 10.1128/aem.00250-16

Offre, P., Kerou, M., Spang, A., and Schleper, C. (2014). Variability of the transporter gene complement in ammonia-oxidizing archaea. *Trends Microbiol.* 22, 665–675. doi: 10.1016/j.tim.2014.07.007

Prosser, J. I, Hink, L., Gubry-Rangin, C., and Nicol, G. W. (2019). Nitrous oxide production by ammonia oxidisers: physiological diversity, niche differentiation and potential mitigation strategies. *Glob. Chang. Biol.* 26, 103–118. doi: 10.1111/gcb.14877

Prosser, J. I., and Nicol, G. W. (2012). Archaeal and bacterial ammonia-oxidisers in soil: the quest for niche specialisation and differentiation. *Trends Microbiol.* 20, 523–531. doi: 10.1016/J.TIM.2012.08.001

R Development Core Team (2012). *R: A Language and Environment for Statistical Computing*. Vienna: R Foundation for Statistical Computing.

Santoro, A. E., Buchwald, C., McIlvin, M. R., and Casciotti, K. L. (2011). Isotopic signature of N2O produced by marine ammonia-oxidizing archaea. *Science* 333, 1282–1285. doi: 10.1126/science.1208239

Santoro, A. E., and Casciotti, K. L. (2011). Enrichment and characterization of ammonia-oxidizing archaea from the open ocean: phylogeny, physiology and stable isotope fractionation. *ISME J.* 5:1796. doi: 10.1038/ismej.2011.58

Santoro, A. E., Dupont, C. L., Richter, R. A., Craig, M. T., Carini, P., McIlvin, M. R., et al. (2015). Genomic and proteomic characterization of "Candidatus Nitrosopelagicus brevis": an ammonia-oxidizing archaeon from the open ocean. *Proc. Natl. Acad. Sci. U.S.A.* 112, 1173–1178. doi: 10.1073/pnas.1416223112

Shen, T., Stieglmeier, M., Dai, J., Urich, T., and Schleper, C. (2013). Responses of the terrestrial ammonia-oxidizing archaeon Ca. Nitrososphaera viennensis and the ammonia-oxidizing bacterium Nitrosospira multiformis to nitrification inhibitors. *FEMS Microbiol. Lett.* 344, 121–129. doi: 10.1111/1574-6968.12164

Sigman, D. M., and Casciotti, K. L. (2001). "Nitrogen isotopes in the ocean," in *Encyclopedia of Ocean Sciences*, ed. J. H. Steele (Cambridge, MA: Academic Press), 1884–1894. doi: 10.1006/rwos.2001.0172

Simon, J., and Klotz, M. G. (2013). Diversity and evolution of bioenergetic systems involved in microbial nitrogen compound transformations. *Biochim. Biophys. Acta Bioenerget.* 1827, 114–135. doi: 10.1016/j.bbabio.2012.07.005

Sørensen, P., and Jensen, E. S. (1991). Sequential diffusion of ammonium and nitrate from soil extracts to a polytetrafluoroethylene trap for 15N

determination. *Anal. Chim. Acta* 252, 201–203. doi: 10.1016/0003-2670(91)87215-s

Stieglmeier, M., Klingl, A., Alves, R. J. E., Rittmann, S. K.-M. R., Melcher, M., Leisch, N., et al. (2014a). *Nitrososphaera viennensis* gen. nov., sp. nov., an aerobic and mesophilic, ammonia-oxidizing archaeon from soil and a member of the archaeal phylum Thaumarchaeota. *Int. J. Syst. Evol. Microbiol.* 64, 2738–2752. doi: 10.1099/ijs.0.063172-0

Stieglmeier, M., Mooshammer, M., Kitzler, B., Wanek, W., Zechmeister-Boltenstern, S., Richter, A., et al. (2014b). Aerobic nitrous oxide production through N-nitrosating hybrid formation in ammonia-oxidizing archaea. *ISME J.* 8, 1135–1146. doi: 10.1038/ismej.2013.220

Tourna, M., Stieglmeier, M., Spang, A., Könneke, M., Schintlmeister, A., Urich, T., et al. (2011). Nitrososphaera viennensis, an ammonia oxidizing archaeon from soil. *Proc. Natl. Acad. Sci. U.S.A.* 108, 8420–8425. doi: 10.1073/pnas.1013488108

van Kessel, M. A. H. J., Speth, D. R., Albertsen, M., Nielsen, P. H., den Camp, H. J. M. O., Kartal, B., et al. (2015). Complete nitrification by a single microorganism. *Nature* 528, 555–559. doi: 10.1038/nature16459

Vitousek, P. M., Menge, D. N. L., Reed, S. C., and Cleveland, C. C. (2013). Biological nitrogen fixation: rates, patterns and ecological controls in terrestrial ecosystems. *Philos. Trans. R. Soc. B Biol. Sci.* 368:20130119. doi: 10.1098/rstb.2013.0119

Walker, C. B., De La Torre, J. R., Klotz, M. G., Urakawa, H., Pinel, N., Arp, D. J., et al. (2010). Nitrosopumilus maritimus genome reveals unique mechanisms for nitrification and autotrophy in globally distributed marine crenarchaea. *Proc. Natl. Acad. Sci. U.S.A.* 107, 8818–8823. doi: 10.1073/pnas.0913533107

Yoshida, N. (1988). 15N-depleted N2O as a product of nitrification. *Nature* 335:528. doi: 10.1038/335528a0

Yoshida, N., and Toyoda, S. (2000). Constraining the atmospheric N2O budget from intramolecular site preference in N2O isotopomers. *Nature* 405, 330–334. doi: 10.1038/35012558

Conflict of Interest: The authors declare that the research was conducted in the absence of any commercial or financial relationships that could be construed as a potential conflict of interest.

Citation: Mooshammer M, Alves RJE, Bayer B, Melcher M, Stieglmeier M, Jochum L, Rittmann SK-MR, Watzka M, Schleper C, Herndl GJ and Wanek W (2020) Nitrogen Isotope Fractionation During Archaeal Ammonia Oxidation: Coupled Estimates From Measurements of Residual Ammonium and Accumulated Nitrite. Front. Microbiol. 11:1710. doi: 10.3389/fmicb.2020.01710

frontiers in Microbiology

ORIGINAL RESEARCH
published: 04 August 2020
doi: 10.3389/fmicb.2020.01736

Nitrite Oxidizer Activity and Community Are More Responsive Than Their Abundance to Ammonium-Based Fertilizer in an Agricultural Soil

Yang Ouyang[1,2] *and Jeanette M. Norton*[1]*

[1]Department of Plants, Soils and Climate, Utah State University, Logan, UT, United States, [2]Department of Microbiology and Plant Biology, Institute for Environmental Genomics, University of Oklahoma, Norman, OK, United States

Autotrophic nitrification is mediated by ammonia oxidizing bacteria (AOB) or ammonia oxidizing archaea (AOA) and nitrite oxidizing bacteria (NOB). Mounting studies have examined the impact of nitrogen (N) fertilization on the dynamic and diversity of AOA and AOB, while we have limited information on the response of the activity, abundance, and diversity of NOB to N fertilization. We investigated the influence of organic and inorganic N fertilizers on soil NOB in silage corn field plots that received contrasting nitrogen (N) treatments: control (no additional N), ammonium sulfate (AS 100 and 200 kg N ha^{-1}), and compost (200 kg N ha^{-1}). Nitrifying community was examined using a universal marker (16S rRNA gene), functional gene markers (AOB *amoA* and *Nitrospira nxrB*), and metagenomics. The overall nitrifying community was not altered after the first fertilization but was significantly shifted by 4-year repeated application of ammonium fertilizers. *Nitrospira* were the dominant NOB (>99.7%) in our agricultural soil. Both community compositions of AOB and *Nitrospira* were significantly changed by ammonium fertilizers but not by compost after 4 years of repeated applications. All nitrifiers, including comammox, were recovered in soil metagenomes based on a gene-targeted assembly, but their sequence counts were very low. Although N treatment did not affect the abundance of *Nitrospira nxrB* determined by real-time quantitative PCR, ammonium fertilizers significantly promoted rates of potential nitrite oxidation determined at 0.15 mM nitrite in soil slurries. Understanding the response of both ammonia oxidizers and nitrite oxidizers to N fertilization may initiate or improve strategies for mitigating potential environmental impacts of nitrate production in agricultural ecosystems.

Keywords: nitrifying community, nitrite oxidizing bacteria, nitrogen fertilizer, *nxrB*, *Nitrospira*, potential nitrite oxidation

OPEN ACCESS

Edited by:
Sebastian Lücker, Radboud University Nijmegen, Netherlands

Reviewed by:
Michael Pester, German Collection of Microorganisms and Cell Cultures GmbH (DSMZ), Germany
Ping Han, East China Normal University, China

***Correspondence:**
Jeanette M. Norton
jeanette.norton@usu.edu

Specialty section:
This article was submitted to Microbiological Chemistry and Geomicrobiology, a section of the journal Frontiers in Microbiology

Received: *28 April 2020*
Accepted: *02 July 2020*
Published: *04 August 2020*

Citation:
Ouyang Y and Norton JM (2020) Nitrite Oxidizer Activity and Community Are More Responsive Than Their Abundance to Ammonium-Based Fertilizer in an Agricultural Soil. Front. Microbiol. 11:1736. doi: 10.3389/fmicb.2020.01736

INTRODUCTION

Nitrification, the oxidation of ammonium to nitrite and nitrate, mobilizes soil nitrogen (N), and promotes N loss through nitrate leaching and denitrification and, therefore, often reduces N use efficiency in agricultural ecosystems (Norton and Ouyang, 2019). Autotrophic nitrification has generally thought to be a two-step process: ammonia oxidation to nitrite by ammonia oxidizing

bacteria (AOB) and ammonia oxidizing archaea (AOA) and nitrite oxidation to nitrate by nitrite oxidizing bacteria (NOB). Remarkably, recent research has uncovered that some *Nitrospira*, a diverse and widespread known NOB, are able to convert ammonia to nitrate within one organism in the complete oxidation of ammonia to nitrate known as comammox (Daims et al., 2015; van Kessel et al., 2015). Since nitrifiers are generally slow growing and recalcitrant to isolation, culture-independent molecular techniques, targeting 16S ribosomal RNA (rRNA) or functional marker genes, have been primarily used to investigate the quantity and diversity of these organisms in natural and managed ecosystems (Rotthauwe et al., 1997; Purkhold et al., 2000; Leininger et al., 2006; Attard et al., 2010; Prosser, 2011; Pester et al., 2012, 2014). High throughput sequencing of 16S rRNA genes detects the diversity and richness of all nitrifying groups in a whole microbial community without using specific functional markers (Purkhold et al., 2000; Zhou et al., 2015). The *amoA* gene, which encodes the alpha subunit of ammonia monooxygenase, is a frequently and widely used functional marker gene for ammonia oxidizers (Rotthauwe et al., 1997; Leininger et al., 2006; Pjevac et al., 2017). The genes encoding the alpha or beta subunit of nitrite oxidoreductase (*nxrA* or *nxrB*) have been developed to detect and quantify NOB in pure cultures and environmental samples (Poly et al., 2008; Pester et al., 2014). Functional marker genes of nitrifiers, such as *amoA* and *nxrB*, often provide a higher phylogenetic resolution than 16S rRNA for discriminating nitrifiers on the strain and species levels (Norton et al., 2002; Pester et al., 2014, Aigle et al., 2019).

Nitrogen fertilization is an important management practice for crop production that exerts a significant influence on the nitrifying community in agricultural systems. Several research groups have documented that AOB are more responsive than AOA to N fertilization in agricultural soils (Jia and Conrad, 2009; Taylor et al., 2012; Carey et al., 2016; Ouyang et al., 2016, 2018). Although the response of ammonia oxidizers to N fertilization has been extensively examined, we have limited information about the ecology of NOB in agricultural systems. The NOB belong to seven genera in the phyla of *Proteobacteria*, *Nitrospirae*, *Nitrospinae*, and *Choloroflexi* (Daims et al., 2016). The genera *Nitrobacter* and *Nitrospira* are considered as the two main players in soils (Poly et al., 2008; Wertz et al., 2008; Attard et al., 2010). Previous studies found that *Nitrobacter* spp. were more responsive than *Nitrospira* spp. to tillage practices (Attard et al., 2010), organic amendments (Ollivier et al., 2013; Han et al., 2018), and N fertilization (Han et al., 2018).

In a previous study, we assessed temporal changes in the abundance and diversity of AOA and AOB, using *amoA* as marker gene, under organic and conventional N management, and showed that the abundance and community of AOB, but not AOA, were significantly shifted by 3-year repeated mineral N fertilization (Ouyang et al., 2016). The objective of the current study was to complement our previous examination using 16S rRNA gene marker in the same field. A more commonly used primer set (amoA1F/2R) was applied to re-examine the diversity of AOB *amoA* using high-throughput sequencing. We expected to find the similar results as our previous study. Since our 16S rRNA gene-based high throughput sequencing revealed that *Nitrospira* were the dominant nitrite oxidizers (>99.7%) recovered in our soil, a newly developed gene marker, *nxrB* of *Nitrospira*, was used to expand our understanding of the abundance and diversity of nitrite oxidizers under contrasting N treatment. Understanding the response of both ammonia oxidizers and nitrite oxidizers to N fertilization may initiate or improve strategies for mitigating potential environmental impacts of nitrate production in agricultural ecosystems.

MATERIALS AND METHODS

Soil Characterization

The details of the agricultural site (North Logan, Utah, USA), experimental design, treatments, soil sampling, and soil characteristics have been previously described (Ouyang et al., 2016, 2017). The soil is an irrigated, very strongly calcareous Millville silt loam (Coarse-silty, carbonatic, mesic Typic Haploxeroll) with a pH of approximately 8.0. The experimental design is a randomized complete block with four blocks and four nitrogen treatments: control (no N fertilization), ammonium sulfate (AS 100 and 200 kg N ha^{-1}), and steer-waste compost (200 kg total N ha^{-1}). Treatments were surface applied in May of each year and incorporated by tilling immediately after application. Silage corn was planted within 2 days and irrigation was applied according to general agricultural practice in the area.

Potential Nitrite Oxidation

We measured potential nitrite oxidation (PNO) for soils sampled in 2015. PNO was determined using a modified method of Wertz et al. (2007). Samples of 3 g of fresh soil were placed in a 100 ml Erlenmeyer flask, and then 30 ml of a solution of $NaNO_2$ (final 0.15 mM $NaNO_2$) was added. Preliminary experiments measured PNO with a range of final nitrite concentrations (0.05, 0.1, 0.15, 0.3, and 1 mM) and showed that there was no nitrite inhibition and enough nitrite left after 24 h with 0.15 mM nitrite. Flasks were covered with foil with small hole and incubated at 30°C for 24 h with shaking (200 rpm). After incubation for 1, 6, 20, and 24 h, 1.5 ml of the suspension was sampled using pipette with a wide mouth tip, and centrifuged (10,000 *g*) for 5 min. Supernatants were then transferred to a new tube and nitrite concentration in the supernatants was analyzed spectrophotometrically using the Griess reagent (Mulvaney, 1996). The change in nitrite was used to calculate the linear rate of nitrite consumption over the 24 h period.

Soil DNA Extraction and Real-Time Quantitative PCR

Soil DNA was extracted following the MoBio Power Soil DNA isolation protocol (MoBio Laboratories Inc., Carlsbad, USA) using 0.25 g moist soil. DNA extracts were quantified by using a NanoDrop spectrophotometer (NanoDrop Technologies, Wilmington, DE). Quantitative PCR (qPCR) of *Nitrospira nxrB* gene was performed using the SsoAdvanced SYBR Green Supermix and a CFX CONNECT real-time PCR detection system (Bio-Rad laboratories, Hercules, CA, USA). Primers, nxrB169R and nxrB638F, were used to quantify *Nitrospira nxrB*

gene abundance (Pester et al., 2014). Standard curve was constructed with plasmids containing cloned *nxrB* products from environmental DNA. The 25 µl reaction mixture contained 12.5 µl SsoAdvanced SYBR Green Supermix (Bio-Rad laboratories, Hercules, CA, USA), 0.5 µM of both reverse and forward primers, and 10 µl of 10-fold diluted soil DNA extract. Amplifications were carried out as follows: an initial denaturation step of 95°C for 10 min, 40 cycles of 95°C for 45 s, 56.2°C for 1 min, and 72°C for 45 s, and a final extension step of 72°C for 10 min. Fluorescence intensity was read during the 72°C step of each cycle. Reaction efficiencies ranged from 94 to 105%, and R^2 values ranged from 0.992 to 0.999.

Illumina Sequencing and Data Analysis for Bacterial *amoA* and *Nitrospira nxrB*

Sequencing of the bacterial *amoA* and *Nitrospira nxrB* amplicon libraries was accomplished for soils sampled in June 2014. The primer set (amoA1F/2R) was used to examine the diversity of AOB *amoA* (Rotthauwe et al., 1997). The same *Nitrospira nxrB* primers described above were used for high-throughput sequencing. The preparation and Miseq sequencing were the same as our previous study (Ouyang and Norton, 2020). Raw forward and reverse reads were merged using the USEARCH workflow (Edgar, 2013). High quality *amoA* and *nxrB* sequences were extracted from merged reads in each sample using the RDP SeqFilters with a read Q score cutoff of 20 (Cole et al., 2014). The obtained sequences were further processed using the FrameBot tool (Wang et al., 2013) to fix frame shifts. Sequences were dereplicated and clustered at 90% nucleotide similarity using USEARCH. Operational taxonomic unit (OTU) table and taxonomy file were organized for diversity analysis using R package phyloseq (McMurdie and Holmes, 2013). A neighbor-joining phylogenetic tree was constructed from top 20 OTUs using a Kimur 2-parameter distance with 1,000 bootstrap replicates with MEGA 6 (Tamura et al., 2013).

Soil Metagenome Processing and Gene Targeted Assembly

Metagenomes were also obtained from soils samples in June 2014 (Ouyang and Norton, 2020). DNA samples from four replicates of each N treatment were pooled with equal amount of DNA. DNA were then sequenced on the Illumina HiSeq 2,500 platform with 2 × 150 bp paired-end format, processed at the Joint Genome Institute (JGI) and data are available at the IMG/M website (Chen et al., 2017). Gene-targeted assembly was conducted for the quality-filtered metagenomes using Xander (Wang et al., 2015). Five genes involved in nitrification (AOA *amoA*, AOB *amoA*, comammox *amoA*, *Nitrobacter nxrB*, and *Nitrospira nxrB*) and *rplB* (encoding ribosomal protein L2) were included for the assembly. For each gene of interest, seed sequences, hidden Markov models (HMMs), and nucleotide and protein reference sequences were downloaded from FunGene (Fish et al., 2013). Default assembly parameters were used and sequences were clustered at 95% amino acid similarity. A representative sequence from each cluster was searched against the reference gene database and the nonredundant database (nr) from NCBI using BLAST (Camacho et al., 2009). Some sequences of *nxrB* were removed if they were not a match with *Nitrospira* or *Nitrobacter*.

Identify Nitrifying Community With 16S Illumina Sequencing

The detailed information about Illumina sequencing with 16S rRNA gene and bioinformatics analysis was described in Ouyang and Norton (2020). Soil nitrifying community, including AOA, AOB, and NOB, was evaluated by screening 16S rRNA gene sequences. The relative abundance of AOA, AOB, NOB, and their specific OTUs were calculated by dividing the total 16S rRNA sequences in each sample. The OTU representatives of NOB were selected to create a phylogenetic tree, which was constructed by neighbor-joining using a Kimur 2-parameter distance with 1,000 bootstrap replicates with MEGA 6 (Tamura et al., 2013).

Statistical Analysis

Statistical analysis of the effect of N treatment and year on AOA, AOB, NOB, and selected OTU relative abundances was completed using two-way analysis of variance (ANOVA) with the Proc Mixed model in SAS 9.2 (SAS Institute, Inc., Cary, NC, USA). Treatment and year were used as fixed effects and block as a random effect. One-way ANOVA was used to the effect of N treatment on the relative abundance of *amoA* and *nxrB* top 20 OTUs. Data were log transformed as necessary to meet normality assumptions. Repeated measures ANOVA was used to analyze effects of treatment on *nxrB* copy numbers and PNO rates in soils sampled in 2015. Any values of $p \leq 0.05$ were considered to be statistically significant. The Bray-Curtis distance matrix was created by using the relative abundance of all OTUs from nitrifying community. To carry out the beta-diversity analysis, the AOB *amoA* and *Nitrospira nxrB* libraries were first normalized to 432 and 380 reads, respectively (fewest sequences per sample). The rarefaction curves showed that these normalized reads were sufficient to capture the diversity of *amoA* and *nxrB*. Nonmetric multidimensional scaling (NMDS) and permutational multivariate ANOVA (PerMANOVA) were conducted to visualize and assess the Bray-Curtis distance matrix in *vegan* package of R software[1].

RESULTS

The Activity and Abundance of *Nitrospira*

PNO rates ranged from 4 to 20 mg N kg^{-1} d^{-1}. Repeated ANOVA analysis indicated that both treatment (F = 116.72, p < 0.0001) and sampling time (F = 116.55, p < 0.0001) significantly influenced PNO rates, and there was a treatment and sampling time interaction effect (F = 11.86, p < 0.001). PNO rates were significantly increased by AS treatments, but unchanged by compost, compared with control treatment (**Figure 1A**). PNO rates were lowest for soils sampled before fertilization. In addition, PNO rates were relative higher for soils sampled 14 days after fertilization compared with other sampling times in both AS treatments. *Nitrospira nxrB* copy

[1]http://www.r-project.org

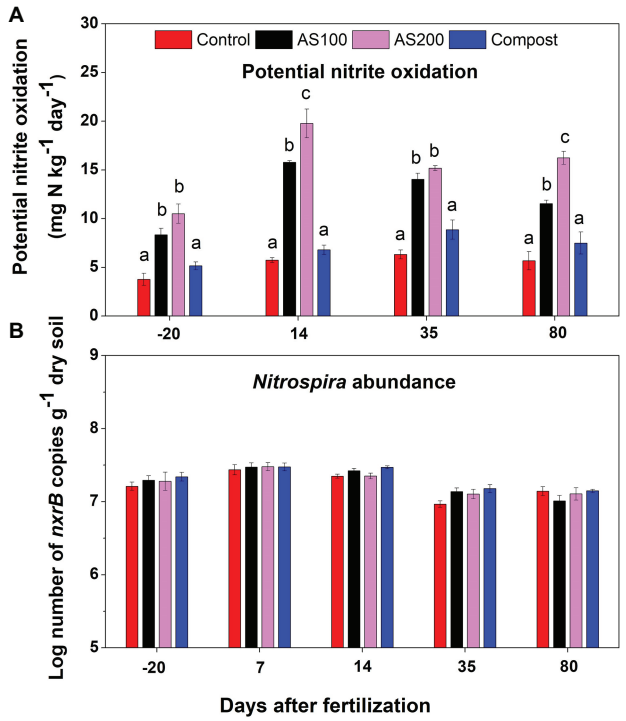

FIGURE 1 | (A) Nitrite oxidation potentials in 2015 before and after fertilization across four Nitrogen (N) treatments [control (no N fertilization), ammonium sulfate (AS 100 and 200 kg N ha^{-1}), and compost (200 kg N ha^{-1})]. Nitrite oxidation potential was measured by soil slurry assay supplemented with 0.15 mM NO_2^-. Error bars represent standard errors (n = 4). Different letters above the bars indicate a significant difference among treatments within a specific sampling time ($p < 0.05$) based on repeated measures ANOVA. **(B)** Abundance of *Nitrospira nxrB* gene copy numbers (log_{10} transformed) across four N treatments. Error bars represent standard errors (n = 4).

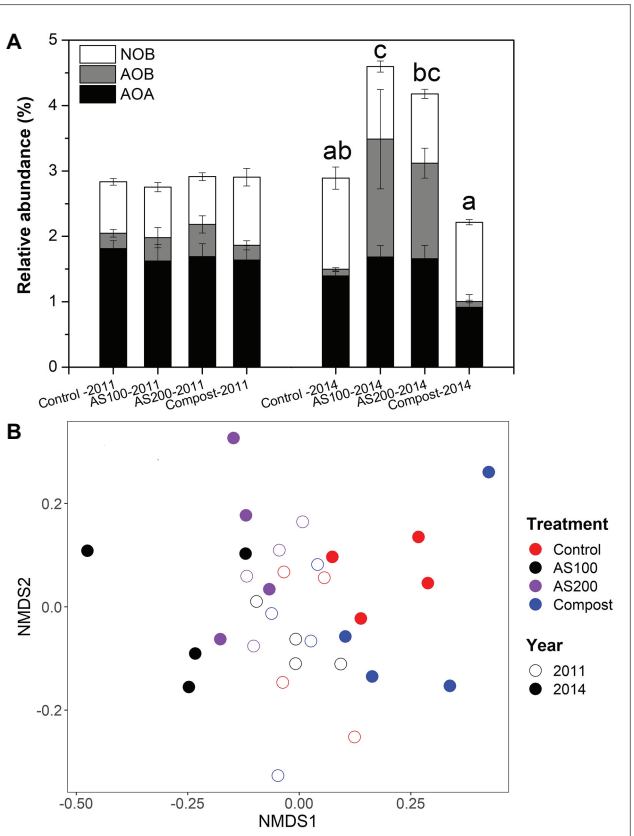

FIGURE 2 | (A) Relative abundance of nitrifying populations based on differences in 16S rRNA genes for four N treatments. Error bars represent standard errors (n = 4). Different letters above the bars indicate a significant different in total nitrifying populations in 2014. Abbreviation: AOA, ammonia oxidizing archaea; AOB, ammonia oxidizing bacteria; NOB, nitrite oxidizing bacteria. **(B)** Nonmetric multidimensional scaling (NMDS) ordination based on the abundance of 16S rRNA gene operational taxonomic units (OTUs) of all nitrifying populations. Colors denote treatment (red = control, black = AS100, purple = AS200, blue = compost). Fill denotes sampling time (open = 2011, solid = 2014).

numbers, ranging from 7.94×10^6 to 2.95×10^7 per gram of dry soils, showed no treatment effect (F = 1.66, p = 0.24), but has significant time effect (F = 72.70, $p < 0.001$). *Nitrospira nxrB* copy numbers were highest on 7 days after fertilization across all N treatments (**Figure 1B**). *Nitrospira nxrB* copy numbers were not significantly correlated with PNO rates (r = 0.02, p = 0.89).

Nitrifying Community Composition Recovered in 16S rRNA Gene Illumina Sequencing

The structure of nitrifying community was examined by screening 16S rRNA gene sequences of AOA, AOB, and NOB for Aug 2011 and Jun 2014 samples. We obtained 30,405, 11,181, and 19,236 sequence reads for AOA, AOB, and NOB, respectively, with 19, 8, and 22 unique OTUs, respectively. We only obtained one OTU, which grouped with *Nitrobacter*. *Nitrospira* were the dominant nitrite oxidizers (>99.7%) recovered in all soil samples. Soil nitrifiers represent 3–5% of total prokaryotic community. The relative abundance of soil nitrifiers was not changed by N treatment in 2011, but their relative abundance was significantly increased by AS treatments but decreased by compost treatment in 2014 (**Figure 2A** and **Supplementary Table S1**). Specifically, in 2014, AOB proportion was strongly increased by AS treatments, and AOA proportion was significantly reduced by compost treatment, but NOB proportion was unchanged by N treatments (**Figure 2A**).

Nitrifying community structures were different between 2011 and 2014, and N treatment strongly changed nitrifying community in 2014 (**Figure 2B**). Two-way PerMANOVA confirmed that nitrifying community composition was significantly affected by year ($p < 0.001$), treatment ($p < 0.001$), and their interaction (p = 0.002). Seven OTUs were selected for detailed statistical analysis that had relative abundances higher than 0.1% of total prokaryotic community. None of those seven OTUs showed a N treatment effect in 2011 (**Supplementary Figure S1** and **Supplementary Table S1**). The relative abundance of AOB OTU 23, related to *Nitrosospira multiformis*, was increased significantly by AS treatments in 2014. Three selected AOA OTUs, belonged to the *Nitrososphaera* cluster, were reduced by compost treatment

in 2014. *Nitrospira* OTU_13 and OTU_276 belonged to Lineage II, but OTU_202 belongs to Lineage V (**Supplementary Figure S2**). The relative abundance of *Nitrospira* OTU_13 was decreased by all N fertilizers and OTU_202 was increased by AS treatment while OTU_276 was increased by compost treatment in 2014.

Diversity of Bacterial *amoA* and *Nitrospira nxrB*

The structure of AOB and *Nitrospira* communities was also evaluated using Illumina high-throughput sequencing analysis of *amoA* and *nxrB* genes, respectively. A total of 22,980 and 27,061 high-quality raw sequence reads were obtained for AOB and *Nitrospira*, respectively, with 44 and 70 unique OTUs, respectively (90% identity cut off). One of the samples from control treatment was removed due to low reads (<150).

AOB community structure was significantly affected by N treatment (R^2 = 0.47, p = 0.002). Pairwise comparison indicated that there was no difference between control and compost treatments. However, AS treatments were significantly different from control and compost treatments (**Figure 3A**). Phylogenetic analysis of top 20 abundant OTUs (contributing 98.2% of total sequences) showed that these abundant OTUs were all affiliated with the *Nitrosospira* Cluster 3 lineage (**Figure 4**). Nine abundant OTUs were significantly changed by N treatment (ANOVA, p < 0.05). Specifically, AOB1 (closely related to *Nitrosospira multifomis* ATCC 25196) was significantly higher in N fertilized treatments than control treatments (**Figure 6A**). AOB6, AOB7, AOB14, and AOB15, which were all closely related to *Nitrosospira briensis* Nsp10, were significantly higher in AS treatments than control and compost treatments. However, AOB11, AOB12, AOB16, and AOB17, which were all closely related to *Nitrosospira* sp. Wyke8, were significantly higher in control and compost treatments than in AS treatments.

Nitrospira community structure was also significantly affected by N treatment (R^2 = 0.55, p = 0.002). Similarly, pairwise comparison indicated that there was no difference between control and compost treatments. However, AS treatments were significantly different from control and compost treatments (**Figure 3B**). Phylogenetic analysis indicated that those top 20 abundant OTUs (contributing 94.9% of total sequence OTUs) were affiliated with at least five different *Nitrospira* lineages (**Figure 5**). Eight abundant OTUs were significantly changed by N treatment (**Figure 6B**; ANOVA, p < 0.05). For example, in compost treatment, nxrB16 (lineage V) was significantly higher than in control treatment, while nxrB2 and nxrB4, nxrB43, and nxrB6, which belonged to lineage II, were significantly lower. In AS treatments, nxrB2, nxrB4, nxrB43 and nxrB14 were significantly higher than control treatments, while nxrB1, nxrB3, and nxrB16 were significantly lower.

Gene-Targeted Assembly for Nitrifiers

Five selected nitrification genes were all recovered in soil metagenomes based on gene-targeted assembly (**Supplementary Table S2**). The number of OTUs recovered at 95% amino acid identity for these nitrification genes ranged from 2 to 8, and their rplB normalized abundances ranged from 0 to 3.8% in four soil metagenomes. There were six OTUs for AOA, belonging to *Nitrososphaera* and *Nitrosocosmicus* (**Supplementary Table S3**). There were seven OTUs for AOB and most of them were closely related to *Nitrosospira*. AS treatments had relatively higher AOB abundance than control and compost treatments. Interestingly, two comammox OTUs were recovered in our metagenomes with very high similarity (>98%) to current available comammox genome bins (**Supplementary Table S3**, *Nitrospira* sp. SG-bin1).

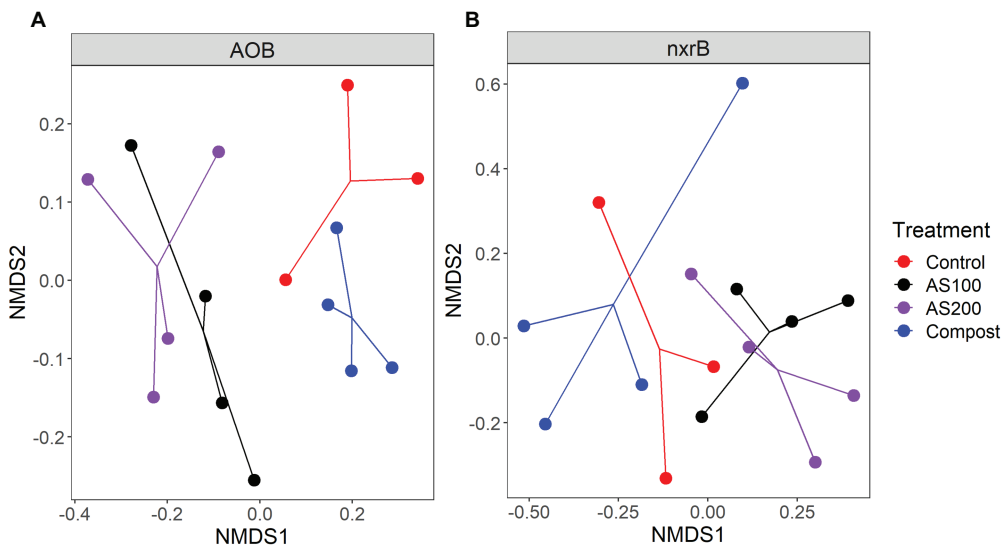

FIGURE 3 | NNMDS ordination based on the Bray-Curtis distance matrices showing the change in AOB **(A)** and *Nitrospira* **(B)** community composition for four N treatments.

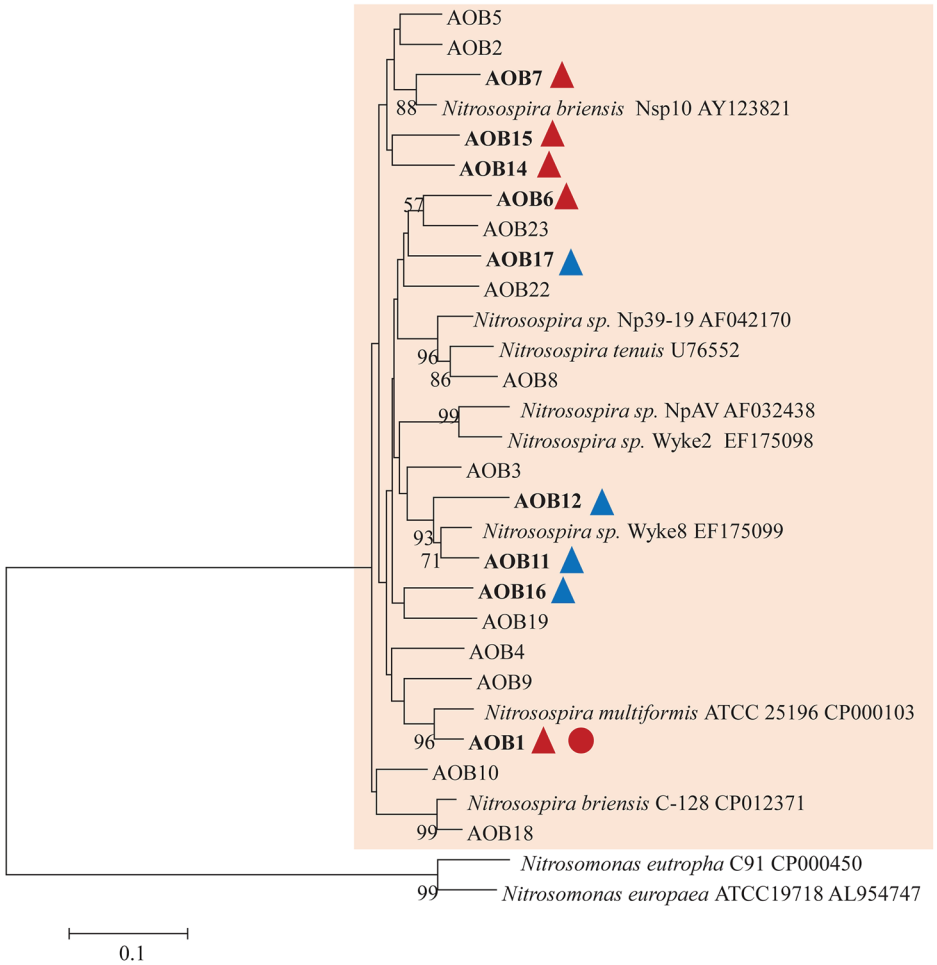

FIGURE 4 | Neighbor joining tree for AOB partial *amoA* top 20 OTUs (covered 98.2% of total sequences). The scale bar represents 10% nucleic acid sequence divergence, and bootstrap values (>50%) are showed at branch points. OTUs are shown in bold if they were significantly changed by N treatment. Up triangles indicate a significant difference between values for control and AS treatments while circles indicate a significant difference between values for control and compost treatments. Red color indicates a significant higher abundance than control while blue color indicates a lower abundance.

Nitrospira were recovered in all four metagenomes, while *Nitrobacter* were only present in AS treatments.

DISCUSSION

Ammonium-Based Fertilizer Changed the Activity and Community Composition, but Not the Abundance of *Nitrospira*

Ammonia oxidation has generally been considered the rate-limiting step of nitrification. Recent studies also showed that PNO was much higher than potential ammonia oxidation (Ke et al., 2013). However, compared to our nitrification potentials (NP), PNO rates were much lower than NPs in the same soil samples (Ouyang et al., 2017). We also measured the dynamic of nitrite during the NP assays for soils sampled in Aug 2015. The result showed that nitrite accumulated linearly during the 24 h shaking-period, with the proportion increasing from 6 to 43% (**Supplementary Figure S3**). Taken together, our observation suggested that nitrite oxidation is the rate-limiting step during the NP assay with non-limiting ammonium availability and continuous shaking. It is noteworthy that the accumulation of nitrite during the NP assay may not be representative of field conditions. Ammonium availability is limited for most of the growing season in field soils causing ammonia oxidation rates to be constrained by diffusion to the cell surface in the soil matrix (Stark and Firestone, 1995).

We observed that PNO was increased by ammonium-based fertilization but not by compost fertilization. The high nitrite concentration from ammonia oxidation shortly after ammonium-based fertilization may stimulate the enzyme production of nitrite oxidoreductase. However, *nxrB* copy numbers were not changed by either ammonium-based fertilization or compost. One of the reasons may be that the genomes of *Nitrospira* often contains multiple copies of *nxrB*, ranging from 2 to 6 copies in currently available *Nitrospira* genomes (Pester et al., 2014).

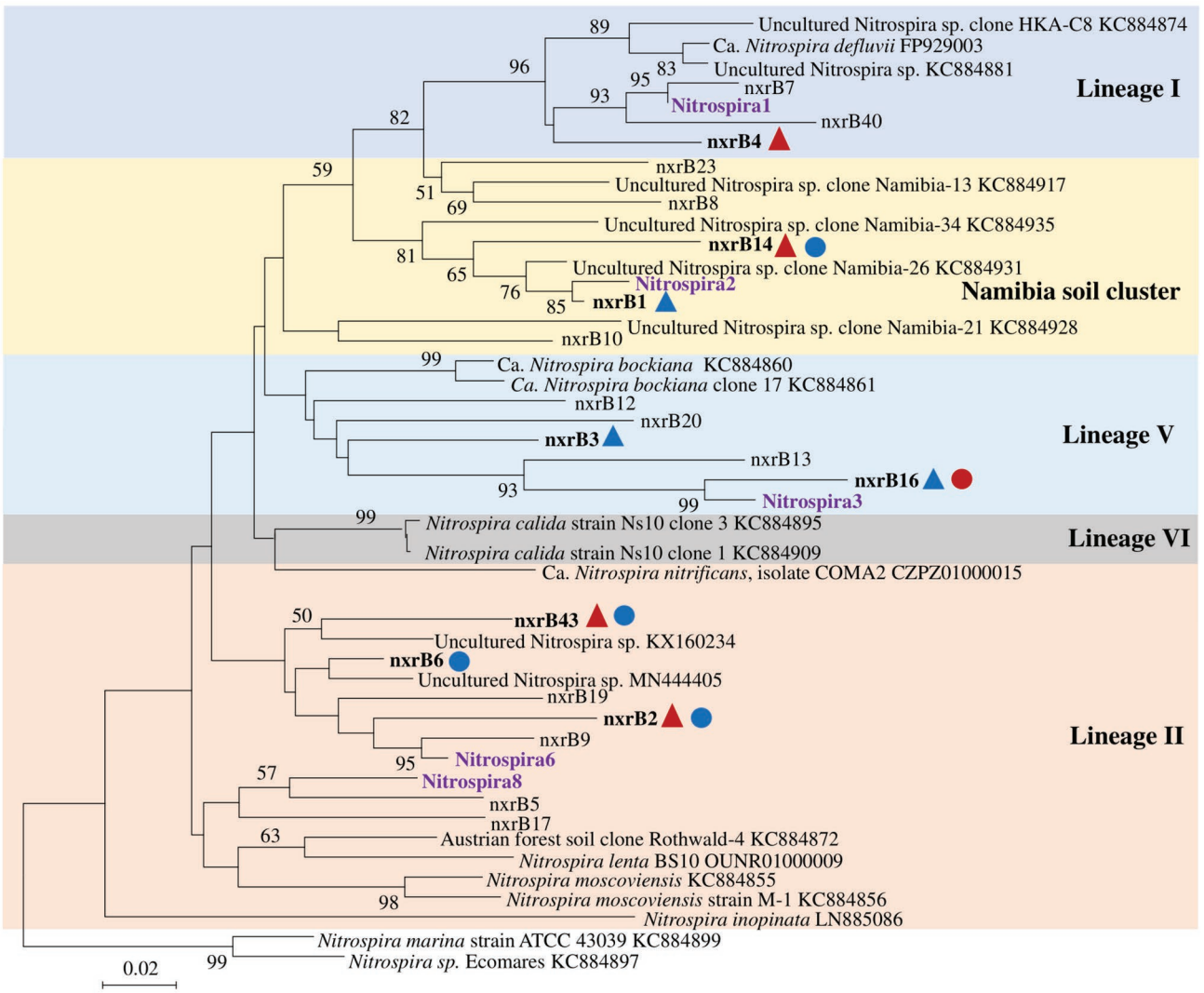

FIGURE 5 | Neighbor joining tree for *Nitrospira* partial *nxrB* top 20 OTUs (covered 94.9% of total sequences). The scale bar represents 1% nucleic acid sequence divergence, and bootstrap values (>50%) are showed at branch points. OTUs are shown in bold if they were significantly changed by N treatment. Up triangles indicate a significant difference between values for control and AS treatments, while circles indicate a significant difference between values of control and compost treatments. Red color indicates a significant higher abundance than control treatment, while blue color indicates a lower abundance.

Therefore, detection of *nxrB* copies may neither reflect actual changes in the abundance of *Nitrospira* nor the actual enzyme. In our study, PNO was not correlated with *nxrB* gene copy numbers. Several previous studies reported that PNO was strongly and significantly correlated with the abundance of *Nitrobacter*-like NOB but weakly correlated with the abundance of *Nitrospira*-like NOB (Attard et al., 2010; Han et al., 2018). Although *Nitrobacter* were recovered in 16S and metagenomic analysis in our study, their relative abundance was extremely low compared to that of *Nitrospira*. Ongoing investigations will use qPCR and high-throughput amplicon sequencing to further examine any contribution of *Nitrobacter* to nitrite oxidation in our soils.

Based on the high-throughput sequencing analysis of *Nitrospira nxrB*, *Nitrospira* community composition was significantly changed by ammonium-based fertilizers but not organic fertilizers. However, Han et al. (2018) showed that both inorganic and organic fertilization significantly influenced the *Nitrospira* community composition. Manure, with relatively higher N availability than the compost used in our case, was continuously applied for 26 years in their study. We might also observe effects of organic fertilization if followed over decades. Interestingly, at the OTU level, abundant OTUs could be both increased and decreased by organic and inorganic N fertilization. The pattern was relatively consistent to each specific lineage. The variety of patterns of *Nitrospira* OTUs in response to N fertilization indicates that the *Nitrospira* community is physiologically diverse in their response (Daims et al., 2016). We have been conducting an enrichment of this NOB experiment in our lab, detailed investigation at the single cell level may provide new insight in the response of NOB to N availability.

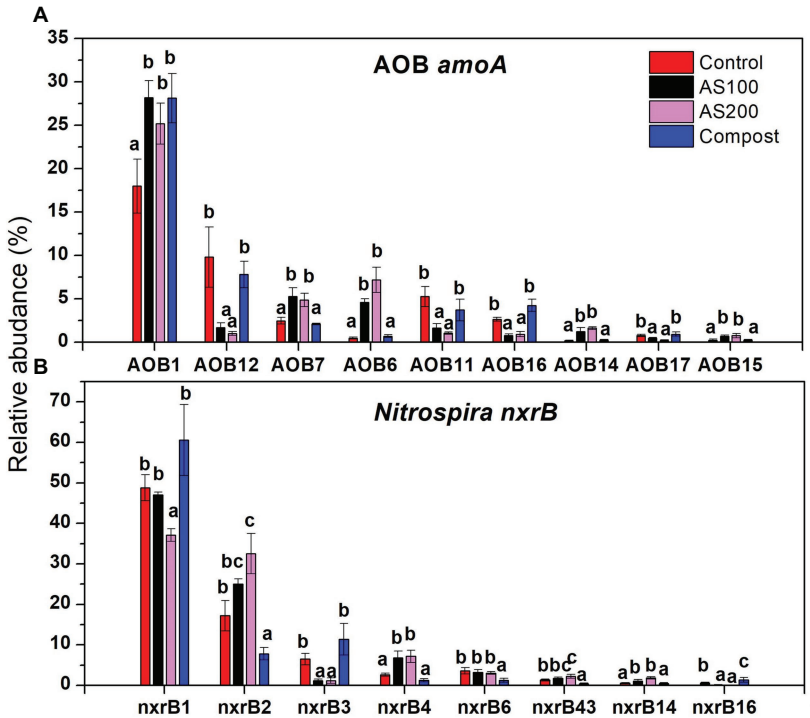

FIGURE 6 | Relative abundances of selected AOB **(A)** and *Nitrospira* **(B)** top 20 OTUs, which were significantly changed by N treatments. Error bars represent standard errors (n = 4). Different lowercase letters indicate significant differences in relative abundance among the N treatments within an OTU ($p < 0.05$).

Most described comammox belong to *Nitrospira* lineage II (Daims et al., 2015; van Kessel et al., 2015). Similar *Nitrospira* were recovered from three of four of our soil metagenomes. We could not examine the response of comammox to N fertilization using the limited sequences recovered from soil metagenomes.

Comparison of Molecular Techniques for Soil Nitrifiers

Illumina sequencing targeting 16S rRNA genes provided comparable numbers of sequence reads to pyrosequencing of *amoA* genes performed in our earlier study (Ouyang et al., 2016), suggesting that high-throughput sequencing of 16S rRNA genes is powerful enough to detect the nitrifying community, even though they are a small fraction (2–5%) of the total microbial community. Therefore, nitrifying community can be examined using the same universal primers targeting the 16S rRNA genes when accomplished with a very high sequencing depth. However, it is noteworthy that the 16S rRNA gene has low phylogenetic resolution for some closely related nitrifiers. For example, phylogenetic analysis of AOB *amoA* indicated 20 or 44 different OTUs from *Nitrosospira*, while 16S rRNA gene showed only one AOB OTU which belongs to *Nitrosospira*. In comparisons of full-length *amoA* genes with 16S rRNA genes, *Nitrosospira multiformis* ATCC 25196 and *Nitrosospira multiformis* 24-C showed 97% identity in the 16S rRNA gene sequence but approximately 88% similarity in the full-length *amoA* gene (Norton et al., 2002).

High-throughput sequencing of 16S rRNA genes enabled us to examine the changes in relative frequencies of AOA, AOB, and NOB in response to N treatment. Similar to our previous work, AOB was more responsive than AOA to ammonium fertilizers after 4 years of repeated application (Ouyang et al., 2016). In addition, it is interesting to observe the reduction of relative abundance of AOA in compost treatment, possibly due to the increase of other members of the microbial community, such as *proteobacteria* (Ouyang and Norton, 2020). Different primers for *amoA* are often used to examine the abundance and diversity of ammonia oxidizers (Meinhardt et al., 2015; Ouyang et al., 2018). We got similar community-level and species-level result with a more commonly used primer set (amoA1F/2R) for the diversity of AOB *amoA* compared with our previous study (Ouyang et al., 2016). Specifically, the overall AOB community was significantly changed by ammonium fertilizers. Several OTUs closely affiliated with *Nitrosospira* sp. Wyke8 were reduced by AS treatments suggestive that this group may be inhibited by high ammonium concentrations as found previously (Webster et al., 2005). Our study suggests that the selection of primers had relatively limited impact on the analysis of AOB community.

Shotgun metagenomics has been previously used to examine the diversity of soil nitrifiers (Wang et al., 2015; Orellana et al., 2018). However, this approach has a limitation to the detection of low-abundance genes of interest, such as genes involved in nitrification, in complex soil samples (Rodriguez-R et al., 2018). In our study, we only recovered 2–8 OTUs for nitrifiers in metagenomes with relative high sequence depth (>33 Gb). With few counts in each OTU, we were unable to assess relative abundance by this method. Therefore, the nitrifiers recovered

from soil metagenomes have low coverage and provide a relative weak statistical power for the comparison of treatment or temporal dynamics. However, soil metagenomes may provide the preliminary data for the discovery of novel organisms or functions. For example, even though we recovered limited sequences putatively related to comammox and *Nitrobacter*, this information confirmed the presence of those two nitrifiers and stimulated their further detailed examination.

CONCLUSION

Our investigation of nitrifying community using 16S rRNA gene marker complemented previous reports using the *amoA* gene marker, indicating that 4-year repeated N fertilization but not one time N fertilization significantly change the relative abundance and composition of the nitrifying community. Inorganic N fertilizers strongly stimulated the rates of potential nitrite oxidation. N fertilizers, regardless of inorganic or organic, had no effect on the abundance of *nxrB* of *Nitrospira*, although the abundance of *nxrB* showed significant temporal variation. Nitrite oxidizers were found to be dominated by *Nitrospira* by 16S rRNA sequencing. Their community composition as indicated by *Nitrospira* targeted *nxrB* genes was shifted by ammonium-based fertilization.

DATA AVAILABILITY STATEMENT

The datasets presented in this study can be found in online repositories. The names of the repository/repositories and accession number(s) can be found at: https://www.ncbi.nlm.nih.gov/, SRP109290, SRP109299, SRP109302, SRP109289. MiSeq amplicon reads may be accessed from PRJNA597781.

AUTHOR CONTRIBUTIONS

JN designed the study and revised the manuscript. YO conducted the experiment, analyzed the data, and wrote the draft of the manuscript. All authors have read and approved the final manuscript.

FUNDING

The first author YO published portions of this work as part of his dissertation (Ouyang, 2016). The USDA National Institute of Food and Agriculture funded this work under awards 2011-67019-30178 and 2016-35100-25091. The research was supported by the Utah Agricultural Experiment Station, Utah State University and approved as journal paper number 9331. Some of the work, including 16S Illumina sequencing and metagenomic sequencing, was conducted by the U.S. Department of Energy Joint Genome Institute, an Office of Science User Facility, and was supported by the Office of Science of the U.S. Department of Energy under contract DE-AC02-05CH11231.

ACKNOWLEDGMENTS

We would like to thank Marlen Craig Rice, Henry Linford, John Graves, and Lili Song for laboratory and field assistance.

SUPPLEMENTARY MATERIAL

The Supplementary Material for this article can be found online at: https://www.frontiersin.org/articles/10.3389/fmicb.2020.01736/full#supplementary-material.

REFERENCES

Aigle, A., Prosser, J. I., and Gubry-Rangin, C. (2019). The application of high-throughput sequencing technology to analysis of *amoA* phylogeny and environmental niche specialisation of terrestrial bacterial ammonia-oxidisers. *Environ. Microbiome* 14:3. doi: 10.1186/s40793-019-0342-6

Attard, E., Poly, F., Commeaux, C., Laurent, F., Terada, A., Smets, B. F., et al. (2010). Shifts between *Nitrospira*- and *Nitrobacter*-like nitrite oxidizers underlie the response of soil potential nitrite oxidation to changes in tillage practices. *Environ. Microbiol.* 12, 315–326. doi: 10.1111/j.1462-2920.2009.02070.x

Camacho, C., Coulouris, G., Avagyan, V., Ma, N., Papadopoulos, J., Bealer, K., et al. (2009). BLAST+: architecture and applications. *BMC Bioinformatics* 10:421. doi: 10.1186/1471-2105-10-421

Carey, C. J., Dove, N. C., Beman, J. M., Hart, S. C., and Aronson, E. L. (2016). Meta-analysis reveals ammonia-oxidizing bacteria respond more strongly to nitrogen addition than ammonia-oxidizing archaea. *Soil Biol. Biochem.* 99, 158–166. doi: 10.1016/j.soilbio.2016.05.014

Chen, I. M. A., Markowitz, V. M., Chu, K., Palaniappan, K., Szeto, E., Pillay, M., et al. (2017). IMG/M: integrated genome and metagenome comparative data analysis system. *Nucleic Acids Res.* 45, D507–D516. doi: 10.1093/nar/gkw929

Cole, J. R., Wang, Q., Fish, J. A., Chai, B., McGarrell, D. M., Sun, Y., et al. (2014). Ribosomal database project: data and tools for high throughput rRNA analysis. *Nucleic Acids Res.* 42, D633–D642. doi: 10.1093/nar/gkt1244

Daims, H., Lebedeva, E. V., Pjevac, P., Han, P., Herbold, C., Albertsen, M., et al. (2015). Complete nitrification by *Nitrospira* bacteria. *Nature* 528, 504–509. doi: 10.1038/nature16461

Daims, H., Lücker, S., and Wagner, M. (2016). A new perspective on microbes formerly known as nitrite-oxidizing bacteria. *Trends Microbiol.* 24, 699–712. doi: 10.1016/j.tim.2016.05.004

Edgar, R. C. (2013). UPARSE: highly accurate OTU sequences from microbial amplicon reads. *Nat. Methods* 10, 996–998. doi: 10.1038/nmeth.2604

Fish, J. A., Chai, B., Wang, Q., Sun, Y., Brown, C. T., Tiedje, J. M., et al. (2013). FunGene: the functional gene pipeline and repository. *Front. Microbiol.* 4:291. doi: 10.3389/fmicb.2013.00291

Han, S., Zeng, L., Luo, X., Xiong, X., Wen, S., Wang, B., et al. (2018). Shifts in *Nitrobacter*- and *Nitrospira*-like nitrite-oxidizing bacterial communities under long-term fertilization practices. *Soil Biol. Biochem.* 124, 118–125. doi: 10.1016/j.soilbio.2018.05.033

Jia, Z., and Conrad, R. (2009). Bacteria rather than archaea dominate microbial ammonia oxidation in an agricultural soil. *Environ. Microbiol.* 11, 1658–1671. doi: 10.1111/j.1462-2920.2009.01891.x

Ke, X., Angel, R., Lu, Y., and Conrad, R. (2013). Niche differentiation of ammonia oxidizers and nitrite oxidizers in rice paddy soil. *Environ. Microbiol.* 15, 2275–2292. doi: 10.1111/1462-2920.12098

Leininger, S., Urich, T., Schloter, M., Schwark, L., Qi, J., Nicol, G. W., et al. (2006). Archaea predominate among ammonia-oxidizing prokaryotes in soils. *Nature* 442, 806–809. doi: 10.1038/nature04983

McMurdie, P. J., and Holmes, S. (2013). Phyloseq: an R package for reproducible interactive analysis and graphics of microbiome census data. *PLoS One* 8:e61217. doi: 10.1371/journal.pone.0061217

Meinhardt, K. A., Bertagnolli, A., Pannu, M. W., Strand, S. E., Brown, S. L., and Stahl, D. A. (2015). Evaluation of revised polymerase chain reaction

primers for more inclusive quantification of ammonia-oxidizing archaea and bacteria. *Environ. Microbiol. Rep.* 7, 354–363. doi: 10.1111/1758-2229.12259

Mulvaney, R. L. (1996). "Nitrogen—inorganic forms" in *Methods of soil analysis*. eds. D. L. Sparks, A. L. Page, P. A. Helmke, R. H. Loeppert, P. N. Soltanpour, M. A. Tabatabai, et al. (Madison, WI, USA: Soil Science Society America, American Society of Agronomy), 1123-1184.

Norton, J. M., Alzerreca, J. J., Suwa, Y., and Klotz, M. G. (2002). Diversity of ammonia monooxygenase operon in autotrophic ammonia-oxidizing bacteria. *Arch. Microbiol.* 177, 139–149. doi: 10.1007/s00203-001-0369-z

Norton, J., and Ouyang, Y. (2019). Controls and adaptive management of nitrification in agricultural soils. *Front. Microbiol.* 10:1931. doi: 10.3389/fmicb.2019.01931

Ollivier, J., Schacht, D., Kindler, R., Groeneweg, J., Engel, M., Wilke, B. -M., et al. (2013). Effects of repeated application of sulfadiazine-contaminated pig manure on the abundance and diversity of ammonia and nitrite oxidizers in the root-rhizosphere complex of pasture plants under field conditions. *Front. Microbiol.* 4:22. doi: 10.3389/fmicb.2013.00022

Orellana, L. H., Chee-Sanford, J. C., Sanford, R. A., Löffler, F. E., and Konstantinidis, K. T. (2018). Year-round shotgun metagenomes reveal stable microbial communities in agricultural soils and novel ammonia oxidizers responding to fertilization. *Appl. Environ. Microbiol.* 84, e01646–e01717. doi: 10.1128/AEM.01646-17

Ouyang, Y. (2016). Agricultural nitrogen management affects microbial communities, enzyme activities, and functional genes for nitrification and nitrogen mineralization. All Graduate Theses and Dissertations. 5068. Available at: https://digitalcommons.usu.edu/etd/5068

Ouyang, Y., Evans, S. E., Friesen, M. L., and Tiemann, L. K. (2018). Effect of nitrogen fertilization on the abundance of nitrogen cycling genes in agricultural soils: a meta-analysis of field studies. *Soil Biol. Biochem.* 127, 71–78. doi: 10.1016/j.soilbio.2018.08.024

Ouyang, Y., and Norton, J. M. (2020). Short-term nitrogen fertilization affects microbial community composition and nitrogen mineralization functions in an agricultural soil. *Appl. Environ. Microbiol.* 86, e02278–e02319. doi: 10.1128/AEM.02278-19

Ouyang, Y., Norton, J. M., and Stark, J. M. (2017). Ammonium availability and temperature control contributions of ammonia oxidizing bacteria and archaea to nitrification in an agricultural soil. *Soil Biol. Biochem.* 113, 161–172. doi: 10.1016/j.soilbio.2017.06.010

Ouyang, Y., Norton, J. M., Stark, J. M., Reeve, J. R., and Habteselassie, M. Y. (2016). Ammonia-oxidizing bacteria are more responsive than archaea to nitrogen source in an agricultural soil. *Soil Biol. Biochem.* 96, 4–15. doi: 10.1016/j.soilbio.2016.01.012

Pester, M., Maixner, F., Berry, D., Rattei, T., Koch, H., Lücker, S., et al. (2014). NxrB encoding the beta subunit of nitrite oxidoreductase as functional and phylogenetic marker for nitrite-oxidizing *nitrospira*. *Environ. Microbiol.* 16, 3055–3071. doi: 10.1111/1462-2920.12300

Pester, M., Rattei, T., Flechl, S., Gröngröft, A., Richter, A., Overmann, J., et al. (2012). AmoA-based consensus phylogeny of ammonia-oxidizing archaea and deep sequencing of amoA genes from soils of four different geographic regions. *Environ. Microbiol.* 14, 525–539. doi: 10.1111/j.1462-2920.2011.02666.x

Pjevac, P., Schauberger, C., Poghosyan, L., Herbold, C. W., van Kessel, M. A. H. J., Daebeler, A., et al. (2017). AmoA-targeted polymerase chain reaction primers for the specific detection and quantification of comammox *Nitrospira* in the environment. *Front. Microbiol.* 8:1508. doi: 10.3389/fmicb.2017.01508

Poly, F., Wertz, S., Brothier, E., and Degrange, V. (2008). First exploration of *Nitrobacter* diversity in soils by a PCR cloning-sequencing approach targeting functional gene *nxrA*. *FEMS Microbiol. Ecol.* 63, 132–140. doi: 10.1111/j.1574-6941.2007.00404.x

Prosser, J. I. (2011). "Soil nitrifiers and nitrification" in *Nitrification*. eds. B. B. Ward, D. J. Arp and M. G. Klotz (Washington, DC: American Society for Microbiology), 347–383.

Purkhold, U., Pommerening-Röser, A., Juretschko, S., Schmid, M. C., Koops, H. P., and Wagner, M. (2000). Phylogeny of all recognized species of ammonia oxidizers based on comparative 16S rRNA and amoA sequence analysis: implications for molecular diversity surveys. *Appl. Environ. Microbiol.* 66, 5368–5382. doi: 10.1128/AEM.66.12.5368-5382.2000

Rodriguez-R, L. M., Gunturu, S., Tiedje, J. M., Cole, J. R., and Konstantinidis, K. T. (2018). Nonpareil 3: fast estimation of metagenomic coverage and sequence diversity. *mSystems* 3, e00039–e00118. doi: 10.1128/mSystems.00039-18

Rotthauwe, J. H., Witzel, K. P., and Liesack, W. (1997). The ammonia monooxygenase structural gene amoA as a functional marker: molecular fine-scale analysis of natural ammonia-oxidizing populations. *Appl. Environ. Microbiol.* 63, 4704–4712. Available at: http://www.ncbi.nlm.nih.gov/pubmed/9406389

Stark, J. M., and Firestone, M. K. (1995). Mechanisms for soil moisture effects on activity of nitrifying bacteria. *Appl. Environ. Microbiol.* 61, 218–221. Available at: http://www.ncbi.nlm.nih.gov/pubmed/16534906

Tamura, K., Stecher, G., Peterson, D., Filipski, A., and Kumar, S. (2013). MEGA6: molecular evolutionary genetics analysis version 6.0. *Mol. Biol. Evol.* 30, 2725–2729. doi: 10.1093/molbev/mst197

Taylor, A. E., Zeglin, L. H., Wanzek, T. A., Myrold, D. D., and Bottomley, P. J. (2012). Dynamics of ammonia-oxidizing archaea and bacteria populations and contributions to soil nitrification potentials. *ISME J.* 6, 2024–2032. doi: 10.1038/ismej.2012.51

van Kessel, M. A. H. J., Speth, D. R., Albertsen, M., Nielsen, P. H., Op den Camp, H. J. M., Kartal, B., et al. (2015). Complete nitrification by a single microorganism. *Nature* 528, 555–559. doi: 10.1038/nature16459

Wang, Q., Fish, J. A., Gilman, M., Sun, Y., Brown, C. T., Tiedje, J. M., et al. (2015). Xander: employing a novel method for efficient gene-targeted metagenomic assembly. *Microbiome* 3:32. doi: 10.1186/s40168-015-0093-6

Wang, Q., Quensen, J. F., Fish, J. A., Lee, T. K., Sun, Y., Tiedje, J. M., et al. (2013). Ecological patterns of nifH genes in four terrestrial climatic zones explored with targeted metagenomics using FrameBot, a new informatics tool. *mBio.* 4, e00592–e00613. doi: 10.1128/mBio.00592-13

Webster, G., Embley, T. M., Freitag, T. E., Smith, Z., and Prosser, J. I. (2005). Links between ammonia oxidizer species composition, functional diversity and nitrification kinetics in grassland soils. *Environ. Microbiol.* 7, 676–684. doi: 10.1111/j.1462-2920.2005.00740.x

Wertz, S., Degrange, V., Prosser, J. I., Poly, F., Commeaux, C., Guillaumaud, N., et al. (2007). Decline of soil microbial diversity does not influence the resistance and resilience of key soil microbial functional groups following a model disturbance. *Environ. Microbiol.* 9, 2211–2219. doi: 10.1111/j.1462-2920.2007.01335.x

Wertz, S., Poly, F., Le Roux, X., and Degrange, V. (2008). Development and application of a PCR-denaturing gradient gel electrophoresis tool to study the diversity of *Nitrobacter*-like *nxrA* sequences in soil. *FEMS Microbiol. Ecol.* 63, 261–271. doi: 10.1111/j.1574-6941.2007.00416.x

Zhou, X., Fornara, D., Wasson, E. A., Wang, D., Ren, G., Christie, P., et al. (2015). Effects of 44 years of chronic nitrogen fertilization on the soil nitrifying community of permanent grassland. *Soil Biol. Biochem.* 91, 76–83. doi: 10.1016/j.soilbio.2015.08.031

Conflict of Interest: The authors declare that the research was conducted in the absence of any commercial or financial relationships that could be construed as a potential conflict of interest.

frontiers in Microbiology

PERSPECTIVE
published: 11 August 2020
doi: 10.3389/fmicb.2020.01900

It Takes a Village: Discovering and Isolating the Nitrifiers

*Christopher J. Sedlacek**

Division of Microbial Ecology, Centre for Microbiology and Environmental Systems Science, University of Vienna, Vienna, Austria

It has been almost 150 years since Jean-Jacques Schloesing and Achille Müntz discovered that the process of nitrification, the oxidation of ammonium to nitrate, is a biological process carried out by microorganisms. In the following 15 years, numerous researchers independently contributed paradigm shifting discoveries that formed the foundation of nitrification and nitrification-related research. One of them was Sergei Winogradsky, whose major accomplishments include the discovery of both lithotrophy (in sulfur-oxidizing bacteria) and chemoautotrophy (in nitrifying bacteria). However, Winogradsky often receives most of the credit for many other foundational nitrification discoveries made by his contemporaries. This accumulation of credit over time is at least in part due to the increased attention, Winogradsky receives in the scientific literature and textbooks as a "founder of microbiology" and "the founder of microbial ecology." Here, some light is shed on several other researchers who are often overlooked, but whose work was instrumental to the emerging field of nitrification and to the work of Winogradsky himself. Specifically, the discovery of the biological process of nitrification by Schloesing and Müntz, the isolation of the first nitrifier by Grace and Percy Frankland, and the observation that nitrification is carried out by two distinct groups of microorganisms by Robert Warington are highlighted. Finally, the more recent discoveries of the chemolithoautotrophic ammonia-oxidizing archaea and complete ammonia oxidizers are put into this historical context.

Keywords: nitrification, nitrogen cycle, ammonia oxidizers, nitrite oxidizers, comammox

OPEN ACCESS

Edited by:
Sebastian Lücker, Radboud University Nijmegen, Netherlands

Reviewed by:
Hidetoshi Urakawa, Florida Gulf Coast University, United States
Alyson E. Santoro, University of California, Santa Barbara, United States

***Correspondence:**
Christopher J. Sedlacek
chris.j.sedlacek@gmail.com

Specialty section:
This article was submitted to Microbial Physiology and Metabolism, a section of the journal Frontiers in Microbiology

Received: *07 April 2020*
Accepted: *20 July 2020*
Published: *11 August 2020*

Citation:
Sedlacek CJ (2020) It Takes a Village: Discovering and Isolating the Nitrifiers. Front. Microbiol. 11:1900. doi: 10.3389/fmicb.2020.01900

INTRODUCTION

It has been almost 150 years since the discovery of microbially mediated nitrification (the oxidation of ammonium to nitrate), and ever since scientists have been working toward identifying and characterizing the microorganisms responsible. The ability to regulate the process of nitrification in the environment is essential in a world battling to reduce greenhouse gas emissions, prevent the eutrophication of aquatic ecosystems, and increase the efficiency of drinking and waste water treatment (Galloway et al., 2003, 2017; Fields, 2004; Erisman et al., 2008; Houlton et al., 2019). With that in mind, the study of nitrification and the microbes that carry this process out is arguably more relevant than ever. Here, a look back at several groundbreaking discoveries that form the foundation for nitrification-related research is presented.

Many independent researchers and research groups contributed to these groundbreaking discoveries, but one researcher in particular receives the lion's share of the credit for the initial work surrounding nitrification and nitrifying microorganisms, the Russian microbiologist Sergei Winogradsky. Winogradsky is often broadly credited with the discovery of nitrification, the

isolation of the first nitrifiers, and the observation that nitrification occurs as a two-step process. Interestingly, he is most likely not responsible for any of these particular discoveries (albeit determining who really had the first pure nitrifier culture is not without controversy). This accumulation of credit is in part a consequence of the increased attention Winogradsky receives in the scientific literature and textbooks – due to his impressive body of work. In fact, Winogradsky's seminal papers on nitrification cite the foundational work performed by the lesser known researchers highlighted here (Winogradsky, 1890, 1891).

Winogradsky did of course make numerous pioneering contributions to the field of nitrification and to the microbiological sciences as a whole. While at the Swiss Polytechnic Institute in Zurich, he discovered that nitrifiers were chemoautotrophic (first example of microbial autotrophy), proposed that nitrification was performed by a particular type of microorganism, championed the enrichment culturing technique that is still widely utilized today and possibly isolated the first nitrite-oxidizing bacterium (Winogradsky, 1890). Combined with his discovery of microbial lithotrophy while working with the sulfur-oxidizing *Beggiota* at the University of Strasbourg (Winogradsky, 1887; Doetsch, 1960), and his doctrine of pleomorphism (Winogradsky, 1936; Doolittle, 2013), it is easy to see why he is referred to as a "founder of microbiology" and "the founder of microbial ecology." Consequently, his life and scientific discoveries have been well documented several times over (Waksman, 1953; Penn and Dworkin, 1976; Zavarzin, 2006; Ackert, 2007; Dworkin, 2011). So, while the works of Winogradsky will be mentioned here for context, his (and his longtime research assistant, Viselli Omelianski's) work will not be the focus of this piece.

Instead, some light will be shed on a few of the other less well known but nonetheless critical researchers responsible for key nitrification-related discoveries between 1877 and 1892, which often get credited to, or grouped with, Winogradsky's accomplishments. Their discoveries are put into a timeline highlighting some of the large scientific leaps made in nitrification research during this early period. In addition, this timeline was extended to include the more recent paradigm shifting discoveries of the ammonia-oxidizing archaea and complete ammonia oxidizers.

NITRIFICATION IS A BIOTIC PROCESS

Up until the late 1870s, ammonium and nitrates held quite of bit of mystery in both agricultural and drinking water quality research. For instance, it was unknown how nitrates were replenished in unfertilized soils. Common hypotheses centered around abiotic chemical reactions, such as reactions of atmospheric nitrogen and oxygen, organic nitrogen with oxygen or ozone, or ammonia with ferric oxide (reviewed by Warington, 1878a). In addition, it was Edmund Davy, an Irish medical doctor and professor of forensic medicine at the Royal College of Surgeons in Ireland, who first observed that ammonium concentrations decreased while nitrite (and he assumed nitrate) increased over time in sewage contaminated drinking water. Therefore, in order to rule out sewage contamination, Davy argued that drinking water should be tested for not only just ammonium but also nitrite and nitrate (Davy, 1883). Notably, although Davy did not attempt to answer whether nitrification was a biotic process or not, he detailed how the process of nitrification: (1) is inhibited by high amounts of organic matter, (2) requires air or free oxygen, and (3) proceeds at an optimal temperature of between 21 and 27°C.

The first person to hypothesize that ammonia oxidation may in fact be a biological process was the French chemist/microbiologist Luis Pasteur, who in 1862 suggested that ammonia may be oxidized to nitrate in a similar manner as alcohol is oxidized to acetic acid (Pasteur, 1862). A decade later, Alexander Müller, a German agricultural chemist, would put forward that ammonia oxidation must be performed by microorganisms. While investigating water quality from wells in Berlin, Müller noted that ammonium was stable in sterilized solutions in the laboratory but readily nitrified in natural waters (Müller, 1875). Even with these observations, it would be ~25 years (1877) after Pasteur's initial hypothesis until two French agricultural chemists working in Paris, Jean-Jacques Schloesing and Achille Müntz, demonstrated that the oxidation of ammonium in sewage and soils was indeed a microbially mediated process (Schloesing and Müntz, 1877a,b).

In order to demonstrate the biological nature of nitrification, Schloesing and Müntz slowly passaged liquid sewage through an artificial soil matrix column consisting of sterilized sand and powered chalk. With this experimental setup, they were able to make four key observations: (1) there was an initial lag phase, (2) as the ammonia concentration decreased the nitrate concentration increased in the filtrate, (3) nitrification irreversibly ceased when the column was exposed to chloroform or high heat, and (4) nitrification could be restarted by adding small amounts of soil washings (Schloesing and Müntz, 1877a,b). These results were independently confirmed by the English agricultural chemist Robert Warington who was investigating the nitrification ability of garden soil at the (still operational today) Rothamsted experimental station in Harpenden England. Warington was also able to demonstrate that soil added to dilute solutions of ammonium would produce nitrate, and that these nitrifying solutions could seed new nitrifying solutions – with this, nitrifier enrichment/cultivation was born (Warington, 1878b). Together, these seminal studies kick-started the study of microbial nitrification.

Interestingly, one of the still remaining open questions in nitrification research became a topic of debate during these early years. Several researchers published observations very early on as to whether or not direct sunlight inhibited the process of nitrification, with varied results (Warington, 1878b, 1879, 1884; Davy, 1883; Munro, 1886). However, the effect of 24-hour illumination on nitrification could not be studied, as the incandescent light bulb was still being developed.

NITRIFICATION IS A TWO-STEP PROCESS

In 1879, Warington made the first observation that nitrification proceeds as a two-step process, involving the oxidation of ammonia to nitrite and the oxidation of nitrite to nitrate. Here, Warington

described and propagated individual ammonia- and nitrite-oxidizing enrichment cultures. In addition, he observed that fully nitrifying cultures only built up nitrite as an intermediate if the rate of ammonia oxidation was sufficiently high (Warington, 1879). The two-step process of nitrification would be later confirmed by the English chemist John Munro working at the College of Agriculture at Downton (Munro, 1886). These observations were made well before the isolation of the first nitrifier in 1890. However, the hypothesis at the time was that the ammonia- and nitrite-oxidizing cultures represented different life phases or character traits of the single nitrifying microorganism (Warington, 1884, 1891).

NITRIFIER ISOLATION ATTEMPTS

Once it was confirmed that nitrification was a microbially mediated process, the race was on to be the first researcher to isolate and characterize the microorganism(s) responsible. Over the course of the next ~15 years (1877-1890), several researchers made claims that they isolated cultures that had (or previously had) full nitrifying capabilities (the ability to oxidize ammonium to nitrate). At the time, it was still hotly debated whether microorganisms were pleomorphic – able to radically change their abilities or characteristics under different circumstances, sometimes irreversibly in short periods of time (Winogradsky, 1936; Doolittle, 2013). With the pleomorphic hypothesis in mind, some researchers observed that nitrifying microorganisms irreversibly lost their nitrifying capabilities through the process of isolation. These studies attempted to isolate single nitrifier colonies on solid growth medium containing high amounts of organic carbon. In a somewhat ironic twist, this exact approach (growth in or on medium containing high amounts of organic carbon) is now common practice in order to detect heterotrophic contaminants in pure nitrifier cultures. However, because each researcher isolated their own unique environmental cultures and some of these cultures had seemingly lost their nitrifying capabilities by the time of publication, independent conformational studies were difficult if not impossible.

As a notable exception, the German chemist Wilhelm Heraeus, working at the Institute of Hygiene in Berlin, published in 1886 that in addition to cultures, he freshly isolated from sites around Hanau Germany, several well-known bacterial cultures, including *Bacillus anthracis* and *Bacillus ramosus* had nitrifying capabilities. In his publication, Heraeus notes that some of these isolated cultures produced detectable but not quantifiable amounts of nitrite and nitrate when cultured in dilute urine (Heraeus, 1886). As these *Bacillus* strains were more widely available to the scientific community, others could attempt to replicate the results. Indeed, the English agricultural chemist Percy Frankland attempted but could not independently verify Heraeus's results. Frankland determined that Heraeus was most likely detecting small amounts of nitrate present in the urine, and that the *Bacillus* cultures were reducing this nitrate to nitrite. By inoculating the *Bacillus* cultures into ammonium solutions instead of dilute urine, Frankland was able to refute Heraeus's claims as no nitrite or nitrate was produced (Frankland, 1888). It would not be until 1890 that Percy and Grace Frankland, two English scientists working in Dundee Scotland would publish about the isolation of what is most likely the first pure nitrifier (ammonia-oxidizing) culture (Frankland and Frankland, 1890). This breakthrough was made possible by the combined expertise of Grace as a bacteriologist and Percy as an agricultural chemist.

ISOLATION OF THE FIRST NITRIFIERS

For years researchers (including the Frankland's) failed to isolate actively nitrifying cultures using Robert Koch's solid medium isolation techniques (Koch, 1882). However, Warington, Winogradsky, and the Frankland's were all able to establish and propogate nitrifying enrichment cultures (Warington, 1878b; Frankland and Frankland, 1890; Winogradsky, 1890). Ultimately Frankland and Frankland were the first to isolate a pure nitrifier (ammonia-oxidizing bacteria) from their enrichment cultures. In order to achieve a pure culture, they employed a system of serial dilutions with very low inoculum over the period of several years (Frankland and Frankland, 1890). This method of serial dilution to extinction is a tried and true method that is still used for the (painstakingly slow) isolation of nitrifiers today.

In 1890, both Winogradsky as well as Frankland and Frankland would both claim that they were the first to have a pure nitrifier culture (Frankland and Frankland, 1890; Winogradsky, 1890). However, at this time, Winogradsky's pure culture was still a fully nitrifying culture, and he would later disclose through personal communications (~40 years later) that his nitrifying cultures were suitable for nitrification studies but not pure in the strictest sense of the word (Hanks and Weintraub, 1936). With the more recent discovery of complete ammonia oxidizers in mind, it is tempting to speculate that Winogradsky did in fact have a pure culture of a complete ammonia oxidizer capable of fully nitrifying. However, based on his work in the years to come, this culture was much more likely a co-culture of ammonia- and nitrite-oxidizing bacteria. Winogradsky was able to separate the ammonia- and nitrite-oxidizing bacteria just a year later (Winogradsky, 1891).

In contrast to other researchers before them, both the team of Frankland and Frankland as well as Winogradsky took many steps in order to ensure they had an actively nitrifying pure culture. Both noted that pure nitrifying cultures did not produce any growth on solid media, and that the nitrifying liquid medium remained clear throughout the entirety of nitrification. Additionally, they monitored and quantified the conversion of ammonium into nitrite and nitrate (Frankland and Frankland, 1890; Winogradsky, 1890, 1891).

Although Frankland and Frankland were confident that they had isolated the microorganism responsible for nitrification, the isolate only oxidized ammonium to nitrite when in its pure form (Frankland and Frankland, 1890). Warington had observed a similar phenomenon years ago, noting that after several passages in the laboratory nitrifying cultures would often produce nitrite rather than fully nitrifying (Warington, 1879, 1884). There were several hypotheses to explain this partial nitrification: (1) the oxidation of nitrite to nitrate was completed by a second uncultured microorganism, (2) the conditions for full ammonia oxidation were not met in the laboratory, or (3)

part of the microorganism's physiology present when in soil was lost rapidly during laboratory cultivation. In hindsight, Warington as well as Frankland and Frankland, were unknowingly separating ammonia- and nitrite-oxidizing bacteria through the use of different growth mediums and transfer techniques.

As is the case with the ammonia-oxidizing bacteria, determining which researcher(s) truly isolated the first nitrite-oxidizing bacteria, is not without uncertainty. Again, there were researchers that claimed to isolate nitrite-oxidizing bacteria that quickly lost their nitrite oxidation abilities once grown and isolated on or in organic growth medium (Beijerinck, 1914), which were most likely not pure nitrite-oxidizing bacteria. In addition, some seemingly pure cultures were later discovered to be highly enriched cultures with only a few bacterial members (Burri and Stutzer, 1895). But there are about 10 research groups, who between 1900 and 1960 claim to have purified nitrite-oxidizing bacteria, which did not produce noticeable growth when inoculated on or in growth medium containing high amounts of organic matter (reviewed by Zavarzin and Legunkova, 1959; but missing Fred and Davenport, 1921). As with the ammonia oxidizers, Winogradsky was the first to claim a pure nitrite-oxidizing culture (Winogradsky, 1891). Unfortunately, unlike with the isolation of the first ammonia oxidizers, where there was a clear difference between theoretically pure cultures that produce nitrite versus those that produce nitrate from ammonium; here, all theoretically pure nitrite oxidizer cultures share the same reported physiology (nitrite consumption and nitrate production). Therefore, without preserved cultures, it is difficult if not impossible to say with certainty which cultures contained no heterotrophic contaminants.

Nitrite oxidizer isolation represents another close call for Robert Warington. After being the first to observe the two steps of nitrification (even if the significance of the observation was not immediately clear), he spent years attempting to isolate nitrite-oxidizing microorganisms through the serial dilution technique shown to be successful by Frankland and Frankland with ammonia oxidizers, but to no avail. He would end his scientific career before he was able to produce a pure nitrite-oxidizing isolate (Warington, 1891).

NEW NITRIFIERS DISCOVERED IN THE 21ST CENTURY

Since the inaugural era of nitrification research discussed so far, there has been a wealth of studies that have propelled the field of nitrification forward during the subsequent ~100 years. These advances include (but are not limited to) the (1) discovery of many phylogenetically and physiologically distinct ammonia- and nitrite-oxidizing bacteria, (2) a deeper understanding of nitrifier (eco)physiology/enzymology, and (3) extensive environmental surveys. These discoveries, isolations, and characterizations have previously been thoroughly reviewed throughout the years (Watson et al., 1981, 1989; Prosser, 1989; Koops and Pommerening-Röser, 2001; Kowalchuk and Stephen, 2001; Koops et al., 2006; Arp et al., 2007; Daims et al., 2011; Stahl and de la Torré, 2012).

Even with this immense increase in the diversity of known nitrifiers, up until just over 15 years ago, it was widely accepted that (1) there was a complete division of labor in nitrification and (2) nitrification was carried out solely by bacteria. Then, over the course of a 10-year period both of these century-old paradigms were shattered with the discovery and isolation of ammonia-oxidizing archaea and complete ammonia oxidizers. Just as with the discovery and isolation of the ammonia- and nitrite-oxidizing bacteria, these discoveries too, took a village.

Ammonia-Oxidizing Archaea

In 2004, two independent research groups identified putative ammonia monooxygenase genes (the main functional genes used to identify ammonia oxidizers) in genomic sequence material belonging to a *Crenarchaeota* microorganism (Treusch et al., 2004; Venter et al., 2004).

Almost immediately, these findings were followed key genomic comparisons (Schleper et al., 2005) and environmental survey studies (Francis et al., 2005). Amazingly, the first isolated ammonia-oxidizing archaea culture, *Nitrosopumilus maritimus*, was published within the next year (Könneke et al., 2005), and the first genome of an ammonia-oxidizing archaea (*Candidatus Cenarchaeum symbiosum*) was published soon after (Hallam et al., 2006a,b). Since these works, there have been hundreds of studies focusing on the diversity, physiology, and environmental distribution of ammonia-oxidizing archaea, highlighting to what extent they have changed the field of nitrification in such a short time (reviewed by Erguder et al., 2009; Schleper and Nicol, 2010; Urakawa et al., 2011; Hatzenpichler, 2012; Prosser and Nicol, 2012; Stahl and de la Torré, 2012; Alves et al., 2018).

Complete Ammonia Oxidizers

Although a complete ammonia oxidizer had never been described, their existence was by no means a new hypothesis. The whole field of nitrification began with the belief that nitrification was completed by one microorganism (a nitrifying ferment). In addition, a recent theoretical kinetic study hypothesized that complete ammonia oxidizers would be found in environments that select for slow growing but high yield microorganisms (Costa et al., 2006). In 2015, just 10 years after the discovery of the ammonia-oxidizing archaea, the existence of complete ammonia oxidizers was published in parallel by two research groups. Both studies yielded metagenomic evidence for, and enrichment cultures of, a complete ammonia oxidizer (Daims et al., 2015; van Kessel et al., 2015). Within a year, two additional research groups published evidence supporting these findings (Pinto et al., 2015; Palomo et al., 2016). The isolation of *Nitrospira inopinata*, the first complete ammonia oxidizer brought into pure culture, followed shortly thereafter (Daims et al., 2015; Kits et al., 2017). In the same manner as the discovery of the ammonia-oxidizing archaea before them, studies focusing on the diversity, physiology, and environmental distribution of complete ammonia oxidizers are now increasing at a rapid pace (reviewed by Daims et al., 2016; Palomo et al., 2018; Xia et al., 2018; Koch et al., 2019). It took about 150 years,

but the field of nitrification has now come full circle – a fully nitrifying microorganism with the ability to oxidize ammonia all the way to nitrate.

IN SUMMARY

While Winogradsky has certainly earned his title of "the founder of microbial ecology," the breakthroughs illustrated here highlight the work of many of his often-overlooked contemporaries. Schloeing, Muntz, Warington, Frankland, and Frankland among others, all contributed essential observations and discoveries that now form the foundation of nitrification-related research. With the surprising discoveries of new types of nitrifiers within just the past 15 years, the future of nitrification research looks bright. It will be exciting to see whether there are even more fundamentally different types of nitrifiers including nitrite-oxidizing or complete ammonia-oxidizing archaea out there waiting to be discovered and isolated.

AUTHOR CONTRIBUTIONS

The author confirms being the sole contributor of this work and has approved it for publication.

FUNDING

CS was supported by the Wittgenstein Award of the Austrian Science Fund presented to Michael Wagner, the Austrian Science Fund (FWF, project P30570-B29), and the Comammox Research Platform of the University of Vienna.

ACKNOWLEDGMENTS

I would like to thank Michael Wagner, Holger Daims, Petra Pjevac, Andrew Giguere, Anna Aplenc, and Heather Beck for fruitful discussions and helpful comments on the manuscript.

REFERENCES

Ackert, L. T. (2007). The "cycle of life" in ecology: Sergei Vinogradskii's soil microbiology, 1885–1940. *J. Hist. Biol.* 40, 109–145. doi: 10.1007/s10739-006-9104-6

Alves, R. J., Minh, B. Q., Urich, T., Haeseler, A., and Schleper, C. (2018). Unifying the global phylogeny and environmental distribution of ammonia-oxidising archaea based on amoA genes. *Nat. Commun.* 9:1517. doi: 10.1038/s41467-018-03861-1

Arp, D. J., Chain, P. S. G., and Klotz, M. G. (2007). The impact of genome analyses on our understanding of ammonia-oxidizing bacteria. *Annu. Rev. Microbiol.* 61, 503–528. doi: 10.1146/annurev.micro.61.080706.093449

Beijerinck, W. (1914). Ueber das Nitratferment und ueber physiologische Artbildung. *Folio Microbiol.* 3, 91–113.

Burri, R., and Stutzer, A. (1895). Ueber einen auf Nährgelatine gedeihenden nitratbildenden *Bacillus*. *Central. Bakt.* 2, 721–740.

Costa, E., Pérez, J., and Kreft, J. U. (2006). Why is metabolic labour divided in nitrification? *Trends Microbiol.* 14, 213–219. doi: 10.1016/j.tim.2006.03.006

Daims, H., Lebedeva, E. V., Pjevac, P., Han, P., Herbold, C., Albertsen, M., et al. (2015). Complete nitrification by *Nitrospira* bacteria. *Nature* 528, 504–509. doi: 10.1038/nature16461

Daims, H., Lücker, S., Le Paslier, D., and Wagner, M. (2011). "Diversity, environmental genomics, and ecophysiology of nitrite-oxidizing bacteria" in *Nitrification*. eds. B. Ward, D. Arp and M. Klotz (Washington, DC: ASM Press), 295–322.

Daims, H., Lücker, S., and Wagner, M. (2016). A new perspective on microbes formerly known as nitrite-oxidizing bacteria. *Trends Microbiol.* 24, 699–712. doi: 10.1016/j.tim.2016.05.004

Davy, E. W. (1883). Notes of some observations on nitrification. *Proc. R. Ir. Acad. Sci.* 3, 242–247.

Doetsch, R. M. (1960). *Historical contribution from 1776 to 1908 by Spallanzani, Schwann, Pasteur, Cohn, Tyndall, Koch, Lister, Schloesing, Burrill, Ehrlich, Winogradsky, Warrington, Beijerinck, Smith, Orla-Jensen*. New Brunswick, NJ: Rutgers University Press.

Doolittle, W. F. (2013). Microbial neopleomorphism. *Biol. Philos.* 28, 351–378. doi: 10.1007/s10539-012-9358-7

Dworkin, M. (2011). Sergei Winogradsky: a founder of modern microbiology and the first microbial ecologist. *FEMS Microbiol. Rev.* 36, 364–379. doi: 10.1111/j.1574-6976.2011.00299.x

Erguder, T. H., Boon, N., Wittebolle, L., Marzorati, M., and Verstraete, W. (2009). Environmental factors shaping the ecological niches of ammonia-oxidizing archaea. *FEMS Microbiol. Rev.* 33, 855–869. doi: 10.1111/j.1574-6976.2009.00179.x

Erisman, J., Sutton, M., Galloway, J., Klimont, Z., and Winiwarter, W. (2008). How a century of ammonia synthesis changed the world. *Nat. Geosci.* 1, 636–639. doi: 10.1038/ngeo325

Fields, S. (2004). Global nitrogen: cycling out of control. *Environ. Health Perspect.* 112, A556–A563. doi: 10.1289/ehp.112-a556

Francis, C. A., Roberts, K. J., Beman, J. M., Santoro, A. E., and Oakley, B. B. (2005). Ubiquity and diversity of ammonia-oxidizing archaea in water columns and sediments of the ocean. *Proc. Natl. Acad. Sci. U. S. A.* 102, 14683–14688. doi: 10.1073/pnas.0506625102

Frankland, P. F. (1888). The action of some specific microorganisms on nitric acid. *J. Chem. Soc. Trans.* 53, 373–391. doi: 10.1039/CT8885300373

Frankland, P. F., and Frankland, G. C. (1890). The nitrifying process and its specific ferment. Part I. *Philos. Trans. R. Soc. Lond. B* 181, 107–128. doi: 10.1098/rstb.1890.0005

Fred, E. B., and Davenport, A. (1921). The effect of organic nitrogenous compounds on the nitrate-forming organism. *Soil Sci.* 11, 389–407. doi: 10.1097/00010694-192105000-00006

Galloway, J. N., Aber, J. D., Erisman, J. W., Seitzinger, S. P., Howarth, R. W., Cowling, E. B., et al. (2003). The nitrogen cascade. *Bioscience* 53, 341–356. doi: 10.1641/0006-3568(2003)053[0341:TNC]2.0.CO;2

Galloway, J. N., Leach, A. M., Erisman, J. W., and Bleeker, A. (2017). Nitrogen: the historical progression from ignorance to knowledge, with a view to future solutions. *Soil Res.* 55, 417–424. doi: 10.1071/SR16334

Hallam, S. J., Konstantinidis, K. T., Putnam, N., Schleper, C., Watanabe, Y., Sugahara, J., et al. (2006a). Genomic analysis of the uncultivated marine crenarchaeote *Cenarchaeum symbiosum*. *Proc. Natl. Acad. Sci. U. S. A.* 103, 18296–18301. doi: 10.1073/pnas.0608549103

Hallam, S. J., Mincer, T. J., Schleper, C., Preston, C. M., Roberts, K., Richardson, P. M., et al. (2006b). Pathways of carbon assimilation and ammonia oxidation suggested by environmental genomic analyses of marine *Crenarchaeota*. *PLoS Biol.* 4:e95. doi: 10.1371/journal.pbio.0040095

Hanks, J. H., and Weintraub, R. L. (1936). The pure culture isolation of ammonia-oxidizing bacteria. *J. Bacteriol.* 32, 653–670. doi: 10.1128/JB.32.6.653-670.1936

Hatzenpichler, R. (2012). Diversity, physiology, and niche differentiation of ammonia-oxidizing archaea. *Appl. Environ. Microbiol.* 78, 7501–7510. doi: 10.1128/AEM.01960-12

Heraeus, W. (1886). Ueber das Verhalten der Bacterien im Brunnenwasser, sowie uber reducirende und oxydirende Eigenschaften der bacterien. *Z. Hyg.* 1, 193–242. doi: 10.1007/BF02188450

Houlton, B. Z., Almaraz, M., Aneja, V., Austin, A. T., Bai, E., Cassman, K. G., et al. (2019). A world of cobenefits: solving the global nitrogen challenge. *Earth's Future* 7, 865–872. doi: 10.1029/2019EF001222

Kits, K. D., Sedlacek, C. J., Lebedeva, E. V., Han, P., Bulaev, A., Pjevac, P., et al. (2017). Kinetic analysis of a complete nitrifier reveals an oligotrophic lifestyle. *Nature* 549, 269–272. doi: 10.1038/nature23679

Koch, R. (1882). "Die aetiologie der tuberculose. Berl. Klin. Wchnschr., xix: 221-230" in *Milestones in microbiology: 1556 to 1940*. ed. T. D. Brock (Washington, DC, USA: ASM Press), 109.

Koch, H., van Kessel, M. A. H. J., and Lücker, S. (2019). Complete nitrification: insights into the ecophysiology of comammox *Nitrospira*. *Appl. Microbiol. Biotechnol.* 103, 177–189. doi: 10.1007/s00253-018-9486-3

Könneke, M., Bernhard, A. E., de la Torre, J. R., Walker, C. B., Waterbury, J. B., and Stahl, D. A. (2005). Isolation of an autotrophic ammonia-oxidizing marine archaeon. *Nature* 437, 543–546. doi: 10.1038/nature03911

Koops, H. P., and Pommerening-Röser, A. (2001). Distribution and ecophysiology of the nitrifying bacteria emphasizing cultured species. *FEMS Microbiol. Ecol.* 37, 1–9. doi: 10.1111/j.1574-6941.2001.tb00847.x

Koops, H. P., Purkhold, U., Pommerening-Röser, A., Timmermann, G., and Wagner, M. (2006). "The lithoautotrophic ammonia-oxidizing bacteria" in *The Prokaryotes. Vol. 5.* eds. M. Dworkin, S. Falkow, E. Rosenberg, K. H. Schleifer and E. Stackebrandt (New York, NY: Springer), 778–811.

Kowalchuk, G. A., and Stephen, J. R. (2001). Ammonia-oxidizing bacteria: a model for molecular microbial ecology. *Annu. Rev. Microbiol.* 55, 485–529. doi: 10.1146/annurev.micro.55.1.485

Müller, A. (1875). "Ammoniakgehalt des Spree- und Wasserleitungs wassers in Berlin" in *Fortsetzung der Vorarbeiten zu einer zukünftigen Wasser-Versorgung der Stadt Berlin ausgeführt in den Jahren 1868 und 1869*. Berlin, Germany: Deitrich Reimer, 121–123.

Munro, J. H. M. (1886). The formation and destruction of nitrates and nitrites in artificial solution and in river and well waters. *J. Chem. Soc. Trans.* 49, 632–681. doi: 10.1039/CT8864900632

Palomo, A., Fowler, J. S., Gülay, A., Rasmussen, S., Sicheritz-Ponten, T., and Smets, B. F. (2016). Metagenomic analysis of rapid gravity sand filter microbial communities suggests novel physiology of *Nitrospira* spp. *ISME J.* 10, 2569–2581. doi: 10.1038/ismej.2016.63

Palomo, A., Pedersen, A. G., Fowler, S. J., Dechesne, A., Sicheritz-Pontén, T., and Smets, B. F. (2018). Comparative genomics sheds light on niche differentiation and the evolutionary history of comammox *Nitrospira*. *ISME J.* 12, 1779–1793. doi: 10.1038/s41396-018-0083-3

Pasteur, L. (1862). Etudes sur les mycoderme. *C. R. Acad. Sci.* 54, 265–270.

Penn, M., and Dworkin, M. (1976). Robert Koch and two visions of microbiology. *Bacteriol. Rev.* 40, 276–283. doi: 10.1128/MMBR.40.2.276-283.1976

Pinto, A. J., Marcus, D. N., Ijaz, U. Z., Bautista-de Lose Santos, Q. M., Dick, G. J., and Raskin, L. (2015). Metagenomic evidence for the presence of comammox *Nitrospira*-like bacteria in a drinking water system. *mSphere* 1:e00054–15. doi: 10.1128/mSphere.00054-15

Prosser, J. I. (1989). Autotrophic nitrification in bacteria. *Adv. Microb. Physiol.* 30, 125–181. doi: 10.1016/s0065-2911(08)60112-5

Prosser, J. I., and Nicol, G. W. (2012). Archaeal and bacterial ammonia-oxidisers in soil: the quest for niche specialisation and differentiation. *Trends Microbiol.* 20, 523–531. doi: 10.1016/j.tim.2012.08.001

Schleper, C., Jurgens, G., and Jonuscheit, M. (2005). Genomic studies of uncultivated archaea. *Nat. Rev. Microbiol.* 3, 479–488. doi: 10.1038/nrmicro1159

Schleper, C., and Nicol, G. W. (2010). "Ammonia-oxidising archaea—physiology, ecology and evolution" in *Advances in microbial physiology*. ed. K. P. Robert (NY, USA: Academic Press New York), 1–41.

Schloesing, J. J. T., and Müntz, A. (1877a). Sur la nitrification pas les ferments organisés. *C. R. Acad. Sci.* 84, 301–303.

Schloesing, J. J. T., and Müntz, A. (1877b). Sur la nitrification pas les ferments organisés. *C. R. Acad. Sci.* 85, 1018–1020.

Stahl, D. A., and de la Torré, J. R. (2012). Physiology and diversity of ammonia-oxidizing archaea. *Annu. Rev. Microbiol.* 66, 83–101. doi: 10.1146/annurev-micro-092611-150128

Treusch, A. H., Kletzin, A., Raddatz, G., Ochsenreiter, T., Quaiser, A., Meurer, G., et al. (2004). Characterization of large-insert DNA libraries from soil for environmental genomic studies of archaea. *Environ. Microbiol.* 6, 970–980. doi: 10.1111/j.1462-2920.2004.00663.x

Urakawa, H., Martens-Habbena, W., and Stahl, D. A. (2011). "Physiology and genomics of ammonia-oxidizing archaea" in *Nitrification*. eds. B. B. Ward, D. J. Arp and M. G. Klotz (Washington, DC: ASM Press), 460.

van Kessel, M. A. H. J., Speth, D. R., Albertsen, M., Nielsen, P. H., den Camp, H. J. O., Kartal, B., et al. (2015). Complete nitrification by a single microorganism. *Nature* 528, 555–559. doi: 10.1038/nature16459

Venter, J. C., Remington, K., Heidelberg, J. F., Halpern, A. L., Rusch, D., Eisen, J. A., et al. (2004). Environmental genome shotgun sequencing of the Sargasso Sea. *Science* 304, 66–74. doi: 10.1126/science.1093857

Waksman, S. (1953). *Sergei N. Winogradsky his life and work*. New Brunswick, New Jersey: Rutgers University Press.

Warington, R. (1878a). Nitrification. *Nature* 17, 367–369. doi: 10.1038/017367a0

Warington, R. (1878b). On nitrification. *J. Chem. Soc. Trans.* 33, 44–51. doi: 10.1039/CT8783300044

Warington, R. (1879). On nitrification part II. *J. Chem. Soc. Trans.* 35, 429–456. doi: 10.1039/CT8793500429

Warington, R. (1884). On nitrification part III. *J. Chem. Soc. Trans.* 45, 637–672. doi: 10.1039/CT8844500637

Warington, R. (1891). On nitrification part IV. *J. Chem. Soc. Trans.* 59, 484–529. doi: 10.1039/CT8915900484

Watson, S. W., Bock, E., Harms, H., Koops, H. P., and Hooper, A. B. (1989). "Nitrifying bacteria" in *Bergey's manual of systematic bacteriology*. *Vol. 3.* eds. J. T. Staley, M. P. Bryant, N. Pfennig and J. G. Holt (Baltimore, MD: Williams and Wilkins), 1808–1834.

Watson, S. W., Valois, F. W., and Waterbury, J. B. (1981). "The family nitrobacteraceae" in *The prokaryotes. Vol. 1.* eds. M. P. Starr, H. Stolp and H. Trüper, (Berlin, Germany: Springer-Verlag), 1005–1022.

Winogradsky, S. (1887). Ueber Schwefelbacterien. *Bot. Zeit.* 45, 489–610.

Winogradsky, S. (1890). Sur les organisms de la nitrification. *Ann. Inst. Pasteur* 4, 215–231, 257–275, 760–771.

Winogradsky, S. (1891). Sur les organisms de la nitrification. *Ann. Inst. Pasteur* 5, 92–100, 577–616.

Winogradsky, S. (1936). The doctrine of pleomorphism in bacteriology. *Soil Sci.* 43, 327–340. doi: 10.1097/00010694-193705000-00001

Xia, F., Wang, J. G., Zhu, T., Zou, B., Rhee, S. K., and Quan, Z. X. (2018). Ubiquity and diversity of complete ammonia oxidizers (comammox). *Appl. Environ. Microbiol.* 84:e01390–18. doi: 10.1128/AEM.01390-18

Zavarzin, G. A. (2006). Winogradsky and modern microbiology. *Microbiology* 75, 501–511. doi: 10.1134/S0026261706050018

Zavarzin, G. A., and Legunkova, R. (1959). The morphology of *Nitrobacter winogradskyi*. *J. Gen. Microbiol.* 21, 186–190. doi: 10.1099/00221287-21-1-186

Conflict of Interest: The author declares that the research was conducted in the absence of any commercial or financial relationships that could be construed as a potential conflict of interest.

frontiers in Microbiology

ORIGINAL RESEARCH
published: 08 September 2020
doi: 10.3389/fmicb.2020.551925

Autotrophic Fixed-Film Systems Treating High Strength Ammonia Wastewater

Hussain Aqeel[1] *and Steven N. Liss*[1,2,3]*

[1] School of Environmental Studies, Queen's University, Kingston, ON, Canada, [2] Department of Chemistry and Biology, Ryerson University, Toronto, ON, Canada, [3] Department of Microbiology, Stellenbosch University, Stellenbosch, South Africa

The aim of the study was enrichment of nitrifying bacteria and to investigate the potential of autotrophic fixed-film and hybrid bioreactors to treat high strength ammonia wastewater (up to 1,000 mg N/L). Two types of fixed-film systems [moving bed biofilm reactor (MBBR) and BioCord^{TM}] in two different configurations [sequencing batch reactor (SBR) and a continuous stirred tank reactor (CSTR)] were operated for 306 days. The laboratory-scale bioreactors were seeded with activated sludge from a municipal wastewater treatment plant and fed synthetic wastewater with no organics. Strategies for acclimation included biomass reseeding (during bioreactor start-up), and gradual increase in the influent ammonia concentration [from 130 to 1,000 mg N/L (10% every 5 days)]. Stable ammonia removal was observed up to 750 mg N/L from 45 to 145 days in the MBBR SBR (94–100%) and CSTR (72–100%), and BioCord^{TM} SBR (96–100%) and CSTR (92–100%). Ammonia removal declined to 87% ± 6, in all bioreactors treating 1,000 mg N/L (on day 185). Following long-term operation at 1,000 mg N/L (on day 306), ammonia removal was 93–94% in both the MBBR SBR and BioCord^{TM} CSTR; whereas, ammonia removal was relatively lower in MBBR CSTR (20–35%) and BioCord^{TM} SBR (45–54%). Acclimation to increasing concentrations of ammonia led to the enrichment of nitrifying (*Nitrosomonas*, *Nitrospira*, and *Nitrobacter*) and denitrifying (*Comamonas*, *OLB8*, and *Rhodanobacter*) bacteria [16S rRNA gene sequencing (Illumina)] in all bioreactors. In the hybrid bioreactor, the nitrifying and denitrifying bacteria were relatively more abundant in flocs and biofilms, respectively. The presence of dead cells (in biofilms) suggests that in the absence of an organic substrate, endogenous decay is a likely contributor of nutrients for denitrifying bacteria. The nitrite accumulation and abundance of denitrifying bacteria indicate partial denitrification in fixed-film bioreactors operated under limited carbon conditions. Further studies are required to assess the contribution of organic material produced in autotrophic biofilms (by endogenous decay and soluble microbial products) to the overall treatment process. Furthermore, the possibility of sustaining autotrophic nitrogen in high strength waste-streams in the presence of organic substrates warrants further investigation.

Keywords: biofilms, moving bed biofilm reactors, hybrid systems, BioCord^{TM}, ammonia removal, microbial community dynamics, nitrifying and denitrifying bacteria

OPEN ACCESS

Edited by:
Holger Daims,
University of Vienna, Austria

Reviewed by:
Jeseth Delgado Vela,
Howard University, United States
Achlesh Daverey,
Doon University, India

****Correspondence:***
Steven N. Liss
steven.liss@ryerson.ca

Specialty section:
This article was submitted to Aquatic Microbiology, a section of the journal Frontiers in Microbiology

Received: *14 April 2020*
Accepted: *12 August 2020*
Published: *08 September 2020*

Citation:
Aqeel H and Liss SN (2020) Autotrophic Fixed-Film Systems Treating High Strength Ammonia Wastewater. Front. Microbiol. 11:551925. doi: 10.3389/fmicb.2020.551925

INTRODUCTION

Increasing populations, urbanization, and commercial activities contribute to high strength wastewaters rich in organics and/or ammonia. Landfill leachate, return sludge from the anaerobic digesters, and several industries (e.g., oil refining, fertilizer production and use, and meat processing) can generate high strength ammonia wastewaters ranging from 500 to 2,500 mg N/L (Savci, 2012; Syron et al., 2015; Tabassum et al., 2018). Nutrients entering water bodies poses a serious threat to aquatic life and human health (Constable et al., 2003). Effluent regulations require treatment options and new approaches to treating high strength wastewaters in order to ensure water resources are protected.

Nitrifying bacteria oxidize ammonia to nitrate in two steps: in the first step, ammonia-oxidizing bacteria (AOB) (e.g., *Nitrosomonas*) oxidize ammonia to nitrite, and in second step nitrite-oxidizing bacteria (NOB) (e.g., *Nitrospira*) oxidize nitrite to nitrate. However, a subgroup of *Nitrospira* (comammox) can oxidize ammonia directly to nitrate in one step (Daims et al., 2015). There are several factors that can influence nitrification, including free nitrous acid, and the development and accumulation of sufficient nitrifying biomass (Yao and Peng, 2017; Tabassum et al., 2018; Du et al., 2019). The relative abundance of nitrifying bacteria in biomass is typically low since nitrifying bacteria are relatively slow-growing microorganisms, and are sensitive to environmental and operational stresses (Yao and Peng, 2017; Tabassum et al., 2018). The proportion of nitrifying bacteria observed in the biological nutrient removal systems varies and has been reported to be as low as 0.4% in a full-scale activated sludge wastewater treatment plant (Dionisi et al., 2002), 8.7% in a nitrifying sequencing batch reactor (SBR) (Li et al., 2007), 13% in biofilms and 17% in suspended biomass of a hybrid bioreactor (You et al., 2003), and as high as 41% in moving bed biofilm reactors (MBBR) (Hoang et al., 2014).

The partial nitritation and anammox (PN/A) is an attractive energy-efficient technology for the treatment of high strength ammonia wastewater (Lackner et al., 2014; van Loosdrecht and Brdjanovic, 2014). The application of PN/A technology is dependent on balancing the competition between the ammonia oxidizing bacteria (AOB), nitrite oxidizing bacteria (NOB), and anammox bacteria. Several operational conditions (e.g., dissolved oxygen concentration and temperature) have been engineered to support the growth of anammox bacteria, limit AOB and inhibit NOB (Lackner et al., 2014; Aqeel et al., 2019). The NOB are selectively washed-out from the system by elevating the temperature (>30°C). Therefore, the PN/A technology is applied to treat the digester effluent, on the side-stream; whereas, the relatively low temperatures of the mainstream wastewater is a challenge for the application of PN/A technology (Lackner et al., 2014; Laureni et al., 2019). Alternatively, partial denitrification and anammox (PD/A) technology has the potential to treat mainstream high strength ammonia wastewater. The PD/A process is advantageous (compared to the PN/A) because it does not require the operational conditions to washout the NOB. In the PD/A process, nitrates are partially denitrified to nitrite that is used by the anammox bacteria resulting in nitrogen removal from the system (Du et al., 2019; Zhang et al., 2020).

Fixed-film technologies are attractive due to its small footprint, and capability to support the slow-growing microorganisms (Mahendran et al., 2012; Wang et al., 2019). The first full-scale installations of MBBR and bio-cord or bio-lace, were first reported in the mid-1990s (Rusten et al., 1995; Randall and Sen, 1996). MBBR technology is relatively more widely adopted worldwide for biological nutrient removal (Forrest et al., 2016). The biocord^{TM} is composed of a central cord that supports the rings of the interwoven cord. Several different polymers have been tested to optimize the performance of biocord^{TM} (Tian et al., 2019). Both the MBBR and biocord^{TM} based bioreactors can be easily set up within conventional wastewater treatment plants to increase the capacity and efficiency of biological nutrient removal.

We report on a study that investigated the potential of autotrophic nitrifying fixed-film bioreactors to treat high strength ammonia wastewater. The main objectives of this study included: (a) an investigation of the acclimation of biomass to high strength ammonia wastewater (up to 1,000 mg/L) and enrichment of the nitrifying bacteria, and (b) a comparative examination of distinctive hybrid and fixed-film bioreactors to treat high strength ammonia wastewater.

MATERIALS AND METHODS

Experimental Setup

Four laboratory-scale fixed-film bioreactors with an effective working volume of 2.2 L each, were operated for 10 months. Two configurations of fixed-film systems, including moving bed biofilm reactor (MBBR) and BioCord^{TM}, each set up as a sequencing batch reactor (SBR) and continuous stirred tank reactor (CSTR) configuration, were operated for 10 months. The MBBR SBR was a hybrid bioreactor because it has a relatively higher amount of mixed liquor suspended solids (MLSS) along with the fixed-films. The BioCord^{TM} (Bishop Water Technologies, Canada) carrier media is composed of interwoven rings of polymers (vinylon and polypropylene) attached to a central cord to support the growth of the attached biomass (**Supplementary Figures S1, S2**). The same BioCord^{TM} carrier media was used for the SBR and CSTR configuration. The MBBR carrier media were made of polyethylene. The total available surface area for the fixed-films in the MBBRs (protected surface area) and BioCord^{TM} bioreactors were maintained in the range of 0.58–0.62 m^2. A range of surface area is given to reflect the loss of carrier media during sampling. The protected surface area of the MBBR carrier media was used for the comparison owing to little or no biofilm accumulating on the outer surface of the MBBR media (Mahendran et al., 2012).

All bioreactors were equipped with peristaltic pumps for feeding and draining (Cole Parmer model 7520-35), air pumps (Optima LR-91926), and pH meters. All bioreactors were fed and aerated (with diffused air store) from the bottom of the bioreactors. The CSTRs were drained from the top of the bioreactors at 2.2 L mark; whereas, the SBRs were drained

from the draining port at 1.1 L mark on the bioreactors. The SBRs were programmed (using programmed timers) for the 12 h sequencing batch cycles (15 min of feeding, 11 h and 15 min of reacting, 15 min of settling, and 15 min of draining phases). The CSTRs and SBRs were programmed to maintain a constant hydraulic retention time (HRT) of 24 h. The feeding and draining tubes were regularly either flushed or replaced to minimize any impact on operations as a result of clogging due to fouling. The HRT of the bioreactors was calibrated biweekly to maintain a constant HRT.

The treated effluent water was filtered (using a 0.45 μ syringe filter) prior to the measurement of ammonia, nitrite, and nitrate concentrations using HACH assays (HACH, London, ON, Canada). Dissolved oxygen (DO) and pH were measured using a DO probe (Oakton) and an online pH measurement system, respectively. The sludge volume index (SVI), mixed liquor suspended solids (MLSS) and effluent suspended solids (ESS) were measured following standard protocols (Eaton et al., 2005). The bioreactors were operated at room temperature (22°C ± 1), pH 7.5 ± 0.3, and dissolved oxygen (DO) concentration was maintained at 6–7 mg/L (Tian et al., 2019). The operational conditions of the bioreactors are summarized in **Table 1**.

The attached biomass on the carrier media was measured on day 45, as previously described (Mahendran et al., 2012). Briefly, the carrier media were dried at 100°C for 1 h. After weighing, the carrier media were washed twice in 100 ml of 0.1 M NaOH solution at 80°C for 30 min. The clean carrier media were washed in running deionized water and dried at 100°C for 1 h. The difference in weight of the dry carrier media before and after the cleaning was used to estimate the attached biomass on the carrier media.

Bioreactor Seeding

The bioreactors were seeded with activated sludge from a municipal wastewater treatment plant (Cataraqui Bay wastewater treatment plant, Kingston, ON, Canada). The final concentration of biomass following inoculation was 2 g/L MLSS seed in all bioreactors. The reactors were operated without wasting for the first 48 h. To further support biomass retention and biofilm formation, following an initial seeding, all bioreactors were reseeded on days 5, 10, 15, and 20. The biomass for reseeding was taken from a separate batch reactor (without biomass wasting) established and operated (for 5–10 days) under conditions similar to the experimental bioreactors (e.g., synthetic feed, aeration, pH, and HRT). All bioreactors were treated similarly, and reseeded for uniformity in bioreactor operations. The amount of biomass required for reseeding was calculated based on the hybrid MBBR SBR, to a final concentration of 2 g/L MLSS.

Synthetic Wastewater and Ammonia Feeding Regime

The bioreactors were fed with ammonia-rich synthetic wastewater that was prepared (twice or thrice a week) with no organics. The recipe used in this study was a modified version of Tian et al. (2019). The macro and micronutrient composition for synthetic feed were $(NH4)_2SO_4$: 130–1,000 mg N/L, $NaHCO_3$: 354.32 mg/L, $MgSO_4{\cdot}7H_2O$: 70.98 mg/L, $CaCl_2{\cdot}2H_2O$: 29.34 mg/L, KH_2PO_4: 79.09 mg/L, $FeSO_4{\cdot}7H_2O$: 4.98 mg/L. The micronutrients were $MnCl_2{\cdot}4H_2O$: 0.1 mg/L, $Na_2MoO_4{\cdot}2H_2O$: 0.025 mg/L, $CuSO_4{\cdot}5H_2O$: 0.103 mg/L, $CoCl_2{\cdot}6H_2O$: 0.001 mg/L, $ZnSO_4{\cdot}7H_2O$: 0.03 mg/L. The startup ammonia concentration in the feed was 130 mg N/L. After an acclimatization period of 45 days, the ammonia concentration was increased by (approximately) 10% every 5 days, to a final ammonia concentration of 1,000 mg N/L in the synthetic feed on day 180 (**Figure 1**). However, when the ammonia removal efficiency declined below 90% (in all bioreactors), the influent ammonia concentration was kept constant for another period of 5 days. The ammonia removal declined below 90% twice on days (on days 150 and 165), and recovered to more than 90% within 10 days. The increase in the influent ammonia concentration was resumed to 10% every 5 days when ammonia removal efficiency recovered to higher than 90% in all bioreactors.The pH in all bioreactors was maintained at 7.5 ± 0.3 by adjusting the concentration of sodium bicarbonate in the synthetic feed. The feed tank was placed on the stirrer plate, and the synthetic feed was continuously mixed with a magnetic stirrer.

Live/Dead Cells

Live/dead cell in the biofilms was estimated based on the fluorescent staining and confocal laser scanning microscopy (CLSM) (Zeiss LSM 710). The biofilm samples were collected on day 185 for the analysis. The MBBR and BioCord^{TM} carrier media were sliced with a surgical blade to obtain a cross-section of the biofilms. The samples were stained as described previously (Aqeel et al., 2016; Lishman et al., 2020). Briefly, a combination of SYTO 9 and propidium iodide stains were used for the estimation of live and dead cells, respectively. The biofilms were stained in a dark and humid Petri dish (2.5 cm diameter) for 30 min. After staining, samples were gently rinsed with deionized water to remove excess stain. All images were captured using a 10× magnification lens, using ZEN 2009 software (Zeiss LSM 710). ZEN 2012 (Zeiss) software was used for image analysis, including mean intensity measurements.

DNA Extraction and Amplicon Sequencing

The biomass from the carrier media was collected as previously described (Mahendran et al., 2012; Lishman et al., 2020). Briefly, the biofilms were scrapped from the carrier media using a sterilized surgical blade and suspended in phosphate buffered saline. The suspension was centrifuged at 9,000 *g* for 10 min at 4°C, and the pellet was used for the genomic DNA extraction. Genomic DNA was extracted from the biofilms of all bioreactors and MLSS of MBBR SBR, using the PowerSoil DNA Isolation Kit (Mo Bio Laboratories Inc.). The compositions of the bacterial communities in biofilms and suspended biomass were assessed using 16S rRNA gene sequencing. The V3–V4 region of the 16S rRNA gene was amplified using primers 341F (CCTACGGGNGGCWGCAG) and 805R (GACTACHVGGGTATCTAATCC), with sample-specific barcodes. The PCR product was sequenced (Genome

TABLE 1 | Operational conditions of the fixed-film and hybrid bioreactors.

	MBBR SBR	BioCord^{TM} SBR	MBBR CSTR	BioCord^{TM} CSTR
Biofilm carrier material	Polyethylene	Polypropylene and vinylon	Polyethylene	Polypropylene and vinylon
Surface area	0.58–0.6 m^2	0.58–0.6 m^2	0.58–0.6 m^2	0.58–0.6 m^2
Attached biomass (g/m^2)	1.41	5.36	1.02	3.14
Live/dead cells	1.4 ± 0.2	3.0 ± 0.7	2.6 ± 0.3	2.7 ± 0.4
HRT (hours)	24	24	24	24
pH	7.5 ± 0.3	7.5 ± 0.3	7.5 ± 0.3	7.5 ± 0.3
DO	6–7 mg/L	6–7 mg/L	6–7 mg/L	6–7 mg/L

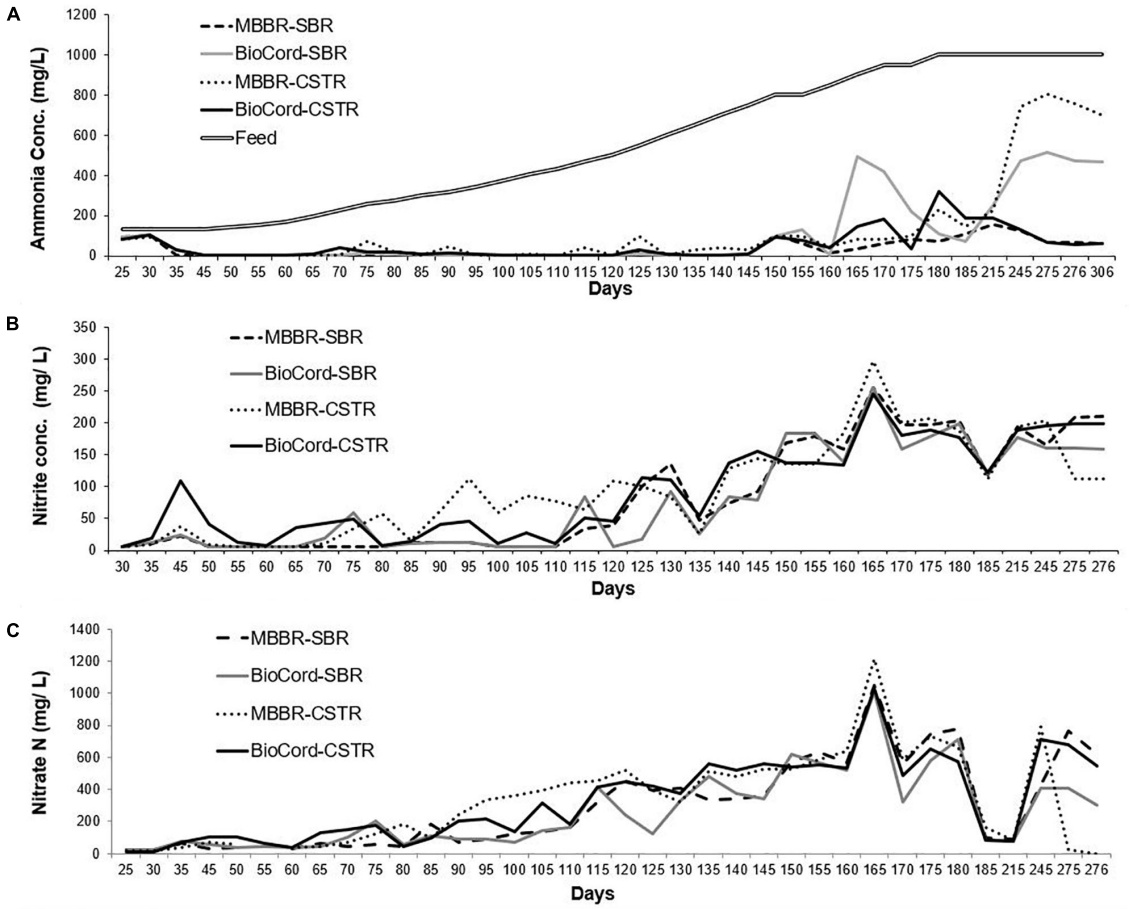

FIGURE 1 | (A) Ammonia concentration in the synthetic feed and the final effluents of all bioreactors. **(B)** The nitrite accumulation in the final effluent, and **(C)** final nitrate effluent concentrations in al bioreactors.

Quebec) using Illumina MiSeq. The forward and reverse sequences from the Illumina paired-end sequences were merged using the DADA2 software. The markers, adapters and the errors in the sequences (including chimera sequences) were removed using the DADA2 pipeline (Callahan et al., 2016), Taxonomic classification, α (based on observed species) and β (based on Bray–Curtis metrics) diversity were performed using Microbiome Analyst software. The assignment of the sequences was performed using SILVA taxonomy (Dhariwal et al., 2017; Chong et al., 2020). The low abundance (less than 10%) features were removed from the downstream analyses for α and β diversities. The graphs for the relative abundance of bacterial families and genera were prepared by selecting the top ten, and top 25 relatively abundant bacterial families, and by eliminating the bacterial genera with less than 35,000 sequences. A total of 5.9 million sequences were obtained that clustered into more than 13 thousand oligo taxonomic units. The predominant bacterial groups were selected to demonstrate the relative abundance of these microbes in the community. The less abundant bacterial genera or families are represented as "other" in the relative abundance graphs. The bioreactor sample metadata (accession number, SAMN14427038), and

sequencing data (accession number, PRJNA614475) are available from the National Center for Biotechnology Information (NCBI) database[1].

RESULTS

Fixed-film bioreactors (MBBR and BioCord^{TM}) were operated in SBR and CSTR mode, where the MBBR SBR was a hybrid system consisting of a fixed-film and suspended growth. To support the acclimation of the biomass to increasing concentrations of ammonia, and enrichment of nitrifying bacteria, the influent ammonia concentration was gradually increased over the duration of the study from 130 to 1000 mg N/L at a rate of 10% every 5 days.

Reactor Performance and Biomass Retention

Activated sludge from a municipal wastewater treatment plant was used to inoculate the bioreactors. Partial biomass washout from the laboratory-scale SBRs and CSTRs was anticipated due to the shift from municipal wastewater to synthetic wastewater, and relatively a short settling time of 15 min in the SBRs. A biomass reseeding strategy was employed for the development and retention of nitrifying bacteria through the early acclimation following start-up. The amount of biomass (for reseeding) in all bioreactors was calculated based on the hybrid MBBR SBR. The MLSS in the MBBR SBR was found to decline to 0.5–1.2 g/L MLSS (during first 20 days of bioreactor start-up). Bioreactors were supplemented with the biomass (acclimated to the autotrophic bioreactor conditions) to a final concentration of 2 g/L MLSS.

The MLSS in the hybrid bioreactor gradually increased from 400 ± 100 mg/L (on day 45) to 2,000 ± 600 mg/L by day 180 following startup and over the duration of increasing the influent ammonia concentration to 1,000 mg N/L. The MLSS gradually decreased in the BioCord^{TM} SBR and MBBR CSTR, and BioCord^{TM} CSTR to 15 ± 4, 37 ± 7, 25 ± 10, respectively, by day 180 (**Table 2**). The MLSS and effluent suspended solids (ESS) were the same in the fixed-film bioreactors. Overall, the ESS gradually declined in all bioreactors with time. The ESS was relatively lower in the BioCord^{TM} bioreactors compared to the MBBR bioreactors, for example, on days 120 and 180. In BioCord^{TM} reactors, the ESS was lower in SBR compared to the CSTR. Whereas in MBBRs, the ESS was higher in SBR compared to the CSTR (**Table 2**).

The SVI of the seed biomass was typical of a municipal activated sludge plant (154 ml/g MLSS), producing a good-quality effluent. It was observed that with a gradual increase in the influent ammonia concentration of synthetic wastewater, the SVI of the suspended biomass gradually decreased. The SVI of the suspended biomass in the hybrid system (MBBR SBR) was 123.0, 55.48, 33.8, and 27.69 at influent ammonia concentration of 130, 250, 500, and 1,000 mg N/L, respectively (**Supplementary Figure S3**).

[1]https://www.ncbi.nlm.nih.gov/bioproject/PRJNA614475

TABLE 2 | Mixed liquor suspended solids (MLSS) and Effluent suspended solids (ESS) in the fixed-film and hybrid bioreactors.

	Ammonia conc. in feed (mg N/L)	MBBR SBR	BioCord^{TM} SBR	MBBR CSTR	BioCord^{TM} CSTR
MLSS (mg/L)	Seed	2000 ± 10	2000 ± 10	2000 ± 10	2000 ± 10
	130	400 ± 100	40–70	30–60	10–20
	250	1730 ± 50	20–70	30–60	34–140
	500	1720 ± 10	17–27	24–48	14–26
	1000	2000 ± 600	11–19	30–44	15–35
ESS (mg/L)	130	50–90	40–70	30–60	10–20
	250	20–90	20–70	30–60	34–140
	500	40–70	17–27	24–48	14–26
	1000	36–54	11–19	30–44	15–35

The attached biomass on the carrier media was relatively higher in the MBBR and BioCord^{TM} SBRs compared to the respective CSTRs. The attached biomass on the MBBR SBR and CSTR were 1.41 and 1.01 g/m^2, respectively, on day 45. The attached biomass on the BioCord^{TM} SBR and CSTR were 5.36 and 3.14 g/m^2, respectively, on day 45 (**Table 1**). The developing biofilms on the BioCord^{TM} fibers were loosely bound and subject to detachment when fibers were sampled. The frequency of biofilm sampling was adjusted during biofilm development to minimize the destabilization of the reactor. The frequency of effluent sampling remained the same throughout the study. As the biofilm developed in the BioCord^{TM} bioreactors, there was minimal biomass detachment and low ESS during regular operation and sample collection from the bioreactors (**Table 2**).

The ammonia concentration (130 mg N/L) in synthetic feed was kept constant during the initial stabilization phase (45 days). The ammonia removal efficiency after seeding and reseeding increased from 30% ± 10 (on day 25) to more than 99% (by day 45), in all bioreactors (**Figure 2**). After an initial stabilization period of 45 days, the influent ammonia concentration was increased at the rate of about 10% every 5 days. The rate of increase in influent ammonia concentration was adjusted to 10% every 10 days (instead of every 5 days) when the ammonia removal efficiency decreased below 90%. This occurred on two occasions (at 800 and 900 mg N/L influent ammonia). The maximum influent ammonia concentration of 1,000 mg N/L was attained on day 180 and was maintained through day 300 of operation. Ammonia removal efficiency was relatively more stable in the MBBR SBR (94–100%), BioCord^{TM} SBR (96–100%), and BioCord^{TM} CSTR (92–100%) compared to the MBBR CSTR (72–100%) up to ammonia concentrations of 750 mg N/L, on day 145 (**Figure 2**). The ammonia removal efficiency at 1,000 mg N/L, on day 185, in both MBBR and BioCord^{TM} SBRs was 91% ± 2, and was relatively higher compared to the respective CSTRs (with an ammonia removal of 83% ± 2) (**Figure 2**). All bioreactors became unstable following day 215 of the bioreactor operation, with a decline in ammonia removal efficiency. The decline in ammonia removal efficiency may have been triggered by an operational stressor, unrelated to the high concentration of the influent ammonia. All bioreactors were capable of retaining the

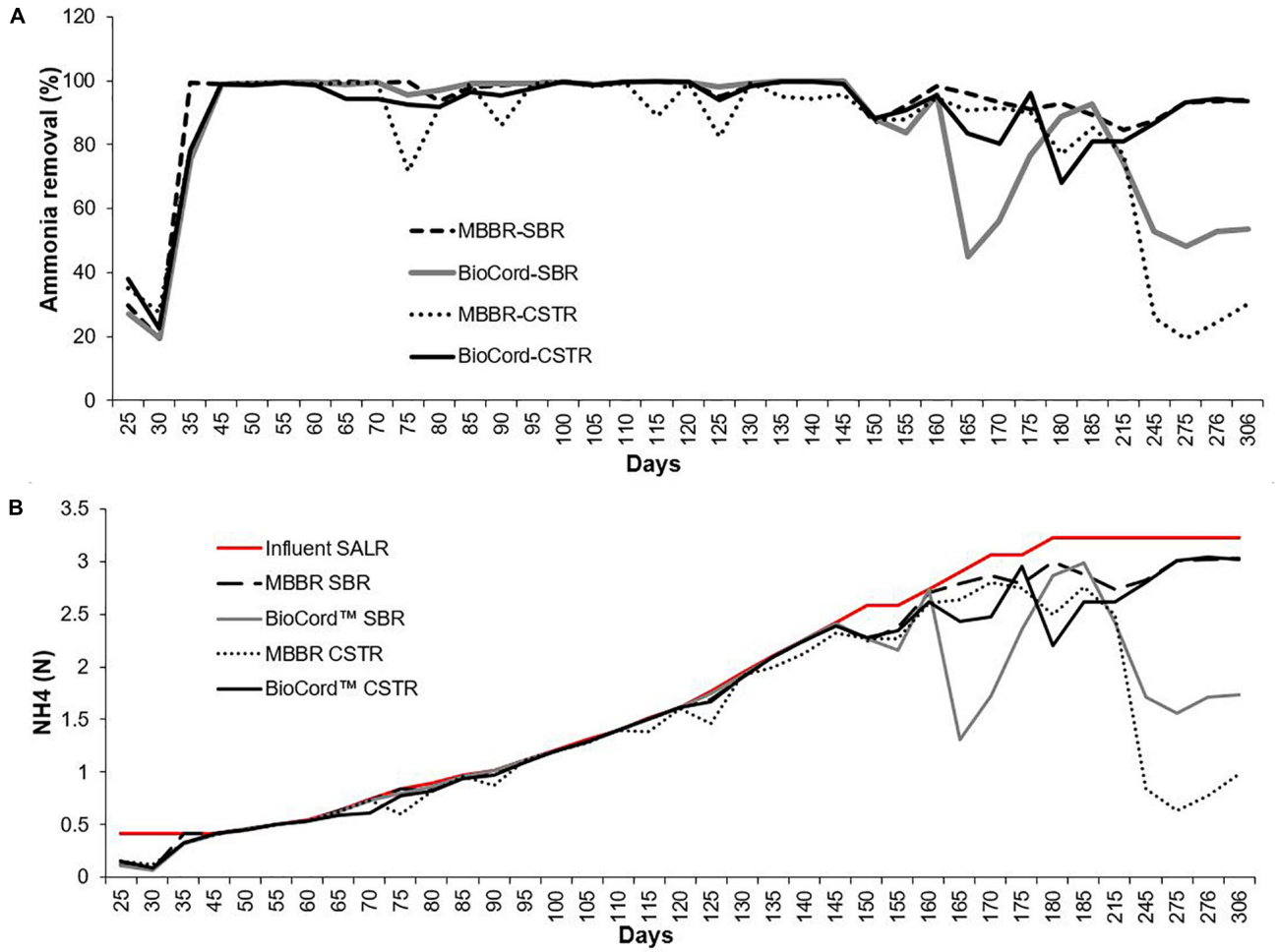

FIGURE 2 | (A) The ammonia removal efficiency in the hybrid and fixed-film bioreactors. **(B)** The ammonia removal rate [NH_4 (N) g/m^2.day] in all bioreactors with the influent surface area loading rate (SALR).

biomass during this phase, except the MBBR CSTR, where major biofilm sloughing and biomass washout was observed. Longer-term operation of the bioreactors at high strength ammonia concentrations (1,000 mg N/L) led to the recovery of elevated (93% ± 1), and stable ammonia removal efficiency in the MBBR SBR and BioCord^{TM} CSTR (days 275–306). However, ammonia removal in MBBR CSTR and BioCord^{TM} SBR declined to 20–30% and 48–54%, respectively, after long term operation of bioreactors (days 275–306) (**Figure 2**).

The surface area loading rate (SALR) was 0.42 NH^4 (N) g/m^2.day in all bioreactors, during the first 45 days following start-up. The SALR was gradually increased to 3.33 g N/m^2.day, from 45 to 180 days (**Figure 2**). The surface area removal rate (SARR) was initially 0.09–0.15 NH_4 (N) g/m^2.day, and increased to 0.42 g N/m^2.day on day 24. The ammonia removal rate was 0.42–2.39 g N/m^2.day from 45 to 145 days. The SARR on day 185 was 2.9–3.0, and 2.6–2.8 g N m^2.day in SBRs and CSTRs, respectively (**Figure 2**). The ammonia removal rate improved to 3.01–3.02 g N/m^2.day in the hybrid MBBR SBR and BioCord^{TM} CSTR (from 275 to 306 days).

Overall, nitrate and nitrite accumulation was higher in the CSTRs compared to the SBRs. The concentrations of nitrite and nitrate were relatively lower in the BioCord^{TM} SBR and CSTR compared to the respective MBBR SBR and CSTR during the acclimation phase (**Figure 1**). There was a trend of gradual increase in the accumulation of nitrate and nitrite in the bioreactors with increasing influent ammonia concentrations. The total nitrate and nitrite accumulation on day 50 was 44 and 46 mg N/L in the MBBR and BioCord^{TM} SBR, respectively, indicating that 68–70% of nitrate and nitrite were removed from the system. The total nitrite and nitrate accumulation on day 110 [435 mg (NH_4) N/L in feed] increased to 169 mg N/L in the MBBR and BioCord^{TM} SBR, corresponding to 61% of nitrate and nitrite being removed. The total nitrate and nitrite accumulation on day 180 [1,000 mg (NH_4) N/L] was 980 and 914 mg N/L in the MBBR and BioCord^{TM} SBRs, respectively. After long term operation of the bioreactors (days 275–300), the nitrate and nitrite levels were relatively lower in the BioCord^{TM} SBR and MBBR CSTR compared to the MBBR SBR and BioCord^{TM} CSTR. The lower levels of nitrite and nitrate were observed in these

bioreactors and correlated to the lower ammonia removal in the BioCord™ SBR and MBBR CSTR (on day 306).

Microbial Community Dynamics

The rarefaction curves showing the alpha diversity of the bacterial communities indicate that the sequencing depth was enough to identify the rare microbial species. The microbial communities of the suspended biomass and biofilms were merged to represent the alpha diversity of the hybrid MBBR SBR. The alpha diversity index based on the observed species of the microbial communities shows that fixed-films of BioCord™ reactors were more diverse compared to the MBBRs (**Figure 3**). Furthermore, the microbial communities of MBBR SBR and BioCord™ SBR were relatively more diverse compared to the microbial communities of MBBR CSTR, and BioCord™ CSTR, respectively. The alpha diversity of the samples collected at different time points shows that the group dispersion was relatively low in MBBR CSTR compared to the other bioreactors (**Figure 3**).

The alpha diversity of the seed biomass was higher and declined over the duration of the operation of the bioreactors (**Figure 3**). The observed species richness was lowest on day 180 (1,000 mg N/L influent ammonia). The microbial community diversity increased when the influent ammonia concentration was kept constant at 1,000 mg N/L for a relatively longer time period (from days 180 to 300). The group dispersion in the microbial communities of the bioreactors indicates that the species diversity in all bioreactors was relatively close to each other on day 45 (prior to increasing the concentration of ammonia in the feed); whereas, by day 120, and at an ammonia concentration of 500 mg N/L, the reactor communities (all bioreactors) were distinctive and diverse with respect to each other.

The beta diversity index was characterized, based on the Bray–Curtis, using principal coordinate analyses (PCoA) and non-metric multidimensional scaling (NMDS). The PCoA measures fixed distances between the microbes based on the presence and absence of the bacterial species, genera or the families, whereas the NMDS also accounts for the abundance of a bacterial group. The PCoA analyses show that the seed biomass was very distinct from the microbial communities of the bioreactors over time. The microbial community continued to evolve during the operation of the bioreactors. The microbial communities of the seed biomass, on days 45 and 120 were distinct from each other; whereas, the microbial communities on day 180 overlapped the microbial communities of the bioreactors on days 120 and 300 (**Figure 4**). The NMDS analyses, accounting for the abundance of the bacterial groups, show that each of the reactor communities were distinct.

Composition and Dynamics of Bacterial Populations in the Fixed-Films Communities

A total of 5,877,269 sequences from Illumina MiSeq were obtained. There was an average of 217,677 sequences per sample, which clustered into 13,288 oligo taxonomic units (OTUs). The OTUs were annotated based on SILVA taxonomy, where 5,546 OTUs were with two or more than two counts. A total of 1,138 low abundance features were removed based on prevalence (less than 10%). The number of features remaining after the data filtering steps was 4,408. The identification and abundance of microbial populations at the bacterial class and family level show that the fixed-film communities were very diverse

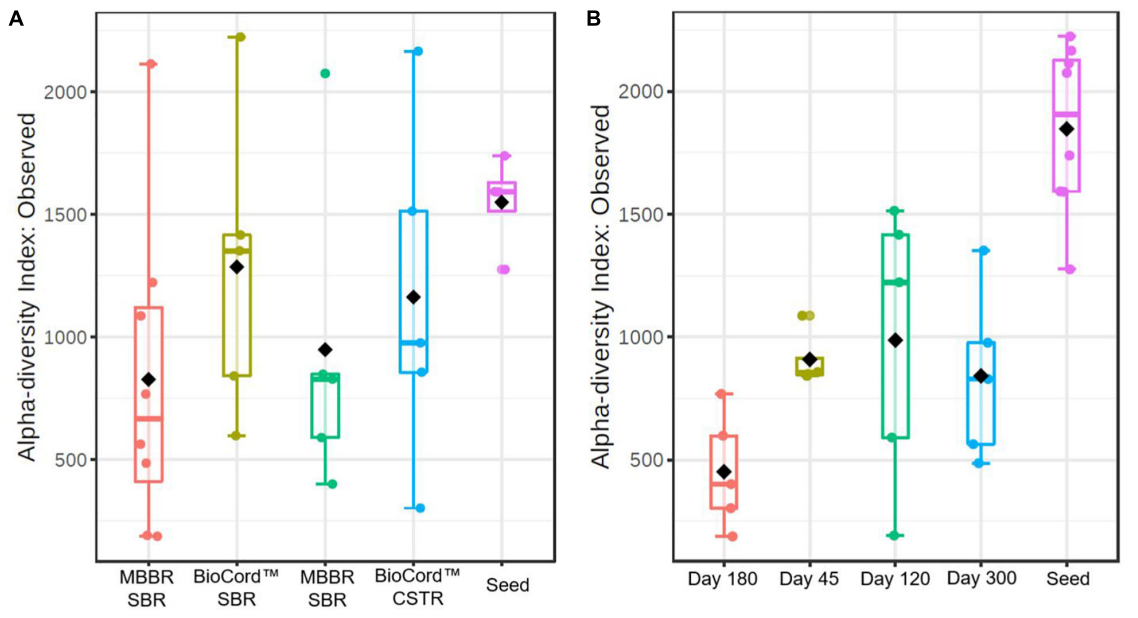

FIGURE 3 | The box plots showing alpha diversity in hybrid and fixed film bioreactors **(A)**, and during the operation of the bioreactors at different time points **(B)**.

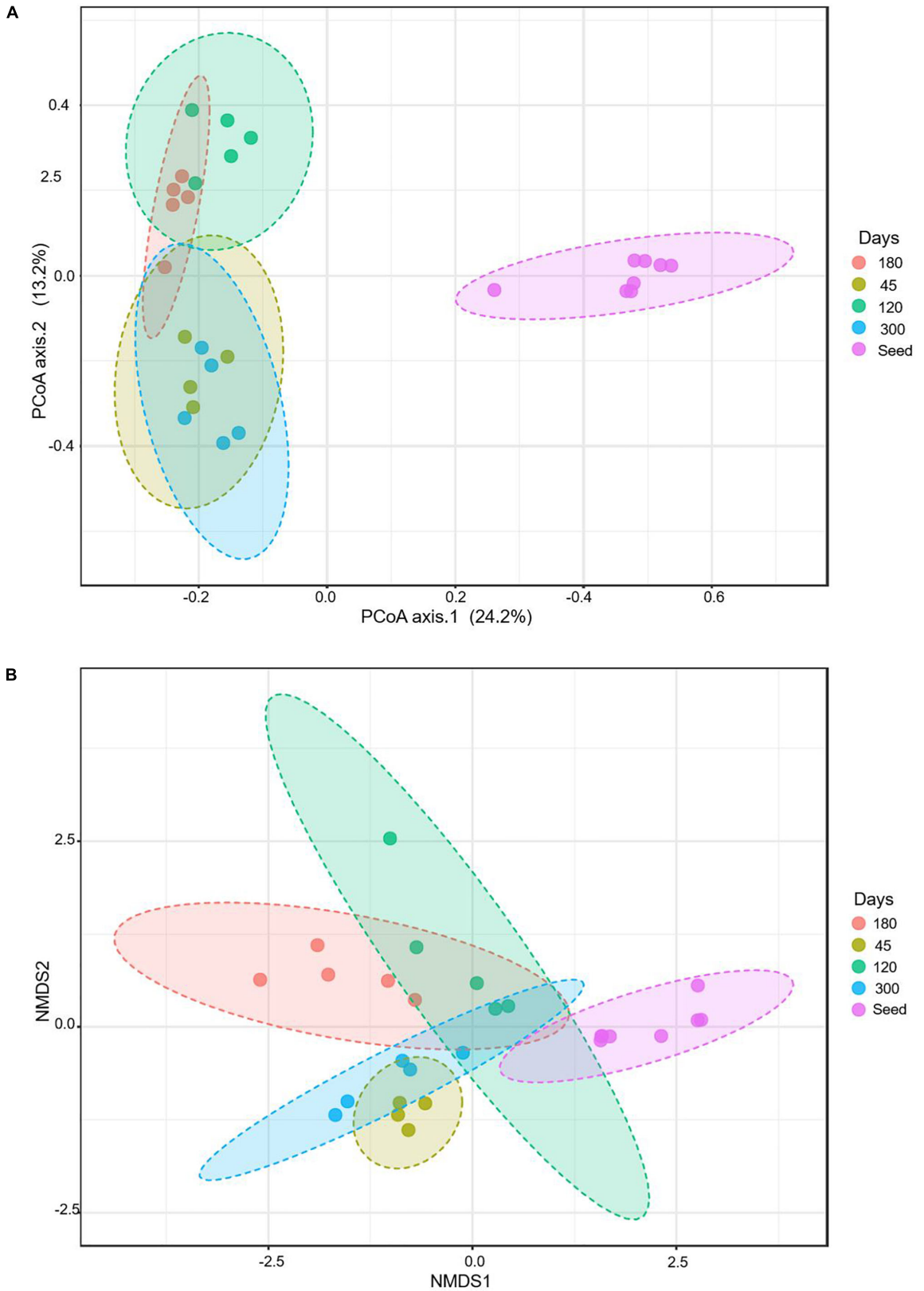

FIGURE 4 | Beta diversity during evolutions of the microbial communities at different time points, based on Bray–Curtis metrics: **(A)** using principal coordinate analyses (PCoA), and **(B)** non-metric multidimensional scaling (NMDS).

(**Supplementary Figures S4, S5**). The microbial community analyses at the genus level using the top 10 predominant genera show that the nitrifying and denitrifying bacterial populations were predominant in fixed-film communities (**Supplementary Figure S6**). The predominant nitrifying and denitrifying bacterial populations were selected to understand the composition and dynamics of these bacteria in the communities of the hybrid and fixed-film biomass, treating high strength ammonia wastewater (**Figure 5** and **Supplementary Figure S7**). It is important to note that estimations of the microbial communities were performed using amplicon sequencing, a semi-quantitative method revealing the relative abundance of the bacterial population in a microbial community.

Nitrifying Bacteria

The relative abundance of *Nitrosomonas*, in the microbial communities of all bioreactors, increased from the point of inoculation (0.03%), during reseeding (0.2–2.0%, day 20), stabilization (3–21%, by day 45) and acclimation phases, and gradually increased following increasing concentrations of influent ammonia from days 45 to 180 (**Figure 5** and **Supplementary Figure S7**).

The relative abundance of *Nitrosomonas* was higher in the flocs compared to the biofilms of the hybrid bioreactor, and gradually increased from 6.3 to 18.4%, 49.2, and 60.4% on days 45, 120, 180, and 300 of operation, respectively. *Nitrosomonas* remained relatively constant (6–10%) in the biofilm community from days 45 to 180; however, the relative abundance in the biofilms of hybrid bioreactor increased more than sevenfold from days 180 to 300 (from 6.2 to 45.6%) at influent ammonia concentrations of 1,000 mg N/L. While the relative abundance of *Nitrosomonas* increased in the microbial communities of the flocs and biofilms in the hybrid bioreactor from days 180 to 300, a decrease was observed in the fixed-film bioreactors [BioCord^{TM} (SBR and CSTR) and MBBR CSTR] from days 180 to 300 (**Figure 5** and **Supplementary Figure S7**).

The relative abundance of *Nitrosomonas* was highest (21% on day 45 of bioreactor operation) in the biofilms of MBBR CSTR compared to the other three bioreactor configurations (**Figure 5**). The MBBR CSTR biofilm was observed to be thinner with less biomass, compared to the other three configurations of the bioreactors, suggesting that *Nitrosomonas* was among the early biofilm colonizers that resulted in the highest relative abundance on carriers with relatively lower biomass. Levels of *Nitrosomonas*, *however*, were found to fluctuate in the MBBR CSTR throughout the duration of the study, increasing to 21% by day 45, followed by a decline to 4% by day 120, and then an increase to 16.4% by day 180. By day 300, the relative abundance of *Nitrosomonas* declined to 0.4% (**Figure 5** and **Supplementary Figure S7**), and was associated with a major biofilm sloughing event and biomass washout from the MBBR CSTR as noted above (see section "Microbial Community Dynamics" acclimation of the bioreactors to high strength ammonia feed).

In the BioCord^{TM} systems, the relative abundance of *Nitrosomonas* bacteria was higher in the SBR compared to the CSTR configuration. The relative abundance of the *Nitrosomonas* in the fixed-films of the SBR was 6.3% by day 45 and increased to 9.9% by day 120 when the influent ammonia concentration was increased from 130 to 500 mg N/L. However, a greater than fourfold increase in the relative abundance of *Nitrosomonas* (41.7%) was observed by day 180 when influent ammonia concentration was increased from 500 to 1,000 mg N/L (**Figure 5** and **Supplementary Figure S7**). The relative abundance of *Nitrosomonas* decreased to 9.4% by day 300 upon the end of the experimental period.

Within the BioCord^{TM} CSTR on day 45, the relative abundance of *Nitrosomonas* was estimated to be 2.4% (**Figure 5**). This increased approximately threefold (6.9%) from days 45

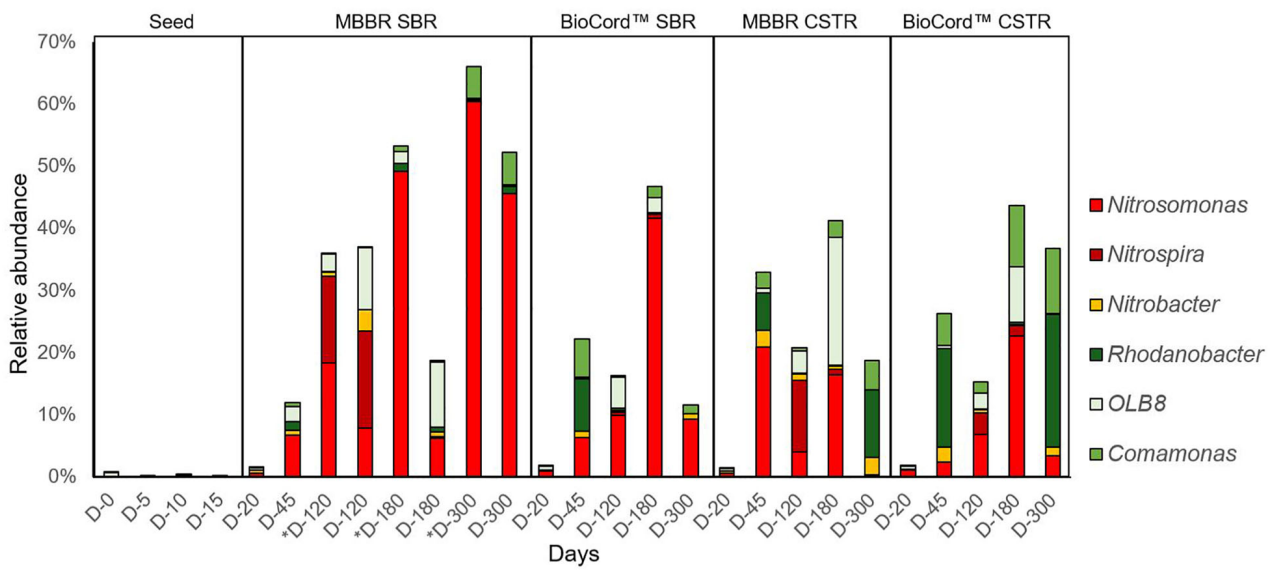

FIGURE 5 | The relative abundance of predominant nitrifying and denitrifying bacterial genera in the hybrid and fixed-film bioreactors.

to 120 and more than threefold (22.8%) from days 120 to 180 when the influent ammonia concentration increased from 130 to 1,000 mg N/L by day 180. The relative abundance of *Nitrosomonas* declined to 3.5% by day 300; the same trend was observed in all fixed-film bioreactors where the relative abundance of *Nitrosomonas* declined when the influent ammonia concentration was kept constant at 1,000 mg N/L, from days 180 to 300.

Nitrobacter was estimated to be more abundant in the microbial communities of the MBBR CSTR and BioCord^{TM} CSTR (2.6 and 2.5%, respectively) compared to the flocs and biofilms of the hybrid bioreactor (0.8%) and biofilms of the BioCord^{TM} SBR (1.1%), on day 45. The relative abundance of *Nitrobacter* gradually declined in the microbial communities of all bioreactors (except in the biofilms of hybrid bioreactors) during the increase in the influent ammonia concentration. *Nitrobacter* increased to 3.4% in the microbial communities of the biofilms of the hybrid biofilms by day 120, followed by a decline to 0.7% by day 180. The relative abundance of *Nitrobacter* increased in the fixed-film communities of all bioreactors (except in the biofilms of the hybrid bioreactors), from days 180 to 300 when the influent ammonia concentration was kept constant at 1,000 mg N/L (**Figure 5** and **Supplementary Figure S6**).

Nitrospira was relatively higher in the MBBR SBR (hybrid) and MBBR CSTR compared to the respective BioCord^{TM} SBR and CSTR (**Figure 5** and **Supplementary Figure S6**). The relative abundance of *Nitrospira* spiked in the fixed-film (15.6%) and flocs (14.0%) of the hybrid bioreactor and the fixed-film (11.5%) of MBBR CSTR by day 120. Furthermore, in MBBR CSTR and hybrid bioreactors, the relative abundance *Nitrospira* was higher compared to the relative abundance of *Nitrosomonas* in the respective biofilm communities by day 120. In the BioCord^{TM} bioreactors, the abundance of *Nitrospira* was relatively higher in the microbial communities of CSTR biofilms (3.5%) compared to the SBR biofilms (0.6%) by day 120 when the influent ammonia concentration was at 500 mg N/L.

Denitrifying Bacteria

Rhodanobacter, *OLB8*, and *Comamonas* were the predominant denitrifying bacteria in the microbial communities of the hybrid and fixed-film bioreactors. The relative abundance of *Comamonas* was relatively higher in the BioCord^{TM} SBR (6.2%) and CSTR (5.1%) bioreactors compared to the MBBRs SBR (0.6%) and CSTR (2.6%) biofilms by day 45. The relative abundance of *Comamonas* declined to 0.2–2.0% in all bioreactors with the gradual increase in the influent ammonia concentration from 130 to 500 mg N/L, day 120. However, after an initial drop, the relative abundance of the *Comamonas* increased when the influent ammonia concentration was increased from 500 to 1,000 mg N/L. The relative abundance of *Comamonas* by day 180 was highest in the BioCord^{TM} CSTR (10.5%) followed by MBBR CSTR (2.7%), BioCord^{TM} SBR (1.7%), and MBBR SBR (0.3%) biofilms (**Figure 5**).

The relative abundance of *Rhodanobacter* followed a similar trend to *Comamonas*. *Rhodanobacter* was relatively higher in the biofilms of BioCord^{TM} SBR (8.5%) and CSTR (15.9%) compared to the MBBR SBR (1.3%) and CSTR (6%) by day 45. The relative abundance of *Rhodanobacter* was relatively higher by day 45 and by day 300 when ammonia influent concentrations were constant for extended periods of time compared to the periods leading to 120 and 180 when influent ammonia concentrations were gradually being increased. The abundance of *Rhodanobacter* was relatively higher in the biofilms of CSTRs BioCord^{TM} (21.4%) and MBBR (10.9%) compared to the respective SBRs by day 300 (**Figure 5** and **Supplementary Figure S7**).

The relative abundance of *OLB8* throughout the experiment displayed a different trend compared to the other denitrifying bacteria (*Rhodanobacter* and *Comamonas*). The relative abundance of *OLB8* increased three to more than 10-fold during the phase when the influent ammonia concentration was gradually increasing (from days 45 to 180), followed by a decline in the relative abundance of *OLB8* when the influent ammonia concentration was kept constant from days 180 to 300. The relative abundance of *OLB8* was relatively higher in the biofilms of the hybrid bioreactor (2.5%) compared to the biofilms of fixed-film bioreactors (less than 0.1%), by day 45 (**Figure 5**). The relative abundance of *OLB8* was more than fourfold higher in biofilms (9.9 and 10.5% by days 120 and 180, respectively) compared to the flocs (2.8 and 2% by days 120 and 180, respectively) of the hybrid bioreactor (**Figure 5** and **Supplementary Figure S7**). The relative abundance of *OLB8* increased (from less than 0.1%, on day 45) to 3.6 and 20.6% by days 120 and 180, respectively (in MBBR CSTR), and 2.6 and 8.9% by days 120 and 180, respectively (in BioCord^{TM} CSTR). Whereas, in the BioCord^{TM} SBR, the relative abundance of BioCord^{TM} increased to 5% by day 120, followed by a decline in relative abundance to 2.5% by day 180 (**Figure 5** and **Supplementary Figure S7**).

The presence and abundance of heterotrophic denitrifying bacteria indicate that endogenous decay may have provided a source of organic substrate in the absence of organics in the influent wastewater. The presence of decaying cells in all biofilms was evident in microscopic images and image analyses. The ratio of live and dead cells in the biofilms was estimated using the fluorescent staining coupled with the confocal laser scanning microscopy. The live to dead ratio in the MBBR (SBR and CSTR), and BioCord^{TM} (SBR, and CSTR) was 1.4 $\pm$ 0.2, 2.6 $\pm$ 0.3, 3.0 $\pm$ 0.7, and 2.7 $\pm$ 0.4, respectively (**Table 1**).

DISCUSSION

This study provides unique insights into the development of the biofilms and changes in the microbial community of autotrophic nitrifying fixed-films and hybrid systems capable of treating high strength ammonia containing wastewaters. Two distinct fixed-film systems, MBBR and BioCord^{TM} in both SBR and CSTR configurations, were examined. The MBBR SBR represented a hybrid system consisting of both fixed and suspended growth forms. In anticipation of challenges in retaining biomass and growth of slow-growing autotrophs following inoculation from municipal activated sludge, a strategy was employed, including a reseeding regime from biomass adapted to initial conditions in the experimental reactors. The study demonstrates the

potential for seamless acclimation to increasing concentrations of ammonia from 130 to 1,000 mg N/L over a period of 145 days. This period of acclimation was associated with the growth of nitrifying bacteria (*Nitrosomonas*, *Nitrospira*, and *Nitrobacter*) and denitrifying bacteria (*Comamonas*, *Rhodanobacter*, and *OLB8*). The relative distribution of the nitrifiers and denitrifiers in suspended biomass and fixed-films in the hybrid reactors, and the relative ammonia removal performance of the MBBR SBR and CSTR systems, suggests there are benefits to a hybrid system. The presence and abundance of the denitrifying bacteria in the bioreactors (fed without an organic substrate) indicates that endogenous decay and soluble microbial products, likely contribute to the growth of heterotrophic bacteria.

Acclimation to High Strength Ammonia Wastewater

Reseeding is a common practice in the activated sludge system, where the settled biomass (in a separate tank) is reseeded in the system to maintain the higher biomass concentration for biological nutrient removal (Pehrson et al., 2008). The initial startup of the bioreactors entailed inoculating with the seed biomass, and a regime of reseeding to achieve a state where biomass levels were maintained over the initial 20 days to support the growth of slow-growing autotrophs in the biofilms. This was followed by a period of increasing concentrations of influent ammonia beginning on day 45. The biomass used for reseeding was developed from the original seed biomass and acclimated (in a batch bioreactor fed with a synthetic feed rich in ammonia lacking organic substrate) for 5–10 days before reseeding the experimental bioreactors. The selection and enrichment of autotrophs are essential because nitrifying bacteria are slow-growing autotrophs that require long solid retention time (Liu et al., 2004; Chung et al., 2007). Several studies have used biofilms or suspended biomass from nitrifying bioreactors to inoculate the bioreactors for easy startup and selection of the microbial community to treat high strength ammonia wastewater (Tian et al., 2019; Wang et al., 2019). The acclimation of the initial seed biomass was crucial because, in this study, the seed biomass was collected from the aeration tank of a municipal wastewater treatment plant. The acclimation of seed biomass resulted in gradual enrichment of *Nitrosomonas* from 0.03% (in seed biomass), to 0.2–2.0% (after reseeding on day 20), and 3–21% (by day 45), in all bioreactors.

Recently, the gradual increase in the influent ammonia concentration (from 54 to 800 mg N/L in 200 days) have been used for the optimization of partial denitrification/anammox (PD/A) technology (Du et al., 2019). In this study, the influent ammonia concentration was gradually increased (after 45 days of bioreactor startup) at a rate of approximately 10% every 5 days. The timing of the increase to influent ammonia was increased to 10 days when the ammonia removal efficiency decreased below 90%. This occurred on two occasions (at 800 and 900 mg N/L influent ammonia). The 10 days were sufficient for the recovery of ammonia removal efficiency. The goal was a seamless acclimation to support the enrichment of nitrifying bacteria to effectively treat high strength ammonia wastewater. The maximum relative abundance of nitrifying bacteria was observed in the hybrid bioreactor (60.4% in suspended biomass and 45.6% in fixed-films) on day 300. The relative abundance of nitrifying bacteria was 49.2%, 6.3% (in suspended biomass and fixed-films, respectively), 41.7, 16.9, and 24.4% in hybrid, BioCord^{TM} SBR, MBBR CSTR, and BioCord^{TM} CSTR, respectively, at the end of the gradual increase in the influent ammonia concentration on day 180 (**Figure 5**).

The gradual increase in the ammonia influent (up to 750 mg N/L, or 2.39 g N/m^2.day) resulted in elevated ammonia removal (>98%) that was relatively more stable in the MBBR and BioCord^{TM} SBRs compared to the respective CSTRs (**Figure 2**). The ammonia removal efficiency declined in the SBRs (91% ± 2), and CSTRs (83% ± 2), when influent ammonia concentration was increased to 1,000 mg N/L. The maximum ammonia removal rate of 3 g N/m^2.d was observed in the hybrid MBBR SBR and BioCord^{TM} CSTR (**Figure 2**). Tian et al. (2019) successfully employed BioCord^{TM} CSTR to treat a relatively high strength synthetic wastewater, but at lower concentrations than examined in this study (128 mg N/L), with ammonia removal efficiencies between of 92 and 97%. Several other studies (using different biofilm bioreactors) have shown relatively poor ammonia removal efficiency to treat high strength ammonia wastewater. For example, the ammonia removal efficiency was 75% in a hybrid membrane bioreactor (Downing and Nerenberg, 2007), and 87 and 38% in membrane-aerated biofilm bioreactors (Terada et al., 2003; Wang et al., 2019).

Effectiveness of MBBRs and BioCord^{TM} in Treating High Strength Ammonia Wastewaters

The loss of planktonic and sloughed biomass can impede the startup of fixed-film and hybrid bioreactors. Growing and developing biofilm entails the involvement of bacteria cycling between fixed and planktonic forms (Bester et al., 2013). Developed films exhibit reversible and irreversible attachment, followed by sloughing (Telgmann et al., 2004; Aqeel et al., 2019). The sloughed biomass may be retained in the hybrid bioreactor and associate with the suspended biomass contributing to stable and elevated biological nutrient removal in the hybrid bioreactors. This was not the case in the MBBR CSTR where the sloughed biomass was washed out from the system. A decline in ammonia removal efficiency was observed in both MBBRs on day 215 (**Figure 2**). The ammonia removal efficiency improved to 93% ± 1 in the hybrid bioreactor, whereas a major biomass sloughing event and biomass washout in the MBBR CSTR resulted in poor ammonia removal efficiency (25% ± 10) that did not recover (days 245–306). Conditions that support higher biomass retention in a system can improve biological nutrient removal. Fixed-film, and hybrid systems, in particular, are more resilient to operational or nutritional stressors compared to conventional biological treatment systems (Mahendran et al., 2012; Aqeel et al., 2019).

Further insights into the stability of the reactors can be drawn from the alpha diversity analyses (observed species richness) based on group dispersion, which revealed that the microbial

communities of the MBBR SBR were more diverse than the CSTR configuration (**Figure 3**). A biological nutrient removal system with a more diverse microbial community is likely more resilient and resistant to operational and nutritional stresses (Zhu et al., 2013; Aqeel et al., 2019).

The suspended biomass decreased initially (up to day 45), followed by a gradual increase in the hybrid bioreactor (**Table 2**). Biomass did decrease initially due to loss of slow settling biomass and selection of the fast settling biomass. The SVI of the suspended biomass decreased gradually with the time of operation of the bioreactors. The decrease in SVI of the suspended biomass was associated with an increase in the influent ammonia concentration and enrichment of the nitrifying bacteria and other changes in the community structure, leading to improved settling properties (**Supplementary Figure S3**). There was no evidence of granule formation or granular structures.

The structure of the BioCord^{TM} carrier media contributes to the entrapment of suspended biomass within the web of interwoven rings. The retention of loosely bound biomass resulted in higher biomass in the BioCord^{TM} reactors compared to the MBBRs. Early in the development of the biofilm, biomass loss during sampling was problematic due to loosely bound biomass that was readily detached. Over time a compact biofilm was established. The greater levels of attached biomass on BioCord^{TM} could be attributed to the ability to entrap biomass as well as the nature of aeration and hydrodynamic conditions compared to the MBBR system. In contrast, the MBBR media are subjected to physical interactions and hydrodynamic conditions that minimize biofilm accumulation, particularly on the outer surfaces of the carrier media, reducing the biomass accumulation in the MBBRs. Therefore, only the inner surface area of the MBBR media was used to standardize the surface area (Mahendran et al., 2012).

The attached biomass was relatively higher in the BioCord^{TM} SBR compared to the BioCord^{TM} CSTR (**Table 2**). It is suggested that the attached biomass was higher in the BioCord^{TM} SBR because the long SBR cycle (12 h cycles) allows the sloughed biomass to reattach to the carrier media. Whereas, in a BioCord^{TM} CSTR, the sloughed biomass was more prone to be washed-out from the system as indicated by the consistently higher ESS from the BioCord^{TM} CSTR compared to the SBR (**Table 2**). Biomass loss coincided with the decline in ammonia removal. The higher biomass retention in the BioCord^{TM} SBR resulted in relatively elevated and consistent ammonia removal during the stable phase (from 45 to 145 days).

Dynamics of Nitrifying and Denitrifying Bacteria

The predominant nitrifying bacteria in the hybrid and fixed-film bioreactors were *Nitrosomonas* [ammonia-oxidizing bacteria (AOB)], *Nitrospira* and *Nitrobacter* [nitrite-oxidizing bacteria (NOB)]. The nitrifying bacteria were relatively more abundant in the suspended biomass compared to the fixed-films in the hybrid bioreactor (MBBR SBR). Several phenomena can contribute to the higher relative abundance of the nitrifying bacteria in the suspended solids. These include (a) the oxygen penetration is complete in the flocs to support the growth of nitrifying bacteria; whereas, biofilms have stratified structures with oxic, anoxic and anaerobic zones, (b) the sloughing or erosion of the outer layer of biofilms where nitrifying bacteria are predominant, and (c) the enrichment of nitrifying bacteria found associated with microbial aggregates with improved settleability (low SVI). The conditions in the SBR appeared to enhance the enrichment of fast settling flocs containing nitrifying bacteria. Laureni et al. (2019) have also observed, relatively higher abundance of the nitrifying bacteria in the flocs compared to biofilms of hybrid MBBR SBR.

The *Nitrosomonas* bacteria were relatively more abundant in the fixed-films of the MBBR CSTR compared to the SBR fixed-films. However, the ammonia removal was relatively more stable and elevated in the hybrid bioreactor compared to the MBBR CSTR. The suspended biomass in the hybrid bioreactor complements the nitrification capability of the fixed-film that results in the functional stability of the system. Biofilm sloughing is an integral part of biofilm development that can be triggered depending upon the internal or external stressors (Picioreanu et al., 2001; Aqeel et al., 2019). In conventional fixed-film bioreactors, the biofilm sloughing results in a transient decline in the efficiency of wastewater treatment. Whereas, a major biofilm sloughing can result in biomass washout and system failure.

The relative abundance of NOB is dependent on the AOB in the nitrifying bacterial communities (Winkler et al., 2012). Therefore, the relative abundance of AOB is usually about twofold higher than the NOB (Winkler et al., 2012; Aqeel et al., 2019). In the present study, the relative abundance of AOB was mostly more than 10-fold higher compared to the well-known NOBs (*Nitrobacter* and *Nitrospira*) (**Figure 5**). However, the abundance of *Nitrospira* (NOB) was relatively higher compared to the *Nitrosomonas* (AOB) in the samples collected during a gradual increase in the influent ammonia concentration. Specifically, the relative abundance of *Nitrospira* was two to threefold higher in the fixed-films of the MBBRs (both SBR and CSTR) on day 120 (**Figure 5** and **Supplementary Figure S7**). Some of the bacterial species related to *Nitrospira* are comammox that are capable of complete ammonia oxidation to nitrate (Daims et al., 2015). Therefore, it is possible that during a gradual increase in ammonia concentration, the comammox *Nitrospira* outcompete *Nitrosomonas* for ammonia oxidation.

Additionally, nitrite loop and ping-pong theories have been proposed to justify the higher abundance of NOB compared to AOB (Winkler et al., 2012; Aqeel et al., 2019). Nitrite loop is described as oxidation of nitrite by NOB to nitrate, followed by a reduction of nitrate by denitrifying bacteria to nitrite. The recycled nitrite is again available for NOB metabolism that results in a higher relative abundance of NOB compared to the AOB. According to the ping-pong theory, the NOB is capable of oxidizing nitrite to nitrate, followed by heterotrophic denitrification of the nitrates. *Rhodanobacter* is capable of complete denitrification that can metabolize nitrite, nitrate and nitrous oxide for complete denitrification (Green et al., 2012; Prakash et al., 2012; Aqeel et al., 2016). In the present study, *Rhodanobacter* was predominant in the BioCord^{TM} SBR and CSTR on days 45 and 300.

The predominant denitrifying bacteria in the hybrid and fixed-film bioreactors were *Rhodanobacter*, *OLB8*, and *Comamonas*. The higher relative abundance of *Rhodanobacter* was also observed in the microbial community of granular sludge in the bioreactors that were seeded with the biomass from the same wastewater treatment plant in an earlier study (Aqeel et al., 2016). This further reinforces that nitrifiers and denitrifiers in biomass at low levels can be easily enriched and selected for in the development of microbial structures and in supporting nitrifying and denitrifying activities.

The abundance of denitrifying bacteria was relatively higher in the fixed-films compared to the suspended biomass of the hybrid bioreactors, and is consistent with the observation that denitrifying bacteria are predominantly present in the anoxic layer of the biofilms (Mahendran et al., 2012; Aqeel et al., 2019). The abundance of the denitrifying bacteria in fixed-films indicates that the sloughing/erosion of the biofilms was resulting in the detachment of bacteria, predominantly from the outer oxic layer of the biofilms. Nitrifying bacteria were predominant in the suspended biomass of the hybrid reactor. The relative distribution of nitrifying and denitrifying bacteria in suspended biomass and fixed-films, respectively, further suggests interactions and possible synergy between the fixed and suspended biomass in biological nutrient removal in hybrid bioreactors (Randall and Sen, 1996; Aqeel et al., 2019).

The relative abundance of the denitrifying bacteria gradually increased in all bioreactors, with increasing influent ammonia concentration and biofilm growth (**Figure 5**). The anoxic layer of a biofilm increases with the growth of biofilm that can support denitrifying bacteria. However, in the absence of organics in the influent, the observation of dead cells in the fixed-films suggests that the endogenous decay might have supported the growth of the heterotrophic denitrifying bacteria. The development of unfavorable conditions in the deeper layer of the fixed-film limits the growth of aerobic bacteria. Bacteria may produce toxic metabolites that trigger the cell lysis of competitor microbes (Adav et al., 2010; Aqeel et al., 2016). In the present study, bacteria related to *Isosphaeraceae* (phylum, planctomycetes) were predominant in the fixed-film microbial communities. The relative abundance of *Isosphaeraceae* in fixed-film communities increased gradually with biofilm development (**Supplementary Figure S5**). The bacteria related to *Isosphaeraceae* are capable of synthesizing enzymes that can hydrolyze the complex microorganism-based carbohydrates; and synthesize the secondary metabolites that have potential bacteriocin and antibiotic activity (Kulichevskaya et al., 2016; Ivanova et al., 2017). The resulting soluble organic matter provides a nutrient source for heterotrophic denitrifying bacteria in the anoxic layer. Additionally, experimental and modeling studies indicate that autotrophic NOB produce soluble microbial products (SMP) that may serve as an organic substrate for the growth of heterotrophic denitrifying bacteria (Ni et al., 2011). Heterotrophs are also capable of producing the SMP that can further support the growth of denitrifying bacteria and nitrogen removal (Xie et al., 2012).

There was a gradual increase in nitrate and nitrite accumulation in the bioreactors (**Figure 1**). This was expected to decline with an anticipated increase in denitrifying bacteria (**Figure 5**). The nitrate and nitrite removal declined from 80–81% (at start-up) to 2–9% in the SBRs (on day 180 when the NH_4 in the feed was at 1,000 mg (NH_4 N/L). The bioreactors were operated under organic carbon limiting conditions (without external organics, but with endogenous decay). Carbon limiting conditions are known to support only partial denitrification (Aqeel et al., 2019) that result in the accumulation of nitrite in the system (Zhang et al., 2020). The accumulation of nitrite during partial denitrification is an exciting avenue for the application of PD/A technology for the treatment of mainstream high strength wastewater (Du et al., 2019; Zhang et al., 2020). The aim of this study was not partial nitritation, or partial denitrification; however, nitrite accumulation was observed in the system that suggests further studies are required to study the system by seeding the fixed-film bioreactors with biomass that have nitrifying and anammox bacteria. Further assessment of the contribution of organic material produced in autotrophic biofilms to the overall treatment process would be valuable. The possibility of sustaining autotrophic nitrogen in high strength waste-streams in the presence of organic substrates warrants further investigation.

CONCLUSION

The enrichment of nitrifying bacteria from municipal wastewater biomass was achieved in fixed-film bioreactors, by acclimation of the seed biomass and gradual ramping-up of the influent ammonia concentration. Two types of fixed-film bioreactors (MBBR and BioCord^{TM}) in two different configurations (SBR and CSTR) were operated for 306 days. Elevated (up to 99–100%) ammonia removal efficiency was observed at the ammonia loading rate of 2.39 g (NH_4) N/m^2.day (750 mg N/L), and was relatively more stable in the MBBR and BioCord^{TM} SBRs compared to the CSTRs. The maximum ammonia loading rate was 3.23 g N/m^2.day (1,000 mg N/L), where the hybrid MBBR SBR and BioCord^{TM} CSTR removed ammonia at a rate of 3.01 g N/m^2.day. The nitrifying (*Nitrosomonas*, *Nitrospira*, and *Nitrobacter*) and denitrifying (*Comamonas*, *OLB*8, and *Rhodanobacter*) bacteria were predominant in the microbial communities of the fixed-film and hybrid bioreactors. The presence of dead cells (in the absence of organics in the synthetic feed) suggests endogenous decay supported the growth of the denitrifying bacteria. The limiting organic carbon might have resulted in partial denitrification and accumulation of nitrite in the fixed-film bioreactors. The observation of nitrite accumulation is interesting because it shows that the fixed-film and hybrid bioreactors have the potential to support PD/A processes. Further studies are required to understand the contribution of cellular material (decaying cells, storage polymers, and SMP) in autotrophic ammonia removal from high strength wastewater.

DATA AVAILABILITY STATEMENT

The datasets generated in this study can be found in online repositories. The names of the repository/repositories and accession number(s) can be found at: https://www.ncbi.nlm.nih.gov/, PRJNA614475.

AUTHOR CONTRIBUTIONS

HA conducted the experiments and wrote the first draft. HA and SL contributed to the interpretation of the data, manuscript revision, read, and approved the manuscript. Both authors contributed to the article and approved the submitted version.

FUNDING

This research was funded by the Natural Sciences and Engineering Research Council of Canada (NSERC).

ACKNOWLEDGMENTS

The authors acknowledge the city of Kingston for providing the biomass to inoculate the bioreactors; Bishop Waters for the kind gift of the BioCord^{TM} carrier media; and Genome Quebec for 16S rRNA sequencing.

SUPPLEMENTARY MATERIAL

The Supplementary Material for this article can be found online at: https://www.frontiersin.org/articles/10.3389/fmicb.2020.551925/full#supplementary-material

FIGURE S1 | The BioCord^{TM} carrier media, the rings of biocord interwoven on a central cord to support biofilm formation.

FIGURE S2 | The attached biomass during the early stage and the relatively mature biofilms on MBBR and BioCord^{TM} carrier media.

FIGURE S3 | The sludge volume index (SVI) of the suspended biomass of hybrid bioreactor gradually decreased with increasing influent ammonia concentration.

FIGURE S4 | Heat map tree illustrating microbial diversity at **(A)** the bacterial class level, and **(B)** family level.

FIGURE S5 | The relative abundance of predominant bacterial families (top 20) in the hybrid and fixed-film bioreactors.

FIGURE S6 | The relative abundance of predominant bacterial genera (top 10) in the hybrid and fixed-film bioreactors.

FIGURE S7 | The relative abundance and dynamics of predominant **(A)** nitrifying bacteria, and **(B)** denitrifying bacteria with influent ammonia concentration in the hybrid and fixed-film bioreactors.

REFERENCES

Adav, S. S., Lee, D. J., and Lai, J. Y. (2010). Potential cause of aerobic granular sludge breakdown at high organic loading rates. *Appl. Microbiol. Biotechnol.* 85, 1601–1610. doi: 10.1007/s00253-009-2317-9

Aqeel, H., Basuvaraj, M., Hall, M., Neufeld, J. D., and Liss, S. N. (2016). Microbial dynamics and properties of aerobic granules developed in a laboratory-scale sequencing batch reactor with an intermediate filamentous bulking stage. *Appl. Microbiol. Biotechnol.* 100, 447–460. doi: 10.1007/s00253-015-6981-7

Aqeel, H., Weissbrodt, D. G., Cerruti, M., Wolfaardt, G. M., Wilén, B. M., and Liss, S. N. (2019). Drivers of bioaggregation from flocs to biofilms and granular sludge. *Environ. Sci. Water Res. Technol.* 5, 2072–2089. doi: 10.1039/C9EW00450E

Bester, E., Wolfaardt, G. M., Aznaveh, N. B., and Greener, J. (2013). Biofilms' role in planktonic cell proliferation. *Int. J. Mol. Sci.* 14, 21965–21982. doi: 10.3390/ijms141121965

Callahan, B. J., McMurdie, P. J., Rosen, M. J., Han, A. W., Johnson, A. J. A., and Holmes, S. P. (2016). DADA2: high-resolution sample inference from Illumina amplicon data. *Nat. Methods* 13, 581–583. doi: 10.1038/nmeth.3869

Chong, J., Liu, P., Zhou, G., and Xia, J. (2020). Using MicrobiomeAnalyst for comprehensive statistical, functional, and meta-analysis of microbiome data. *Nat. Protoc.* 15, 799–821. doi: 10.1038/s41596-019-0264-1

Chung, J., Bae, W., Lee, Y. W., and Rittmann, B. E. (2007). Shortcut biological nitrogen removal in hybrid biofilm/suspended growth reactors. *Process Biochem.* 42, 320–328. doi: 10.1016/j.procbio.2006.09.002

Constable, M., Charlton, M., Jensen, F., McDonald, K., Craig, G., and Taylor, K. W. (2003). An ecological risk assessment of ammonia in the aquatic environment. *Hum. Ecol. Risk Assess.* 9, 527–548. doi: 10.1080/713609921

Daims, H., Lebedeva, E. V., Pjevac, P., Han, P., Herbold, C., Albertsen, M., et al. (2015). Complete nitrification by *Nitrospira* bacteria. *Nature* 528, 504–509. doi: 10.1038/nature16461

Dhariwal, A., Chong, J., Habib, S., King, I. L., Agellon, L. B., and Xia, J. (2017). MicrobiomeAnalyst: a web-based tool for comprehensive statistical, visual and meta-analysis of microbiome data. *Nucleic Acids Res.* 45, W180–W188. doi: 10.1093/nar/gkx295

Dionisi, H. M., Layton, A. C., Harms, G., Gregory, I. R., Robinson, K. G., and Sayler, G. S. (2002). Quantification of *Nitrosomonas oligotropha*-like ammonia-oxidizing bacteria and *Nitrospira* spp. from full-scale wastewater treatment plants by competitive PCR. *Appl. Environ. Microbiol.* 68, 245–253. doi: 10.1128/aem.68.1.245-253.2002

Downing, L. S., and Nerenberg, R. (2007). Performance and microbial ecology of the hybrid membrane biofilm process for concurrent nitrification and denitrification of wastewater. *Water Sci. Technol.* 55, 355–362. doi: 10.2166/wst.2007.277

Du, R., Cao, S., Li, B., Zhang, H., Li, X., Zhang, Q., et al. (2019). Step-feeding organic carbon enhances high-strength nitrate and ammonia removal via DEAMOX process. *Chem. Eng. J.* 360, 501–510. doi: 10.1016/j.cej.2018.12.011

Eaton, A. D., Clesceri, L. S., Rice, E. W., Greenberg, A. E., and Franson, M. A. H. A. (2005). *APHA: Standard Methods for The Examination of Water and Wastewater*. Washington, DC: APHA, AWWA, WEF.

Forrest, D., Delatolla, R., and Kennedy, K. (2016). Carrier effects on tertiary nitrifying moving bed biofilm reactor: an examination of performance, biofilm and biologically produced solids. *Environ. Technol.* 37, 662–671. doi: 10.1080/09593330.2015.1077272

Green, S. J., Prakash, O., Jasrotia, P., Overholt, W. A., Cardenas, E., Hubbard, D., et al. (2012). Denitrifying bacteria from the genus Rhodanobacter dominate bacterial communities in the highly contaminated subsurface of a nuclear legacy waste site. *Appl. Environ. Microbiol.* 78, 1039–1047. doi: 10.1128/aem.06435-11

Hoang, V., Delatolla, R., Abujamel, T., Mottawea, W., Gadbois, A., Laflamme, E., et al. (2014). Nitrifying moving bed biofilm reactor (MBBR) biofilm and biomass response to long term exposure to 1 C. *Water Res.* 49, 215–224. doi: 10.1016/j.watres.2013.11.018

Ivanova, A. A., Naumoff, D. G., Miroshnikov, K. K., Liesack, W., and Dedysh, S. N. (2017). Comparative genomics of four Isosphaeraceae planctomycetes: a common pool of plasmids and glycoside hydrolase genes shared by *Paludisphaera borealis* PX4T, *Isosphaera pallida* IS1BT, *Singulisphaera acidiphila*

DSM 18658T, and strain SH-PL62. *Front. Microbiol.* 8:412. doi: 10.3389/fmicb.2017.00412

Kulichevskaya, I. S., Ivanova, A. A., Suzina, N. E., Rijpstra, W. I. C., Damste, J. S. S., and Dedysh, S. N. (2016). *Paludisphaera borealis* gen. nov., sp. nov., a hydrolytic planctomycete from northern wetlands, and proposal of Isosphaeraceae fam. nov. *Int. J. Syst. Evol. Microbiol.* 66, 837–844. doi: 10.1099/ijsem.0.000799

Lackner, S., Gilbert, E. M., Vlaeminck, S. E., Joss, A., Horn, H., and van Loosdrecht, M. C. (2014). Full-scale partial nitritation/anammox experiences–an application survey. *Water Res.* 55, 292–303. doi: 10.1016/j.watres.2014.02.032

Laureni, M., Weissbrodt, D. G., Villez, K., Robin, O., De Jonge, N., Rosenthal, A., et al. (2019). Biomass segregation between biofilm and flocs improves the control of nitrite-oxidizing bacteria in mainstream partial nitritation and anammox processes. *Water Res.* 154, 104–116. doi: 10.1016/j.watres.2018.12.051

Li, B., Irvin, S., and Baker, K. (2007). The variation of nitrifying bacterial population sizes in a sequencing batch reactor (SBR) treating low, mid, high concentrated synthetic wastewater. *J. Environ. Eng. Sci.* 6, 651–663. doi: 10.1139/S07-008

Lishman, L., Aqeel, H., Basuvaraj, M., Liao, B., Wang, R., and Liss, S. N. (2020). Biofouling of an aerated membrane reactor: four distinct microbial communities. *Environ. Eng. Sci.* 37, 3–12. doi: 10.1089/ees.2019.0209

Liu, Y., Yang, S. F. and Tay, J. H. (2004). Improved stability of aerobic granules by selecting slow-growing nitrifying bacteria. *J. Biotechnol.* 108, 161–169. doi: 10.1016/j.jbiotec.2003.11.008

Mahendran, B., Lishman, L., and Liss, S. N. (2012). Structural, physicochemical and microbial properties of flocs and biofilms in integrated fixed-film activated sludge (IFFAS) systems. *Water Res.* 46, 5085–5101. doi: 10.1016/j.watres.2012.05.058

Ni, B. J., Xie, W. M., Chen, Y. P., Fang, F., Liu, S. Y., Ren, T. T., et al. (2011). Heterotrophs grown on the soluble microbial products (SMP) released by autotrophs are responsible for the nitrogen loss in nitrifying granular sludge. *Biotechnol. Bioeng.* 108, 2844–2852. doi: 10.1002/bit.23247

Pehrson, R. L., Flournoy, W. J., and Hubbell, S. B. (2008). *System for Treating Wastewater and a Controlled Reaction-Volume Module Usable Therein*. U.S. Patent US7445715B2. Chapel Hill, NC: Entex Technologies Inc.

Picioreanu, C., Van Loosdrecht, M. C., and Heijnen, J. J. (2001). Two-dimensional model of biofilm detachment caused by internal stress from liquid flow. *Biotechnol. Bioeng.* 72, 205–218. doi: 10.1002/1097-0290(20000120)72:2<205::aid-bit9>3.0.co;2-l

Prakash, O., Green, S. J., Jasrotia, P., Overholt, W. A., Canion, A., Watson, D. B., et al. (2012). *Rhodanobacter denitrificans* sp. nov., isolated from nitrate-rich zones of a contaminated aquifer. *Int. J. System. Evol. Microbiol.* 62, 2457–2462. doi: 10.1099/ijs.0.035840-0

Randall, C. W., and Sen, D. (1996). Full-scale evaluation of an integrated fixed-film activated sludge (IFAS) process for enhanced nitrogen removal. *Water Sci. Technol.* 33, 155–162. doi: 10.1016/0273-1223(96)00469-6

Rusten, B., Hem, L. J., and Ødegaard, H. (1995). Nitrification of municipal wastewater in moving-bed biofilm reactors. *Water Environ. Res.* 67, 75–86. doi: 10.2175/106143095X131213

Savci, S. (2012). An agricultural pollutant: chemical fertilizer. *Int. J. Environ. Sci. Dev.* 3:73. doi: 10.7763/ijesd.2012.v3.191

Syron, E., Semmens, M. J., and Casey, E. (2015). Performance analysis of a pilot-scale membrane aerated biofilm reactor for the treatment of landfill leachate. *Chem. Eng. J.* 273, 120–129. doi: 10.1016/j.cej.2015.03.043

Tabassum, S., Li, Y., Chi, L., Li, C., and Zhang, Z. (2018). Efficient nitrification treatment of comprehensive industrial wastewater by using novel mass bio system. *J. Clean. Prod.* 172, 368–384. doi: 10.1016/j.jclepro.2017.10.022

Telgmann, U., Horn, H., and Morgenroth, E. (2004). Influence of growth history on sloughing and erosion from biofilms. *Water Res.* 38, 3671–3684. doi: 10.1016/j.watres.2004.05.020

Terada, A., Hibiya, K., Nagai, J., Tsuneda, S., and Hirata, A. (2003). Nitrogen removal characteristics and biofilm analysis of a membrane-aerated biofilm reactor applicable to high-strength nitrogenous wastewater treatment. *J. Biosci. Bioeng.* 95, 170–178. doi: 10.1016/S1389-1723(03)80124-X

Tian, X., Ahmed, W., and Delatolla, R. (2019). Nitrifying bio-cord reactor: performance optimization and effects of substratum and air scouring. *Environ. Technol.* 40, 480–488. doi: 10.1080/09593330.2017.1397760

van Loosdrecht, M. C., and Brdjanovic, D. (2014). Anticipating the next century of wastewater treatment. *Science* 344, 1452–1453. doi: 10.1126/science.1255183

Wang, R., Zeng, X., Wang, Y., Yu, T., and Lewandowski, Z. (2019). Two-step startup improves pollutant removal in membrane-aerated biofilm reactors treating high-strength nitrogenous wastewater. *Environ. Sci.: Water Res. Technol.* 5, 39–50. doi: 10.1039/C8EW00668G

Winkler, M. K., Bassin, J. P., Kleerebezem, R., Sorokin, D. Y., and van Loosdrecht, M. C. (2012). Unravelling the reasons for disproportion in the ratio of AOB and NOB in aerobic granular sludge. *Appl. Microbiol. Biotechnol.* 94, 1657–1666. doi: 10.1007/s00253-012-4126-9

Xie, W. M., Ni, B. J., Seviour, T., Sheng, G. P., and Yu, H. Q. (2012). Characterization of autotrophic and heterotrophic soluble microbial product (SMP) fractions from activated sludge. *Water Res.* 46, 6210–6217. doi: 10.1016/j.watres.2012.02.046

Yao, Q., and Peng, D. C. (2017). Nitrite oxidizing bacteria (NOB) dominating in nitrifying community in full-scale biological nutrient removal wastewater treatment plants. *AMB Express* 7:25. doi: 10.1186/s13568-017-0328-y

You, S. J., Hsu, C. L., Chuang, S. H., and Ouyang, C. F. (2003). Nitrification efficiency and nitrifying bacteria abundance in combined AS-RBC and A2O systems. *Water Res.* 37, 2281–2290. doi: 10.1016/S0043-1354(02)00636-X

Zhang, Z., Zhang, Y., and Chen, Y. (2020). Recent advances in partial denitrification in biological nitrogen removal: from enrichment to application. *Bioresour. Technol.* 298:122444. doi: 10.1016/j.biortech.2019.122444

Zhu, L., Yu, Y., Dai, X., Xu, X., and Qi, H. (2013). Optimization of selective sludge discharge mode for enhancing the stability of aerobic granular sludge process. *Chem. Eng. J.* 217, 442–446. doi: 10.1016/j.cej.2012.11.132

Conflict of Interest: The authors declare that the research was conducted in the absence of any commercial or financial relationships that could be construed as a potential conflict of interest.

frontiers in Microbiology

ORIGINAL RESEARCH
published: 15 September 2020
doi: 10.3389/fmicb.2020.545190

Genomic and Physiological Characteristics of a Novel Nitrite-Oxidizing *Nitrospira* Strain Isolated From a Drinking Water Treatment Plant

Hirotsugu Fujitani[1,2†‡], Kengo Momiuchi[3†], Kento Ishii[3†], Manami Nomachi[3], Shuta Kikuchi[3], Norisuke Ushiki[3], Yuji Sekiguchi[1] and Satoshi Tsuneda[2,3]*

[1] Biomedical Research Institute, National Institute of Advanced Industrial Science and Technology, Tsukuba, Japan, [2] Research Organization for Nano & Life Innovation, Waseda University, Tokyo, Japan, [3] Department of Life Science and Medical Bioscience, Waseda University, Tokyo, Japan

OPEN ACCESS

Edited by:
Holger Daims,
University of Vienna, Austria

Reviewed by:
Eva Spieck,
University of Hamburg, Germany
Graeme W. Nicol,
Université de Lyon, France

***Correspondence:**
Satoshi Tsuneda
stsuneda@waseda.jp

[†] These authors have contributed equally to this work

[‡] **Present address:**
Hirotsugu Fujitani,
Department of Biological Sciences,
Faculty of Science and Engineering,
Chuo University, Tokyo, Japan

Specialty section:
This article was submitted to Microbial Physiology and Metabolism, a section of the journal Frontiers in Microbiology

Received: 24 March 2020
Accepted: 24 August 2020
Published: 15 September 2020

Citation:
Fujitani H, Momiuchi K, Ishii K, Nomachi M, Kikuchi S, Ushiki N, Sekiguchi Y and Tsuneda S (2020) Genomic and Physiological Characteristics of a Novel Nitrite-Oxidizing Nitrospira Strain Isolated From a Drinking Water Treatment Plant. Front. Microbiol. 11:545190. doi: 10.3389/fmicb.2020.545190

Nitrite-oxidizing bacteria (NOB) catalyze the second step of nitrification, which is an important process of the biogeochemical nitrogen cycle and is exploited extensively as a biological nitrogen removal process. Members of the genus *Nitrospira* are often identified as the dominant NOB in a diverse range of natural and artificial environments. Additionally, a number of studies examining the distribution, abundance, and characterization of complete ammonia oxidation (comammox) *Nitrospira* support the ecological importance of the genus *Nitrospira*. However, niche differentiation between nitrite-oxidizing *Nitrospira* and comammox *Nitrospira* remains unknown due to a lack of pure cultures. In this study, we report the isolation, physiology, and genome of a novel nitrite-oxidizing *Nitrospira* strain isolated from a fixed-bed column at a drinking water treatment plant. Continuous feeding of ammonia led to the enrichment of *Nitrospira*-like cells, as well as members of ammonia-oxidizing genus *Nitrosomonas*. Subsequently, a microcolony sorting technique was used to isolate a novel nitrite-oxidizing *Nitrospira* strain. Sequences of strains showing the growth of microcolonies in microtiter plates were checked. Consequently, the most abundant operational taxonomic unit (OTU) exhibited high sequence similarity with *Nitrospira japonica* (98%) at the 16S rRNA gene level. The two other *Nitrospira* OTUs shared over 99% sequence similarities with *N. japonica* and *Nitrospira* sp. strain GC86. Only one strain identified as *Nitrospira* was successfully subcultivated and designated as *Nitrospira* sp. strain KM1 with high sequence similarity with *N. japonica* (98%). The half saturation constant for nitrite and the maximum nitrite oxidation rate of strain KM1 were orders of magnitude lower than the published data of other known *Nitrospira* strains; moreover, strain KM1 was more sensitive to free ammonia compared with previously isolated *Nitrospira* strains. Therefore, the new *Nitrospira* strain appears to be better adapted to oligotrophic environments compared with other known non-marine nitrite oxidizers. The complete

genome of strain KM1 was 4,509,223 bp in length and contained 4,318 predicted coding sequences. Average nucleotide identities between strain KM1 and known cultured *Nitrospira* genome sequences are 76.7–78.4%, suggesting at least species-level novelty of the strain in the *Nitrospira* lineage II. These findings broaden knowledge of the ecophysiological diversity of nitrite-oxidizing *Nitrospira*.

Keywords: ammonia, comammox, genome, isolation, kinetics, nitrite, *Nitrospira*, *Nitrosomonas*

INTRODUCTION

Nitrification is a key process in the biogeochemical nitrogen cycle. Conventionally, this reaction takes place in two-steps: the first step is ammonia oxidation, which is carried out by ammonia-oxidizing archaea (AOA) and ammonia-oxidizing bacteria (AOB), and the second step is nitrite oxidation, which is carried out by the nitrite-oxidizing bacteria (NOB). Recently, it has been reported that a group of *Nitrospira* species that are conventionally recognized as NOB, carry out complete ammonia oxidation (comammox), transforming ammonia to nitrate (Daims et al., 2015; van Kessel et al., 2015). This surprising finding suggests the ecological importance of *Nitrospira* and indicates that our understanding about nitrification is still insufficient.

Nitrospira are chemolithoautotrophic bacteria and are categorized into six different lineages, of which lineage II exhibits a huge phylogenetic diversity and environmental distribution (Daims et al., 2001; Lebedeva et al., 2008, 2011). To date, many environmental sequences within the *Nitrospira* lineage II have been identified from different environments, such as wastewater treatment plants (Schramm et al., 1998; Maixner et al., 2006; Park and Noguera, 2008; Fujitani et al., 2013; Gruber-Dorninger et al., 2015), freshwater habitats (Nowka et al., 2015b), permafrost soils (Nowka et al., 2015b), volcanic grassland soils (Daebeler et al., 2014), and rhizosphere (Okabe et al., 2012; Caliz et al., 2015). Additionally, recent metagenomic analysis revealed the presence of comammox *Nitrospira* in activated sludge (Chao et al., 2016; Camejo et al., 2017), soils (Orellana et al., 2018; Shi et al., 2018), freshwater (Liu et al., 2020), and drinking water treatment plants (DWTPs) (Pinto et al., 2015; Wang et al., 2017).

In systems producing drinking water, nitrification plays a key role in decreasing monochloramine and producing nitrate in DWTPs (Wang et al., 2014). Culture-independent approaches revealed that nitrite-oxidizing *Nitrospira* were more abundant than *Nitrobacter* in DWTPs (Regan et al., 2003; Tatari et al., 2017). As nitrite concentration is suggested as an important environmental factor differentiates niches among NOB (Daims et al., 2016) and between lineages I and II *Nitrospira* (Maixner et al., 2006; Fujitani et al., 2013), an increase of nitrite concentration selected for *Nitrotoga* rather than *Nitrospira* on biofilm systems fed with tap water (Kinnunen et al., 2017). To examine niche differentiation within NOB, it is important to characterize pure strains kinetically (Nowka et al., 2015a; Ushiki et al., 2017; Kitzinger et al., 2018). In rapid sand filters flowing into DWTPs in Denmark, *Nitrospira* were found to be present in abundance as a core taxon based on metagenomic approaches (Gülay et al., 2016; Palomo et al., 2016). Further analysis demonstrated that comammox *Nitrospira* were more abundant than AOB based on *amoA* gene abundance (Fowler et al., 2018) and had metabolic versatility allowing niche-partitioning among ammonia oxidizers (Palomo et al., 2018). Consequently, ammonia oxidation by comammox *Nitrospira* was functionally demonstrated by DNA and RNA stable isotope probing (Gülay et al., 2019). Although these culture-independent approaches revealed the occurrence of *Nitrospira* in oligotrophic environments, little is known about the physiology and genome of a *Nitrospira* strain from DWTPs. Recently, *Nitrospira inopinata*, the only comammox pure culture, was isolated from microbial biofilm on the surface of a pipe and characterized kinetically (Kits et al., 2017). Surprisingly, this strain seemed to be adapted to oligotrophic environments with a high affinity for ammonia but low affinity for nitrite. This finding raised additional questions about niche differentiation among NOB and between comammox *Nitrospira* and nitrite-oxidizing *Nitrospira*. To answer these questions, isolation and characterization of novel *Nitrospira* species from oligotrophic environments is essential. Here, we report a novel nitrite-oxidizing *Nitrospira* strain that was isolated from a fixed-bed column present at a DWTP. Continuous feeding of ammonia to imitate the natural environment successfully led to the enrichment of diverse nitrifiers, including *Nitrospira* species belonging to lineage II and AOB. Subsequently, nitrite-oxidizing *Nitrospira* belonging to lineage II was purified based on a microcolony sorting technique. Finally, the morphology, physiology, kinetics, and genome of a novel *Nitrospira* strain were characterized.

MATERIALS AND METHODS

Sample Source and Continuous Feeding Bioreactor

Zeolite as a water purification material was set up at the drinking water treatment plant. Zeolite has an ability to adsorb ammonium, creating a suitable habitat for nitrifiers. Zeolite was sampled as seed biomass to cultivate the nitrifiers in May 2010. To enrich nitrifiers, a continuous feeding bioreactor to supply substrate in low concentration was set up (**Supplementary Figure S1**). The volume of the bioreactor used was 1.1 L. Non-woven fabric materials were used as a biomass carrier. The inorganic medium was comprised of NH_4Cl (0.0038–0.304 g L^{-1}; 0.071–5.683 mM), NaCl (0.116 g L^{-1}; 1.985 mM), $MgSO_4{\cdot}7H_2O$ (0.040 g L^{-1}; 0.332 mM), $CaCl_2{\cdot}2H_2O$ (0.073 g L^{-1}; 0.497 mM), KCl (0.038 g L^{-1}; 0.510 mM), KH_2PO_4 (0.034 g L^{-1}; 0.250 mM), and trace elements (1 mL). The composition of trace elements was the same as described in our previous research study (Abe

et al., 2017). An aerobic culture condition was maintained at a pH of around 6.9 and incubated in the dark to avoid light inhibition. In the drinking water treatment plant, the influent ammonia concentration was below 1 mg-N L^{-1} (0.071 mM). Therefore, the influent ammonia concentration was also maintained at 1 mg-N L^{-1} in the primary culture. Flow rate was 4.4 L day^{-1}. The hydraulic retention time was adjusted to around 6 h. Loading was also carried out at a rate of 4.4 mg-N L^{-1} day^{-1}. During a 0–100 days period from the cultivation start, zeolites and non-woven fabric materials were placed in the continuous feeding bioreactor. On days 100–200, only zeolites were removed. After 200 days, influent ammonia concentration was increased gradually to reach up to 70 mg-N L^{-1} (5 mM) on day 350. During this period, ammonia concentration in the bioreactor was maintained below 1 mg-N L^{-1} (0.071 mM).

Chemical Analysis of Nitrogen Compounds During Enrichment Process

During the enrichment process, chemical properties were assessed. Ammonia concentration was measured by performing the colorimetric analysis with indophenol (Kandeler and Gerber, 1988). Additionally, nitrite and nitrate concentrations were measured according to the protocol described in a previous study (Fujitani et al., 2014).

Sorting of Nitrifiers' Microcolonies, Pure Cultivation, and Purity Check

Nitrifiers' microcolonies from the enrichment samples were separated using the cell sorter as described in previous research studies (Ushiki et al., 2013; Fujitani et al., 2014, 2015; Abe et al., 2017). The sorted microcolonies were incubated for 1–2 months in the 96 well microtiter plates containing inorganic medium as described previously. However, it is important to note that the medium contained both, 5 mg-N L^{-1} ammonia (NH_4Cl; 0.36 mM) and 5 mg-N L^{-1} nitrite ($NaNO_2$; 0.36 mM), and the pH was adjusted to 7.5. Incubation was performed at 23°C under dark and static conditions. Cell growth and identification were confirmed by fluorescence *in situ* hybridization (FISH) and 16S rRNA gene sequence analyses. Pure strains identified as *Nitrospira* were transferred into test tubes and Erlenmeyer flasks, and were supplemented with 10 mg-N L^{-1} of nitrite (0.71 mM) in the medium every month for further characterization. Likewise, pure strains identified as *Nitrosomonas* were sub-cultivated with 10 mg-N L^{-1} of ammonia (0.71 mM) in the medium. Purity checks were carried out by microscopic observations based on FISH analysis and by using the heterotrophic media. The strain KM1 was transferred to 200-fold diluted Luria-Bertani (BD, NJ, United States), Nutrient Broth (BD) and R2A [polypeptone 500 mg L^{-1}, casamino acid 500 g L^{-1}, soluble starch 500 mg L^{-1}, yeast extract 500 mg L^{-1}, sodium pyruvate 300 mg L^{-1}, KH_2PO_4 500 mg L^{-1} (3.67 mM), $MgSO_4{\cdot}7H_2O$ 50.0 mg L^{-1} (0.415 mM)] media in the form of agar plates and liquid cultures.

Fluorescence *in situ* Hybridization (FISH)

Fluorescence *in situ* hybridization was performed according to a previously described standard protocol (Amann et al., 1990). Oligonucleotide probes were fluorescently labeled with the hydrophilic sulfoindocyanine dye (Cy3) (Fasmac Co. Ltd., Atsugi, Japan) and are listed (**Supplementary Table S1**). Observations were carried out according to a previous study (Fujitani et al., 2014).

DNA Extraction, PCR, and Cloning

DNA was extracted from the enrichment samples according to the standard protocol of the ISOIL extraction kit (Nippon Gene, Tokyo, Japan). Fragments of 16S rRNA and *amoA* genes were amplified using the total DNA with the listed primer sets (**Supplementary Table S1**). The PCR mixtures and purification of PCR products were conducted based on previously described protocols (Fujitani et al., 2013). Purified PCR products were cloned according to the protocol provided in the Qiagen PCR cloning plus kit (QIAGEN). To identify 16S rRNA gene sequences of pure strains cultivated in 96 well microtiter plates, bacterial DNA was extracted by heating at 95°C. The 16S rRNA gene was amplified with the 27f/1492r primer set. The sequences of about 750 bases were obtained by using the primer 27f. The cloning of the comammox *Nitrospira amoA* genes was performed according to the protocol described in a previous study (Fujitani et al., 2020).

Phylogenetic Analysis

The regions of sequences with low quality were trimmed, and the contaminated sequences were removed. The cloned sequences of 16S rRNA genes were grouped into operational taxonomic units (OTU) with a similarity threshold of 98.7%. The OTUs were classified using the SILVA SINA algorithm (Pruesse et al., 2012). In addition, the closest strain to each OTU was searched using the NCBI Web BLASTn program. The 16S rRNA gene sequences of AOB, NOB, and comammox *Nitrospira* were aligned using the ClustalW tool of the MEGAX software (Kumar et al., 2018). Maximum-likelihood trees were constructed in MEGAX using the Tamura-Nei model. Bootstrap values were calculated by performing the iteration 1,000 times. The phylogenetic analysis of comammox *Nitrospira amoA* gene was conducted according to a previously described protocol (Fujitani et al., 2020).

Electron Microscopy

Morphology of a *Nitrospira* pure strain was observed by scanning electron microscopy (SEM) and transmission electron microscopy (TEM), according to a previous study (Fujitani et al., 2014).

Physiological Activity Test to Determine Optimum Temperature and Generation Time

Mean nitrite oxidation rates (μM day^{-1}) were calculated during a 3 days incubation period at 4, 13, 22, 26, 30, 34, and 38°C using the exponentially growing pure strain. We used a fresh medium containing less than 1 mM nitrite in the pre-incubation step. After the cells were incubated with the medium for a few days, we checked the cells were in the exponential growth phase. The oxidation rates were often measured to evaluate the optimum

temperature of NOB pure cultures (Nowka et al., 2015b; Kitzinger et al., 2018). The cell number and the amount of oxidized nitrite showed a good positive correlation (Nowka et al., 2015a; Ushiki et al., 2017; Ishii et al., 2020). The culture experiment for determining the generation time (see below) showed that the isolated cells grew exponentially 2–4 days after nitrite addition. To investigate the generation time, the isolate was incubated at 28°C after replacing the supernatant in order to remove the nitrate and by-products by centrifugation. Nitrite and nitrate concentrations were measured using the ion chromatography with a TSKgel SuperIC-Anion HS (IC-2010; Tosoh, Tokyo, Japan) according to the protocol described in our previous studies (Fujitani et al., 2020; Ishii et al., 2020). Cell numbers were estimated by performing qPCR analysis of the *nxrB* gene as described in a previous study (Ushiki et al., 2017). The *nxrB* gene was amplified by using a specific primer set (**Supplementary Table S1**). The purified *nxrB* products at known concentrations were diluted to 10–10^8 copies μL^{-1} to generate a standard curve. The PCR efficiency was 103% with an R^2 value of 0.99. The thermal cycler program used was as follows: an initial denaturing step at 98°C for 2 min, followed by 40 cycles of denaturation at 98°C for 10 s, annealing at 52°C for 10 s, and extension at 68°C for 40 s. The estimated *nxrB* gene copy number was divided by two, because the *Nitrospira* strain possesses two copies of the *nxrB* gene. The average generation time was determined based on the change in the number of cells in the period between the confirmation of cell growth and the depletion of nitrite. The minimum generation time was also calculated using two time points from the log phase.

Kinetic Parameters for Nitrite Oxidation

As described in previous studies (Ishii et al., 2017; Ushiki et al., 2017), the kinetic parameters were calculated from multiple nitrite oxidation rates using exponentially growing cells. The cells were harvested by centrifugation, and resuspended using fresh mineral nitrite medium. The cell suspensions in glass containers were incubated at room temperature with shaking until the available nitrite content was depleted. Every 5–30 min, aliquots of 50 μL of the samples were collected and heated at 95°C for 5 min to inactivate the *Nitrospira* cells. Nitrite concentrations were measured by a colorimetric method using the Griess reagent (Hewitt and Nicholas, 1964). The experimental data were fitted to the following Michaelis–Menten kinetic equation: $V = (V_{max}[S])/(K_m + [S])$. Here, K_m is the apparent half-saturation constant for nitrite (μM NO_2^-), V_{max} is the maximum nitrite oxidation rate (μmol NO_2^-/mg protein/h), V is the nitrite oxidation rate, and $[S]$ is the nitrite concentration (μM NO_2^-). For protein measurements, the cells were lysed using 0.15 M NaOH solution at 90°C for 30 min. Protein concentrations were measured by using the BCA protein assay kit (Takara).

Inhibition Effect With Free Ammonia

The inhibitory constant for free ammonia was determined upon amending the medium with 0–3.6 mM NH_4Cl. The estimated half-saturation constant (K'_m) values in the presence of free ammonia were fitted to the following inhibitory constant equation: $K'_m = K_m\ (1 + [I]/K_i)$. Here, K_i is the inhibitory constant for free ammonia (μM NO_2^-), and $[I]$ is the free ammonia concentration (mg-NH_3 L^{-1} and μM NH_3), which was calculated by assessing the NH_4Cl concentration, temperature, and pH (Anthonisen et al., 1976). The other materials and methods were in accordance with the procedures that are described above.

Genome Reconstruction and Annotation

DNA was extracted from the purified strain KM1 according to the standard protocol of the NucleoSpin Tissue DNA extraction kit (Takara). DNA sequencing, assembly, and manual curation of the genomes of different strains were performed as previously described (Sekiguchi et al., 2015; Ushiki et al., 2018). Coding sequences (CDS) were automatically predicted and annotated by using the DFAST ver. 1.2.3 (Tanizawa et al., 2018) and a published *Nitrospira* genome sequence (Koch et al., 2015). Average nucleotide identities (ANI) were calculated using fastANI with the default settings (Jain et al., 2018). Orthologous genes were identified using the OrthoVenn 2 web service tool (Xu et al., 2019) with an *E*-value of 1e-05. Toxin-antitoxin modules were searched using the TAfinder with *E*-value of 1e-06 for BLAST and *E*-value of 1e-03 for HMMer (Xie et al., 2018).

RESULTS AND DISCUSSION

Enrichment of Nitrifiers Using a Continuous Feeding Bioreactor

Nitrifiers from a drinking water treatment plant were cultivated using zeolites as primary samples from a continuous feeding bioreactor with non-woven fabric materials to maintain the biomass (**Supplementary Figure S1**). Influent ammonia, effluent ammonia, nitrite, and nitrate concentrations were monitored during the enrichment process (**Figure 1A**). To increase the biomass in the non-woven fabric materials, zeolites and non-woven fabric materials were set up for an initial 200 days incubation. During this period, ammonia and nitrite concentrations in the bioreactor were maintained at nearly 0 mg-N L^{-1}. After 200 days, the influent ammonia concentration was gradually increased from 1 to 70 mg-N L^{-1}, in order to enhance the growth activities of the nitrifiers. Even during this period, ammonia and nitrite concentrations were maintained at nearly 0 mg-N L^{-1}. Although the ammonia concentration in the bioreactor temporarily increased around the 300 days, the nitrate concentration increased with an increase in the influent ammonia concentration. Therefore, complete nitrification reaction occurred in the bioreactor throughout the enrichment process. FISH observations revealed the growth pattern of nitrifiers in the enrichment samples. Although almost no nitrifiers were identified due to low influent ammonia concentration during the first 200 days, the cells of *Nitrosomonas* and *Nitrospira* species were observed on day 250. Finally, the ratios of species belonging to the *Nitrosomonas* and *Nitrospira* lineage II on day 350 were around 30 and 40%, respectively, based on the cell counts. The species of *Nitrosomonas* and *Nitrospira* that were observed in this study formed spherical and dense microcolonies (**Figure 1B** and **Supplementary Figure S2A**).

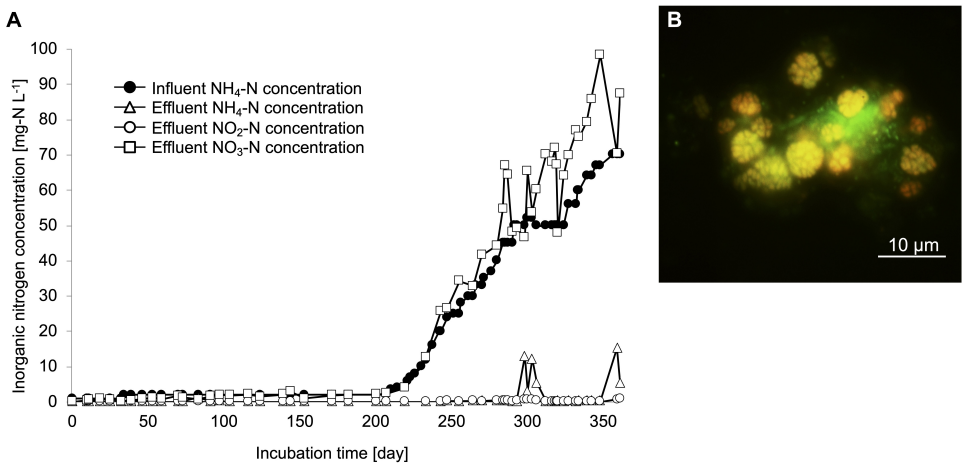

FIGURE 1 | Enrichment culture of nitrifiers in the continuous feeding bioreactor. **(A)** Influent ammonium concentration, and effluent ammonium, nitrite, nitrate concentrations recorded during the incubation period. **(B)** FISH analysis. The yellow cells indicate the Ntspa662-stained *Nitrospira* cells and the green cells indicate the SYTOX green-stained other microorganisms.

During this enrichment process, AOA and species belonging to *Nitrospira* lineage I were not detected.

Subsequently, 16S rRNA gene sequences in the enrichment culture were cloned on day 350. In total, 87 clones were obtained, out of which 5 and 36 clones were identified to belong to the genus *Nitrosomonas* and *Nitrospira*, respectively (**Figure 2**, **Supplementary Table S2**, and **Supplementary Figure S2B**). The most abundant OTU, OTU1 (35/87 clones) exhibited high sequence similarity with the *Nitrospira* sp. strain GC86 (99.9%). OTU2 (1/87 clones) exhibited high sequence similarity with *Nitrospira japonica* (98.0%). Five clones that were affiliated to the genus *Nitrosomonas* were grouped into three OTUs. Additionally, a total of 48 clones were subjected to sequencing using the primer set for *Nitrospira amoA* gene that was designed in a previous study (Fujitani et al., 2020) and grouped as one OTU (**Supplementary Figure S3** and **Supplementary Table S2**).

Sorting of Single Microcolonies, Pure Cultivation, and Identification

Enrichment samples were allowed to pass through the cell sorter for sorting single microcolonies according to the method described in the previous studies (Ushiki et al., 2013; Fujitani et al., 2014, 2015; Abe et al., 2017). By sorting an area with a large forward scatter (FSC) value and a small side scatter (SSC) value, we could successfully sort the nitrifiers' microcolonies (**Supplementary Figure S4**). Each microcolony was inoculated and cultured in 96 well microtiter plates containing both, ammonia and nitrite inorganic medium. After 1–2 months of incubation period, the cells in each well were subjected to sequencing. In total, 13 isolates that were cultured with the medium containing both ammonia and nitrite belonged to the genus *Nitrospira*. The most abundant OTU, OTU34 (11/13 isolates) exhibited high sequence similarity with *N. japonica* (98%) at the 16S rRNA gene level. OTU35 and OTU36 exhibited over 99% sequence identity with *N. japonica* and *Nitrospira* sp. strain GC86, respectively (**Figure 2** and **Supplementary Table S2**). Additionally, 10 isolates that were cultured with the medium containing both ammonia and nitrite belonged to the genus *Nitrosomonas* (**Supplementary Table S2** and **Supplementary Figure S2B**). Strains that were identified as either *Nitrosomonas* or *Nitrospira* were transferred from the 96 well microtiter plates to test tubes and Erlenmeyer flasks. At that time, the *Nitrosomonas* strains were cultivated using inorganic medium containing only ammonia and the *Nitrospira* strains were cultivated using inorganic medium containing only nitrite. Although some strains might be comammox *Nitrospira*, we identified the organisms with 16S rRNA gene only and could not discriminate comammox *Nitrospira* from nitrite-oxidizing *Nitrospira*. After that, we could not sub-cultivate all the 10 strains that were identified as *Nitrosomonas* in the ammonia-containing medium, and only one strain (OTU34) that was identified as *Nitrospira* grew successfully in the nitrite medium. This successfully cultivated nitrite-oxidizing strain was designated as *Nitrospira* sp. strain KM1. Most of the clones cultivated from the enrichment culture (OTU1, 35 clones) were closely related to *Ca. N. nitrificans* and *Ca. N. nitrosa*, whereas the identified strains (OTU34, 11 clones) were distant from the lineage including *Ca. N. nitrificans* and *Ca. N. nitrosa* (**Figure 2**). After that, we carefully confirmed the purity of the strain KM1 using heterotrophic media, PCR, FISH.

Physiological Characterization of Strain KM1

Using scanning electron microscopy, we confirmed that dozens of cells aggregated densely (**Supplementary Figure S5A**) and that each cell formed a spiral shape (**Supplementary Figure S5B**). The strain KM1 produced low amounts of extracellular polymeric substances (EPS) (**Supplementary Figure S5C**) and formed weak flocs in a manner similar to that observed for *Nitrospira lenta*, which also belongs to lineage

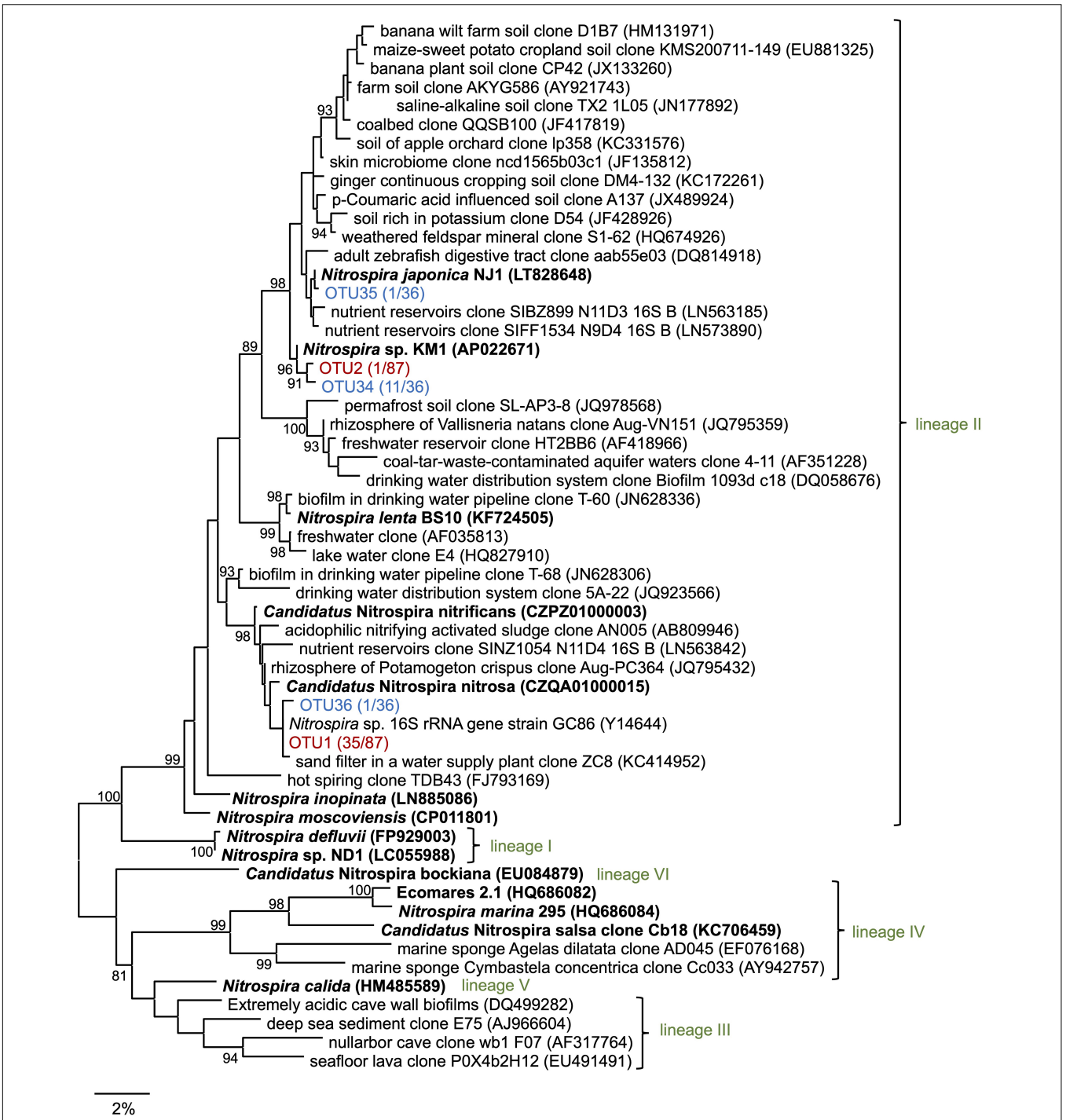

FIGURE 2 | Phylogenetic tree of the genus *Nitrospira* based on the 16S rRNA gene sequence. The tree was constructed using the maximum likelihood (ML) algorithm. Bootstrap values at the branch nodes were iterated 1,000 times. Known isolates and enriched cultures are indicated in bold. For the *Nitrospira* sequences obtained in this study, enrichment clones and isolates are presented in red and blue, respectively. The number of OTUs are specified in brackets. Each lineage belonging to the genus *Nitrospira* is indicated in green. The scale bar corresponds to 2% of the estimated sequence divergence. Accession numbers are shown toward the right side of the organism's names/descriptions.

II of *Nitrospira* (Nowka et al., 2015b). Transmission electron microscopy revealed that the strain KM1 formed a cell cluster embedded in the EPS (**Supplementary Figure S5D**).

The strain KM1 showed nitrite oxidation activity over a temperature range from 4 to 38°C and the optimum temperature was identified as 30°C (**Figure 3A**). This trend was nearly similar

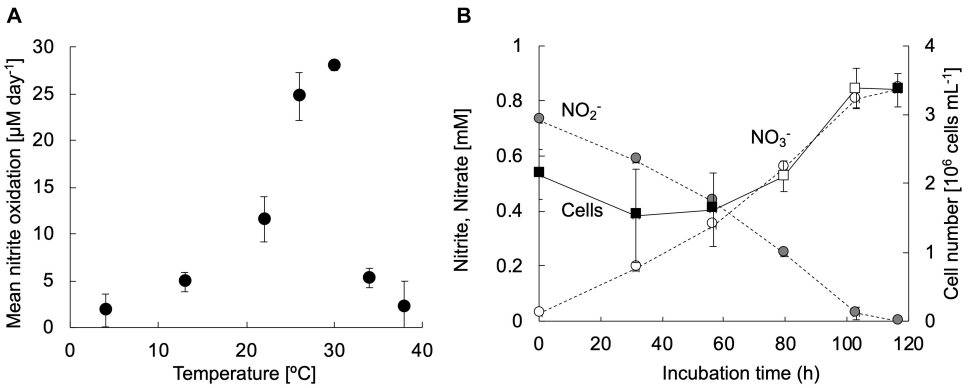

FIGURE 3 | Physiological characteristics of strain KM1. **(A)** The exponentially growing strain KM1 was incubated at a temperature range from 4 to 38°C for 3 days, and the mean nitrite oxidation rates were calculated. **(B)** The strain KM1 was incubated at 28°C in mineral nitrite medium in batch cultures. Gray and white circles indicate the concentrations of nitrite and nitrate, respectively. Filled squares indicate the cell numbers estimated by qPCR analysis targeting the *nxrB* gene. The estimated *nxrB* gene copy number was divided by two, because the *Nitrospira* strain possesses two copies of the *nxrB* gene. The average generation time was determined based on the change in the number of cells in the period between the confirmation of cell growth and the depletion of nitrite. The time points for calculating the minimum generation time were marked by open squares. The experiments were performed in biological triplicate. Error bars indicate the standard deviation (SD).

those observed for other nitrite-oxidizing *Nitrospira* species (Spieck and Lipski, 2011; Ushiki et al., 2013; Fujitani et al., 2014; Nowka et al., 2015b). To evaluate the generation time and growth yield, the strain KM1 was incubated at 28°C in mineral nitrite medium. It oxidized 0.73 mM of nitrite to nitrate in 117 h. The minimum generation time of the strain KM1 was estimated as 34 h, while the average was estimated as 65 h (**Figure 3B** and **Supplementary Figure S6**). Growth yield of the strain KM1 was calculated based on the number of cells and nitrite consumption. The growth yield was estimated as 9.38 log cell mmol NO_2^-. Therefore, the growth rate of the strain KM1 was found to be very similar to that of other *Nitrospira* pure cultures (**Table 1**).

Nitrite oxidation by strain KM1 followed Michalis–Menten kinetics (**Figure 4A** and **Supplementary Table S3**), with a mean apparent half-saturation constant $K_{m(app)}$ = 0.81 ± 0.19 μM of nitrite and without ammonium. The mean of maximum oxidation rate of nitrite (V_{max}) was 2.46 ± 0.33 μM of nitrite (mg of protein h^{-1}). The values of $K_{m(app)}$ and V_{max} were compared among different nitrite-oxidizing *Nitrospira* species (**Table 1**). Surprisingly, the measured $K_{m(app)}$ (NO_2^-) and V_{max} values of strain KM1 were orders of magnitude lower than the published values for other known *Nitrospira* strains. Note that most other $K_{m(app)}$ values for NOB were determined by measuring nitrite-dependent oxygen consumption. Although *Nitrospira inopinata* is not strictly a nitrite oxidizer, the genus *Nitrospira* in oligotrophic environments indicated a wide range of affinity for nitrite. Additionally, the values of $K_{m(app)}$ and V_{max} in strain KM1 were compared with other NOB (**Supplementary Table S4**). Strain KM1 had the lowest value among cultured NOB from non-marine habitats. According to a recent study, *in situ* kinetic values for nitrite oxidation in the dark ocean were at nanomolar levels and orders of magnitude lower than the $K_{m(app)}$ values of cultured NOB (Zhang et al., 2020). This would suggest uncultured NOB are well-adapted to oligotrophic environments in nature. NOB in marine samples might have a higher affinity for nitrite than NOB in non-marine habitat. As there is still a gap between *in situ* kinetic values and kinetic values of the cultured representatives, we should continue efforts to characterize uncultured NOB.

Meanwhile, the value of $K_{m(app)}$ was shown to increase in the presence of NH_4Cl, which means that in this condition, the affinities for nitrite decreased in the strain KM1 (**Figure 4B**). Intriguingly, the strain KM1 seemed to lose the ability to oxidize low concentration of nitrite in the condition where it was exposed to higher concentration of ammonia. The inhibitory constant for free ammonia (K_i) for the strain KM1 was calculated as 0.68 ± 0.03 mg-NH_3 L^{-1} = 40.0 ± 1.89 μM NH_3, which was lower than that of lineage I *Nitrospira* sp. strain ND1 (8.5 ± 0.9 mg-NH_3 L^{-1} = 500 ± 52.9 μM NH_3), and lineage II *N. japonica* strain NJ1 (16 ± 2.3 mg-NH_3 L^{-1} = 941 ± 135 μM NH_3) (Ushiki et al., 2017). Additionally, the thermophilic NOB that is related to *Nitrospira calida* showed a tolerance for free ammonia with an IC50 value of 5.0 mg NH_3-N L^{-1} (Courtens et al., 2016). Therefore, the strain KM1 was more sensitive to ammonia than other strains, such as ND1, NJ1, and thermophilic NOB. Since the *Nitrospira* NXR is located in the periplasm, nitrite transporters most likely play no role in nitrite oxidation (Lücker et al., 2010). Nitrite oxidation by the periplasmic NXR itself seems to be inhibited by ammonia (Courtens et al., 2016; Ushiki et al., 2017), and the mechanism is in need of further study.

The different sensitivity to free ammonia might distinguish the niches of different species of *Nitrospira*. Based on previous microscopic and spatial analysis, *Nitrospira* sp. belonging to lineage I tend to localize in the vicinity of AOB, whereas such close proximity was not observed for the *Nitrospira* sp. belonging to lineage II in nitrifying biofilms (Maixner et al., 2006). This unique distribution was explained based on the small-scale nitrite gradient that forms around the AOB. Furthermore, similar analysis revealed that the preferred nitrite concentrations were different among the members of *Nitrospira*

TABLE 1 | Comparative physiological characteristics among pure *Nitrospira* strains.

Cultures	Lineage	Sample source	K_m (μM NO_2^-)	V_{max} (μmol NO_2^-·(mg protein)$^{-1}$·h^{-1})	K_{i_K} (mg-NH_3 L^{-1})	Generation time (h)	Growth yield (log cell mmol NO_2^-)	Reference
Nitrospira defluvii A17	I	Activated sludge	6 ± 1	48 ± 2	N.D.	37	9.93	a
Nitrospira sp. ND1	I	Activated sludge	9 ± 3	45 ± 7	8.5 ± 0.9	14 (74)*	9.61	b
Nitrospira moscoviensis M-1	II	Corroded iron pipe	9 ± 3	18 ± 1	N.D.	32	10.55	a
Nitrospira lenta BS10	II	Activated sludge	27 ± 11	20 ± 2	N.D.	37	10.40	a
Nitrospira japonica NJ1	II	Activated sludge	10 ± 2	31 ± 5	16 ± 2.3	19 (39)*	9.37	b
Nitrospira sp. KM1	II	Freshwater	0.81 ± 0.19	2.46 ± 0.33	0.68 ± 0.03	34 (65)*	9.38	In this study
Nitrospira inopinata (Comammox)	II	Biofilm on pipe	449.2 ± 65.8	16.88 ± 0.21	N.D.	N.D.	N.D.	c
Nitrospira sp. Ecomares 2.1	IV	Aquaculture system	54 ± 11.9	21.4 ± 1.2	N.D.	N. D.	N. D.	d

*(a) Nowka et al. (2015a). (b) Ushiki et al. (2017). (c) Kits et al. (2017). (d) Jacob et al. (2017). *Numbers in brackets indicate average generation time.*

linage I (Gruber-Dorninger et al., 2015). In this context, a gradient of ammonia concentration in the biofilms might be formed depending on the distance from AOB. If ammonia influenced the nitrite affinity of *Nitrospira* species, ammonia seems to be a key factor that influences and regulates niche differentiation among different *Nitrospira* species. Apart from nitrite-oxidizing *Nitrospira*, *N. inopinata*, the only comammox pure culture, possesses a high affinity for ammonia and a high $K_{m(app)}$ value for nitrite and therefore appears to be well-adapted to oligotrophic environments (Kits et al., 2017). Considering this point, comammox *Nitrospira* might flourish more than nitrite-oxidizing *Nitrospira* in low ammonia conditions. If AOA and AOB with a high affinity for ammonia coexist with nitrite-oxidizing *Nitrospira*, the competition between comammox *Nitrospira* and nitrite-oxidizing *Nitrospira* seems to maintain the balance in low ammonia conditions. Meanwhile, nitrite-oxidizing *Nitrospira* with high affinity for nitrite would be more abundant than comammox *Nitrospira* in low nitrite and no ammonia conditions. Additionally, continuous feeding with low concentration of ammonia would be effective to enrich comammox *Nitrospira* as demonstrated in our previous study (Fujitani et al., 2020). However, there is a big hurdle to isolate uncultured comammox *Nitrospira*. Although pure microcolonies including comammox *Nitrospira* were probably sorted in this study, we could not confirm cell growth of comammox *Nitrospira*. Considering comammox *Nitrospira* could be adapted to lower oxygen concentrations (Koch et al., 2019), ammonia and oxygen concentration should be strictly controlled in 96 well microtiter plates after sorting. Otherwise, small-scale devices to continuously feed substrate such as microfluidics might be effective to monitor cell growth in single cell levels during long-term incubation.

Genomic Composition

Genomic properties of the strain KM1 are summarized in **Table 2**. The sequence coverage was 119.5-fold genome equivalents. The sequence reads obtained from the strain KM1 were assembled into one contig. The reconstructed complete genome sequence of the strain KM1 is 4,509,223 bp in length and with a 56.0% GC content, 4,318 predicted CDS, 46 tRNA, and single copy rRNA genes (5S, 16S, and 23S). The strain KM1 shares high similarity to *N. japonica* strain NJ1 with respect to the 16S rRNA (98.9%), and *nxrB* (93.2%) gene sequences. The genome of strain KM1 contains no *amoA* gene. The ANI between the genome sequences of *Nitrospira* strains ranges from 76.7% to 78.4%. The predicted metabolic features encoded by the genome of strain KM1 are schematically represented in **Supplementary Figure S7**. We rechecked the purity of strain KM1 from whole genome sequencing data and found no contamination.

Like other *Nitrospira* sp., gene sets belonging to the nitrite oxidation pathway and the tricarboxylic acid cycle were identified in the genome sequence of strain KM1. NXR is a key enzyme that catalyzes nitrite oxidation, and is encoded by *nxrA*, *nxrB*, and *nxrC* genes coding for the alpha, beta, and gamma subunits, respectively (Daims et al., 2015). Three copies of potential *nxrA* and *nxrC* genes and two copies of *nxrB* gene were also found in the genome sequence. One of the three *nxrA* genes

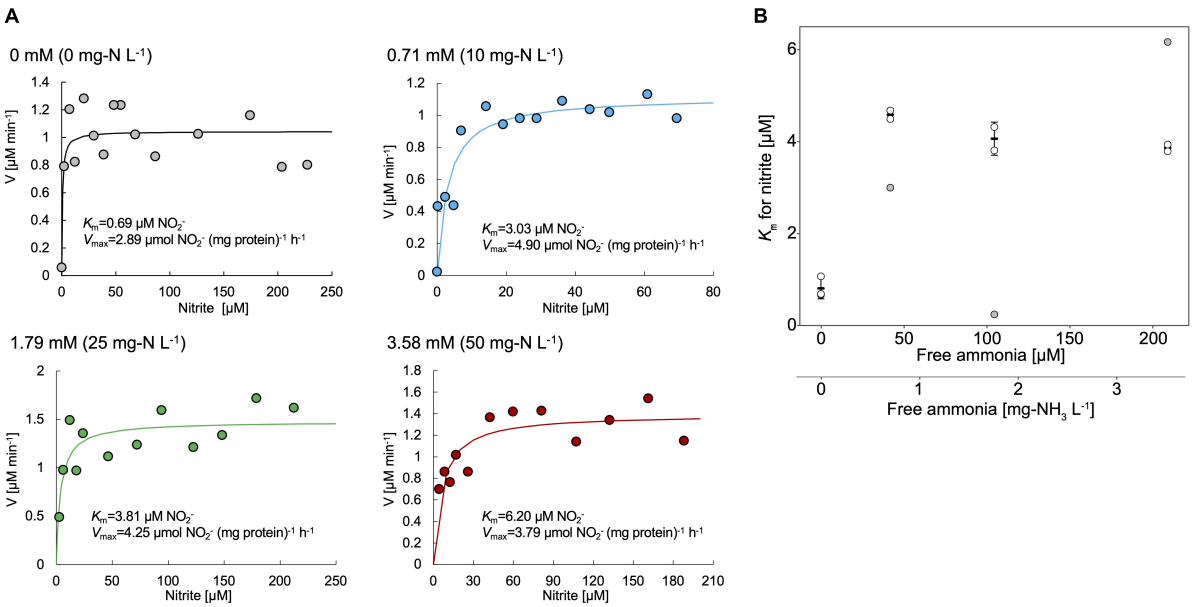

FIGURE 4 | (A) Representative data of the kinetic parameters of the strain KM1. Cell pellets of strain KM1 were resuspended in mineral nitrite medium containing different concentrations of NH_4Cl and were incubated at room temperature with continuous agitation. Circle plots indicate the nitrite consumption in the absence or presence of NH_4Cl (0 – 3.58 mM). Lines indicate the fitted Michaelis–Menten kinetic equations. **(B)** K_m values for nitrite (μM) plotted against free ammonia concentration (mg-NH_3 L^{-1} and mM). The experiments were performed using biological triplicates. The values outside the mean ± standard deviation (68.3% confidence interval) of three data in each condition were removed, which are shown as gray circles. The shown mean and standard deviation were recalculated using the remaining plots. All the kinetic data is shown in **Supplementary Table S3**.

TABLE 2 | Key genomic features of pure strains affiliated with *Nitrospira* lineage II.

Strain	***Nitrospira* sp. KM1**	***Nitrospira moscoviensis* M-1**	***Nitrospira japonica* NJ1**	***Nitrospira lenta* BS10**	***Nitrospira inopinata***
Sample source	**Drinking water**	**Corroded iron pipe**	**Activated sludge**	**Activated sludge**	**Biofilm on pipe**
Genome size (bp)	4,509,223	4,589,485	4,084,817	3,756,190	3,295,117
GC (%)	56	62	59	58	59
Number of CDSs	4,318	4,863	4,150	3,907	3385
Protein coding density (%)	85.8	90.6	90.3	92.8	89.4
rRNA genes	3	4	3	3	3
tRNA genes	46	47	45	46	48
nxrA	3*	5	3	2	1
nxrB	2	4**	3	1	1
nxrC	3	5***	3	2	4
Nitrogen assimilation	1 (ONR)	1 (ONR)	1 (ONR)	2 (ONR and NirA)	1 (NrfA)
Cyanase	1	1	1	1	0
Urease	1 (UreABCDFG)	1 (UreABCDFGH)	1 (UreABCDEFG)	1 (UreABCDFG)	1 (UreABCDFG)
Hydrogenase	–	1 (group 2a)	–	–	1 (group 3b)
Carbonic anhydrase	1	0	0	1	1
Toxin-antitoxin system	18	50	4	13	16
Reference	In this study	a, b	c	d	e

*CDS, coding sequence; ONR, octaheme nitrite reductase. *The length of one of three NxrA (W02_10680) is 4,515 bp, whereas the other NxrA (W02_21980 and W02_23210) are 3,438 and 3,447 bp, respectively. **Two of five nxrB genes (NITMOv2_4533 and 4537) are fused after genome deletion event. ***Two of five NxrC (NITMOv2_0740 and 3640) has C-terminal transmembrane helix besides N-terminal signal peptide recognized by the Sec pathway. (a) Koch et al. (2015). (b) Mundinger et al. (2019). (c) Ushiki et al. (2018). (d) Sakoula et al. (2018). (e) Daims et al. (2015).*

has a length of 4515 bp, whereas the others are 3437 and 3446 bp in length. A gene likely encoding a sigma-54 dependent transcriptional regulator is directly located in the upstream region of the two *nxrA* genes. Considering the fact that the NXR operons in most *Nitrospira* strains are preceded by sigma-54 (Lücker et al., 2010; Koch et al., 2015), the expression of multicopy *nxrA* and *nxrB* genes might be controlled by the regulator. However, recent transcriptional analysis revealed

that the sigma-54 dependent transcriptional regulator exhibited low expression levels during nitrite oxidation in *Nitrospira moscoviensis* (Mundinger et al., 2019).

Nitrite-oxidizing *Nitrospira* utilize nitrite as a major source of nitrogen as well as energy. For reduction of nitrite to ammonia, a gene likely encoding octaheme cytochrome c nitrite reductase (ONR) was found in strain KM1, similar to *Nitrospira moscoviensis* (Koch et al., 2015). NirA-dependent ferredoxin relevant to nitrite reduction was identified in *N. defluvii*, *Nitrospira* sp. ND1 in linage I, and *Nitrospira lenta* in lineage II (Lücker et al., 2010; Koch et al., 2015; Ushiki et al., 2018). Additionally, *Nitrospira inopinata* as a comammox species has a potential *nrfAH* gene, encoding cytochrome c nitrite reductase (Daims et al., 2015). These findings suggest that members of the genus *Nitrospira* possess versatile nitrogen assimilation ability. Genes likely relevant to nitrogen assimilation include *glnA*, glutamine synthetase and *glnK*, and the P-II protein controlling nitrogen assimilation were located close to ONR in the genome of the strain KM1.

In the urease and urea transporter gene clusters, the strain KM1 lacks *ureE* and *ureH* genes, which encode for urease accessory proteins. *UreDEFG* is an accessory protein operon that supports the maturation of urease and controls the activity of urease (Lee et al., 1992). Urease contains Ni in its active center. *UreE* and *UreH* function as a Ni donor and Ni transporter, respectively (Mobley et al., 1995). Although *N. moscoviensis* lacks *ureE* gene, the hydrogenase maturation factors HypA and HypB are expected to exhibit the same function as UreE (Koch et al., 2014, 2015). *Nitrospira* sp. ND1 was shown to perform urease degradation despite the lack of a *ureE* gene, which indicates that urease might be activated with an increase in Ni concentration in the cells because the strain ND1 possesses a gene likely encoding nickel/cobalt transporter with high affinity (Ushiki et al., 2018). However, no chaperon protein and nickel/cobalt transporter with high affinity was identified in the genome sequence of the strain KM1 and may result in low urease activity.

Cyanate hydratase and three copies of an Amt-type ammonium transporter, which may help utilize ammonium as nitrogen source, were also identified in the KM1 genome. Intriguingly, nitrite-oxidizing *Nitrospira* encode three homologs of Amt-type transporters clustering separately in phylogenetic analysis (Koch et al., 2019). If Amt-type transporters among *Nitrospira* are functionally different, *Nitrospira* might possess the potential to survive in environments with fluctuating ammonia concentration. *N. japonica* reduced transcripts of the gene likely encoding octaheme cytochrome *c* nitrite reductase (NSJP_2412) in medium amended by nitrite and ammonium compared to medium with nitrite as a sole nitrogen source (Ushiki et al., 2018). Ammonium addition can also promote growth and allow cultivation of NOB from other genera (Sorokin et al., 2012; Sayavedra-Soto et al., 2015; Ishii et al., 2017; Wegen et al., 2019; Spieck et al., 2020). Therefore, some types of NOB might utilize ammonium from their surroundings instead of assimilatory nitrite reduction. Although it is unknown whether the strain KM1 utilizes ammonium as a nitrogen source, ammonium availability in the environment for NOB would be an important factor.

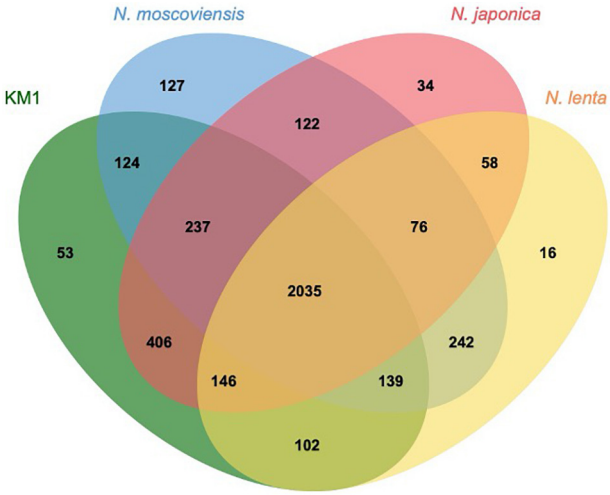

FIGURE 5 | Comparative genomics of isolated *Nitrospira* lineage II. Orthologous genes were clustered by OrthoVenn2 (Xu et al., 2019). The numbers indicate the shared orthologous clusters among the four strains.

Upon comparing the genomes of strain KM1, *N. moscoviensis*, *N. japonica*, and *N. lenta* within *Nitrospira* lineage II, 2035 out of 3917 clusters were shared among all the four strains as orthologous clusters (**Figure 5**). Carbonic anhydrase (CA) that catalyzes reversible the reaction between carbon dioxide and carbonic acid was identified in strain KM1 and *N. lenta* genome sequences (Sakoula et al., 2018). Additionally, two isolated *Nitrospira* strains in lineage I have CA (Lücker et al., 2010; Ushiki et al., 2018). According to previous studies, the growth of *Haemophilus influenza* lacking CA was inhibited by atmospheric concentrations (~0.04% CO_2), which indicates that CA plays an important role in CO_2 poor conditions (Langereis et al., 2013). Considering that CA is essential for survival in many microorganisms (Kusian et al., 2002; Aguilera et al., 2005; Burghout et al., 2011), CA might be one of the factors that could facilitate ecological niche differentiation among different *Nitrospira* species. Additionally, 18 sets of genes likely encoding for a toxin-antitoxin (TA) system in a stress response module (Williams and Hergenrother, 2012) were identified in the genome of strain KM1. In *Nitrosomonas europaea*, a toxin endoribonuclease designated as $MazF_{NE1181}$ may improve a resistance to mercury in heavy metal stress environments (Miyamoto et al., 2016). This suggests that strain KM1 might respond to different environmental stresses using its TA system.

CONCLUSION

This study reported the isolation, morphology, physiology, kinetics, and genome of a novel nitrite-oxidizing *Nitrospira* strain from a fixed-bed column present at a drinking water treatment plant. Although morphological and genomic features were typical of *Nitrospira*, the values of $K_{m(app)}$ and V_{max} for nitrite of the strain KM1were orders of magnitude lower than the cultured NOB in non-marine habitat. Therefore, the strain KM1

is well-adapted to oligotrophic environments with a high affinity for nitrite. To bridge the gap between *in situ* kinetic values and kinetic values of the cultured representatives, further studies including the isolation and characterization of novel NOB strains would be required. Additionally, strain KM1 had high sensitivity to free ammonia. Considering ammonia influenced $K_{m(app)}$ for nitrite, ammonia as well as nitrite concentration could be the main determinants for niche differentiation among NOB. These findings broaden known physiological features of nitrite-oxidizing *Nitrospira*, an ecologically important group in the biogeochemical nitrogen cycle.

DATA AVAILABILITY STATEMENT

The National Center for Biotechnology Information (NCBI) BioProject number for genome sequencing of *Nitrospira* sp. strain KM1 is PRJDB5488 (https://www.ncbi.nlm.nih.gov/bioproject/608100). Illumina raw reads were deposited at the DDBJ Sequence Read Archive (SRA) under the accession number DRR084142 (https://trace.ncbi.nlm.nih.gov/Traces/sra/?run=DRR084142). The reconstructed genome sequence of the strain KM1 is deposited in the NCBI under the accession number AP022671 (https://www.ncbi.nlm.nih.gov/nuccore/AP022671.1/). Sequences obtained by cloning are also available in the NCBI under the accession numbers LC521604 – LC521648.

AUTHOR CONTRIBUTIONS

HF and ST contributed to the conception and design of the study. HF and KM sampled out the zeolite from the drinking water treatment plant and enriched the nitrifiers. KM and NU performed the isolation of nitrifiers and cloning based on 16S rRNA gene. MN and KI carried out the cloning based on *amoA* gene. KI conducted the physiological experiments. HF and KI analyzed the physiological data. YS performed the genome sequencing and assembly. HF, KI, and SK carried out the genome analysis. HF, KI, YS, and ST wrote the manuscript. All authors contributed to the article and approved the submitted version.

FUNDING

This research was supported by a grant-in-aid for young scientists (16K18609 and 19K16218) and a platform for advanced genome science (16H06279) provided by the Japan Society for the Promotion of Science (JSPS) (to HF), and by a domestic research grant (16A070 and 17K012) provided by the Kurita Water and Environment Foundation (to HF).

ACKNOWLEDGMENTS

We thank the technical staff in the drinking water plant for sampling zeolite for this study. We also appreciate the dedicated efforts put together by Masaru Jinno, a member of Tsuneda laboratory in Waseda University, in order to maintain the pure cultures.

SUPPLEMENTARY MATERIAL

The Supplementary Material for this article can be found online at: https://www.frontiersin.org/articles/10.3389/fmicb.2020.545190/full#supplementary-material

REFERENCES

Abe, T., Ushiki, N., Fujitani, H., and Tsuneda, S. (2017). A rapid collection of yet unknown ammonia oxidizers in pure culture from activated sludge. *Water Res.* 108, 169–178. doi: 10.1016/j.watres.2016.10.070

Aguilera, J., Van Dijken, J. P., De Winde, J. H., and Pronk, J. T. (2005). Carbonic anhydrase (Nce103p): an essential biosynthetic enzyme for growth of *Saccharomyces cerevisiae* at atmospheric carbon dioxide pressure. *Biochem. J.* 391, 311–316. doi: 10.1042/BJ20050556

Amann, R. I., Binder, B. J., Olson, R. J., Chisholm, S. W., Devereux, R., and Stahl, D. A. (1990). Combination of 16S rRNA-targeted oligonucleotide probes with flow cytometry for analyzing mixed microbial populations. *Appl. Environ. Microbiol.* 56, 1919–1925.

Anthonisen, A. C., Loehr, R. C., Prakasam, T. B., and Srinath, E. G. (1976). Inhibition of nitrification by ammonia and nitrous acid. *J. Water Pollut. Control. Fed.* 48, 835–852.

Burghout, P., Vullo, D., Scozzafava, A., Hermans, P. W., and Supuran, C. T. (2011). Inhibition of the beta-carbonic anhydrase from *Streptococcus pneumoniae* by inorganic anions and small molecules: toward innovative drug design of antiinfectives? *Bioorg. Med. Chem.* 19, 243–248. doi: 10.1016/j.bmc.2010.11.031

Caliz, J., Montes-Borrego, M., Triado-Margarit, X., Metsis, M., Landa, B. B., and Casamayor, E. O. (2015). Influence of edaphic, climatic, and agronomic factors on the composition and abundance of nitrifying microorganisms in the rhizosphere of commercial olive crops. *PLoS One* 10:e0125787. doi: 10.1371/journal.pone.0125787

Camejo, P. Y., Santo Domingo, J., McMahon, K. D., and Noguera, D. R. (2017). Genome-enabled insights into the ecophysiology of the comammox bacterium *Candidatus Nitrospira nitrosa*. *mSystems* 2:e0059-17.

Chao, Y., Mao, Y., Yu, K., and Zhang, T. (2016). Novel nitrifiers and comammox in a full-scale hybrid biofilm and activated sludge reactor revealed by metagenomic approach. *Appl. Microbiol. Biotechnol.* 100, 8225–8237. doi: 10.1007/s00253-016-7655-9

Courtens, E. N., Spieck, E., Vilchez-Vargas, R., Bodé, S., Boeckx, P., Schouten, S., et al. (2016). A robust nitrifying community in a bioreactor at 50°C opens up the path for thermophilic nitrogen removal. *ISME J.* 10, 2293–2303. doi: 10.1038/ismej.2016.8

Daebeler, A., Bodelier, P. L., Yan, Z., Hefting, M. M., Jia, Z., and Laanbroek, H. J. (2014). Interactions between *Thaumarchaea*, *Nitrospira* and methanotrophs modulate autotrophic nitrification in volcanic grassland soil. *ISME J.* 8, 2397–2410. doi: 10.1038/ismej.2014.81

Daims, H., Lebedeva, E. V., Pjevac, P., Han, P., Herbold, C., Albertsen, M., et al. (2015). Complete nitrification by *Nitrospira* bacteria. *Nature* 528, 504–509.

Daims, H., Lücker, S., and Wagner, M. (2016). A new perspective on microbes formerly known as nitrite-oxidizing bacteria. *Trends Microbiol.* 24, 699–712. doi: 10.1016/j.tim.2016.05.004

Daims, H., Ramsing, N. B., Schleifer, K. H., and Wagner, M. (2001). Cultivation-independent, semiautomatic determination of absolute bacterial cell numbers in environmental samples by fluorescence *in situ* hybridization. *Appl. Environ. Microbiol.* 67, 5810–5818. doi: 10.1128/aem.67.12.5810-5818.2001

Fowler, S. J., Palomo, A., Dechesne, A., Mines, P. D., and Smets, B. F. (2018). Comammox *Nitrospira* are abundant ammonia oxidizers in diverse

groundwater-fed rapid sand filter communities. *Environ. Microbiol.* 20, 1002–1015. doi: 10.1111/1462-2920.14033

Fujitani, H., Aoi, Y., and Tsuneda, S. (2013). Selective enrichment of two different types of *Nitrospira*-like nitrite-oxidizing bacteria from a wastewater treatment plant. *Microbes Environ.* 28, 236–243. doi: 10.1264/jsme2.me12209

Fujitani, H., Kumagai, A., Ushiki, N., Momiuchi, K., and Tsuneda, S. (2015). Selective isolation of ammonia-oxidizing bacteria from autotrophic nitrifying granules by applying cell-sorting and sub-culturing of microcolonies. *Front. Microbiol.* 6:1159. doi: 10.3389/fmicb.2015.01159

Fujitani, H., Nomachi, M., Takahashi, Y., Hasebe, Y., Eguchi, M., and Tsuneda, S. (2020). Successful enrichment of low-abundant comammox *Nitrospira* from nitrifying granules under ammonia-limited conditions. *FEMS Microbiol.* 367:fnaa025.

Fujitani, H., Ushiki, N., Tsuneda, S., and Aoi, Y. (2014). Isolation of sublineage I *Nitrospira* by a novel cultivation strategy. *Environ. Microbiol.* 16, 3030–3040. doi: 10.1111/1462-2920.12248

Gruber-Dorninger, C., Pester, M., Kitzinger, K., Savio, D. F., Loy, A., Rattei, T., et al. (2015). Functionally relevant diversity of closely related *Nitrospira* in activated sludge. *ISME J.* 9, 643–655. doi: 10.1038/ismej.2014.156

Gülay, A., Fowler, S. J., Tatari, K., Thamdrup, B., Albrechtsen, H., Al-Soud, W. A., et al. (2019). DNA-and RNA-SIP reveal *Nitrospira* spp. As key drivers of nitrification in groundwater-fed biofilters. *mBio* 10:e001870-19.

Gülay, A., Musovic, S., Albrechtsen, H. J., Al-Soud, W. A., Sorensen, S. J., and Smets, B. F. (2016). Ecological patterns, diversity and core taxa of microbial communities in groundwater-fed rapid gravity filters. *ISME J.* 10, 2209–2222. doi: 10.1038/ismej.2016.16

Hewitt, E. J., and Nicholas, D. J. D. (1964). "Enzymes of inorganic nitrogen metabolism," in *Modern Methods of Plant Analysis*, Vol. 7, eds H. F. Linskens, B. D. Sanwal, and M. V. Tracey (Heidelberg: Springer), 167–172.

Ishii, K., Fujitani, H., Sekiguchi, Y., and Tsuneda, S. (2020). Physiological and genomic characterization of a new '*Candidatus* Nitrotoga' isolate. *Environ. Microbiol.* 22, 2365–2382. doi: 10.1111/1462-2920.15015

Ishii, K., Fujitani, H., Soh, K., Nakagawa, T., Takahashi, R., and Tsuneda, S. (2017). Enrichment and physiological characterization of a cold-adapted nitrite-oxidizing *Nitrotoga* sp. from an eelgrass sediment. *Appl. Environ. Microbiol.* 83:e00549-17.

Jacob, J., Nowka, B., Merten, V., Sanders, T., Spieck, E., and Dähnke, K. (2017). Oxidation kinetics and inverse isotope effect of marine nitrite-oxidizing isolates. *Aquatic Microb. Ecol.* 80, 289–300. doi: 10.3354/ame01859

Jain, C., Rodriguez-R, L. M., Phillippy, A. M., Konstantinidis, K. T., and Aluru, S. (2018). High throughput ANI analysis of 90K prokaryotic genomes reveals clear species boundaries. *Nat. Commun.* 9:5114. doi: 10.1038/s41467-018-07641-9

Kandeler, E., and Gerber, H. (1988). Short-term assay of soil urease activity using colorimetric determination of ammonium. *Biol. Fert. Soils* 6, 68–72.

Kinnunen, M., Gülay, A., Albrechtsen, H. J., Dechesne, A., and Smets, B. F. (2017). *Nitrotoga* is selected over *Nitrospira* in newly assembled biofilm communities from a tap water source community at increased nitrite loading. *Environ. Microbiol.* 19, 2785–2793. doi: 10.1111/1462-2920.13792

Kits, K. D., Sedlacek, C. J., Lebedeva, E. V., Han, P., Bulaev, A., Pjevac, P., et al. (2017). Kinetic analysis of a complete nitrifier reveals an oligotrophic lifestyle. *Nature* 549, 269–272. doi: 10.1038/nature23679

Kitzinger, K., Koch, H., Lücker, S., Sedlacek, C. J., Herbold, C., Schwarz, J., et al. (2018). Characterization of the first *Candidatus* Nitrotoga isolate reveals metabolic versatility and separate evolution of widespread nitrite-oxidizing bacteria. *mBio* 9:e01186-18.

Koch, H., Galushko, A., Albertsen, M., Schintlmeister, A., Gruber-Dorninger, C., Lücker, S., et al. (2014). Growth of nitrite-oxidizing bacteria by aerobic hydrogen oxidation. *Science* 345, 1052–1054. doi: 10.1126/science.1256985

Koch, H., Lücker, S., Albertsen, M., Kitzinger, K., Herbold, C., Spieck, E., et al. (2015). Expanded metabolic versatility of ubiquitous nitrite-oxidizing bacteria from the genus *Nitrospira*. *Proc. Natl. Acad. Sci. U.S.A.* 112, 11371–11376.

Koch, H., van Kessel, M. A. H. J., and Lücker, S. (2019). Complete nitrification: insights into the ecophysiology of comammox *Nitrospira*. *Appl. Microbiol. Biotechnol.* 103, 177–189. doi: 10.1007/s00253-018-9486-3

Kumar, S., Stecher, G., Li, M., Knyaz, C., and Tamura, K. (2018). MEGA X: molecular evolutionary genetics analysis across computing platforms. *Mol. Biol. Evol.* 35, 1547–1549. doi: 10.1093/molbev/msy096

Kusian, B., Sültemeyer, D., and Bowien, B. (2002). Carbonic anhydrase is essential for growth of *Ralstonia eutropha* at ambient CO_2 concentrations. *J. Bacteriol.* 184, 5018–5026. doi: 10.1128/jb.184.18.5018-5026.2002

Langereis, J. D., Zomer, A., Stunnenberg, H. G., Burghout, P., and Hermans, P. W. (2013). Nontypeable *Haemophilus influenzae* carbonic anhydrase is important for environmental and intracellular survival. *J. Bacteriol.* 195, 2737–2746. doi: 10.1128/jb.01870-12

Lebedeva, E. V., Alawi, M., Maixner, F., Jozsa, P. G., Daims, H., and Spieck, E. (2008). Physiological and phylogenetic characterization of a novel lithoautotrophic nitrite-oxidizing bacterium, '*Candidatus Nitrospira bockiana*'. *Int. J. Syst. Evol. Microbiol.* 58, 242–250. doi: 10.1099/ijs.0.65379-0

Lebedeva, E. V., Off, S., Zumbragel, S., Kruse, M., Shagzhina, A., Lücker, S., et al. (2011). Isolation and characterization of a moderately thermophilic nitrite-oxidizing bacterium from a geothermal spring. *FEMS Microbiol. Ecol.* 75, 195–204. doi: 10.1111/j.1574-6941.2010.01006.x

Lee, M. H., Mulrooney, S. B., Renner, M. J., Markowicz, Y., and Hausinger, R. P. (1992). Klebsiella aerogenes urease gene cluster: sequence of ureD and demonstration that four accessory genes (ureD, ureE, ureF, and ureG) are involved in nickel metallocenter biosynthesis. *J. Bacteriol.* 174, 4324–4330. doi: 10.1128/jb.174.13.4324-4330.1992

Liu, S., Wang, H., Chen, L., Wang, J., Zheng, M., Liu, S., et al. (2020). Comammox *Nitrospira* within the Yangtze River continuum: community, biogeography, and ecological drivers. *ISME J.* doi: 10.1038/s41396-020-0701-8

Lücker, S., Wagner, M., Maixner, F., Pelletier, E., Koch, H., Vacherie, B., et al. (2010). A *Nitrospira* metagenome illuminates the physiology and evolution of globally important nitrite-oxidizing bacteria. *Proc. Natl. Acad. Sci. U.S.A.* 107, 13479–13484. doi: 10.1073/pnas.1003860107

Maixner, F., Noguera, D. R., Anneser, B., Stoecker, K., Wegl, G., Wagner, M., et al. (2006). Nitrite concentration influences the population structure of *Nitrospira*-like bacteria. *Environ. Microbiol.* 8, 1487–1495. doi: 10.1111/j.1462-2920.2006.01033.x

Miyamoto, T., Yokota, A., Tsuneda, S., and Noda, N. (2016). AAU-specific RNA cleavage mediated by MazF toxin endoribonuclease conserved in Nitrosomonas Europaea. *Toxins* 8:174. doi: 10.3390/toxins8060174

Mobley, H. L. T., Island, M. D., and Hausinger, R. P. (1995). Molecular biology of microbial ureases. *Microbiol. Rev.* 59, 451–480. doi: 10.1128/mmbr.59.3.451-480.1995

Mundinger, A. B., Lawson, C. E., Jetten, M. S. M., Koch, H., and Lücker, S. (2019). Cultivation and transcriptional analysis of a canonical *Nitrospira* under stable growth conditions. *Front. Microbiol.* 10:1325. doi: 10.3389/fmicb.2015.01325

Nowka, B., Daims, H., and Spieck, E. (2015a). Comparison of oxidation kinetics of nitrite-oxidizing bacteria: nitrite availability as a key factor in niche differentiation. *Appl. Environ. Microbiol.* 81, 745–753. doi: 10.1128/aem.02734-14

Nowka, B., Off, S., Daims, H., and Spieck, E. (2015b). Improved isolation strategies allowed the phenotypic differentiation of two *Nitrospira* strains from widespread phylogenetic lineages. *FEMS Microbiol. Ecol.* 91:fiu031.

Okabe, S., Nakamura, Y., and Satoh, H. (2012). Community structure and in situ activity of nitrifying bacteria in *Phragmites* root-associated biofilms. *Microb. Environ.* 27, 242–249. doi: 10.1264/jsme2.me11314

Orellana, L. H., Chee-Sanford, J. C., Sanford, R. A., Löffler, F. E., and Konstantinidis, K. T. (2018). Year-round shotgun metagenomes reveal stable microbial communities in agricultural soils and novel ammonia oxidizers responding to fertilization. *Appl. Environ. Microbiol.* 84:e01646-17.

Palomo, A., Jane Fowler, S., Gülay, A., Rasmussen, S., Sicheritz-Ponten, T., and Smets, B. F. (2016). Metagenomic analysis of rapid gravity sand filter microbial communities suggests novel physiology of *Nitrospira* spp. *ISME J.* 10, 2569–2581. doi: 10.1038/ismej.2016.63

Palomo, A., Pedersen, A. G., Fowler, S. J., Dechesne, A., Sicheritz-Ponten, T., and Smets, B. F. (2018). Comparative genomics sheds light on niche differentiation and the evolutionary history of comammox *Nitrospira*. *ISME J.* 12, 1779–1793. doi: 10.1038/s41396-018-0083-3

Park, H. D., and Noguera, D. R. (2008). *Nitrospira* community composition in nitrifying reactors operated with two different dissolved oxygen levels. *J. Microbiol. Biotechnol.* 18, 1470–1474.

Pinto, A. J., Marcus, D. N., Ijaz, U. Z., Bautista-de Lose Santos, Q. M., Dick, G. J., and Raskin, L. (2015). Metagenomic evidence for the presence of comammox nitrospira-like bacteria in a drinking water system. *mSphere* 1:e0054-15.

Pruesse, E., Peplies, J., and Glockner, F. O. (2012). SINA: accurate high-throughput multiple sequence alignment of ribosomal RNA genes. *Bioinformatics* 28, 1823–1829. doi: 10.1093/bioinformatics/bts252

Regan, J. M., Harrington, G. W., Baribeau, H., Leon, R. D., and Noguera, D. R. (2003). Diversity of nitrifying bacteria in full-scale chloraminated distribution systems. *Water Res.* 37, 197–205. doi: 10.1016/s0043-1354(02)00237-3

Sakoula, D., Nowka, B., Spieck, E., Daims, H., and Lücker, S. (2018). The draft genome sequence of *Nitrospira lenta* strain BS10, a nitrite oxidizing bacterium isolated from activated sludge. *Stand. Genomic Sci.* 13:32.

Sayavedra-Soto, L., Ferrell, R., Dobie, M., Mellbye, B., Chaplen, F., Buchanan, A., et al. (2015). *Nitrobacter winogradskyi* transcriptomic response to low and high ammonium concentrations. *FEMS Microbiol. Lett.* 362, 1–7. doi: 10.1093/femsle/fnu040

Schramm, A., De Beer, D., Wagner, M., and Amann, R. (1998). Identification and activities in situ of *Nitrosospira* and *Nitrospira* spp. as dominant populations in a nitrifying fluidized bed reactor. *Appl. Environ. Microbiol.* 64, 3480–3485. doi: 10.1128/aem.64.9.3480-3485.1998

Sekiguchi, Y., Ohashi, A., Parks, D. H., Yamauchi, T., Tyson, G. W., and Hugenholtz, P. (2015). First genomic insights into members of a candidate bacterial phylum responsible for wastewater bulking. *PeerJ* 3:e740. doi: 10.7717/peerj.740

Shi, X., Hu, H., Wang, J., He, J., Zheng, C., Wan, X., et al. (2018). Niche separation of comammox *Nitrospira* and canonical ammonia oxidizers in an acidic subtropical forest soil under long-term nitrogen deposition. *Soil Biol. Biochem.* 126, 114–122. doi: 10.1016/j.soilbio.2018.09.004

Sorokin, D. Y., Lücker, S., Vejmelkova, D., Kostrikina, N. A., Kleerebezem, R., Rijpstra, W. I., et al. (2012). Nitrification expanded: discovery, physiology and genomics of a nitrite-oxidizing bacterium from the phylum *Chloroflexi*. *ISME J.* 6, 2245–2256. doi: 10.1038/ismej.2012.70

Spieck, E., and Lipski, A. (2011). Cultivation, growth physiology, and chemotaxonomy of nitrite-oxidizing bacteria. *Methods Enzymol.* 486, 109–130. doi: 10.1016/b978-0-12-381294-0.00005-5

Spieck, E., Spohn, M., Wendt, K., Bock, E., Shively, J., Frank, J., et al. (2020). Extremophilic nitrite-oxidizing *Chloroflexi* from Yellowstone hot springs. *ISME J.* 14, 364–379. doi: 10.1038/s41396-019-0530-9

Tanizawa, Y., Fujisawa, T., and Nakamura, Y. (2018). DFAST: a flexible prokaryotic genome annotation pipeline for faster genome publication. *Bioinformatics* 34, 1037–1039. doi: 10.1093/bioinformatics/btx713

Tatari, K., Musovic, S., Gülay, A., Dechesne, A., Albrechtsen, H. J., and Smets, B. F. (2017). Density and distribution of nitrifying guilds in rapid sand filters for drinking water production: dominance of *Nitrospira* spp. *Water Res.* 127, 239–248. doi: 10.1016/j.watres.2017.10.023

Ushiki, N., Fujitani, H., Aoi, Y., and Tsuneda, S. (2013). Isolation of *Nitrospira* belonging to sublineage II from a wastewater treatment plant. *Microbes Environ.* 28, 346–353. doi: 10.1264/jsme2.me13042

Ushiki, N., Fujitani, H., Shimada, Y., Morohoshi, T., Sekiguchi, Y., and Tsuneda, S. (2018). Genomic analysis of two phylogenetically distinct *Nitrospira* species reveals their genomic plasticity and functional diversity. *Front. Microbiol.* 8:2637. doi: 10.3389/fmicb.2015.02637

Ushiki, N., Jinno, M., Fujitani, H., Suenaga, T., Terada, A., and Tsuneda, S. (2017). Nitrite oxidation kinetics of two *Nitrospira* strains: the quest for competition and ecological niche differentiation. *J. Biosci. Bioeng.* 123, 581–589. doi: 10.1016/j.jbiosc.2016.12.016

van Kessel, M. A., Speth, D. R., Albertsen, M., Nielsen, P. H., Op den Camp, H. J., Kartal, B., et al. (2015). Complete nitrification by a single microorganism. *Nature* 528, 555–559. doi: 10.1038/nature16459

Wang, H., Proctor, C. R., Edwards, M. A., Pryor, M., Domingo, J. W. S., Ryu, H., et al. (2014). Microbial community response to chlorine conversion in a chloraminated drinking water distribution system. *Environ. Sci. Technol.* 48, 10624–10633. doi: 10.1021/es502646d

Wang, Y., Ma, L., Mao, Y., Jiang, X., Xia, Y., Yu, K., et al. (2017). Comammox in drinking water systems. *Water Res.* 116, 332–341. doi: 10.1016/j.watres.2017.03.042

Wegen, S., Nowka, B., and Spieck, E. (2019). Low temperature and neutral pH define *Candidatus* Nitrotoga sp. as a competitive nitrite oxidizer in coculture with *Nitrospira defluvii*. *Appl. Environ. Microbiol.* 85:e002569-18.

Williams, J. J., and Hergenrother, P. J. (2012). Artificial activation of toxin-antitoxin systems as an antibacterial strategy. *Trends Microbiol.* 20, 291–298. doi: 10.1016/j.tim.2012.02.005

Xie, Y., Wei, Y., Shen, Y., Li, X., Zhou, H., Tai, C., et al. (2018). TADB 2.0: an updated database of bacterial type II toxin-antitoxin loci. *Nucleic Acids Res.* 46, D749–D753.

Xu, L., Dong, Z., Fang, L., Luo, Y., Wei, Z., Guo, H., et al. (2019). OrthoVenn2: a web server for whole-genome comparison and annotation of orthologous clusters across multiple species. *Nucleic Acids Res.* 47, W52–W58.

Zhang, Y., Qin, W., Hou, L., Zakem, E. J., Wan, X., Zhao, Z., et al. (2020). Nitrifier adaptation to low energy flux controls inventory of reduced nitrogen in the dark ocean. *Proc. Natl. Acad. Sci. U.S.A.* 117, 4823–4830.

Conflict of Interest: The authors declare that the research was conducted in the absence of any commercial or financial relationships that could be construed as a potential conflict of interest.

frontiers in Microbiology

ORIGINAL RESEARCH
published: 06 October 2020
doi: 10.3389/fmicb.2020.589268

Distribution and Diversity of Comammox *Nitrospira* in Coastal Wetlands of China

*Dongyao Sun[1], Xiufeng Tang[1], Mengyue Zhao[1], Zongxiao Zhang[2], Lijun Hou[2], Min Liu[1,3], Baozhan Wang[4], Uli Klümper[5] and Ping Han[1,2,3]**

[1] Key Laboratory of Geographic Information Science (Ministry of Education), School of Geographic Sciences, East China Normal University, Shanghai, China, [2] State Key Laboratory of Estuarine and Coastal Research, East China Normal University, Shanghai, China, [3] Institute of Eco-Chongming, East China Normal University, Shanghai, China, [4] Key Laboratory of Microbiology for Agricultural Environment (Ministry of Agriculture), College of Life Sciences, Nanjing Agricultural University, Nanjing, China, [5] Institute for Hydrobiology, Technische Universität Dresden, Dresden, Germany

OPEN ACCESS

Edited by:
Anne E. Taylor, Oregon State University, United States

Reviewed by:
Aqiang Ding, Chongqing University, China
Hirotsugu Fujitani, Chuo University, Japan

***Correspondence:**
Ping Han
phan@geo.ecnu.edu.cn

Specialty section:
This article was submitted to Microbial Physiology and Metabolism, a section of the journal Frontiers in Microbiology

Received: *30 July 2020*
Accepted: *15 September 2020*
Published: *06 October 2020*

Citation:
Sun D, Tang X, Zhao M, Zhang Z, Hou L, Liu M, Wang B, Klümper U and Han P (2020) Distribution and Diversity of Comammox Nitrospira in Coastal Wetlands of China. Front. Microbiol. 11:589268. doi: 10.3389/fmicb.2020.589268

Complete ammonia oxidizers (comammox), able to individually oxidize ammonia to nitrate, are considered to play a significant role in the global nitrogen cycle. However, the distribution of comammox *Nitrospira* in estuarine tidal flat wetland and the environmental drivers affecting their abundance and diversity remain unknown. Here, we present a large-scale investigation on the geographical distribution of comammox *Nitrospira* along the estuarine tidal flat wetlands of China, where comammox *Nitrospira* were successfully detected in 9 of the 16 sampling sites. The abundance of comammox *Nitrospira* ranged from 4.15×10^5 to 6.67×10^6 copies/g, 2.21- to 5.44-folds lower than canonical ammonia oxidizers: ammonia-oxidizing bacteria (AOB) and ammonia-oxidizing archaea (AOA). Phylogenetic analysis based on the alpha subunit of the ammonia monooxygenase encoding gene (*amoA*) revealed that comammox Nitrospira Clade A, mainly originating from upstream river inputs, accounts for more than 80% of the detected comammox *Nitrospira*, whereas comammox *Nitrospira* clade B were rarely detected. Comammox *Nitrospira* abundance and dominant comammox *Nitrospira* OTUs varied within the estuarine samples, showing a geographical pattern. Salinity and pH were the most important environmental drivers affecting the distribution of comammox *Nitrospira* in estuarine tidal flat wetlands. The abundance of comammox *Nitrospira* was further negatively correlated with high ammonia and nitrite concentrations. Altogether, this study revealed the existence, abundance and distribution of comammox *Nitrospira* and the driving environmental factors in estuarine ecosystems, thus providing insights into the ecological niches of this recently discovered nitrifying consortium and their contributions to nitrification in global estuarine environments.

Keywords: comammox, *Nitrospira*, estuarine tidal flat wetlands of China, distribution, salinity

INTRODUCTION

Nitrification, a key process of the biogeochemical nitrogen cycle (Konneke et al., 2005), was for over a century considered to exclusively be a two-step microbial process: first, ammonia is oxidized to nitrite by ammonia-oxidizing archaea (AOA) or ammonia-oxidizing bacteria (AOB) (Purkhold et al., 2000; Konneke et al., 2005), with nitrite then being further oxidized to nitrate by nitrite-oxidizing bacteria (NOB) (Winogradsky, 1890). Based on kinetic theory of optimal metabolic processes, the hypothetical existence of complete ammonia-oxidizing (comammox) microorganisms had been proposed (Costa et al., 2006). Their discovery in 2015 (Daims et al., 2015; van Kessel et al., 2015) redefined this key process of the biogeochemical nitrogen cycle.

In contrast to canonical ammonia oxidizers and NOB, comammox *Nitrospira* were confirmed to genes encoding ammonia monooxygenase (AMO) and hydroxylamine dehydrogenase (HAO) genes for initial ammonia oxidation, as well as nitrite oxidoreductase (NXR) genes necessary for nitrite oxidation (Daims et al., 2015; van Kessel et al., 2015; Camejo et al., 2017). Based on phylogenetic analysis using the 16S rRNA gene, all currently known comammox bacteria are members of the genus *Nitrospira*, which is the most abundant and widespread group of NOB (Daims et al., 2015; Pinto et al., 2016). Nevertheless, phylogenetic analysis based on either, the 16S rRNA or *nxr* genes, is not able to distinguish between comammox *Nitrospira* and classical NOB (Pjevac et al., 2017). Consequently, specific primers targeting the *amoA* gene, encoding the alpha subunit of *amo*, were used to screen for the presence of comammox *Nitrospira* in various environments (Pjevac et al., 2017; Abujabhah et al., 2018), owing to the comammox *Nitrospira amoA* genes forming a distinct cluster from canonical ammonia oxidizers. According to similarity analysis of the *amoA* gene comammox *Nitrospira* were subdivided into clade A (including subclade A1 and A2) and clade B (Daims et al., 2015; Xia et al., 2018).

Metagenomic screening of published databases of environmental samples revealed the existence of comammox *Nitrospira* in a wide variety of natural and engineered ecosystems, such as agricultural soils, forest soil, wastewater treatment plants (WWTPs) and drinking water systems (Daims et al., 2015; Pjevac et al., 2017; Wang et al., 2017b, 2019). Intriguingly, there is so far no evidence supporting the existence of comammox *Nitrospira* in marine environments. However, recent evidence indicates the presence of complete ammonia-oxidizing bacteria in estuarine tidal flat wetlands (Yu et al., 2018), the key transition zone of land and marine interaction. Yet, environmental factors affecting the dynamics of comammox *Nitrospira* in these complex habitats remain poorly understood.

In China, with its large population and rapid development of agriculture and economy, considerable amounts of reactive nitrogen (Nr) are released into the environment. Large amounts of Nr are transported into estuarine and coastal ecosystems through river runoff (Cui et al., 2013; Hou et al., 2015a). Consequently, the estuaries and coastal areas of China have become highly Nr-enriched regions, with extreme eutrophication and the formation of algal blooms regularly appearing (Hou et al., 2015b). Located along the long Chinese coastline, there are dozens of estuaries with variable sizes, spanning tropical, subtropical and temperate zones of distinct temperature from north to south (Cao and Wong, 2007). Temperature has been identified as an important factor affecting the distribution and community structure of ammonia oxidizing microorganisms (Urakawa et al., 2008). Further, in estuarine tidal flat wetlands with large amounts of Nr, the present, ammonia-oxidizing microbes responded with high nitrification rates (Zheng et al., 2014). As relatively recently discovered members of the ammonia oxidizing consortia, comammox *Nitrospira* have not yet been identified in marine environments, and there is lack of knowledge about the dynamics of comammox *Nitrospira* in environments affected by their proximity to marine environments, such as estuarine tidal flat wetlands. Estuarine tidal flat wetland ecosystems possess unique environmental characteristics compared to other ecosystems, due to the interaction of land and sea. Estuaries and adjacent areas often experience tidal changes, salinity intrusions, high Nr concentrations and nutrient pulses, which can have a key impact on the community dynamics of ammonia oxidizers (Zheng et al., 2013). We here aimed at revealing comammox *Nitrospira* abundance and environmental factors affecting their dynamics in this complex habitat.

Consequently, the purpose of this study was to (i) examine the diversity and distribution of comammox *Nitrospira* in the estuarine tidal flat wetlands of China; (ii) determine important environmental factors affecting the dynamics of the community structure of comammox *Nitrospira* in estuarine tidal flat wetland systems under marine and land effects; and (iii) elucidate the occurrence of comammox *Nitrospira* and canonical ammonia oxidizers in coastal ecosystems. This is the first study to systematically investigate the environmental drivers of comammox *Nitrospira* abundance and diversity and its interplay with canonical ammonia oxidizers (AOA and AOB) in this natural environment with high salinity content.

MATERIALS AND METHODS

Study Site and Sampling

In this study, surface sediment samples were collected from 16 sites along the estuarine tidal flat wetlands of China (**Figure 1**), including Liaohe (LH), Beidaihe (BDH), Haihe (HH), Yellow River (YR), Sheyanghe (SYH), Bingchayunhe (BCYH), Yangtze River (CJ), and Jiaojiang (JJ), Oujiang (OJ), Minjiang (MJ), Mulanxi (MLX), Jiulongjiang (JLJ), Yifuxi (YFX), Zhujiang (ZJ), Yangjiang (YJ), Nanliujiang (NLJ). Fieldwork was conducted from March to April 2019. At each site, surface sediment samples (0–5 cm) from 6 to 8 plots (50 cm by 50 cm) per site were collected with sterile, stainless steel tubes by S-shaped sampling. The collected sediment samples were stored in sterile plastic bags, sealed, refrigerated and transported back to the laboratory. Upon return to the laboratory, the sediment samples obtained from individual plots at each site were combined at equal proportions inside a sterile plastic bag and mixed using sterile gloves to

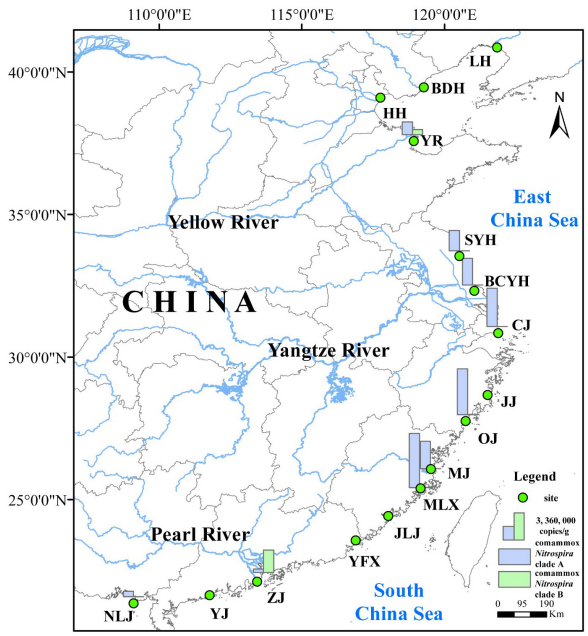

FIGURE 1 | Location of sampling sites in the estuarine tidal flat wetlands of China.

obtain a homogenized, composite sample for each individual sampling site. Finally, the composite samples were divided into two parts, one was stored at 4°C for the determination of nitrification rates and sediment physicochemical properties, and the second preserved at −20°C for DNA extraction and subsequent molecular analysis.

Physicochemical Analysis

At each site, *in situ* determination of sediment temperature was carried out with a portable electronic thermometer. A YSI Model 30 salinity meter and a Mettler-Toledo pH meter were used to measure sediment salinity and pH, by mixing sediments with deionized, CO_2-free water at a sediment to water ratio of 1:2.5 (Lin et al., 2016). Water content of the sediment was measured based on weight loss after drying a known quantity of wet sediment at 80° to constant weight. Sediment particle size was analyzed using a Beckman Coulter LS13320 laser granulometer (United States). Exchangeable ammonium (NH_4^+-N), nitrite (NO_2^--N), and nitrate (NO_3^--N) were extracted by adding five parts 2 M KCl to one part of fresh sediment, with the solution subsequently analyzed by spectrophotometry on a continuous-flow nutrient analyzer (SAN Plus, Skalar Analytical B.V., The Netherlands), with detection limits of 0.5 μM for NH_4^+-N and 0.1 μM for NO_2^--N and NO_3^--N (Gao et al., 2017). Ferric oxides in sediments were extracted with a mixture of 0.5 M HCl and 0.25 M hydroxylamine hydrochloride and analyzed with the ferrozine-based colorimetric method (Roden and Lovley, 1993; Wei et al., 2020). After treatment with 0.1 M HCl to remove sedimentary carbonate, Organic carbon (OC) was measured on a carbon-hydrogen-nitrogen elementary analyzer (VVarioELIII, Elementary, Germany) (Lin et al., 2017). Total nitrogen (TN) and Total carbon (TC) in sediments were measured using a Carbon nitrogen analyzer (Elementar Vario MAX CN, Germany). All sediment physicochemical parameters were analyzed in triplicate.

DNA Extraction and PCR Amplification

Total genomic DNA of each sediment sample was extracted in duplicate from 0.5 g of the homogenized sediments using the FastDNA Spin Kit for Soil (QBIOgene, Carlsbad, CA, United States) following the manufacturer's instruction. Duplicate extracts were combined for down-stream molecular analyses. A NanoDrop-2000 UV-Vis Spectrophotometer (Thermo Scientific) and 1% agarose gel electrophoresis were applied to determine the concentration and quality of extracted DNA. The ammonia monooxygenase alpha subunit encoding genes (*amoA*) of AOA, AOB and comammox *Nitrospira* clade A and comammox *Nitrospira* clade B were amplified by PCR with primers targeting each individual group (Rotthauwe et al., 1997; Pester et al., 2012; Pjevac et al., 2017; Yu et al., 2018). Detailed information about PCR primers used in this study is summarized in **Supplementary Table S1**. All PCR reactions were performed in a total volume of 20 μL, containing 10 μL 2 × Hieff® PCR Master Mix (Yeasan, China), 1 μL of each primer (10 μM), 1 μL template DNA and 8 μL of ddH_2O. PCRs were carried out with 5 min (for AOA and AOB) or 8 min (for comammox *Nitrospira*) at 95°C; 35 cycles of 95°C for 30 s, 53°C (for AOA and AOB) or 52°C (for comammox *Nitrospira*) for 30 s, and 72°C for 1 min; and a final 10 min extension cycle at 72°C. During PCR amplifications, negative (without template DNA) and positive controls were always included. DNA extracts obtained from pure cultures of the respective ammonia-oxidizers (*N. nitrosa* 18-3D for AOB, *N. gargensis* for AOA and *N. inopinata* for comammox *Nitrospira*) served as positive controls.

Real-Time qPCR

To analyze the abundance of AOA, AOB, comammox *Nitrospira* clade A, and comammox *Nitrospira* clade B, quantitative real-time PCR was performed in triplicate with an ABI 7500 sequence detection system (Applied Biosystems, Canada) using the SYBR green quantitative PCR (qPCR) method. Primer pairs, CamoA-19F/616R, amoA-1F/2R, comaAF/R and comaB-244F/659R (**Supplementary Table S1**), targeting the alpha subunit of the *amo* encoding gene of AOA, AOB, comammox *Nitrospira* clade A and comammox *Nitrospira* clade B, respectively, were used to estimate abundance through qPCR assays. The 21 μL qPCR mixture contained 10 μL of Hieff® qPCR SYBR Green Master Mix with Low Rox Plus (Yeasan, China), 0.4 μL of each primer (10 μM), 1 μL template DNA and 9.2 μL of ddH_2O. The qPCR was performed with the following protocols: 50°C for 2 min and 95°C for 10 min, followed by 40 cycles of 15 s at 95°C, 30 s at 53°C (for AOA and AOB) and 52°C (for comammox *Nitrospira*), and 40 s at 72°C. To create standard curves, the respective PCR products were purified using the QIAquick PCR Purification Kit (Qiagen, Germany) following the manufacturer's protocol. The concentration of purified PCR product was

estimated with a Nanodrop-2000 Spectrophotometer (Thermo, United States) and copies of purified PCR product calculated as: Copy number = (C × 10^{-9}/MW) × NA, with C: template concentration ng/μL, MW: template molecular weight in Daltons, NA: Avogadro's constant, 6.022 × 10^{23}. Then the purified PCR product was serial diluted into a gradient to serve as standards for standard curves. Standard curves with an amplification efficiency 0.94–1.14 and $R^2 \geq 0.99$ were accepted and melting curve analysis was performed to assess the amplicon specificity. For each qPCR assay, negative controls containing no template DNA simultaneously analyzed to detect and rule out any potential contamination.

Potential Nitrification Rates (PNRs)

Potential Nitrification Rates measurements for each sediment sample were carried out in triplicate by referring to the methods previously published by Kurola et al. (2005) and Gao et al. (2016b). In brief, 5 g of sediment and 25 mL of phosphate buffer solution (pH = 7.4: NaCl 8.0 g/L; KCl 0.2 g/L; Na_2HPO_4 0.2 g/L; NaH_2PO_4 0.2 g/L; $(NH_4)_2SO_4$ 0.132 g/L) were added to 50 mL Falcon tubes. The initial ammonia concentration in this solution was 1 mM. To inhibit nitrite oxidation, 10mM $KClO_3$ was added to the solution. Tubes were then incubated in the dark at 25° for 24 h with shaking speed of 120 rpm. After incubation, nitrite was extracted using 2M KCl-solution as described above and analyzed on a continuous flow nutrient analyzer (SAN plus, Skalar Analytical B.V., Netherlands). PNRs were determined through the changes in nitrite concentrations during the incubation period.

High-Throughput Sequencing and Phylogenetic Analysis

From all samples with positive comammox *Nitrospira*, AOB or AOA detection, PCR products of the *amoA* genes from AOA, AOB and comammox *Nitrospira* were sequenced using Illumina MiSeq by Shanghai Meiji Biomedical Technology Company (Shanghai, China). The raw data was processed using Quantitative Insight into Microbial Ecology (QIIME)[1] (Caporaso et al., 2010). First, the FLASH plugin was used to stitch paired-end reads based on matched overlapping regions. Using Usearch 7.0[2], the sequences were clustered to operational taxonomic unit (OTUs) according to 95% nucleic acid similarity and chimeras were eliminated (Schloss, 2013). Sequences of *amoA* gene were analyzed using the BLASTn tool[3] to select closely related reference sequences. All obtained sequences were aligned using ClustalX (Thompson et al., 1997). Neighbor-joining phylogenetic trees from one representative sequence and its closest reference sequence for each OTU retrieved from GenBank (Kumar et al., 2004) were created using MEGA 7.0 with 1000 bootstrap replicates to evaluate the reliability of the tree topologies (Tamura et al., 2007). The AOA, AOB and comammox sequences obtained in the present study have been deposited in GenBank, with accession numbers MT809785–MT809998, MT797386–MT797560, and MT790359–MT790492.

Statistical Analysis

.+5The Chao1 species richness and α-diversity indices were calculated in R V3.4 using the Vegan packages V2.5-4 (Oksanen et al., 2013; R Core Team, 2013). The coverage was estimated as the number of observed OTUs divided by the Chao1 species richness estimate (Mohamed et al., 2010). Redundancy analysis (RDA) was performed using the software Canoco 4.5 to evaluate variations in ammonia oxidizing community structure in connection with environmental variables. Correlations between comammox *Nitrospira* clade A OTU abundances and environmental variables were explored with canonical correspondence analysis (CCA). The maximum gradient length determined by detrended correspondence analysis (DCA) in Canoco 4.5 was higher than 4 standard deviations (SD) for ammonia oxidizers, showing that the environmental variables were unimodal (ter Braak and Smilauer, 2002; Zheng et al., 2014). Similarity and clustering of sediment ammonia-oxidizer communities were explored with principal coordinates analysis (PCoA) (Lozupone et al., 2011). Pearson correlation analyses were conducted to test correlations between diversity, abundance and environmental factors. One-way analysis of variance (ANOVA) tests were performed to compare PNRs rates (Gao et al., 2016a). Significance for all tests was accepted at $p \leq 0.05$. All statistical analyses were performed using SPSS 22.0.

RESULTS

Physicochemical Characteristics of the Sediment Samples

Among the sampling sites, located along the estuarine tidal flat wetlands of China, the latitude varied from 21°34′ to 40°51′ N, while longitude varied from 109°05′ to 121°53′ E (**Figure 1**). The physicochemical characteristics of the sediment samples varied significantly across the different sampling locations (**Supplementary Table S2**): The sediment temperature was between 12 and 29.9°, salinity ranged from 0.14 to 8.80 ppt and sediment pH varied from 6.41 to 8.91. Sediments were mainly composed of clay, silt, and smaller amounts of sands, with the average particle size ranging from 6.2 to 136.2 μm and water content ranging from 21 to 54%. Sediments consisted of 0.38–2.87% TC, 0.24–3.18% TOC, and 0.04–0.31% TN. Among the observed Nr concentrations, ammonia (6.51–53.76 μg/g) was significantly and positively correlated with nitrate (1.80–11.97 μg/g; $r = 0.356$, $p < 0.05$, $n = 48$) and nitrite (0.14–0.90 μg/g; $r = 0.404$, $p < 0.01$, $n = 48$). Further, concentrations of Fe^{2+} (0.14–0.69 mg/g) were significantly negative correlated with Fe^{3+} (0.16–0.86 mg/g; $r = 0.336$, $p < 0.05$, $n = 48$) (**Supplementary Figure S1**).

Potential Nitrification Rates

PNRs in the estuarine tidal flat wetland samples varied from as low as 8.84 up to 174.32 nmol N $L^{-1}h^{-1}$

[1]http://qiime.org/

[2]http://drive5.com/uparse/

[3]http://www.ncbi.nlm.nih.gov/BLAST

(**Supplementary Figure S2**), with significant differences in PNRs in estuaries in different latitudes ($p < 0.05$): PNRs of estuaries located in central latitudes were generally higher (97.44 ± 48.67 nmol N $L^{-1}h^{-1}$) than those found in northern (42.10 ± 40.79 nmol N $L^{-1}h^{-1}$) and southern latitudes (46.49 ± 25.58 nmol N $L^{-1}h^{-1}$). PNRs were further positively correlated to pH ($r = 0.316$, $p < 0.05$, $n = 48$) and Fe^{2+} concentrations ($r = 0.445$, $p < 0.01$, $n = 48$). Significant negative correlations were found between the PNRs and salinity ($r = -0.519$, $p < 0.01$, $n = 48$), particle size ($r = -0.375$, $p < 0.01$, $n = 48$) as well as ammonia ($r = -0.459$, $p < 0.01$, $n = 48$). However, between temperature and PNRs no significant relationship ($p > 0.05$) was observed. Unsurprisingly, PNRs were significantly correlated with the abundances of each of the three ammonium oxidizing groups: AOA ($r = 0.324$, $p < 0.05$, $n = 48$), AOB ($r = 0.582$, $p < 0.01$, $n = 48$) and comammox *Nitrospira* ($r = 0.770$, $p < 0.01$, $n = 48$).

Abundance of Comammox *Nitrospira* and Canonical Ammonia Oxidizers

In the ammonia oxidizing community comammox *Nitrospira* was significantly less abundant than canonical ammonia-oxidizers (**Supplementary Figure S3**). While AOA and AOB were detected in all tested sediment samples, comammox *Nitrospira* were detected in only 9 of the 16 samples. Among those 9 samples, all contained Comammox *Nitrospira* clade A *amoA*, with abundances between 4.15×10^5 and 6.67×10^6 copies/g dry soil. Comammox *Nitrospira* clade B *amoA* was only detected in 2 samples, but dominated comammox *Nitrospira* abundance in these samples (6.28×10^5–4.01×10^6 copies/g dry soil). Comammox *Nitrospira* was widespread in most parts of the tested wetland areas, and their abundance showed spatial patterns, similar to those detected for the PNRs, with higher abundance in the central ($9.41 \times 10^6 \pm 1.28 \times 10^6$ copies/g dry soil) than southern ($2.77 \times 10^6 \pm 2.53 \times 10^6$ copies/g dry soil) and northern ($1.55 \times 10^6 \pm 6.3 \times 10^5$ copies/g dry soil) latitudes (**Figure 4**). The highest copy number of comammox *Nitrospira amoA* genes was detected at central latitude site MLX (6.66×10^6 copies/g dry soil), and the lowest one was recorded at the most southern site NLJ (6.47×10^5 copies/g dry soil). Again, no significant correlation with temperature ($p > 0.05$), but a significant positive correlation with Fe_2C ($r = 0.403$, $p < 0.01$, $n = 27$) and a negative correlation with salinity ($r = -0.321$, $p < 0.05$, $n = 27$) were detected (**Supplementary Figure S1**), further indicating the strong effect of salinity and metal ions on ammonia oxidation.

Among the canonical ammonia oxidizers, which were detected in all samples, abundance ranged from 1.15×10^6 to 3.66×10^7 copies/g dry soil (AOA) and 1.76×10^5 to 1.73×10^7 copies/g dry soil (AOB) (**Supplementary Figure S3**). In 10 of the 16 estuarine tidal flat wetland samples AOA showed higher abundance than AOB (**Supplementary Figure S4**). The abundance of AOA was positively correlated with temperature ($r = 0.44$, $p < 0.01$, $n = 48$) with highest abundance in estuaries of central and southern latitudes. Contrary, AOB were mainly distributed across the central and northern latitudes, and dominated ammonia oxidizer abundances at the northern latitudes.

Diversity of Comammox *Nitrospira*

In total 69,858 high-quality comammox *Nitrospira amoA* gene sequences were generated from the 9 samples where comammox *Nitrospira* were detected. Comammox *Nitrospira amoA* gene sequences were clustered into 118 OTUs based on 95% nucleotide similarity, with the number of OTUs for each sample ranges from 17 to 70. Chao1 richness estimates ranged from 17.5 (for site BCYH) to 76.9 (for site CJ), with coverage for comammox *Nitrospira* detection ranging from 89–100%. Salinity was the only environmental factor showing significant negative effects ($r = -0.768$, $p < 0.05$, $n = 9$) on the Chao1 richness as well as the Shannon diversity of comammox *Nitrospira* communities ($r = 0.698$, $p < 0.05$, $n = 9$). In addition, TC was positively correlated with Shannon diversity ($r = 0.793$, $p < 0.05$, $n = 9$) while not affecting richness (**Supplementary Table S4**).

The phylogenetic tree (**Figure 2**) generated for the comammox *Nitrospira amoA* gene supported the division of comammox *Nitrospira* into two clades (clade A: 118, clade B: 16). Clade A can further be subdivided into clade A1 and A2 (Xia et al., 2018). Clade A1 had slightly more representative OTUs (68/118 clade A OTUs) than clade A2 (50/118), however among the 50 most abundantly detected comammox *Nitrospira* OTUs, 43 (86%) belonged to clade A1. Clade B was present in 2 samples only (YR and ZJ). Again, a latitudinal pattern emerged on the OTU abundance level: While OTU55 and OTU119 dominated comammox *Nitrospira* abundance in the southern latitude estuaries, a wider variety of OTUs were observed in those estuaries from central or northern latitude (**Supplementary Figure S5**).

Based on the same methodology for canonical ammonia-oxidizers, 214 AOA and 175 AOB, OTUs were detected. Most AOA sequences (107 OTUs) were divided into the *Nitrosopumilus* cluster (group1.1b), while 94 OTUs belonged to the *Nitrososphaera* cluster (group1.1a) (**Supplementary Figure S6**). The remaining OTUs were affiliated with the *Nitrosotalea* cluster (group1.1a – associated). Although the number of OTUs in group 1.1a was slightly lower than in group 1.1b, 78.53% of the detected sequences were affiliated with group 1.1a. For AOB, all sequences were grouped within known species of *Betaproteobacteria*, *Nitrosomonas* (119 OTUs) and *Nitrosospira* (56 OTUs). More than half of the AOB sequences belonged to the 6 *Nitrosomonas*-related clusters, and grouped with the lineages *N. communis, N. europaea*, *N. oligotropha*, *N. marina*, *N. cryotolerans,* and *N.* sp. Nm143. The *Nitrosospira* were subdivided into 4 clusters and a single *Nitrosospira-like* strain (**Supplementary Figure S7**). Base on Pearson correlation analysis, none of the environmental factors showed significant effects on the Shannon diversity within both AOA and AOB communities (Data not shown).

The Effects of Environmental Factors

Redundancy analysis was performed to evaluate variations in ammonia oxidizing community structure in connection

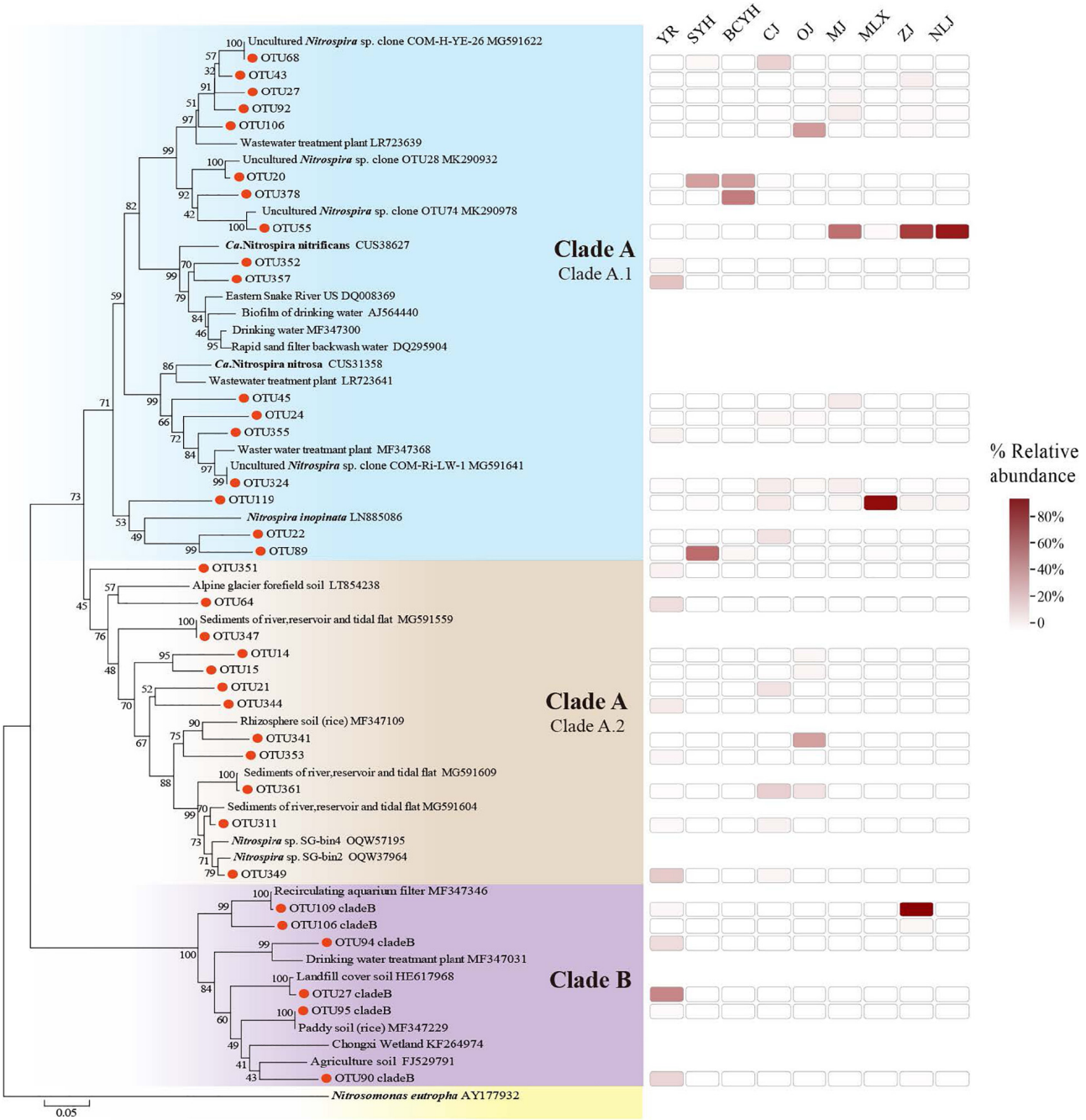

FIGURE 2 | Phylogenetic tree of comammox *Nitrospira amoA* genes constructed by neighbor joining methods. Sequences were collected from this study and the GenBank database. Bootstrap values are given on the branches of the neighbor-joining tree. The scale bar represents 5% nucleic acid sequence divergence.

with environmental variables (**Figure 3A**). The first two RDA dimensions explained 98.62% of the cumulative variance. Higher temperatures were promoting the growth of AOA, but had no significant effect on AOB and comammox *Nitrospira* abundance. Different forms of iron ions significantly promoted the abundance of ammonia-oxidizers, and ammonia, particle size and pH were also showing varying degrees of influence on their abundance (**Figure 3A**).

The correlations of comammox *Nitrospira* clade A OTU abundances in the different communities with environmental variables were tested by CCA. The first two CCA dimensions accounted for 38.55% of the cumulative variance of the comammox *Nitrospira* community environmental correlation (**Figure 3B**). Comammox *Nitrospira* clade A community diversity in the sediments of Chinese estuarine tidal flat wetlands were significantly correlated to TOC (P = 0.004,

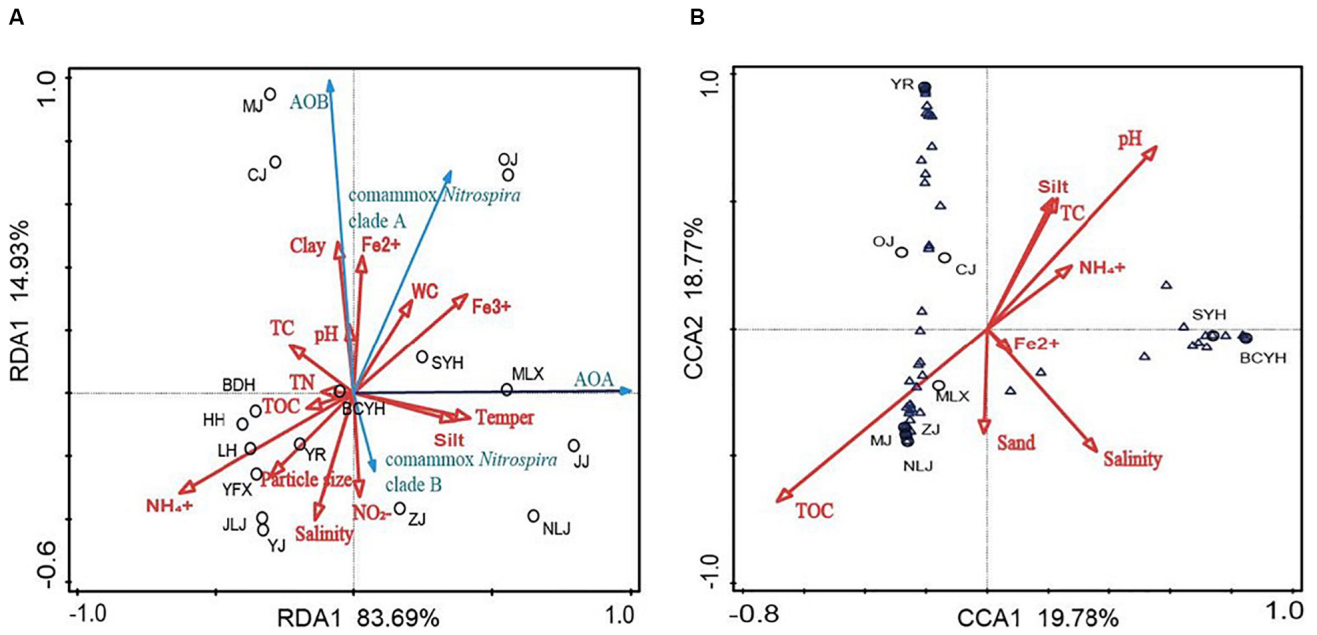

FIGURE 3 | (A) RDA plot based on the relative abundances of all ammonia-oxidizers (qPCR results); **(B)** CCA plot based on comammox *Nitrospira* clade A OTU abundances (high-throughput sequencing results). Black circles: samples, Blue arrows: ammonia-oxidizers, Blue triangles: Comammox *Nitrospira* clade A OTUs, Red arrows: environmental factors

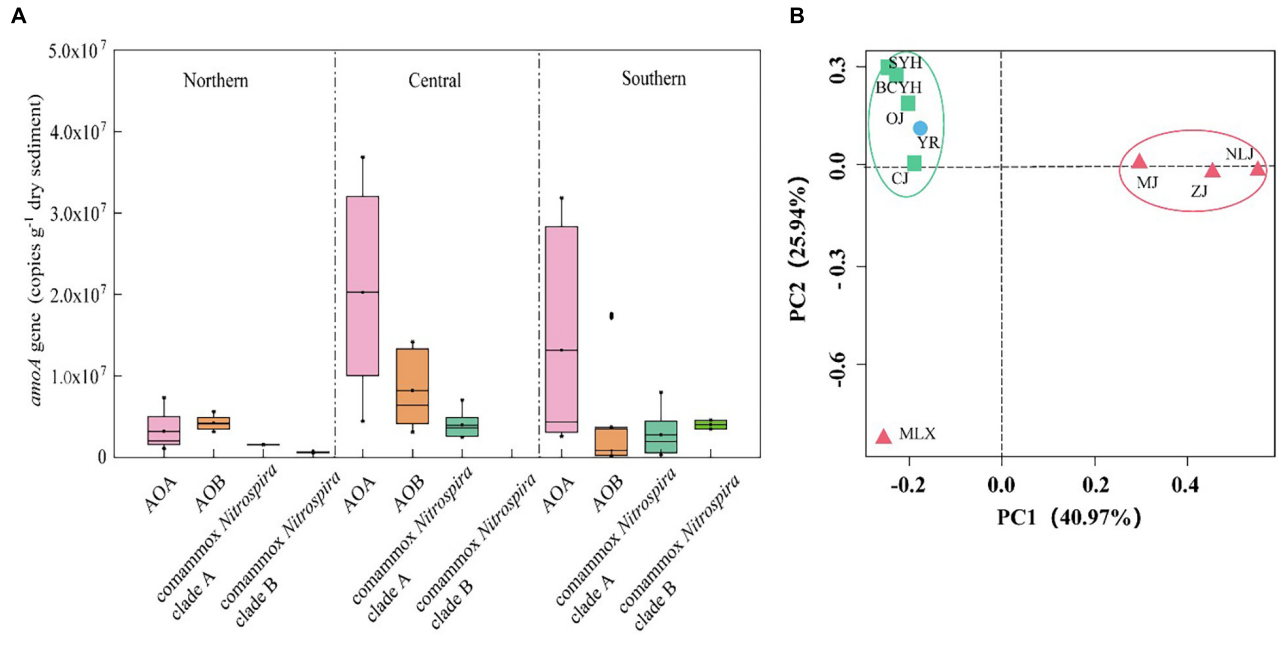

FIGURE 4 | (A) Abundance of ammonia-oxidizers in the distinct areas based on qPCR results. **(B)** UniFrac weighted PCoA analysis of comammox *Nitrospira* communities in the estuary tidal flat wetlands of China. Red triangle: Southern estuaries (MJ, ZJ, MLX, NLJ); Green square: Central estuaries (BCYH, SYH, CJ, OJ); Blue circle: Northern estuaries (YR).

F = 1.6), pH (P = 0.04, F = 1.5) and salinity (P = 0.013, F = 1.5), accounted for half of the total expositive power. Despite the contribution of other environmental variables (including ammonia levels, TN, particle size) were not significant ($P > 0.05$), they also contributed considerably to the CCA's expositive power.

DISCUSSION

Distribution of Comammox *Nitrospira* in Estuarine Tidal Flat Wetlands of China

Comammox *Nitrospira* were detected from 9 of the 16 sampling sites. The abundance of comammox *Nitrospira* ranged from 4.15×10^5 to 6.66×10^6 copies/g, 2.21- to 5.44-folds lower than canonical ammonia oxidizers: AOA and AOB, which were both detected at every sampling location. The three types of microorganisms use ammonia as an energy substance, and hence are in direct nutrient competition. However, they are able to coexist in most environments. In the estuarine tidal flat wetlands nitrifying microbial network (AOA, AOB, and comammox *Nitrospira*) (**Figure 5**), the correlation between all species is mainly positive (98.17%) and their abundance is equally correlated with the detected PNRs. The average ratio of comammox *Nitrospira* to AOA and AOB is 0.18 and 0.46. From the proportion of abundance, the contribution of comammox *Nitrospira* to the PNRs and hence nitrification may be smaller than that of AOA and AOB. The abundance of AOA was higher than that of AOB in 10 of the 16 sediment samples, with the AOA/AOB ratio ranging from 0.22 up to 205. No significant decreases of PNRs could be observed in intertidal sediment after AOB were inhibited by ampicillin, implying that AOA might play the most important role for the nitrification potential in this specific ecosystem (Zheng et al., 2014).

Recent studies of ammonia oxidizing microbial communities based on *amoA* genes revealed that relative proportions of comammox *Nitrospira*, AOB and AOA are highly variable across environmental matrixes including both natural and engineered systems (**Table 1**). While in most ecosystems (e.g., river water, grassland, agricultural and paddy soil) AOA or AOB were the dominating organisms (Kits et al., 2017; Zhang et al., 2019), comammox *Nitrospira* were found to mainly dominate in engineered systems (Bartelme et al., 2017; Tatari et al., 2017), but also in some natural environments, such as specific freshwater lakes (Shi et al., 2020) or the river water and sediments of the Yangtze River (Liu et al., 2020). Contrary, no marine comammox organisms have been identified so far.

Here, comammox *Nitrospira amoA* sequences obtained from the estuarine tidal flat wetland of China were affiliated with those previously identified in terrestrial sources from China (Yu et al., 2018; Zhao et al., 2019). Comammox *Nitrospira* clade A1 mainly found in fresh water, and engineered ecosystems (Pjevac et al., 2017; Zhao et al., 2019) was more abundant and widely distributed than clade A2 that mainly occupies agriculture soils (Xu et al., 2020). The lower abundance of comammox *Nitrospira* clade B compared comammox *Nitrospira* clade A observed in this study was also in line with previous studies

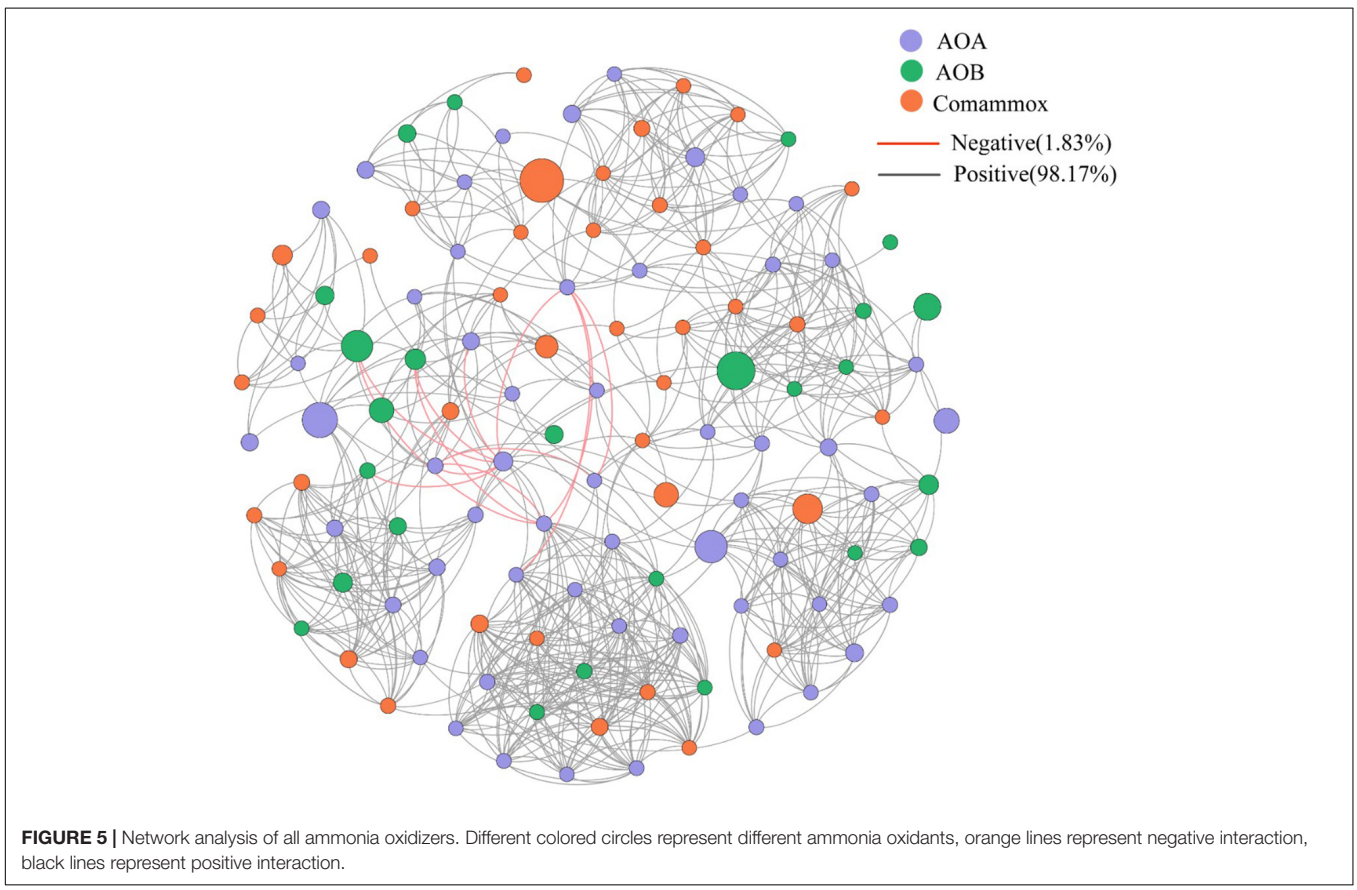

FIGURE 5 | Network analysis of all ammonia oxidizers. Different colored circles represent different ammonia oxidants, orange lines represent negative interaction, black lines represent positive interaction.

TABLE 1 | Distribution of ammonia-oxidizers in different ecosystems.

Country	Ecosystem	AOA	AOB	comammox *Nitrospira* clade A	comammox *Nitrospira* clade B	References
America	Recirculating aquaculture systems	0.94×10^8–3.4×10^8 (copies/g)	2.6×10^3–5.0×10^5 (copies/g)	1.6×10^8–4.2×10^8 (copies/g)	–	Bartelme et al., 2017
Denmark	Drinking water	1.2×10^3–3.4×10^3 (copies/m^3)	1.6×10^7–10.0×10^7 (copies/m^3)	0.82×10^8–2.58×10^8 (copies/m^3)	–	Tatari et al., 2017
Austria	Waste water treatment plant	–	1.3×10^3–2.1×10^3 (copies/ng DNA)	3.4×10^2–6.8×10^2 (copies/ng DNA)	–	Pjevac et al., 2017
China	Overlying water in river	3.34×10^3–2.18×10^7 (copies/L)	1.06×10^5–2.98×10^7 (copies/L)	1.25×10^4 (copies/L)	–	Zhang et al., 2019
China	Agriculture soil	–	–	4.14×10^4–1.65×10^7 (copies/g)	9.44×10^2–2.12×10^6 (copies/g)	Xu et al., 2020
Italy	Rice paddy soil	2.1×10^3–3.1×10^3 (copies/ng DNA)	–	3.6×10^2–4.6×10^2 (copies/ng DNA)	3.5×10^2–4.5×10^2 (copies/ng DNA)	Pjevac et al., 2017
Italy	Forest soil	1.4×10^2–2.6×10^2 (copies/ng DNA)	1.7×10^3–3.5×10^3 (copies/ng DNA)	–	2.9×10^2–4.9×10^2 (copies/ng DNA)	Pjevac et al., 2017
China	River sediment	1.84×10^2–3×10^2 (copies/ng DNA)	9.3×10^1–3.4×10^3 (copies/ng DNA)	1.8×10^2–2.8×10^2 (copies/ng DNA)	–	Zhao et al., 2019
China	Intertidal sediment	1.7×10^2–4.9×10^3 (copies/ng DNA)	2.2×10^2–5.4×10^3 (copies/ng DNA)	1.6×10^2–3.2×10^2 (copies/ng DNA)	–	Zhao et al., 2019
China	**Estuary tidal wetland sediment**	**1.15×10^6–1.66×10^7 (copies/g) or 5.71×10^1–6.27×10^3 (copies/ng DNA)**	**1.76×10^5–1.73×10^7 (copies/g) or 1.05×10^1–1.57×10^3 (copies/ng DNA)**	**4.15×10^5–6.67×10^6 (copies/g) or 2.74×10^1–7.02×10^2 (copies/ng DNA)**	**6.28×10^5–4.01×10^6 (copies/g) or 1.1×10^2–2.65×10^2 (copies/ng DNA)**	**This study**

(Pjevac et al., 2017; Xu et al., 2020). Overall, this indicates that the main source of comammox *Nitrospira* in the estuarine tidal flat wetland ecosystem is upstream river runoff input with only minor contributions from soil and sediments (clade A2 and clade B).

The Influence of Environmental Factors on the Abundance and Structure of Comammox *Nitrospira* Flora

The major environmental factors associated with comammox *Nitrospira* abundance and defining comammox *Nitrospira community* structure were identified as pH, salinity, the availability of iron ions, TOC, ammonia, nitrite and particle size.

The pH in the study area ranged between 6.74 and 8.65, and displayed a positive correlation with comammox *Nitrospira* abundance. Blum et al. (2018) found ammonia oxidizers to preferentially grow in slightly alkaline environments, due to the optimal pH range (7–8) for key nitrifying enzymes (e.g., *amo* and *hao*). Although the *amo* enzyme of comammox *Nitrospira is* different from that of traditional AOB (Palomo et al., 2016), it still showed similar pH adaptability. While some studies have shown that pH will impact the niche distinction between different ammonia-oxidizing groups, the number of comammox *Nitrospira* found in low pH environments such as forest soils (pH < 6.0) can on occasion still exceed that of AOA and AOB (Hu and He, 2017). No significant effect of pH on AOA and AOB has been shown in this study, so the exact effect of environmental pH on *amo* of comammox *Nitrospira* in comparison with canonical ammonia oxidizer enzymes remains to be determined.

Salinity displayed a significant negative correlation with comammox *Nitrospira* abundance and PNRs, as well as comammox *Nitrospira* community diversity. Oceans were previously speculated to not provide a suitable habitat for any known comammox *Nitrospira*, based on the higher salinity levels (Kuypers, 2017; Santos et al., 2017). Here, the highest richness of comammox *Nitrospira is* detected in the estuaries with lowest salinity in the central latitudes. The highest number of OTU were found in these central estuaries, with 29 of the Top 30 OTUs present and 14 of them dominating. Clade A1 was mostly abundant, but clade A2 was considerably distributed in the lower salinity CJ and OJ estuaries, indicating that clade A1 can adapt to environments with a wider range of salinity, while clade A2 is exclusively adapted to habitats with low salinity.

In the southern estuaries with intermediate salinity, due to strong evaporation rates at high temperature, but also high amounts of river runoff, still considerable comammox *Nitrospira* abundance can be detected. However, the comammox *Nitrospira* community was dominated by exclusively two species. Specifically, OTU 55, which was close to an uncultured *Nitrospira* sp. clone OTU74 discovered by Zhao et al. (2019), was most abundantly found in the southern estuary (MJ, ZJ, NLJ). It dominated the southern comammox *Nitrospira* community together with *Nitrospira* species OTU119, which might be better adapt to the higher-salinity sampling sites in the MLX, clustering with *Nitrospira inopinata* (Daims et al., 2015).

Moreover, comammox *Nitrospira* was not detected in areas with higher salinity (e.g., HH 8.80 ppt and LH 5.92 ppt). These northern rivers have small amounts of river runoffs and are mostly affected by the ocean, which might be the reason that no comammox *Nitrospira* was detected in samples from these areas. An exception in this area was the Yellow River, which is an aboveground river with an estuary located higher than sea level, hence less affected by the ocean. Intriguingly, the Yellow River sediment was the only one hosting comammox *Nitrospira* clade A2 and clade B, mainly associated with soil and sediment ecosystems (Yu et al., 2018). This correlates with the large amount of sediment input in the upper Yellow River and might further mask the influence of the higher salinity generally observed in the northern regions. Although there were differences in the dominant OTU species in the central and northern estuaries, the overall community structure was not significantly different, while there are differences with the community structure of the southern estuaries, which was also verified by PCoA analysis (**Figure 4B**).

Iron exists in the active center of various enzymes in nitrifying bacteria, which is involved in the transport of molecular oxygen and the transformation of nitrogen (Wang et al., 2013). It was found in this study that Fe^{2+} has a positive correlation with the PNRs, and abundance of comammox *Nitrospira*. Fe^{2+} acts on enzymes (e.g., *amo, nxr*) in the metabolic nitrification process and as part of various cofactors and proteins that are beneficial to nitrification. Although there are differences in *amo* between AOB and comammox *Nitrospira*, Fe^{2+} can increase the microbial activity and increase the nitrification reaction by increasing the enzyme activity of *amo* (Ren et al., 2011) for both AOB and comammox *Nitrospira*. Interestingly, Fe^{3+} showed a positive correlation with the abundance of AOA, indicating different impact mechanisms on archaea. The cells of most nitrifying organisms have complex inner membrane pleated structures (flaky, vesicular and tubular), and iron as a chemical catalyst can increase the permeability of the cell membrane, thereby accelerating the transmission rate of nutrients (Wang et al., 2003), which could be a potential mode of effect.

It has been shown that in low oxygen environments, high TOC concentrations will mutually strengthen the effect on nitrification (Zhang et al., 2002). While oxygen concentrations in the estuarine tidal flats were indeed low, no effect of TOC on the PNRs was found in this study. However, the community structure of comammox *Nitrospira* was affected by TOC to a certain extent. The complex interaction mechanism between comammox *Nitrospira* and TOC requires further investigation.

Both AOA and comammox *Nitrospira* displayed significant negative correlation with ammonia in this study, indicating better adaptions to oligotrophic environments. Levels of ammonia are known to affect various nitrifying microorganisms during the nitrification process (Santoro, 2016). The affinity for ammonia is much higher in AOA than AOB (Martens-Habbena et al., 2009), and comammox *Nitrospira* species *Nitrospira inopinata* has been shown to possess a higher affinity for ammonia than non-marine AOA and many AOB, resulting in a competitive advantage at low ammonia concentrations (Kits et al., 2017). Due to the large accumulation of reactive nitrogen in estuarine tidal flat wetlands the higher concentrations of ammonia might have put comammox *Nitrospira* at a competitive disadvantage as nitrogen affinity did not play a significant role.

A negative correlation between comammox *Nitrospira* and the availability of nitrite was found, suggesting that low levels of nitrite may be beneficial for comammox *Nitrospira*. Comammox *Nitrospira* is phylogenetically closely related to lineage II NOB, but, other than for NOB, nitrite is not a necessary substrate or final metabolite of comammox *Nitrospira*. Comammox *Nitrospira* have, compared with canonical NOB, a poor affinity for nitrite (Kits et al., 2017) and might thus have a competitive disadvantage against these strictly nitrite oxidizing bacteria in this environment rich in reactive nitrogen.

The final observed factor, particle size, controls the physicochemical characteristics of the sediments which can subsequently affect the structure of the microbiome (Dang et al., 2010), but the specific influence mechanism of particle size on comammox *Nitrospira* is not obvious.

Distribution of Canonical Ammonia Oxidizers

Among the canonical ammonia oxidizers AOB generally had a lower diversity of *amoA* genes than AOA in the estuarine tidal flat wetlands (**Supplementary Table S4**), was consistent with studies on other estuarine and coastal environments (Jin et al., 2011; Zheng et al., 2014). Temperature was positively correlated with AOA abundance. Significant correlations were also found between salinity and the distribution, but not the abundance, of AOA and AOB. AOB is more abundant than AOA in the northern estuaries with higher salinity, whereas AOA dominated in the regions with lower salinity and higher temperatures, previous studies also verified this result (Mosier and Francis, 2008; Bernhard et al., 2010).

Ammonia-oxidizing archaea detected in the study were divided into two major development branches, sediment group1.1a and soil group1.1b. 78.5% of the AOA sequence obtained belongs to sediment group1.1a, which is the dominant group. Clustered with AOA from sedimentary environments such as estuaries and oceans (Bernhard et al., 2010; Zheng et al., 2013), it is widely distributed in all regions. The remaining 21.5% of the sequences belong to group 1.1b, clustered with AOA in soil environments such as paddy soil and irrigated desert soil (Wang et al., 2015, 2017a), mainly distributed in the north and south estuaries of higher salinity.

Ammonia-oxidizing bacteria is divided into 6 *Nitrosomonas* branches and 2 *Nitrosospira* branches. *Nitrosomonas* under branch OTU637 was the most dominant AOB group in the sediments, accounting for 19.9% of the total sequences. It showed high homology with *Nitrosomonas* sp. Nm143 isolated from saltmarsh sediment (Purkhold et al., 2003; Bernhard et al., 2019), explaining its wide distribution of higher salinity estuaries in the north and south. Among *Nitrosospira* species, we found that a *Nitrosospira*-like branch occupies a dominant position with 89% similarity to the other four pure culture clusters, clustered with some sediment samples in the estuary environment (Jin et al., 2011); further analysis of this strain branch is required. From cluster 3 most OTUs were found exclusively in the Yellow River

estuary in the northern region, which implies the particularity of AOB distribution in this estuary, potentially based on the introduction of soil in the upper Yellow river.

CONCLUSION

Comammox *Nitrospira* was found widely distributed in the estuarine tidal flat wetland of China, but with lower abundances and diversity compared to canonical AOB and AOA. Comammox *Nitrospira* communities were dominated by clade A1, indicating input of river runoff as the main source. The abundance and diversity of comammox *Nitrospira* in tidal flat wetlands of estuaries of China were larger in the central parts than in the South or the North, which was consistent with observed PNRs. The comammox *Nitrospira* community structures were different in southern, central and northern China estuaries. In general, comammox *Nitrospira* is distributed more in estuaries with high runoff and lower salinity. For estuarine tidal flat wetland systems, salinity, pH and iron were important factors affecting the distribution of comammox *Nitrospira*. Ammonia, nitrite and TOC also influence the distribution of comammox *Nitrospira* to some extent. Our findings provide new insights into the distribution of comammox *Nitrospira* in the natural ecosystem, was an important supplement to the biogeochemical Nitrogen cycle.

DATA AVAILABILITY STATEMENT

The datasets presented in this study can be found in online repositories. The names of the repository/repositories and accession number(s) can be found in the article/ **Supplementary Material**.

AUTHOR CONTRIBUTIONS

PH and DS contributed to the development of the research plan and project goals. DS, XT, and MZ performed laboratory work, and contributed to data analysis. XT and ZZ participated in the analysis of the sequencing data. LH, ML, and PH contributed to sources of project funding. BW and UK helped with the data interpretation. DS and PH wrote the manuscript with the input of all other authors. All authors contributed to the article and approved the submitted version.

FUNDING

This work was supported by the National Natural Science Foundation of China (NSFC) (Grant Nos. 41807465, 41725002, 41730646, and 41761144062) and the Chinese National Key Programs for Fundamental Research and Development (No. 2016YFA0600904). UK was supported through the DSWAP project [European Union (Grant: 1822)].

SUPPLEMENTARY MATERIAL

The Supplementary Material for this article can be found online at: https://www.frontiersin.org/articles/10.3389/fmicb.2020.589268/full#supplementary-material

REFERENCES

Abujabhah, I. S., Doyle, R. B., Bound, S. A., and Bowman, J. P. (2018). Assessment of bacterial community composition, methanotrophic and nitrogen-cycling bacteria in three soils with different biochar application rates. *J. Soils Sediments* 18, 148–158. doi: 10.1007/s11368-017-1733-1

Bartelme, R. P., McLellan, S. L., and Newton, R. J. (2017). Freshwater recirculating aquaculture system operations drive biofilter bacterial community shifts around a stable nitrifying consortium of ammonia-oxidizing archaea and comammox *Nitrospira*. *Front. Microbiol.* 8:101. doi: 10.3389/fmicb.2017.00101

Bernhard, A. E., Chelsky, A., Giblin, A. E., and Roberts, B. J. (2019). Influence of local and regional drivers on spatial and temporal variation of ammonia−oxidizing communities in Gulf of Mexico salt marshes. *Environ. Microbiol. Rep.* 11, 825–834. doi: 10.1111/1758-2229.12802

Bernhard, A. E., Landry, Z. C., Blevins, A., José, R., Giblin, A. E., and Stahl, D. A. (2010). Abundance of ammonia-oxidizing archaea and bacteria along an estuarine salinity gradient in relation to potential nitrification rates. *Appl. Environ. Microbiol.* 76, 1285–1289.

Blum, J. M., Su, Q., Ma, Y., Valverde−Pérez, B., Domingo−Félez, C., Jensen, M. M., et al. (2018). The pH dependency of N−converting enzymatic processes, pathways and microbes: effect on net N_2O production. *Environ. Microbiol.* 20, 1623–1640. doi: 10.1111/1462-2920.14063

Camejo, P. Y., Santo Domingo, J., McMahon, K. D., and Noguera, D. R. (2017). Genome-enabled insights into the ecophysiology of the comammox bacterium "*Candidatus* Nitrospira nitrosa". *mSystems* 2:e00059-17. doi: 10.1128/mSystems.00059-17

Cao, W., and Wong, M. H. (2007). Current status of coastal zone issues and management in China: a review. *Environ. Int.* 33, 985–992. doi: 10.1016/j.envint.2007.04.009

Caporaso, J. G., Kuczynski, J., Stombaugh, J., Bittinger, K., Bushman, F. D., Costello, E. K., et al. (2010). QIIME allows analysis of high-throughput community sequencing data. *Nat. Methods* 7, 335–336. doi: 10.1038/nmeth.f.303

Costa, E., Perez, J., and Kreft, J. (2006). Why is metabolic labour divided in nitrification. *Trends. Microbiol.* 14, 213–219. doi: 10.1016/j.tim.2006.03.006

Cui, S., Shi, Y., Groffman, P. M., Schlesinger, W. H., and Zhu, Y. (2013). Centennial-scale analysis of the creation and fate of reactive nitrogen in China (1910-2010). *Proc. Natl. Acad. Sci. U.S.A.* 110, 2052–2057. doi: 10.1073/pnas.1221638110

Daims, H., Lebedeva, E. V., Pjevac, P., Han, P., Herbold, C. W., Albertsen, M., et al. (2015). Complete nitrification by *Nitrospira* bacteria. *Nature* 528, 504–509. doi: 10.1038/nature16461

Dang, H., Li, J., Chen, R., Wang, L., Guo, L., Zhang, Z., et al. (2010). Diversity, abundance, and spatial distribution of sediment ammonia-oxidizing betaproteobacteria in response to environmental gradients and coastal eutrophication in Jiaozhou Bay. *China. Appl. Environ. Microbiol.* 76, 4691–4702. doi: 10.1128/AEM.02563-09

Gao, D., Li, X., Lin, X., Wu, D., Jin, B., Huang, Y., et al. (2017). Soil dissimilatory nitrate reduction processes in the Spartina alterniflora invasion chronosequences of a coastal wetland of southeastern China: dynamics and environmental implications. *Plant. Soil* 421, 383–399. doi: 10.1007/s11104-017-3464-x

Gao, J., Hou, L., Zheng, Y., Liu, M., Yin, G., Li, X., et al. (2016b). nirS-Encoding denitrifier community composition, distribution, and abundance along the coastal wetlands of China. *Appl. Microbiol. Biotechnol.* 100, 8573–8582. doi: 10.1007/s00253-016-7659-5

Gao, J., Hou, L., Zheng, Y., Liu, M., Yin, G., Yu, C., et al. (2016a). Shifts in the community dynamics and activity of ammonia-oxidizing prokaryotes along the yangtze estuarine salinity gradient. *J. Geophys. Res. Biogeol.* 123, 3458–3469. doi: 10.1029/2017JG004182

Hou, L., Yin, G., Liu, M., Zhou, J., Zheng, Y., Gao, J., et al. (2015a). Effects of sulfamethazine on denitrification and the associated N_2O release in estuarine and coastal sediments. *Environ. Sci. Technol.* 49, 326–333. doi: 10.1021/es504433r

Hou, L., Zheng, Y., Liu, M., Li, X., Lin, X., Yin, G., et al. (2015b). Anaerobic ammonium oxidation and its contribution to nitrogen removal in China's coastal wetlands. *Sci. Rep.* 5:15621. doi: 10.1038/srep15621

Hu, H., and He, J. (2017). Comammox-a newly discovered nitrification process in the terrestrial nitrogen cycle. *J. Soils Sediments* 17, 2709–2717. doi: 10.1007/s11368-017-1851-9

Jin, T., Zhang, T., Ye, L., Lee, O. O., Wong, Y. H., and Qian, P. (2011). Diversity and quantity of ammonia-oxidizing archaea and bacteria in sediment of the Pearl River Estuary. *China. Appl. Microbiol. Biot.* 90, 1137–1145. doi: 10.1007/s00253-011-3107-8

Kits, K. D., Sedlacek, C. J., Lebedeva, E. V., Han, P., Bulaev, A., Pjevac, P., et al. (2017). Kinetic analysis of a complete nitrifier reveals an oligotrophic lifestyle. *Nature* 549, 269–272. doi: 10.1038/nature23679

Konneke, M., Bernhard, A. E., La Torre, J. R., Walker, C. B., Waterbury, J. B., and Stahl, D. A. (2005). Isolation of an autotrophic ammonia-oxidizing marine archaeon. *Nature* 437, 543–546. doi: 10.1038/nature03911

Kumar, S., Tamura, K., and Nei, M. (2004). MEGA3: integrated software for molecular evolutionary genetics analysis and sequence alignment. *Brief. Bioinform.* 5, 150–163. doi: 10.1093/bib/5.2.150

Kurola, J., Salkinojasalonen, M., Aarnio, T., Hultman, J., and Romantschuk, M. (2005). Activity, diversity and population size of ammonia-oxidising bacteria in oil-contaminated landfarming soil. *FEMS Microbiol. Lett.* 250, 33–38. doi: 10.1016/j.femsle.2005.06.057

Kuypers, M. M. (2017). Microbiology: a fight for scraps of ammonia. *Nature* 549, 162–163. doi: 10.1038/549162a

Lin, X., Hou, L., Liu, M., Li, X., Zheng, Y., Yin, G., et al. (2016). Nitrogen mineralization and immobilization in sediments of the East China Sea: spatiotemporal variations and environmental implications. *J. Geophys. Res. Biogeo.* 121, 2842–2855.

Lin, X., Liu, M., Hou, L., Gao, D., Li, X., Lu, K., et al. (2017). Nitrogen losses in sediments of the East China Sea: spatiotemporal variations, controlling factors and environmental implications. *J Geophys. Res. Biogeo.* 122, 2699–2715. doi: 10.1002/2017JG004036

Liu, S., Wang, H., Chen, L., Wang, J., Zheng, M., Liu, S., et al. (2020). Comammox *Nitrospira* within the Yangtze River continuum: community, biogeography, and ecological drivers. *ISME J.* 14, 2488–2504. doi: 10.1038/s41396-020-0701-8

Lozupone, C. A., Lladser, M. E., Knights, D., Stombaugh, J., and Knight, R. (2011). UniFrac: an effective distance metric for microbial community comparison. *ISME J.* 5, 169–172. doi: 10.1038/ismej.2010.133

Martens-Habbena, W., Berube, P. M., Urakawa, H., La Torre, J. R., and Stahl, D. A. (2009). Ammonia oxidation kinetics determine niche separation of nitrifying archaea and bacteria. *Nature* 461, 976–979. doi: 10.1038/nature08465

Mohamed, N. M., Saito, K., Tal, Y., and Hill, R. T. (2010). Diversity of aerobic and anaerobic ammonia-oxidizing bacteria in marine sponges. *ISME J.* 4, 38–48. doi: 10.1038/ismej.2009.84

Mosier, A. C., and Francis, C. A. (2008). Relative abundance and diversity of ammonia-oxidizing archaea and bacteria in the San Francisco Bay estuary. *Environ. Microbiol.* 10, 3002–3016.

Oksanen, J., Blanchet, F. G., Kindt, R., Legendre, P., Minchin, P. R., O'hara, R., et al. (2013). *Vegan: Community Ecology Package, R Package Version 2.0.* Available online at: http://CRAN.Rproject.org/package=vegan

Palomo, A., Fowler, S. J., Gulay, A., Rasmussen, S., Sicheritzponten, T., and Smets, B. F. (2016). Metagenomic analysis of rapid gravity sand filter microbial communities suggests novel physiology of *Nitrospira* spp. *ISME J.* 10, 2569–2581. doi: 10.1038/ismej.2016.63

Pester, M., Rattei, T., Flechl, S., Grongroft, A., Richter, A., Overmann, J., et al. (2012). *AmoA*-based consensus phylogeny of ammonia-oxidizing archaea and deep sequencing of *amoA* genes from soils of four different geographic regions. *Environ. Microbiol.* 14, 525–539.

Pinto, A. J., Marcus, D. N., Ijaz, U. Z., Bautista-de lose Santos, Q. M., Dick, G. J., and Raskin, L. (2016). Metagenomic evidence for the presence of comammox *Nitrospira*-like bacteria in a drinking water system. *mSphere* 1:e00054-15. doi: 10.1128/mSphere.00054-15

Pjevac, P., Schauberger, C., Poghosyan, L., Herbold, C. W., Van Kessel, M. A., Daebeler, A., et al. (2017). *AmoA*-Targeted polymerase chain reaction primers for the specific detection and quantification of comammox *Nitrospira* in the environment. *Front. Microbiol.* 8:1508. doi: 10.3389/fmicb.2017.01508

Purkhold, U., Pommereningroser, A., Juretschko, S., Schmid, M., Koops, H., and Wagner, M. (2000). Phylogeny of all recognized species of ammonia oxidizers based on comparative 16S rRNA and *amoA* sequence analysis: implications for molecular diversity surveys. *Appl. Environ. Microbiol.* 66, 5368–5382. doi: 10.1128/AEM.66.12.5368-5382.2000

Purkhold, U., Wagner, M., Timmermann, G., Pommereningroser, A., and Koops, H. (2003). 16S rRNA and *amoA*-based phylogeny of 12 novel betaproteobacterial ammonia-oxidizing isolates: extension of the dataset and proposal of a new lineage within the nitrosomonads. *Int. J. Syst. Evol. Micr.* 53, 1485–1494. doi: 10.1099/ijs.0.02638-0

R Core Team (2013). *R: A Language and Environment for Statistical Computing*. Vienna: R Foundation for Statistical Computing.

Ren, X., Bi, X., Cheng, L., Zhu, Z., and Chang, G. (2011). Research on enhanced biological nitrogen and phosphorus removal by compound ferric enzymatic actived sludge (in Chinese). *China Water Wastewater* 17, 24–28.

Roden, E. E., and Lovley, D. R. (1993). Evaluation of 55Fe as a tracer of Fe (III) reduction in aquatic sediments. *Geomicrobiol. J.* 11, 49–56. doi: 10.1080/01490459309377931

Rotthauwe, J. H., Witzel, K. P., and Liesack, W. (1997). The ammonia monooxygenase structural gene *amoA* as a functional marker: molecular fine-scale analysis of natural ammonia-oxidizing populations. *Appl. Environ. Microbiol.* 63, 4704–4712. doi: 10.1128/aem.63.12.4704-4712.1997

Santoro, A. E. (2016). The do-it-all nitrifier. *Science* 351, 342–343.

Santos, J. P., Mendes, D., Monteiro, M., Ribeiro, H., Baptista, M. S., Borges, M., et al. (2017). Salinity impact on ammonia oxidizers activity and *amoA* expression in estuarine sediments. *Estuar. Coast. Shelf S* 211, 177–187. doi: 10.1016/j.ecss.2017.09.001

Schloss, P. D. (2013). Secondary structure improves OTU assignments of 16S rRNA gene sequences. *ISME J.* 7, 457–460. doi: 10.1038/ismej.2012.102

Shi, Y., Jiang, Y., Wang, S., Wang, X., and Zhu, G. (2020). Biogeographic distribution of comammox bacteria in diverse terrestrial habitats. *Sci. Total. Environ.* 717, 137257.

Tamura, K., Dudley, J., Nei, M., and Kumar, S. (2007). MEGA4: molecular evolutionary genetics analysis (MEGA) software version 4.0. *Mol. Biol. Evol.* 24, 1596–1599. doi: 10.1093/molbev/msm092

Tatari, K., Musovic, S., Gulay, A., Dechesne, A., Albrechtsen, H., and Smets, B. F. (2017). Density and distribution of nitrifying guilds in rapid sand filters for drinking water production: dominance of *Nitrospira* spp. *Water Res.* 127, 239–248. doi: 10.1016/j.watres.2017.10.023

ter Braak, C. J. F., and Smilauer, P. (2002). *CANOCO Reference Manual and CanoDraw for Windows User's Guide: Software for Canonical Community Ordination (version 4.5). (Microcomputer Power)*. Ithaca NY: Canoco.

Thompson, J. D., Gibson, T. J., Plewniak, F., Jeanmougin, F., and Higgins, D. G. (1997). The CLUSTAL_X windows interface: flexible strategies for multiple sequence alignment aided by quality analysis tools. *Nucleic. Acids. Res.* 25, 4876–4882. doi: 10.1093/nar/25.24.4876

Urakawa, H., Tajima, Y., Numata, Y., and Tsuneda, S. (2008). Low temperature decreases the phylogenetic diversity of ammonia-oxidizing archaea and bacteria in aquarium biofiltration systems. *Appl. Environ. Microbiol.* 74, 894–900. doi: 10.1128/AEM.01529-07

van Kessel, M. A., Speth, D. R., Albertsen, M., Nielsen, P. H., den Camp, H. J. O., Kartal, B., et al. (2015). Complete nitrifification by a single microorganism. *Nature* 528, 555–559. doi: 10.1038/nature16459

Wang, B., Zhao, J., Guo, Z., Ma, J., Xu, H., and Jia, Z. (2015). Differential contributions of ammonia oxidizers and nitrite oxidizers to nitrification in four paddy soils. *ISME J.* 9, 1062–1075. doi: 10.1038/ismej.2014.194

Wang, J. C., Wang, J. L., Rhodes, G., He, J. Z., and Ge, Y. (2019). Adaptive responses of comammox *Nitrospira* and canonical ammonia oxidizers to long-term fertilizations: implications for the relative contributions of different ammonia oxidizers to soil nitrogen cycling. *Sci. Total. Environ.* 668, 224–233. doi: 10.1016/j.scitotenv.2019.02.427

Wang, X., Ren, N., Wang, A., and Ma, F. (2003). Study on the effect of iron and manganese iron from nitration. (in Chinese). *J. Harbin Inst. Tech.* 35, 122–125.

Wang, Y., Li, J., Zhai, S., and Feng, J. (2013). Effect of Fe0 on acrylic fiber wastewater treatment in SBBR. (in Chinese). *J.Chem. Ind. Eng.* 64, 2996–3002. doi: 10.3969/j.issn.0438-1157.2013.08.042

Wang, Y., Liu, Y., Liu, R., Zhang, A., Yang, S., Liu, H., et al. (2017b). Biochar amendment reduces paddy soil nitrogen leaching but increases net global warming potential in Ningxia irrigation. *China. Sci. Rep.* 7:1592. doi: 10.1038/s41598-017-01173-w

Wang, Y., Ma, L., Mao, Y., Jiang, X., Xia, Y., Yu, K., et al. (2017a). Comammox in drinking water systems. *Water Res.* 116, 332–341. doi: 10.1016/j.watres.2017.03.042

Wei, H., Gao, D., Liu, Y., and Lin, X. (2020). Sediment nitrate reduction processes in response to environmental gradients along an urban river-estuary-sea continuum. *Sci. Total. Environ.* 718:137185. doi: 10.1016/j.scitotenv.2020.137185

Winogradsky, S. (1890). The morphology of the contributions of nitrification system. *Arch. Biol. Sci.* 4, 257–275.

Xia, F., Wang, J., Zhu, T., Zou, B., Rhee, S., and Quan, Z. (2018). Ubiquity and diversity of complete ammonia oxidizers (comammox). *Appl. Environ. Microbiol.* 84:e01390-18.

Xu, S., Wang, B., Li, Y., Jiang, D., Zhou, Y., Ding, A., et al. (2020). Ubiquity, diversity, and activity of comammox *Nitrospira* in agricultural soils. *Sci. Total. Environ.* 706:135684. doi: 10.1016/j.scitotenv.2019.135684

Yu, C., Hou, L., Zheng, Y., Liu, M., Yin, G., Gao, J., et al. (2018). Evidence for complete nitrification in enrichment culture of tidal sediments and diversity analysis of clade a comammox *Nitrospira* in natural environments. *Appl. Microbiol. Biot.* 102, 9363–9377. doi: 10.1007/s00253-018-9274-0

Zhang, S., Xia, X., Li, S., Zhang, L., Wang, G., Li, M., et al. (2019). Ammonia oxidizers in high-elevation rivers of the Qinghai-tibet plateau display distinctive distribution patterns. *Appl. Environ. Microbiol.* 85:e01701-19. doi: 10.1128/AEM.01701-19

Zhang, X., Peng, D., Wang, Z., and Yuan, L. (2002). Influence of organic matters on nitrification at low DO in biological turbulent bed reactor. *China Water Wastewater* 5, 10–13. doi: 10.1007/s11769-002-0041-9 (in Chinese).

Zhao, Z., Huang, G. H., He, S., Zhou, N., Wang, M., Dang, C., et al. (2019). Abundance and community composition of comammox bacteria in different ecosystems by a universal primer set. *Sci. Total. Environ.* 691, 146–155. doi: 10.1016/j.scitotenv.2019.07.131

Zheng, Y., Hou, L., Liu, M., Lu, M., Zhao, H., and Yin, G. (2013). Diversity, abundance, and activity of ammonia-oxidizing bacteria and archaea in Chongming eastern intertidal sediments. *Appl. Microbiol. Biot.* 97, 8351–8363. doi: 10.1007/s00253-012-4512-3

Zheng, Y., Hou, L., Newell, S. E., Liu, M., Zhou, J., Zhao, H., et al. (2014). Community dynamics and activity of ammonia-Oxidizing prokaryotes in intertidal sediments of the Yangtze estuary. *Appl. Environ. Microbiol.* 80, 408–419. doi: 10.1128/AEM.03035-13

Conflict of Interest: The authors declare that the research was conducted in the absence of any commercial or financial relationships that could be construed as a potential conflict of interest.

frontiers in Microbiology

ORIGINAL RESEARCH
published: 26 November 2020
doi: 10.3389/fmicb.2020.574815

The Response of Estuarine Ammonia-Oxidizing Communities to Constant and Fluctuating Salinity Regimes

João Pereira Santos[1,2], António G. G. Sousa[1], Hugo Ribeiro[1,3] and Catarina Magalhães[1,4,5,6]*

[1] Centro Interdisciplinar de Investigação Marinha e Ambiental (CIIMAR), Universidade do Porto, Terminal de Cruzeiros do Porto de Leixões, Matosinhos, Portugal, [2] Department F.A. Forel for Environmental and Aquatic Sciences, Section of Earth and Environmental Sciences, Institute for Environmental Sciences, University of Geneva, Geneva, Switzerland, [3] Abel Salazar Institute of Biomedical Sciences, University of Porto (ICBAS-UP), Porto, Portugal, [4] Faculdade de Ciências, Universidade do Porto, Porto, Portugal, [5] School of Science & Engineering, University of Waikato, Hamilton, New Zealand, [6] Ocean Frontier Institute, Dalhousie University, Halitax, NS, Canada

OPEN ACCESS

Edited by:
Laura E. Lehtovirta-Morley, University of East Anglia, United Kingdom

Reviewed by:
Li-mei Zhang, Chinese Academy of Sciences, China
Silvia Newell, Wright State University, United States

***Correspondence:**
João Pereira Santos
joaofs21@gmail.com

Specialty section:
This article was submitted to Microbiological Chemistry and Geomicrobiology, a section of the journal Frontiers in Microbiology

Received: *21 June 2020*
Accepted: *02 November 2020*
Published: *26 November 2020*

Citation:
Santos JP, Sousa AGG, Ribeiro H and Magalhães C (2020) The Response of Estuarine Ammonia-Oxidizing Communities to Constant and Fluctuating Salinity Regimes. Front. Microbiol. 11:574815. doi: 10.3389/fmicb.2020.574815

Aerobic nitrification is a fundamental nitrogen biogeochemical process that links the oxidation of ammonia to the removal of fixed nitrogen in eutrophicated water bodies. However, in estuarine environments there is an enormous variability of water physicochemical parameters that can affect the ammonia oxidation biological process. For instance, it is known that salinity can affect nitrification performance, yet there is still a lack of information on the ammonia-oxidizing communities behavior facing daily salinity fluctuations. In this work, laboratory experiments using upstream and downstream estuarine sediments were performed to address this missing gap by comparing the effect of daily salinity fluctuations with constant salinity on the activity and diversity of ammonia-oxidizing microorganisms (AOM). Activity and composition of AOM were assessed, respectively by using nitrogen stable isotope technique and 16S rRNA gene metabarcoding analysis. Nitrification activity was negatively affected by daily salinity fluctuations in upstream sediments while no effect was observed in downstream sediments. Constant salinity regime showed clearly higher rates of nitrification in upstream sediments while a similar nitrification performance between the two salinity regimes was registered in the downstream sediments. Results also indicated that daily salinity fluctuation regime had a negative effect on both ammonia-oxidizing bacteria (AOB) and ammonia-oxidizing archaea (AOA) community's diversity. Phylogenetically, the estuarine downstream AOM were dominated by AOA (0.92–2.09%) followed by NOB (0.99–2%), and then AOB (0.2–0.32%); whereas NOB dominated estuarine upstream sediment samples (1.4–9.5%), followed by AOA (0.27–0.51%) and AOB (0.01–0.23%). Analysis of variance identified the spatial difference between samples (downstream and upstream) as the main drivers of AOA and AOB diversity. Our study indicates that benthic AOM inhabiting different estuarine sites presented distinct plasticity toward

the salinity regimes tested. These findings help to improve our understanding in the dynamics of the nitrogen cycle of estuarine systems by showing the resilience and consequently the impact of different salinity regimes on the diversity and activity of ammonia oxidizer communities.

Keywords: salinity, nitrification (*amoA* AOA, *amoA* AOB), ^{15}N isotope, 16S rRNA gene, AOB and AOA, estuarine communities

INTRODUCTION

Nitrification, the oxidation of ammonium (NH_4^+) to nitrite (NO_2^-), and subsequently to nitrate (NO_3^-), plays an important role in the nitrogen (N) cycle (Kowalchuk and Stephen, 2001; Prosser and Embley, 2002). This process represents a critical link between mineralization of organic matter and the loss of fixed N via coupled nitrification–denitrification (Marchant et al., 2016; Zhu et al., 2018) and nitrification–anammox (Fernandes et al., 2016), being responsible for the removal of anthropogenic N in estuarine and marine environments. Nowadays, three functional groups of nitrifying prokaryotes have been identified based on their capacity to perform the nitrification process. The first group, which oxidizes ammonia or ammonium to nitrite (first step of the nitrification), are represented by the ammonia-oxidizing bacteria (AOB) with species within the β- and γ-*Proteobacteria* classes (Purkhold et al., 2000; Junier et al., 2010), and the ammonia-oxidizing archaea (AOA) represented by species affiliated with the *Thaumarchaeota* phylum (Stahl and de la Torre, 2012). The second group of microorganisms oxidizes nitrite to nitrate (second step of the nitrification), hence being identified as the nitrite-oxidizing bacteria (NOB). NOB are a phylogenetically heterogeneous group with species within the *Proteobacteria* (classes Alpha, Beta, and Gamma), *Nitrospirae*, *Nitrospinae*, and *Chloroflexi* (Daims et al., 2016). The third group is characterized by species able to perform the complete oxidation of ammonia to nitrate also known as comammox (Daims et al., 2015; van Kessel et al., 2015), with species within the *Nitrospirae* phylum (Lawson and Lucker, 2018).

Several studies have demonstrated that both archaeal and bacterial ammonia oxidizers are present in estuarine sediments (Magalhaes et al., 2007; Mosier and Francis, 2008; Monteiro et al., 2017; Zhu et al., 2018), with some areas dominated by AOA (Bernhard et al., 2010) and others by AOB (Li et al., 2015). Differences between AOA and AOB ratios have been linked to the elevated variability in terms of hydrodynamic, physical and chemical conditions observed in estuarine and intertidal sediments (Magalhães et al., 2009; Monteiro et al., 2017). In fact, key environmental factors thought to impact the distribution and activity of ammonia-oxidizing prokaryotes have been reported, and includes nitrogen forms (Dang et al., 2010; Sudarno et al., 2011), temperature (Sahan and Muyzer, 2008; Zeng et al., 2014), oxygen (Liu and Wang, 2015), pH (Guo et al., 2017), salinity (Bernhard et al., 2007; Zhang et al., 2015c; Santos et al., 2018), anthropogenic pollutants, like heavy metals (Beddow et al., 2016) among others. In the particular case of salinity, the high gradients of salinity along the estuarine areas have been shown to affect the magnitudes of nitrification rates (Berounsky and Nixon, 1993; Bernhard et al., 2007) by playing a major role in controlling NH_4^+ adsorption capacity of the sediment (Rysgaard et al., 1999; Weston et al., 2010). Also, salinity limits the distribution and functionality of the ammonia oxidizers by affecting their activity (Santos et al., 2018), abundance (Li et al., 2015), and diversity (Zhang et al., 2015c). Several studies have shown spatial differences in terms of nitrification activity in estuarine systems, with downstream communities displaying higher tolerance to salinity in comparison with upstream communities (Bernhard et al., 2007; Wang and Gu, 2014; Zhang et al., 2015c; Monteiro et al., 2017; Santos et al., 2018).

In terms of the key players involved in the nitrification process, previous studies showed some contradictory results in terms of AOA/AOB ratios across salinity gradient (Santoro et al., 2008; Bernhard et al., 2010; Li et al., 2015), suggesting the action of other parameters in ruling the prevalence of AOA or AOB (e.g., NH_4^+ levels). Despite the efforts to understand the dynamics of this process in estuarine systems, it is still unclear how the environmental parameters along the estuarine gradient control ammonia oxidizers diversity and activity. For instance, there is a lack of information about how the effect of short-term salinity fluctuation, experienced in estuarine systems, will influence the ammonia oxidation and the organisms that mediate this transformation. Yet, estuarine ammonia-oxidizing microorganisms (AOM) are exposed to different magnitudes of daily salinity fluctuations (Giblin et al., 2010; Yan et al., 2015), which varies according to the estuary location (e.g., upper estuary has low salinity variation compared with lower estuary).

In this study, we isolated through a controlled laboratory experiment, the effect of different salinity regimes (constant and daily fluctuation) on the activity and diversity of AOM from upstream and downstream estuarine sediments. We hypothesize that AOM sediments from upstream (Crestuma) and downstream (Afurada) estuarine locations would display distinct resilience toward short term salinity fluctuations.

MATERIALS AND METHODS

Site Description and Sample Collection

The Douro River estuary is a mesotidal estuary with 21.6 km long located on the northwest coast of Portugal (Vieira and Bordalo, 2000). It is located in a highly urbanized area, promoting several anthropogenic activities, and consequently the increase of pollutants in water and sediments (Madureira et al., 2010; Cruzeiro et al., 2017; Ribeiro et al., 2018). In July 2015, intertidal sediments from two sites (Afurada and Crestuma)

along the salinity gradient of the Douro River estuary were collected. Afurada (AF) is located in the downstream estuary, being characterized by a highly dynamic site with marked daily salinity changes due to the influence of coastal Atlantic saltwater. Crestuma (CR) is located in the upstream estuary and highly influenced by freshwater riverine input. Information about the *in situ* physical and chemical characteristics of Douro River estuary and more precisely Afurada and Crestuma locations have been reported previously in other studies (Monteiro et al., 2017; Santos et al., 2018).

Surface sediments (2 cm depth) were randomly collected from 10 sub-locations of each site (approximately 5 kg), homogenized in sterile plastic boxes (10 L) and stored in refrigerated ice chests. In the laboratory, sub-samples of homogenized sediment were collected into sterile plastic bags (VWR Sterile Sample Bags) and stored at −80°C for later DNA extraction, while other sub-samples were used to set up the different salinity regimes experiments. Water used for the incubation experiment was collected from the Douro River (around 1200 L) using a firetruck and stored in appropriated and cleaned tanks at CIIMAR.

Experimental Setup

Experiments were designed to simulate different salinity regimes which consisted of two salinity treatments *per* site (AF and CR) in triplicate. The two salinity regimes consisted of a constant salinity treatment (with salinity at 0 psu for CR (upstream) sediments and with salinity at 15 psu for AF (downstream) sediments) based on the predominant site salinity characteristics (Santos et al., 2018), and a salinity fluctuation treatment which consisted on gradual daily oscillations between salinities of 0, 15, and 30 psu. The sediments subjected to a constant salinity regime of 0 and 15 psu were labeled as CR_C and AF_C, respectively for CR and AF sediment reactors. The AF and CR sediments under the salinity fluctuation regime were labeled as CR_Δ and AF_Δ, respectively.

An autonomous water agitation system was built with 12 acrylic reactors, each with 14 cm diameter and 33 cm height (**Supplementary Figure S1**), with a rotation set at 32 rpm to maintain water homogenized and oxygenized. The photoperiod was simulated, starting at 7:30 am and switching off at 7:30 pm. All materials in contact with water and sediments were acid cleaned (10% HCl) before the beginning of the experiment. The sediments from upstream (CR) and downstream (AF) locations were added to six reactors (final volume of 708.47 cm^3, 10 cm depth) in a total of 12 reactors. Douro River water (1.2 L) adjusted to the desired salinities (0, 15, and 30 psu) with marine salts (Tropic Marin) and supplemented with 20 μM of NH_4Cl was also added to each reactor. Every 12 h, this water (1.2 L) was renewed in each treatment (constant and fluctuation) with its respective salinity and NH_4Cl supplementation. The water used for the incubations had a pH of 8.14, and the following nutrients concentrations: 111.3 μM of NO_3^-, 0.1 μM of NO_2^- and 0.1 μM of NH_4^+/NH_3. Salinity and water temperature were monitored before water renewal using a conductivity meter CO 310 (VWR Collection).

In the 30th day of incubation, the renewed 1.2 L water was supplemented with 20 μM of labeled $[^{15}N]H_4Cl$ to measure nitrification rates directly in the reactors (Denk et al., 2017; Xia et al., 2017; Jäntti et al., 2018). Site sediment treatments had the same salinity (Afurada treatments = 15 psu and Crestuma treatments = 0 psu) when exposed to labeled $^{15}NH_4Cl$.

After 36 days of incubation, composed surface sediment samples (2 cm depth) from the triplicate reactors (CR_C, CR_Δ, AF_C, and AF_Δ) were also collected to measure nitrification activity by performing slurries incubations. For those measurements both CR sediments were incubated with water at salinity of 0 psu, while AF sediments were incubated with salinity at 15 psu. To each 100 mL serum bottle, it was added 35.3 ± 1.2 g of wet weight of sediment. Water (50 mL) was amended with 100 μM of $[^{15}N]H_4^+$ to measure nitrification rates in the different conditions (constant vs. fluctuation).

In both cases, 8 mL of overlying water was collected from each slurry after 2 h of incubation, centrifuged at 420 × *g* (Compact Star CS4), filtered at 0.2 μm (VWR Syringe Filters) and stored at −20°C for later isotopic analyses. During incubation, serum flasks were held in a dark room at constant temperature (20°C) with constant agitation at 100 rpm.

Chemical Analysis

Nitrification Rates

Potential nitrification rates were measured using the stable isotope technique, where samples were amended with $[^{15}N]H_4^+$ and the production of $[^{15}N]O_2^-$ and $[^{15}N]O_3^-$ were measured, giving an estimate of the potential uncoupled nitrification occurring in the water. The analyses were determined using the denitrifier method (Sigman et al., 2001) at Appalachian Lab, University of Maryland. Potential nitrification rates were calculated based on the $[^{15}N]$ fractional change ($R\frac{15}{14}N$) after 2 h of incubation, and the $[NO_3^-]$ and $[NO_2^-]$ existent at the same period, using the equation described by Jantti et al. (2012).

$$N[\mu molNx^{-x}h^{-1}] = (([NO_3^- + NO_2^-] \times vol)/ \text{weigth or area}) \times R\frac{15}{14}N)/\Delta t$$

where N correspond to the potential uncoupled nitrification, $[NO_3^- + NO_2^-]$ is the NO_3^- and NO_2^- concentration at the end of the incubation (μM), vol is the volume of water in the system (L), weight is the weight of sediment in the slurries (x = g) and area is the area corresponding to the reactors (x = cm^2), $R\frac{15}{14}N$ is the ratio between atom 15 and atom 14 in the samples after 2 h of incubation, Δt is the incubation time (2 h).

Molecular Analysis

Nucleic Acid Extraction and Quantification

Total DNA was extracted from 0.5 g wet weight of homogenized sediment (from *in situ* AF and CR sediments, as well as from each reactor at the end of the salinity regimes experiment) using the PowerSoil DNA isolation kit (MoBio Laboratories Inc., Solana Beach, CA, United States). Similarly, total RNA was extracted from 2 g wet weight of homogenized sediment from each reactor at the end of the salinity regimes experiment using the Power Soil RNA isolation kit (MoBio Laboratories Inc.) according to

MoBio instructions. DNA was digested from the RNA pool by being treated with 1 U μL^{-1} of DNase I (Sigma) using DNA- and RNA-free reagents, followed by PCR using general 16S rRNA gene bacterial primers to check for traces of genomic DNA contamination. Reverse transcription (RT) was performed using the Omniscript RT kit (Qiagen) by adding 13 μL of total RNA to an 18 μL RT mixture following the manufacturer's instructions. The DNA and cDNA were quantified by the Qubit® dsDNA HS assay and Qubit® ssDNA Kit (Life Technologies), respectively, according to manufacturer's instructions.

Next-Generation Sequencing of the 16S rRNA Gene Amplicons

DNA extracted from sediment samples from AF and CR at the beginning of the experiment (AF_i and CR_i) as well as from two of the triplicate reactors subjected to the different salinity regimes (AF_C, CR_C, AF_△, and CR_△) was used for sequencing the 16S rRNA gene. The primer set 515F-Y (5′-GTGYCAGCMGCCGCGGTAA-3′) (Caporaso et al., 2012) and 926R (5′-CCGYCAATTYMTTTRAGTTT-3′) (Parada et al., 2016) targeting the V4-V5 region of the archaeal and bacterial 16S rRNA genes was used to assess the whole prokaryotic community diversity (Wear et al., 2018). This primer set yielded accurate estimates of complex prokaryotic mock communities increasing the *Thaumarchaeota* coverage relatively to other primer sets (Parada et al., 2016). Although 16S rRNA primers will not cover the entire diversity of ammonia oxidizers, the monophyly of most of AOA and AOB groups facilitate the use of 16S rRNA gene to study the diversity of ammonia oxidizers, being its phylogeny mostly congruent with *amoA* gene phylogeny (Alves et al., 2018). Amplicons were used to build Illumina paired-end libraries (2 × 300 bp) sequenced on an Illumina MiSeq platform using V3 Chemistry (Illumina). These steps were carried out by LGC Genomics (LGC Genomics GmbH, Berlin, Germany).

PCR Amplification and Denaturing Gradient Gel Electrophoresis (DGGE)

PCR amplification of β-proteobacterial *amoA* genes and transcript fragments were performed using the primer set amoA-1F (5′-GGGGTTTCTACTGGTGGT) with a GC clamp (CGCCCGCCGCGC CCCGCGCCCGGCCCGCCGCCC CCGCCCC) (Muyzer et al., 1993) and amoA-2R (5′-CC CCTCKGSAAAGCCTTCTTC) (Rotthauwe et al., 1997). For the amplification of fragments of archaeal *amoA*, it was used the primer set CrenamoA23f (5′-ATGGTCTGGCTWAGACG) and CrenamoA616r (5′-GCCATCCATCTGTATGTCCA) (Tourna et al., 2008). All conditions used were the same described in Santos et al. (2018).

The denaturing gradient gel electrophoresis (DGGE) technique was performed using a DCode Universal Mutation Detection System (Bio-Rad, Hertfordshire, United Kingdom). The conditions were established according to Yamamoto et al. (2010). Afterward, gels were silver stained based on Karpouzas and Singh (2010) and scanned using a GS-800 Calibrated Densitometer (Bio-Rad, Hertfordshire, United Kingdom). The DGGE gel images were converted to a densitometry scan and aligned using image analysis software (Quantity One software). The software records a density profile through each DGGE lane, detects the bands, and calculates the relative contribution of each band to the total band signal in the lane after applying a rolling disk function as background subtraction. Then, values corresponding to the band position were imported into the Primer 6 software package (version 6.1.11) (Clarke and Gorley, 2006). Based on the presence/absence of individual bands in each lane, a binary matrix was created using Primer 6 and hierarchical cluster analysis based on Bray–Curtis similarity (Clarke and Warwick, 2001). DGGE results and the respective gel profiles images can be found in **Supplementary Figures S2–S6**.

Data Analysis

Statistical Analysis

Data from the nitrification rates were analyzed in triplicate for all relevant parameters. Data were tested for normality using the Kolmogorov–Smirnov test, and for homoscedasticity using Levene's test. In both tests the null hypothesis was not rejected (P-value > 0.5) meaning that the data is not statistically different from a normal distribution with equal variance across the groups being compared. Significant differences between pairwise means were assessed using t-tests. All analyses were performed at the 95% confidence level and the statistical tests were performed using the software STATISTICA (version 13, StatSoft, Inc.).

Bioinformatic Analysis of NGS 16S rRNA Gene Amplicons

16S rRNA gene amplicons from different samples were sequenced in three different sequencing runs: run 1 (samples AF_C1, AF_C2, AF_Δ2, CR_C2, CR_Δ2), run 2 (AF_Δ1, CR_C3, CR_Δ1), and run 3 (AF_i and CR_i). Primer clipped forward and reverse fastq files were imported, filtered, truncated, trimmed, merged and denoised using DADA2 package (v.1.14.0) (Callahan et al., 2016) implemented in R (v.3.4.1) (R Core Team, 2017). Forward and reverse reads were truncated according to the quality of each sequencing run: 200 and 190 bp for the run 1, 200 and 200 bp for the run 2, and 220 and 220 bp for the run 3. Reads with ambiguities (i.e., N) were discarded and filtered with a truncation quality score of two and maximum expected error of eight for both reads. Then, forward and reverse fastq reads were dereplicated into unique reads and pooled independently for each run to estimate the error rates using the default $1e^8$ number of bases (randomized) and to denoize sequences into Amplicon Sequence Variants (ASV). The denoised unique forward and reverse reads were merged using the default parameters (without allowing mismatches and with a minimum overlap of 12 bp) and the sequences out of the target range (367–377 bp) were discarded. Chimeras were removed using the consensus method implemented in the DADA2 R package (v.1.14.0). Finally, the ASVs were taxonomically classified against the SILVA SSU Ref NR database (v.132) (Quast et al., 2013) using the RDP Naive Bayesian Classifier algorithm (Wang et al., 2007; Callahan, 2018) with a minimum bootstrap confidence for assigning a taxonomic level of 60%. Additionally, the ASVs that matched exactly with one reference fasta sequence within the SILVA database were classified until the species level.

The ASVs fasta sequences were imported to QIIME2 (v.2018.4) (Bolyen et al., 2019) to use the available plugins to build a phylogenetic tree. First, MAFFT (v.7) (Katoh and Standley, 2013) plugin was used to perform a multiple sequence alignment (MSA). The MSA was masked to eliminate the highly variable positions and the masked MSA was used to build a maximum-likelihood tree with FastTree 2 (Price et al., 2010) plugin. Ultimately, the phylogenetic tree was rooted through the midpoint rooting method.

The ASV table, taxonomy table and phylogenetic tree were imported to the phyloseq R package (v.1.28.0) (McMurdie and Holmes, 2013) in order to perform beta-diversity analyses. Whereas the beta-diversity metrics estimated were the unweighted and weighted UniFrac (Lozupone and Knight, 2005; Lozupone et al., 2007) visualized through the Principal Coordinate Analysis (PCoA) method. For beta-diversity analysis, the compositional table of ASVs was transformed in the following way: ASVs that appeared less than six times, in less than three samples were excluded; sequence reads *per* sample were transformed to counts *per* million; and kept only the top 10 phyla (*Proteobacteria, Bacteroidetes, Planctomycetes, Cyanobacteria, Acidobacteria, Nitrospirae, Thaumarchaeota, Gemmatimonadetes, Verrucomicrobia, and Chloroflexi*). This represents in average *ca.* 85% of reads in relation to the initial number of sequences. The final plots were visualized and compiled using the ggplot2 (v.3.3.0) (Wickham, 2009) and the gridExtra (v.2.3) (Auguie and Antonov, 2017) R packages, respectively. Multivariate homogeneity of groups dispersions and permutational multivariate analysis of variance of unweighted and weighted UniFrac distance matrices were performed to assess the within- and between-group variation with the *betadisper*() and *adonis()* functions from the vegan (v. 2.5.6) R package (Oksanen et al., 2018). It was only rejected the null hypothesis of the second test, when the null of the first was not rejected, i.e., only when there was not found statistically significant differences within-group variation, it was tested between-group variation hypothesis.

Nitrifying ASVs were retrieved by searching the "*Nitro*" prefix throughout all the taxonomic levels (from phylum to genus). Then, the putative nitrifying taxa were manually checked. The ASV_3095 and ASV_6335 classified as *Methylophaga* (genus), the ASV_3517 as *Leptospirillum* (genus) and ASV_6835 as *Thermodesulfovibrionia* (until class) were removed because do not constitute potential nitrifying taxa and due to the lack of confidence. In addition, all unclassified ASVs at genus level or environmental clones/sequences were also removed due to the lack of confidence.

Sequences data sets from 16S rRNA amplicon used in this study were deposited in the European Nucleotide Archive under the project accession number PRJEB38114.

RESULTS

Experimental System

Sediments exposure to different salinity regimes was performed at room temperature (18.8 ± 2.2°C) during 36 days. Water temperature and salinity measurements from the different reactors (AF_C, CR_C, AF_Δ, and CR_Δ) are presented in **Supplementary Table S1**. Salinity was maintained steady, with minor variations in constant treatments triplicate reactors (AF_C and CR_C). On salinity fluctuation treatments (AF_Δ and CR_Δ), the salinity ranged between 1.2 and 29.3 psu in the upstream sediments reactors (Crestuma) and between 1.5 and 29.3 psu in the sediment reactors from downstream station (Afurada).

Potential Nitrification Rates

Nitrification rates in constant (AF_C and CR_C) and fluctuation (AF_Δ, CR_Δ) conditions were estimated directly in the reactors (**Figures 1A,B**) as well as in sediment slurries incubations (**Figures 1C,D**). Nitrification measurements in the reactors and in sediment slurries were comparable, with estuarine downstream sediments (AF) presenting similar (t-test, $P \geq 0.05$) nitrification rates between the two salinity regimes tested (AF_C and AF_Δ) (**Figures 1A,C**). In contrast, nitrification rates under the constant salinity regime in the upstream site (CR) were significantly (t-test, $P < 0.05$) higher than those subjected to the fluctuating salinity regime (CR_Δ). Again, these results were similar for direct reactors measurements and for slurries incubations (**Figures 1B,D**). Nitrification rates measured directly in the reactors and in slurries for each salinity treatment are presented in **Supplementary Tables S2**, **S3**, respectively.

Denaturing Gradient Gel Electrophoresis of Archaeal and Bacterial *amoA* Genes and Transcripts

Fingerprinting analysis of the archaeal and bacterial *amoA* gene fragments (DNA) and transcripts (cDNA) of Afurada (AF_i, AF_Δ and AF_C) and Crestuma (CR_i, CR_Δ and CR_C) sediments are presented in **Supplementary Figures S2**, **S3**.

For the constant salinity treatment, results from the downstream sediments (AF) showed that DGGE bands of AOA genes and transcripts decreased compared to the initial samples (Figure S2A). However, in the salinity fluctuation treatment, the number of DGGE bands from AOA genes and transcripts remained similar to the initial samples (Figure S2A). In the upstream (CR) sediments higher number of DGGE bands of AOA genes were found in the constant salinity treatment compared with the salinity fluctuation regime (t-test, $P < 0.05$; Figure S2B). DGGE profiles of archaeal *amoA* gene transcripts were also more diverse in the constant salinity treatment compared with the salinity fluctuation regime.

In AF sediments, the DGGE profile (Figure S3A) of bacterial *amoA* gene showed differences (t-test, $P < 0.05$) between the number of DGGE bands of *amoA* gene fragments exposed to the different salinity regimes (AF_C and AF_Δ). However, similar (t-test, $P \geq 0.05$) number of DGGE bands of AOB *amoA* transcripts was observed for AF_Δ treatment and constant salinity regime. In CR sediments, a clear increase (t-test, $P < 0.05$) of the DGGE bands of the bacterial *amoA* gene were observed between CR_i, CR_C, and CR_Δ. However, in

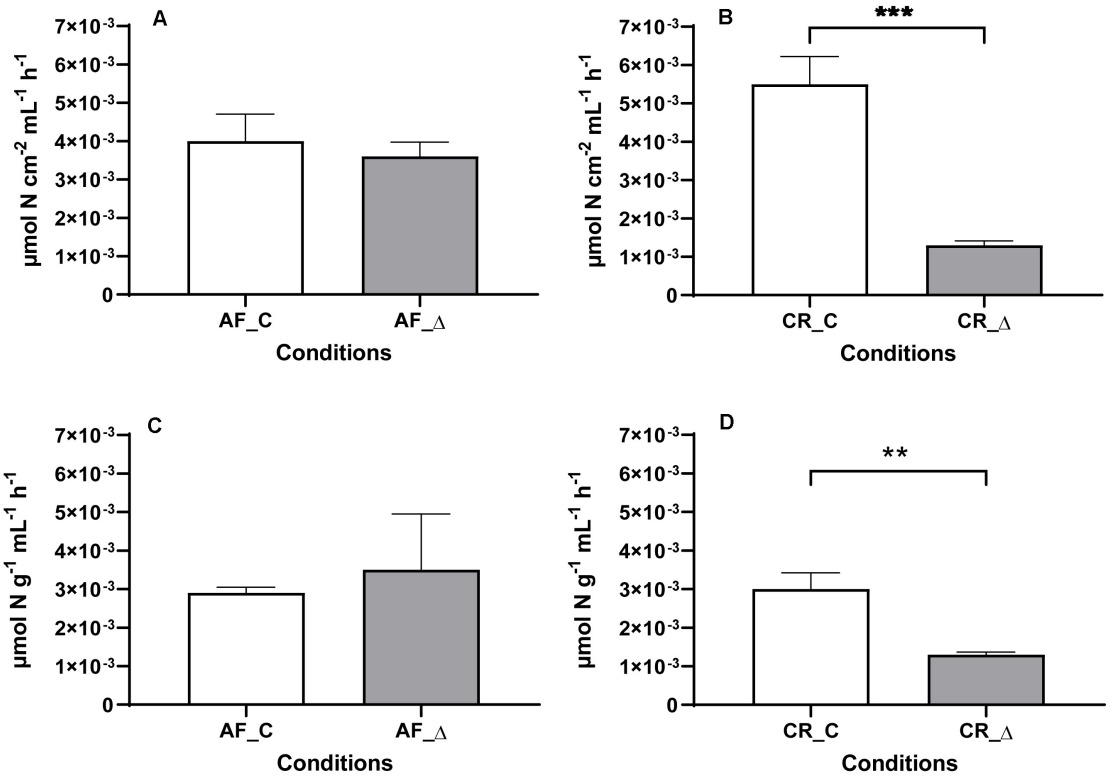

FIGURE 1 | Mean and standard deviation (n = 3) of potential nitrification rates ($[^{15}N]O_2^- + [^{15}N]O_3^-$ produced) measured in the sediments subjected to daily salinity fluctuations (AF_Δ and CR_Δ) and constant salinity (AF_C and CR_C) treatments. Rates were measured with the same salinity (0 psu for Crestuma sediments, and 15 for Afurada sediments). Nitrification rates are displayed in four different charts corresponding to Afurada (AF) reactors **(A)** and Crestuma (CR) reactors **(B)** after addition of 20 μM of $[^{15}N]H_4^+$), and Afurada slurries **(C)** and Crestuma slurries **(D)** after addition of 100 μM of $[^{15}N]H_4^+$). Symbol ** and *** means a $P < 0.01$ and $P < 0.001$, respectively.

CR sediments, the bacterial *amoA* gene transcripts were not detected (Figure S3B).

Prokaryotic Community

The Illumina Miseq platform originated ∼680000 raw reads of the 16S rRNA gene (V4–V5) amplicons from the ten samples analyzed. After the quality filtering steps and chimera removal, it was obtained a total of 489414 16S rRNA gene amplicon sequences ranging from 19636 (AF_i sample) to 113330 (AF_Δ1 sample) sequences *per* sample. Due to the nature of Illumina sequencing, the number of obtained sequences varied among samples. A total of 98.3% good-quality sequences were taxonomically classified as Bacteria, 1.7% as Archaea and 0.0045% as Eukaryote.

The top 20 phyla are presented in **Figure 2**. *Proteobacteria* was the most abundant phylum in all samples analyzed. *Bacteroidetes*, *Cyanobacteria*, and *Verrucomicrobia* phyla relative abundance decreased in all treatments in comparison with initial sediment (AF_i and CR_i). *Planctomycetes* phylum relative abundance increased in AF treatments while CR treatments maintained a similar relative abundance with initial sediment. *Acidobacteria* phylum only increased in AF_C treatment while decreased in CR_Δ treatment in comparison with each respective initial sediment. The relative abundance of *Thaumarchaeota* phylum was similar across all treatments, with a considerable higher abundance in AF samples. Lastly, *Nitrospirae* phylum presents a tremendous increase in CR_C treatment in comparison with initial sediment and CR_Δ. Detailed information about the relative abundance of each phyla across all samples can be found in **Supplementary Table S4**.

The differences in the prokaryotic composition, across sediment samples from the salinity regimes tested (AF_i, CR_i, CR_C, AF_C, AF_Δ, and CR_Δ) were explored in the PCoA based on unweighted and weighted UniFrac distances (**Figures 3A,B**). The prokaryotic composition between replicates were found to be highly homogeneous (**Figure 3**) highlighting that despite some of the replicates have been sequenced in different runs, the data is highly reliable and comparable (e.g., CR_Δ2, run 1 and CR_Δ1, run 2). Principal coordinate 1 (PC1) explained the majority of the variance (62%) in the prokaryotic communities based on the presence/absence of the phylogenetic distance of the ASVs – unweighted UniFrac distance – belonging to the 10 most abundant phyla (**Figure 3A**). The variance explained by the abundance of the phylogenetic distance of the ASVs (of the top 10 phyla) – weighted UniFrac distance – was similar (**Figure 3B**). In both analyses, the permutational multivariate analysis of variance (permanova) found that site

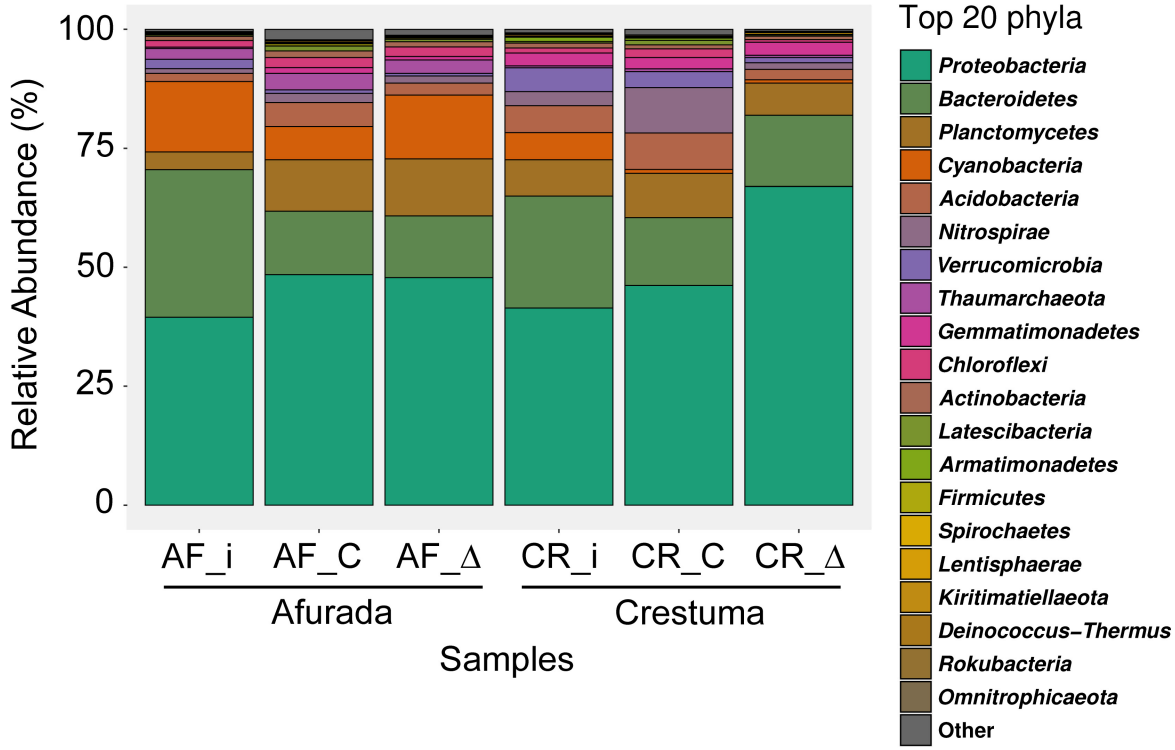

FIGURE 2 | Bar plot representing the relative abundance of the top 20 most abundant prokaryotic phyla from the initial sediment (AF_i and CR_i) and from the sediment samples of the different salinity treatments (constant – AF_C and CR_C, and fluctuation – AF_Δ and CR_Δ). Samples under different salinity treatments were depicted as mean relative abundances of phyla from original sample replicates (n = 2).

location (downstream and upstream stations) was a strong driver on differences in microbial composition (R^2 = 0.58 and P-value = 0.008 and R^2 = 0.54 and P-value = 0.01, **Figures 3A,B**).

Taxonomic Composition of Nitrifying Prokaryotes

The relative abundance of the nitrifying organisms at the genus level in all samples is presented in **Figure 4**. In the version 132 of SILVA SSU Ref NR database β-*Proteobacteria* class was rearranged under the *Betaproteobacteriales* order within the class γ-*Proteobacteria*. Therefore, what is known as AOB β- and γ-*Proteobacteria* in some taxonomies and literature, in 132 version of SILVA database is rearranged under the γ-*Proteobacteria* class, particularly within the family *Nitrosomonadaceae* (*Betaproteobacteriales* order). *Nitrosomonas* was the only AOB genus identified with higher relative abundance in the constant salinity treatments of AF and CR (**Supplementary Figure S7** and **Supplementary Table S5**). Regarding the AOA taxonomic groups, one family was identified, the *Nitrosopumilaceae* which included representatives of "*Ca.* Nitrosopumilus", "*Ca.* Nitrosoarchaeum", and "*Ca.* Nitrosotenuis".

"*Ca.* Nitrosopumilus" was found to be highly representative in AF sediments, while "*Ca.* Nitrosoarchaeum" and "*Ca.* Nitrosotenuis" are over-represented in CR sediments with a pronounced increase of "*Ca.* Nitrosotenuis" in the freshwater treatment (CR_C). Two genera belonging to the NOB group were also identified in the data set. While *Nitrospira* presented higher relative abundance in downstream sediments, *Nitrospina* showed an opposite pattern with the highest values registered at the constant salinity treatment in upstream sediments (**Supplementary Figure S7** and **Supplementary Table S5**).

DISCUSSION

The objective of this study was to test whether upstream and downstream AOM communities would display different responses to salinity fluctuations. For that, we simulated different salinity regimes in controlled reactors with estuarine sediments and overlying water from the Douro River to mimic natural physiochemical conditions.

It can be assumed that laboratory experiments do not reflect the natural conditions, which are extremely dynamic and complex; however it can provide valuable insights of how short-term constant and salinity fluctuations can shape and affect AOM activity and diversity.

The downstream estuarine site (Afurada) is characterized by its marked daily salinity amplitudes [e.g., 3.4–14.0 psu variation in December 2014 (Santos et al., 2018)]. These amplitudes are expected to select communities more resilient to the natural salinity regime (Crump et al., 2004; Wang et al., 2018). Our results showed no significant differences between nitrification rates in

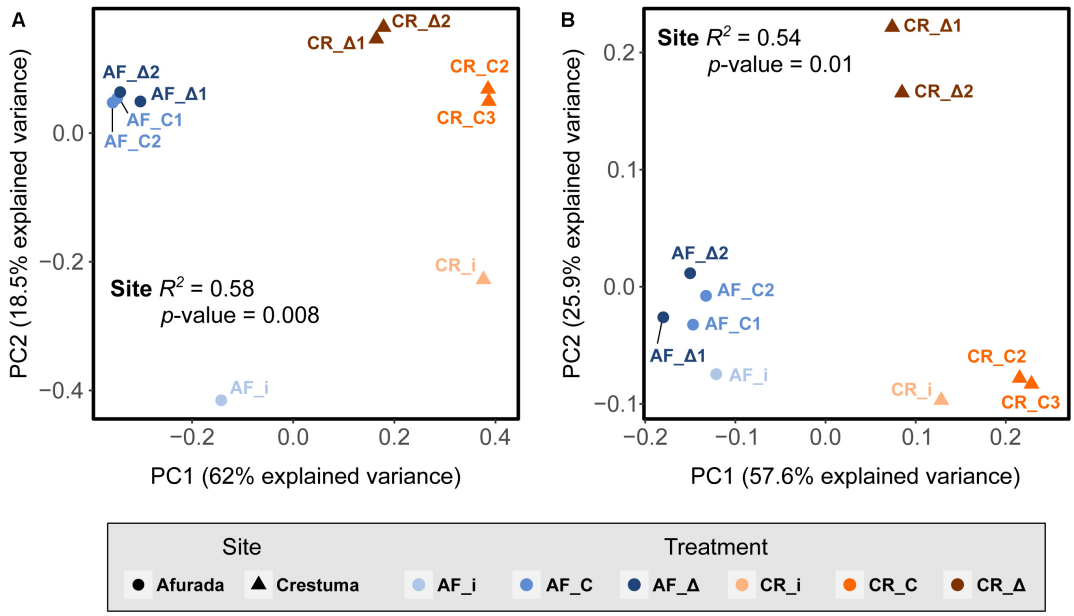

FIGURE 3 | Principal Coordinates Analysis (PCoA) of **(A)** unweighted and **(B)** weighted UniFrac distances of ASVs belonging to the top 10 phyla from the initial sediment (AF_i and CR_i) as well as in the sediment samples of the different salinity treatments (constant – AF_C and CR_C, and fluctuation – AF_Δ and CR_Δ). The R^2 and *P*-values that resulted from the Adonis analysis of unweighted and weighted UniFrac distance matrices grouped by site and treatment are highlighted inside the PCoA. Samples were grouped by site (Afurada – AF_i, AF_C1, AF_C2, AF_Δ1, AF_Δ2; and Crestuma – CR_i, CR_C2, CR_C3, CR_Δ1, CR_Δ2) and treatment (Afurada *in situ* sample – AF_i; Afurada constant salinity – AF_C1, AF_C2; Afurada fluctuation salinity – AF_Δ1, AF_Δ2; and Crestuma *in situ* sample – CR_i; Crestuma constant salinity – CR_C2, CR_C3; Crestuma fluctuation salinity – CR_Δ1, CR_Δ2).

downstream estuarine sediments exposed to constant salinity vs. fluctuating regime. Thus, suggesting that AOM from estuarine downstream sediments display an elevated plasticity to different salinity regimes which can be advantageous when inhabiting environments with high salinity amplitudes. Although, to the best of our knowledge, the effect of daily salinity fluctuations has not been tested directly, some previous works point that AOM communities from downstream estuarine systems displayed similar potential nitrification rates under salinities ranges of 15 and 30 psu (Magalhaes et al., 2005; Bernhard et al., 2007; Santos et al., 2018). Yet, it should be noted that within the AOM, AOB and AOA activity may differ in response to different salinities, as previously reported in other high salinity amplitude environments such as Weeks Bay (Caffrey et al., 2007), Douro River estuary (Magalhães et al., 2009), Plum Island Sound estuary (Bernhard et al., 2007, 2010), Huntington Beach subterranean estuary (Santoro et al., 2008), Cochin estuary (Puthiya Veettil et al., 2015), and Colne estuary (Li et al., 2015).

Prokaryotic beta diversity analysis showed a high similarity between Afurada *in situ* communities and the ones exposed to 36 days of constant and daily salinity fluctuations, highlighting the elevated resilience of the prokaryotic communities from Afurada site to salinity shifts. With primers able to capture archaeal and bacterial 16S rRNA genes simultaneously and with particularly good coverage and resolution for *Thaumarchaeota* (Parada et al., 2016), we were able to identify known genera of AOA and AOB. However, it is important to recognize that this analysis does not target specifically the 16S rRNA gene nor the functional genes of AOM communities. The prokaryotic composition analysis in Afurada treatments identified higher relative abundance of the AOA "*Ca.* Nitrosopumilus" genus in both constant and fluctuation salinity treatments in comparison with *in situ* sediments (2.0 and 1.4%, for AF_C and AF_Δ, respectively). In addition, relative low abundance of the other AOA genera ("*Ca.* Nitrosoarchaeum" and "*Ca.* Nitrosotenuis") was registered in AF_C and AF_Δ treatments. The higher detection of "*Ca.* Nitrosopumilus" genus in both salinity treatments in comparison with the other two genera can be explained by the fact that *Nitrosopumilus* taxa has been often associated to saline environments (Bouskill et al., 2012; Xie et al., 2014). For instance, Jin et al. (2010) reported the dominance of *Nitrosopumilus maritimus*-like in a laboratory-scale bioreactor treating saline wastewater under 10 psu. Whereas, Wu et al. (2013) hypothesized that a high salinity condition could promote the growth of the marine group representative, *N. maritimus*. Similarly, Qin et al. (2017) reported *Nitrosopumilus* species capable of growing over a wide salinity range, suggesting even a possible adaptation to seasonal salinity fluctuations in estuarine environments, which is in agreement with our findings.

Concerning the AOB groups, only the *Nitrosomonas* genus was identified in our analysis with an increase (compared to initial *in situ* sediment – CR_i) in constant salinity and no difference in the salinity fluctuation, suggesting a good adaptation of Afurada AOB to the salinity regimes tested. After incubating sediments from Jiulong River during 28 days, Wang et al. (2018) reported that the abundance of AOB increased at intermediate

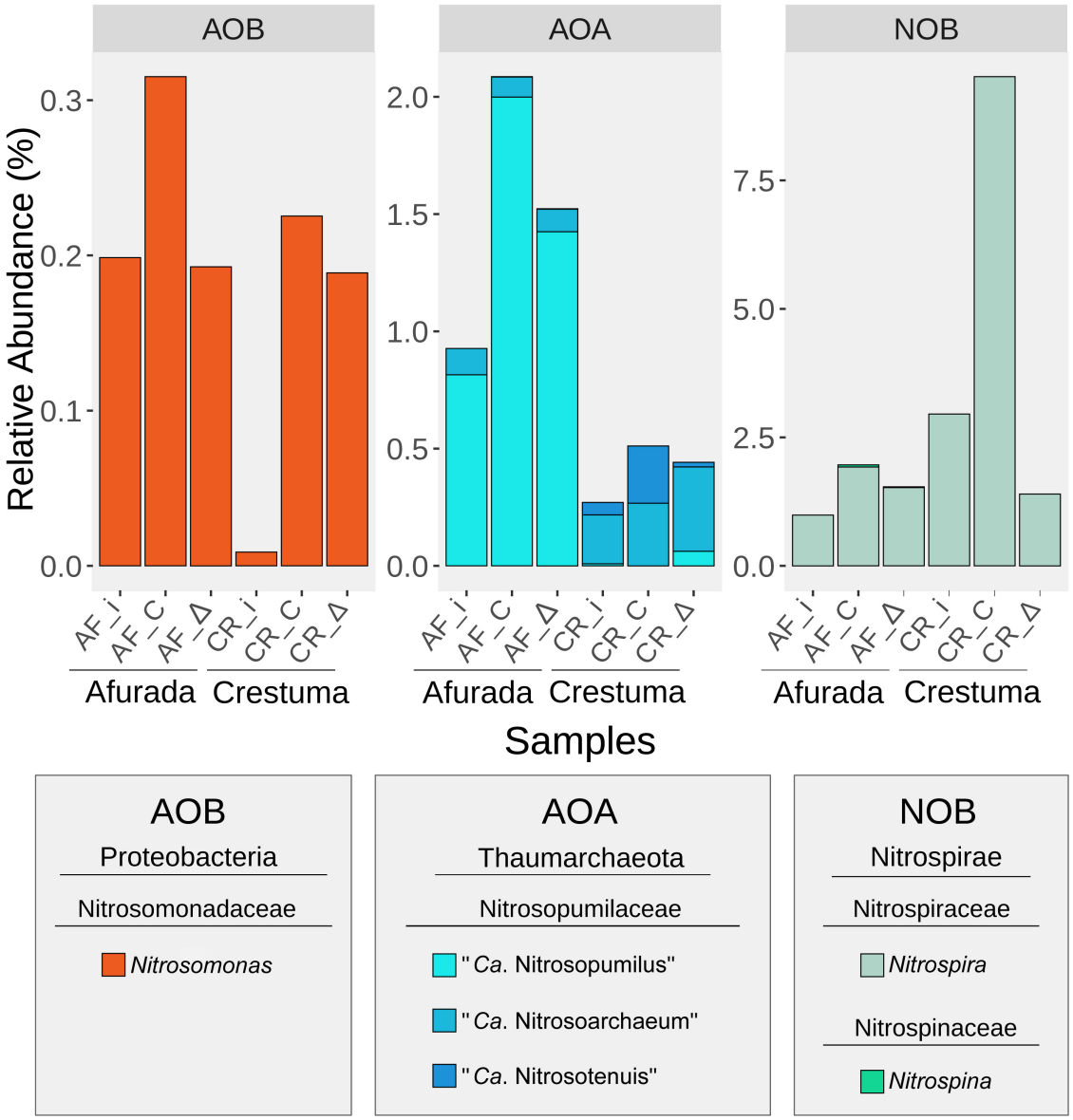

FIGURE 4 | Bar plot representing the relative abundance of the identified nitrifying taxa at genus level in the initial sediment (AF_i and CR_i) as well as in the sediment samples of the different salinity treatments (constant – AF_C and CR_C, and fluctuation – AF_Δ and CR_Δ). Samples under different salinity treatments were depicted as mean relative abundances of genera from original sample replicates (n = 2).

salinity levels (ranging from 0, 10, 20, and 30 psu). The capacity of AOB to be more resilient in higher salinities compared to lower salinities has also been previously reported (Gonzalez-Silva et al., 2016; Zhou et al., 2017). Indeed, our targeted analysis of *amoA* gene fragments supported this assumption with high similarity between treatments and initial *in situ* sediments in the hierarchical cluster analysis.

The upstream estuarine site (Crestuma) is characterized by low salinity amplitudes (Azevedo et al., 2010), and thus, expected to promote the development of communities with low tolerance to high salinity amplitudes. As a consequence, the different experimental incubation conditions (constant salinity of 0 psu, similar to *in situ* conditions; and salinity fluctuations quite different from *in situ* conditions) would be expected to have a distinct impact in these community's activity and structure. Indeed, significantly higher nitrification rates were detected in Crestuma constant salinity regime when compared with fluctuation regime. This is in agreement with the differences in the prokaryotic communities observed between the CR_Δ and CR_C treatments (see **Figure 3**). These results support our initial hypothesis that prokaryotic communities in the different sites are well established toward their *in situ* natural salinity regimes. Previously, Santos et al. (2018) exposed *in situ* Crestuma sediments to three constant salinities (0, 15, and 30 psu)

and found a significant decrease in nitrification rates when sediments were exposed to higher salinities. Similarly, (Bernhard et al., 2007) found a significant nitrification rate decrease when exposing sediments (form upstream region) to high salinity (30 psu). In agreement Zhang et al. (2015c) through the incubation of estuarine sediments found that AOB showed the highest transcriptional activity in the low-salinity microcosms.

The AOA groups identified by the 16S rRNA gene sequencing analysis showed the appearance of the saline-associated "*Ca.* Nitrosopumilus" (Bouskill et al., 2012) on the fluctuation treatment suggesting a shift from the initial natural community. "*Ca.* Nitrosotenuis" was more abundant at the freshwater treatment (CR_C) as expected since previous studies identified this group as non-halophilic (Lebedeva et al., 2013; Li et al., 2016; Sauder et al., 2018). In the case of "*Ca.* Nitrosoarchaeum," despite being associated with low salinity habitats (Mosier et al., 2012; Lebedeva et al., 2013), it was favored in both salinity conditions suggesting a certain tolerance of this genus to salinity fluctuations.

Differences on AOA phylotypes within the different salinity treatments, based on the 16S rRNA gene sequencing analysis, were also reflected in the fingerprinting *amoA* gene transcripts analysis that showed 30% of relative dissimilarity between the DGGE profile of AOA *amoA* gene transcripts of the different salinity treatments.

The AOB group identified in Crestuma sediments was also the *Nitrosomonas* genus, which increased after 36 days of incubation in both salinity treatments, although with higher relative abundance in the constant salinity treatment. The fingerprinting β-AOB *amoA* transcript analysis suggested an increase number of β-AOB phylotypes in both salinity treatments (mainly in the salinity fluctuation regime) since a higher detection of DGGE bands were registered in the experimental salinity treatments in comparison with the Crestuma *in situ* sediment. Yet, hierarchical cluster analysis of the β-AOB *amoA* DGGE bands profiles suggests that the β-AOB phylotypes of both salinity treatments are quite distinct and therefore could contribute to a certain extent to the different nitrification rates obtained. In fact, Cortés-Lorenzo et al. (2015) showed that the increase of concentrations of NaCl of 24.1 g L^{-1} in a freshwater water effluent resulted in a remarkable decrease of the NH_4^+ oxidation capacity of the system and a shift in AOB species present.

Changes in Crestuma community structure facing the different salinity regimes is likely to occur especially within the salinity fluctuation treatment due to the low *in-situ* salinity amplitudes that characterize Crestuma site (Santos et al., 2018), and thus the adaptation of its communities to lower osmotic pressures (Moussa et al., 2006; Jeffries et al., 2012).

Yet, the differences found between initial *in situ* communities and salinity treatments might suggest that other constant experimental factors could have played an important role in the results obtained. Indeed, studies have been shown the importance of salinity in estuarine salinity gradient environments (Zhang et al., 2015a; Gao et al., 2018; Li et al., 2018), however other factors have also been shown to contribute substantially to the shaping of the AOM communities – e.g., NH_4^+ levels (Verhamme et al., 2011; Zhang et al., 2015b; Gao et al., 2016). Thus, the addition of 20 μM of NH_4Cl every 12 h could have played an important role in the development of AOM, such as AOB communities (under both salinity conditions), since Crestuma site is characterized by low ammonium concentrations in the water column.

The prokaryotic composition among the different incubated sediments suggests that comammox process, carried out by some *Nitrospira* species (Daims et al., 2015; Zhao et al., 2019) could have played an important role in the nitrification rates differences seen between Crestuma salinity regimes (CR_C and CR_Δ). This assumption is to a certain extent supported by the non-detection of AOB *amoA* transcripts (see **Supplementary Figures S3**, **S6B**) under Crestuma constant and salinity fluctuation treatments (CR_C and CR_Δ). Similar results were reported by Santos et al. (2018) and Monteiro et al. (2017) for sediments from the same Douro estuarine location collected within different years. Monteiro et al. (2017) not only found greater abundances of NOB at Crestuma site, but also a positive correlation with *Nitrospira* genus and the potential nitrification rates. In our study, we observed a substantial increase of *Nitrospira* genus from 2.95% (*in-situ*, prior to the incubation) to 9.52% in CR_C, and at the same time a decrease to 1.40% in CR_Δ. These differences between treatments can be related with the higher sensitivity of *Nitrospira* genus found in Crestuma location to salinity fluctuation. The sensitiveness of *Nitrospira* to salinity has been shown in previous studies. For instance, Bassin et al. (2011) reported that *Nitrospira* spp. disappeared in systems with elevated salinity. In accordance, Moussa et al. (2006) identified *Nitrospira* sp. as the dominant NOB within the salinity range until 10 g NaCl L^{-1}. Therefore, our salinity fluctuation regime had most likely an important impact on this taxon. This is in agreement with Liu Z. et al. (2020), who performed a study on comammox communities in various mangrove ecosystems and found out that temperature and salinity were important factors shaping the comammox community. Although studies focusing on comammox species and their distribution have been emerging (Jiang et al., 2019; Zhao et al., 2019; Liu S. et al., 2020; Liu Z. et al., 2020), we still require future studies aiming toward this group of organisms to account for their actual role in the nitrification process in estuarine ecosystems.

CONCLUSION

By controlling the effect of environmental factors, our microcosm experiment proved to be a good approach to assess the plasticity of estuarine AOM to different salinity regimes, showing that the presence of marked salinity gradients in estuarine systems shape communities with different functional resilience toward salinity fluctuations. The results of this study demonstrated that AOM inhabiting natural high salinity amplitude sites (our study: Afurada) displayed an elevated plasticity in terms of nitrification activity and community structure toward the incubation salinity conditions tested (constant and salinity fluctuation regimes). The AOM that inhabit the upstream sediments of the same estuarine system, that naturally experience low salinity amplitudes, were deeply affected when exposed under daily salinity fluctuation

conditions. Our results suggested that *Nitrosomonas* and "*Ca.* Nitrosopumilus" have a higher influence on the nitrification process in downstream sediments, while *Nitrospira*, "*Ca.* Nitrosoarchaeum" and "*Ca.* Nitrosotenuis" genus displayed an important role on the nitrification process in the upstream sediments. Specific studies that target *Nitrospira* phylotypes including comammox are required to understand their functional contribution in estuarine systems. Finally, further research focusing on the adaptation of AOM toward salinity regimes are required to improve our understanding on the mechanisms that control the selection of this group of prokaryotes and their contributions to estuarine nitrification budgets.

DATA AVAILABILITY STATEMENT

The datasets presented in this study can be found in online repositories. The names of the repository/repositories and accession number(s) can be found below: https://www.ebi.ac.uk/ena, PRJEB38114.

AUTHOR CONTRIBUTIONS

JS and CM designed the study. JS performed the experiments, analyzed the samples, and wrote the manuscript. JS and AS analyzed the data and produced plots. AS, HR, and CM assisted in writing the manuscript. AS did the bioinformatic analysis. CM provided conceptual contributions to the experiments. All authors contributed conceptually and reviewed the manuscript.

FUNDING

The Portuguese Science and Technology Foundation (FCT) funded this study through a grant to CM (PTDC/CTA-AMB/30997/2017) and within the scope of UIDB/04423/2020 and UIDP/04423/2020.

ACKNOWLEDGMENTS

We thank M. Monteiro for performing the RNA extractions, CIIMAR – BOGA team for their laboratory assistance during the microcosms experimental set up as well as Américo Santos and Ramiro Santos for building the agitation system.

SUPPLEMENTARY MATERIAL

The Supplementary Material for this article can be found online at: https://www.frontiersin.org/articles/10.3389/fmicb.2020.574815/full#supplementary-material

REFERENCES

Alves, R. J. E., Minh, B. Q., Urich, T., von Haeseler, A., and Schleper, C. (2018). Unifying the global phylogeny and environmental distribution of ammonia-oxidising archaea based on *amoA* genes. *Nat. Commun.* 9:1517.

Auguie, B., and Antonov, A. (2017). *gridExtra: Miscellaneous Functions for "Grid" Graphics [Internet]*. 2016. Available online at: https://cran.r-project.org/web/packages/gridExtra/index.html (accessed March 31, 2017).

Azevedo, I. C., Bordalo, A. A., and Duarte, P. M. (2010). Influence of river discharge patterns on the hydrodynamics and potential contaminant dispersion in the Douro estuary (Portugal). *Water Res.* 44, 3133–3146. doi: 10.1016/j.watres.2010.03.011

Bassin, J. P., Pronk, M., Muyzer, G., Kleerebezem, R., Dezotti, M., and van Loosdrecht, M. C. (2011). Effect of elevated salt concentrations on the aerobic granular sludge process: linking microbial activity with microbial community structure. *Appl. Environ. Microbiol.* 77, 7942–7953. doi: 10.1128/AEM.05016-11

Beddow, J., Stolpe, B., Cole, P. A., Lead, J. R., Sapp, M., Lyons, B. P., et al. (2016). Nanosilver inhibits nitrification and reduces ammonia−oxidising bacterial but not archaeal *amoA* gene abundance in estuarine sediments. *Environ. Microbiol.* 19, 500–510. doi: 10.1111/1462-2920.13441

Bernhard, A. E., Landry, Z. C., Blevins, A., de la Torre, J. R., Giblin, A. E., and Stahl, D. A. (2010). Abundance of ammonia-oxidizing archaea and bacteria along an estuarine salinity gradient in relation to potential nitrification rates. *Appl. Environ. Microbiol.* 76, 1285–1289. doi: 10.1128/AEM.02018-2019

Bernhard, A. E., Tucker, J., Giblin, A. E., and Stahl, D. A. (2007). Functionally distinct communities of ammonia-oxidizing bacteria along an estuarine salinity gradient. *Environ. Microbiol.* 9, 1439–1447. doi: 10.1111/j.1462-2920.2007.01260.x

Berounsky, V. M., and Nixon, S. W. (1993). Rates of nitrification along an estuarine gradient in Narragansett Bay. *Estuaries* 16, 718–730. doi: 10.2307/1352430

Bolyen, E., Rideout, J. R., Dillon, M. R., Bokulich, N. A., Abnet, C. C., Al-Ghalith, G. A., et al. (2019). Reproducible, interactive, scalable and extensible microbiome data science using QIIME 2. *Nat. Biotechnol.* 37, 852–857.

Bouskill, N. J., Eveillard, D., Chien, D., Jayakumar, A., and Ward, B. B. (2012). Environmental factors determining ammonia-oxidizing organism distribution and diversity in marine environments. *Environ. Microbiol.* 14, 714–729. doi: 10.1111/j.1462-2920.2011.02623.x

Caffrey, J. M., Bano, N., Kalanetra, K., and Hollibaugh, J. T. (2007). Ammonia oxidation and ammonia-oxidizing bacteria and archaea from estuaries with differing histories of hypoxia. *ISME J.* 1, 660–662. doi: 10.1038/ismej.2007.79

Callahan, B. (2018). Silva Taxonomic Training Data Formatted for DADA2 (Silva Version 132). Zenodo. doi: 10.5281/zenodo.1172783

Callahan, B. J., McMurdie, P. J., Rosen, M. J., Han, A. W., Johnson, A. J. A., and Holmes, S. P. (2016). DADA2: high-resolution sample inference from Illumina amplicon data. *Nat. Methods* 13:581. doi: 10.1038/nmeth.3869

Caporaso, J. G., Lauber, C. L., Walters, W. A., Berg-Lyons, D., Huntley, J., Fierer, N., et al. (2012). Ultra-high-throughput microbial community analysis on the Illumina HiSeq and MiSeq platforms. *ISME J.* 6, 1621–1624. doi: 10.1038/ismej.2012.8

Clarke, K., and Gorley, R. (2006). *Primer v6: User Manual/Tutorial (Plymouth Routines in Multivariate Ecological Research)*. Plymouth: Primer-E.

Clarke, K., and Warwick, R. (2001). *Change in Marine Communities: An Approach to Statistical Analysis and Interpretation*, 2nd Edn. Plymouth: Primer-E.

Cortés-Lorenzo, C., Rodríguez-Díaz, M., Sipkema, D., Juárez-Jiménez, B., Rodelas, B., Smidt, H., et al. (2015). Effect of salinity on nitrification efficiency and structure of ammonia-oxidizing bacterial communities in a submerged fixed bed bioreactor. *Chem. Eng. J.* 266, 233–240. doi: 10.1016/j.cej.2014.12.083

Crump, B. C., Hopkinson, C. S., Sogin, M. L., and Hobbie, J. E. (2004). Microbial biogeography along an estuarine salinity gradient: combined influences of bacterial growth and residence time. *Appl. Environ. Microbiol.* 70, 1494–1505. doi: 10.1128/aem.70.3.1494-1505.2004

Cruzeiro, C., Amaral, S., Rocha, E., and Rocha, M. J. (2017). Determination of 54 pesticides in waters of the Iberian Douro river estuary and risk assessment of environmentally relevant mixtures using theoretical approaches and *Artemia salina* and *Daphnia magna* bioassays. *Ecotoxicol. Environ. Saf.* 145, 126–134. doi: 10.1016/j.ecoenv.2017.07.010

Daims, H., Lebedeva, E. V., Pjevac, P., Han, P., Herbold, C., Albertsen, M., et al. (2015). Complete nitrification by *Nitrospira* bacteria. *Nature* 528, 504–509. doi: 10.1038/nature16461

Daims, H., Lucker, S., and Wagner, M. (2016). A new perspective on microbes formerly known as nitrite-oxidizing bacteria. *Trends Microbiol.* 24, 699–712. doi: 10.1016/j.tim.2016.05.004

Dang, H., Li, J., Chen, R., Wang, L., Guo, L., Zhang, Z., et al. (2010). Diversity, abundance, and spatial distribution of sediment ammonia-oxidizing Betaproteobacteria in response to environmental gradients and coastal eutrophication in Jiaozhou Bay, China. *Appl. Environ. Microbiol.* 76, 4691–4702. doi: 10.1128/aem.02563-09

Denk, T. R., Mohn, J., Decock, C., Lewicka-Szczebak, D., Harris, E., Butterbach-Bahl, K., et al. (2017). The nitrogen cycle: a review of isotope effects and isotope modeling approaches. *Soil Biol. Biochem.* 105, 121–137. doi: 10.1016/j.soilbio.2016.11.015

Fernandes, S. O., Javanaud, C., Michotey, V. D., Guasco, S., Anschutz, P., and Bonin, P. (2016). Coupling of bacterial nitrification with denitrification and anammox supports N removal in intertidal sediments (Arcachon Bay, France). *Estuar. Coast. Shelf Sci.* 179, 39–50. doi: 10.1016/j.ecss.2015.10.009

Gao, J., Hou, L., Zheng, Y., Liu, M., Yin, G., Yu, C., et al. (2018). Shifts in the community dynamics and activity of ammonia−oxidizing prokaryotes along the Yangtze estuarine salinity gradient. *J. Geophys. Res.* 123, 3458–3469. doi: 10.1029/2017jg004182

Gao, J.-F., Fan, X.-Y., Pan, K.-L., Li, H.-Y., and Sun, L.-X. (2016). Diversity, abundance and activity of ammonia-oxidizing microorganisms in fine particulate matter. *Sci. Rep.* 6:38785.

Giblin, A. E., Weston, N. B., Banta, G. T., Tucker, J., and Hopkinson, C. S. (2010). The effects of salinity on nitrogen losses from an Oligohaline Estuarine sediment. *Estuaries Coast.* 33, 1054–1068. doi: 10.1007/s12237-010-9280-7

Gonzalez-Silva, B. M., Jonassen, K. R., Bakke, I., Østgaard, K., and Vadstein, O. (2016). Nitrification at different salinities: biofilm community composition and physiological plasticity. *Water Res.* 95, 48–58. doi: 10.1016/j.watres.2016.02.050

Guo, J., Ling, N., Chen, H., Zhu, C., Kong, Y., Wang, M., et al. (2017). Distinct drivers of activity, abundance, diversity and composition of ammonia-oxidizers: evidence from a long-term field experiment. *Soil Biol. Biochem.* 115, 403–414. doi: 10.1016/j.soilbio.2017.09.007

Jantti, H., Leskinen, E., Stange, C. F., and Hietanen, S. (2012). Measuring nitrification in sediments–comparison of two techniques and three 15NO(-)3 measurement methods. *Isotopes Environ. Health Stud.* 48, 313–326. doi: 10.1080/10256016.2012.641543

Jäntti, H., Ward, B. B., Dippner, J. W., and Hietanen, S. (2018). Nitrification and the ammonia-oxidizing communities in the central Baltic Sea water column. *Estuar. Coast. Shelf Sci.* 202, 280–289. doi: 10.1016/j.ecss.2018.01.019

Jeffries, T., Seymour, J., Newton, K., Smith, R., Seuront, L., and Mitchell, J. (2012). Increases in the abundance of microbial genes encoding halotolerance and photosynthesis along a sediment salinity gradient. *Biogeosciences* 9, 815–825. doi: 10.5194/bg-9-815-2012

Jiang, Q., Xia, F., Zhu, T., Wang, D., and Quan, Z. (2019). Distribution of comammox and canonical ammonia-oxidizing bacteria in tidal flat sediments of the Yangtze River estuary at different depths over four seasons. *J. Appl. Microbiol.* 127, 533–543. doi: 10.1111/jam.14337

Jin, T., Zhang, T., and Yan, Q. (2010). Characterization and quantification of ammonia-oxidizing archaea (AOA) and bacteria (AOB) in a nitrogen-removing reactor using T-RFLP and qPCR. *Appl. Microbiol. Biotechnol.* 87, 1167–1176. doi: 10.1007/s00253-010-2595-2

Junier, P., Molina, V., Dorador, C., Hadas, O., Kim, O. S., Junier, T., et al. (2010). Phylogenetic and functional marker genes to study ammonia-oxidizing microorganisms (AOM) in the environment. *Appl. Microbiol. Biotechnol.* 85, 425–440. doi: 10.1007/s00253-009-2228-9

Karpouzas, D. G., and Singh, B. K. (2010). Application of fingerprinting molecular methods in bioremediation studies. *Methods Mol. Biol.* 599, 69–88. doi: 10.1007/978-1-60761-439-5_5

Katoh, K., and Standley, D. M. (2013). MAFFT multiple sequence alignment software version 7: improvements in performance and usability. *Mol. Biol. Evol.* 30, 772–780. doi: 10.1093/molbev/mst010

Kowalchuk, G. A., and Stephen, J. R. (2001). Ammonia-oxidizing bacteria: a model for molecular microbial ecology. *Annu. Rev. Microbiol.* 55, 485–529. doi: 10.1146/annurev.micro.55.1.485

Lawson, C. E., and Lucker, S. (2018). Complete ammonia oxidation: an important control on nitrification in engineered ecosystems? *Curr. Opin. Biotechnol.* 50, 158–165. doi: 10.1016/j.copbio.2018.01.015

Lebedeva, E. V., Hatzenpichler, R., Pelletier, E., Schuster, N., Hauzmayer, S., Bulaev, A., et al. (2013). Enrichment and genome sequence of the group I. 1a ammonia-oxidizing Archaeon "Ca. Nitrosotenuis uzonensis" representing a clade globally distributed in thermal habitats. *PLoS One* 8:e80835. doi: 10.1371/journal.pone.0080835

Li, J., Nedwell, D. B., Beddow, J., Dumbrell, A. J., McKew, B. A., Thorpe, E. L., et al. (2015). *amoA* Gene abundances and nitrification potential rates suggest that benthic ammonia-oxidizing bacteria and not archaea dominate N cycling in the Colne Estuary, United Kingdom. *Appl. Environ. Microbiol.* 81, 159–165. doi: 10.1128/AEM.02654-14

Li, M., Wei, G., Shi, W., Sun, Z., Li, H., Wang, X., et al. (2018). Distinct distribution patterns of ammonia-oxidizing archaea and bacteria in sediment and water column of the Yellow River estuary. *Sci. Rep.* 8:1584. doi: 10.1038/s41598-018-20044-6

Li, Y., Ding, K., Wen, X., Zhang, B., Shen, B., and Yang, Y. (2016). A novel ammonia-oxidizing archaeon from wastewater treatment plant: its enrichment, physiological and genomic characteristics. *Sci. Rep.* 6: 23747.

Liu, G., and Wang, J. (2015). Quantifying the chronic effect of low DO on the nitrification process. *Chemosphere* 141, 19–25. doi: 10.1016/j.chemosphere.2015.05.088

Liu, S., Wang, H., Chen, L., Wang, J., Zheng, M., Liu, S., et al. (2020). Comammox nitrospira within the Yangtze River continuum: community, biogeography, and ecological drivers. *ISME J.* 14, 2488–2504. doi: 10.1038/s41396-020-0701-8

Liu, Z., Zhang, C., Wei, Q., Zhang, S., Quan, Z., and Li, M. (2020). Temperature and salinity drive comammox community composition in mangrove ecosystems across southeastern China. *Sci. Total Environ.* 742:140456. doi: 10.1016/j.scitotenv.2020.140456

Lozupone, C., and Knight, R. (2005). UniFrac: a new phylogenetic method for comparing microbial communities. *Appl. Environ. Microbiol.* 71, 8228–8235. doi: 10.1128/aem.71.12.8228-8235.2005

Lozupone, C. A., Hamady, M., Kelley, S. T., and Knight, R. (2007). Quantitative and qualitative β diversity measures lead to different insights into factors that structure microbial communities. *Appl. Environ. Microbiol.* 73, 1576–1585. doi: 10.1128/aem.01996-06

Madureira, T. V., Barreiro, J. C., Rocha, M. J., Rocha, E., Cass, Q. B., and Tiritan, M. E. (2010). Spatiotemporal distribution of pharmaceuticals in the Douro River estuary (Portugal). *Sci. Total Environ.* 408, 5513–5520. doi: 10.1016/j.scitotenv.2010.07.069

Magalhaes, C., Bano, N., Wiebe, W., Hollibaugh, J., and Bordalo, A. (2007). Composition and activity of beta−Proteobacteria ammonia−oxidizing communities associated with intertidal rocky biofilms and sediments of the Douro River estuary, Portugal. *J. Appl. Microbiol.* 103, 1239–1250. doi: 10.1111/j.1365-2672.2007.03390.x

Magalhaes, C. M., Joye, S. B., Moreira, R. M., Wiebe, W. J., and Bordalo, A. A. (2005). Effect of salinity and inorganic nitrogen concentrations on nitrification and denitrification rates in intertidal sediments and rocky biofilms of the Douro River estuary, Portugal. *Water Res.* 39, 1783–1794. doi: 10.1016/j.watres.2005.03.008

Magalhães, C. M., Machado, A., and Bordalo, A. A. (2009). Temporal variability in the abundance of ammonia- oxidizing bacteria vs. archaea in sandy sediments of the Douro River estuary, Portugal. *Aquat. Microb. Ecol.* 56, 13–23. doi: 10.3354/ame01313

Marchant, H. K., Holtappels, M., Lavik, G., Ahmerkamp, S., Winter, C., and Kuypers, M. M. (2016). Coupled nitrification–denitrification leads to extensive N loss in subtidal permeable sediments. *Limnol. Oceanogr.* 61, 1033–1048. doi: 10.1002/lno.10271

McMurdie, P. J., and Holmes, S. (2013). phyloseq: an R package for reproducible interactive analysis and graphics of microbiome census data. *PLoS One* 8:e61217. doi: 10.1371/journal.pone.0061217

Monteiro, M., Séneca, J., Torgo, L., Cleary, D. F., Gomes, N. C., Santoro, A. E., et al. (2017). Environmental controls on estuarine nitrifying communities along a salinity gradient. *Aquat. Microb. Ecol.* 80, 167–180. doi: 10.3354/ame01847

Mosier, A. C., Allen, E. E., Kim, M., Ferriera, S., and Francis, C. A. (2012). Genome sequence of "*Candidatus* Nitrosoarchaeum limnia" BG20, a low-salinity

ammonia-oxidizing archaeon from the San Francisco Bay estuary. *J. Bacteriol.* 194, 2119–2120. doi: 10.1128/JB.00007-12

Mosier, A. C., and Francis, C. A. (2008). Relative abundance and diversity of ammonia-oxidizing archaea and bacteria in the San Francisco Bay estuary. *Environ. Microbiol.* 10, 3002–3016. doi: 10.1111/j.1462-2920.2008.01764.x

Moussa, M. S., Sumanasekera, D. U., Ibrahim, S. H., Lubberding, H. J., Hooijmans, C. M., Gijzen, H. J., et al. (2006). Long term effects of salt on activity, population structure and floc characteristics in enriched bacterial cultures of nitrifiers. *Water Res.* 40, 1377–1388. doi: 10.1016/j.watres.2006.01.029

Muyzer, G., de Waal, E. C., and Uitterlinden A. G. (1993). Profiling of complex microbial populations by denaturing gradient gel electrophoresis analysis of polymerase chain reaction-amplified genes coding for 16S rRNA. *Appl. Environ. Microbiol.* 59, 695–700. doi: 10.1128/aem.59.3.695-700.1993

Oksanen, J., Blanchet, F., Friendly, M., Kindt, R., Legendre, P., McGlinn, D., et al. (2018). *Vegan: Community Ecology Package. R Package Version* 2.5-2. 2018.

Parada, A. E., Needham, D. M., and Fuhrman, J. A. (2016). Every base matters: assessing small subunit rRNA primers for marine microbiomes with mock communities, time series and global field samples. *Environ. Microbiol.* 18, 1403–1414. doi: 10.1111/1462-2920.13023

Price, M. N., Dehal, P. S., and Arkin, A. P. (2010). FastTree 2–approximately maximum-likelihood trees for large alignments. *PLoS One* 5:e9490. doi: 10.1371/journal.pone.0009490

Prosser, J. I., and Embley, T. M. (2002). Cultivation-based and molecular approaches to characterisation of terrestrial and aquatic nitrifiers. *Antonie Van Leeuwenhoek* 81, 165–179. doi: 10.1023/A:1020598114104

Purkhold, U., Pommerening-Roser, A., Juretschko, S., Schmid, M. C., Koops, H. P., and Wagner, M. (2000). Phylogeny of all recognized species of ammonia oxidizers based on comparative 16S rRNA and *amoA* sequence analysis: implications for molecular diversity surveys. *Appl. Environ. Microbiol.* 66, 5368–5382. doi: 10.1128/aem.66.12.5368-5382.2000

Puthiya Veettil, V., Abdulaziz, A., Chekidhenkuzhiyil, J., Kalanthingal Ramkollath, L., Karayadi Hamza, F., Kizhakkepat Kalam, B., et al. (2015). Bacterial domination over archaea in ammonia oxidation in a monsoon-driven tropical estuary. *Microb. Ecol.* 69, 544–553. doi: 10.1007/s00248-014-0519-x

Qin, W., Heal, K. R., Ramdasi, R., Kobelt, J. N., Martens-Habbena, W., Bertagnolli, A. D., et al. (2017). *Nitrosopumilus maritimus* gen. nov., sp. nov., *Nitrosopumilus cobalaminigenes* sp. nov., *Nitrosopumilus oxyclinae* sp. nov., and *Nitrosopumilus ureiphilus* sp. nov., four marine ammonia-oxidizing archaea of the phylum Thaumarchaeota. Int. J. Syst. Evol. Microbiol. 67, 5067–5079. doi: 10.1099/ijsem.0.002416

Quast, C., Pruesse, E., Yilmaz, P., Gerken, J., Schweer, T., Yarza, P., et al. (2013). The SILVA ribosomal RNA gene database project: improved data processing and web-based tools. *Nucleic Acids Res.* 41, D590–D596. doi: 10.1093/nar/gks1219

R Core Team (2017). *R: A Language and Environment for Statistical Computing*. Vienna: R Foundation for Statistical Computing. https://www.R-project.org/

Ribeiro, C., Couto, C., Ribeiro, A. R., Maia, A. S., Santos, M., Tiritan, M. E., et al. (2018). Distribution and environmental assessment of trace elements contamination of water, sediments and flora from Douro River estuary, Portugal. *Sci. Total Environ.* 639, 1381–1393. doi: 10.1016/j.scitotenv.2018.05.234

Rotthauwe, J. H., Witzel, K. P., and Liesack, W. (1997). The ammonia monooxygenase structural gene amoA as a functional marker: molecular fine-scale analysis of natural ammonia-oxidizing populations. *Appl. Environ. Microbiol.* 63, 4704–4712. doi: 10.1128/aem.63.12.4704-4712.1997

Rysgaard, S., Thastum, P., Dalsgaard, T., Christensen, P. B., and Sloth, N. P. (1999). Effects of salinity on NH4+ adsorption capacity, nitrification, and denitrification in Danish estuarine sediments. *Estuaries Coast.* 22, 21–30. doi: 10.2307/1352923

Sahan, E., and Muyzer, G. (2008). Diversity and spatio-temporal distribution of ammonia-oxidizing archaea and bacteria in sediments of the Westerschelde estuary. *FEMS Microbiol. Ecol.* 64, 175–186. doi: 10.1111/j.1574-6941.2008.00462.x

Santoro, A. E., Francis, C. A., de Sieyes, N. R., and Boehm, A. B. (2008). Shifts in the relative abundance of ammonia-oxidizing bacteria and archaea across physicochemical gradients in a subterranean estuary. *Environ. Microbiol.* 10, 1068–1079. doi: 10.1111/j.1462-2920.2007.01547.x

Santos, J. P., Mendes, D., Monteiro, M., Ribeiro, H., Baptista, M. S., Borges, M. T., et al. (2018). Salinity impact on ammonia oxidizers activity and *amoA* expression in estuarine sediments. *Estuar. Coast. Shelf Sci.* 211, 177–187. doi: 10.1016/j.ecss.2017.09.001

Sauder, L. A., Engel, K., Lo, C.-C., Chain, P., and Neufeld, J. D. (2018). "*Candidatus* Nitrosotenuis aquarius," an ammonia-oxidizing archaeon from a freshwater aquarium biofilter. *Appl. Environ. Microbiol.* 84:e1430-18.

Sigman, D. M., Casciotti, K. L., Andreani, M., Barford, C., Galanter, M., and Bohlke, J. K. (2001). A bacterial method for the nitrogen isotopic analysis of nitrate in seawater and freshwater. *Anal. Chem.* 73, 4145–4153. doi: 10.1021/ac010088e

Stahl, D. A., and de la Torre, J. R. (2012). Physiology and diversity of ammonia-oxidizing archaea. *Annu. Rev. Microbiol.* 66, 83–101. doi: 10.1146/annurev-micro-092611-150128

Sudarno, U., Winter, J., and Gallert, C. (2011). Effect of varying salinity, temperature, ammonia and nitrous acid concentrations on nitrification of saline wastewater in fixed-bed reactors. *Bioresour. Technol.* 102, 5665–5673. doi: 10.1016/j.biortech.2011.02.078

Tourna, M., Freitag, T. E., Nicol, G. W., and Prosser, J. I. (2008). Growth, activity and temperature responses of ammonia-oxidizing archaea and bacteria in soil microcosms. *Environ. Microbiol.* 10, 1357–1364. doi: 10.1111/j.1462-2920.2007.01563.x

van Kessel, M. A. H. J., Speth, D. R., Albertsen, M., Nielsen, P. H., den Camp, H. J. M., Kartal, B., et al. (2015). Complete nitrification by a single microorganism. *Nature* 528, 555–559. doi: 10.1038/nature16459

Verhamme, D. T., Prosser, J. I., and Nicol, G. W. (2011). Ammonia concentration determines differential growth of ammonia-oxidising archaea and bacteria in soil microcosms. *ISME J.* 5, 1067–1071. doi: 10.1038/ismej.2010.191

Vieira, M. E. C., and Bordalo, A. A. (2000). The Douro estuary (Portugal): a mesotidal salt wedge. *Oceanol. Acta* 23, 585–594. doi: 10.1016/s0399-1784(00)01107-5

Wang, H., Gilbert, J. A., Zhu, Y., and Yang, X. (2018). Salinity is a key factor driving the nitrogen cycling in the mangrove sediment. *Sci. Total Environ.* 63, 1342–1349. doi: 10.1016/j.scitotenv.2018.03.102

Wang, Q., Garrity, G. M., Tiedje, J. M., and Cole, J. R. (2007). Naive Bayesian classifier for rapid assignment of rRNA sequences into the new bacterial taxonomy. *Appl. Environ. Microbiol.* 73, 5261–5267. doi: 10.1128/aem.00062-07

Wang, Y. F., and Gu, J. D. (2014). Effects of allylthiourea, salinity, and pH on ammonia/ammonium-oxidizing prokaryotes in mangrove sediment incubated in laboratory microcosms. *Appl. Microbiol. Biotechnol.* 98, 3257–3274. doi: 10.1007/s00253-013-5399-3

Wear, E. K., Wilbanks, E. G., Nelson, C. E., and Carlson, C. A. (2018). Primer selection impacts specific population abundances but not community dynamics in a monthly time-series 16S rRNA gene amplicon analysis of coastal marine bacterioplankton. *Environ. Microbiol.* 20, 2709–2726. doi: 10.1111/1462-2920.14091

Weston, N. B., Giblin, A. E., Banta, G. T., Hopkinson, C. S., and Tucker, J. (2010). The effects of varying salinity on ammonium exchange in estuarine sediments of the Parker River, Massachusetts. *Estuaries Coast.* 33, 985–1003. doi: 10.1007/s12237-010-9282-5

Wickham, H. (2009). Elegant graphics for data analysis. *Media* 35:211.

Wu, Y. J., Whang, L. M., Fukushima, T., and Chang, S. H. (2013). Responses of ammonia-oxidizing archaeal and betaproteobacterial populations to wastewater salinity in a full-scale municipal wastewater treatment plant. *J. Biosci. Bioeng.* 115, 424–432. doi: 10.1016/j.jbiosc.2012.11.005

Xia, X., Liu, T., Yang, Z., Michalski, G., Liu, S., Jia, Z., et al. (2017). Enhanced nitrogen loss from rivers through coupled nitrification-denitrification caused by suspended sediment. *Sci. Total Environ.* 579, 47–59. doi: 10.1016/j.scitotenv.2016.10.181

Xie, W., Zhang, C., Zhou, X., and Wang, P. (2014). Salinity-dominated change in community structure and ecological function of archaea from the lower Pearl River to coastal South China Sea. *Appl. Microbiol. Biotechnol.* 98, 7971–7982. doi: 10.1007/s00253-014-5838-9

Yamamoto, N., Otawa, K., and Nakai, Y. (2010). Diversity and abundance of ammonia-oxidizing bacteria and ammonia-oxidizing archaea during cattle manure composting. *Microb. Ecol.* 60, 807–815. doi: 10.1007/s00248-010-9714-6

Yan, N., Marschner, P., Cao, W., Zuo, C., and Qin, W. (2015). Influence of salinity and water content on soil microorganisms. *Int. Soil Water Conserv. Res.* 3, 316–323. doi: 10.1016/j.iswcr.2015.11.003

Zeng, J., Zhao, D., Yu, Z., Huang, R., and Wu, Q. L. (2014). Temperature responses of ammonia-oxidizing prokaryotes in freshwater sediment microcosms. *PLoS One* 9:e100653. doi: 10.1371/journal.pone.0100653

Zhang, Q., Tang, F., Zhou, Y., Xu, J., Chen, H., Wang, M., et al. (2015a). Shifts in the pelagic ammonia-oxidizing microbial communities along the eutrophic estuary of Yong River in Ningbo City, China. *Front. Microbiol.* 6:1180. doi: 10.3389/fmicb.2015.01180

Zhang, Y., Chen, L., Dai, T., Sun, R., and Wen, D. (2015b). Ammonia manipulates the ammonia-oxidizing archaea and bacteria in the coastal sediment-water microcosms. *Appl. Microbiol. Biotechnol.* 99, 6481–6491. doi: 10.1007/s00253-015-6524-2

Zhang, Y., Chen, L., Dai, T., Tian, J., and Wen, D. (2015c). The influence of salinity on the abundance, transcriptional activity, and diversity of AOA and AOB in an estuarine sediment: a microcosm study. *Appl. Microbiol. Biotechnol.* 99, 9825–9833. doi: 10.1007/s00253-015-6804-x

Zhao, Z., Huang, G., He, S., Zhou, N., Wang, M., Dang, C., et al. (2019). Abundance and community composition of comammox bacteria in different ecosystems by a universal primer set. *Sci. Total Environ.* 691, 146–155. doi: 10.1016/j.scitotenv.2019.07.131

Zhou, M., Butterbach-Bahl, K., Vereecken, H., and Bruggemann, N. (2017). A meta-analysis of soil salinization effects on nitrogen pools, cycles and fluxes in coastal ecosystems. *Glob. Chang. Biol.* 23, 1338–1352. doi: 10.1111/gcb.13430

Zhu, W., Wang, C., Hill, J., He, Y., Tao, B., Mao, Z., et al. (2018). A missing link in the estuarine nitrogen cycle? Coupled nitrification-denitrification mediated by suspended particulate matter. *Sci. Rep.* 8:2282. doi: 10.1038/s41598-018-20688-4

Conflict of Interest: The authors declare that the research was conducted in the absence of any commercial or financial relationships that could be construed as a potential conflict of interest.

frontiers in Microbiology

ORIGINAL RESEARCH
published: 04 February 2021
doi: 10.3389/fmicb.2020.622454

Effect of Long-Term Fertilization on Ammonia-Oxidizing Microorganisms and Nitrification in Brown Soil of Northeast China

Fangfang Cai[1,2,3], Peiyu Luo[1,2,3], Jinfeng Yang[1,2,3], Muhammad Irfan[4], Shiyu Zhang[1,2,3], Ning An[1,2,3], Jian Dai[1,2,3] and Xiaori Han[1,2,3]**

[1] College of Land and Environment, Shenyang Agricultural University, Shenyang, China, [2] National Engineering Laboratory for Efficient Utilization of Soil and Fertilizer Resources, Tai'an, China, [3] Northeast Scientific Observation Station of Corn Nutrition and Fertilization of Ministry of Agriculture, Shenyang, China, [4] Department of Biotechnology, University of Sargodha, Sargodha, Pakistan

OPEN ACCESS

Edited by:
Anne E. Taylor,
Oregon State University,
United States

Reviewed by:
Christoph Mueller,
University of Giessen, Germany
Cuijing Zhang,
Shenzhen University, China

***Correspondence:**
Peiyu Luo
ibtyoufe@syau.edu.cn
Xiaori Han
hanxiaori@163.com

Specialty section:
This article was submitted to Microbiological Chemistry and Geomicrobiology, a section of the journal Frontiers in Microbiology

Received: 28 October 2020
Accepted: 22 December 2020
Published: 04 February 2021

Citation:
Cai F, Luo P, Yang J, Irfan M, Zhang S, An N, Dai J and Han X (2021) Effect of Long-Term Fertilization on Ammonia-Oxidizing Microorganisms and Nitrification in Brown Soil of Northeast China. Front. Microbiol. 11:622454. doi: 10.3389/fmicb.2020.622454

The objective of this study was to find out changes in ammonia oxidation microorganisms with respect to fertilizer as investigated by real-time polymerase chain reaction and high-throughput sequencing. The treatments included control (CK); chemical fertilizer nitrogen low (N) and high (N_2); nitrogen and phosphorus (NP); nitrogen phosphorus and potassium (NPK) and organic manure fertilizer (M); MN; MN_2; MNPK. The results showed that long-term fertilization influenced soil fertility and affected the abundance and community of ammonia-oxidizing microorganisms by changing the physical and chemical properties of the soil. The abundance and community structure of ammonia-oxidizing archaea (AOA) and ammonia-oxidizing bacteria (AOB) was influenced by soil organic carbon, total nitrogen, total soil phosphorus, available phosphorus, available potassium, and soil nitrate. Soil environmental factors affected the nitrification potential by affecting the structure of ammonia-oxidizing microorganisms; specific and rare AOA and AOB rather than the whole AOA or AOB community played dominant role in nitrification.

Keywords: ammonia-oxidizing archaea, ammonia-oxidizing bacteria, potential nitrification rate, brown soil, long-term fertilization

INTRODUCTION

Agricultural nitrogen cycling is a crucial part in global nitrogen cycling, and ammoxidation is one of critical process of agricultural nitrogen cycling, which turns ammonia to nitrite and then to nitrate. Ammonia-oxidizing organisms, limiting the rate, play an important role in the first step of nitrification. As Könneke et al. (2005) found that archaea could oxidize ammonia to nitrite, researchers studied the comparison between ammonia-oxidizing archaea (AOA) and ammonia-oxidizing bacteria (AOB) about which one was more important under different environmental conditions (Adair and Schwartz, 2008; Chen et al., 2008, 2015; Li et al., 2010; Tao et al., 2017). However, it is controversial whether AOA or AOB play a dominant role under different environmental conditions (Li et al., 2010; Liu et al., 2015; Gan et al., 2016), which may be due to that ammonia-oxidizing microorganisms community structure were affected by physiochemical

properties of soil (Li et al., 2010; Huang et al., 2013). In a previous study, AOA might be dominant within nitrogen cycling under extreme environmental conditions (Erguder et al., 2009); AOA rather than AOB could adapt to oxygenated/hypoxic water conditions (Liu et al., 2015). However, AOB rather than AOA dominated in potential nitrification in other environment (Dang et al., 2018). Different NH_4^+-N concentration and different levels of total carbon and total nitrogen in soils influenced the composition and AOA and AOB abundance in various environmental conditions (Huang et al., 2013; Li and Gu, 2013; Wang et al., 2013).

Long-term fertilization, a good way to investigate agricultural soil, changed physicochemical properties and microbial community structure, such as soil pH, dissolved organic carbon (DOC), available phosphorus, etc. (Luo et al., 2015). Crop rotation could also change the physiochemical properties of soil and microbial community structure (Belay et al., 2002; Bhattacharyya et al., 2010). Whether fertilization changed the ammonia-oxidizing microorganisms' community structure and quantities, which ammonia-oxidizing microorganisms play a dominant role in the nitrification process under the condition of long-term rotation and fertilization is still unclear. In this study, we evaluated the effects of fertilization on the changing of AOA and AOB because of a long-term (38 years) rotation and fertilization experiment. Our objectives were (i) to determine whether AOA and AOB had different responses to variations under the condition of long-term fertilization and rotation, (ii) to identify which taxa play a more crucial role during nitrification process, and (iii) to assess the relative contribution of those variables to changes in AOA and AOB activities and function.

MATERIALS AND METHODS

Experimental Site and Soil Sampling

This 38 years fertilization experiment was established in 1979; the field soil properties and block design were described by Hua et al. (2020). The field experiment was conducted under a rotation of maize–maize–soybean. The crop-growing season started at the end of April and ended at the end of September. In this study, we have chosen nine treatments as follows: CK (no fertilizer), N (mineral nitrogen fertilizer), N_2 (high mineral nitrogen fertilizer), NP (N and phosphate fertilizer), NPK (N, P, and potassium fertilizer), and M (manure), MN, MN_2, MNPK. N was applied in the form of urea, whereas P was calcium superphosphate, and K was potassium sulfate, and the manure fertilizer used was pig manure; the specific application rates are detailed in **Supplementary Table S1**. Soil samples were collected from surface soil layer (0–20 cm) and plow pan soil layer (20–40 cm) on each plot on October 7, 2016. Three soil cores (5 cm diameter) were taken from each layer of soil in each plot, respectively. All samples were shifted through a 2.0 mm sieve. Some part of fresh soil samples was used for DNA extraction, whereas some part was used to determine the soil moisture content, and the rest was air-dried and ground for physiochemical properties determination.

Chemical Analysis

Soil properties determined was soil pH, DOC, soil organic carbon (SOC), total nitrogen (TN), total phosphorus (TP), total potassium (TK), and available phosphorus (AP) and potassium (AK), as described earlier (Luo et al., 2015). The fresh soil samples were used to determine soil ammonium (NH_4^+-N) and nitrate (NO_3^--N), extracted with 1 M KCl and determined by a continuous flow analyzer (AutoAnalyzer 3; SEAL Analytical Ltd., Germany). Soil potential nitrification rate (PNR) was determined using the method of Kandeler (1995).

DNA Extraction and Quantitative Polymerase Chain Reaction Amplification

DNA was extracted from soil (0.250 g) using the PowerSoil™ DNA Isolation Kit (MoBio Laboratories Inc., United States). Purified DNA extracts were stored at −20°C until further determination. Amplification of archaeal and bacterial *amo*A genes was performed using the primer, which is listed in **Supplementary Table S2**. The reaction mixture (20 μL) contained 1 μL of DNA template (20–40 ng per reaction), 0.8 μL of forward and reverse primers (10 μM), respectively, and 10 μL of TB Green Premix Ex Taq (2X) 10 μL (Takara Biomedical Technology Co. Ltd., Beijing, China). The quantitative polymerase chain reaction (qPCR) amplification procedure of *amo*A gene was performed as prime denaturation at 95°C for 30 s, followed with 40 cycles of denaturation for 5 s at 95°C, annealing for 30 s at 55°C, and extension for 30 s at 72°C. The qPCR amplification procedure of arch-amoA gene was performed as prime denaturation at 94°C for 30 s, followed with 45 cycles of denaturation for 30 s at 94°C, annealing for 60 s at 55°C, and extension for 60 s at 72°C.

High-Throughput Sequencing

The pure PCR product equimolar and paired end was sequenced according to the standard protocols by Majorbio Bio-Pharm Technology Co., Ltd. (Shanghai, China) (Zhang et al., 2020). The raw *amo*A gene sequencing reads were demultiplexed, quality-filtered by fast p version 0.20.0 (Chen et al., 2018), and merged by FLASH version 1.2.7 (Magoč and Salzberg, 2011) with the same following criteria as described by Zhang et al. (2020).

UPARSE version 7.1 clustering was used to identify and remove chimeric sequences of operation classification unit (OTUs) with 97% similarity truncation (Edgar, 2013). RDP version 2.2 was used for classification analysis of *amo*A database, and the confidence threshold was 0.7 (Wang et al., 2007).

Statistical Analysis

Redundancy analysis (RDA) (CANOCO 4.5 for Windows) was used to evaluate the relationships among high-throughput sequencing results, quantity PCR results, and physicochemical properties of fertilization treatments. The measured data were used to analyze the variation, using IBM SPSS Statistics 19.0 for Windows (IBM, Inc., Armonk, NY, United States). Analysis of variance and non-metric multidimensional scaling (NMDS) analysis (calculated by Qiime, and analysis and mapping by

Vegan software package for R) were used to analyze the environmental factors and microbes index. A probability level of 5% was adopted for accepting or rejecting null hypotheses.

RESULTS

Soil Physicochemical Properties

Long-term fertilization prominently changed the brown soil properties from both physical and chemical aspects (**Table 1**). Soil pH was varied from 5.03 to 6.95 and 5.78 to 6.86; SOC contents varied from 13.91 to 23.32 g · kg^{-1} and 10.42 to 20.51 g · kg^{-1}; AP contents varied from 1.65 to 136.75 mg · kg^{-1} and 1.45 to 117.90 mg · kg^{-1}; and NO_3^--N contents varied from 2.65 to 27.32 mg · kg^{-1} and 1.50 to 19.80 mg · kg^{-1}. PNR was varied from 0.86 to 5.06 mg · kg^{-1} · d^{-1} and 0.93 to 3.99 mg · kg^{-1} · d^{-1}; DOC contents varied from 21.83 to 36.04 mg · kg^{-1} and 3.72 to 14.05 mg · kg^{-1} in surface arable soil layer (0–20 cm) and plow pan soil layer (20–40 cm), respectively. The application of manure significantly ($P < 0.05$) increased the soil pH, PNR, and the stocks of SOC, TN, TP, AP, AK, and NO_3^--N of soil in both surface arable soil layer and plow pan soil layer. It had no remarkable difference ($P > 0.05$) in the stocks of TK and NH_4^+-N in all fertilization treatments.

In addition to organic fertilizer treatments, contents of SOC in chemical phosphorus fertilizer treatments (NP, NPK) were significantly higher ($P < 0.05$) than that in N and N_2 treatments. The content of PNR in organic fertilizer treatments was significantly higher ($P < 0.05$) than that in chemical fertilizer treatments, and that in surface arable soil was significantly higher ($P < 0.05$) than that in plow pan soil. It was highest in M treatment in both soil layers. The stock of DOC in surface arable soil in the M treatment was the highest in all treatments, and contents of DOC in plow pan soil in N, MN, and MN_2 treatments were the highest in all treatments.

Abundance and Community Structures of AOB and AOA in Soil

The *aom*A gene (AOB) quantified by qPCR ranging from 4.68×10^5 to 7.28×10^6 copy numbers per gram of dry soil in surface arable soil layer (**Figure 1A**) and 7.44×10^5 to 6.1×10^6 copy numbers per gram of dry soil in plow pan soil layer (**Figure 1B**) in this experiment. The abundance of *amo*A gene in both soil layers in organic fertilizer treatments was prominently higher ($P < 0.05$) than that in chemical fertilizer treatments. Except for N_2 and MNPK treatments, the abundance of *amo*A gene in surface arable soil layer was higher than that in plow pan soil layer.

Community structures of AOB were similar in both of two soil layers under long-term fertilization (**Figures 1A,B**). The abundance of uncultured bacterium MF323203.1 (MNPK 23.49 and 50.90%, MN 24.99 and 10.21%, MN_2 30.86 and 8.91%, M 11.52 and 5.92% in surface arable soil layer and plow pan soil layer, respectively), uncultured bacterium MF323620.1 (MNPK 22.25 and 81.09%, MN 14.22 and 3.88%, MN_2 28.83 and 9.14%, M 13.95 and 3.40% in surface arable soil layer and plow pan soil layer, respectively), and *Nitrosospira* PJA1 (MNPK 19.00 and 74.35%, MN 22.97 and 9.78%, MN_2 37.87 and 10.68%, M 3.27 and 0.76% in surface arable soil layer and plow pan soil layer, respectively) in organic fertilizer treatments was prominently higher ($P < 0.05$) than that in other treatments. The abundance of unclassified *Nitrosomonadaceae* in NP (27.70 and 7.67% in surface arable soil layer and plow pan soil layer, respectively), NPK (46.70 and 10.24% in surface arable soil layer and plow pan soil layer, respectively), and *Nitrosospira*.L115 in NP (27.34% in surface arable soil layer) and NPK (25.24% in surface arable soil layer) treatments were significantly higher ($P < 0.05$) than that in other treatments. The abundance of *Nitrosomonadaceae* (40.78 and 40.02% in surface arable soil layer and plow pan soil layer, respectively) was the highest in N_2 treatment. The abundance of uncultured *Nitrosomonadales* bacterium was the highest in M treatment (87.62 and 62.64% in surface arable soil layer and plow pan soil layer, respectively). The abundance of *Nitrosospira*.Ka3, uncultured AOB and *Nitrosospira*.Nsp12 in fertilizer treatments were prominently higher ($P < 0.05$) than that in CK treatment (*Nitrosospira*.Ka3 0.62 and 5.82%, uncultured AOB 0.73 and 0.07% in surface arable soil layer and plow pan soil layer, respectively). Unclassified *Nitrosospira* in surface arable soil layer was different from that in plow pan soil layer. The quantities of unclassified *Nitrosospira* were dominantly higher in NP (11.52%), NPK (20.01%) treatments, and organic fertilizer treatments (MNPK 23.11%, MN 11.86%, MN2 25.40%, M 3.83%) than that in other treatments in surface arable soil, whereas the quantities of unclassified *Nitrosospira* were significantly higher ($P < 0.05$) in organic fertilizer treatments (MNPK 69.69%, MN 5.09%, MN_2 11.79%, M 5.68%) than that in chemical fertilizer treatments in plow pan soil.

The *arch-amo*A gene (AOA) quantified by qPCR ranging from 9.82×10^5 to 6.49×10^6 copy numbers per gram of dry soil in surface arable soil layer (**Figure 2A**) and 2.07×10^6–9.09×10^6 copy numbers per gram of dry soil in plow pan soil layer (**Figure 2B**). The abundance of *arch-amo*A gene of soil in MN_2 treatment was significantly higher ($P < 0.05$) than that in other treatments in surface arable soil layer, and the abundance of *arch-amo*A gene of soil in M treatment was significantly higher ($P < 0.05$) than that in other treatments in plow pan soil layer. There was no prominent difference ($P > 0.05$) in *arch-amo*A gene abundance in surface arable soil layer of N, NPK, MN, and MNPK treatments. The abundance of *arch-amo*A gene in NP, N_2, and CK treatments were significantly lower ($P < 0.05$) than that in other treatments in surface arable soil. The abundance of *arch-amo*A gene in M, MNPK, N_2, and N treatments were significantly higher than CK treatment, and CK treatment had no significant difference with MN and MN_2 treatments in plow pan soil. Except for MN_2 and NPK treatments, the abundance of *arch-amo*A gene in surface arable soil layer was significantly higher ($P < 0.05$) than that in plow pan soil layer.

Community structures of AOA were similar in both of two soil layers under long-term fertilization (**Figures 2A,B**). The abundance of *Crenarchaeota* in M (0.37 and 0.56% in surface arable soil layer and plow pan soil layer, respectively) and CK (1.28 and 0.93% in surface arable soil layer and plow pan soil layer, respectively) treatments was dominantly lower ($P < 0.05$) than that in other treatments; MN_2 treatment (27.69%) was

TABLE 1 | Physicochemical properties of soils in different fertilization treatments after 38 years of long-term fertilization.

	Soil layers	CK	N	N_2	NP	NPK	M	MN	MN_2	MNPK
pH	0–20 cm	5.97 ± 0.1*c*	5.24 ± 0.07*e*	5.03 ± 0.07*f*	5.72 ± 0.12*d*	5.77 ± 0.08*d*	6.95 ± 0.07*a*	6.2 ± 0.02*b*	5.93 ± 0.07*c*	6.13 ± 0.02*b*
	20–40 cm	5.93 ± 0.01*e*	6.06 ± 0.04*d*	5.78 ± 0.06*f*	6.42 ± 0.07*c*	6.14 ± 0.07*d*	6.86 ± 0.03*a*	6.56 ± 0.03*b*	6.55 ± 0.07*b*	6.42 ± 0.05*c*
TN ($g \bullet kg^{-1}$)	0–20 cm	0.99 ± 0.01*e*	1.08 ± 0.03*d*	0.99 ± 0.04*e*	1.15 ± 0.07*c*	1.07 ± 0.01*d*	1.53 ± 0.01*a*	1.46 ± 0.02*b*	1.56 ± 0.02*a*	1.55 ± 0.02*a*
	20–40 cm	0.87 ± 0.01*de*	0.73 ± 0.02*f*	0.84 ± 0.02*ef*	0.82 ± 0.05*g*	0.83 ± 0.02*ef*	0.92 ± 0.01*c*	0.88 ± 0.01*d*	0.98 ± 0.03*bc*	1.17 ± 0.01*a*
SOC ($gkg \bullet^{-1}$)	0–20 cm	13.91 ± 0.03*f*	15.26 ± 0.03*d*	14.44 ± 0.51*e*	17.29 ± 0.68*c*	16.33 ± 0.07*c*	23.31 ± 0.17*a*	21.6 ± 0.02*b*	23.32 ± 0.11*a*	22.82 ± 0.01*a*
	20–40 cm	12.15 ± 0.03*f*	10.42 ± 0.18*h*	11.59 ± 0.12*g*	12.61 ± 0.01*e*	12.49 ± 0.13*e*	14.5 ± 0*c*	13.34 ± 0.14*d*	15.35 ± 0.04*b*	20.51 ± 0.23*a*
TP ($g \bullet kg^{-1}$)	0–20 cm	0.2 ± 0.01*e*	0.22 ± 0.01*e*	0.21 ± 0.03*e*	0.27 ± 0.02*d*	0.27 ± 0.03*d*	0.7 ± 0.04*b*	0.6 ± 0.01*c*	0.68 ± 0.03*b*	0.83 ± 0.02*a*
	20–40 cm	0.24 ± 0.02*f*	0.24 ± 0.01*f*	0.23 ± 0.01*f*	0.26 ± 0.01*f*	0.31 ± 0.01*e*	0.48 ± 0.03*b*	0.35 ± 0*d*	0.43 ± 0*c*	0.63 ± 0.02*a*
TK ($g \bullet kg^{-1}$)	0–20 cm	22.11 ± 2.42*abcde*	20.26 ± 1.03*e*	21.51 ± 2.29*bcde*	20.81 ± 0.77*de*	21.06 ± 1.3*cde*	23.38 ± 0.4*ab*	24.17 ± 1.02*a*	23.8 ± 0.38*ab*	23.27 ± 0.51*abcd*
	20–40 cm	23.85 ± 0.51*ab*	22.29 ± 1.64*b*	23.08 ± 0.59*ab*	24.11 ± 0.56*ab*	23.17 ± 0.84*ab*	24.31 ± 0.28*a*	23.68 ± 1.04*ab*	23.21 ± 1.17*ab*	23.7 ± 1.26*ab*
AP ($mg \bullet kg^{-1}$)	0–20 cm	4.05 ± 0.2*f*	1.65 ± 0.69*f*	2.74 ± 0.4*f*	10.89 ± 0.89*ef*	18.78 ± 3.68*e*	98.12 ± 9.55*c*	74.21 ± 15.44*d*	100.63 ± 1.87*b*	136.75 ± 0.82*a*
	20–40 cm	3.32 ± 0.31*e*	1.62 ± 0.27*e*	1.45 ± 0.15*e*	5.46 ± 0.82*e*	4.57 ± 0.27*e*	68.01 ± 5.35*b*	31.61 ± 0.97*d*	42.58 ± 2.12*c*	117.9 ± 6.69*a*
AK ($mg \bullet kg^{-1}$)	0–20 cm	86.83 ± 6.45*e*	79.21 ± 0.95*e*	58.58 ± 2.76*f*	89.73 ± 11.9*e*	148.38 ± 9.19*c*	114.01 ± 13*d*	153.59 ± 7.16*bc*	164.91 ± 10.62*ab*	169.5 ± 9.23*a*
	20–40 cm	73.25 ± 4.63*cd*	73.58 ± 4.01*cd*	72.91 ± 4.94*d*	62.23 ± 3.79*e*	77.25 ± 8.1*cd*	87.6 ± 1*b*	77.25 ± 1.53*cd*	83.6 ± 5.58*bc*	104.63 ± 9.86*a*
NH_4^+-N ($mg \bullet kg^{-1}$)	0–20 cm	3.62 ± 0.2*ab*	3.49 ± 0.2*b*	3.45 ± 0.08*b*	4.07 ± 0.55*a*	3.32 ± 0.13*b*	3.4 ± 0.17*b*	3.71 ± 0.33*ab*	4.08 ± 0.37*a*	3.37 ± 0.08*b*
	20–40 cm	3.54 ± 0.2*a*	3.62 ± 0.27*a*	3.47 ± 0.04*a*	3.59 ± 0.27*a*	3.67 ± 0.37*a*	3.34 ± 0.03*a*	3.64 ± 0.12*a*	3.58 ± 0.19*a*	3.5 ± 0.06*a*
PNR ($mg \bullet kg^{-1} \bullet d^{-1}$)	0–20 cm	0.86 ± 0.02*h*	1.83 ± 0.07*e*	1.4 ± 0.08*g*	1.6 ± 0.05*f*	1.68 ± 0*ef*	5.06 ± 0.17*a*	2.59 ± 0.05*c*	2.4 ± 0.06*d*	3.46 ± 0.11*b*
	20–40 cm	1.16 ± 0.04*d*	0.96 ± 0.04*e*	1.45 ± 0.11*c*	0.54 ± 0.03*f*	0.64 ± 0.1*f*	3.99 ± 0.19*a*	2.54 ± 0.04*b*	1.61 ± 0.11*c*	2.52 ± 0.09*b*
NO_3^--N ($mg \bullet kg^{-1}$)	0–20 cm	2.56 ± 0.15*c*	8.12 ± 0.49*b*	7.00 ± 0.31*bc*	5.65 ± 0.49*bc*	5.01 ± 0.3*bc*	27.32 ± 2.15*a*	23.22 ± 6.44*a*	22.45 ± 1.72*a*	25.51 ± 3.79*a*
	20–40 cm	1.5 ± 0.31*f*	5.23 ± 0.34*e*	7.76 ± 0.56*d*	2.17 ± 0.75*f*	2.49 ± 0.31*f*	19.8 ± 0.8*a*	12.88 ± 1.19*c*	16.76 ± 1.71*b*	12.53 ± 1.21*c*
DOC ($mg \bullet kg^{-1}$)	0–20 cm	15.58 ± 2.9*e*	25.56 ± 2.02*cd*	36.04 ± 3.48*a*	34.59 ± 5.85*ab*	26.55 ± 1.78*cd*	22.26 ± 4.26*d*	21.83 ± 0.27*d*	29.03 ± 0.9*bc*	27.27 ± 5.44*cd*
	20–40 cm	3.72 ± 0.04*c*	12.44 ± 1.12*a*	4.17 ± 1.38*c*	4.66 ± 2.35*c*	5.19 ± 0.82*c*	4.88 ± 1.22*c*	9.21 ± 2.53*b*	14.05 ± 2.51*a*	6.3 ± 1.39*c*
SMC (%)	0–20 cm	20.76 ± 0.1*c*	20.99 ± 0.2*c*	20.30 ± 0.2*c*	18.16 ± 1.1*d*	19.94 ± 0.7*c*	23.72 ± 1.0*a*	22.54 ± 0.2*b*	22.36 ± 0.1*b*	22.68 ± 0.4*b*
	20–40 cm	21.98 ± 0.5*abc*	21.33 ± 1.1*abc*	20.68 ± 0.4*c*	21.42 ± 1.4*abc*	21.23 ± 0.7*bc*	21.93 ± 0.7*abc*	21.50 ± 0.8*abc*	22.66 ± 0.4*ab*	22.79 ± 0.4*a*

CK, no fertilizer, N, mineral nitrogen fertilizer; N_2, high mineral nitrogen fertilizer; NP, mineral nitrogen and phosphate fertilizer; NPK, mineral nitrogen, phosphate and potassium fertilizer; M, pig manure; MN, pig manure and mineral nitrogen fertilizer; MN_2, pig manure and high mineral nitrogen fertilizer; MNPK, pig manure, mineral phosphate, potassium fertilizer and mineral nitrogen fertilizer; SOC, soil organic carbon; TN, total nitrogen; TP, total phosphorus; TK, total potassium; AP, available phosphorus; AK, available potassium; NH_4^+-N, ammonia nitrogen; NO_3^--N, nitrate nitrogen; PNR, potential nitrite rate; DOC, dissolved organic carbon; SMC, soil moisture carbon. The mean value ± SD (n = 3). Different letters in the same row represent significantly differences among fertilization treatments (LSD method, and $p < 0.05$).

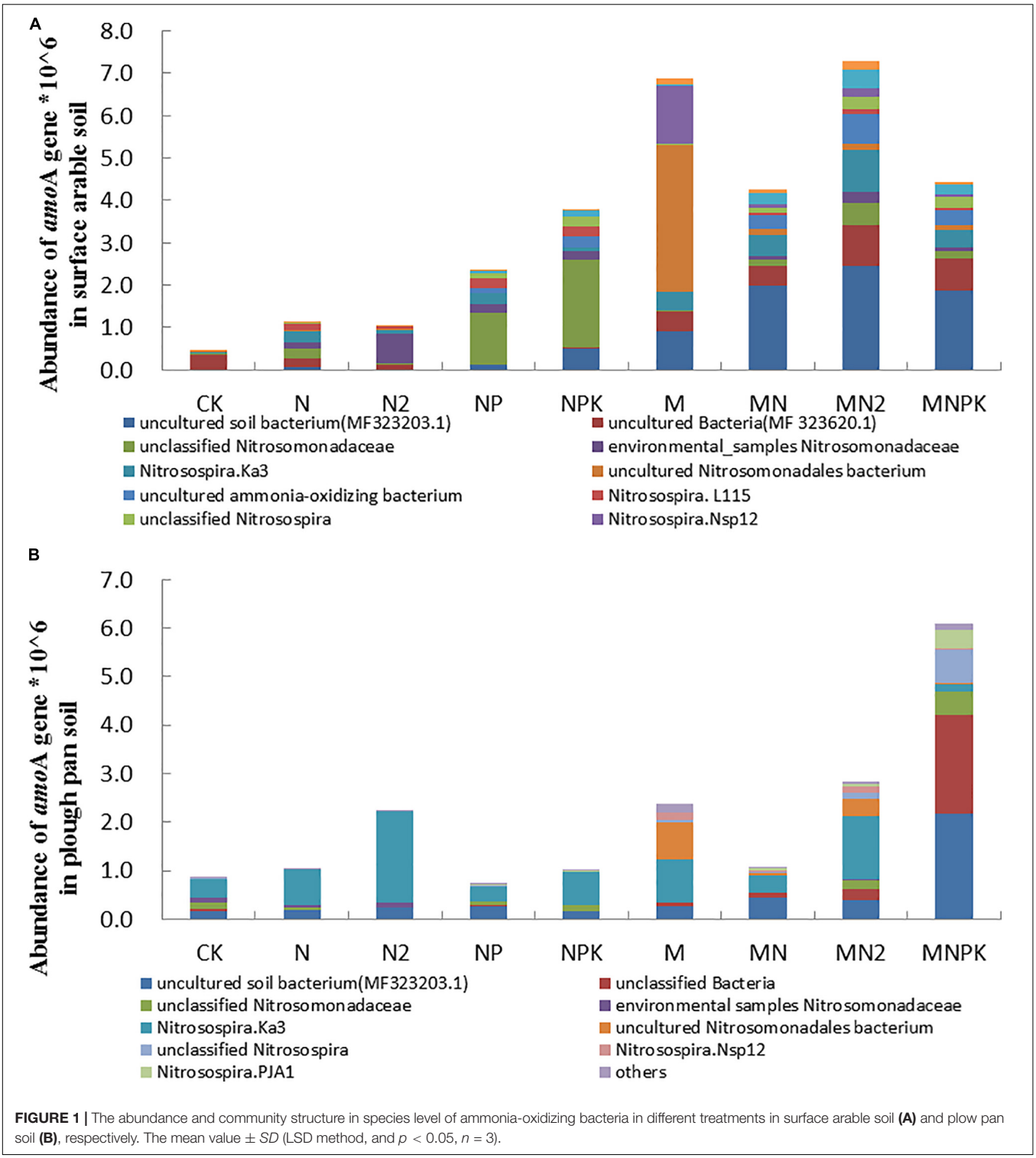

FIGURE 1 | The abundance and community structure in species level of ammonia-oxidizing bacteria in different treatments in surface arable soil **(A)** and plow pan soil **(B)**, respectively. The mean value ± *SD* (LSD method, and $p < 0.05$, $n = 3$).

the highest than other treatments in surface arable soil, and N_2 treatment (31.58%) was the highest treatment than other treatments in plow pan soil. It indicated that excessive nitrogen was good to *Crenarchaeota*, and the increment of *Crenarchaeota* increased with the increase of chemical nitrogen fertilizer; in opposite, organic manure alone inhibited *Crenarchaeota*. The abundance of uncultured AOA in NPK (22.22 and 9.11% in surface arable soil layer and plow pan soil layer, respectively) and M (19.31 and 34.69% in surface arable soil layer and plow pan soil layer, respectively) treatments was dominantly higher ($P < 0.05$) than that in other treatments. The abundance of *Nitrososphaera*.JG1 (MNPK 13.75 and 27.33%, MN 18.69

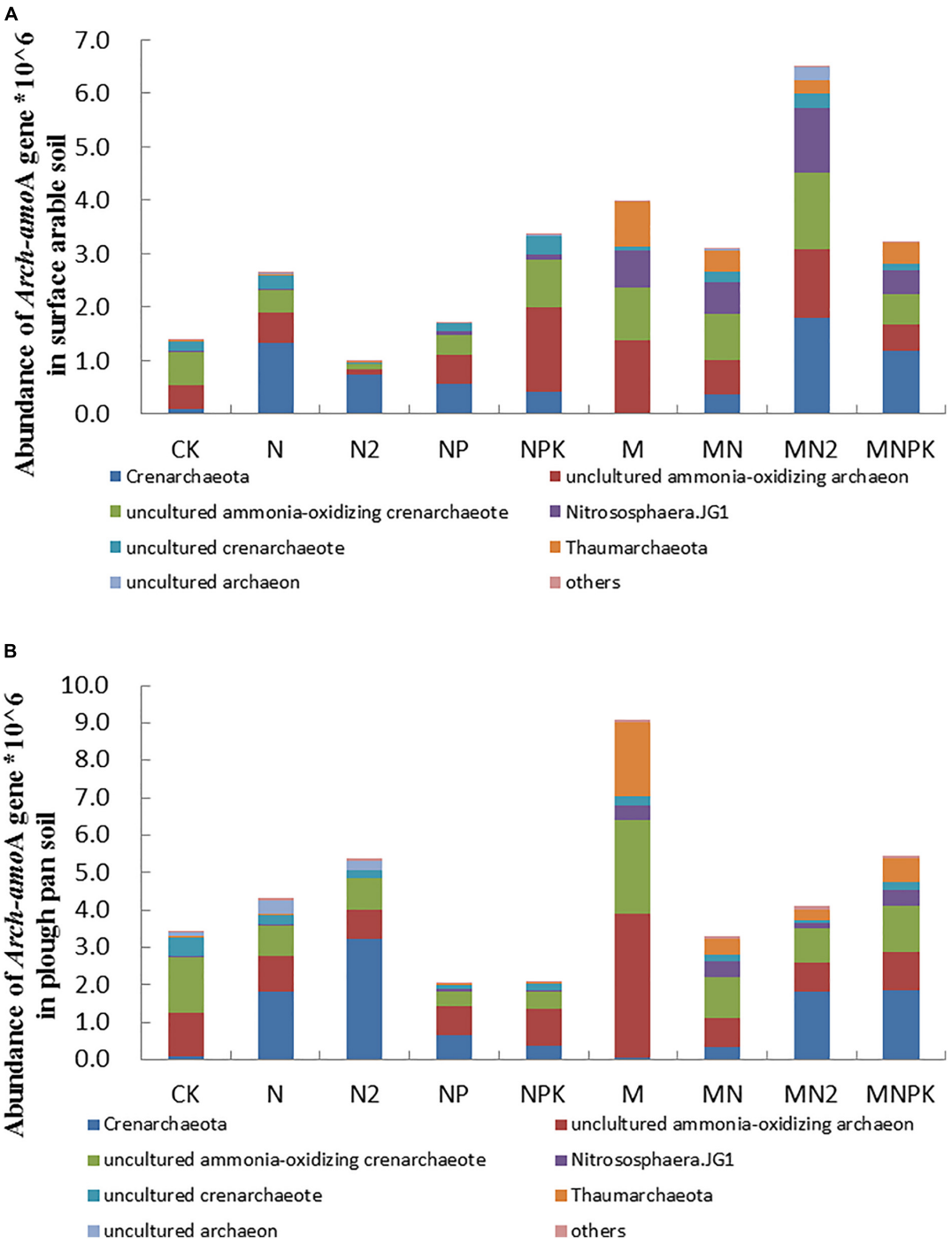

FIGURE 2 | The abundance and community structure in species level of ammonia-oxidizing archaea in different treatments in surface arable soil **(A)** and plow pan soil **(B)**, respectively. The mean value ± *SD* (LSD method, and $p < 0.05$, $n = 3$).

and 27.70%, MN_2 38.52 and 10.08%, M 22.21 and 25.37% in surface arable soil layer and plow pan soil layer, respectively) and *Thaumarchaeota* (MNPK 20.50 and 17.97%, MN 20.44 and 12.88%, MN_2 12.68 and 8.18%, and M 44.44 and 56.92% in surface arable soil layer and plow pan soil layer, respectively) in organic fertilizer treatments was significantly higher ($P < 0.05$) than that in chemical fertilizer treatments. The abundance of uncultured ammonia-oxidizing *Crenarchaeote* and uncultured *Crenarchaeote* were different between two soil layers. The abundance of uncultured ammonia-oxidizing *Crenarchaeote* in organic manure treatments (MNPK 9.41%, MN 13.88%, MN_2 22.87%, M 15.64%) was significantly higher ($P < 0.05$) than

that in other treatments in surface arable soil, whereas that in M (15.21%) and CK (25.67%) treatments was significantly higher ($P < 0.05$) as compared to other treatments in plow pan soil. The abundance of uncultured *Crenarchaeota* in NPK (19.75%), N (15.89%), MN (12.37%), and MN_2 (17.13%) was significantly higher ($P < 0.05$) than that in other treatments in surface arable soil, whereas that in CK treatment (25.95%) was significantly higher ($P < 0.05$) with respect to other treatments in plow pan soil.

Community Structures of AOB and AOA in Soil Under Relative Abundance

The relative abundance of AOB community structures was different between surface arable soil with plow pan soil under long-term fertilization (**Supplementary Figures S1A,B**). The relative quantity of *Nitrosospira*.Ka3 in CK treatment was prominently lower than that in other treatments in surface arable soil (**Supplementary Figure S1A**). The relative abundance of unclassified *Nitrosomonadaceae*, unclassified environmental samples *Nitrosomonadaceae*, and *Nitrosospira*.L115 in chemical treatments was prominently higher than that in other treatments, and the relative abundance of unclassified environmental samples *Nitrosomonadaceae* in N and N_2 treatments was prominently higher as compared to other treatments. The relative abundance of uncultured bacterium MF323203.1 in MNPK, MN, and MN_2 treatments was significantly higher than that in other treatments. It indicated that application of organic in combination with chemical fertilizer could increase the relative quantity of uncultured AOB. The relative abundance of unclassified *Nitrosomonadaceae*, unclassified environmental samples *Nitrosomonadaceae* in CK treatment, was significantly higher than that in other treatments in plow pan soil (**Supplementary Figure S1B**). The relative abundance of *Nitrosospira*.Ka3 in chemical fertilizer treatments was significantly higher than that in other treatments. The relative abundance of uncultured *Nitrosomonadales* bacterium and *Nitrosospira*.Nsp12 in M treatment was prominently higher than that in other treatments. The relative abundance of unclassified *Nitrosospira*, *Nitrosospira*.PJA1 in N, N_2, M, and CK treatments was significantly lower among all other treatments. The relative abundance of AOA community structures was similar in both soil layers under long-term fertilization (**Supplementary Figures S2A,B**). The relative abundance of *Crenarchaeota* in M and CK treatments was dominantly lower than that in other treatments. *Crenarchaeota* in chemical fertilizer treatments was significantly higher than that in organic manure treatments; N_2 treatment was higher than N treatment; MN_2 treatment was higher than MN treatment. The relative abundance of uncultured ammonia-oxidizing *Crenarchaeote* and uncultured *Crenarchaeote* in CK treatment was significantly higher than that in other treatments. Uncultured *Crenarchaeote* of relative abundance in chemical fertilizer treatments was higher than that in organic fertilizer treatments. The relative quantity of *Thaumarchaeota* in M treatment was higher than that in other treatments, whereas the relative abundance of *Nitrososphaera*.JG1 in organic manure treatments was significantly higher than that in chemical fertilizer treatments. It indicated that application of organic manure fertilizer increased the quantity.

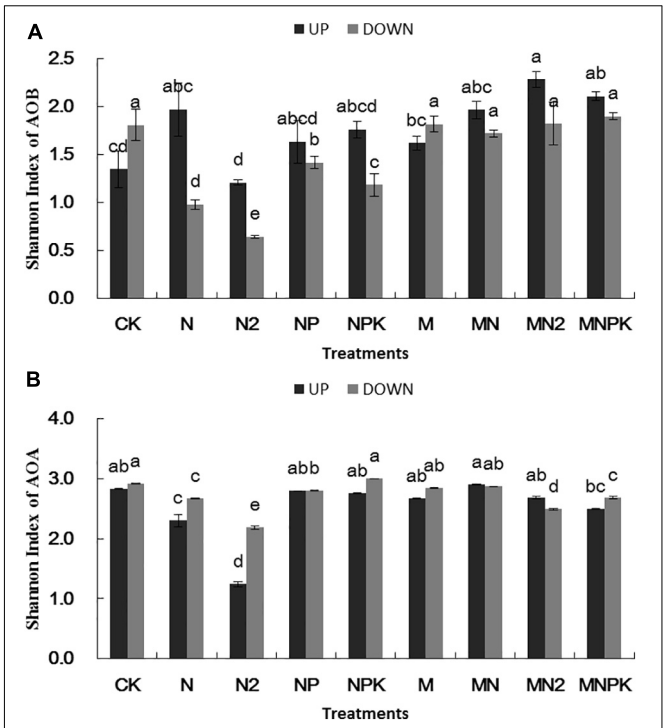

FIGURE 3 | Shannon index of ammonia-oxidizing bacteria **(A)** and archaea **(B)** in different treatments in surface arable soil and plow pan soil, respectively. The mean value ± *SD* ($n = 3$). Different letters represent significant differences among fertilization treatments (LSD method, and $p < 0.05$). UP represented surface arable soil (0–20 cm), and Down represented plow pan soil (20–40 cm).

Shannon Index of AOA and AOB

Shannon index of AOB (**Figure 3A**) in the N_2 treatment was significantly lower ($P < 0.05$) than other treatments in both of two soil layers. Shannon index of AOB was higher in surface arable soil than that in plow pan soil. There was no significant difference ($P > 0.05$) between organic fertilizer treatments and CK treatment in Shannon index of AOB in plow pan soil, whereas the Shannon index of AOB was higher in organic manure treatments than that in chemical fertilizer treatments.

Shannon index of AOA (**Figure 3B**) in N and N_2 treatments was significantly lower ($P < 0.05$) than that in other treatments in surface arable soil layer, whereas Shannon index of AOA in N, N_2, and MN_2 treatments in plow pan soil layer was significantly lower ($P < 0.05$) than that in other treatments. Shannon index of AOA in plow pan soil layer was higher than that in surface arable soil layer.

NMDS Analysis of AOA and AOB

In order to determine whether long-term fertilization and soil layers were related to changes in soil ammonia-oxidizing microbial community structure, we used NMDS based on Bray–Curtis dissimilarities to analyze the overall archaeal and

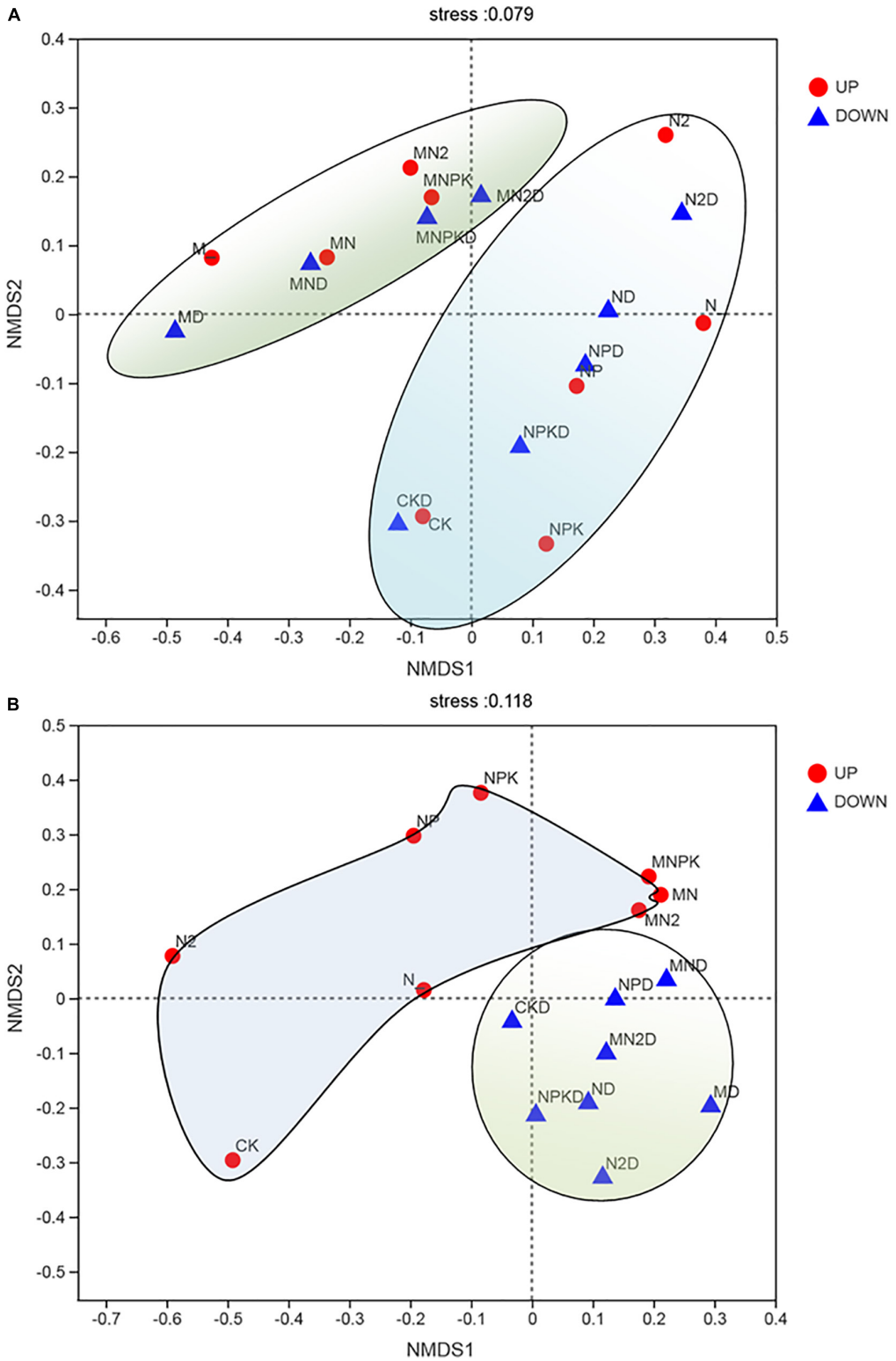

FIGURE 4 | Non-metric multidimensional scaling (NMDS) of AOA **(A)** and AOB **(B)** in two soil layers under different fertilization treatments. UP represented surface arable soil (0–20 cm) and Down represented plow pan soil (20–40 cm). Points of different colors or shapes represent samples of different groups. The closer the two sample points are, the more similar the species composition of the two samples. The abscissa and ordinate indicate the relative distance and have no practical meaning. Stress: Test the pros and cons of NMDS analysis results. It is generally believed that when stress is less than 0.2, it can be represented by a two-dimensional dot diagram of NMDS, which has a certain explanatory meaning; when stress is less than 0.1, it can be considered as a good ranking.

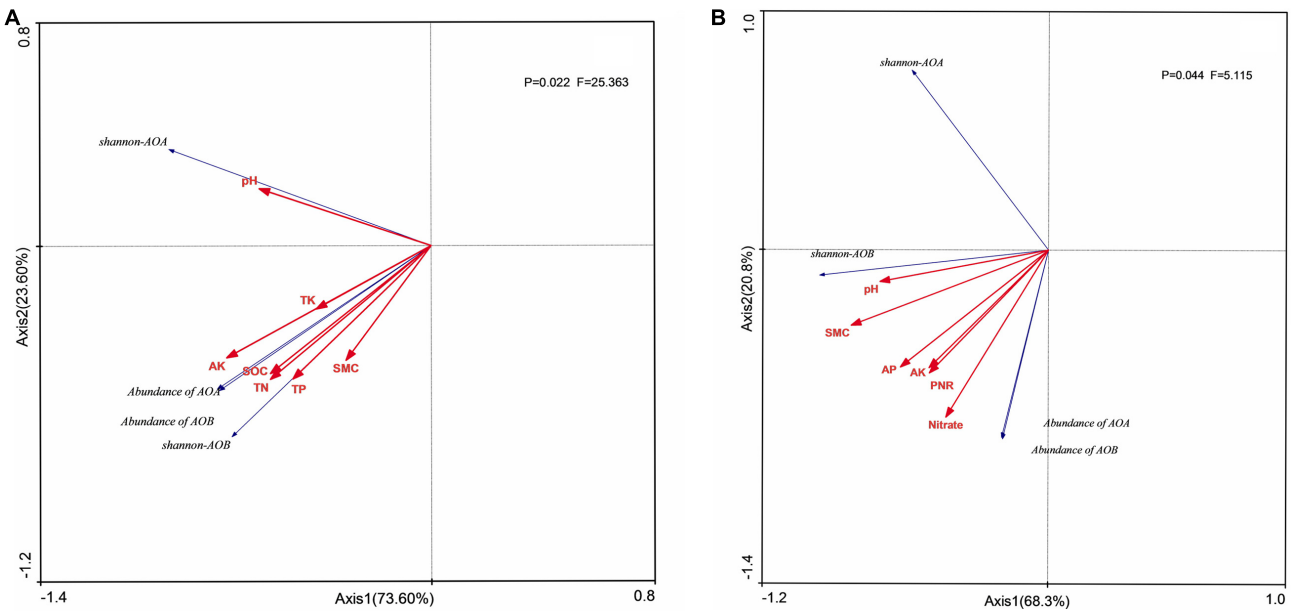

FIGURE 5 | Redundancy analysis (RDA) of AOB and AOA in diversity and quantity in surface arable soil layer **(A)** and plow pan soil layer **(B)**. RDA correlation plot showed changes in ammonia oxidizers diversity and quantity explained by soil environmental factors. SOC, soil organic carbon; TN, total nitrogen; TP, total phosphorus; TK, total potassium; AP, available phosphorus; AK, available potassium; NO_3^--N, nitrate nitrogen; PNR, potential nitrite rate; SMC, soil moisture carbon.

bacterial community structural changes in **Figure 4**. The NMDS ordinations showed that the AOA (**Figure 4A**) community structure was divided into two parts: the organic fertilizer treatment and chemical fertilizer treatments. The community structure of AOB (**Figure 4B**) had a significant correlation with the soil layer, and the community structure of AOB was divided into two parts: the surface arable soil and the plow pan soil.

The Relationship Among Soil Physicochemical Properties, Abundance, and Community Structure of AOA and AOB

The quantities of AOB in both soil layers (**Figure 5**) and AOA in surface arable soil layer (**Figure 5A**) had significant positive correlation ($P < 0.05$) with stocks of SOC, TN, TP, AP, AK, and NO_3^--N under long-term fertilization, and the quantities of AOB in surface soil (**Figure 5A**) had significant positive correlation ($P < 0.05$) with PNR, whereas the quantity of AOA had significant positive correlation ($P < 0.05$) with PNR and NO_3^--N in plow pan soil layer and had significant negative correlation with NH_4^+-N.

Shannon index of AOA had no relationship with environmental factors in both two soil layers (**Figure 5**), whereas the Shannon index of AOB had significant positive correlation ($P < 0.05$) with stocks of SOC, TN, and AK in both two soil layers. Unclassified *Nitrosomonadaceae*, *Nitrosomonadaceae*, and *Nitosospira*.L115 had no significant correlation ($P > 0.05$) with environmental factors, whereas uncultured bacterium MF323203.1, uncultured *Nitrosomonadaceae* bacterium, and *Nitrosospira*.Nsp12 had significant positive correlation ($P < 0.05$) with PNR and stocks of SOC, TN, TP, and NO_3^--N in surface arable soil layer (**Figure 6A**). Uncultured bacterium MF323203.1 had prominently positive correlation ($P < 0.05$) with TK, AP, and AK, whereas *Nitrosospira*.PJA1 had prominent correlation ($P < 0.05$) with SOC, TK, AP, and AK, and unclassified *Nitrosospira* only had significant correlation ($P < 0.05$) with AK. *Nitrosospira*.Ka3, uncultured bacterium MF323203.1, and environmental samples of *Nitrosomonadaceae* had no correlation ($P < 0.05$) with environmental factors. Uncultured *Nitrosomonadaceae* bacterium and unclassified *Nitrosospira* had significant positive correlation ($P < 0.05$) with PNR and stocks of TP, AP, and NO_3^--N in plow pan soil layer (**Figure 6B**). Uncultured *Nitrosomonadaceae* bacterium had prominent correlation with soil pH. Uncultured bacterium MF323203.1, uncultured bacterium MF323620.1, and unclassified *Nitrosospira* were significantly correlated with SOC, TP, TK, AP, and AK, whereas *Nitrosospira*.PJA1 had significant correlation with pH, SOC, and TP.

Crenarchaeota, unclassified AOA, uncultured *Crenarchaeota*, and uncultured archaea had no significant correlation ($P < 0.05$) with the environmental factors, whereas *Nitrososphaera*.JG1 and *Thaumarchaeota* had significant positive correlation ($P < 0.05$) with PNR, soil pH, and stocks of SOC, TN, TP, TK, and NO_3^--N in surface arable soil layer (**Figure 6C**). Unclassified AOA, uncultured ammonia-oxidizing *Crenarchaeota*, *Nitrososphaera*.JG1, and *Thaumarchaeota* had significant positive correlation ($P < 0.05$) with PNR and soil pH in plow pan soil layer, whereas *Nitrososphaera*.JG1 and *Thaumarchaeota* had significant positive correlation ($P < 0.05$) with soil pH and stocks of SOC, TN, TP, AP, AK, and NO_3^--N in plow pan soil layer (**Figure 6D**).

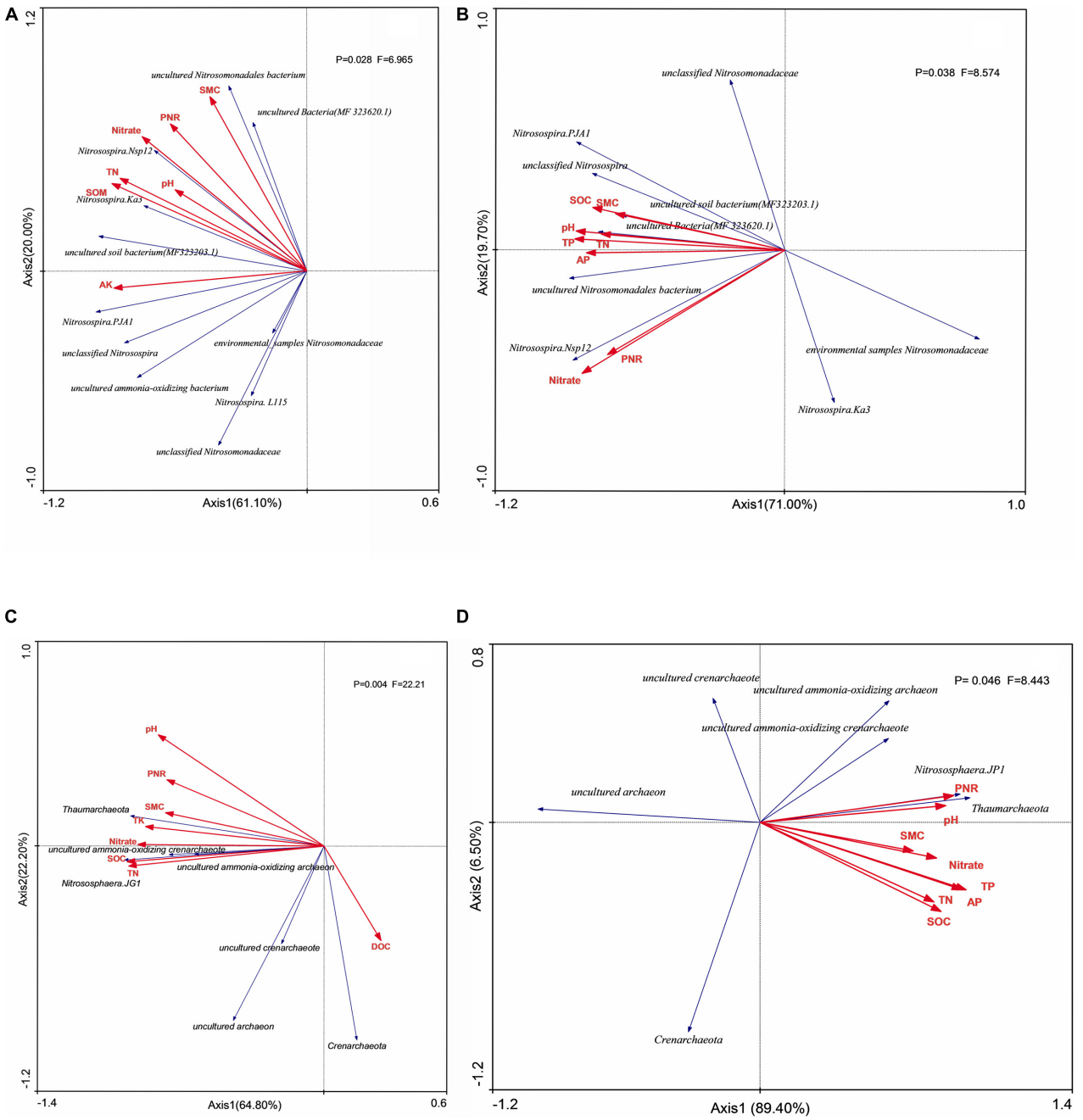

FIGURE 6 | Redundancy analysis (RDA) of AOB taxa on surface arable soil **(A)** and plow pan soil **(B)**, respectively, and of AOA taxa on surface arable soil **(C)** and plow pan soil **(D)**. RDA correlation plot showed variance in taxa of ammonia-oxidation microorganisms explained by soil environmental factors. SOC, soil organic carbon; TN, total nitrogen; TP, total phosphorus; TK, total potassium; AP, available phosphorus; AK, available potassium; NO_3^--N, nitrate nitrogen; PNR, potential nitrite rate; DOC, dissolved organic carbon; SMC, soil moisture carbon.

DISCUSSION

Long-term application of manure with chemical fertilizer could effectively increase soil nutrient content, improve soil physicochemical properties, and increase crop yields, thereby influencing microorganisms (Oehl et al., 2004; Shi et al., 2008; Feitosa de Souza et al., 2016; Lin et al., 2018), whereas long-term application of chemical nitrogen fertilizer alone was likely to decrease soil pH and microbial biomass and damage soil microbial structure (Sun et al., 2017; Huang et al., 2018; Li et al., 2019). Our experiment showed the same results, and the phosphorus fertilizer application could increase organic matters of soil (**Table 1**). Long-term application of manure with chemical fertilizer effectively slowed down soil

acidification and increased SOC, TN, TP, AP, and NO_3^--N in both soil layers, which might be due to the application of manure that could effectively improve physicochemical property of soil.

Our experiment showed that application of organic fertilizer could significantly increase the abundance of *amo*A gene in both soil layers (**Figure 1**). This result was consistent with results reported as the abundance of AOB in organic fertilizer treatment was higher than that in chemical fertilizer (Li et al., 2017, 2018), which was due to the enrichment of soil nutrients caused the increase of bacterial abundance. Our result has supported the above conjecture, and RDA in abundance of *amo*A gene with environment showed that the abundance of *amo*A gene was significant positively correlated with the stocks of SOC, TN, TP, AP, AK, and NO_3^--N in both layers of soil (**Figure 5**).

The results of absolute abundance (**Figures 1**, **2**) and relative abundance (**Supplementary Figures S1, S2**) analysis were different from each other on community structure of ammonia-oxidizing microorganisms. We adopted the combined determination results of absolute abundance with the proportion of relative abundance of each taxon in different treatments for subsequent analysis in order to get the analysis results closer to the real situation.

The application of organic fertilizer, balanced application of chemical fertilizer, and rational application of nitrogen fertilizer could improve the abundance of *arch-amo*A gene in surface arable soil (**Figure 2A**), whereas the application of organic fertilizer and nitrogen fertilizer could keep the abundance of *arch-amo*A gene constant in plow pan soil layer (**Figure 2B**). The abundance of *arch-amo*A gene was higher in plow pan soil layer than that in surface arable soil layer. This might be due to the oxygen content in surface arable soil layer being higher than that in plow pan soil layer, and parts of AOA belong to anaerobic heterotrophic bacteria under our experimental condition. Previous studies have confirmed that AOA could adapt to lower oxygen conditions (Liu et al., 2015), and AOB quantities were more easily decreased along with the sediment depth (Wang et al., 2014).

The results of NMDS (**Figure 4**) showed that the community structure of AOB was divided into two parts in all treatments according to soil layers. This result indicated that the taxa of AOB in different soil layers were significantly different. On the one hand, soil nutrient of plow pan soil layer was significantly lower than that of surface arable soil layer; on the other hand, dissolved oxygen could greatly affect the growth of bacteria (Canziani et al., 2006), whereas AOB were significantly increased in less bioturbated zone (Chen and Gu, 2017). Therefore, community structure of AOB in plow pan soil layer was significantly different from that in surface arable soil layer due to less soil nutrient, oxygen, and disturbance in plow pan soil layer.

The results of NMDS (**Figure 4A**) showed that the community structure of AOA was divided into two parts in both soil layers due to application of organic fertilizer. This result indicated that AOA had different requirements for nutrient forms. This was consistent with the result reported for readily mineralized organic matter, which was important for AOA (Jiang et al., 2012), and addition of glucose could influence the community of AOA in Beijing Miyun Reservoir (Wang et al., 2015).

PNR was the ability of soil to oxidize ammonium nitrogen to nitrate nitrogen. In our experiment, long-term application of organic fertilizer was more conducive to improving soil PNR; this might be due to that organic fertilizer enhanced the PNR, whereas chemical fertilizer suppressed PNR (Fan et al., 2011). Han et al. (2016) found that PNR was significant positively correlated with abundance of AOB but not AOA. Some studies (Qin et al., 2012; Xu et al., 2012) found that AOA, but not AOB, was significantly correlated with PNR in acidic soils of slope land, and Nguyen et al. (2018) found that PNR was significantly correlated with both AOA and AOB. However, we found that PNR was significantly correlated with the abundance of *amo*A of AOB in surface arable soil layer (**Figure 5A**) and significantly correlated with the abundance of AOA in plow pan soil layer (**Figure 5B**). The abundance of uncultured bacterium MF323203.1, uncultured *Nitrosomonadaceae* bacterium, and *Nitrosospira*.Nsp12 had significant correlation with PNR and were mostly influenced by the soil phosphorus (**Figures 6A,B**), whereas the stock of P was significantly higher in surface arable soil than that in plow pan soil (**Table 1**). Thus, we hypothesized that this might be related to the beneficial effects of phosphorus on the growth and reproduction of these AOB. The abundance of unclassified AOA, uncultured ammonia-oxidizing *Crenarchaeota*, *Nitrososphaera*.JG1, and *Thaumarchaeota* had significant correlation with PNR and was prominently higher in manure fertilizer treatments than that in chemical fertilizer treatments (**Figures 2A,B**). NMDS ordinations (**Figure 4A**) showed that AOA was divided into two parts by organic fertilizer. Thus, we hypothesized that abundance of these AOA could be increased by complex changes in the soil physical and chemical properties, which were due to organic fertilizer. These results might be due to that uncultured bacterium MF323203.1, uncultured *Nitrosomonadaceae* bacterium, *Nitrosospira*.Nsp12, *Nitrososphaera*.JG1, and *Thaumarchaeota* played a dominant role in PNR (**Figure 6**). However, the changes of abundance of uncultured bacterium MF323203.1, uncultured *Nitrosomonadaceae* bacterium, and *Nitrosospira*.Nsp12 that were positively correlated with PNR were consistent with the total abundance of AOB. The changes of abundance of *Nitrososphaera*.JG1 and *Thaumarchaeota* that had positive correlation with PNR were different from the total abundance of AOA in surface arable soil layer. The changes of abundance of unclassified AOA, uncultured ammonia-oxidizing *Crenarchaeota*, *Nitrososphaera*.JG1, and *Thaumarchaeota* were positively correlated with PNR and consistent with the total abundance of AOA. The changes of abundance of uncultured *Nitrosomonadaceae* bacterium and *Nitrosospira*.NSP12 were positively correlated with PNR and different from the total abundance of AOB in plow pan soil layer. PNR was correlated with unclassified AOA, uncultured ammonia-oxidizing *Crenarchaeota*, *Nitrososphaera*.JG1, *Thaumarchaeota* (AOA)

and uncultured bacterium MF323203.1, uncultured *Nitrosomonadaceae* bacterium, and *Nitrosospira*.Nsp12 (AOB). PNR was also positively related to the abundance of AOB in surface arable layer and AOA in plow pan layer macroscopically. The essence was that these taxa affected the ammonia oxidation under long-term fertilization in brown soil. It might be a good explanation for some studies suggesting that AOA or AOB played a dominant role in various environments.

CONCLUSION

In conclusion, long-term fertilization changed soil PNR by influencing specific ammonia-oxidizing microorganisms, which are influenced by soil physiochemical properties in the brown soil. Only specific and rare AOA and AOB instead of the whole AOA or AOB community played a dominant role in nitrification in brown soil under long-term fertilization.

DATA AVAILABILITY STATEMENT

The datasets presented in this study can be found in online repositories. The names of the repository/repositories and accession number(s) can be found in the article/ **Supplementary Material**.

AUTHOR CONTRIBUTIONS

FC, XH, and PL conceived, designed the study, and wrote the manuscript. JY, MI, SZ, NA, and JD collected and analyzed the data. All authors read and approved the final manuscript.

FUNDING

This work was supported by the National Key Research and Development Program of China (Grant No. 2018YFD0300308) and the National Natural Science Foundation of China (Grant No. 31972511).

SUPPLEMENTARY MATERIAL

The Supplementary Material for this article can be found online at: https://www.frontiersin.org/articles/10.3389/fmicb.2020.622454/full#supplementary-material

REFERENCES

Adair, K. L., and Schwartz, E. (2008). Evidence that ammonia-oxidizing archaea are more abundant than ammonia-oxidizing bacteria in semiarid soils of northern Arizona. *Microb. Ecol.* 56, 420–426. doi: 10.1007/s00248-007-9360-9

Belay, A., Claassens, A., and Wehner, F. (2002). Effect of direct nitrogen and potassium and residual phosphorus fertilizers on soil chemical properties, microbial components and maize yield under long-term crop rotation. *Biol. Fertil. Soils* 35:420427. doi: 10.1007/s00374-002-0489-x

Bhattacharyya, R., Prakash, V., and Kundu, S. (2010). Long term effects of fertilization on carbon and nitrogen sequestration and aggregate associated carbon and nitrogen in the Indian sub-Himalayas. *Nutr. Cycl. Agroecosyst.* 86:116. doi: 10.1007/s10705-009-9270-y

Canziani, R., Emondi, V., Garavaglia, M., Malpei, F., Pasinetti, E., and Buttiglieri, G. (2006). Effect of oxygen concentration on biological nitrification and microbial kinetics in a cross-flow membrane bioreactor (MBR) and moving-bed biofilm reactor (MBBR) treating old landfill leachate. *J. Membr. Sci.* 286:202212. doi: 10.1016/j.memsci.2006.09.044

Chen, J., and Gu, J. (2017). Faunal burrows alter the diversity, abundance, and structure of AOA, AOB, anammox and n-Damo communities in coastal mangrove sediments. *Microb. Ecol.* 74:140156. doi: 10.1007/s00248-017-0939-5

Chen, J., Zhang, H., Liu, W., Lian, J., Ye, W., and Shen, W. (2015). Spatial distribution patterns of ammonia-oxidizing archaea abundance in subtropical forests at early and late successional stages. *Sci. Rep.* 5:16587.

Chen, S., Zhou, Y., Chen, Y., and Gu, J. (2018). fastp: an ultra-fast all-in-one FASTQ preprocessor. *Bioinformatics* 34, i884–i890. doi: 10.1093/bioinformatics/bty560

Chen, X. P., Zhu, Y. G., Xia, Y., Shen, J. P., and He, J. Z. (2008). Ammonia-oxidizing archaea: important players in paddy rhizosphere soil? *Environ. Microbiol.* 10, 1978–1987. doi: 10.1111/j.1462-2920.2008.01613.x

Dang, C., Liu, W., Lin, Y., Zheng, M., Jiang, H., Chen, Q., et al. (2018). Dominant role of ammonia-oxidizing bacteria in nitrification due to ammonia accumulation in sediments of Danjiangkou reservoir, China. *Appl. Microbiol. Biotechnol.* 102:33993410. doi: 10.1007/s00253-018-8865-0

Edgar, R. C. (2013). UPARSE: highly accurate OTU sequences from microbial amplicon reads. *Nat. Methods* 10, 996–998. doi: 10.1038/nmeth.2604

Erguder, T. H., Boon, N., Wittebolle, L., Marzorati, M., and Verstraete, W. (2009). Environmental factors shaping the ecological niches of ammonia-oxidizing archaea. *FEMS Microbiol. Rev.* 33, 855–869. doi: 10.1111/j.1574-6976.2009.00179.x

Fan, F., Yang, Q., Li, Z., Wei, D., Cui, X. A., and Liang, Y. (2011). Impacts of organic and inorganic fertilizers on nitrification in a cold climate soil are linked to the bacterial ammonia oxidizer community. *Microb. Ecol.* 62, 982–990.

Feitosa, de Souza, T. A., Rodrígues, A. F., and Marques, L. F. (2016). The trend of soil chemical properties, and rapeseed productivity under different long-term fertilizations and stubble management in a Ferralsols of Northeastern Brazil. *Org. Agric.* 7, 353–363. doi: 10.1007/s13165-016-0164-4

Gan, X. H., Zhang, F. Q., Gu, J. D., Guo, Y. D., Li, Z. Q., Zhang, W. Q., et al. (2016). Differential distribution patterns of ammonia-oxidizing archaea and bacteria in acidic soils of nanling national nature reserve forests in subtropical China. *Antonie Van Leeuwenhoek* 109, 237–251. doi: 10.1007/s10482-015-0627-8

Han, J., Shi, J., Zeng, L., Xu, J., and Wu, L. (2016). Impacts of continuous excessive fertilization on soil potential nitrification activity and nitrifying microbial community dynamics in greenhouse system. *J. Soils Sediments* 17, 471–480. doi: 10.1007/s11368-016-1525-z

Hua, W., Luo, P., An, N., Cai, F., Zhang, S., Chen, K., et al. (2020). Manure application increased crop yields by promoting nitrogen use efficiency in the soils of 40-year soybean-maize rotation. *Sci. Rep.* 10:14882. doi: 10.1038/s41598-020-71932-9

Huang, L., Dong, H., Wang, S., Huang, Q., and Jiang, H. (2013). Diversity and abundance of ammonia-oxidizing archaea and bacteria in diverse chinese paddy soils. *Geomicrobiol. J.* 31, 12–22. doi: 10.1080/01490451.2013.797523

Huang, X., Liu, Y., Li, Y., Guo, P., Fang, X., and Yi, Z. (2018). Foliage application of nitrogen has less influence on soil microbial biomass and community composition than soil application of nitrogen. *J. Soils Sediments* 19, 221–231. doi: 10.1007/s11368-018-2027-y

Jiang, X., Liu, W., Liu, Q., Jia, Z., Wright, A. L., and Cao, Z. (2012). Soil N mineralization, nitrification and dynamic changes in abundance of ammonia-oxidizing bacteria and archaea along a 2000 year chronosequence of rice cultivation. *Plant Soil* 365, 59–68. doi: 10.1007/s11104-012-1377-2

Kandeler, E. (1995). "Potential nitrification," in *Methods in Soil Biology*, eds F. Schinner, R. Öhlinger, E. Kandeler, and A. Margesin (Berlin; Heidelberg: Springer), 146149.

Könneke, M., Bernhard, A. E., de la Torre, J. R., Walker, C. B., Waterbury, J. B., and Stahl, D. A. (2005). Isolation of an autotrophic ammonia-oxidizing marine archaeon. *Nature* 437, 543–546. doi: 10.1038/nature03911

Li, D., Chen, L., Xu, J., Ma, L., Olk, D. C., Zhao, B., et al. (2018). Chemical nature of soil organic carbon under different long-term fertilization regimes is coupled with changes in the bacterial community composition in a Calcaric Fluvisol. *Biol. Fertil. Soils* 54, 999–1012. doi: 10.1007/s00374-018-1319-0

Li, F., Chen, L., Zhang, J., Yin, J., and Huang, S. (2017). Bacterial community structure after long-term organic and inorganic fertilization reveals important associations between soil nutrients and specific taxa involved in nutrient transformations. *Front. Microbiol.* 8:187.

Li, M., and Gu, J. D. (2013). Community structure and transcript responses of anammox bacteria, AOA, and AOB in mangrove sediment microcosms amended with ammonium and nitrite. *Appl. Microbiol. Biotechnol.* 97, 9859–9874. doi: 10.1007/s00253-012-4683-y

Li, M., Cao, H., Hong, Y., and Gu, J. D. (2010). Spatial distribution and abundances of ammonia-oxidizing archaea (AOA) and ammonia-oxidizing bacteria (AOB) in mangrove sediments. *Appl. Microbiol. Biotechnol.* 89, 1243–1254. doi: 10.1007/s00253-010-2929-0

Li, N., Kumar, P., Lai, L., Abagandura, G. O., Kumar, S., Nleya, T., et al. (2019). Response of soil greenhouse gas fluxes and soil properties to nitrogen fertilizer rates under camelina and carinata nonfood oilseed crops. *BioEnergy Res.* 12, 524–535. doi: 10.1007/s12155-019-09987-4

Lin, Y., Slessarev, E. W., Yehl, S. T., D'Antonio, C. M., and King, J. Y. (2018). Long-term nutrient fertilization increased soil carbon storage in california grasslands. *Ecosystems* 22, 754–766. doi: 10.1007/s10021-018-0300-y

Liu, S., Hu, B., He, Z., Zhang, B., Tian, G., Zheng, P., et al. (2015). Ammonia-oxidizing archaea have better adaptability in oxygenated/hypoxic alternant conditions compared to ammonia-oxidizing bacteria. *Appl. Microbiol. Biotechnol.* 99, 8587–8596. doi: 10.1007/s00253-015-6750-7

Luo, P., Han, X., Wang, Y., Han, M., Shi, H., Liu, N., et al. (2015). Influence of long-term fertilization on soil microbial biomass, dehydrogenase activity, and bacterial and fungal community structure in a brown soil of northeast China. Ann. Microbiol. 65, 533–542. doi: 10.1007/s13213-014-0889-9

Magoč, T., and Salzberg, S. L. (2011). FLASH: fast length adjustment of short reads to improve genome assemblies. *Bioinformatics* 27, 2957–2963. doi: 10.1093/bioinformatics/btr507

Nguyen, L. T. T., Osanai, Y., Anderson, I. C., Bange, M. P., Braunack, M., Tissue, D. T., et al. (2018). Impacts of waterlogging on soil nitrification and ammonia-oxidizing communities in farming system. *Plant Soil* 426, 299–311. doi: 10.1007/s11104-018-3584-y

Oehl, F., Sieverding, E., Mader, P., Dubois, D., Ineichen, K., Boller, T., et al. (2004). Impact of long-term conventional and organic farming on the diversity of arbuscular mycorrhizal fungi. *Oecologia* 138, 574–583. doi: 10.1007/s00442-003-1458-2

Qin, H., Yuan, H., Zhang, H., Zhu, Y., Yin, C., Tan, Z., et al. (2012). Ammonia-oxidizing archaea are more important than ammonia-oxidizing bacteria in nitrification and NO3–N loss in acidic soil of sloped land. *Biol. Fert. Soils* 49, 767–776. doi: 10.1007/s00374-012-0767-1

Rotthauwe, J.-H., and Witzel, K.-P. (1997). The ammonia monooxygenase structural gene amoA as a functional marker: molecular fine-scale analysis of natural ammonia- oxidizing populations. *Appl. Environ. Microbiol.* 63, 4704–4712. doi: 10.1128/aem.63.12.4704-4712.1997

Shi, Z. H., Chen, L. D., Cai, C. F., Li, Z. X., and Liu, G. H. (2008). Effects of long-term fertilization and mulch on soil fertility in contour hedgerow systems: a case study on steeplands from the three gorges area, China. *Nutr. Cycling Agroecosyst.* 84, 39–48. doi: 10.1007/s10705-008-9223-x

Sun, Y. F., Shen, J. P., Zhang, C. J., Zhang, L. M., Bai, W. M., Fang, Y., et al. (2017). Responses of soil microbial community to nitrogen fertilizer and precipitation regimes in a semi-arid steppe. *J. Soils Sediments* 18, 762–774. doi: 10.1007/s11368-017-1846-6

Tao, R., Wakelin, S. A., Liang, Y., and Chu, G. (2017). Response of ammonia-oxidizing archaea and bacteria in calcareous soil to mineral and organic fertilizer application and their relative contribution to nitrification. *Soil Biol. Biochem.* 114, 20–30. doi: 10.1016/j.soilbio.2017.06.027

Wang, C., Zhu, G., Wang, W., and Yin, C. (2013). Preliminary study on the distribution of ammonia oxidizers and their contribution to potential ammonia oxidation in the plant-bed/ditch system of a constructed wetland. *J. Soils Sediments* 13, 1626–1635. doi: 10.1007/s11368-013-0750-y

Wang, Q., Garrity, G. M., Tiedje, J. M., and Cole, J. R. (2007). Naive bayesian classifier for rapid assignment of rRNA sequences into the new bacterial taxonomy. *Appl. Environ. Microbiol.* 73, 5261–5267. doi: 10.1128/aem.00062-07

Wang, X., Wang, C., Bao, L., and Xie, S. (2015). Impact of carbon source amendment on ammonia-oxidizing microorganisms in reservoir riparian soil. *Ann. Microbiol.* 65, 1411–1418. doi: 10.1007/s13213-014-0979-8

Wang, Z., Wang, Z., Huang, C., and Pei, Y. (2014). Vertical distribution of ammonia-oxidizing archaea (AOA) in the hyporheic zone of a eutrophic river in North China. *World J. Microbiol. Biotechnol.* 30, 1335–1346. doi: 10.1007/s11274-013-1559-y

Xu, Y., Yu, W., Ma, Q., and Zhou, H. (2012). Responses of bacterial and archaeal ammonia oxidisers of an acidic luvisols soil to different nitrogen fertilization rates after 9 years. *Biol. Fert. Soils* 48, 827–837. doi: 10.1007/s00374-012-0677-2

Zhang, H., Gao, Z., Shi, M., and Fang, S. (2020). Soil bacterial diversity and its relationship with soil CO2 and mineral composition: a case study of the Laiwu experimental site. *Int. J. Environ. Res. Public Health* 17:5699. doi: 10.3390/ijerph17165699

Conflict of Interest: The authors declare that the research was conducted in the absence of any commercial or financial relationships that could be construed as a potential conflict of interest.

frontiers in Microbiology

ORIGINAL RESEARCH
published: 23 February 2021
doi: 10.3389/fmicb.2021.624071

Depth Profile of Nitrifying Archaeal and Bacterial Communities in the Remote Oligotrophic Waters of the North Pacific

Miguel Semedo[1], Eva Lopes[1], Mafalda S. Baptista[1,2,3], Ainhoa Oller-Ruiz[4], Javier Gilabert[4], Maria Paola Tomasino[1] and Catarina Magalhães[1,2,5]*

[1] Interdisciplinary Centre of Marine and Environmental Research (CIIMAR), University of Porto, Matosinhos, Portugal, [2] Faculty of Sciences, University of Porto, Porto, Portugal, [3] International Centre for Terrestrial Antarctic Research, University of Waikato, Hamilton, New Zealand, [4] Department of Chemical & Environmental Engineering, Universidad Politécnica de Cartagena (UPCT), Cartagena, Spain, [5] School of Science, Faculty of Science and Engineering, University of Waikato, Hamilton, New Zealand

OPEN ACCESS

Edited by:
Laura E. Lehtovirta-Morley, University of East Anglia, United Kingdom

Reviewed by:
Annette Bollmann, Miami University, United States
Willm Martens-Habbena, University of Florida, United States

***Correspondence:**
Miguel Semedo
msemedo@ciimar.up.pt

Specialty section:
This article was submitted to Aquatic Microbiology, a section of the journal Frontiers in Microbiology

Received: *30 October 2020*
Accepted: *01 February 2021*
Published: *23 February 2021*

Citation:
Semedo M, Lopes E, Baptista MS, Oller-Ruiz A, Gilabert J, Tomasino MP and Magalhães C (2021) Depth Profile of Nitrifying Archaeal and Bacterial Communities in the Remote Oligotrophic Waters of the North Pacific. Front. Microbiol. 12:624071. doi: 10.3389/fmicb.2021.624071

Nitrification is a vital ecosystem function in the open ocean that regenerates inorganic nitrogen and promotes primary production. Recent studies have shown that the ecology and physiology of nitrifying organisms is more complex than previously postulated. The distribution of these organisms in the remote oligotrophic ocean and their interactions with the physicochemical environment are relatively understudied. In this work, we aimed to evaluate the depth profile of nitrifying archaea and bacteria in the Eastern North Pacific Subtropical Front, an area with limited biological surveys but with intense trophic transferences and physicochemical gradients. Furthermore, we investigated the dominant physicochemical and biological relationships within and between ammonia-oxidizing archaea (AOA), ammonia-oxidizing bacteria (AOB), and nitrite-oxidizing bacteria (NOB) as well as with the overall prokaryotic community. We used a 16S rRNA gene sequencing approach to identify and characterize the nitrifying groups within the first 500 m of the water column and to analyze their abiotic and biotic interactions. The water column was characterized mainly by two contrasting environments, warm O_2-rich surface waters with low dissolved inorganic nitrogen (DIN) and a cold O_2-deficient mesopelagic layer with high concentrations of nitrate (NO_3^-). Thaumarcheotal AOA and bacterial NOB were highly abundant below the deep chlorophyll maximum (DCM) and in the mesopelagic. In the mesopelagic, AOA and NOB represented up to 25 and 3% of the total prokaryotic community, respectively. Interestingly, the AOA community in the mesopelagic was dominated by unclassified genera that may constitute a novel group of AOA highly adapted to the conditions observed at those depths. Several of these unclassified amplicon sequence variants (ASVs) were positively correlated with NO_3^- concentrations and negatively correlated with temperature and O_2, whereas known thaumarcheotal genera exhibited the opposite behavior. Additionally, we found a large network of positive interactions

within and between putative nitrifying ASVs and other prokaryotic groups, including 13230 significant correlations and 23 sub-communities of AOA, AOB, NOB, irrespective of their taxonomic classification. This study provides new insights into our understanding of the roles that AOA may play in recycling inorganic nitrogen in the oligotrophic ocean, with potential consequences to primary production in these remote ecosystems.

Keywords: nitrification, thaumarchaeota, AOA, NOB, Pacific Subtropical Front

INTRODUCTION

Nitrogen (N) is an essential element of important biomolecules, such as amino acids, chlorophyll, ATP, and nucleic acids, with a crucial role in regulating ecosystem productivity. In the oligotrophic open ocean, fixed nitrogen is often the growth-limiting nutrient for photosynthetic organisms such as algae and marine bacteria (Tyrrell, 1999). In these environments, pelagic bacteria and archaea can also use the oxidation of inorganic N as their main energy source, in a series of reactions within the nitrification process, performed by ammonia-oxidizing bacteria (AOB) and ammonia-oxidizing archaea (AOA), nitrite-oxidizing bacteria (NOB), and comammox organisms (Winogradsky, 1890; Könneke et al., 2005; Daims et al., 2015; van Kessel et al., 2015).

Until recently, it has been accepted that these nitrifying organisms gain energy in the two-step oxidation of ammonia (NH_3) to nitrite (NO_2^-). In the first step, NH_3 is oxidized to hydroxylamine (NH_2OH), by the ammonia monooxygenase (AMO) and in the second step NH_2OH is oxidized into NO_2^-, by hydroxylamine oxidoreductase (HAO). However, recent discoveries proposed a new model for AOB ammonia oxidation where NH_2OH and also NO are produced as intermediates of these reactions (Caranto and Lancaster, 2017). A HAO homolog remains to be discovered for AOA, thus it is still unclear if archaeal AMO catalyzes the same reactions described for AOB (Lehtovirta-Morley, 2018). While archaea ammonia oxidation pathway is still not resolved, the models that have been developed suggest that this oxidation releases two net electrons that can enter the respiratory chain in both AOA and AOB (Lehtovirta-Morley, 2018).

Ammonia-oxidizing bacteria are rather restricted in their phylogeny and only found in the γ-Proteobacteria and in the formerly β-Proteobacteria, now Betaproteobacteriales (Zehr and Ward, 2002). AOA are only found in the Thaumarchaeota phylum, formerly known as Crenarchaeota (Beman et al., 2010). A recent comparison of whole genome sequences, however, suggests the revision of AOA to the class Nitrososphaeria within the Thermoproteota phylum (Parks et al., 2020). NOB can be found in α-Proteobacteria and the Nitrospirae phylum, but species assigned to the recently proposed Nitrospinae phylum are the dominant NOB in the marine environment (Luecker et al., 2013; Levipan et al., 2014; Sun et al., 2019). The phylogeny of marine nitrifying organisms has been extensively studied and constrained by previous works using nitrification genes sequencing as well as by shotgun metagenomics, supporting the use of 16S-derived phylogeny to infer nitrifier populations (Kowalchuk and Stephen, 2001; Santoro et al., 2010; Sun et al., 2019; Zhong et al., 2020).

In the open ocean, nitrification is a key process for nitrate-based new production and it is partly responsible for the nitrate standing stock in the subeuphotic zone (Zehr and Ward, 2002; Mincer et al., 2007). Nitrifying organisms in these environments occur mainly in the bottom of the euphotic zone, where they can avoid light inhibition and competition by phototropic phytoplankton for fixed N (Pajares and Ramos, 2019). With depth, light becomes limited and nitrifiers can thrive and dominate NH_4^+ consumption. The physiochemical environment also has a significant influence in the relative distribution of the different groups of nitrifying organisms in the water column. Thaumarchaeotal AOA, for instance, can make up more than 30% of the total marine picoplankton below the photic zone (Karner et al., 2001) and tend to predominate over AOB in oligotrophic environments due to their higher affinity for NH_4^+ (Martens-Habbena et al., 2009; Horak et al., 2013; Kits et al., 2017). AOA are also better adapted to low O_2 conditions than AOB, which makes them highly abundant in vast oxygen minimum zones of the open ocean (Holtappels et al., 2011; Hollibaugh, 2017). On the other hand, AOA are reported to be more sensitive to light than AOB which, in turn, makes them more vulnerable in the upper layers of the water column (Merbt et al., 2012). Despite all cultured NOB being obligate aerobes, abundant and highly active NOBs can also be found in O_2-poor waters (Sun et al., 2017, 2019).

Nitrifying organisms are essential to generate accessible forms of N that support primary production below the euphotic zone. Notwithstanding the current knowledge about their ecology and physiology, the interactions between the different groups of nitrifying organisms and with the surrounding environment are still relatively unknown. Especially in the remote oligotrophic ocean due to the inherent limitations accessing the planktonic communities in these areas. Improved knowledge of the dynamics and physicochemical constraints of nitrifying archaea and bacteria is thus crucial for a better understanding of current and future ocean functioning. The goal of this study is to evaluate the depth profile of nitrifying archaea and bacteria in the Eastern North Pacific Subtropical Front, an area with limited biological surveys but with intense trophic transferences and physicochemical gradients (Olson et al., 1994; Sow et al., 2020). Additionally, we aimed to determine the dominant physicochemical and biological relationships within and between the two prokaryotic groups of nitrifying organisms, thaumarchaeotal AOA and nitrifying bacteria (AOB and NOB), as well as with the overall prokaryotic community. We used 16S rRNA gene high-throughput sequencing and physicochemical analyses to identify and characterize the

nitrifying groups present within the first 500 m of the water column as well as to describe their interactions with the abiotic environment and among taxa.

MATERIALS AND METHODS

Site Description and Water Sampling

Water column samples were collected in two different transects along the Eastern North Pacific Subtropical Front (ENPSF), 1000 nautical miles off the coast of Southern California, on board of the Schmidt Ocean Institute (SOI) research vessel "Falkor" (**Figure 1**). The sampled area presents an average bottom depth of around 4500 m. A total of 31 samples were collected in the top 500 m of the water column with a Rosette multi-sampler, between the 1st and 14th of June, 2018 (**Table 1**). Sea water samples of 3.75 L were filtered with a Sterivex® filter (0.2 μm pore size) for microplankton analysis. The collection filters were stored on board at −80°C and transported in dry ice to CIIMAR for later DNA extraction. The detailed methodology can be found in de Sousa et al. (2019). Samples were classified according to their depth and *in situ* chlorophyll concentrations. Four different depth layers were used in this study: surface (3–5 m, n = 11), deep chlorophyll maximum (DCM), (107–130 m, n = 11), below DCM (175–200 m, n = 4), and mesopelagic (500 m, n = 5). The DCM depths observed in this study were similar to the DCM depths previously observed in the Pacific Ocean (Letelier et al., 2004; Sauzède et al., 2020).

Physicochemical Parameters

Physicochemical properties of the collected water samples were obtained *in situ* with a Seabird SBE 9 Plus conductivity-temperature-depth (CTD) profiler, deployed with the Rosette. Conductivity (mS/cm), temperature (°C), depth (m), salinity (PSU), oxygen (ml/L), turbidity (NTU), and fluorescence (mg/m^3) were measured simultaneously in each cast and the complete results from the CTD dataset are publicly available in PANGAEA international archive[1]. Additionally, seawater samples were collected for the quantification of inorganic nitrogen, namely, ammonium (NH_4^+), nitrite (NO_2^-), and nitrate (NO_3^-), at the stations and depths where microplankton samples were collected. These samples were also stored onboard at −80°C. Upon arrival to shore, nutrient samples were transported in dry ice to Technical University of Cartagena, Spain, to be analyzed using a SEAL AA3-HD continuous flow autoanalyzer according to previously described methodology (Strickland and Parsons, 1977; Gordon et al., 1993).

DNA Extraction and Amplicon Sequencing

Planktonic DNA was extracted from the Sterivex filters using the DNeasy® PowerWater® Sterivex DNA Isolation Kit protocol (Qiagen), following manufacturer's instructions. The 16S rRNA gene was amplified with the degenerate primer pair 515YF (5′–GTGYCAGCMGCCGCGGTAA–3′) and Y926R-jed (5′–CCGYCAATTYMTTTRAGTTT–3′), targeting the hypervariable V4–V5 region (Caporaso et al., 2011, 2012; Apprill et al., 2015; Parada et al., 2016). This primer set has a broad spectrum of diversity, including the Crenarchaeota/Thaumarchaeota phylum (degeneracy at 515YF), as well as the freshwater and marine clade SAR11 (Alphaproteobacterial class, degeneracy at Y926R-jed) (Apprill et al., 2015; Parada et al., 2016).

The initial PCR reaction included 12.5 ng of template DNA in a total volume of 25 μL. The PCR protocol involved a 3 min denaturation step, followed by 25 cycles of 98°C for 20 s, 60°C for 30 s, and 72°C for 30 s, and, finally, an extension stage at 72°C for 5 min. A second PCR reaction was performed to add indexes and sequencing adapters to the target region, according to manufacturer's recommendations (Illumina, 2013). Negative controls without template were included in all PCR reactions. Lastly, PCR products were one-step purified and normalized using SequalPrep 96-well plate kit (Thermo Fisher Scientific, Waltham, MA, United States), pooled, and pair-end sequenced in the Illumina MiSeq® sequencer using 2 × 300 bp with the V3 chemistry, according to manufacturer instructions (Illumina, San Diego, CA, United States) at Genoinseq (Cantanhede, Portugal). The results from this 16S amplicon sequencing are publicly available in ENA-EMBL archive with the project accession number PRJEB32783.

Bioinformatic Analysis

The raw FASTQ files obtained with Illumina MiSeq sequencing were trimmed for primer removal using "cutadapt" v.1.16 and imported into R (version 3.5.1) using "DADA2" package v.1.10.1 (Callahan et al., 2016a). Sample filtering, trimming, error rates learning, dereplication, and amplicon sequence variant (ASV) inference were performed with default settings. Chimeras were removed with the *removeBimeraDenovo* function using the method "consensus." Taxonomy was assigned with the native implementation of the naive Bayesian classifier and a DADA2-formatted reference database for the SILVA v128 database (Quast et al., 2013). Additionally, for disambiguation, taxonomy was further assigned with the GTDB database (Parks et al., 2018) and with the "DECIPHER" package v.2.10.2 (Wright, 2016) using the IDTAXA classifier (Murali et al., 2018) and the modified training sets provided, namely GTDB 16S (revision 95) and SILVA SSU (v138). These pre-processing steps resulted in 6262 ASVs found, with a median number of 43408 reads per sample (16004–71932), corresponding to 60.1% of the initial number of the sequences (**Supplementary Table 1**). Taxonomy filtering was performed by removing eukaryotic, mitochondrial, and chloroplast sequences (426 ASVs removed). Relative abundances of each ASV per sample were calculated in the filtered dataset by dividing the absolute abundance (counts) of each ASV by the sum of counts of all ASVs.

To explore the nitrifying communities, taxa were categorized into guilds based on the presence of genes that code for proteins in the pathways of nitrification. These guilds were identified at different taxonomic levels to mitigate the effects

[1]https://doi.pangaea.de/10.1594/PANGAEA.903405

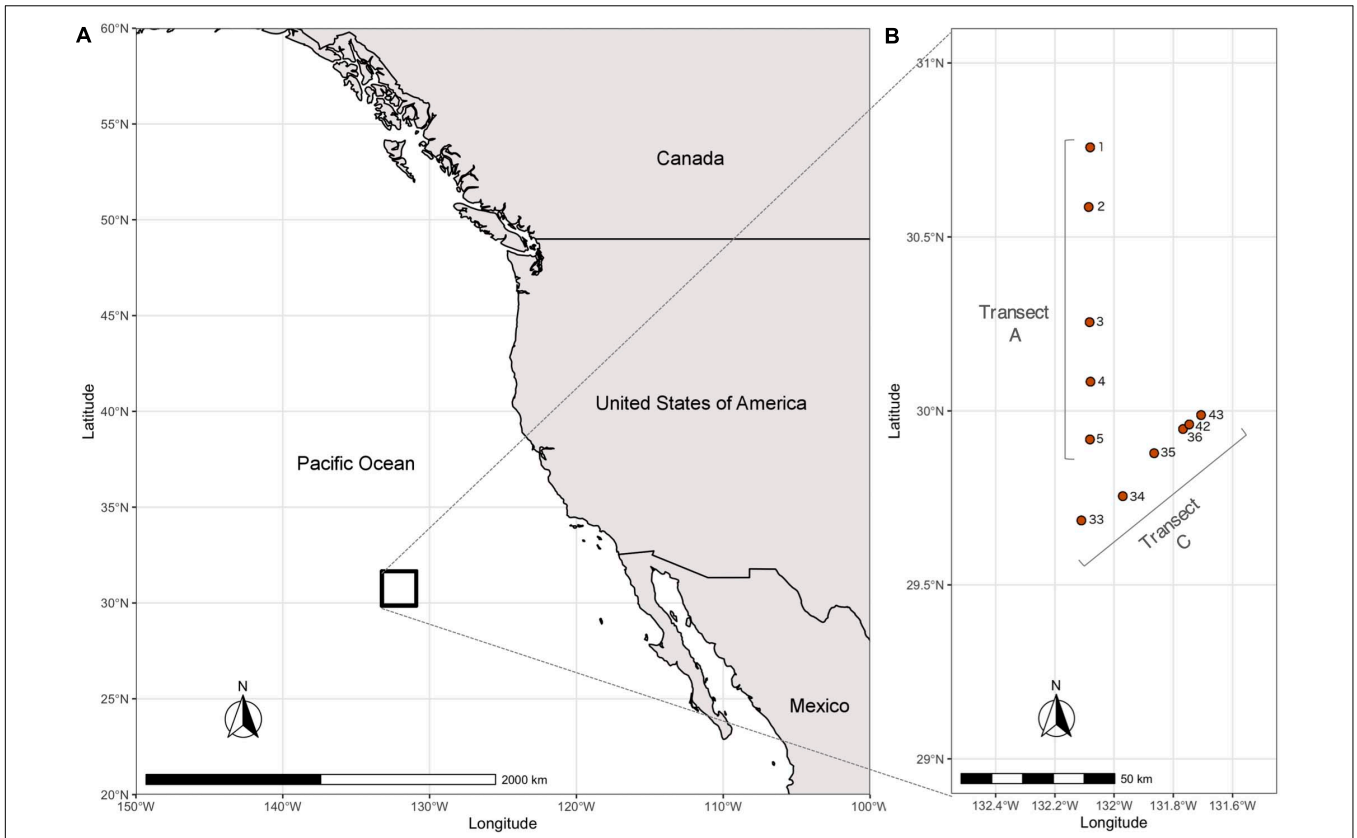

FIGURE 1 | Map of the sampling area and sampling sites. **(A)** Map of North America and Pacific Ocean with sampling area denoted by a black rectangle. **(B)** Sampling sites identified by cast number (information on casts and corresponding samples is detailed in **Table 1**).

of unclassified sequences: Thaumarchaeota, Nitrospinae, Nitrospirae, and Nitrospinota were selected at the phylum level; Nitrosomonadaceae and Nitrosococcaceae at the family level; and *Nitrosococcus*, *Nitrospirae*, *Nitrobacter*, *Candidatus Nitrotoga*, *Nitrotoga*, *Nitrospina*, *Nitrococcus*, *Nitrolancea*, *Candidatus Nitromaritima*, and *Nitromaritima* at the genus level. This taxonomic selection resulted in a final number of 302 putative nitrifying ASVs.

To estimate species richness and α-diversity of selected nitrifying communities, Chao and Shannon indexes were calculated, respectively. β-diversity among these communities was evaluated using the Bray-Curtis dissimilarity calculator and a principal coordinate analysis (PCoA). Due to the presence of samples without any thaumarcheotal or nitrifying bacterial ASVs, a mock ASV with an abundance of 0.0001 was added to all samples. Significant effects of depth in community dissimilarity were tested by multivariate permutational ANOVA (PERMANOVA) using the adonis function of the vegan package in R (Oksanen et al., 2017). Multivariate homogeneity of group dispersion was evaluated using the betadisper function of the same R package. To normalize the α- and β-diversity estimates (based on absolute abundances), the original samples (before taxonomic selection of nitrifying groups) were randomly subsampled to the lowest number of sequences (n = 16004 sequences per sample). These estimates were calculated using the phyloseq package in R (McMurdie and Holmes, 2013).

A neighbor-joining phylogenetic tree was constructed with all 6262 ASVs found in these samples using the decipher (Wright, 2016) and phangorn (Schliep, 2011) packages in R according to the workflow provided by Callahan et al. (2016b). The phylogenetic tree of thaumarcheotal ASVs was then visualized and annotated in iTOL v. 5.6.3. (Letunic and Bork, 2019).

Statistical Analysis

Differences in the α-diversity estimators between the different depth groups (surface, DCM, below DCM, and mesopelagic) were analyzed using one-way analysis of variances (ANOVAs) and a Tukey's HSD test to perform multiple comparisons. Significant relationships were considered at $\alpha < 0.05$. Normality and homoscedasticity were assessed with Q-Q plots and residual plots for each variable. Due to the non-homoscedasticity of the observed number of ASVs and the Chao index, these data were square-root-transformed to meet ANOVA assumptions.

Spearman's rank correlation coefficients were employed to assess the correlations between individual ASVs abundance and the concentrations of inorganic N and the physicochemical parameters. Only samples from transect A were selected due to the lack of O_2, turbidity, and fluorescence data in eight of the 12 samples from transect C. Low abundance ASVs (that

TABLE 1 | Geospatial description of samples used in this study.

Depth Layer	Transect	Sample ID	Cast	Depth (m)	Latitude	Longitude
Surface (3–5 m)	A	4A	1	5	30.586	−132.086
		8A	2	5	29.918	−132.082
		12A	3	5	30.084	−132.080
		16A	4	5	30.255	−132.083
		20A	5	5	30.758	−132.081
	C	53A	33	3	29.878	−131.865
		55A	34	3	29.948	−131.767
		57A	35	3	29.961	−131.746
		59A	36	3	29.988	−131.706
		71A	42	3	29.685	−132.111
		73A	43	3	29.755	−131.970
DCM* (107–130 m)	A	3A	1	120	30.586	−132.086
		7A	2	110	29.918	−132.082
		11A	3	108	30.084	−132.080
		15A	4	122	30.255	−132.083
		18A	5	130	30.758	−132.081
	C	52A	33	123	29.878	−131.865
		54A	34	115	29.948	−131.767
		56A	35	115	29.961	−131.746
		58A	36	115	29.988	−131.706
		70A	42	107	29.685	−132.111
		72A	43	127	29.755	−131.970
Below DCM (175–200 m)	A	2A	1	195	30.586	−132.086
		6A	2	200	29.918	−132.082
		14A	4	175	30.255	−132.083
		10A	3	180	30.084	−132.080
Mesopelagic (500 m)	A	1A	1	500	30.586	−132.086
		5A	2	500	29.918	−132.082
		9A	3	500	30.084	−132.080
		13A	4	500	30.255	−132.083
		17A	5	500	30.758	−132.081

**DCM, Deep Chlorophyll Maximum.*

do not appear more than two times in at least four samples) were excluded from this analysis to avoid low degrees of freedom. Correlations were obtained on a centered log ratio transformed ASV table (Gloor et al., 2017). Spearman's rank correlation coefficients were also calculated between all ASVs using the ELSA pipeline (Xia et al., 2011, 2013). A network analysis for the significant correlations found between ASVs was created with the igraph R package (Csardi and Nepusz, 2006) and subcommunities/modules were found using the Louvain method (Blondel et al., 2008). A cut off of $\rho > |0.7|$, with a p-value < 0.001, was imposed to consider the Spearman's correlations significant. For both physicochemical and biological correlation analyses, only the samples from below DCM and mesopelagic were used to avoid the effect of auto-correlation among several variables in largely distinct water column sections.

All statistical analyses were conducted in the R environment (version 3.2.2. Copyright 2015, the R Foundation for Statistical Computing). Most plots were obtained with base R and the ggplot2 R package, while maps were created with "rnaturalearth," "ggplot2," "sf," and "ggspatial" R packages, and edited with Gimp (v.2.8.14).

RESULTS

Physicochemical Context

The physicochemical parameters and inorganic N concentrations measured at the different depths are shown in **Figure 2** (see **Supplementary Figure 1** for the full CTD profiles). The temperature dropped consistently with depth, from mean 19°C at the surface to 6°C in the mesopelagic. Salinity was generally higher in samples from the surface and DCM, especially when compared to samples collected just below the DCM. The variability in salinity values was also considerably higher in surface and DCM samples. The studied region has very clear waters, with low turbidity levels across the different water column depths. The fluorescence levels peaked at the DCM while the other depth layers had near-zero values in most samples. Oxygen concentrations dropped from around

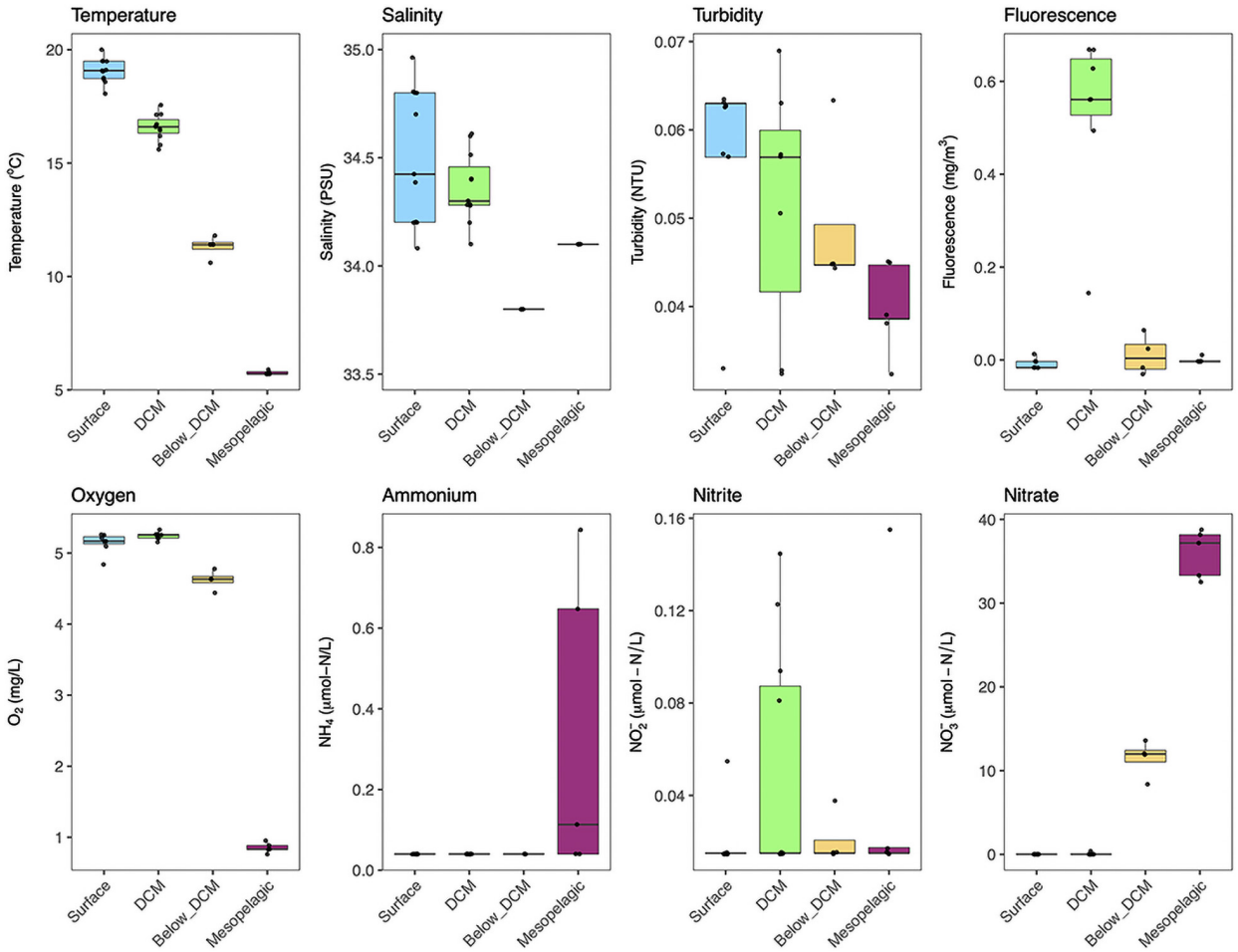

FIGURE 2 | Physicochemical and dissolved inorganic nitrogen (DIN) conditions at the different sampling depths. Each sample is represented by one point. The boxes represent the first and third quartiles, with median value bisecting each box. The whiskers extend to the largest/smallest value, excluding outliers (data beyond 1.5× inter-quartile range).

5.2 mg L^{-1} at the surface and the DCM to 4.6 mg L^{-1} below the DCM and 0.85 mg L^{-1} in the mesopelagic. Considering inorganic nitrogen, we measured NH_4^+, NO_2^-, and NO_3^- concentrations at the different depths. Dissolved NH_4^+ concentrations were below the limit of quantification (0.04 µM) in almost all samples, with the exception of the mesopelagic, that presented average values of 0.34 µM. Nitrite (NO_2^-) concentrations presented high variability in most depths. Nonetheless, a peak in NO_2^- concentrations was observed in samples collected at the DCM. Nitrate, on the other hand, accumulated in deeper samples, with concentrations in the mesopelagic (36 µM) and below DCM (12 µM) being three orders of magnitude higher than those found at the DCM (0.036 µM). In surface waters, NO_3^- levels were always below the quantification limit (0.015 µM). Overall, the four different depths were clearly distinct based on the measured physicochemical parameters and dissolved inorganic nitrogen (DIN) concentrations (see **Supplementary Figure 2** for a principal component analysis plot).

Community Composition of Nitrifying Archaea and Bacteria

The relative abundances of thaumarchaeotal and nitrifying bacterial genera are shown in **Figure 3** (overall prokaryotic community shown in **Supplementary Figure 3**). Considering Thaumarchaeota, a strong depth preference was observed. Despite the presence of the genus *Candidatus Nitrosopelagicus* in almost all depths sampled, the total relative abundance of thaumarcheotal genera increased from an average of less than 1% at the surface to around 15% below the DCM and almost 25% in the mesopelagic. This increment was mainly driven by the substantial increase in the relative abundance of unclassified Thaumarchaeota belonging to the Nitrosopumilaceae family, a well-known family of putative AOA. In fact, unclassified Nitrosopumilaceae dominated in the deeper layers, with more than 90% of the thaumarcheotal sequences in the mesopelagic and more than 50% below the DCM.

The phylogenetic distance between these unclassified ASVs and the other Thaumarchaeota present in this dataset is shown

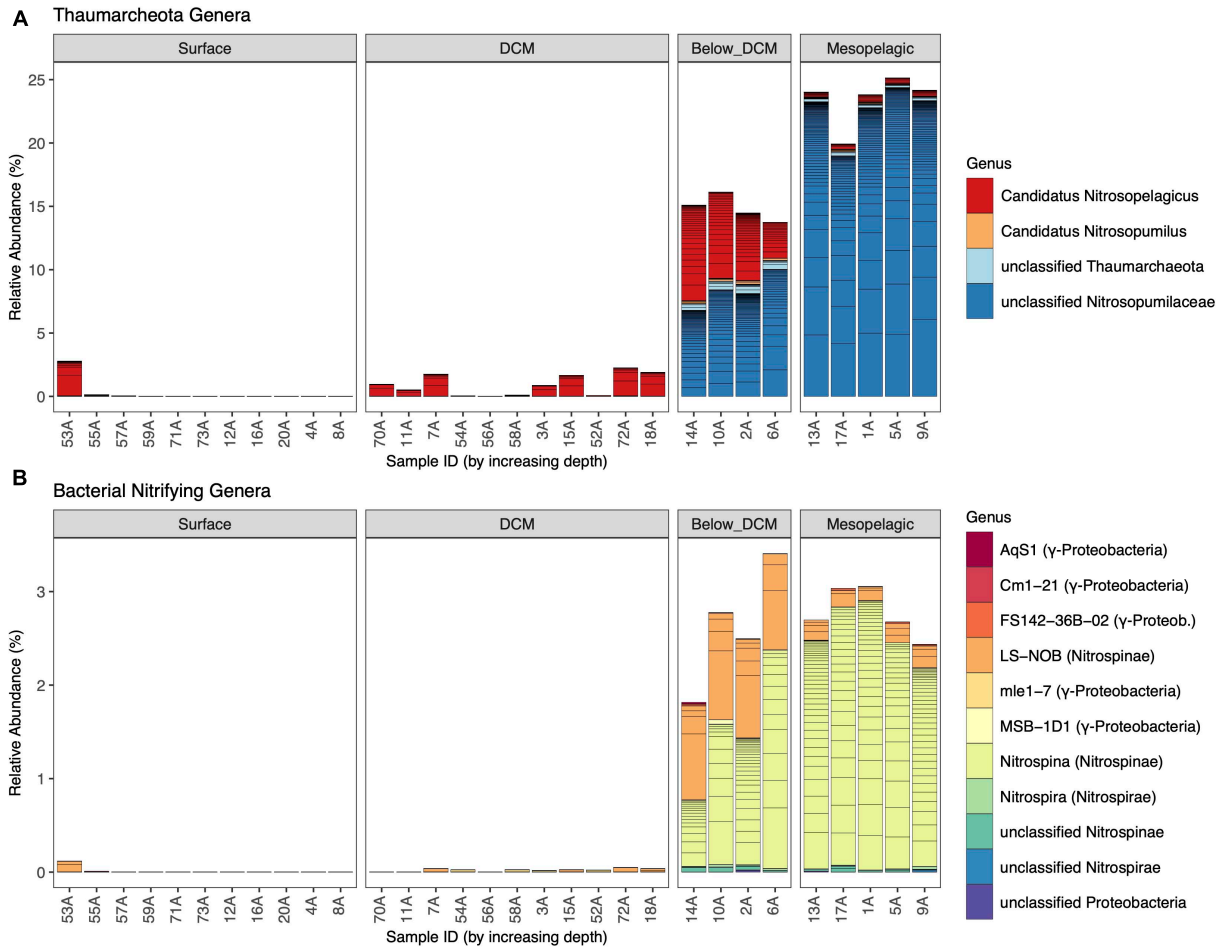

FIGURE 3 | Thaumarcheotal **(A)** and nitrifying bacterial **(B)** community composition at the different depths. Each line of a stacked bar represents a unique amplicon sequence variant (ASV) and different genera are represented by different colors. Relative abundances of each ASV per sample were calculated by dividing the absolute abundance (counts) of each ASV by the sum of counts of all prokaryotic ASVs.

in **Figure 4**. The majority of unclassified ASVs at the genus level are closer to the *Candidatus Nitrosopumilus* genus than to the *Ca. Nitrosopelagicus*. However, four of the top five most abundant ASVs, namely ASV 16, ASV 33, ASV 39, and ASV 98, present a high genetic distance to both genera. To further explore these unknown classifications, we applied a different classifier and reference database to the sequence data. These alternative taxonomic classifications are shown in **Table 2**. The ambiguity persisted, i.e., the top five ASVs (with the exception of ASV 24, which had previously been found to be closer to *Ca. Nitrosopumilus*) could be assigned to either *Ca. Nitrosopumilus*, *Ca. Nitrosopelagicus*, or unclassified, depending on the classifier and classification algorithm used.

When considering putative nitrifying bacteria (**Figure 3B**), these followed the same depth preference as Thaumarchaeota, although with substantially lower levels than their archaeal counterparts. Their maximum total prokaryotic community relative abundance was around 3%, below the DCM and in the mesopelagic. Concerning AOB, we identified the presence of four genera (AqS1, Cm1-21, FS142-36B-02, and MSB-1D1) and unclassified ASVs belonging to the Nitrosococcaceae family (Nitrosococcales order of γ-Proteobacteria) and the mle1-7 genus belonging to the Nitrosomonadaceae family (Betaproteobacteriales order of γ-Proteobacteria) at very low relative abundances (<0.05%). All other nitrifying bacteria identified were putative NOB, belonging to the Nitrospinae or Nitrospirae phyla. *Nitrospina* was the most abundant NOB genus, especially in the mesopelagic, representing around 90% of all putative nitrifying bacteria. Other important nitrite oxidizers, like *Nitrobacter*, were not found to be present in this dataset.

Richness and Diversity of Nitrifying Archaea and Bacteria

A principal coordinate analysis (PCoA) was performed to represent the β-diversity of nitrifier communities based on the calculated dissimilarities among samples (**Figure 5**). The dissimilarity among samples was based on the distribution of 196 thaumarchaeotal ASVs and 95 putative nitrifying bacterial ASVs, representing 98 and 92% of the total number of ASVs

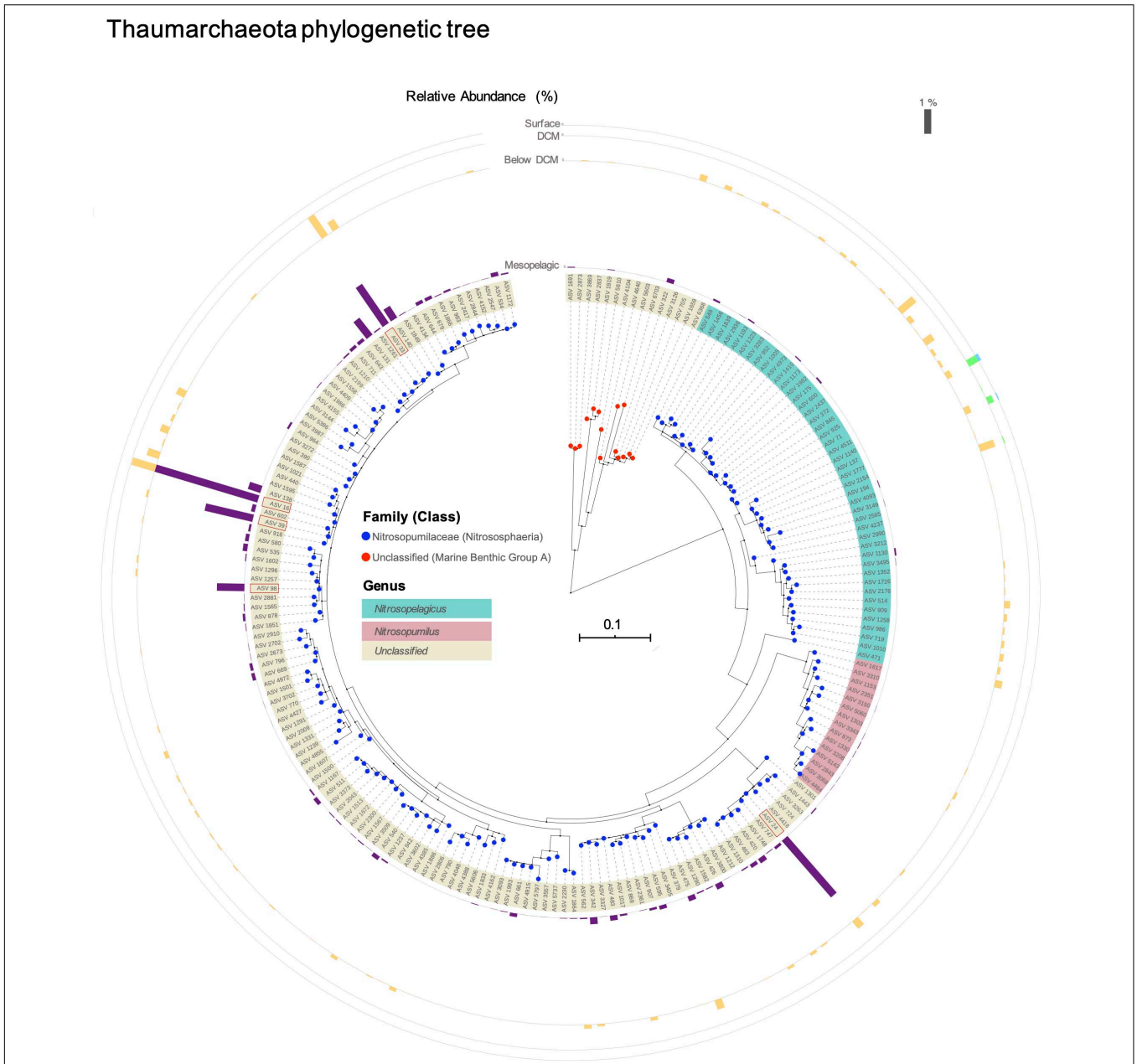

FIGURE 4 | Neighbor-joining phylogenetic tree of all thaumarcheotal ASVs found in this study. Taxonomy was assigned with the silva v128 database. The bars in the outer circle represent the mean relative abundance of each ASV at the different depths in the water column (scale bar on the top right). The top 5 ASVs are highlighted with a red rectangle (ASV 33, ASV 16, ASV 39, ASV 98, and ASV 24). The tree was visualized and annotated using the iTOL software.

in each nitrifiers' community, respectively. The first two principal coordinates represented 54.3 and 54.4% of the variation in thaumarcheotal and nitrifying bacterial communities, respectively. Thaumarchaeotal β-diversity (**Figure 5A**) was significantly affected by depth (PERMANOVA, $p < 0.05$). Samples from the mesopelagic and below DCM are generally similar to each other while the samples from the surface and the DCM cluster further apart. This is possibly explained by the shift observed from a *Ca. Nitrosopelagicus* dominated thaumarchaeotal community at the surface and DCM to a more diverse community below the DCM and in the mesopelagic. Nitrifying bacteria (AOB and NOB) β-diversity (**Figure 5B**) was also significantly affected by depth (PERMANOVA, $p < 0.05$) and presented the same mesopelagic/below DCM cluster, positioned further away from the surface and DCM samples. The drastic increase in Nitrospinae bacteria, especially *Nitrospina*, below the DCM and the mesopelagic possibly caused this shift. The significant depth effect in structuring the thaumarcheotal and nitrifying bacterial communities was also observed for the overall prokaryotic communities (**Supplementary Figure 4**).

TABLE 2 | Taxonomic assignments of the five most abundant thaumarchaeotal ASVs.

ASV	Classifier	Database	Class	Order	Family	Genus
ASV 16	DADA2-Bayesian	Silva	Nitrososphaeria	Nitrosopumilales	Nitrosopumilaceae	NA
		GTDB	NA	Nitrosopumilales	Nitrosopumilaceae	Nitrosopumilus
	IDTAXA	Silva	Nitrososphaeria	Nitrosopumilales	Nitrosopumilaceae	NA
		GTDB	Nitrososphaeria	Nitrososphaerales	Nitrosopumilaceae	Nitrosopelagicus
ASV 24	DADA2-Bayesian	Silva	Nitrososphaeria	Nitrosopumilales	Nitrosopumilaceae	NA
		GTDB	NA	Nitrosopumilales	Nitrosopumilaceae	Nitrosopumilus
	IDTAXA	Silva	Nitrososphaeria	Nitrosopumilales	Nitrosopumilaceae	NA
		GTDB	Nitrososphaeria	Nitrososphaerales	Nitrosopumilaceae	NA
ASV 39	DADA2-Bayesian	Silva	Nitrososphaeria	Nitrosopumilales	Nitrosopumilaceae	NA
		GTDB	NA	Nitrosopumilales	Nitrosopumilaceae	Nitrosopumilus
	IDTAXA	Silva	Nitrososphaeria	Nitrosopumilales	Nitrosopumilaceae	NA
		GTDB	Nitrososphaeria	Nitrososphaerales	Nitrosopumilaceae	Nitrosopelagicus
ASV 33	DADA2-Bayesian	Silva	Nitrososphaeria	Nitrosopumilales	Nitrosopumilaceae	NA
		GTDB	NA	Nitrosopumilales	Nitrosopumilaceae	Nitrosopumilus
	IDTAXA	Silva	Nitrososphaeria	Nitrosopumilales	Nitrosopumilaceae	NA
		GTDB	Nitrososphaeria	Nitrososphaerales	Nitrosopumilaceae	Nitrosopelagicus
ASV 98	DADA2-Bayesian	Silva	Nitrososphaeria	Nitrosopumilales	Nitrosopumilaceae	NA
		GTDB	NA	Nitrosopumilales	Nitrosopumilaceae	Nitrosopumilus
	IDTAXA	Silva	Nitrososphaeria	Nitrosopumilales	Nitrosopumilaceae	Nitrosopumilus
		GTDB	Nitrososphaeria	Nitrososphaerales	Nitrosopumilaceae	Nitrosopelagicus

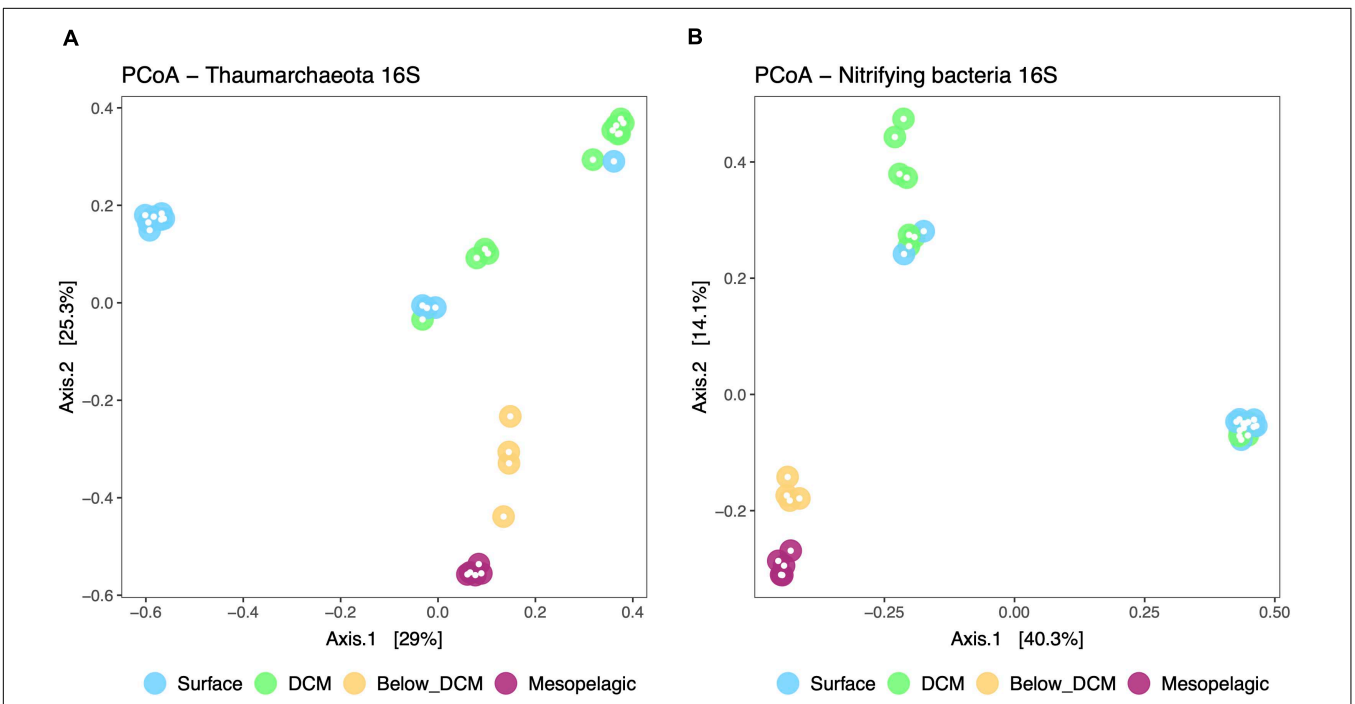

FIGURE 5 | Principal coordinate analysis (PCoA) plot representing the β-diversity of the thaumarchaeotal **(A)** and nitrifying bacterial **(B)** community from the different depths in the water column. Sample dissimilarity and distance analysis were calculated using the Bray-Curtis dissimilarity index. The group dispersion was not significantly different across depths for the Thaumarcheotal community (permdisp, $p = 0.256$) but it was marginally different in the nitrifying bacterial community (permdisp, $p = 0.016$).

The depth effect in species richness and α-diversity of putative nitrifying prokaryotes is displayed in **Figure 6**. Species richness of thaumarchaeota, estimated by the number of observed ASVs and the Chao index, increased significantly below the DCM and in the mesopelagic, when compared to the surface and DCM (one-way ANOVA, $p < 0.05$). Thaumarcheotal α-diversity, estimated through the Shannon index (H′), peaked in samples collected just below the DCM and it was significantly higher at

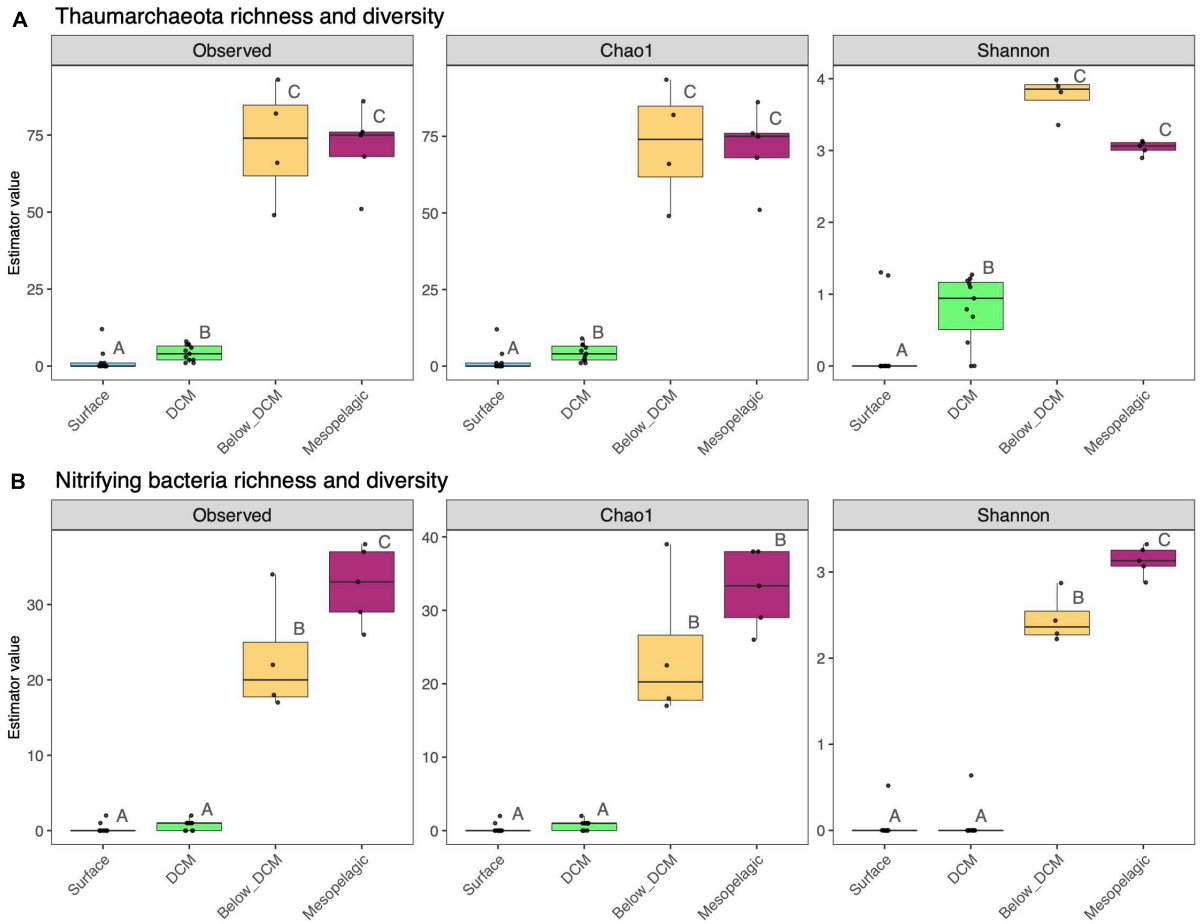

FIGURE 6 | Species richness and α-diversity of thaumarchaeotal **(A)** and nitrifying bacterial **(B)** communities from the different depths in the water column. Each sample is represented by one point. The boxes represent the first and third quartiles, with median value bisecting each box. The whiskers extend to the largest/smallest value, excluding outliers (data beyond 1.5× inter-quartile range). Dissimilar letters denote a significant difference (one-way ANOVA, $p < 0.05$) between the depth layers.

this depth and in the mesopelagic than in surface and DCM samples (one-way ANOVA, $p < 0.05$). A similar pattern was observed for putative nitrifying bacteria as well as the overall prokaryotic community (**Supplementary Figure 5**), with an increase in species richness and diversity with depth. The highest values, however, were observed at the mesopelagic, not below the DCM, as it happened with the Thaumarchaeota.

Environmental and Biological Interactions

The abundance of putative nitrifying thaumarchaeota and bacteria was higher at below DCM and mesopelagic sampling sites, where concomitantly the concentrations of dissolved NH_4^+ and NO_3^- were higher. To inspect the relationships between the abundance of thaumarchaeotal and nitrifying bacterial ASVs with the concentrations of DIN, we employed Spearman's rank correlation coefficients (**Figure 7**). Nineteen unclassified thaumarchaeotal ASVs, all belonging to the Nitrosopumilaceae family, showed a significant positive relationship with NO_3^- concentrations, while known AOA, mainly assigned to the *Ca. Nitrosopelagicus* genus, showed a negative relationship. Eight positive correlations and one negative were found between NH_4^+ and thaumarchaeotal ASVs, mostly with unclassified ASVs from the Nitrosopumilaceae family, but it's worth noting that ASV 1691 lowest assignment was to phylum Thaumarchaeota, and ASV 1919 lowest assignment was to class Marine Benthic Group A.

Putative NOB identified as being associated with changes in DIN concentrations could be assigned either to *Nitrospina* sp. or LS-NOB, both in the family Nitrospinaceae, with the exception of ASV 2550, with the lowest taxonomic assignment at the phylum level (Nitrospinae). Further inspection of all correlations showed that ASVs assigned to LS-NOB predominantly exhibited a negative correlation with NO_3^- concentrations and a positive correlation with NH_4^+, as shown in **Figure 7**. On the other hand, *Nitrospina* sp., in spite of showing predominantly positive correlations with DIN concentrations, also displayed two ASVs negatively correlated with N-NH_4^+ and N-NO_3^- concentrations. Other bacterial groups of interest, such as AOB,

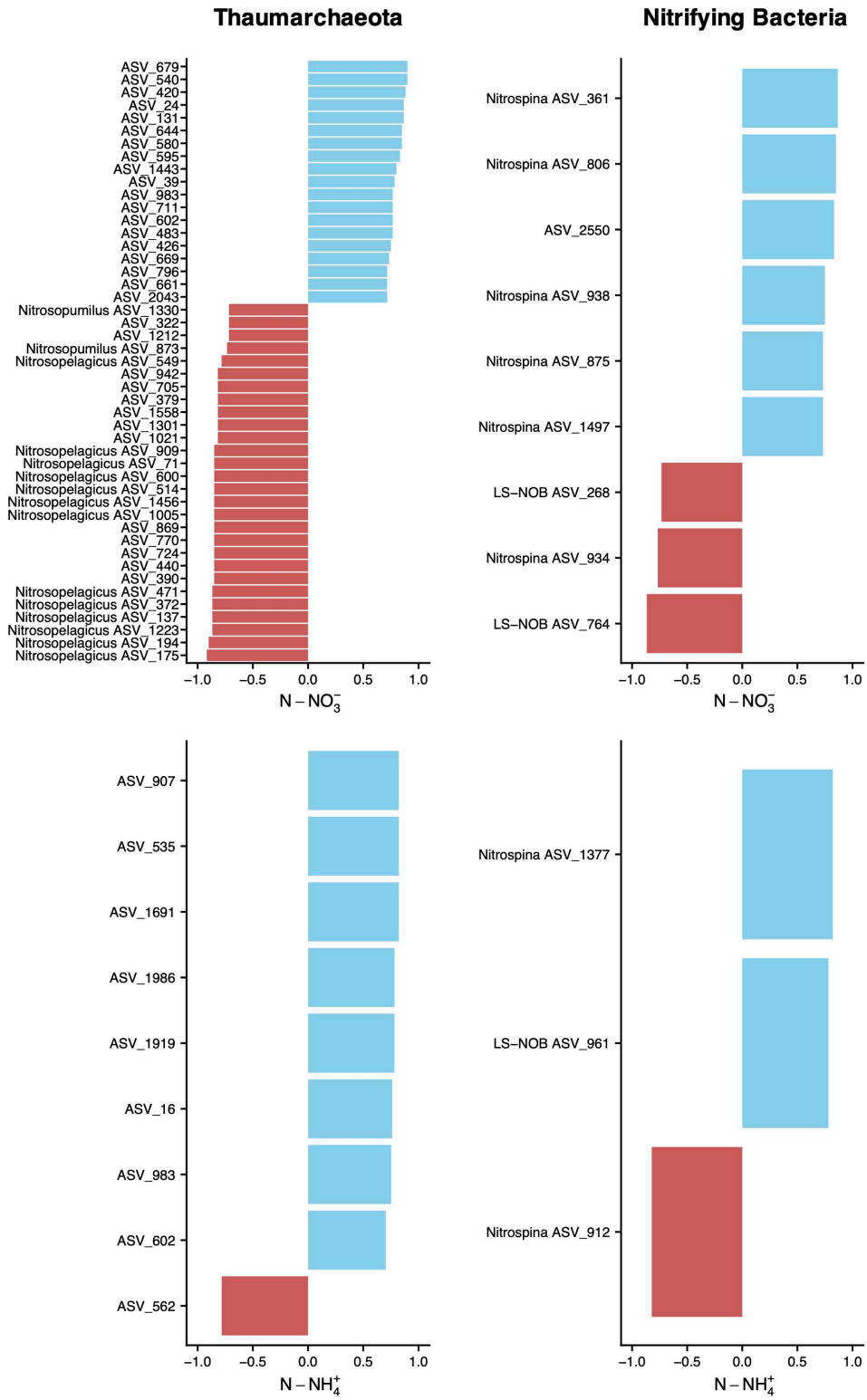

FIGURE 7 | Relationship between dissolved inorganic N and ASV abundance. ASVs without a genus name in the vertical axis represent unclassified ASVs at the genus level. Correlations were assessed by Spearman's rank coefficients (horizontal axis) for archaeal and nitrifying bacterial ASVs. Spearman's ranks are shown for $\rho > |0.7|$, with a p-value < 0.001 and were obtained on a centered log ratio transformed biological dataset, after selecting for ASVs that occur more than two times in at least four sampling sites of transect A. Only samples from below DCM and mesopelagic were included to avoid the auto-correlation effect among several variables caused by the sharp gradients across the different water column sections.

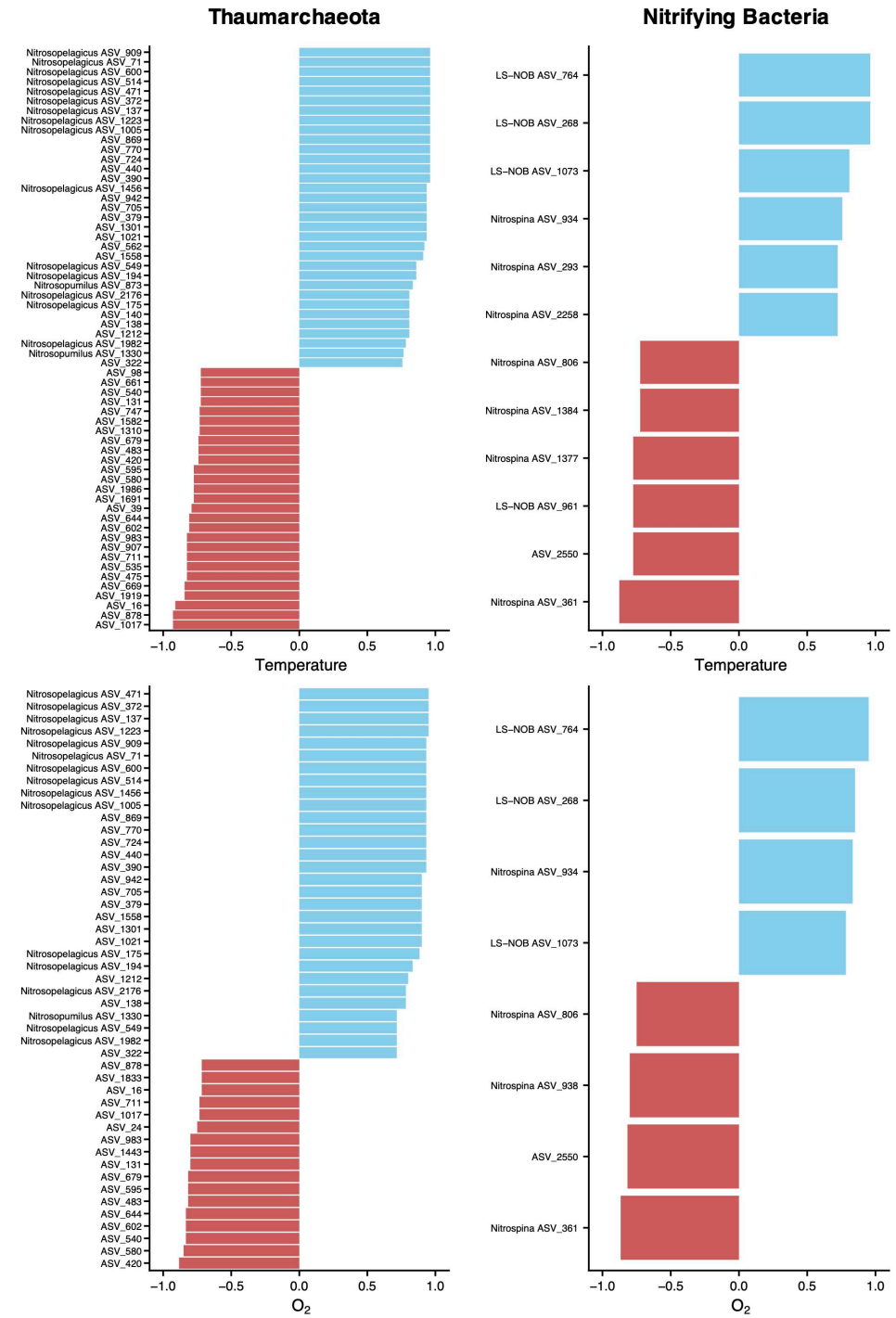

FIGURE 8 | Relationship between physicochemical parameters and ASV abundance. ASVs without a genus name in the vertical axis represent unclassified ASVs at the genus level. Correlations were assessed by Spearman's rank coefficients (horizontal axis) for archaeal and nitrifying bacterial ASVs. Spearman's ranks are shown for $\rho > |0.7|$, with a p-value < 0.001 and were obtained on a centered log ratio transformed biological dataset, after selecting for ASVs that occur more than two times in at least four sampling sites of transect A. Only samples from below DCM and mesopelagic were included to avoid the auto-correlation effect among several variables caused by the sharp gradients across the different water column sections.

could not be correlated with DIN concentration. ASVs assigned to families Nitrospiraceae and Nitrosomonadaceae only occurred in one or two sampling sites, making correlations unfeasible.

To explore the interactions between putative nitrifying ASVs and the abiotic environment of the water column, we performed a Spearman's rank analysis between the abundance of selected

ASVs, temperature, and oxygen (**Figure 8**). The relationships between thaumarchaeotal ASVs and these variables showed that AOA assigned to the *Ca. Nitrosopelagicus*, *Ca. Nitrosopumilus*, and some unclassified genera correlated positively with temperature and O_2. However, the negative correlations with temperature and O_2 were found exclusively with unclassified thaumarchaeotal ASVs. When considering putative NOB, our correlation analysis showed significant positive and negative correlations, regardless of the taxonomic classification.

Quantitative associations within and between nitrifying ASVs and the overall microbiome present in below DCM and mesopelagic samples were evaluated through Spearman correlations and a corresponding network analysis (**Figure 9**). A total of 13230 significant correlations (edges) were found between 872 unique ASVs (717 non-nitrifying and 155 potential nitrifiers). A median number of 19 significant interactions per ASV was found across the network. The large majority of these interactions (99.5%) were positive correlations. By employing the Louvain method, 23 subcommunities/modules were found. It is worth noticing that AOA and NOB co-occur within several nodules and that all subcommunities included ASVs from different genera. No modules were found to be taxonomically or functionally exclusive. In fact, a large diversity of non-nitrifying taxa, from 20 different phyla, correlated strongly with nitrifying ASVs. Among those, unclassified Chloroflexi, Marinimicrobia, α- and γ-Proteobacteria had the highest number of correlations, with 5821 significant correlations in total and an average of 11.1–19.2 significant correlations/ASV (**Supplementary Table 2**). If unclassified genera are not considered, the non-nitrifying genera with the highest number of correlations with nitrifying ASVs were Rhodopirellula (Planctomycetes), Marinoscillum (Bacteroidetes), Pseudohongiella (γ-Proteobacteria), and Woeseia (γ-Proteobacteria), with 440 significant correlations in total and an average of 15.5–31.8 significant correlations/ASV (**Supplementary Table 2**).

DISCUSSION

In this study, we found extremely contrasting environments in the top 500 m of the water column, similarly to previous studies in the Pacific Ocean and other stratified water columns (Sun et al., 2019; Faull et al., 2020). In surface waters (3–5 m deep) and in the DCM (107–130 m deep), relatively high temperatures and oxygen levels were measured (**Figure 2**). The salinity and turbidity levels at these two depths suggest a well-mixed surface layer. Moving down the water column, below the DCM and in the mesopelagic, the environment was much colder and oxygen-poor, especially in the mesopelagic, where the O_2 concentrations reached average levels of around 50 μM, still 10–100 times higher than levels found in oxygen minimum zones, such as the one located in the Eastern Tropical North Pacific (Faull et al., 2020). The DIN concentrations also showed a clear depth gradient. Surface and DCM waters were practically depleted of DIN (with the exception of NO_2^- in the DCM), while below DCM and mesopelagic water masses accumulated high amounts of DIN, especially NO_3^-, the end-product of nitrification. In summary, two main contrasting environments were noted, a warmer O_2-rich surface layer depleted in DIN and a colder O_2-poor water below 150 m with high NO_3^- concentrations.

This oceanographic split between surface/DCM and below DCM/mesopelagic was also evident in the community composition and β-diversity of putative nitrifying archaea and bacteria (**Figures 3**, **5**). Thaumarchaeotal and nitrifying bacterial ASVs were rare in surface and DCM layers while relatively abundant (especially Thaumarchaeota) below the DCM and in the mesopelagic, as previously reported in this region as well as in microplankton communities from other regions, such as the Mediterranean Sea (Mincer et al., 2007; Santoro et al., 2010; Besseling et al., 2019; Mende et al., 2019). In deeper water columns, such as in the Marianas Trench, the increase in thaumarcheotal relative abundance is observed deeper than the mesopelagic (Zhong et al., 2020). In other regions, such as the northeastern South China Sea, thaumarcheotal abundance can remain homogeneously low throughout the water column, hypothetically due to an intense vertical mixing (Liu et al., 2017).

The exclusion of nitrifying microorganisms in nitrogen-limited sunlit layers is expected in mid-latitude oceans due to the high nitrogen assimilation capacity of dominating photosynthetic organisms (Harrison et al., 1996; Zakem et al., 2018) and to the indirect photoinhibition caused by reactive oxygen species (Tolar et al., 2016). This ecological competition also explains the overall low levels of all DIN species observed in the upper layers of the water column, with the exception of the NO_2^- peak at the DCM (**Figure 2**). A NO_2^- peak near the DCM has been previously observed in the Pacific (Shiozaki et al., 2016; Smith et al., 2016) and the Atlantic Ocean (Liu et al., 2018) and can be explained by differences in redox chemistry and cell size between ammonia- and nitrite-oxidizing organisms (Zakem et al., 2018). Smaller AOA grow faster and oxidize NH_4^+ to NO_2^- at higher rates than larger NOB can oxidize NO_2^- to NO_3^- (Kuypers et al., 2018). This explanation is, in fact, consistent with the observation in our study of a subtle increase of AOA in the DCM without a concomitant increase in NOB.

Besides this broader split in community composition between shallower and deeper layers, we also observed some finer differences within each nitrifying group that may represent ecological and physiological differences. Most thaumarcheotal ASVs at the DCM were assigned to the *Ca. Nitrosopelagicus* genus (**Figure 3**). This genus has been shown to dominate thaumarcheotal sequences near the surface of the open ocean, probably due to its high genomic potential to survive in oligotrophic conditions (Santoro et al., 2015). With the increase in depth, the relative number of ASVs assigned to *Ca. Nitrosopelagicus* decreased and the majority of thaumarchaeotal sequences were unclassified at the genus level. In the North Pacific, the presence of diverse and abundant thaumarcheotal sequences that are unclassified at the genus level has been previously observed around the DCM and in the mesopelagic (Lund et al., 2012; Mende et al., 2019), which is probably explained by the high AOA diversity observed at these depths (Mincer et al., 2007; Santoro et al., 2010). The decrease in the abundance of *Ca. Nitrosopelagicus* can be

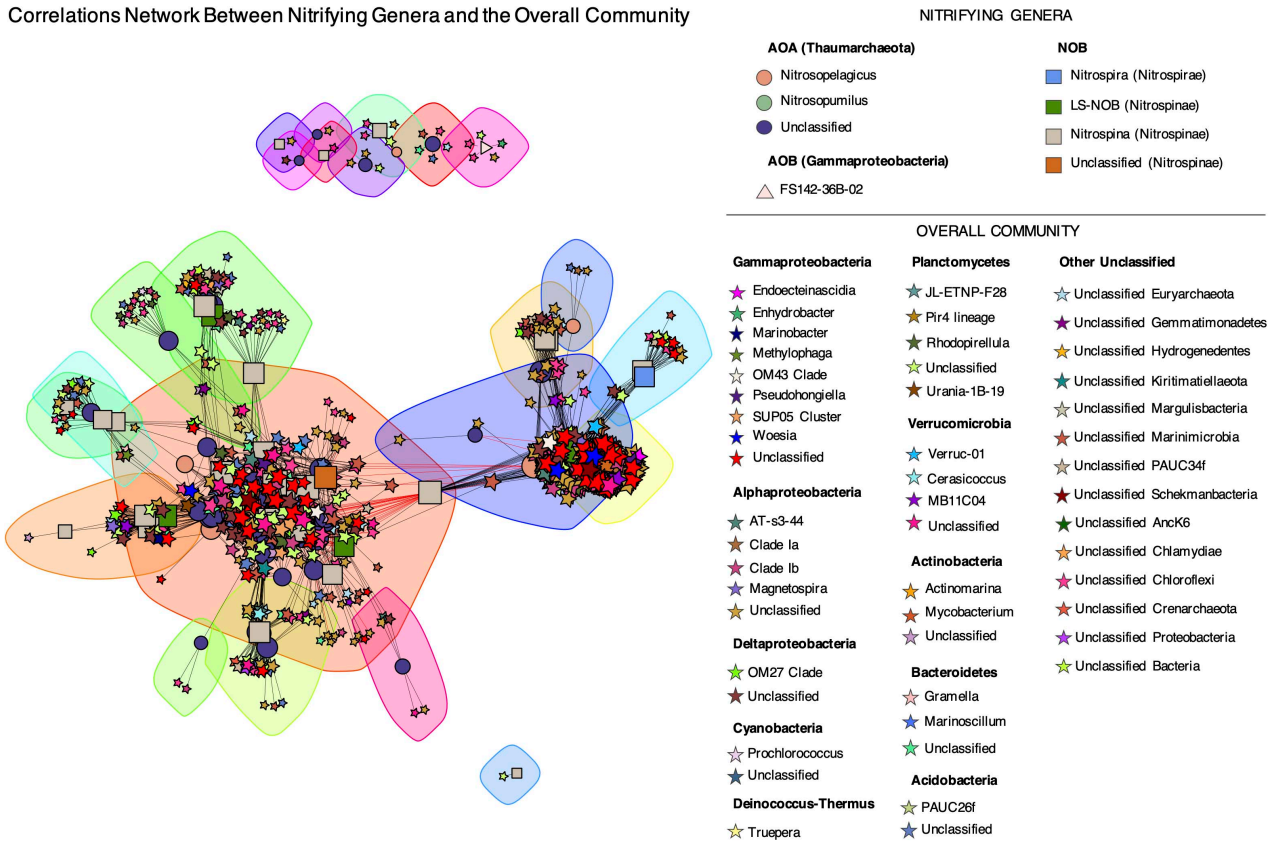

FIGURE 9 | Network analysis of putative nitrifying ASVs and the overall community below the DCM and in the mesopelagic. Relationships were assessed by Spearman's rank coefficients and only correlations with $\rho > |0.7|$, p-value < 0.001, and degree > 0 are shown. Edge color indicates sign of correlation: negative (red) and positive (black). Node size is proportional to node degree (number of significant correlations). Node taxon is represented by different colors while the shapes represent functional guilds: AOA (circles), AOB (triangles), NOB (squares), and overall community (stars). Sub-communities are highlighted with shaded areas and were found using the Louvain method (Blondel et al., 2008). The network layout was obtained with the force-directed layout algorithm by Fruchterman and Reingold using the igraph R package (Csardi and Nepusz, 2006).

partially caused by its growth temperature optimum of ∼22°C and completely halted growth in temperatures below 10°C (Santoro et al., 2015), such as the ones observed here in the mesopelagic.

Our phylogenetic analysis revealed that the unknown Thaumarchaeota that dominated the mesopelagic environment were closer to the *Ca. Nitrosopumilus* genus than to the *Ca. Nitrosopelagicus* (**Figure 4**). A depth-stratified population structure within phylogenetically related clades has been previously observed (Mende et al., 2019). A predominance of *Ca. Nitrosopumilus* over *Ca. Nitrosopelagicus* in deeper and colder waters could be attributed to the high thermal range observed for different *Ca. Nitrosopumilus* species (Walker et al., 2010; Bayer et al., 2019). The diverse unclassified sequences we found to be highly abundant in the mesopelagic may thus represent a new clade of *Ca. Nitrosopumilus* AOA or even a larger taxonomic division. However, due to the limited size of our 16S reads and the ambiguous classification from different databases (**Table 2**), we cannot confidently conclude that these unknown sequences would fall into the *Ca. Nitrosopumilus* or to a putative new genus. For a finer phylogenetic placement of these unknown sequences, larger DNA fragments need to be sequenced. Nevertheless, our data strongly suggests that an unknown group of closely related AOA is very well adapted to the conditions observed in the deeper layers of this water column.

When considering the abundance and depth distribution of NOB, we observed a sharp increase below the DCM and in the mesopelagic, marked by a strong dominance of Nitrospinae ASVs (**Figure 3B**). *Nitrospina*-like sequences dominated the NOB community across all samples, but they were particularly abundant below the DCM and in the mesopelagic, which is in accordance with previous studies from other regions showing a successful adaptation of *Nitrospina* to O_2-poor mesopelagic waters (Zaikova et al., 2010; Füssel et al., 2012; Sun et al., 2019).

Much less is known about the α-diversity patterns of nitrifying organisms in the water column. In our study, the highest values of thaumarcheotal diversity were observed below the DCM and not in the mesopelagic, where their relative abundance was highest (**Figures 6A**, **3A**). This result, together with the non-significant difference in species richness between the two depth layers, indicates that the community was more evenly

distributed below the DCM while the mesopelagic was dominated by a fewer number of ASVs. When considering the richness and diversity of putative nitrifying bacteria, their highest values were observed in the mesopelagic (**Figures 6B**, **3B**), despite the dominance of the *Nitrospina* genus. This result suggests that diversity within this NOB is particularly high, at least in O_2-poor cold waters, which may contribute to their adaptability in this presumptive harsh environment for an obligate aerobe (Sun et al., 2019).

Our correlation analysis also revealed striking differences within thaumarcheotal ASVs between their abundances, DIN concentrations, and physicochemical parameters. Interestingly, only ASVs with unknown genus correlated positively with NO_3^- (**Figure 7**), which suggests a crucial role of this group in regenerating NO_3^- in this oligotrophic region. The importance of ammonia oxidation as the rate-limiting step of nitrification in the oceans is widely recognized (Lehtovirta-Morley, 2018), but our results suggest the existence of a particular thaumarcheotal group with stronger relevance than previously identified *Ca. Nitrosopelagicus* or *Ca. Nitrosopumilus* organisms, since the latter had non-significant or negative correlations with NO_3^-. The significant negative correlations of most unassigned ASVs with temperature and O_2 (**Figure 8**) further indicate that these unknown AOA may be particularly well adapted to the colder O_2-poor waters of the mesopelagic. This finding contrasts with general trends of increased AOA activity with temperature, previously documented for terrestrial, freshwater, and cultivated AOA (Lehtovirta-Morley, 2018). However, it is in agreement with previous work demonstrating high functional diversity and metabolic versatility among closely related thaumarchaeotal strains (Bayer et al., 2016).

Sometimes overlooked in environmental studies, biological interactions between different groups of nitrifying organisms play also a vital role in community structure (Jones and Hallin, 2019) and consequently, ecosystem functioning. Despite the oligotrophic nature of our study site, positive interactions dominated the correlations network between nitrifying ASVs (**Figure 9**). This observation indicates a strong co-occurrence between the microorganisms involved in nitrification, often reported in the literature (Daebeler et al., 2014; Bartelme et al., 2017; Jones and Hallin, 2019), and supports a theoretical hypothesis that a nutrient-limited environment would lead to stronger positive than negative interactions. Besides the interactions within nitrifying ASVs, we also observed a complex network of correlations between this group and diverse taxa of non-nitrifying prokaryotes (**Figure 9**). The highest degree of correlations was found for unclassified ASVs belonging to Chloroflexi, Marinimicrobia (formerly known as Marine Group A and SAR406), α- and γ-Proteobacteria (**Supplementary Table 2**). Both α- and γ-Proteobacteria are dominant classes of heterotrophic bacteria in the marine environment (Sanz-Sáez et al., 2020), while Chloroflexi organisms represent a diverse range of metabolisms, such as aerobic/anaerobic heterotrophy or anoxygenic photosynthesis, and are present in multiple habitats around the planet, from the human oral cavity to sponges or the deep sea (Bayer et al., 2018). Marinimicrobia, with no cultured representatives so far, is globally distributed in the oceans and appears to have a wide diversity of metabolic properties and syntrophic interactions (Hawley et al., 2017). A recent metagenomic and metatranscriptomic study showed that some Marinimicrobia lineages can participate in strong co-metabolic interactions within the nitrogen cycle, particularly by expressing the nitrous oxide (N_2O) reductase gene (*nosZ*), which allows the coupling to thaumarchaeotal AOA that produce N_2O as a byproduct of ammonia oxidation (Santoro et al., 2011; Hawley et al., 2017). This potential link to AOA may contribute to explain the high relative abundance of unclassified Marinimicrobia observed in the below DCM and mesopelagic samples (**Supplementary Figure 3**). In our study, the network community modules found were taxonomically and functionally diverse. All subcommunities found included several AOA and NOB with different taxonomic assignments. Tight correlations between some specific nitrifying groups, such as AOA and Nitrospina species in open ocean waters have been previously documented (Mincer et al., 2007; Santoro et al., 2010), but a cosmopolitan interaction, such as the one observed in our study is seldom observed, probably because only specific groups are targeted in most studies.

Overall, the results from this study show that a diverse and potentially unknown group of thaumarchaeotal ASVs are crucial for NO_3^- production below the euphotic zone in the subtropical North Pacific. Moreover, it indicates that this group is composed of organisms well-adapted to the colder and O_2-poor waters of the mesopelagic, where they thrive and become critical for N recycling. This study further demonstrates that, despite their dominance below the DCM and in the mesopelagic, this group is tightly linked to multiple NOB and that diverse subcommunities are present in the oligotrophic deep ocean. Future research addressing this large group of unclassified Thaumarchaeotal organisms will certainly contribute to improve our understanding about the role of AOA in recycling inorganic nitrogen in the remote oligotrophic ocean.

DATA AVAILABILITY STATEMENT

The datasets presented in this study can be found in online repositories. The web links and accession numbers can be found below: https://www.ebi.ac.uk/ena, PRJEB32783 (16S amplicon sequencing data); and https://doi.pangaea.de/10.1594/PANGAEA.903405 (CTD dataset).

AUTHOR CONTRIBUTIONS

CM conceived and designed the field sampling for this study. JG, MT, and CM performed the field sampling and data collection. MT performed the sample preparation for sequencing. MS, EL, MB, and MT analyzed the sequencing data. AO and JG analyzed the nutrient data. MS, EL, MB, and CM wrote the manuscript. All authors approved the final submitted manuscript.

FUNDING

The authors acknowledge the support of the Schmidt Ocean Institute (SOI) for providing the R/V Falkor for a 3 week cruise within the "Exploring Fronts with Multiple Robots" expeditionw (https://schmidtocean.org/cruise/exploring_fronts_with_multiple_aerial-surface-underwater-vehicles/). The Portuguese Science and Technology Foundation (FCT) funded this study through a grant to CM (PTDC/CTA-AMB/30997/2017) and partially supported this research through the projects UIDB/04423/2020, and UIDB/04565/2020.

ACKNOWLEDGMENTS

The authors are grateful to João Sousa and Kanna Rajan for leading and coordinating the "Exploring Fronts with Multiple Robots" expedition. Our most sincere thanks also go to Francisco López for his assistance during sample collection and preparation in the wet lab as well as to António Gaspar G. de Sousa for assistance in the laboratory during sample processing for sequencing.

SUPPLEMENTARY MATERIAL

The Supplementary Material for this article can be found online at: https://www.frontiersin.org/articles/10.3389/fmicb.2021.624071/full#supplementary-material

Supplementary Figure 1 | Water column profiles of temperature, salinity, turbidity, fluorescence, and oxygen from casts performed along with sample collection.

Supplementary Figure 2 | Principal component analysis of environmental parameters between samples collected at the different depths in the water column.

Supplementary Figure 3 | Prokaryotic community composition at the different depths of the water column.

Supplementary Figure 4 | Principal coordinate analysis (PCoA) plot representing the β-diversity of the overall prokaryotic community from the different depths in the water column.

Supplementary Figure 5 | Species richness and α-diversity of prokaryotic communities from the different depths in the water column.

Supplementary Table 1 | Summary of sequence processing in collected samples.

Supplementary Table 2 | Taxonomic affiliation of non-nitrifying ASVs co-occurring with nitrifying ASVs.

REFERENCES

Apprill, A., Mcnally, S., Parsons, R., and Weber, L. (2015). Minor revision to V4 region SSU rRNA 806R gene primer greatly increases detection of SAR11 bacterioplankton. *Aquat. Microb Ecol.* 75, 129–137. doi: 10.3354/ame01753

Bartelme, R. P., McLellan, S. L., and Newton, R. J. (2017). Freshwater recirculating aquaculture system operations drive biofilter bacterial community shifts around a stable nitrifying consortium of ammonia-oxidizing archaea and comammox nitrospira. *Front. Microbiol.* 8:101.

Bayer, B., Vojvoda, J., Offre, P., Alves, R. J. E., Elisabeth, N. H., Garcia, J. A. L., et al. (2016). Physiological and genomic characterization of two novel marine thaumarchaeal strains indicates niche differentiation. *ISME J.* 10, 1051–1063. doi: 10.1038/ismej.2015.200

Bayer, B., Vojvoda, J., Reinthaler, T., Reyes, C., Pinto, M., and Herndl, G. J. (2019). *Nitrosopumilus adriaticus* sp. nov. and *Nitrosopumilus piranensis* sp. nov., two ammonia-oxidizing archaea from the Adriatic sea and members of the class Nitrososphaeria. *Int. J. Syst. Evol. Microbiol.* 69, 1892–1902. doi: 10.1099/ijsem.0.003360

Bayer, K., Jahn, M. T., Slaby, B. M., Moitinho-Silva, L., and Hentschel, U. (2018). Marine sponges as chloroflexi hot spots: genomic insights and high-resolution visualization of an abundant and diverse symbiotic clade. *mSystems* 3:e150-118.

Beman, J. M., Sachdeva, R., and Fuhrman, J. A. (2010). Population ecology of nitrifying archaea and bacteria in the southern california bight. *Environ. Microbiol.* 12, 1282–1292. doi: 10.1111/j.1462-2920.2010.02172.x

Besseling, M. A., Hopmans, E. C., Koenen, M., van der Meer, M. T. J., Vreugdenhil, S., Schouten, S., et al. (2019). Depth-related differences in archaeal populations impact the isoprenoid tetraether lipid composition of the mediterranean Sea water column. *Org. Geochem.* 135, 16–31. doi: 10.1016/j.orggeochem.2019.06.008

Blondel, V. D., Guillaume, J. L., Lambiotte, R., and Lefebvre, E. (2008). Fast unfolding of communities in large networks. *J. Stat. Mech. Theory Exp.* 2008:P10008.

Callahan, B. J., McMurdie, P. J., Rosen, M. J., Han, A. W., Johnson, A. J. A., and Holmes, S. P. (2016a). DADA2: high-resolution sample inference from Illumina amplicon data. *Nat. Methods* 13, 581–583. doi: 10.1038/nmeth.3869

Callahan, B. J., Sankaran, K., Fukuyama, J. A., McMurdie, P. J., and Holmes, S. P. (2016b). Bioconductor workflow for microbiome data analysis: from raw reads to community analyses [version 2; peer review: 3 approved]. *F1000Research* 5:1492. doi: 10.12688/f1000research.8986.2

Caporaso, J. G., Lauber, C. L., Walters, W. A., Berg-Lyons, D., Huntley, J., Fierer, N., et al. (2012). Ultra-high-throughput microbial community analysis on the Illumina HiSeq and MiSeq platforms. *ISME J.* 6, 1621–1624. doi: 10.1038/ismej.2012.8

Caporaso, J. G., Lauber, C. L., Walters, W. A., Berg-Lyons, D., Lozupone, C. A., Turnbaugh, P. J., et al. (2011). Global patterns of 16S rRNA diversity at a depth of millions of sequences per sample. *Proc. Natl. Acad. Sci. U.S.A.* 108, 4516–4522. doi: 10.1073/pnas.1000080107

Caranto, J. D., and Lancaster, K. M. (2017). Nitric oxide is an obligate bacterial nitrification intermediate produced by hydroxylamine oxidoreductase. *Proc Natl Acad Sci U S A.* 114, 8217–8222. doi: 10.1073/pnas.1704504114

Csardi, G., and Nepusz, T. (2006). The igraph software package for complex network research. *InterJ. Complex Syst.* 5, 1–9.

Daebeler, A., Bodelier, P. L. E., Yan, Z., Hefting, M. M., Jia, Z., and Laanbroek, H. J. (2014). Interactions between thaumarchaea, nitrospira and methanotrophs modulate autotrophic nitrification in volcanic grassland soil. *ISME J.* 8, 2397–2410. doi: 10.1038/ismej.2014.81

Daims, H., Lebedeva, E. V., Pjevac, P., Han, P., Herbold, C., and Albertsen, M. (2015). Complete nitrification by Nitrospira bacteria. *Nature* 528, 504–509. doi: 10.1038/nature16461

de Sousa, A. G. G., Tomasino, M. P., Duarte, P., Fernández-Méndez, M., Assmy, P., Ribeiro, H., et al. (2019). Diversity and composition of pelagic prokaryotic and protist communities in a thin arctic sea-ice regime. *Microb. Ecol.* 78, 388–408. doi: 10.1007/s00248-018-01314-2

Faull, L. M., Mara, P., Taylor, G. T., and Edgcomb, V. P. (2020). Imprint of trace dissolved oxygen on prokaryoplankton community structure in an oxygen minimum zone. *Front. Mar. Sci.* 7:360.

Füssel, J., Lam, P., Lavik, G., Jensen, M. M., Holtappels, M., Günter, M., et al. (2012). Nitrite oxidation in the namibian oxygen minimum zone. *ISME J.* 6, 1200–1209. doi: 10.1038/ismej.2011.178

Gloor, G. B., Macklaim, J. M., Pawlowsky-Glahn, V., and Egozcue, J. J. (2017). Microbiome datasets are compositional: and this is not optional. supplementary materials. *Front. Microbiol.* 8:2224.

Gordon, L., Jennings, J., Ross, A., and Krest, J. (1993). A suggested protocol for continuous flow automated analysis of seawater nutrients (phosphate, nitrate, nitrite and silicic acid) in the WOCE hydrographic program and the joint global ocean fluxes study. *Methods Man WHPO.* 91.

Harrison, W. G., Harris, L. R., and Irwin, B. D. (1996). The kinetics of nitrogen utilization in the oceanic mixed layer: nitrate and ammonium interactions at

nanomolar concentrations. *Limnol. Oceanogr.* 41, 16–32. doi: 10.4319/lo.1996.41.1.0016

Hawley, A. K., Nobu, M. K., Wright, J. J., Durno, W. E., Morgan-Lang, C., Sage, B., et al. (2017). Diverse marinimicrobia bacteria may mediate coupled biogeochemical cycles along eco-thermodynamic gradients. *Nat. Commun.* 8:1507.

Hollibaugh, J. T. (2017). Oxygen and the activity and distribution of marine thaumarchaeota. *Environ. Microbiol. Rep.* 9, 186–188. doi: 10.1111/1758-2229.12534

Holtappels, M., Lavik, G., Jensen, M. M., and Kuypers, M. M. M. (2011). "Chapter ten - 15N-labeling experiments to dissect the contributions of heterotrophic denitrification and anammox to nitrogen removal in the OMZ waters of the ocean," in *Research on Nitrification and Related Processes, Part A*, ed. M. G. Klotz (Cambridge, MA: Academic Press), 223–251. doi: 10.1016/b978-0-12-381294-0.00010-9

Horak, R. E. A., Qin, W., Schauer, A. J., Armbrust, E. V., Ingalls, A. E., Moffett, J. W., et al. (2013). Ammonia oxidation kinetics and temperature sensitivity of a natural marine community dominated by Archaea. *ISME J.* 7, 2023–2033. doi: 10.1038/ismej.2013.75

Jones, C. M., and Hallin, S. (2019). Geospatial variation in co-occurrence networks of nitrifying microbial guilds. *Mol. Ecol.* 28, 293–306. doi: 10.1111/mec.14893

Karner, M. B., DeLong, E. F., and Karl, D. M. (2001). Archaeal dominance in the mesopelagic zone of the Pacific ocean. *Nature* 409, 507–510. doi: 10.1038/35054051

Kits, K. D., Sedlacek, C. J., Lebedeva, E. V., Han, P., Bulaev, A., and Pjevac, P. (2017). Kinetic analysis of a complete nitrifier reveals an oligotrophic lifestyle. *Nature* 549, 269–272. doi: 10.1038/nature23679

Könneke, M., Bernhard, A. E., De La Torre, J. R., Walker, C. B., Waterbury, J. B., and Stahl, D. A. (2005). Isolation of an autotrophic ammonia-oxidizing marine archaeon. *Nature* 437, 543–546. doi: 10.1038/nature03911

Kowalchuk, G. A., and Stephen, J. R. (2001). Ammonia-oxidizing bacteria: a model for molecular microbial ecology. *Annu. Rev. Microbiol.* 55, 485–529. doi: 10.1146/annurev.micro.55.1.485

Kuypers, M. M. M., Marchant, H. K., and Kartal, B. (2018). The microbial nitrogen-cycling network. *Nat. Rev. Microbiol.* 16, 263–276.

Lehtovirta-Morley, L. E. (2018). Ammonia oxidation: ecology, physiology, biochemistry and why they must all come together. *FEMS Microbiol. Lett.* 365.

Letelier, R. M., Karl, D. M., Abbott, M. R., and Bidigare, R. R. (2004). Light driven seasonal patterns of chlorophyll and nitrate in the lower euphotic zone of the North Pacific subtropical gyre. *Limnol. Oceanogr.* 49, 508–519. doi: 10.4319/lo.2004.49.2.0508

Letunic, I., and Bork, P. (2019). Interactive tree of life (iTOL) v4: recent updates and new developments. *Nucleic Acids Res.* 47, W256–W259.

Levipan, H. A., Molina, V., and Fernandez, C. (2014). Nitrospina-like bacteria are the main drivers of nitrite oxidation in the seasonal upwelling area of the Eastern South Pacific (Central Chile 36°S). *Environ. Microbiol. Rep.* 6, 565–573. doi: 10.1111/1758-2229.12158

Liu, H., Zhang, C. L., Yang, C., Chen, S., Cao, Z., Zhang, Z., et al. (2017). Marine group II dominates planktonic archaea in water column of the northeastern south china sea. *Front. Microbiol.* 8:1098.

Liu, Q., Tolar, B. B., Ross, M. J., Cheek, J. B., Sweeney, C. M., Wallsgrove, N. J., et al. (2018). Light and temperature control the seasonal distribution of thaumarchaeota in the South Atlantic bight. *ISME J.* 12, 1473–1485. doi: 10.1038/s41396-018-0066-4

Luecker, S., Nowka, B., Rattei, T., Spieck, E., and Daims, H. (2013). The genome of *Nitrospina gracilis* illuminates the metabolism and evolution of the major marine nitrite oxidizer. *Front. Microbiol.* 4:27.

Lund, M. B., Smith, J. M., and Francis, C. A. (2012). Diversity, abundance and expression of nitrite reductase (nirK)-like genes in marine thaumarchaea. *ISME J.* 6, 1966–1977. doi: 10.1038/ismej.2012.40

Martens-Habbena, W., Berube, P. M., Urakawa, H., de la Torre, J. R., and Stahl, D. A. (2009). Ammonia oxidation kinetics determine niche separation of nitrifying Archaea and bacteria. *Nature* 461, 976–979. doi: 10.1038/nature08465

McMurdie, P. J., and Holmes, S. (2013). Phyloseq: an r package for reproducible Interactive analysis and graphics of microbiome census data. *PLoS One* 8:e61217. doi: 10.1371/journal.pone.0061217

Mende, D. R., Boeuf, D., and DeLong, E. F. (2019). Persistent core populations shape the microbiome throughout the water column in the north pacific subtropical gyre. *Front. Microbiol.* 10:2273.

Merbt, S. N., Stahl, D. A., Casamayor, E. O., Martí, E., Nicol, G. W., and Prosser, J. I. (2012). Differential photoinhibition of bacterial and archaeal ammonia oxidation. *FEMS Microbiol. Lett.* 327, 41–46. doi: 10.1111/j.1574-6968.2011.02457.x

Mincer, T. J., Church, M. J., Taylor, L. T., Preston, C., Karl, D. M., and DeLong, E. F. (2007). Quantitative distribution of presumptive archaeal and bacterial nitrifiers in monterey bay and the North Pacific subtropical gyre. *Environ. Microbiol.* 9, 1162–1175. doi: 10.1111/j.1462-2920.2007.01239.x

Murali, A., Bhargava, A., and Wright, E. S. (2018). IDTAXA: a novel approach for accurate taxonomic classification of microbiome sequences. *Microbiome* 6:140.

Oksanen, J., Blanchet, F. G., Friendly, M., Kindt, R., Legendre, P., McGlinn, D., et al. (2017). *vegan: Community Ecology Package*.

Olson, D., Hitchcock, G., Mariano, A., Ashjian, C., Peng, G., Nero, R., et al. (1994). Life on the edge: marine life and fronts. *Oceanography* 7, 52–60. doi: 10.5670/oceanog.1994.03

Pajares, S., and Ramos, R. (2019). Processes and microorganisms involved in the marine nitrogen cycle: knowledge and gaps. *Front. Mar. Sci.* 6:739.

Parada, A. E., Needham, D. M., and Fuhrman, J. A. (2016). Every base matters: assessing small subunit rRNA primers for marine microbiomes with mock communities, time series and global field samples. *Environ. Microbiol.* 18, 1403–1414. doi: 10.1111/1462-2920.13023

Parks, D. H., Chuvochina, M., Waite, D. W., Rinke, C., Skarshewski, A., Chaumeil, P. -A., et al. (2018). A standardized bacterial taxonomy based on genome phylogeny substantially revises the tree of life. *Nat. Biotechnol.* 36, 996–1004. doi: 10.1038/nbt.4229

Parks, D. H., Chuvochina, M., Chaumeil, P.-A., Rinke, C., Mussig, A. J., and Hugenholtz, P. (2020). A complete domain-to-species taxonomy for bacteria and archaea. *Nat. Biotechnol.* 38, 1079–1086. doi: 10.1038/s41587-020-0501-8

Quast, C., Pruesse, E., Yilmaz, P., Gerken, J., Schweer, T., Yarza, P., et al. (2013). The SILVA ribosomal RNA gene database project: improved data processing and web-based tools. *Nucleic Acids Res.* 41, 590–596.

Santoro, A. E., Buchwald, C., McIlvin, M. R., and Casciotti, K. L. (2011). Isotopic signature of N2O produced by marine ammonia-oxidizing Archaea. *Science* 333, 1282–1285. doi: 10.1126/science.1208239

Santoro, A. E., Casciotti, K. L., and Francis, C. A. (2010). Activity, abundance and diversity of nitrifying archaea and bacteria in the central California current. *Environ. Microbiol.* 12, 1989–2006. doi: 10.1111/j.1462-2920.2010.02205.x

Santoro, A. E., Dupont, C. L., Richter, R. A., Craig, M. T., Carini, P., McIlvin, M. R., et al. (2015). Genomic and proteomic characterization of "candidatus nitrosopelagicus brevis": an ammonia-oxidizing archaeon from the open ocean. *Proc. Natl. Acad. Sci. U.S.A.* 112, 1173–1178. doi: 10.1073/pnas.1416223112

Sanz-Sáez, I., Salazar, G., Sánchez, P., Lara, E., Royo-Llonch, M., Sà, E. L., et al. (2020). Diversity and distribution of marine heterotrophic bacteria from a large culture collection. *BMC Microbiol.* 20:207.

Sauzède, R., Martinez, E., Maes, C., Pasqueron, de Fommervault, O., Poteau, A., et al. (2020). Enhancement of phytoplankton biomass leeward of tahiti as observed by biogeochemical-argo floats. *J. Mar. Syst.* 204:103284. doi: 10.1016/j.jmarsys.2019.103284

Schliep, K. P. (2011). phangorn: phylogenetic analysis in r. *Bioinformatics* 27, 592–593. doi: 10.1093/bioinformatics/btq706

Shiozaki, T., Ijichi, M., Isobe, K., Hashihama, F., Nakamura, K., Ehama, M., et al. (2016). Nitrification and its influence on biogeochemical cycles from the equatorial Pacific to the Arctic Ocean. *ISME J.* 10, 2184–2197. doi: 10.1038/ismej.2016.18

Smith, J. M., Damashek, J., Chavez, F. P., and Francis, C. A. (2016). Factors influencing nitrification rates and the abundance and transcriptional activity of ammonia-oxidizing microorganisms in the dark northeast Pacific ocean. *Limnol. Oceanogr.* 61, 596–609. doi: 10.1002/lno.10235

Sow, S. L. S., Trull, T. W., and Bodrossy, L. (2020). Oceanographic fronts shape Phaeocystis assemblages: a high-resolution 18S rRNA gene survey from the ice-edge to the equator of the South Pacific. *Front. Microbiol.* 11:1847.

Strickland, J. D. H., and Parsons, T. R. (1977). *A Practical Handbook Of Sewater Analysis*. Ottawa: Fisheries Research Board of Canada.

Sun, X., Ji, Q., Jayakumar, A., and Ward, B. B. (2017). Dependence of nitrite oxidation on nitrite and oxygen in low-oxygen seawater. *Geophys. Res. Lett.* 44, 7883–7891. doi: 10.1002/2017gl074355

Sun, X., Kop, L. F. M., Lau, M. C. Y., Frank, J., Jayakumar, A., Lücker, S., et al. (2019). Uncultured Nitrospina-like species are major nitrite oxidizing bacteria in oxygen minimum zones. *ISME J.* 13, 2391–2402. doi: 10.1038/s41396-019-0443-7

Tolar, B. B., Powers, L. C., Miller, W. L., Wallsgrove, N. J., Popp, B. N., and Hollibaugh, J. T. (2016). Ammonia oxidation in the ocean can be inhibited by nanomolar concentrations of hydrogen peroxide. *Front. Mar. Sci.* 3:237.

Tyrrell, T. (1999). The relative influences of nitrogen and phosphorus on oceanic primary production. *Nature* 400, 525–531. doi: 10.1038/22941

van Kessel, M. A. H. J., Speth, D. R., Albertsen, M., Nielsen, P. H., Op, den Camp, H. J. M., et al. (2015). Complete nitrification by a single microorganism. *Nature* 528, 555–559. doi: 10.1038/nature16459

Walker, C. B., de la Torre, J. R., Klotz, M. G., Urakawa, H., Pinel, N., Arp, D. J., et al. (2010). Nitrosopumilus maritimus genome reveals unique mechanisms for nitrification and autotrophy in globally distributed marine crenarchaea. *Proc. Natl. Acad. Sci. U.S.A* 107, 8818–8823. doi: 10.1073/pnas.0913533107

Winogradsky, S. (1890). Recherches sur les organismes des la nitrification. *Ann. Inst. Pasteur.* 4, 213–231.

Wright, E. S. (2016). Using DECIPHER v2.0 to analyze big biological sequence data in r. *R J.* 8, 352–359. doi: 10.32614/rj-2016-025

Xia, L. C., Ai, D., Cram, J., Fuhrman, J. A., and Sun, F. (2013). Efficient statistical significance approximation for local similarity analysis of high-throughput time series data. *Bioinformatics* 29, 230–237. doi: 10.1093/bioinformatics/bts668

Xia, L. C., Steele, J. A., Cram, J. A., Cardon, Z. G., Simmons, S. L., Vallino, J. J., et al. (2011). Extended local similarity analysis (eLSA) of microbial community and other time series data with replicates. *BMC Syst. Biol.* 5:S15.

Zaikova, E., Walsh, D. A., Stilwell, C. P., Mohn, W. W., Tortell, P. D., and Hallam, S. J. (2010). Microbial community dynamics in a seasonally anoxic fjord: saanich inlet, British Columbia. *Environ. Microbiol.* 12, 172–191. doi: 10.1111/j.1462-2920.2009.02058.x

Zakem, E. J., Al-Haj, A., Church, M. J., van Dijken, G. L., Dutkiewicz, S., Foster, S. Q., et al. (2018). Ecological control of nitrite in the upper ocean. *Nat. Commun.* 9:1206.

Zehr, J. P., and Ward, B. B. (2002). Nitrogen cycling in the ocean: new perspectives on processes and paradigms. *Appl. Environ. Microbiol.* 68, 1015–1024. doi: 10.1128/aem.68.3.1015-1024.2002

Zhong, H., Lehtovirta-Morley, L., Liu, J., Zheng, Y., Lin, H., Song, D., et al. (2020). Novel insights into the thaumarchaeota in the deepest oceans: their metabolism and potential adaptation mechanisms. *Microbiome* 8:78.

Conflict of Interest: The authors declare that the research was conducted in the absence of any commercial or financial relationships that could be construed as a potential conflict of interest.

frontiers in Microbiology

HYPOTHESIS AND THEORY
published: 24 March 2021
doi: 10.3389/fmicb.2021.622504

Cyclic Conversions in the Nitrogen Cycle

Robbert Kleerebezem[1]* *and Sebastian Lücker*[2]

[1] Department of Biotechnology, Delft University of Technology, Delft, Netherlands, [2] Department of Microbiology, IWWR, Radboud University, Nijmegen, Netherlands

The cyclic nature of specific conversions in the nitrogen cycle imposes strict limitations to the conversions observed in nature and explains for example why anaerobic ammonium oxidation (anammox) bacteria can only use nitrite – and not nitrate – as electron acceptor in catabolism, and why nitrite is required as additional electron donor for inorganic carbon fixation in anabolism. Furthermore, the biochemistry involved in nitrite-dependent anaerobic methane oxidation excludes the feasibility of using nitrate as electron acceptor. Based on the cyclic nature of these nitrogen conversions, we propose two scenarios that may explain the ecological role of recently discovered complete ammonia-oxidizing (comammox) *Nitrospira* spp., some of which were initially found in a strongly oxygen limited environment: (i) comammox *Nitrospira* spp. may actually catalyze an anammox-like metabolism using a biochemistry similar to intra-oxic nitrite-dependent methane oxidation, or (ii) scavenge all available oxygen for ammonia activation and use nitrate as terminal electron acceptor. Both scenarios require the presence of the biochemical machinery for ammonia oxidation to nitrate, potentially explaining a specific ecological niche for the occurrence of comammox bacteria in nature.

Keywords: nitrification, anammox, thermodynamics, stoichiometry, denitrification

OPEN ACCESS

Edited by:
Marc Strous,
University of Calgary, Canada

Reviewed by:
Po-Heng Lee,
Imperial College London, United Kingdom
Hirotsugu Fujitani,
Chuo University, Japan

***Correspondence:**
Robbert Kleerebezem
r.kleerebezem@tudelft.nl

Specialty section:
This article was submitted to Microbial Physiology and Metabolism, a section of the journal Frontiers in Microbiology

Received: *28 October 2020*
Accepted: *25 February 2021*
Published: *24 March 2021*

Citation:
Kleerebezem R and Lücker S (2021) Cyclic Conversions in the Nitrogen Cycle. Front. Microbiol. 12:622504. doi: 10.3389/fmicb.2021.622504

INTRODUCTION

Catabolic processes in chemotrophic microorganisms either rely on (organic) substrate fermentations or on oxidation of an electron donor with an external electron acceptor. Metabolic energy conservation in non-fermentative catabolic processes typically depends on the transfer of electrons from a reduced electron donor (e.g., organic carbon) to an electron carrier such as NAD under formation of NADH. NADH subsequently serves as electron donor for the respiratory chain where electrons are transferred through a series of respiratory protein complexes to a terminal electron acceptor such as molecular oxygen or oxidized nitrogen compounds like nitrite or nitrate. Metabolic energy available in these redox reactions is used for proton translocation across the cytoplasmic membrane, resulting in a proton motive force. An example process from the nitrogen cycle that is driven by respiration of nitrite or nitrate is heterotrophic denitrification (Strohm et al., 2007; Simon and Klotz, 2013). The versatility of electron carriers like NADH enable an unrestricted flexibility in the number of electrons donated and accepted in the catabolic reaction system, and different electron donor and electron acceptor reactions can be coupled directly.

Other conversions in the nitrogen cycle, primarily autotrophic nitrogen conversions, depend on more direct transfer of electrons from a donor to an acceptor in a dedicated respiratory system that does not involve electron carriers like NADH. In these so-called cyclic conversions electron transfer, the electron donor or an oxidized derivative thereof,

directly reacts with the electron acceptor or an intermediate in the electron acceptor reaction. Due to the more direct reaction of an electron donor with and electron acceptor, cyclic conversions are restricted by tight stoichiometric dependencies that impose strict boundaries to a number of nitrogen conversions (Kartal et al., 2012).

In this manuscript two well-known cyclic conversions in the microbial nitrogen cycle are described and the specific consequences and restrictions associated with the cyclic nature of these conversions are identified. Based on these examples, the ecological implications for the recently discovered comammox metabolism are elaborated and discussed.

WHY ANAEROBIC AMMONIUM OXIDATION WITH NITRITE, AND NOT NITRATE AS ELECTRON ACCEPTOR?

The anammox process concerns the anaerobic oxidation of ammonium with nitrite as electron acceptor as discovered approximately 30 years ago (Strous et al., 1999a,b):

$$1 \cdot NH_4^+ + 1 \cdot NO_2^- \rightarrow 1 \cdot N_2 + 2 \cdot H_2O$$
$$\triangle G^{0'} = -362.8\ kJ \cdot reaction^{-1}$$

All Gibbs free energy change values calculated are corrected for a pH of 7 ($\triangle G^{0'}$) and based on the Gibbs energy of formation values listed in **Table 1**. Microorganisms that are capable of using the anammox reaction for autotrophic growth depend on the oxidation of nitrite to nitrate for reduction of carbon dioxide to biomass precursors, presumably with ammonium as nitrogen source:

$$1 \cdot CO_2 + 2.1 \cdot NO_2^- + 0.2 \cdot NH_4^+ + 0.6 \cdot H_2O \rightarrow 1 \cdot CH_{1.8}O_{0.5}N_{0.2} + 2.1 \cdot NO_3^- + 0.2 \cdot H^+$$
$$\triangle G^{0'} = +311.5\ kJ \cdot reaction^{-1}$$

The growth efficiency as reflected in the biomass yield per mole substrate has been measured to amount $1.30 - 1.70\ g/mol\ NH_4^+$. Using a biomass yield value of $1.70\ g/mol\ NH_4^+$, corresponding to $0.07\ Cmol/mol\ NH_4^+$, the stoichiometry of anammox metabolism becomes:

$$1.00 \cdot NH_4^+ + 1.13 \cdot NO_2^- + 0.07 \cdot CO_2 \rightarrow 0.99 \cdot N_2 + 0.15 \cdot NO_3^- + 0.07 \cdot CH_{1.8}O_{0.5}N_{0.2} + 1.93 \cdot H_2O + 0.01 \cdot H^+$$
$$\triangle G^{0'} = -336.2\ kJ \cdot reaction^{-1}$$

When expressed per mole of biomass formed, the Gibbs free energy change of the anammox process equals $-4865\ kJ/mol\ X$. This value is comparable to the values for other autotrophic conversions that involve reversed electron transfer for carbon dioxide fixation ($-3500\ kJ/mol\ X$, (Heijnen and Kleerebezem, 2010; Kleerebezem and Van Loosdrecht, 2010)), which suggests that the efficiency of the coupling of catabolism and anabolism in the anammox process is comparable to other autotrophic processes that require reversed electron transfer for carbon fixation.

The biochemistry of the anammox process as described by Kartal et al. (2011) is shown in **Figure 1**. In short: The electron acceptor in catabolism, nitrite, is reduced to nitric oxide by a nitrite reductase (*NiR*), and nitric oxide subsequently reacts with ammonium to form hydrazine. Energy-rich hydrazine is oxidized to dinitrogen gas and energy is harvested through formation of a proton motive force. Electrons obtained upon oxidation of hydrazine to dinitrogen gas are used for reducing nitrite to nitric oxide and the condensation of ammonium and nitric oxide to hydrazine. Carbon dioxide reduction to biomass, presumably with ammonium as nitrogen source, uses electrons obtained from nitrite oxidation to nitrate. Since the direct coupling of nitrite oxidation to nitrate and carbon dioxide reduction to biomass precursors is thermodynamically unfavorable, reversed electron transfer is required to drive anabolism. Herewith nitrite plays a peculiar double role in the anammox process: it serves as electron acceptor in catabolism and electron donor in anabolism.

The anammox catabolism is a typical example of a cyclic conversion. There is symmetry in the electron donor and acceptor reactions, where the three electrons gained upon oxidation of ammonium to dinitrogen gas equals the number of electrons required for nitrite reduction to dinitrogen gas. The prerequisite that ammonium in this reaction is activated by nitric oxide determines that ammonium needs to react with nitrite in a one-to-one ratio. In other words, at least one nitric oxide needs to be produced in the electron acceptor reaction to activate one ammonium.

This dependency of the anammox process on nitric oxide for ammonium activation also explains the incapacity of anammox bacteria to use ammonium as electron donor for anabolism: as each ammonium needs to be activated by one nitric oxide molecule, it is impossible to increase the ammonium to nitrite

TABLE 1 | Gibbs energy of formation values for the compounds involved in the reactions described.

compound	formula	phase	$G_f^0[kJ \cdot mol^{-1}]$
dinitrogen	N_2	g	0,0
nitric oxide	NO	g	86,6
nitrous oxide	N_2O	g	104,2
hydroxylamine	NH_2OH	aq	−43,6
hydrazine	N_2H_4	g	159,2
ammonium	NH_4^+	aq	−79,4
nitrite	NO_2^-	aq	−32,2
nitrate	NO_3^-	aq	−111,3
carbon dioxide	CO_2	g	−394,4
biomass	$CH_{1.8}O_{0.5}N_{0.2}$	s	−67,0
methane	CH_4	g	−50,8
methanol	CH_3OH	aq	−175,4
oxygen	O_2	g	0,0
water	H_2O	aq	−237,2
proton	H^+	aq	0,0
electron	e^-	aq	0,0

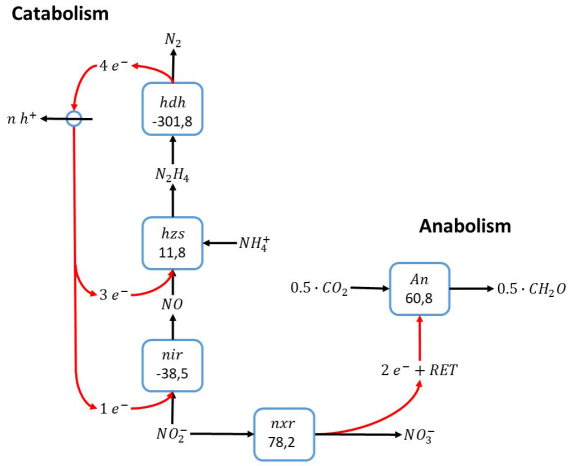

FIGURE 1 | Anammox reaction stoichiometry, assuming ammonium activation with nitric oxide (Kartal et al., 2011). The individual blocks represent enzymatic steps (*hdh*, hydrazine dehydrogenase; *nir*, nitrite reductase; *hzs*, hydrazine synthase; *nxr*, nitrite oxidoreductase) and the corresponding Gibbs free energy change ($\triangle G^{0'}$) of the reaction corrected for a pH of 7. *RET* stands for reversed electron transfer.

ratio to a value higher than one, which would be required if ammonium is used as anabolic electron donor for carbon dioxide reduction. The only remaining compound present in the system to serve as electron donor for carbon fixation is nitrite, which can be oxidized to nitrate. Indeed, growth of anammox is always associated with nitrate production according to a stoichiometry close to the metabolic reaction stoichiometry shown above.

The cyclic nature of the anammox process also explains directly that the potential oxidation of ammonium with nitrate under formation of dinitrogen gas according to

$$1 \cdot NH_4^+ + 0.6 \cdot NO_3^- \rightarrow 1.6 \cdot N_2 + 1.8 \cdot H_2O + 0.4 \cdot H^+$$
$$\triangle G^{0'} = -296.7\ kJ \cdot reaction^{-1}$$

cannot be catalyzed with a biochemistry comparable to the scheme shown in **Figure 1**, because nitric oxide cannot be produced in the required 1:1 ratio with ammonium due to an unbalance in the number of electrons required to reduce nitrate ultimately to dinitrogen gas and electrons gained from ammonium oxidation. This is directly reflected in the ammonium to nitrate ratio of 1:0.6 in the reaction shown above.

A cyclic conversion that facilitates ammonium oxidation with nitrate as electron acceptor can be anticipated if not dinitrogen gas but nitrous oxide would be the end-product of the catabolic process:

$$1 \cdot NH_4^+ + 1 \cdot NO_3^- \rightarrow 1 \cdot N_2O + 2 \cdot H_2O$$
$$\triangle G^{0'} = -179.5\ kJ \cdot reaction^{-1}$$

Even though the Gibbs free energy change of this reaction is much less favorable than the original anammox reaction with nitrite as electron acceptor, there is no direct rational why this reaction would not occur. There is, however, another reason that makes this catabolic reaction unlikely to occur: In absence of nitrite there is no suitable electron donor that can be used to drive the reduction of carbon dioxide to biomass.

On the other hand, the cyclic nature of anammox catabolism allows the use of nitric oxide (NO) as electron acceptor in the process according to:

$$1 \cdot NH_4^+ + 1.5 \cdot NO \rightarrow 1.25 \cdot N_2 + 1.5 \cdot H_2O + 1 \cdot H^+$$
$$\triangle G^{0'} = -446.2\ kJ \cdot reaction^{-1}$$

as has indeed been observed by Hu et al. (2019). In this case, the ammonium to nitric oxide ratio is smaller than 1, which implies that another (unknown) mechanism is available for NO reduction to dinitrogen gas (or ammonium) with electrons from hydrazine oxidation, besides the activation of ammonium like in the reaction scheme shown in **Figure 1**. One of the intriguing possibilities of the use of NO as electron acceptor is that it enables the use of hydrazine as very strong electron donor for carbon dioxide reduction to biomass precursors without the need of reversed electron transfer because anabolism becomes a thermodynamically favorable reaction:

$$1 \cdot CO_2 + 1.05 \cdot N_2H_4 + 0.2 \cdot NH_4^+ \rightarrow 1.05 \cdot N_2$$
$$+1 \cdot CH_{1.8}O_{0.5}N_{0.2} + 1.5 \cdot H_2O + 0.2 \cdot H^+$$
$$\triangle G^{0'} \quad -187.6\ kJ \cdot reaction^{-1}$$

This would exclude the need for anabolic nitrate production as experimentally demonstrated by Hu et al. (2019). Unfortunately, these authors did not report the impact on biomass yield in the process, which is expected to be significantly higher due to the absence of reversed electron transfer for carbon fixation (Kleerebezem and Van Loosdrecht, 2010).

A comparable increase in the energy content of the electrons needed in anabolism can also be achieved with nitrite as electron acceptor, provided that an efficient electron transfer mechanism between *nir* and *nxr* is available to drive nitrite disproportionation. This would then result in nitrite reduction to nitric oxide, combined with nitrite oxidation to nitrate as electron donor reaction as proposed by Hu et al. (2019). To which extent nitrite disproportionation is used in anammox to circumvent reversed electron transfer for carbon fixation remains unclear. The measured biomass yield values and the corresponding Gibbs free energy dissipation values for biomass production (see above) do suggest severe thermodynamic growth inefficiencies as typically associated with reversed electron transfer for carbon fixation.

WHY DIRECT METHANE OXIDATION WITH NITRITE, BUT NOT NITRATE AS ELECTRON ACCEPTOR?

A more recent breakthrough in the microbial nitrogen cycle is the experimental demonstration of methane

oxidation with nitrite and nitrate as electron acceptor (Raghoebarsing et al., 2006):

$$1 \cdot CH_4 + 2.67 \cdot NO_2^- + 2.67 \cdot H^+ \rightarrow 1 \cdot CO_2 + 1.33 \cdot N_2 + 3.33 \cdot H_2O \quad \Delta G^{0'} = -941.8\ kJ \cdot reaction^{-1}$$

$$1 \cdot CH_4 + 1.6 \cdot NO_3^- + 1.6 \cdot H^+ \rightarrow 1 \cdot CO_2 + 0.8 \cdot N_2 + 2.8 \cdot H_2O \quad \Delta G^{0'} = -765.7\ kJ \cdot reaction^{-1}$$

Methane oxidation with nitrite relies on the intracellular production of molecular oxygen from nitric oxide by a nitric oxide dismutase. Since the *Candidatus* Methylomirabilis bacteria that catalyze nitrite-dependent anaerobic methane oxidation use the particulate methane monooxygenase, which requires one molecule of molecular oxygen per methane, the minimum number of nitrite molecules reduced per methane is two (see **Figure 2**). For methane oxidation with nitrite more than two nitrite molecules are required to accept the electrons gained from methane oxidation. Consequently, the remaining electrons from methane oxidation can either be used for inorganic carbon conversion to biomass precursors (Rasigraf et al., 2014) as shown in **Figure 2**, or for more catabolic reduction of nitrite. Overall, there is no reason why methane oxidation with nitrite cannot be catalyzed by a single microorganism, as has indeed been demonstrated experimentally (Raghoebarsing et al., 2006; Ettwig et al., 2010).

The situation is different for methane oxidation with nitrate (Raghoebarsing et al., 2006; Arshad et al., 2015; Welte et al., 2016; Stultiens et al., 2019). In this catabolic system the boundary condition that at least two oxidized nitrogen compounds are required in order to produce one molecular oxygen suggests that in the overall reaction 10 electrons are accepted per oxygen produced. Evidently, this exceeds the eight electrons gained per methane oxidized. This suggests directly that using the biochemistry proposed, there cannot be one microorganism that is capable of catalyzing methane oxidation with nitrate as electron acceptor, as is indeed observed in experiments. Instead, it has been demonstrated that methane oxidation with nitrate can be catalyzed by *Methanoperedens* archaea using the reversed methanogenesis pathway under formation of nitrite or ammonium. This provides the ecological niche for coexistence with either anammox or *Candidatus* Methylomirabilis to establish full conversion of methane and nitrate to dinitrogen gas and carbon dioxide (Stultiens et al., 2019).

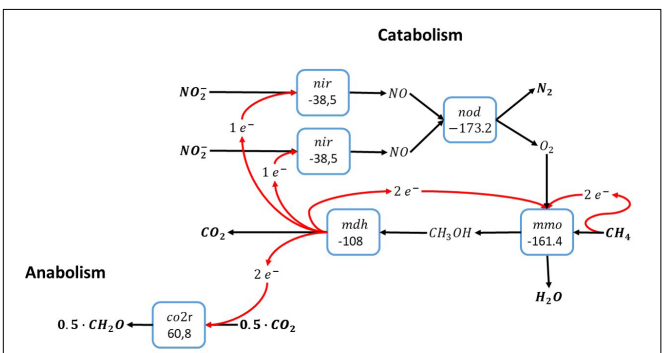

FIGURE 2 | Methane oxidation with nitrite as electron acceptor via anaerobic production of molecular oxygen (Raghoebarsing et al., 2006). The individual blocks represent enzymatic steps (*nod*, nitric oxide dismutase; *nir*, nitrite reductase; *mmo*, methane monooxygenase; *mdh*, methanol dehydrogenase *co2r*, CO_2 fixation); and the corresponding Gibbs free energy change ($\Delta G^{0'}$) of the reactions corrected for a pH of 7.

IS COMAMMOX A CYCLIC CONVERSION?

Until recently aerobic microbial ammonia oxidation to nitrate (nitrification) was regarded as a process catalyzed by two distinct groups of microorganisms that both take care of a distinct part of the process: ammonia oxidizing bacteria (or archaea) oxidize ammonia to nitrite, and nitrite oxidizing bacteria oxidize nitrite to nitrate. Both conversions are aerobic conversions. The reason why this pathway is segregated in two different types of microorganisms has been the topic of intense debate, but to date no convincing hypothesis has been proposed that explains the advantage of pathway segregation. It has been proposed that longer catabolic pathways provide a competitive advantage over short pathways in case of severe substrate limitation because it allows for maximization of the amount of energy that can be harvested per unit of substrate (i.e., ammonia). This maximization of the biomass yield strategy was proposed to enable the enrichment of complete ammonia oxidizing (comammox) microorganisms in case of slow growing substrate-limited systems such as biofilms (Costa et al., 2006).

Recently, convincing proof was presented that ammonia oxidation to nitrate is not necessarily catalyzed by a tandem of an ammonia oxidizer and a nitrite oxidizer, and specific *Nitrospira* species do have the capacity to oxidize ammonia to nitrate (Daims et al., 2015; van Kessel et al., 2015). *Nitrospira* are primarily known as aerobic chemolithoautotrophic nitrite oxidizing bacteria, with the capacity to conduct a number of other functions such as respiration of simple organic carbon molecules or hydrogen (Daims and Wagner, 2018).

Although comammox *Nitrospira* have been detected in a range of natural and engineered environments, their ecological role in many of these systems remains unclear (Daims et al., 2015; van Kessel et al., 2015; Palomo et al., 2016; Camejo et al., 2017; Xia et al., 2018; Li et al., 2019; Poghosyan et al., 2019; Cotto et al., 2020). Some of the first comammox bacteria were initially identified by van Kessel et al. (2015) in a bioreactor fed with effluent water from a recirculating aquaculture system, amended with low concentrations of ammonium, nitrite and nitrate. No molecular oxygen was supplied and therefore only oxygen traces in gases and medium supplied may have entered the bioreactor. Compared to oxygen, an overdose of oxidized nitrogen compounds (nitrite and nitrate) were supplied as electron acceptors to the system. Unfortunately, no mass balance

measurements are available for the nitrogen compounds in the process, so the quantitative ecological role of comammox *Nitrospira* spp. could not be identified. Still, the system described can be considered a strongly oxygen limited system.

Recent studies that aimed for *in situ* detection of comammox *Nitrospira* species have also observed them in significant numbers in systems that are characterized by localized oxygen limitation, such as biofilm systems (Roots et al., 2019). Furthermore, ammonium limitation and long solid retention times seem to favor enrichment of comammox (Kits et al., 2017; Cotto et al., 2020). Here, we focus on the observation by van Kessel at al. (2015) that comammox *Nitrospira* spp. were identified as dominant community members in a severely oxygen limited enrichment culture grown on a mixture of ammonium, nitrite, and nitrate.

Despite the oxygen limitation, comammox *Nitrospira* spp. constituted a considerable fraction of the biomass in this system. It is counterintuitive to assume that oxygen limitation provides a strong competitive advantage for comammox bacteria because the aerobic ammonia oxidation to nitrate *maximizes* oxygen uptake per mole of ammonium. At strongly oxygen limited conditions *minimization* of the stoichiometric needs for oxygen would provide the microorganisms involved with a competitive advantage. However, this would make the unique capacity of comammox to oxidize ammonia to nitrate nothing more than a coincidence. Thus, this raises the question why comammox has been found in this strongly oxygen limited ecosystem and suggests that there must be an intrinsic competitive advantage of having the full catabolic pathway for ammonia oxidation to nitrate.

Overall, it is proven that the specific *Nitrospira* species do have the capacity to catalyze the oxidation of ammonia to nitrate, but to which extent this is the metabolic trait that provides them with a competitive advantage over canonical aerobic autotrophic ammonia oxidisers that produce nitrite remains unclear. Below we will propose two cyclic ammonia oxidation processes that both require the microorganisms involved to possess the capacity to oxidize ammonia to nitrate, and that would be a satisfying explanation why some comammox bacteria have first been encountered in a strongly oxygen limited ecosystem.

SCENARIO 1: IS COMAMMOX FUNCTIONALLY EQUIVALENT TO ANAMMOX IN ANAEROBIC CONDITIONS?

The first pathway that may explain the in-situ activity of comammox bacteria (i) does not require externally supplied oxygen, and (ii) does require the full aerobic ammonia oxidation pathway to nitrate for sustaining the process. The conversion route proposed is based on a combination of the anammox process and the intra-oxic methane oxidation pathway with nitrite as electron acceptor as both described above.

An alternative pathway for the anammox catabolism as shown in **Figure 1** involves the use of reactive oxygen instead of NO for the activation of ammonia, as shown for methane oxidation in **Figure 2**. Molecular oxygen would be produced via nitric oxide dismutation as proposed for anaerobic methane oxidation by *Candidatus* Methylomirabilis oxyfera. As opposed to anaerobic methane oxidation, the catabolic reaction shown in **Figure 3** concerns a perfect cyclic conversion since two of the electrons gained upon oxidation of ammonia to nitrite (6 $emol/mol\ NH_4^+$) are required to reduce two nitrite to nitric oxide, with subsequent dismutation to dinitrogen gas and molecular oxygen, while the remaining four electrons would be required for the reduction of O_2 at the ammonia monooxygenase. The resulting catabolic reaction equals anammox catabolism described before.

The cyclic nature of this anammox-like catabolism via nitric oxide dismutase imposes the necessity of an alternative electron donor for reduction of carbon dioxide to organic biomass precursors, like in anammox. Ammonia cannot be used as electron donor due to the cyclic properties of this catabolism, and the only electron donor available in the autotrophic system is nitrite, which is oxidized to nitrate. As a consequence, the metabolism proposed here requires the biochemical machinery for ammonia oxidation to nitrite in the catabolic system, and nitrite oxidation to nitrate in the anabolic system. In absence of the full oxidation pathway of ammonia to nitrate, this metabolic system cannot exist. Functionally, the overall pathway proposed here is fully equivalent to anammox metabolism as originally described by Strous et al. (1999a).

With regard to the experiments conducted by van Kessel et al. (2015), the reaction proposed here can pose an alternative explanation for the observations in the ^{15}N-ammonium labeling experiments. Activity assays with anammox bacteria and a mixture of ^{15}N-labeled ammonium and unlabeled nitrite typically result in the production of $^{29}N_2$. However, upon partial ammonia oxidation to nitrite as shown in **Figure 3**, also $^{30}N_2$ will be produced, which is in line with the data shown in the paper. Contrastingly, the production $^{30}N_2$ using the comammox

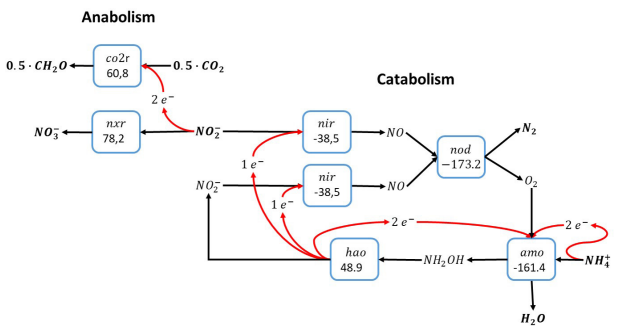

FIGURE 3 | Ammonia oxidation with nitrite as electron acceptor via intracellular production of molecular oxygen (Raghoebarsing et al., 2006). This overall reaction is equivalent to the anammox reaction as shown in **Figure 1**. The individual blocks represent enzymatic steps (*nod*, nitric oxide dismutase; *nir*, nitrite reductase; *amo*, ammonia monooxygenase; *hao*, hydroxylamine dehydrogenase; *nxr*, nitrite oxidoreductase; *co2r*, CO_2 fixation) and the corresponding Gibbs free energy change of the reactions corrected for a pH of 7 ($\Delta G^{0'}$).

metabolism is hard to understand if nitrate is produced from ammonia, since anammox is incapable of using nitrate as electron acceptor. However, the reaction requires the presence of a nitric oxide dismutase as has been proposed for *Ca*. M. oxyfera (Ettwig et al., 2010) that could thus far not be identified in any comammox *Nitrospira* genome.

SCENARIO 2: IS COMAMMOX CAPABLE OF AMMONIA OXIDATION WITH COMBINED USE OF OXYGEN AND NITRATE AS ELECTRON ACCEPTORS IN OXYGEN LIMITED CONDITIONS?

The second pathway we propose is based on the observation that these comammox bacteria have been identified in a system that, while characterized by severe oxygen limitation, might still have received minor amounts of oxygen (van Kessel et al., 2015).

It is counterintuitive that conditions of severe oxygen limitation would select for an ammonia oxidizing microorganism that requires *more* oxygen than canonical ammonia oxidation to nitrite. Under oxygen limiting conditions one would expect the occurrence of metabolic pathways that minimize oxygen requirements. The minimum amount of oxygen required per unit of ammonia evidently is one, due to the consumption of O_2 by the ammonia monooxygenase. Due to this four-electron reduction of oxygen, the oxidation of ammonia to nitrite yields two electrons per mole ammonia:

$$1 \cdot NH_4^+ + 1 \cdot O_2 \rightarrow 1 \cdot NO_2^- + 4 \cdot H^+ + 2 \cdot e^-$$
$$\triangle G^{0'} = -112.5\ kJ \cdot reaction^{-1}$$

Under aerobic conditions the electrons will be accepted by oxygen, but we propose that in case of oxygen limitation nitrate may serve as alternative electron acceptor, with the concomitant formation of nitrite:

$$1 \cdot NO_3^- + 2 \cdot H^+ + 2 \cdot e^- \rightarrow 1 \cdot NO_2^- + 1 \cdot H_2O$$
$$\triangle G^{0'} = -78.2\ kJ \cdot reaction^{-1}$$

Overall, this results in the conversion of ammonia with oxygen and nitrate, forming two nitrite in a so-called nitrite comproportionation reaction (**Figure 4**):

$$1 \cdot NH_4^+ + 1 \cdot O_2 + 1 \cdot NO_3^- \rightarrow 2 \cdot NO_2^- + 1 \cdot H_2O + 2 \cdot H^+$$
$$\triangle G^{0'} = -190.7\ kJ \cdot reaction^{-1}$$

This pathway implies that the nitrite oxidoreductase (*nxr*) is reversible: In case of severe oxygen limitation nitrate can be reduced to nitrite in order to minimize the oxygen requirements for ammonia oxidation. Importantly, this reversibility of the nitrite oxidoreductase has been demonstrated for *Nitrospira moscoviensis*, which was able to couple formate oxidation to nitrate reduction under anaerobic conditions (Koch et al., 2015). In case of oxygen excess, nitrite is oxidized to nitrate facilitating the complete conversion of ammonia to nitrate. As in this reaction scheme the oxidation of ammonia is not directly dependent on products formed during the electron accepting reaction as is the case in the intra-oxic pathway described above, the electrons from ammonia oxidation here can also directly be used for carbon dioxide reduction to biomass precursors.

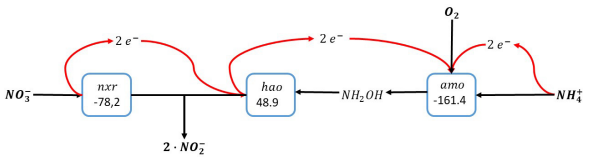

FIGURE 4 | Ammonia oxidation with combined use of oxygen and nitrate as electron acceptors. The individual blocks represent enzymatic steps (*nxr*, nitrite oxidoreductase; *amo*, ammonia monooxygenase; *hao*, hydroxylamine dehydrogenase), and the corresponding Gibbs free energy change ($\triangle G^{0'}$) of the reactions corrected for a pH of 7.

As described for the nitric oxide dismutase-based anammox-like pathway, the formation of $^{30}N_2$ from ^{15}N labeled ammonium as reported by van Kessel et al. (2015) can readily be explained by this pathway, as here the ^{15}N-labeled nitrite formed by comammox *Nitrospira* will serve as substrate for anammox.

DISCUSSION

Cyclic Conversions and the Microbial Nitrogen Cycle

The biochemistry-induced cyclic nature of some nitrogen conversions provides clear limits to the catalytic capacity observed in nature. Why anammox has been found only with nitrite as electron acceptor and not nitrate can readily be explained by the biochemistry of the anammox catabolism. Furthermore, also why anammox uses nitrite as electron donor in anabolism for carbon dioxide reduction to biomass is a direct resultant from the cyclic nature of anammox catabolism. Similarly, the biochemistry of anaerobic nitrite-dependent methane oxidation proposed for *Candidatus* Methylomirabilis oxyfera excludes the direct catabolic use of nitrate as electron acceptor for methane oxidation.

In this paper we have elaborated the consequences of the cyclic nature of nitrogen conversions on the potential ecological role of comammox *Nitrospira* under oxygen-limited conditions. Considering the biochemistry of the known nitrogen conversions, two alternative pathways are proposed to provide an ecological niche for comammox *Nitrospira*: an intra-oxic anammox-like metabolism using nitric oxide dismutase, or nitrite comproportionation, the oxidation of ammonia with both oxygen and nitrate as electron acceptors. Both pathways require the full enzymatic machinery for ammonia oxidation to nitrate in order to proceed, which adds to the plausibility of the pathways proposed. On the other hand, no direct evidence is available to date that either of the two pathways proposed actually occurs in microbial ecosystems, and no genomic evidence supports the existence of a nitric oxide dismutating enzyme system in *Nitrospira*. Furthermore, arguments related to the bioenergetic

growth efficiency and kinetic properties of the processes proposed that may determine ecological niches for specific conversions are excluded from the discussion (Gonzalez-Cabaleiro et al., 2019; Kreft et al., 2020).

Microbial Ecosystems Aim for Thermodynamic Equilibrium

In absence of severe gradients in time or space, one may speculate that microbial ecosystems aim for maximization of the amount of chemical energy that is harvested, provided that the adequate biochemistry is available to do so, and sufficient time is available for the microbes to establish. In other words, microbial ecosystems thrive for a thermodynamic state as close as possible to thermodynamic equilibrium. For example, in absence of external electron acceptors, organic carbon rich environments aim for the production of methane containing biogas because methane is the organic carbon with the lowest energy content per electron ($\triangle G_e^{0'}$) of all organic compounds (Kleerebezem and Van Loosdrecht, 2010). Full conversion of organic carbon to methane can therefore be regarded as the global thermodynamic optimum, whereas the production of intermediate compounds in the process represent local optima. If the thermodynamically most favorable solution for a specific ecosystem does not occur – such as the oxidation of ammonium with nitrate to dinitrogen gas - this implies that either the biochemistry to catalyze this overall reaction does not exist, or has not been discovered yet.

In an oxygen limited environment with non-limiting ammonium as well as oxidized nitrogen compounds (nitrite and nitrate) available, as described by van Kessel et al. (2015), the complete oxidation of ammonia to nitrate with oxygen would thermodynamically be one of the least favorable reactions to catalyze when normalized to one mole of oxygen:

$$0.5 \cdot NH_4^+ + 1 \cdot O_2 \rightarrow 0.5 \cdot NO_3^- + 0.5 \cdot H_2O + 1 \cdot H^+$$
$$\triangle G^{0'} = -174.5\ kJ \cdot mol\ O_2{}^{-1}$$

In comparison, the combined activity of aerobic ammonia oxidation to nitrite by for example *Nitrosomonas* spp. combined with the anammox reaction (**Figure 1**) provides a significantly higher Gibbs free energy yield:

$$1.33 \cdot NH_4^+ + 1 \cdot O_2 \rightarrow 0.67 \cdot N_2 + 1.33 \cdot H^+ + 2 \cdot H_2O$$
$$\triangle G^{0'} = -421.7\ kJ \cdot mol\ O_2{}^{-1}$$

Still, in the presence of nitrate in the medium, and assuming the conversion of part of the ammonium as proposed in Scenario 2 (**Figure 4**) combined with the oxygen independent anammox catabolism, the amount of energy that is harvested is much higher:

$$3 \cdot NH_4^+ + 1 \cdot O_2 + 1 \cdot NO_3^- \rightarrow 2 \cdot N_2 + 2 \cdot H^+ + 5 \cdot H_2O$$
$$\triangle G^{0'} = -916.3\ kJ \cdot reaction^{-1}$$

In an oxygen limited environment where nitrite, nitrate and non-limiting amounts of ammonium are available, maximization of the conversion of ammonium for the production of dinitrogen gas with all electron acceptors available is the global thermodynamic optimum of the reaction network. However, when assuming that no biochemistry for direct ammonium oxidation with nitrate to dinitrogen gas is available in nature, the process described in scenario 2 will maximize the Gibbs energy production per unit of oxygen supplied. Evidently, this provides no evidence that no other local thermodynamic optimum may prevail, but it is tempting to speculate and study to which extent nature and evolution are optimized with the objective to maximize energy production in mind.

Implications for Biofilms and Cell Aggregates

The potential existence of the metabolic pathways proposed here may shed new light on observations made with biofilm systems consisting of aerobic ammonia oxidizing bacteria in the outer layers of the biofilm, and anammox bacteria in the anaerobic core. In these biofilm systems *Nitrospira* is frequently encountered at the aerobic-anaerobic interface (Vlaeminck et al., 2010; Winkler et al., 2012). Traditionally, *Nitrospira* has been associated with aerobic nitrite oxidation to nitrate, and nitrate is not perceived to play a role in the overall conversion of ammonium to dinitrogen gas. Consequently, the appearance of *Nitrospira* in these systems is believed to negatively affect process performance, as it takes away nitrite from anammox and therewith decreases the nitrogen removal efficiency.

The catabolic reactions proposed here in scenarios 1 and 2 provide alternative, mechanistically plausible explanations for the occurrence of *Nitrospira* at the aerobic-anaerobic interface, assuming these have the enzymatic machinery for complete nitrification. According to scenario 1, oxygen may serve as intracellular intermediate in catalyzing anaerobic ammonia oxidation via nitric oxide dismutation, and scenario 2 proposes that at severe oxygen limitation, the use of nitrate besides oxygen in ammonia oxidation provides a competitive advantage over fully aerobic ammonia oxidation to nitrite. At more elevated oxygen concentrations closer to the bulk liquid in the biofilm, aerobic processes will prevail, whereas the anammox metabolism likely dominates at more reduced redox conditions in true absence of oxygen. It is furthermore plausible that when these biofilms are periodically exposed to elevated oxygen concentrations, the comammox *Nitrospira* in the system catalyze the full oxidation of ammonia to nitrate. However, these *Nitrospira* have the advantage that when they compete with canonical ammonia oxidizers for their substrate, they can also return to their core business, nitrite oxidation to nitrate. This may explain why the maximum nitrite oxidation capacity in these systems as determined at elevated dissolved oxygen concentrations usually is much higher than expected in these biofilm systems (Winkler et al., 2012).

In this manuscript we propose that the metabolic versatility of comammox *Nitrospira* spp. may be higher than described to date. The work of Kits et al. (2017) suggests that comammox *Nitrospira* spp. can in specific conditions be an effective competitor for two-step nitrification. In particular, the high affinity for ammonia together with the increased biomass

yield will provide a competitive advantage over canonical ammonia oxidizing microorganisms under conditions of severe ammonium limitation. To which extent severe oxygen limitation provides a similar ecological niche for full oxidation of ammonia to nitrate is unclear, but seems unlikely. Here, we describe that instead of catalyzing ammonia oxidation to nitrate, oxygen limitation may provide an ecological niche for a nitric oxide dismutation-driven anammox-like metabolism, or ammonia oxidation with the combined use of nitrate and oxygen as electron acceptors. Future experiments under oxygen limiting conditions will need to clarify if these conditions specifically enrich for comammox *Nitrospira*, and what their ecological niche is in these kinds of environments.

DATA AVAILABILITY STATEMENT

The original contributions presented in the study are included in the article/supplementary material, further inquiries can be directed to the corresponding author.

AUTHOR CONTRIBUTIONS

All authors listed have made a substantial, direct, and intellectual contribution to the work and approved it for publication.

FUNDING

This work was provided by the Dutch Research Council (NWO, Grant 016.Vidi.189.050) to SL.

ACKNOWLEDGMENTS

Maartje van Kessel, Julio Octavio Perez Cañestro, Tommaso Lotti, Gerben Stouten, Rebeca Gonzalez Cabaleiro, Dimitry Sorokin, Gijs Kuenen, and Mu-En Liu are gratefully acknowledged for numerous discussions on nitrogen cycle conversions.

REFERENCES

Arshad, A., Speth, D. R., de Graaf, R. M., Op den Camp,, Jetten, M. S., and Welte, C. U. (2015). A metagenomics-based metabolic model of nitrate-dependent anaerobic oxidation of methane by methanoperedens-like archaea. *Front. Microbiol.* 6:1423. doi: 10.3389/fmicb.2015.01423

Camejo, P. Y., Santo Domingo, J., McMahon, K. D., and Noguera, D. R. (2017). Genome-enabled insights into the eophysiology of the comammox bacterium "Candidatus Nitrospira nitrosa". *Msystems* 2:e00059-17.

Costa, E., Perez, J., and Kreft, J. U. (2006). Why is metabolic labour divided in nitrification? *Trends Microbiol.* 14, 213–219. doi: 10.1016/j.tim.2006.03.006

Cotto, I., Dai, Z., Huo, L., Anderson, C. L., Vilardi, K. J., Ijaz, U., et al. (2020). Long solids retention times and attached growth phase favor prevalence of comammox bacteria in nitrogen removal systems. *Water Res.* 169:115268. doi: 10.1016/j.watres.2019.115268

Daims, H., Lebedeva, E. V., Pjevac, P., Han, P., Herbold, C. W., Albertsen, M., et al. (2015). Complete nitrification by *Nitrospira bacteria*. *Nature* 528, 504–509. doi: 10.1038/nature16461

Daims, H., and Wagner, M. (2018). Nitrospira. *Trends Microbiol.* 26, 462–463.

Ettwig, K. F., Butler, M. K., Le Paslier, D., Pelletier, E., Mangenot, S., Kuypers, M. M., et al. (2010). Nitrite-driven anaerobic methane oxidation by oxygenic bacteria. *Nature* 464, 543–548.

Gonzalez-Cabaleiro, R., Curtis, T. P., and Ofiteru, I. D. (2019). Bioenergetics analysis of ammonia-oxidizing bacteria and the estimation of their maximum growth yield. *Water Res.* 154, 238–245. doi: 10.1016/j.watres.2019.01.054

Heijnen, J. J., and Kleerebezem, R. (2010). "Bioenergetics of microbial growth," in *Encyclopedia of Industrial Microbiology: Bioprocess, Bioseparation and Cell Technology*, ed. M. C. Flickinger (Hoboken, NJ: John Wiley & Sons, Inc), 594–617.

Hu, Z., Wessels, H., Van Alen, T., Jetten, M. S. M., and Kartal, B. (2019). Nitric oxide-dependent anaerobic ammonium oxidation. *Nat. Commun.* 10:1244.

Kartal, B., Maalcke, W. J., de Almeida, N. M., Cirpus, I., Gloerich, J., Geerts, W., et al. (2011). Molecular mechanism of anaerobic ammonium oxidation. *Nature* 479, 127–159.

Kartal, B., van Niftrik, L., Keltjens, J. T., Op den Camp, H. J., and Jetten, M. S. M. (2012). "Anammox-Growth physiology, cell biology, and metabolism, in advances," in *Microbial Physiology*, Vol. 60, ed. R. K. Poole (Burlington: Academic Press), 211–262. doi: 10.1016/b978-0-12-398264-3.00003-6

Kits, K. D., Sedlacek, C. J., Lebedeva, E. V., Han, P., Bulaev, A., Pjevac, P., et al. (2017). Kinetic analysis of a complete nitrifier reveals an oligotrophic lifestyle. *Nature* 549, 269–272. doi: 10.1038/nature23679

Kleerebezem, R., and Van Loosdrecht, M. C. M. (2010). A generalized method for thermodynamic state analysis of environmental systems. *Crit. Rev. Environ. Sci. Technol.* 40, 1–54. doi: 10.1080/10643380802000974

Koch, H., Lücker, S., Albertsen, M., Kitzinger, K., Herbold, C., Spieck, E., et al. (2015). Expanded metabolic versatility of ubiquitous nitrite-oxidizing bacteria from the genus *Nitrospira*. *Proc. Natl. Acad. Sci. U.S.A.* 112, 11371–11376. doi: 10.1073/pnas.1506533112

Kreft, J. U., Griffin, B. M., and Gonzalez-Cabaleiro, R. (2020). , Evolutionary causes and consequences of metabolic division of labour: why anaerobes do and aerobes don't. *Curr. Opin. Biotechnol.* 62, 80–87. doi: 10.1016/j.copbio.2019.08.008

Li, C. Y., Hu, H. W., Chen, Q. L., Chen, D., and He, J. Z. (2019). Comammox *Nitrospira* play an active role in nitrification of agricultural soils amended with nitrogen fertilizers. *Soil Biol. Biochem.* 138:107609. doi: 10.1016/j.soilbio.2019.107609

Palomo, A., Fowler, J., Gülay, A., Rasmussen, S., Sicheritz-Ponten, T., and Smets, B. F. (2016). Metagenomic analysis of rapid gravity sand filter microbial communities suggests novel physiology of *Nitrospira* spp. *ISME J.* 10, 2569–2581. doi: 10.1038/ismej.2016.63

Poghosyan, L., Koch, H., Lavy, A., Frank, J., van Kessel, M. A. H. J., Jetten, M. S. M., et al. (2019). Metagenomic recovery of two distinct comammox *Nitrospira* from the terrestrial subsurface. *Environ. Microbiol.* 21, 3627–3637. doi: 10.1111/1462-2920.14691

Raghoebarsing, A. A., Pol, A., van de Pas-Schoonen, K. T., Smolders, A. J., Ettwig, K. F., Rijpstra, W. I., et al. (2006). A microbial consortium couples anaerobic methane oxidation to denitrification. *Nature* 440, 918–921. doi: 10.1038/nature04617

Rasigraf, O., Kool, D. M., Jetten, M. S. M., Damste, J. S. S., and Ettwig, K. F. (2014). Autotrophic carbon dioxide fixation via the Calvin-Benson-Bassham cycle by the denitrifying methanotroph "*Candidatus* Methylomirabilis oxyfera". *Appl. Environ. Microbiol.* 80, 2451–2460. doi: 10.1128/AEM.04199-13

Roots, P., Yubo, W., Rosenthal, A., Griffin, J. S., Sabba, F., Petrovich, M., et al. (2019). Comammox *Nitrospira* are the dominant ammonia oxidizers in a mainstream low dissolved oxygen nitrification reactor. *Water Re.* 157, 396–405. doi: 10.1016/j.watres.2019.03.060

Simon, J., and Klotz, M. G. (2013). Diversity and evolution of bioenergetic systems involved in microbial nitrogen compound transformations. *Biochim. Biophy. Acta Bioenerg.* 1827, 114–135. doi: 10.1016/j.bbabio.2012.07.005

Strohm, T. O., Griffin, B., Zumft, W. G., and Schink, B. (2007). Growth yields in bacterial denitrification and nitrate ammonification. *Appl. Environ. Microbiol.* 73, 1420–1424. doi: 10.1128/aem.02508-06

Strous, M., Fuerst, J. A., Kramer, E. H., Logemann, S., Muyzer, G., van de Pas-Schoonen, K. T., et al. (1999a). Missing lithotroph identified as new planctomycete. *Nature* 400, 446–449. doi: 10.1038/22749

Strous, M., Kuenen, J. G., and Jetten, M. S. (1999b). Key physiology of anaerobic ammonium oxidation. *Appl. Environ. Microbiol.* 65, 3248–3250. doi: 10.1128/aem.65.7.3248-3250.1999

Stultiens, K., Cruz, S. G., Van Kessel, M. A. H. J., Jetten, M. S. M., Kartal, B., and Op den Camp, H. J. M. (2019). Interactions between anaerobic ammonium- and methane-oxidizing microorganisms in a laboratory-scale sequencing batch reactor. *Appl. Microbiol. Biotechnol.* 103, 6783–6795. doi: 10.1007/s00253-019-09976-9

van Kessel, M., Speth, D. R., Albertsen, M., Nielsen, P. H., Op den Camp, H. J., Kartal, B., et al. (2015). Complete nitrification by a single microorganism. *Nature* 528, 555–559. doi: 10.1038/nature16459

Vlaeminck, S. E., Terada, A., Smets, B. F., De Clippeleir, H., Schaubroeck, T., Bolca, S., et al. (2010). Aggregate size and architecture determine microbial activity balance for one-stage partial nitritation and anammox. *Appl. Environ. Microbiol.* 76, 900–909. doi: 10.1128/aem.02337-09

Welte, C. U., Rasigraf, O., Vaksmaa, A., Versantvoort, W., Arshad, A., Op den Camp, H. J., et al. (2016). Nitrate- and nitrite-dependent anaerobic oxidation of methane. *Environ. Microbiol. Rep.* 8, 941–955.

Winkler, M. K. H., Bassin, J. P., Kleerebezem, R., Sorokin, D., and Loosdrecht, M. (2012). Unravelling the reasons for disproportion in the ratio of AOB and NOB in aerobic granular sludge. *Appl. Microbiol. Biotechnol.* 94, 1657–1666. doi: 10.1007/s00253-012-4126-9

Xia, F., Wang, J. G., Zhu, T., Zou, B., Rhee, S. K., and Quan, Z. X. (2018). Ubiquity and diversity of complete ammonia oxidizers (Comammox). *Appl. Environ. Microbiol.* 84, e01390-18.

Conflict of Interest: The authors declare that the research was conducted in the absence of any commercial or financial relationships that could be construed as a potential conflict of interest.

frontiers in Microbiology

ORIGINAL RESEARCH
published: 12 July 2021
doi: 10.3389/fmicb.2021.671480

Nutrient-Limited Enrichments of Nitrifiers From Soil Yield Consortia of *Nitrosocosmicus*-Affiliated AOA and *Nitrospira*-Affiliated NOB

*Jonathan Rodriguez†, Seemanti Chakrabarti†, Eunkyung Choi, Nisreen Shehadeh, Samantha Sierra-Martinez, Jun Zhao and Willm Martens-Habbena**

Fort Lauderdale Research and Education Center, Department of Microbiology and Cell Science, University of Florida, Davie, FL, United States

OPEN ACCESS

Edited by:
Laura E. Lehtovirta-Morley, University of East Anglia, United Kingdom

Reviewed by:
Man-Young Jung, Jeju National University, South Korea
Sebastian Lücker, Radboud University, Netherlands

***Correspondence:**
Willm Martens-Habbena
w.martenshabbena@ufl.edu

† These authors have contributed equally to this work

Specialty section:
This article was submitted to Microbial Physiology and Metabolism, a section of the journal Frontiers in Microbiology

Received: *23 February 2021*
Accepted: *22 June 2021*
Published: *12 July 2021*

Citation:
Rodriguez J, Chakrabarti S, Choi E, Shehadeh N, Sierra-Martinez S, Zhao J and Martens-Habbena W (2021) Nutrient-Limited Enrichments of Nitrifiers From Soil Yield Consortia of Nitrosocosmicus-Affiliated AOA and Nitrospira-Affiliated NOB. Front. Microbiol. 12:671480. doi: 10.3389/fmicb.2021.671480

The discovery of ammonia-oxidizing archaea (AOA) and complete ammonia-oxidizing (comammox) bacteria widespread in terrestrial ecosystems indicates an important role of these organisms in terrestrial nitrification. Recent evidence indicated a higher ammonia affinity of comammox bacteria than of terrestrial AOA and ammonia-oxidizing bacteria (AOB), suggesting that comammox bacteria could potentially represent the most low-nutrient adapted nitrifiers in terrestrial systems. We hypothesized that a nutrient-limited enrichment strategy could exploit the differences in cellular kinetic properties and yield enrichments dominated by high affinity and high yield comammox bacteria. Using soil with a mixed community of AOA, AOB, and comammox *Nitrospira*, we compared performance of nutrient-limited chemostat enrichment with or without batch culture pre-enrichment in two different growth media without inhibitors or antibiotics. Monitoring of microbial community composition via 16S rRNA and *amoA* gene sequencing showed that batch enrichments were dominated by AOB, accompanied by low numbers of AOA and comammox *Nitrospira*. In contrast, nutrient-limited enrichment directly from soil, and nutrient-limited sub-cultivation of batch enrichments consistently yielded high enrichments of *Nitrosocosmicus*-affiliated AOA associated with multiple canonical nitrite-oxidizing *Nitrospira* strains, whereas AOB numbers dropped below 0.1% and comammox *Nitrospira* were lost completely. Our results reveal competitiveness of *Nitrosocosmicus* sp. under nutrient limitation, and a likely more complex or demanding ecological niche of soil comammox *Nitrospira* than simulated in our nutrient-limited chemostat experiments.

Keywords: nitrification, competition, nutrient limitation, ammonia-oxidizing bacteria, ammonia-oxidizing archaea, comammox, complete ammonia-oxidizing bacteria

INTRODUCTION

Nitrification, the microbial oxidation of ammonia via nitrite to nitrate, is a central process of the global nitrogen cycle and carried out by an increasingly complex network of bacteria and archaea. Ammonia oxidation, the first and often rate-limiting step of nitrification, is now known to be carried out by three distinct lithoautotrophic microbial groups including ammonia-oxidizing

archaea (AOA) within the archaeal phylum *Thaumarchaeota*, ammonia-oxidizing bacteria (AOB) within the beta- and gamma-subgroup of *Proteobacteria*, and complete ammonia-oxidizing (comammox) bacteria within the bacterial phylum *Nitrospirae* (Daims et al., 2016; Lawson and Lücker, 2018; Norton and Ouyang, 2019; Prosser et al., 2020). Furthermore, several heterotrophic proteobacterial and fungal taxa have been shown to oxidize ammonia (Prosser, 1989; Stein, 2011). Following more than a century of research primarily focusing on the then only known AOB, the discovery of AOA ubiquitous in marine and terrestrial environments, and comammox bacteria widespread in terrestrial ecosystems have vastly expanded the diversity of autotrophic ammonia oxidizers. These discoveries further raised new fundamental questions about the biology and ecology of ammonia oxidation, the distinct physiology, niche preferences, and specific activities of each group and the associated N_2O emissions (Könneke et al., 2005; Prosser and Nicol, 2008, 2012; Tourna et al., 2011; Daims et al., 2015; van Kessel et al., 2015; Kozlowski et al., 2016; Jung et al., 2019; Kits et al., 2019).

Important insights into distinct biological traits of AOA, AOB, and comammox nitrifiers have come from studies on genomes and metagenomes of available isolates, enrichments, and natural ecosystems enriched in ammonia oxidizers (e.g., Treusch et al., 2005; Walker et al., 2010; Bartossek et al., 2012; Stahl and de la Torre, 2012; Daims et al., 2015; Santoro et al., 2015, 2017; van Kessel et al., 2015; Kerou et al., 2016; Palomo et al., 2016, 2018; Sauder et al., 2017; Lawson and Lücker, 2018; Stein, 2019; Spasov et al., 2020). However, understanding of the genetic and physiological diversity of nitrifiers in complex systems such as soils and sediments is still limited due to the challenges associated with obtaining high quality draft genomes or genomic inventories of nitrifiers (e.g., Orellana et al., 2018; Kerou et al., 2021). Furthermore, many important biological traits of ammonia oxidizers, such as kinetic properties, adaptation and response to changing environmental conditions (e.g., pH, temperature, oxygen, organic matter), and maybe most significantly their metabolism of nitric oxide (NO) and nitrous oxide (N_2O), cannot be deducted from genomic sequences alone (Walker et al., 2010; Stahl and de la Torre, 2012; Martens-Habbena et al., 2015; Kozlowski et al., 2016; Lehtovirta-Morley, 2018). Hence, there remains a need for relevant model organisms and integrated physiological studies to inform these complex biological traits and improve interpretation of genetic inventories of nitrifiers (Stahl and de la Torre, 2012; Lehtovirta-Morley, 2018; Stein, 2019; Prosser et al., 2020).

Existing cultivation techniques used to enrich, isolate and study ammonia oxidizers yielded AOB, likely for a combination of reasons including ammonia toxicity, unmatched trace metal requirements or toxicity, pH and temperature adaptation, symbiotic dependencies, such as vitamin and antioxidant requirements (Bollmann et al., 2011; Qin et al., 2014). The recent discoveries of novel nitrifying organisms have benefited from more detailed knowledge of organismal inventories based on molecular studies and also relied on innovative approaches to enrich nitrifiers. For example, the isolation of the first ammonia-oxidizing archaeon, *Nitrosopumilus maritimus* SCM1, came from a marine aquarium devoid of known AOB, spurring the search for novel ammonia oxidizers and enabling systematic variation of cultivation conditions for optimization of ammonia oxidation in the absence of AOB (Könneke et al., 2005; Stahl and de la Torre, 2012; Stahl, 2020). These efforts resulted in identification of the archaeon as the causative agent, and subsequent isolation of strain SCM1 after treatment of the enrichment with bacterial antibiotics (Könneke et al., 2005). Enrichment and isolation of other AOA strains directly from coastal and open ocean seawater and soil also required innovative techniques such as pre-enrichment in original sample water, addition of antioxidants, and application of various antibiotics for enrichment of AOA (e.g., Santoro and Casciotti, 2011; Tourna et al., 2011; French et al., 2012; Qin et al., 2014; Jung et al., 2016). Similarly, the enrichment and isolation of *Ca.* Nitrospira inopinata from the biofilm of a water production pipe of an abandoned oil exploration well at 56°C, was above the growth range of known canonical AOB, facilitating enrichment of the novel organism (Daims et al., 2015). Similarly, *Ca.* Nitrospira nitrosa and *Ca.* Nitrospira nitrificans, two comammox *Nitrospira* species, were successfully enriched along with anammox bacteria from the anaerobic compartment of a trickling filter in a recirculation aquaculture system at low oxygen (3.1 μM), and the enrichment was shown to be devoid of canonical AOB or AOA (van Kessel et al., 2015). However, a vast diversity of ammonia oxidizers inhabit environments where different groups of ammonia oxidizers compete or coexist (e.g., soils, sediments, lakes). Strains representative of the predominant lineages and ecotypes from such environments are still scarce, but are vital to study the adaptations of nitrifiers to these environments and to the competition and coexistence of nitrifiers within the complex ecosystems (Lehtovirta-Morley, 2018; Stein, 2019). Thus, further efforts are needed to improve cultivation success of representative strains.

Kinetic studies on several AOA and *Ca.* N. inopinata indicate that many AOA and comammox bacteria exhibit low apparent half saturation constants [$K_{m(app)}$] for ammonia (Martens-Habbena et al., 2009; Jung et al., 2011; Kits et al., 2017; Straka et al., 2019; Sakoula et al., 2020). Some strains additionally exhibit high specific substrate affinities and thus appear well-adapted to low substrate concentrations (Martens-Habbena et al., 2009; Jung et al., 2011; Kits et al., 2017; Sakoula et al., 2020). However, Kits et al. (2017) found that *Nitrososphaera*-related AOA and AOB from soil may possess rather similar kinetic properties. This raises the question whether kinetic properties are not a significant selective factor for nitrifiers in soils, or if the ammonia concentrations used during the original enrichments may have selected for less oligotrophic and more ammonia tolerant strains. We therefore aimed to test the hypothesis that a nutrient-limited enrichment strategy could yield novel oligotrophic ammonia oxidizers from terrestrial environments harboring mixed assemblages of AOA, AOB, and comammox bacteria. Using soil samples from highly active agricultural soils with a mixed assemblage of nitrifiers we highly enriched a new AOA strain in nutrient-limited continuous culture setups and a new AOB strain in batch cultures. However, only a weak enrichment of a comammox strain predominant in the soil was obtained in batch culture enrichments.

MATERIALS AND METHODS

Soil Physicochemical Analyses

Soil samples for enrichment of nitrifiers were collected in August 2017 and April 2018 from a histosol soil in the Everglades Agricultural Area in South Florida. In a previous study we found that this soil harbors an AOA-dominated community of nitrifiers that also contains AOB and comammox bacteria (Huang et al., 2021). Concentrations of NH_4^+-N and NO_3^--N were determined colorimetrically after extraction with 2M KCl. Briefly, 5 g wet soil was extracted with 45 ml of 2 M KCl solution by shaking for 1 h at 50 rpm. Samples were centrifuged for 10 min at 3,000 *g* and 10 ml supernatant was filtered through a 0.45 μm Nylon filter and refrigerated until analysis within 1–5 days. Ammonium, nitrite and nitrate were determined colorimetrically as described below. Soil pH was determined in a slurry of 1:2 (*w/v*) ratio of soil and deionized water.

Batch Culture Enrichments

After return to the laboratory in August 2017 batch enrichment cultures were established by adding 0.5 g of field-moist soil to 50 ml of synthetic freshwater media (SFCM) in 250 ml Pyrex glass bottles. The bottles were tightly closed and incubated at 28°C in the dark without shaking. The SFCM media contained (per 1 l) 1.0 g NaCl, 0.4 g $MgCl_2.6\ H_2O$, 0.1 g $CaCl_2.2\ H_2O$ and 0.5 g KCl (de la Torre et al., 2008). After autoclaving the media was cooled to room temperature and supplemented with the following sterile stock solutions (per 1.0 l): 2.0 ml $NaHCO_3$ (84 g l^{-1}), 5.0 ml KH_2PO_4 (0.4 g l^{-1}), 1.0 ml FeNaEDTA (2.75 g l^{-1}), 1.0 ml modified non-chelated trace element solution (Martens-Habbena et al., 2009). If not otherwise mentioned the medium was supplemented with 0.5 ml of NH_4Cl (1.0 M) per 1.0 l medium. The pH of this medium at room temperature was ∼7.5.

Enrichment cultures were monitored for ammonia consumption and nitrite production and transferred to fresh media with 1% inoculum once 70–80% of the ammonia was consumed. Following twelve consecutive transfers over ∼ 6-month period the ammonium concentration was reduced to 300 μM, and following another 6 months of consecutive 1% transfers (equivalent to a 10^{58} final dilution of the original soil sample), one culture (batch enrichment culture 9) was selected and scaled up from 50 to 400 ml volume sufficient for DNA extraction (see below).

Bioreactor Enrichments

In order to test the effect of nutrient limitation on the enrichment of nitrifiers, we established three continuous cultures in 3-l bioreactors (New Brunswick Scientific Bioflo 110) with 1.0 l working volume. Reactor A (**Figure 1A**) was established directly from the April 2018 soil sample, and reactors B and C were established from the scaled-up batch enrichment culture 9 described above. The soil sample (4.0 g) was mixed with 40 ml of SFCM media (see above), vortexed vigorously for 3 min to remove cells from soil particles and centrifuged at 300 *g* to remove coarse soil particles. A 5 ml volume of the soil-free sample was then directly introduced into the bioreactor vessel

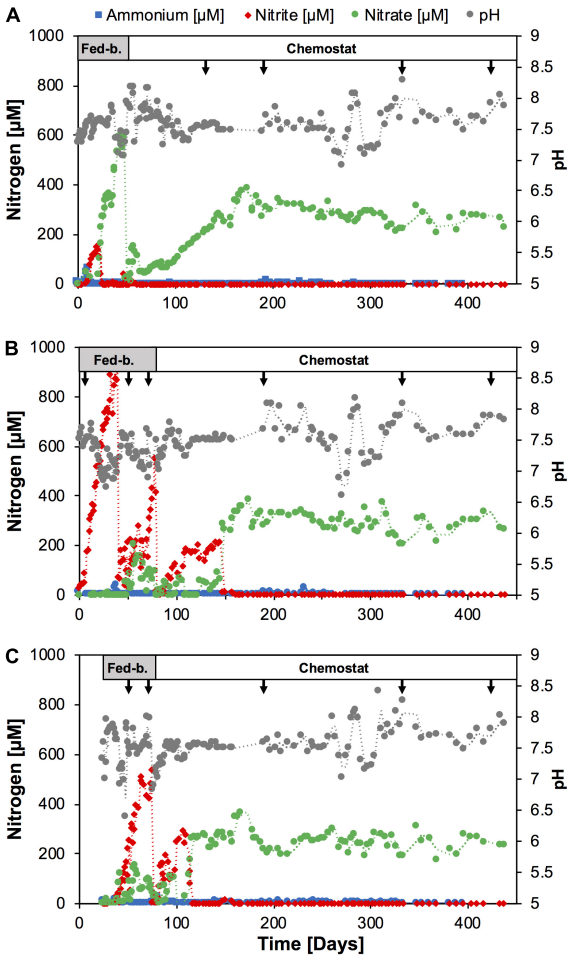

FIGURE 1 | Time course of nutrients and pH during continuous culture enrichments of nitrifiers directly from soil with SFCM media in reactor A **(A)**, and following batch culture pre-enrichment, in SFCM media in reactor B **(B)** and modified NGM media in reactor C **(C)**, respectively. Arrows indicate sampling points for amplicon sequencing analysis. Reactor operation modes are indicated on top. Fed-b., Fed-batch mode; Chemostat, chemostat mode. See **Supplementary Figure 1** for nutrient and pH time course in subculture chemostat reactors.

with 1.0 l working volume of ammonium-free SFCM media (see above) buffered with 20 mM $NaHCO_3$. The reactor feed was composed of the same media amended with 1 mM NH_4Cl (fed-batch period) and subsequently reduced to 0.3 mM (chemostat mode). The reactor was temperature-controlled at 28°C and stirred at 50 rpm. For pH balance and to avoid atmospheric contaminations the reactor was operated under synthetic air headspace (5% CO_2, 95% synthetic air). It was operated in fed-batch mode for the first approximately 40 days. During the first 2 weeks after start-up, the feeding rate was slowly raised from ∼1.5 ml per day to 30 ml per day and maintained at 30 ml per day for approximately 25 days. Once the volume exceeded 2.0 l culture liquid was pumped out to reduce the working volume back to 1.0 l. At a NO_3^- concentration of ∼600 μM the reactor was switched to chemostat mode and operated continuously for

the following 400 days with a 0.3 mM NH_4Cl feed concentration. From Day 41 to Day 120 the feeding rate was slowly raised from 30.0 ml per day (33 days hydraulic retention time) to 200 ml per day (5 days hydraulic time) and remained constant thereafter.

Reactors B and C (**Figures 1B,C**) were established from 5 ml inoculum of batch enrichment culture (see above) in 1.0 l ammonium-free SFCM media and 1.0 l ammonium-free modified NGM media (Sauder et al., 2017), respectively. The modified NGM media was prepared as follows: 50 ml of a 20x basal salt solution (11.68 g NaCl, 3.0 g $CaCl_2.2H_2O$, 1.5 g KCl, 1.0 g $MgSO_4.7H_2O$ per 1.0 l) were added to 930 ml MilliQ water, autoclaved, and cooled to room temperature. The media was supplemented with the following sterile stock solutions (per 1.0 l): 20 ml $NaHCO_3$ (84 g l^1), 5.0 ml KH_2PO_4 (0.4 g l^{-1}), 1.0 ml FeNaEDTA (2.75 g l^{-1}), 1.0 ml trace element solution (Daims et al., 2015). The final pH of this medium at room temperature was ∼7.5. The feed media for both reactors was initially supplemented with 1.0 mM NH_4Cl (fed-batch period) and 0.3 mM NH_4Cl (chemostat period) and both reactors were operated at 28°C with 50 rpm stirring and synthetic air headspace (5% CO_2, 95% synthetic air). Both reactors were operated in fed-batch mode and the feeding rate was raised from 1.5 ml per day to approximately 50 ml per day and 30 ml per day for reactors B and C, respectively. Similar to reactor A, liquid was pumped out to reduce the working volume back to 1.0 l once the volume exceeded 2.0 l in reactors B and C, respectively. The reactors were switched to chemostat mode at Day 78 and Day 74, respectively. Subsequently, both reactors B and C were operated in chemostat mode continuously for the following ∼380 days. The feeding rate was slowly raised to 200 ml per day (5 days hydraulic retention time) until Day 173 and Day 131 in reactor B and C, respectively, and remained constant thereafter.

To test whether higher enrichments could be obtained through either more frequent transfers to fresh reactors, increased NH_4Cl feed concentration, or reduction of organic carbon through removal of EDTA from the Fe-trace metal solution, three consecutive nutrient-limited subculture reactors were run with shorter operation times using the same general operation conditions and feeding rate of 200 ml per day (5-day hydraulic retention time). The first subculture reactors (subculture 1) were set up with 100 ml culture liquid from reactor A, B, and C, respectively. In subculture reactors A and B the feed NH_4Cl concentration was raised to 1.0 mM after 48 days of operation. After approximately 80 days, 800 ml inoculum of subculture 1 were transferred to subculture 2, again operated for approximately 80 days, and subsequently 100 ml inoculum of subculture 2 was used to establish subculture 3. For subcultures 3, the NH_4Cl feed concentration was further raised to 1.8 mM and FeEDTA was replaced with $FeSO_4$ as iron source at the same concentration. From reactor C only one subculture reactor was set up and run for 120 days and the ammonium feed concentration was maintained at 0.3 mM. Samples for DNA isolation and amplicon sequencing were taken before each sub-cultivation.

Samples for nutrient analyses were collected 2–3 times per week (reactors A, B, C) or 1–2 times per week (subculture reactors) and analyzed as described below. Samples for microbial community analysis were collected at time points indicated in **Figure 1** and **Supplementary Figure 1**. Before sampling for DNA sequencing, reactor outflow was stopped to allow accumulation of culture volume to approximately 2 l, with the exception of reactor B at Day 7, when just 200 ml culture sample was taken from the reactor. Glass surfaces were scraped with a silicon spatula to loosen biofilm if present. Then 1-l samples from each reactor were collected in Pyrex bottles for DNA isolation and cells were harvested by filtration onto Sterivex filters (Urakawa et al., 2010). DNA was isolated using the procedure described by Griffiths et al. (2000) with modifications described by Nicol et al. (Nicol and Prosser, 2011).

In order to isolate the predominant AOA strain, duplicate batch cultures were set up with 1–10% inoculum from reactor A or subculture reactor 1A in 250-ml Pyrex glass bottles using 50 ml SFCM media (as described above) with either 50 μM or 1.0 mM NH_4Cl and either of the following antibiotics: streptomycin (50 μg/ml final concentration), kanamycin (50 μg/ml), ampicillin (50 μg/ml), ciprofloxacin (10 μg/ml), azithromycin (10 μg/ml), lincomycin (50 μg/ml), as well as duplicate uninhibited controls. Growth was assessed over a 4-week period by ammonium consumption (50 μM NH_4Cl cultures) or nitrite and nitrate formation (1.0 mM NH_4Cl cultures) relative to uninhibited controls. In additional experiments, the antibiotic treatments were combined with supplementation of either sodium pyruvate, α-ketoglutarate, or malic acid (100 μM final concentration).

Analytical Methods

Ammonium and nitrite concentrations in batch and bioreactor samples and KCl extracts of soil samples were determined using the salicylate-trichloroisocyanuric acid method (Bower and Holm-Hansen, 1980) and sulfanilamide-NED method (Grasshoff et al., 1999), respectively. For accurate determination of ammonium in the bioreactor samples, the pH of the alkaline trichloroisocyanuric acid reagent was adjusted to compensate for the 20 mM bicarbonate buffer in the reactor media without having to dilute the reactor samples. Nitrate concentrations were determined using the method by García-Robledo et al. (2014). Briefly, 150 μL VCl_3 reagent (2% w/v VCl_3 in 6.0 M HCl) and 1.0 ml sample were combined in 1.5 ml reaction tubes, mixed, and incubated at 60°C for exactly 100 min. Combined NO_2^- and NO_3^- were subsequently determined colorimetrically using the modified sulfanilamide-NED reagent as described (García-Robledo et al., 2014).

amoA Gene Sequence Analyses

Gene fragments of target *amoA* were PCR-amplified using previously described primers for archaeal *amoA* (Tourna et al., 2008), bacterial *amoA* (Rotthauwe et al., 1997), and comammox *amoA* (Pjevac et al., 2017). PCR reactions (25 μl) contained 12.5 μl of GoTaq PCR Master Mix (Promega, Fitchburg, WI, United States), 1 μl each of forward and reverse primer (0.5 μM final concentration for archaeal and bacterial *amoA*, 0.25 μM final concentration of each forward primer comaA-244f_a-f and reverse primer comaA-659r_a-f for comammox *amoA*) and 2 μl of DNA template (∼5 ng/μl). PCR cycling conditions were as follows: Initial denaturation at 94°C for 5 min, followed by 30

cycles of denaturation at 94°C for 30 s, annealing at 52°C (53°C for comammox *amoA*) for 30 s, and primer extension at 72°C for 45 s, followed by 10 min final extension at 72°C.

PCR products were purified using Qiagen PCR purification kit (Qiagen, MD, United States) and sequenced by Sanger sequencing at Eurofins Genomics (Huntsville, AL, United States). Sequences were manually quality-checked and imported into ARB (Ludwig et al., 2004). For analysis of comammox *amoA* sequences an ARB-formatted alignment provided by Pjevac et al. (2017) was used and amended with additional sequences from GenBank and the present study. Sequences were aligned and maximum likelihood phylogenetic trees were calculated based on 595, 453, and 383 nucleotide positions for archaeal, bacterial, and comammox *amoA*, respectively, using the RAxML program with GTRGAMMA-25 rate distribution model and rapid hill climbing algorithm.

High-Throughput Amplicon Sequencing of 16S rRNA Genes

The workflow for 16S rRNA gene amplicon sequence analysis followed Earth Microbiome Project standard protocols (Thompson et al., 2017). Briefly, the V4 region of the 16S rRNA gene was amplified using primers 515F (Parada et al., 2016) and 926R (Quince et al., 2011). The forward primer included sequencing adapter sequences and the reverse primer contained the twelve base barcode sequence. PCR reactions consisted of 9.5 μl DNA-Free PCR Water (MoBio, Carlsbad, CA, United States), 12.5 μl 2x AccuStart II PCR ToughMix (Quantabio, Beverly, MA, United States), 1.0 μl 200 pM forward primer, 200 pM Golay barcode-tagged reverse primer, and 1.0 μl template DNA. All PCR template DNA was normalized to ∼20 ng/μl. PCR cycling conditions were: denaturation at 94°C for 3 min, 35 cycles at 94°C for 45 s, 50°C for 60 s, and 72°C for 90 s; and a final extension step of 10 min at 72°C. PCR products were quantified using PicoGreen (Invitrogen, Carlsbad, CA, United States) in a 96 well microplate reader (Infinite 200 PRO, Tecan, Grödig, Austria) and pooled in equimolar amounts, purified using AMPure XP Beads (Beckman Coulter, Brea, CA, United States), quantified by Qubit DNA quantification kit (Invitrogen, Carlsbad, CA, United States), diluted to 2 nM and denatured. Samples were then diluted to final concentration of 6.75 pM with a 10% PhiX spike. The libraries were sequenced on a Illumina MiSeq instrument or a Illumina NovaSeq instrument. PCR amplifications, library preparations and MiSeq DNA sequencing were conducted either at the Environmental Sample Preparation and Sequencing Facility (ESPSF) at Argonne National Laboratory or Novogene, Sacramento, CA, United States.

Amplicon sequences were demultiplexed on the instrument. The command line interface of the QIIME 2 package was used for downstream analyses (Bolyen et al., 2019). DADA2 (Callahan et al., 2016) was used with default settings for quality trimming, denoising and chimera removal and to generate amplicon sequence variants (ASVs). On average 32,164 high quality sequences were obtained per sample, with exception of reactor B (Day 89) and reactor C subculture 1 that had the lowest coverages with 1,822 and 2,553 high quality sequences, respectively. After removing ASVs with less than 4 sequences in at least one sample a total of 2,724 ASVs were identified among all samples. Taxonomic assignments were added to ASVs using the Qiime feature-classifier with sklearn algorithm against the Silva database version 132 (Quast et al., 2012). Sequences of mitochondria and chloroplasts were removed. Sequences of ASVs affiliated with known genera of archaeal and bacterial nitrifiers were imported into ARB and manually aligned. Backbone phylogenetic trees were calculated with near full-length 16S rRNA gene sequences using the accelerated maximum-likelihood method with positional variability filters for *Archaea*, *Betaproteobacteria*, and *Nitrospira*, respectively, and ASV sequences were inserted using the "add sequences using parsimony" option in ARB with the same filters and *Escherichia coli* position limits 534 and 906. Diversity metrics including Shannon Index and Observed_OTUs were calculated using the "qiime diversity core-metrics-phylogenetic" function in Qiime 2 after rarefaction to 1,200 sequences.

RESULTS

In this study we employed two complementary strategies for enrichment of nitrifiers at low substrate concentrations from a highly fertile, unfertilized agricultural soil. We previously found this soil to contain between 1×10^8 and 5×10^8 archaeal *amoA* genes g^{-1} soil and between 1×10^6 and 5×10^6 bacterial and comammox *amoA* genes g^{-1} soil, respectively (Huang et al., 2021). The physicochemical properties of the soil samples were as follows: The pH was 7.3, the concentrations of NH_4^+-N ranged between 5.6 and 8.6 μg N g^{-1} dry soil and NO_3^--N ranged between 43.8 and 116.1 μg N g^{-1} dry soil, respectively.

High throughput sequencing of 16S rRNA gene from April 2018 confirmed our previous results, showing that AOA dominated over bacterial nitrifiers in this soil. In total 4.4% of all 16S rRNA gene sequences belonged to nitrifiers (i.e., AOA, AOB, and *Nitrospira*), of which 90.1% were affiliated with AOA and 9.9% with *Nitrospira*. Similar to our previous study, AOB-affiliated 16S rRNA gene sequences were not detected. AOA-affiliated sequences were dominated by 6 ASVs with proportion of 0.1–2.1%, and the ASV representing the most abundant AOA were assigned to an uncultivated *Nitrososphaera* sister group (NS-δ; **Figures 2**, **3**).

For enrichments we used a basal media composition conducive to cultivation of AOB and AOA (Martens-Habbena et al., 2015). Batch enrichments were carried out initially at 500 μM NH_4Cl, sufficient to allow for growth of AOA, AOB and comammox based on available kinetic data. Out of 10 different enrichments monitored over a 6-month period, 9 enrichments yielded stable nitrite production within 1–2 month. Following repeated approximately bi-weekly transfers over a 6-month period, nitrite accumulation and microscopic analysis suggested similar composition and nitrifying activities in most of the batch cultures. Therefore, one culture (batch enrichment 9) was selected and characterized in detail after additional twelve consecutive 1% transfers over ∼ 6-month period (equivalent

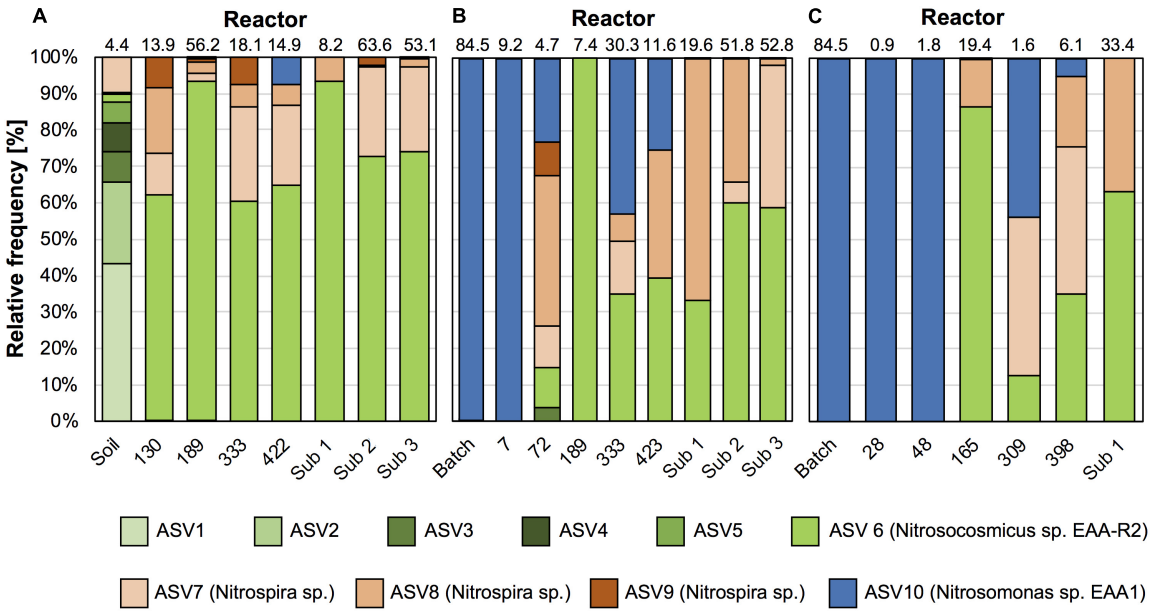

FIGURE 2 | Time series of nitrifier community composition in reactors **A**, **B**, and **C**. Given are relative frequency of 16S rRNA genes affiliated with thaumarchaeal AOA (green), betaproteobacterial AOB (blue), and *Nitrospira* sp. (beige) of all nitrifier-associated sequences. Numbers on top indicate relative abundance of nitrifiers in each whole community sample in%. Sub 1, Sub 2, and Sub 3 refer to sub-culture reactors 1, 2 and 3, respectively.

to a 10^{-58} final dilution of the original soil sample). PCR analysis revealed presence of archaeal, bacterial and comammox *amoA* genes and sequencing of purified PCR products revealed unique and unambiguous *amoA* gene sequences for all three groups (**Figures 3A**, **4A**, **5A**), suggesting dominance of a single *amoA* type of each group in the enrichment. Intriguingly, the AOA *amoA* gene sequence in the batch enrichment was closely related to an AOA phylotype (EAA soil OTU26) within the uncultivated soil *Nitrososphaera*-sister group (NS-δ), previously shown to be frequent in this soil (**Figure 3A**; Huang et al., 2021). The AOB *amoA* sequence in the batch enrichment affiliated with the *Nitrosomonas* sp. Nm173 lineage which we did not previously observe in this soil, and which has not been described in detail. The comammox *amoA* sequence was affiliated with the most frequent comammox *amoA* sequence type previously found in the soil (EAA soil OTU11, **Figure 4A**). Together, these data suggested that environmentally relevant AOA and comammox *Nitrospira* strains were maintained in this culture for more than 1 year. Analysis of 16S rRNA gene amplicons showed that the batch enrichment was highly dominated by the *Nitrosomonas* Nm173-affiliated strain (84.5%) and neither archaeal or comammox ammonia oxidizers, or canonical nitrite oxidizers were detectable in the amplicon dataset (**Figure 2**).

Therefore, we tested in 1.0-l scale bioreactors whether nutrient limited growth conditions would bias the enrichment toward comammox or AOA, or whether the *Nitrosomonas* strain would indeed continue to outcompete other ammonia oxidizers. We seeded one reactor directly with soil biomass (reactor A, **Figures 1A**, **2A**) and two reactors with 5.0 ml inoculum of the batch enrichment 9 using either SFCM medium (reactor B), or a modified NGM medium, similar to that used previously for the isolation of *Ca.* N. inopinata (reactor C). All reactors were initially operated in fed-batch mode and then switched to chemostat mode after stable nitrite or nitrate production was observed (**Figure 1**). Ammonium concentrations remained below 1 μM in all three reactors for the entire operation time with only few exceptions, indicating high specific ammonia oxidation activities at sub-micromolar substrate concentrations (**Figure 1**). In reactor A nitrite initially accumulated for approximately 20 days, before nitrate became the sole detected nitrification product. Reactors B and C seeded with enrichment culture biomass rapidly produced nitrite over the first 20–40 days. Intriguingly, both reactors B and C also began to produce nitrate at day 48 and day 30, respectively, although no nitrate production had been observed in the batch enrichment culture itself. In order to test whether higher ammonium feed concentrations and more frequent sub-cultivation could yield higher relative enrichment of nitrifiers, reactors A and B were sequentially sub-cultivated three times (subculture 1–3, **Supplementary Figure 1**) and ammonium feed concentration was first raised to 1.0 mM (subculture 1) and later to 1.8 mM (subculture 3). Additionally, reactor C was sub-cultured once at the original ammonium feed level. In each of the subculture reactors ammonium was detectable only directly after seeding the reactors, and subsequently fell below 1 μM. Nitrite was only detected at the beginning of subculture B1. As expected, nitrate was the main product and after raising feed concentrations increased as expected to ∼1 mM in subcultures A1 and B2, and ∼1.8 mM in A3 and B3, respectively.

Monitoring of the community composition in all three reactors over approximately 400-day operation, as well as in sub-culture reactors revealed selection for a single *Nitrosocosmicus*-affiliated ASV (ASV 6) in all three reactor sets. Reactor A seeded

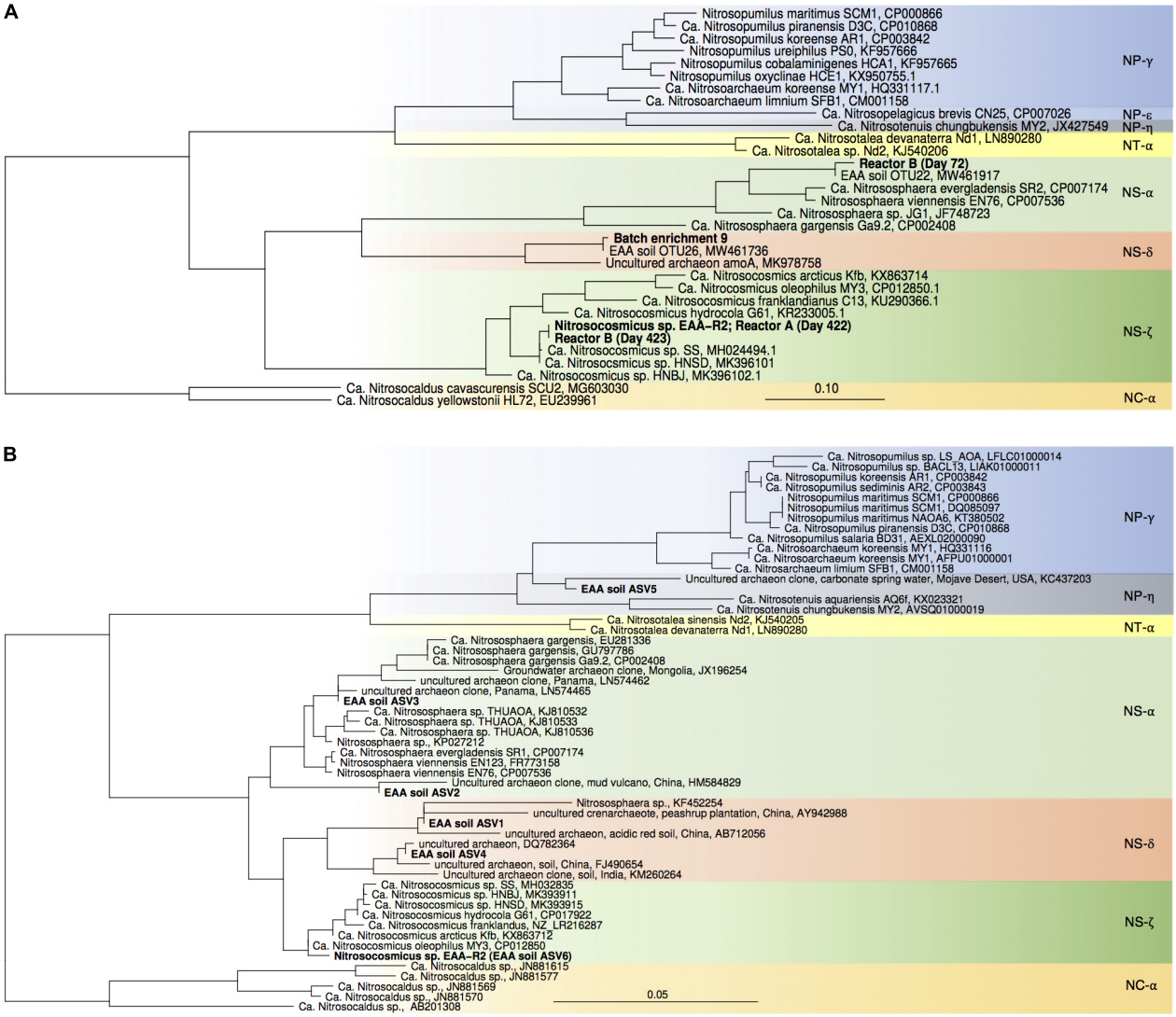

FIGURE 3 | Maximum-likelihood phylogenetic trees of archaeal *amoA* gene sequences **(A)** and thaumarchaeal 16S rRNA gene sequences **(B)**. Sequences obtained in this study are highlighted in bold. *Nitrosocaldus* sp.-associated sequences were used as outgroup. Color codes refer to archaeal lineages (after Alves et al., 2018).

with microbial biomass directly from soil was dominated by this ASV from the first sampling point at Day 130 until the third sub-culture, accounting for 60.6% and 93.3% of all nitrifier-affiliated sequences (**Figures 2**, **3B**). This AOA type was accompanied by three distinct *Nitrospira* strains (ASV 7–9) with proportions between 0.3 and 25.6% of all nitrifier-affiliated sequences in reactor A. Intriguingly, ASV 7 represented the most frequent *Nitrospira* sp. sequence type found in the soil (**Figures 2**, **4B**), and it remained the dominant *Nitrospira* sequence type in reactor A and subsequent sub-culture reactors.

In reactors B and C, seeded with enrichment culture 9, the *Nitrosomonas* strain (ASV 10) remained predominant during the initial fed-batch operation stage irrespective of growth media used (SFCM vs. NGM in reactor B and C, respectively). However, after onset of chemostat operation, its relative abundance dropped below 0.1% after 189 and 165 days in both reactors B and C, respectively (**Figures 2**, **5B**). Concomitantly, the *Nitrosocosmicus* strain (ASV 6) and *Nitrospira* strains (ASV 7–9) rose in relative abundance from Day 72 and thereafter in reactor B, and Day 165 and thereafter in reactor C. However, *Nitrospira* ASV 9 was absent in reactor C. It remains unclear why the *Nitrospira* sp. (ASV 7–9) were below 0.1% at Day 189 in Reactor B, while steady nitrate production was evident during this period.

Notably, *Nitrosomonas* (ASV 10) became significant again at days 333 and 423 in reactor B, and days 309 and 398 in reactor C, respectively, as well as day 422 of operation of reactor A (**Figure 2**). In reactor A it declined again below the detection limit, however, in reactor B and C it remained present. Only in the subculture reactors it was not detected. Although we can only speculate about the reasons for this, pH values fluctuated due to interruption of headspace CO_2 flow over an approximately 2-month period between approximately days 200

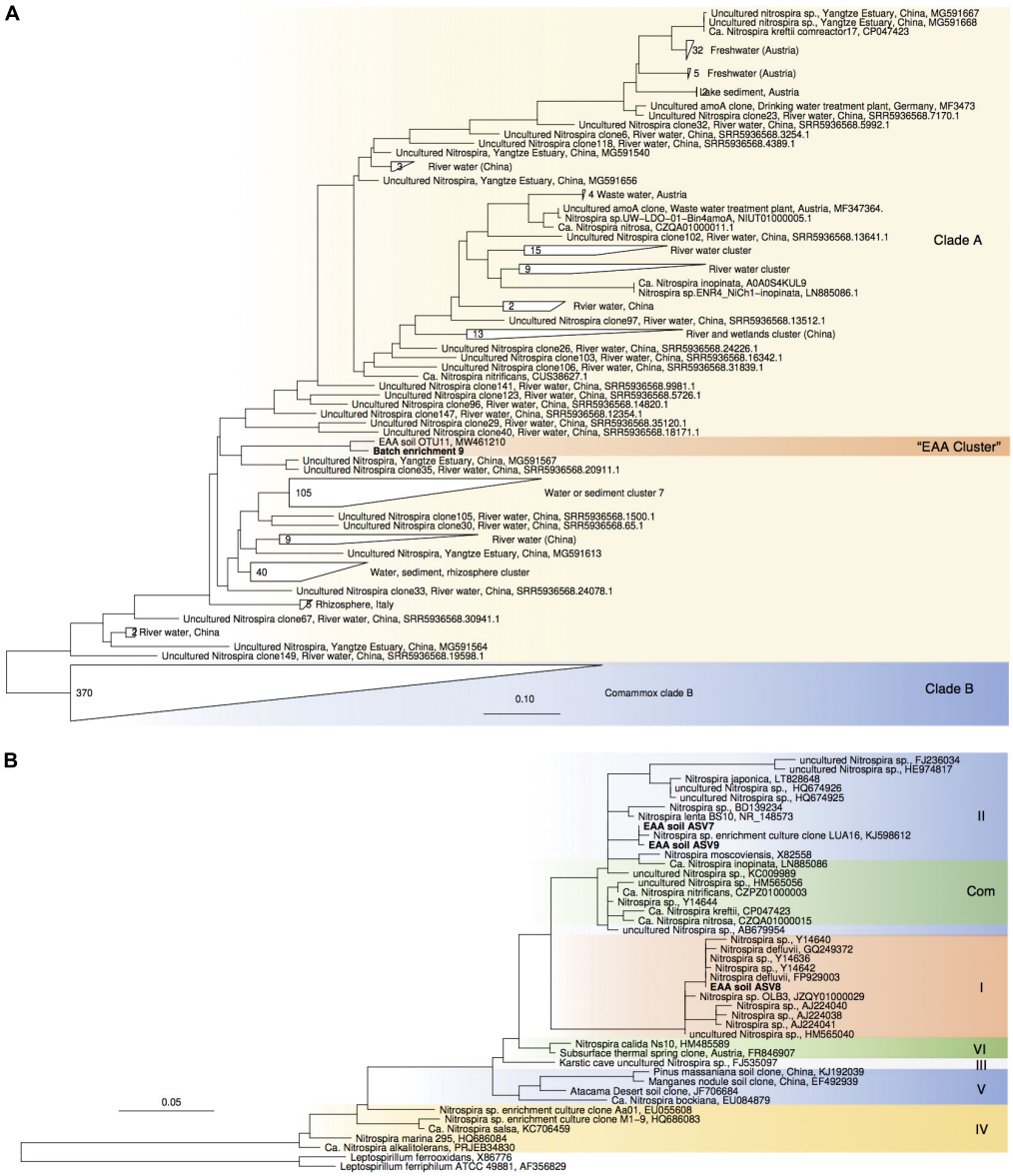

FIGURE 4 | Maximum-likelihood phylogenetic trees of comammox *amoA* gene sequences **(A)** and *Nitrospira* sp.-affiliated 16S rRNA gene sequences **(B)**. Sequences obtained from batch enrichment culture 9 are highlighted in bold. Comammox clade B sequences, and *Leptospirillum* sp. sequences were used as outgroups, respectively.

and 320 (**Figure 1**). Following this period pH values were on average 0.19, 0.26, and 0.21 units higher than during the first 200 days of operation in reactors A, B, and C, respectively. These observations show that despite being undetectable by amplicon sequencing in reactor A for most of the time, a small *Nitrosomonas* population was present and survived for more than 400 days of continuous nutrient limitation and successfully competed for nitrogen when conditions became favorable. Its absence in the subculture reactors may suggest that it primarily resided in biofilms on the glass surface of the reactor vessels.

PCR tests for comammox *amoA* remained negative in all reactor DNA samples with the full combination of comaA-244f_a-f and comaA-659r_a-f, as well as the specific primer combination comaA-244f_a and comaA-659r_c targeting the *amoA* sequence identified in the batch enrichment culture 9. It should be noted that the employed comammox *amoA* primers have been shown to have mismatches to some comammox *amoA* sequence types (Lin et al., 2020). However, since the comammox sequence type predominant in our soil was detected with this primer set in batch cultures, our results indicated that the three detected *Nitrospira* ASVs represented canonical nitrite-oxidizing strains and that *Nitrosocosmicus* was the predominant ammonia oxidizer. Further experiments are needed to test additional conditions and improve the enrichment of comammox *Nitrospira*.

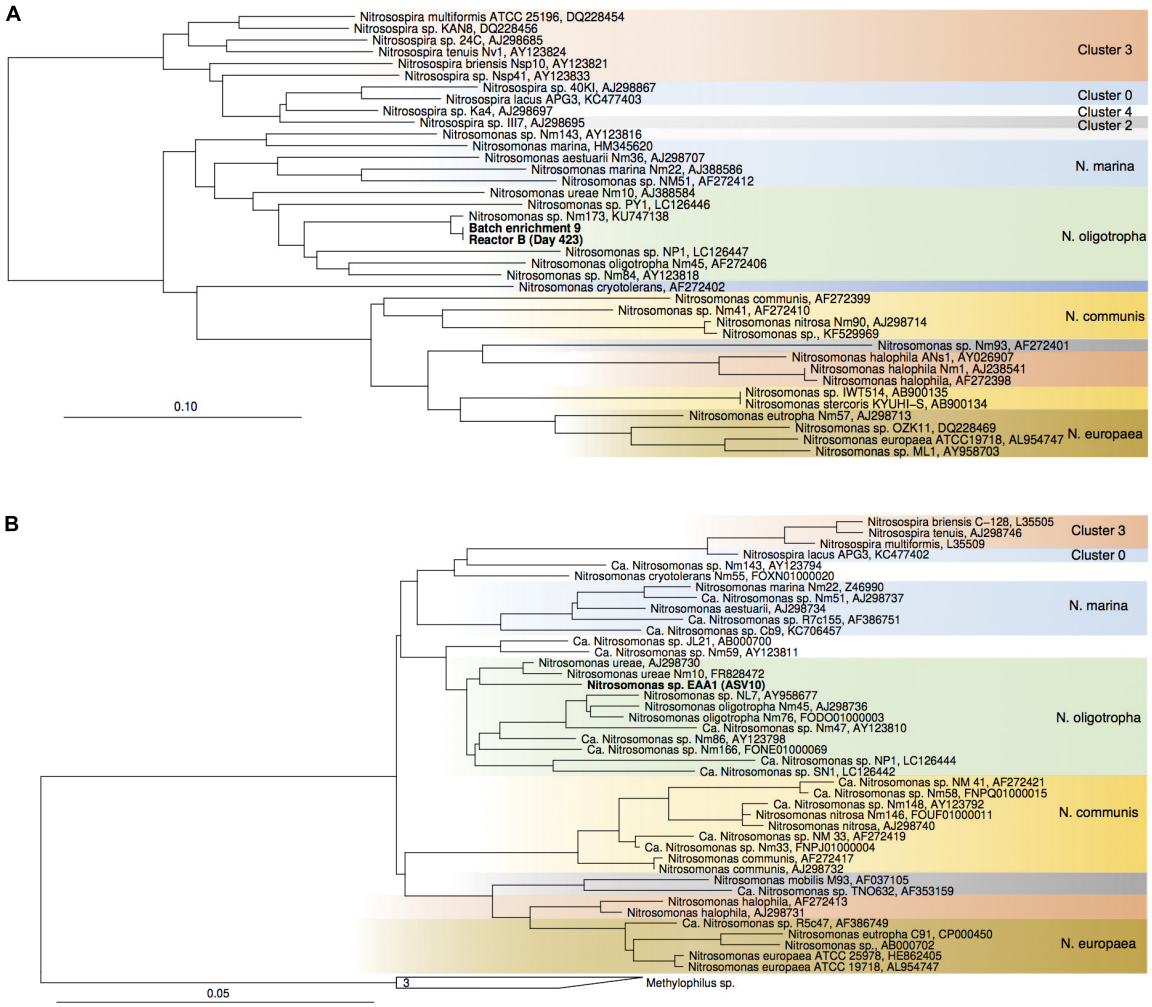

FIGURE 5 | Maximum-likelihood phylogenetic tree of proteobacterial *amoA* gene sequences **(A)** and 16S rRNA genes of *Nitrosomonadaceae*-affiliated AOB **(B)**. Sequences from the current study are highlighted in bold. *Nitrosococcus*- and *Methylophilaceae*-affiliated sequences were used as outgroups, respectively. Color codes highlight *Nitrosospira sp.* clusters and *Nitrosomonas* lineages.

In order to investigate competition between different nitrifiers under nutrient-limited conditions, we adopted an enrichment strategy without selective inhibitors. The overall enrichment of nitrifiers in the reactors was notably low. Based on 16S rRNA amplicon sequences, nitrifiers constituted between 0.9 and 56.2% of all 16S rRNA gene reads in reactor sets A–C and never became highly dominant (**Figure 2**). The highest relative enrichments were observed temporarily at 189 days in reactor A, and in subculture reactors 2 and 3. Increasing the feed ammonium concentration in subculture reactors 1 and 3 led to increased enrichment to above 50%. However, removal of the EDTA solution in subcultures 3 had no instantaneous effect on the community composition or enrichment factor.

Analysis of overall microbial community composition in reactor sets A, B, and C revealed 48 family level archaeal and bacterial taxa with at least 1.0% relative frequency in one of the reactor samples (**Figure 6**). Overall diversity was high in the soil sample, and as expected dropped quickly in the enrichment cultures (**Figure 6A**). However, observed OTU values ranging from 18 to 83, 13 to 191, and 16 to 60 in samples from reactor sets A, B, and C, respectively, indicated a surprisingly high microbial diversity persisting throughout the three reactor series.

Each reactor series showed a unique microbial profile. Besides, the nitrifying taxa, only a few bacterial taxa were found consistently throughout each enrichment time series. In reactor set A, uncultivated *Chlorobi*, *Anaerolineaceae*, and *Pseudomonadaceae*-associated sequences were found frequently throughout the time series, whereas in reactor set B, *Chlorobi* were less common and *Anaerolineaceae*, *Burkholderiaceae*, *Pseudomonadaceae*-associated sequences were more often present. In reactor set C, *Burkholderiaceae* and *Moraxellaceae* were the most commonly found non-nitrifying taxa. However, most taxa were rare and only found once or twice with relative frequencies above 1.0% (**Figure 6B**).

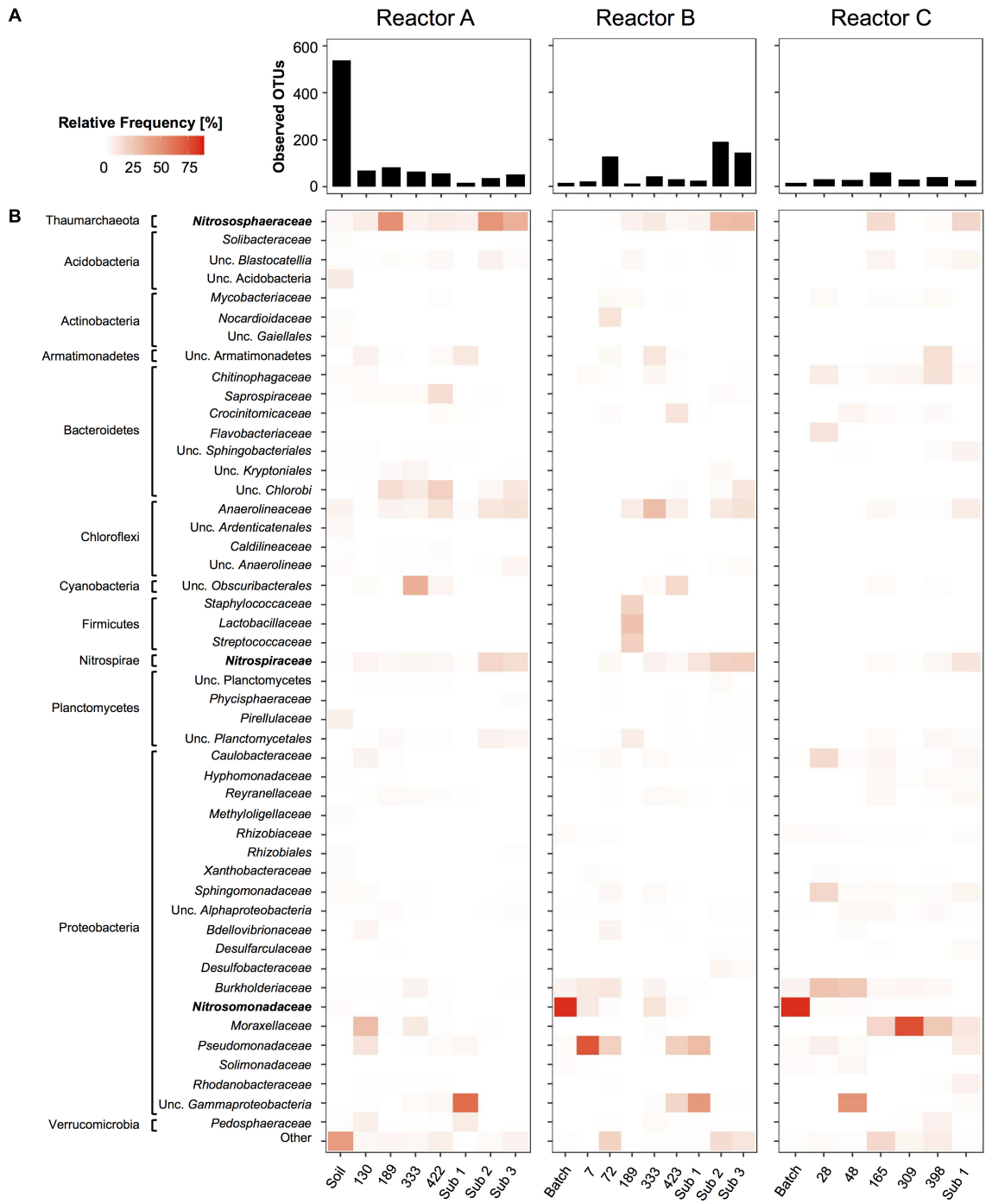

FIGURE 6 | Time series of overall community composition in reactors A, B, and C based on 16S rRNA gene amplicon sequences. Given are overall diversity of bacterial and archaeal taxa as Observed OTU's at ASV level (bar graphs, **A**) and relative frequency of microbial taxa summed and grouped at the family level (heatmaps, **B**). Family level taxa with more than 1% relative frequency in at least one sample are shown on the left. All other less frequent taxa were grouped into "Other." For uncultivated taxa without family level taxonomic names next higher level of taxonomic names are given. Nitrifier taxa highlighted in bold are analyzed in more detail in **Figure 3**. Sub 1, Sub 2, and Sub 3 refer to sub-culture reactors.

In order to isolate the predominant *Nitrosocosmicus* strain into pure culture, batch cultures were set up with low (50 μM) or high (1.0 mM) ammonium concentration. Several antibiotics were tested that have previously been used successfully to enrich or isolate AOA strains (Lehtovirta-Morley et al., 2016; Sauder et al., 2017; Liu et al., 2019). Within 2 weeks of incubation ammonium

was completely consumed in the low ammonium culture controls, and more than 100 μM nitrite/nitrate was produced in the high ammonium culture controls. However, in the kanamycin, ampicillin, ciprofloxacin, azithromycin treatments less than 10 μM ammonia consumption (low ammonium cultures) or combined nitrite and nitrate production (high ammonium cultures) was observed even after more than 4 weeks of incubation. Some ammonia consumption was detected in the streptomycin and lincomycin treatments. However, microscopic examination showed a mixed assemblage of morphotypes in these two treatments, indicating lack of inhibition in these two treatments (data not shown). To further test whether the inhibition of growth in the presence of antibiotics was due to lack of organic carbon source or antioxidants previously shown to be required by some *Nitrosopumilus* and *Nitrososphaera* strains in batch culture (Tourna et al., 2011; Qin et al., 2014; Kim et al., 2016), additional experiments were conducted with combinations of organic carbon compounds (pyruvate, alpha-ketoglutarate, or malic acid) with kanamycin or ampicillin treatment. However, similar to the antibiotic treatments alone, no significant ammonia oxidation activity was observed after more than 1 month incubation (data not shown).

DISCUSSION

The recognition of the vast diversity of AOA and comammox bacteria adapted to low ammonium fluxes still awaiting cultivation and physiological characterization has renewed interest in improved cultivation methods targeting oligotrophic nitrifiers (Bollmann et al., 2011). Significant improvements have been made in overall cultivation success of microbes by better simulating environmental conditions and decreasing nutrient concentrations (Bollmann and Laanbroek, 2001; Overmann, 2010; Lewis et al., 2021). However, enrichment of nitrifiers still remains extremely difficult (Bollmann et al., 2011). Recent studies indicated that available soil AOA strains exhibit kinetic properties similar to low-nutrient adapted soil AOB isolates, e.g., of the *Nitrosomonas oligotropha* lineage, suggesting that kinetic properties may possibly not be a distinguishing factor between these soil AOA and AOB, and that comammox bacteria may be more adapted to nutrient limited conditions (Kits et al., 2017). In support of these results, recently comammox *Nitrospira* were successfully enriched in nutrient-limited membrane bioreactors with biomass retention (Sakoula et al., 2020), sequencing batch reactors (van Kessel et al., 2015; Camejo et al., 2017), and in reactors with fabrics as biomass carriers (Takahashi et al., 2020). Although in our study the comammox *Nitrospira* strain was detected in batch culture after more than a year of bi-weekly transfers (equivalent to a 10^{-58} dilution of the original soil), clearly indicating growth in the batch cultures, no further enrichment of this strain was obtained in the nutrient-limited chemostat setups employed with either of the tested growth media. The low cell density in the cultures and the limited sample DNA from each sampling point did not allow us to further evaluate changes immediately after transfer to the bioreactors or at higher frequency during reactor operation, or to perform additional qPCR tests to characterize populations below the detection limit of the amplicon sequencing dataset.

The main difference between our chemostat setups and the reactor setups employed in the above studies was that our chemostats did not contain a mechanism of biomass retention. Several comammox strains cultivated thus far originate from environmental biofilms (e.g., *Ca.* N. inopinata, *Ca.* N. nitrificans, *Ca.* N. nitrosa, Daims et al., 2015; van Kessel et al., 2015) and have been shown to form aggregates or biofilms in culture (van Kessel et al., 2015; Sakoula et al., 2020; Takahashi et al., 2020). Metagenomic studies have found comammox to be abundant in biofilms, e.g., of groundwater wells, drinking water treatment systems, and freshwater biofilters (Daims et al., 2015; Pinto et al., 2015; Palomo et al., 2016; Bartelme et al., 2017). Together these findings suggest that comammox bacteria may have adopted a biofilm lifestyle, or at least grow best in biofilms or aggregates, or higher cell densities, and may not be as competitive in classical chemostat culture without biomass retention. Indeed, Costa et al. (2006) predicted based on kinetic theory of optimal pathway length that a comammox organisms should be most competitive under slow, substrate-limited growth in flocs, biofilms, or microcolonies. Biomass retention might be especially important and a strong selection factor at low initial cell densities and therefore may have prevented a successful establishment of comammox in our reactors. These results may also suggest that biofilm lifestyle is also the preferred lifestyle of comammox bacteria from EAA soils.

Several additional factors may be responsible for the lack of further enrichment of comammox strains from EAA soils. These include suboptimal temperature, too high oxygen concentrations, and too high starting dilution rates at the transition from fed-batch to chemostat mode (van Kessel et al., 2015; Camejo et al., 2017; Koch et al., 2019). Additionally, metagenomic studies have found urea uptake and metabolism genes frequent in comammox bacteria (Camejo et al., 2017; Palomo et al., 2018), and three urea-decomposing comammox enrichments were recently reported (Li et al., 2021), suggesting widespread capacity for urea utilization among comammox bacteria. Ammonia concentrations in our soils were low in April 2018, as well as in December 2017 (Huang et al., 2021), which could suggest that comammox bacteria in these soils may have adapted to primarily rely on urea and not on ammonia for growth, and that maybe other ammonia oxidizers in the soil may be less competitive for urea. Notably, Sakoula et al., 2020 found that *Ca.* Nitrospira kreftii was partially inhibited at total ammonium concentrations as low as 50 μM, further suggesting a potential importance of urea utilization. Such an ammonia-sensitive strain would have been strongly selected against in our batch enrichments. Further research is needed to elucidate the ecophysiology of comammox bacteria in EAA soils.

To our surprise, all three nutrient-limited reactors yielded a *Nitrosocosmicus* sp. as predominant ammonia oxidizer, accompanied by 2–3 different *Nitrospira* sp.-affiliated canonical nitrite oxidizers, suggesting that at the given temperature, pH, and media composition, this *Nitrosocosmicus* ecotype was the most competitive ammonia oxidizer under nutrient-limited chemostat conditions. Previous studies have suggested a pH

and temperature-based niche separation of different soil AOA lineages based on *amoA* gene phylogeny and distribution (Gubry-Rangin et al., 2011, 2015; Prosser and Nicol, 2012). The observation that the same *Nitrososcosmicus* ecotype was enriched directly from soil and from a batch culture pre-enrichment, may corroborate this hypothesis, as all reactors in our study were maintained under the same temperature and pH regime. Our study joins a notably growing number of enrichment strategies yielding *Nitrososcosmicus* strains (Jung et al., 2016; Lehtovirta-Morley et al., 2016; Sauder et al., 2017; Liu et al., 2019). However, our results are particularly surprising since *Nitrososcosmicus* strains have thus far been noticed mainly for their observed higher tolerance to elevated ammonia concentrations compared to other *Nitrososphaeraceae*- and *Nitrosopumilaceae*-affiliated AOA strains (Lehtovirta-Morley et al., 2016; Sauder et al., 2017). Despite the relatively high ammonia tolerance, the highest growth rates of *Nitrososcosmicus* strains have thus far been reported at lower ammonia concentrations of 0.5 and 2 mM substrate concentrations (Jung et al., 2016; Lehtovirta-Morley et al., 2016; Sauder et al., 2017). Our results clearly indicate that at least some *Nitrososcosmicus* ecotypes also strongly compete under constantly limiting nutrient concentrations at or below 1 μM total ammonium. Thus far no kinetic data have been reported for *Nitrososcosmicus* strains and further physiological studies will be necessary to better understand the metabolism and kinetics of *Nitrososcosmicus* strains. Notably, neither the NS-δ-affiliated AOA strain detected in the batch culture, nor the NS-α-affiliated AOA strain detected in reactor B (Day 72) were further enriched (**Figures 2**, **3A,B**), which may either confirm that these AOA may not be very competitive under nutrient limitation (Kits et al., 2017), or suggest that they may rely on organic carbon sources, antioxidants, or other components lacking in our growth media, or that their general growth conditions were not met well in our experiments.

After pH fluctuations in reactors A, B, and C we observed a small *Nitrosomonas* sp. population to regain in abundance, but then was outcompeted again by the *Nitrososcosmicus* after stabilization of pH (reactor A) and sub-cultivation (reactor B and C). This *Nitrosomonas* strain also highly dominated the original batch enrichment culture at 300 μM starting ammonium concentrations. Assuming that AOA and AOB both use ammonia as their primary substrate (Suzuki et al., 1974; Li et al., 2018), these observations may suggest that the *Nitrososcosmicus* strain exhibited only a marginally higher ammonia affinity compared to the *Nitrosomonas* strain. The rise in NH_3 due to pH-dependent shifts of $NH_3 + H^+ \Leftrightarrow NH_4^+$ equilibrium may have been sufficient for the AOB strain to become more competitive in the chemostats and strongly dominate the batch culture at ammonium concentrations of 300 μM. Alternatively, the pH fluctuation could have impaired activity of the *Nitrososcosmicus* strain and may have caused slightly rising overall NH_4^+ concentrations in the reactors. It should be noted that based on the presented data we cannot determine how much the *Nitrososcosmicus* and *Nitrosomonas* strains each contributed to the overall rate of ammonia oxidation observed in the reactors. Further detailed kinetic studies on both strains and further enrichments targeting a wider range of temperature and pH regimes will be required to examine whether the niche separation hypothesis can be further substantiated with physiological evidence, or whether other cultivation-related biases were responsible for the observed outcome in our reactors.

Analysis of 16S rRNA gene amplicons revealed that a relatively large diversity of heterotrophic bacterial taxa persisted in the chemostat enrichments, suggesting that sufficient organic carbon was available to maintain this diversity of heterotrophs. Similar patterns of diverse heterotrophs maintained in nitrifier enrichments were previously observed in comammox enrichments (Takahashi et al., 2020). In our study enrichments with higher than 50% relative frequency of nitrifiers based on 16S rRNA gene amplicon sequences were obtained only for the *Nitrosomonas* strain in batch culture, at one time point in the original reactors, and more consistently only after additional sub-cultures established in reactors with elevated feed ammonia concentrations of 1.8 mM (**Figure 2**). Indeed, assuming a molar ratio of N oxidation to C fixation of approximately 5 for AOA and 8–12 for AOB, respectively (Billen, 1976; Prosser, 1989; Könneke et al., 2014), it can be estimated that using feed substrate concentrations of 300 μM N, ammonia oxidizers could build up between ∼ 60 μM (AOA) and 35 μM (AOB) biomass carbon under steady-state operation in reactors A–C. For comparison, organic carbon available from the 7.5 μM Fe EDTA [Fe $C_{10}H_{16}N_2O_8$] alone provided approximately 75 μM organic carbon source C. Given a carbon assimilation rate by heterotrophs of approximately 50% (Simon and Azam, 1989), the amount of EDTA supplied with the growth media was sufficient to build up approximately 35 μM biomass carbon. Thus, the biomass yield from organic carbon oxidation and nitrification could have been approximately similar during operation of reactors A–C, therefore explaining the relatively low enrichment factor of nitrifiers in our initial reactors. Interestingly, a notably higher enrichment of the *Nitrosomonas* strain was obtained in batch enrichment culture 9 with only 15.5% accompanying heterotrophs (**Figure 2**). Since we used the exact same media and ammonium feed concentration for reactor B, the frequent transfers and constant presence of nitrite may have limited the number of heterotrophic bacteria over time.

For the purpose of enrichment of nitrifiers long operation times, such as used for reactors A–C, may be detrimental, as in the late stages of the reactor operation the relative enrichment of nitrifiers actually declined (**Figure 2**). This decline may be due to slow accumulation of cell debris or cell aggregates that further fuel heterotrophic growth. Taken together, these observations suggest that 2–3 months reactor operation appears sufficient to obtain initial stable enrichments based on nutrient limitation alone and that further increases in ammonium feed is needed to obtain highly enriched nitrifier cultures. Furthermore, highly purified water and inorganic media sources, or reactor setups with biomass retention, are beneficial when operating reactors at low ammonium feed concentrations. Similar challenges will be associated with enrichment of potential mixotrophic nitrifiers that may rely on amendment of organic carbon or nitrogen compounds. Such organisms are predicted for example among AOA by observation of assimilation of amino acids (Ouverney and Fuhrman, 2000; Dekas et al., 2019) and isotopic signals

of organic carbon assimilation in archaeal membrane lipids (Ingalls et al., 2006).

Treatment of the enrichments with antibiotics or combination of antibiotics and organic carbon sources or antioxidants did not result in pure *Nitrosocosmicus* cultures, instead either ammonia oxidation ceased completely, or if activity was present, the antibiotic treatment did not suppress growth of bacteria. Although it seems unlikely that the *Nitrosocosmicus* strain in our study was directly inhibited by antibiotics since the same antibiotics have previously been used successfully for other *Nitrosocosmicus* enrichments (Lehtovirta-Morley et al., 2016; Liu et al., 2019), we cannot completely rule out cytotoxic effects of the antibiotics on this strain, especially because it was selected for only based on nutrient limitation and in the complete absence of antibiotics. Nonetheless, more likely our results suggest an indirect inhibition via suppression of heterotrophic bacteria, that provide a thus far unknown benefit to the *Nitrosocosmicus* strain. Notably, a similar inhibition of activity in the presence of antibiotics was also observed in *Ca.* Nitrosocosmicus hydrocola G61 (Sauder and Neufeld, personal communication, Sauder et al., 2017). And neither in G61, nor in our enrichment this inhibition could be alleviated by addition of organic carbon compounds shown to stimulate activity of strain G61 (Sauder et al., 2017). Additional experiments will be required to test if supplementation of other potential carbon sources including amino acids, sugars, and complex substrates (peptone, yeast extract, and casamino acids), shown to stimulate activity of other *Nitrosocosmicus* strains (Jung et al., 2016; Sauder et al., 2017) can alleviate this inhibition, or whether more complex kinds of interactions between the *Nitrosocosmicus* strain and heterotrophic bacteria may be responsible for the observed dependence of the *Nitrosocosmicus* strain on heterotrophic bacteria.

DATA AVAILABILITY STATEMENT

DNA sequences obtained in this study have been deposited at NCBI Sequencing Read Archive under BioProject # PRJNA728812 (16S rRNA gene amplicon sequences) and GenBank accession numbers MZ196446-MZ196452 (amoA gene sequences).

AUTHOR CONTRIBUTIONS

SC and WM-H designed the research. SC, JR, EC, NS, SS-M, and WM-H conducted enrichments and bioreactor experiments. JR and WM-H wrote the manuscript. All authors conducted molecular analyses.

FUNDING

This research was supported by startup funds from the Florida Agricultural Experiment Station (Hatch project FLA-FTL-005680) and UF IFAS Early Career award to WM-H.

ACKNOWLEDGMENTS

The authors are indebted to Keelnatham T. Shanmugam and Lonnie O. Ingram (deceased) for their generous donation of bioreactors that made this project possible. Josh Neufeld, Michelle McKnight, and Emilie Spasov are acknowledged for fruitful discussion and for providing cultures of *Ca*. Nitrosocosmicus hydrocola G61. We are sincerely grateful to two reviewers for their detailed and constructive comments that helped to substantially improve this manuscript.

SUPPLEMENTARY MATERIAL

The Supplementary Material for this article can be found online at: https://www.frontiersin.org/articles/10.3389/fmicb.2021.671480/full#supplementary-material

REFERENCES

Alves, R. J. E., Minh, B. Q., Urich, T., von Haeseler, A., and Schleper, C. (2018). Unifying the global phylogeny and environmental distribution of ammonia-oxidising archaea based on amoA genes. *Nat. Commun.* 9:1517. doi: 10.1038/s41467-018-03861-1

Bartelme, R. P., McLellan, S. L., and Newton, R. J. (2017). Freshwater recirculating aquaculture system operations drive biofilter bacterial community shifts around a stable nitrifying consortium of ammonia-oxidizing Archaea and comammox *Nitrospira*. *Front. Microbiol.* 8:101. doi: 10.3389/fmicb.2017.00101

Bartossek, R., Spang, A., Weidler, G., Lanzen, A., and Schleper, C. (2012). Metagenomic analysis of ammonia oxidizing archaea affiliated with the soil group. *Front. Microbiol.* 3:208. doi: 10.3389/fmicb.2012.00208

Billen, G. (1976). Evaluation of nitrifying activity in sediments by dark bicarbonate-C-14 incorporation. *Water Res.* 10, 51–57. doi: 10.1016/0043-1354(76)90157-3

Bollmann, A., French, E., and Laanbroek, H. J. (2011). "Isolation, Cultivation, and Characterization of Ammonia-Oxidizing Bacteria and Archaea Adapted to Low Ammonium Concentrations. *Methods Enzymol.* 486, 55–88. doi: 10.1016/b978-0-12-381294-0.00003-1

Bollmann, A., and Laanbroek, H. J. (2001). Continuous culture enrichments of ammonia-oxidizing bacteria at low ammonium concentrations. *FEMS Microbiol. Ecol.* 37, 211–221. doi: 10.1111/j.1574-6941.2001.tb00868.x

Bolyen, E., Rideout, J. R., Dillon, M. R., Bokulich, N. A., Abnet, C. C., Al-Ghalith, G. A., et al. (2019). Reproducible, interactive, scalable and extensible microbiome data science using QIIME 2. *Nat. Biotechnol.* 37, 852–857.

Bower, C. E., and Holm-Hansen, T. (1980). A salicylate–hypochlorite method for determining ammonia in seawater. *Can. J. Fish. Aquat. Sci.* 37, 794–798. doi: 10.1139/f80-106

Callahan, B. J., McMurdie, P. J., Rosen, M. J., Han, A. W., Johnson, A. J. A., and Holmes, S. P. (2016). DADA2: high-resolution sample inference from Illumina amplicon data. *Nat. Methods* 13, 581–583.

Camejo, P. Y., Santo Domingo, J., McMahon, K. D., and Noguera, D. R. (2017). Genome-enabled insights into the ecophysiology of the comammox bacterium "*Candidatus Nitrospira* nitrosa". *mSystems* 2, e00059–17.

Costa, E., Pérez, J., and Kreft, J.-U. (2006). Why is metabolic labour divided in nitrification? *Trends Microbiol.* 14, 213–219. doi: 10.1016/j.tim.2006.03.006

Daims, H., Lebedeva, E. V., Pjevac, P., Han, P., Herbold, C., Albertsen, M., et al. (2015). Complete nitrification by *Nitrospira* bacteria. *Nature* 528, 504–509. doi: 10.1038/nature16461

Daims, H., Lücker, S., and Wagner, M. (2016). A new perspective on microbes formerly known as nitrite-oxidizing bacteria. *Trends Microbiol.* 24, 699–712. doi: 10.1016/j.tim.2016.05.004

de la Torre, J. R., Walker, C. B., Ingalls, A. E., Könneke, M., and Stahl, D. A. (2008). Cultivation of a thermophilic ammonia oxidizing archaeon synthesizing crenarchaeol. *Environ. Microbiol.* 10, 810–818. doi: 10.1111/j.1462-2920.2007.01506.x

Dekas, A. E., Parada, A. E., Mayali, X., Fuhrman, J. A., Wollard, J., Weber, P. K., et al. (2019). Characterizing chemoautotrophy and heterotrophy in marine archaea and bacteria with single-cell multi-isotope NanoSIP. *Front. Microbiol.* 10:2682. doi: 10.3389/fmicb.2019.02682

French, E., Kozlowski, J. A., Mukherjee, M., Bullerjahn, G., and Bollmann, A. (2012). Ecophysiological characterization of ammonia-oxidizing archaea and bacteria from freshwater. *Appl. Environ. Microbiol.* 78, 5773–5780. doi: 10.1128/aem.00432-12

García-Robledo, E., Corzo, A., and Papaspyrou, S. (2014). A fast and direct spectrophotometric method for the sequential determination of nitrate and nitrite at low concentrations in small volumes. *Mar. Chem.* 162, 30–36. doi: 10.1016/j.marchem.2014.03.002

Grasshoff, K., Kremling, K., and Erhard, M. (1999). *Methods of Seawater Analysis*. Weinheim: Wiley-VCH.

Griffiths, R. I., Whiteley, A. S., O'Donnell, A. G., and Bailey, M. J. (2000). Rapid method for coextraction of DNA and RNA from natural environments for analysis of ribosomal DNA- and rRNA-based microbial community composition. *Appl. Environ. Microbiol.* 66, 5488–5491. doi: 10.1128/aem.66.12.5488-5491.2000

Gubry-Rangin, C., Hai, B., Quince, C., Engel, M., Thomson, B. C., James, P., et al. (2011). Niche specialization of terrestrial archaeal ammonia oxidizers. *Proc. Natl. Acad. Sci. U. S. A.* 108, 21206–21211. doi: 10.1073/pnas.1109000108

Gubry-Rangin, C., Kratsch, C., Williams, T. A., McHardy, A. C., Embley, T. M., Prosser, J. I., et al. (2015). Coupling of diversification and pH adaptation during the evolution of terrestrial *Thaumarchaeota*. *Proc. Natl. Acad. Sci. U. S. A.* 112, 9370–9375. doi: 10.1073/pnas.1419329112

Huang, L., Chakrabarti, S., Cooper, J., Perez, A., John, S. M., Daroub, S. H., et al. (2021). Ammonia-oxidizing archaea are integral to nitrogen cycling in a highly fertile agricultural soil. *ISME Commun.* 1:19. doi: 10.1038/s43705-43021-00020-4

Ingalls, A. E., Shah, S. R., Hansman, R. L., Aluwihare, L. I., Santos, G. M., Druffel, E. R. M., et al. (2006). Quantifying archaeal community autotrophy in the mesopelagic ocean using natural radiocarbon. *Proc. Natl. Acad. Sci. U. S. A.* 103, 6442–6447. doi: 10.1073/pnas.0510157103

Jung, M.-Y., Gwak, J.-H., Rohe, L., Giesemann, A., Kim, J.-G., Well, R., et al. (2019). Indications for enzymatic denitrification to N_2O at low pH in an ammonia-oxidizing archaeon. *ISME J.* 13, 2633–2638. doi: 10.1038/s41396-019-0460-6

Jung, M. Y., Kim, J. G., Damsté, J. S. S., Rijpstra, W. I. C., Madsen, E. L., Kim, S. J., et al. (2016). A hydrophobic ammonia-oxidizing archaeon of the *Nitrosocosmicus* clade isolated from coal tar-contaminated sediment. *Environ. Microbiol. Rep.* 8, 983–992. doi: 10.1111/1758-2229.12477

Jung, M.-Y., Park, S.-J., Min, D., Kim, J.-S., Rijpstra, W. I. C., Sinninghe Damsté, J. S., et al. (2011). Enrichment and characterization of an autotrophic ammonia-oxidizing archaeon of mesophilic crenarchaeal Group I.1a from an agricultural soil. *Appl. Environ. Microbiol.* 77, 8635–8647. doi: 10.1128/aem.05787-11

Kerou, M., Offre, P., Valledor, L., Abby, S. S., Melcher, M., Nagler, M., et al. (2016). Proteomics and comparative genomics of *Nitrososphaera viennensis* reveal the core genome and adaptations of archaeal ammonia oxidizers. *Proc. Natl. Acad. Sci. U. S. A.* 113, E7937–E7946.

Kerou, M., Ponce-Toledo, R. I., Zhao, R., Abby, S. S., Hirai, M., Nomaki, H., et al. (2021). Genomes of *Thaumarchaeota* from deep sea sediments reveal specific adaptations of three independently evolved lineages. *ISME J.* doi: 10.1038/s41396-41021-00962-41396 [Epub Online ahead of print].

Kim, J.-G., Park, S.-J., Sinninghe Damsté, J. S., Schouten, S., Rijpstra, W. I. C., Jung, M.-Y., et al. (2016). Hydrogen peroxide detoxification is a key mechanism for growth of ammonia-oxidizing archaea. *Proc. Natl. Acad. Sci. U. S. A.* 113, 7888–7893. doi: 10.1073/pnas.1605501113

Kits, K. D., Jung, M.-Y., Vierheilig, J., Pjevac, P., Sedlacek, C. J., Liu, S., et al. (2019). Low yield and abiotic origin of N_2O formed by the complete nitrifier *Nitrospira inopinata*. *Nat. Commun.* 10:1836.

Kits, K. D., Sedlacek, C. J., Lebedeva, E. V., Han, P., Bulaev, A., Pjevac, P., et al. (2017). Kinetic analysis of a complete nitrifier reveals an oligotrophic lifestyle. *Nature* 549, 269–272. doi: 10.1038/nature23679

Koch, H., van Kessel, M. A. H. J., and Lücker, S. (2019). Complete nitrification: insights into the ecophysiology of comammox *Nitrospira*. *Appl. Microbiol. Biotechnol.* 103, 177–189. doi: 10.1007/s00253-018-9486-3

Könneke, M., Bernhard, A. E., de la Torre, J. R., Walker, C. B., Waterbury, J. B., and Stahl, D. A. (2005). Isolation of an autotrophic ammonia-oxidizing marine archaeon. *Nature* 437, 543–546. doi: 10.1038/nature03911

Könneke, M., Schubert, D. M., Brown, P. C., Hügler, M., Standfest, S., and Schwander, T. (2014). Ammonia-oxidizing archaea use the most energy-efficient aerobic pathway for CO_2 fixation. *Proc. Natl. Acad. Sci. U. S. A.* 111, 8239–8244. doi: 10.1073/pnas.1402028111

Kozlowski, J. A., Stieglmeier, M., Schleper, C., Klotz, M. G., and Stein, L. Y. (2016). Pathways and key intermediates required for obligate aerobic ammonia-dependent chemolithotrophy in bacteria and *Thaumarchaeota*. *ISME J.* 10, 1836–1845. doi: 10.1038/ismej.2016.2

Lawson, C. E., and Lücker, S. (2018). Complete ammonia oxidation: an important control on nitrification in engineered ecosystems? *Curr. Opin. Biotechnol.* 50, 158–165. doi: 10.1016/j.copbio.2018.01.015

Lehtovirta-Morley, L. E. (2018). Ammonia oxidation: ecology, physiology, biochemistry and why they must all come together. *FEMS Microbiol. Lett.* 365:fny058.

Lehtovirta-Morley, L. E., Ross, J., Hink, L., Weber, E. B., Gubry-Rangin, C., Thion, C., et al. (2016). Isolation of '*Candidatus Nitrosocosmicus* franklandus', a novel ureolytic soil archaeal ammonia oxidiser with tolerance to high ammonia concentration. *FEMS Microbiol. Ecol.* 92:fiw057. doi: 10.1093/femsec/fiw057

Lewis, W. H., Tahon, G., Geesink, P., Sousa, D. Z., and Ettema, T. J. G. (2021). Innovations to culturing the uncultured microbial majority. *Nat. Rev. Microbiol.* 19, 225–240. doi: 10.1038/s41579-020-00458-8

Li, J., Hua, Z.-S., Liu, T., Wang, C., Li, J., Bai, G., et al. (2021). Selective enrichment and metagenomic analysis of three novel comammox *Nitrospira* in a urine-fed membrane bioreactor. *ISME Commun.* 1:7.

Li, P.-N., Herrmann, J., Tolar, B. B., Poitevin, F., Ramdasi, R., Bargar, J. R., et al. (2018). Nutrient transport suggests an evolutionary basis for charged archaeal surface layer proteins. *ISME J.* 12, 2389–2402. doi: 10.1038/s41396-018-0191-0

Lin, C., Xu, H., Qin, W., Xu, S., Tang, X., Kuang, L., et al. (2020). Evaluation of Two Primer Sets for Amplification of Comammox *Nitrospira* amoA Genes in Wetland Soils. *Front. Microbiol.* 11:560942. doi: 10.3389/fmicb.2020.560942

Liu, L., Li, S., Han, J., Lin, W., and Luo, J. (2019). A two-step strategy for the rapid enrichment of *Nitrosocosmicus*-like ammonia-oxidizing Thaumarchaea. *Front. Microbiol.* 10:875. doi: 10.3389/fmicb.2019.00875

Ludwig, W., Strunk, O., Westram, R., Richter, L., Meier, H., Yadhukumar, et al. (2004). ARB: a software environment for sequence data. *Nucleic Acids Res.* 32, 1363–1371. doi: 10.1093/nar/gkh293

Martens-Habbena, W., Berube, P. M., Urakawa, H., Torre, J. R., and Stahl, D. A. (2009). Ammonia oxidation kinetics determine the niche separation of nitrifying archaea and bacteria. *Nature* 461, 976–979. doi: 10.1038/nature08465

Martens-Habbena, W., Qin, W., Horak, R. E. A., Urakawa, H., Schauer, A. J., and Moffett, J. W. (2015). The production of nitric oxide by marine ammonia-oxidizing archaea and inhibition of archaeal ammonia oxidation by a nitric oxide scavenger. *Environ. Microbiol.* 17, 2261–2274. doi: 10.1111/1462-2920.12677

Nicol, G. W., and Prosser, J. I. (2011). "Strategies to determine diversity, growth, and activity of ammonia-oxidizing archaea in soil," in *Methods in Enzymology*, eds G. K. Martin and Y. S. Lisa (Cambridge: Academic Press), 3–34. doi: 10.1016/b978-0-12-386489-5.00001-4

Norton, J., and Ouyang, Y. (2019). Controls and adaptive management of nitrification in agricultural soils. *Front. Microbiol.* 10:1931. doi: 10.3389/fmicb.2019.01931

Orellana, L. H., Chee-Sanford, J. C., Sanford, R. A., Löffler, F. E., and Konstantinidis, K. T. (2018). Year-round shotgun metagenomes reveal stable microbial communities in agricultural soils and novel ammonia oxidizers responding to fertilization. *Appl. Environ. Microbiol.* 84, e01646–17.

Ouverney, C. C., and Fuhrman, J. A. (2000). Marine planktonic archaea take up amino acids. *Appl. Environ. Microbiol.* 66, 4829–4833. doi: 10.1128/aem.66.11.4829-4833.2000

Overmann, J. (2010). "Novel Cultivation Strategies for Environmentally Important Microorganisms," in *Geomicrobiology: Molecular and Environmental Perspective*, eds L. L. Barton, M. Mandl, and A. Loy (Netherlands: Springer), 69–89. doi: 10.1007/978-90-481-9204-5_3

Palomo, A., Fowler, S. J., Gülay, A., Rasmussen, S., Sicheritz-Ponten, T., and Smets, B. F. (2016). Metagenomic analysis of rapid gravity sand filter microbial communities suggests novel physiology of *Nitrospira* spp. *ISME J.* 10, 2569–2581. doi: 10.1038/ismej.2016.63

Palomo, A., Pedersen, A. G., Fowler, S. J., Dechesne, A., Sicheritz-Pontén, T., and Smets, B. F. (2018). Comparative genomics sheds light on niche differentiation and the evolutionary history of comammox *Nitrospira*. *ISME J.* 12, 1779–1793. doi: 10.1038/s41396-018-0083-3

Parada, A. E., Needham, D. M., and Fuhrman, J. A. (2016). Every base matters: assessing small subunit rRNA primers for marine microbiomes with mock communities, time series and global field samples. *Environ. Microbiol.* 18, 1403–1414. doi: 10.1111/1462-2920.13023

Pinto, A. J., Marcus, D. N., Ijaz, U. Z., Bautista-de lose Santos, Q. M., Dick, G. J., and Raskin, L. (2015). Metagenomic evidence for the presence of comammox *Nitrospira*-like bacteria in a drinking water system. *mSphere* 1, e00054–15.

Pjevac, P., Schauberger, C., Poghosyan, L., Herbold, C. W., van Kessel, M. A. H. J., Daebeler, A., et al. (2017). AmoA-targeted polymerase chain reaction primers for the specific detection and quantification of comammox *Nitrospira* in the environment. *Front. Microbiol.* 8:1508. doi: 10.3389/fmicb.2017.01508

Prosser, J. I. (1989). "Autotrophic nitrification in bacteria," in *Advances in Microbial Physiology*, eds A. H. Rose and D. W. Tempest (Cambridge: Academic Press), 125–181. doi: 10.1016/s0065-2911(08)60112-5

Prosser, J. I., Hink, L., Gubry-Rangin, C., and Nicol, G. W. (2020). Nitrous oxide production by ammonia oxidizers: physiological diversity, niche differentiation and potential mitigation strategies. *Glob. Chang. Biol.* 26, 103–118. doi: 10.1111/gcb.14877

Prosser, J. I., and Nicol, G. W. (2008). Relative contributions of archaea and bacteria to aerobic ammonia oxidation in the environment. *Environ. Microbiol.* 10, 2931–2941. doi: 10.1111/j.1462-2920.2008.01775.x

Prosser, J. I., and Nicol, G. W. (2012). Archaeal and bacterial ammonia-oxidisers in soil: the quest for niche specialisation and differentiation. *Trends Microbiol.* 20, 523–531. doi: 10.1016/j.tim.2012.08.001

Qin, W., Amin, S. A., Martens-Habbena, W., Walker, C. B., Urakawa, H., Devol, A. H., et al. (2014). Marine ammonia-oxidizing archaeal isolates display obligate mixotrophy and wide ecotypic variation. *Proc. Natl. Acad. Sci. U. S. A.* 111, 12504–12509. doi: 10.1073/pnas.1324115111

Quast, C., Pruesse, E., Yilmaz, P., Gerken, J., Schweer, T., Yarza, P., et al. (2012). The SILVA ribosomal RNA gene database project: improved data processing and web-based tools. *Nucleic Acids Res.* 41, D590–D596.

Quince, C., Lanzen, A., Davenport, R. J., and Turnbaugh, P. J. (2011). Removing noise from pyrosequenced amplicons. *BMC Bioinformatics* 12:38. doi: 10.1186/1471-2105-12-38

Rotthauwe, J. H., Witzel, K. P., and Liesack, W. (1997). The ammonia monooxygenase structural gene amoA as a functional marker: molecular fine-scale analysis of natural ammonia-oxidizing populations. *Appl. Environ. Microbiol.* 63, 4704–4712. doi: 10.1128/aem.63.12.4704-4712.1997

Sakoula, D., Koch, H., Frank, J., Jetten, M. S. M., van Kessel, M. A. H. J., and Lücker, S. (2020). Enrichment and physiological characterization of a novel comammox *Nitrospira* indicates ammonium inhibition of complete nitrification. *ISME J.* 15, 1010–1024. doi: 10.1038/s41396-41020-00827-41394

Santoro, A. E., and Casciotti, K. L. (2011). Enrichment and characterization of ammonia-oxidizing archaea from the open ocean: phylogeny, physiology and stable isotope fractionation. *ISME J.* 5, 1796–1808. doi: 10.1038/ismej.2011.58

Santoro, A. E., Dupont, C. L., Richter, R. A., Craig, M. T., Carini, P., McIlvin, M. R., et al. (2015). Genomic and proteomic characterization of "*Candidatus* Nitrosopelagicus brevis": an ammonia-oxidizing archaeon from the open ocean. *Proc. Natl. Acad. Sci. U. S. A.* 112, 1173–1178. doi: 10.1073/pnas.1416223112

Santoro, A. E., Richter, R. A., and Dupont, C. L. (2017). Planktonic marine archaea. *Ann. Rev. Mar. Sci.* 11, 131–158. doi: 10.1146/annurev-marine-121916-063141

Sauder, L. A., Albertsen, M., Engel, K., Schwarz, J., Nielsen, P. H., Wagner, M., et al. (2017). Cultivation and characterization of *Candidatus Nitrosocosmicus* exaquare, an ammonia-oxidizing archaeon from a municipal wastewater treatment system. *ISME J.* 11, 1142–1157. doi: 10.1038/ismej.2016.192

Simon, M., and Azam, F. (1989). Protein content and protein synthesis rates of planktonic marine bacteria. *Mar. Ecol. Prog. Ser.* 51, 201–213. doi: 10.3354/meps051201

Spasov, E., Tsuji, J. M., Hug, L. A., Doxey, A. C., Sauder, L. A., Parker, W. J., et al. (2020). High functional diversity among *Nitrospira* populations that dominate rotating biological contactor microbial communities in a municipal wastewater treatment plant. .*ISME J.* 14, 1857–1872. doi: 10.1038/s41396-020-0650-2

Stahl, D. A. (2020). The path leading to the discovery of the ammonia-oxidizing Archaea. *Environ. Microbiol.* 22, 4507–4519. doi: 10.1111/1462-2920.15239

Stahl, D. A., and de la Torre, J. R. (2012). Physiology and diversity of ammonia-oxidizing Archaea. *Ann. Rev. Microbiol.* 66, 83–101. doi: 10.1146/annurev-micro-092611-150128

Stein, L. Y. (2011). "Heterotrophic nitrification and nitrifier denitrification," in *Nitrification*, eds B. B. Ward, D. J. Arp, and M. G. Klotz (Washington: ASM Press), 95–114. doi: 10.1128/9781555817145.ch5

Stein, L. Y. (2019). Insights into the physiology of ammonia-oxidizing microorganisms. *Curr. Opin. Chem. Biol.* 49, 9–15. doi: 10.1016/j.cbpa.2018.09.003

Straka, L. L., Meinhardt, K. A., Bollmann, A., Stahl, D. A., and Winkler, M.-K. H. (2019). Affinity informs environmental cooperation between ammonia-oxidizing archaea (AOA) and anaerobic ammonia-oxidizing (Anammox) bacteria. *ISME J.* 13, 1997–2004. doi: 10.1038/s41396-019-0408-x

Suzuki, I., Dular, U., and Kwok, S. C. (1974). Ammonia or ammonium ion as substrate for oxidation by *Nitrosomonas europaea* cells and extracts. *J. Bacteriol.* 120, 556–558. doi: 10.1128/jb.120.1.556-558.1974

Takahashi, Y., Fujitani, H., Hirono, Y., Tago, K., Wang, Y., Hayatsu, M., et al. (2020). Enrichment of comammox and nitrite-oxidizing *Nitrospira* from acidic soils. *Front. Microbiol.* 11:1737. doi: 10.3389/fmicb.2020.01737

Thompson, L. R., Sanders, J. G., McDonald, D., Amir, A., Ladau, J., Locey, K. J., et al. (2017). A communal catalogue reveals Earth's multiscale microbial diversity. *Nature* 551, 457–463.

Tourna, M., Freitag, T. E., Nicol, G. W., and Prosser, J. I. (2008). Growth, activity and temperature responses of ammonia-oxidizing archaea and bacteria in soil microcosms. *Environ. Microbiol.* 10, 1357–1364. doi: 10.1111/j.1462-2920.2007.01563.x

Tourna, M., Stieglmeier, M., Spang, A., Könneke, M., Schintlmeister, A., Urich, T., et al. (2011). *Nitrososphaera viennensis*, an ammonia oxidizing archaeon from soil. *Proc. Natl. Acad. Sci. U. S. A.* 108, 8420–8425. doi: 10.1073/pnas.1013488108

Treusch, A. H., Leininger, S., Kletzin, A., Schuster, S. C., Klenk, H.-P., and Schleper, C. (2005). Novel genes for nitrite reductase and Amo-related proteins indicate a role of uncultivated mesophilic crenarchaeota in nitrogen cycling. *Environ. Microbiol.* 7, 1985–1995. doi: 10.1111/j.1462-2920.2005.00906.x

Urakawa, H., Martens-Habbena, W., and Stahl, D. A. (2010). High abundance of ammonia-oxidizing Archaea in coastal waters, determined using a modified DNA extraction method. *Appl. Environ. Microbiol.* 76, 2129–2135. doi: 10.1128/aem.02692-09

van Kessel, M. A. H. J., Speth, D. R., Albertsen, M., Nielsen, P. H., Op den Camp, H. J. M., Kartal, B., et al. (2015). Complete nitrification by a single microorganism. *Nature* 528, 555–559. doi: 10.1038/nature16459

Walker, C. B., de la Torre, J. R., Klotz, M. G., Urakawa, H., Pinel, N., Arp, D. J., et al. (2010). *Nitrosopumilus maritimus* genome reveals unique mechanisms for nitrification and autotrophy in globally distributed marine *crenarchaea*. *Proc. Natl. Acad. Sci. U. S. A.* 107, 8818–8823. doi: 10.1073/pnas.0913533107

Conflict of Interest: The authors declare that the research was conducted in the absence of any commercial or financial relationships that could be construed as a potential conflict of interest.

Advantages of publishing in Frontiers

OPEN ACCESS
Articles are free to read for greatest visibility and readership

FAST PUBLICATION
Around 90 days from submission to decision

HIGH QUALITY PEER-REVIEW
Rigorous, collaborative, and constructive peer-review

TRANSPARENT PEER-REVIEW
Editors and reviewers acknowledged by name on published articles

Frontiers
Avenue du Tribunal-Fédéral 34
1005 Lausanne | Switzerland

Visit us: www.frontiersin.org
Contact us: frontiersin.org/about/contact

REPRODUCIBILITY OF RESEARCH
Support open data and methods to enhance research reproducibility

DIGITAL PUBLISHING
Articles designed for optimal readership across devices

FOLLOW US
@frontiersin

IMPACT METRICS
Advanced article metrics track visibility across digital media

EXTENSIVE PROMOTION
Marketing and promotion of impactful research

LOOP RESEARCH NETWORK
Our network increases your article's readership